

# **Investigations of Macrocyclic and Heterobimetallic *N*-Heterocyclic Carbene Metal Complexes**

Zili Li

A thesis submitted in total fulfilment of  
the requirement for the degree of  
Doctor of Philosophy

Department of Chemistry and Physics  
School of Molecular Sciences  
College of Science, Health and Engineering  
La Trobe University  
Victoria, Australia

June 2020

## STATEMENT OF AUTHORSHIP

This thesis includes work by the author that has been published or accepted for publication as described in the text. Except where reference is made in the text of the thesis, this thesis contains no other material published elsewhere or extracted in whole or in part from a thesis accepted for the award of any other degree or diploma. No other person's work had been used without due acknowledgement in the main text of the thesis. This thesis has not been submitted for the award of any degree or diploma in any other tertiary institution.

Zili Li, PhD Candidate

Signature: 

Date: 17/06/2020

## STATEMENT OF CANDIDATE CONTRIBUTION

Chapter 2 contains work that has been published and details of the publication with an estimation of the percentage contribution of each author is indicated:


Li, Z. (85%); Wiratpruk, N. (5%); Barnard, P. J. (10%), *Frontiers in Chemistry* **2019**, 7, 270.

We hereby declare that the individual authors, or the corresponding author, have granted permission to the candidate (Zili Li) to use the results presented in the manuscript above in this thesis.

Supervisor  
Dr Peter Barnard

PhD Candidate  
Zili Li

Signature



Date

17/06/2020

17/06/2020

## ACKNOWLEDGEMENT

Firstly, I sincerely acknowledge my supervisor Dr Peter Barnard for his patience, guidance, advise and support. I would not have achieved so much in chemistry with the absence of your help. I would also like to acknowledge the help from my co-supervisor Dr Jason Dutton. I would like to acknowledge La Trobe University for providing me this opportunity to study as a PhD candidate. This work was supported by a La Trobe University Postgraduate Research Scholarship and a La Trobe University Full Fee Research Scholarship. I would also like to acknowledge all the Barnard group members, past and the present, for their technical and spiritual support. I also want to express my gratitude to Mr Quoc Dat Duong and Mr Joel Mather for sharing the duty to prepare (THT)AuCl, Ms Nuchareenat Wiratpruk for operating the high-resolution mass spectrometer for all the samples in this thesis, Mr Pria Ramkissoon for assisting me with the UV-Vis experiments, Dr Kristoff Basse for the variable temperature NMR experiments and the Dutton group for maintaining the glove box. I also wish to acknowledge Dr Tatiana Soares da Costa and her group for conducting antimicrobial studies. I would also acknowledge the huge sacrifice of the Gram-positive and Gram-negative bacteria whose lives were taken by the Au(I)-Ag(I) heterobimetallic complexes during the antimicrobial studies. I do appreciate the help and I want to say thank you. I am also grateful for all my colleagues and dearest friends in chemistry department particularly Ms Rebecca Karmis, Mr Timothy Gialelis and Dr Rebecca Christoff for proofreading my drafts. Once again, I would like to say thank you to everyone for all kinds of help and support.

Finally, I thank the times and experiences in Australia which I discovered myself much better and learnt:



BE NOT ASHAMED,

BE NOT AFRAID,

BE NOT WHAT THEY SAY,

BE PROUD,

BE LOUD,

BE YOURSELF.

## ABSTRACT

This thesis describes research on the synthesis of *tetra*-imidazolium macrocycles and their *N*-heterocyclic carbene (NHC) metal complexes in addition to the preparation of heterobimetallic NHC complexes. Two types of synthetic strategies were developed and utilized, these being stepwise macrocyclization and a post synthetic modification and metallation method for heterobimetallic complex formation.

The modular stepwise synthetic strategy was developed for the preparation of symmetrical and asymmetrical *tetra*-imidazolium macrocycles. Using this approach, a series of two symmetrical and three asymmetrical *tetra*-imidazolium macrocycles were prepared. These *tetra*-imidazolium macrocycle compounds act as receptors for halide anions and association constants were determined using <sup>1</sup>H-NMR titration studies. These *tetra*-imidazolium macrocycle compounds are precursors for NHC ligands and Au(I), Ag(I) and Pd(II) NHC complexes of these ligands were prepared. A varied of metal complex structures were obtained depending on the chosen macrocyclic NHC pro-ligands and the metal. Mono-, di-, and hexanuclear Au(I) and Ag(I) complexes were prepared while the Pd(II) complexes were found to be mononuclear only. In addition, the modular stepwise method also provides access to asymmetrical macrocycles carrying different azole derivatives (i.e. 1,2,3-triazole and C2-methylated imidazolium). Two imidazolium linked macrocycles incorporating 1,2,3-triazole groups were prepared and association constants between these compounds and halide anions (Cl, Br and I) were also determined using <sup>1</sup>H-NMR titration studies.

Meanwhile, a post synthetic modification and metallation method was utilized for the synthesis of a range of heterobimetallic NHC complexes. Using this method, a series of Au(I)-Ag(I) and Au(I)-Hg(II) heterobimetallic NHC complexes featuring either symmetrical or asymmetrical *bis*-NHC ligands were synthesised. This method offers a new

pathway for the synthesis of heterobimetallic complexes bearing asymmetrical ligands with selective placement of the metal ions. In addition, the antimicrobial property of the homobimetallic Au(I) and Ag(I) complexes and the Au(I)-Ag(I) heterobimetallic complexes were evaluated against two Gram-positive (*A. baumannii* and *E. coli*) and two Gram-negative (*E. faecium* and *S. aureus*) bacterial strains. The minimum inhibitory concentrations (MICs) of the Au(I)-Ag(I) heterobimetallic complexes displayed good activities against both Gram-positive and Gram-negative bacterial strain, with the values obtained being comparable to the currently available antibiotics such as colistin and vancomycin.

# TABLE OF CONTENTS

STATEMENT OF AUTHORSHIP .....	I
STATEMENT OF CANDIDATE CONTRIBUTION .....	II
ACKNOWLEDGEMENT .....	III
ABSTRACT .....	V
TABLE OF CONTENTS.....	VII
LIST OF COMPOUNDS.....	XI
ABBREVIATIONS .....	XXIII
STATEMENT OF AUTHORSHIP .....	I
STATEMENT OF CANDIDATE CONTRIBUTION .....	II
ACKNOWLEDGEMENT .....	III
ABSTRACT .....	IV
TABLE OF CONTENTS.....	VI
LIST OF COMPOUNDS.....	X
ABBREVIATIONS .....	XXII
CHAPTER 1 INTRODUCTION.....	1
1.1 <i>N</i> -Heterocyclic carbenes .....	1
1.1.1    Carbenes .....	1
1.1.2 <i>N</i> -Heterocyclic carbenes (NHCs).....	2
1.2    Imidazolium linked macrocycles .....	4
1.2.1    Synthesis of imidazolium linked macrocycle.....	4
1.2.2    Imidazolium linked macrocycles as anion sensors .....	8
1.3    Metal complexes of NHC ligands .....	12
1.3.1    NHC metal complexes derived from imidazolium linked macrocycles .....	12
1.4    Heterobimetallic complex of NHC ligands.....	21

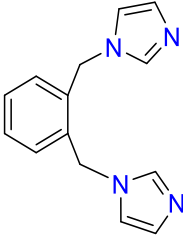
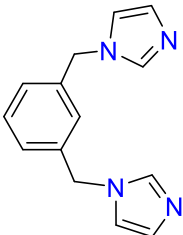
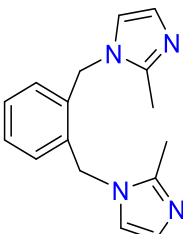
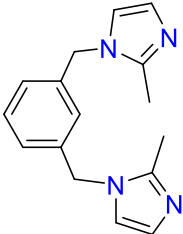
1.4.1	Synthesis of heterobimetallic metal complexes .....	21
1.4.2	Catalytic activities .....	26
1.4.3	Metallophilicity and photophysical properties .....	28
1.5	Biological applications of metal complexes of NHC ligands .....	31
1.5.1	Antimicrobial activities of silver (I) and gold(I) NHC complexes .....	31
1.5.2	Biological applications of heterobimetallic NHC complexes .....	34
1.6	Research overview .....	36
1.7	References .....	40
CHAPTER 2 STEPWISE SYNTHESIS OF <i>TETRA</i> -IMIDAZOLIUM MACROCYCLES		
	AND THEIR <i>N</i> -HETEROCYCLIC CARBENE METAL COMPLEXES.	49
2.1	Introduction .....	49
2.2	Results and discussion.....	51
2.2.1	Synthesis of <i>tetra</i> -imidazolium macrocycles .....	51
2.2.2	Synthesis of Ag(I), Au(I) and Pd(II) complexes .....	54
2.2.3	Structural studies .....	60
2.2.4	Anion binding studies.....	64
2.3	Conclusion.....	67
2.4	Experimental .....	67
2.4.1	<sup>1</sup> H-NMR titration studies .....	67
2.4.2	Jobs plot analysis.....	67
2.4.3	Synthesis.....	68
2.5	References .....	79
CHAPTER 3 SYNTHESIS OF MACROCYCLES INCORPORATING 1,2,3-TRIAZOLE		
	AND IMIDAZOLIUM UNITS AND THEIR METAL COMPLEXES .....	82
3.1	Introduction .....	82
3.2	Results and discussion.....	87

3.2.1	Synthesis of macrocycles containing 1,2,3-triazole and imidazolium groups .....	87
3.2.2	Synthesis of the metal complexes of macrocycle 3.21·Br <sub>2</sub> .....	93
3.2.3	Anion binding studies.....	94
3.3	Conclusion.....	99
3.4	Experimental .....	100
3.4.1	<sup>1</sup> H-NMR titration studies .....	100
3.4.2	Jobs plot analysis.....	100
3.4.3	Synthesis.....	100
3.5	References .....	105
CHAPTER 4 HETEROBIMETALLIC <i>N</i> -HETEROCYCLIC CARBENE COMPLEXES.		
	.....	108
4.1	Introduction .....	108
4.2	Results and discussion.....	110
4.2.1	Synthesis of methylene linked imidazolium salt pro-ligands and corresponding metal complexes .....	110
4.2.2	Synthesis of homobimetallic complexes .....	120
4.2.3	Variable temperature <sup>1</sup> H-NMR studies .....	122
4.2.4	Heterobimetallic complexes of ethylene linked <i>bis</i> -NHC ligands .....	129
4.2.5	Photophysical studies .....	135
4.2.6	Antimicrobial studies .....	136
4.3	Conclusion.....	138
4.4	Experimental .....	140
4.4.1	Synthesis.....	140
4.4.2	Photophysical studies .....	151
4.4.3	Antimicrobial studies .....	151

4.5	References .....	152
CHAPTER 5 CONCLUSION AND FUTURE WORK.....		156
5.1	Conclusion and future work .....	156
5.2	References .....	163
APPENDIX .....		I
A.1	General details.....	i
A.2	Appendix for Chapter 2.....	ii
A.2.1	NMR Spectra for Chapter 2 .....	ii
A.2.2	<sup>1</sup> H-NMR titration spectra for Chapter 2.....	xxi
A.3	Appendix for Chapter 3.....	xxiii
A.3.1	NMR Spectra for Chapter 3 .....	xxiii
A.3.2	<sup>1</sup> H-NMR titration spectra .....	xxxii
A.4	Appendix for Chapter 4.....	xxxvi
A.4.1	NMR Spectra for Chapter 4 .....	xxxvi
A.4.2	Variable temperature NMR studies for Chapter 4 .....	lix
A.5	X-ray crystallography.....	lx
A.5.1	X-ray crystallography detail.....	lx
A.5.2	XRD data for Chapter 2 .....	lxii
A.5.3	XRD data for Chapter 4 .....	lxiii

# LIST OF COMPOUNDS

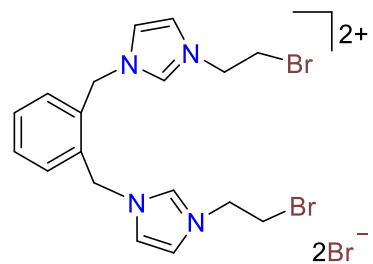
## Chapter 2

Compound Number	Structure
2.7	
2.8	
2.9	
2.10	

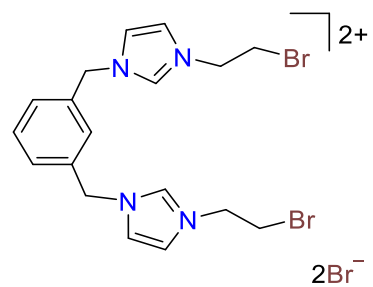


---

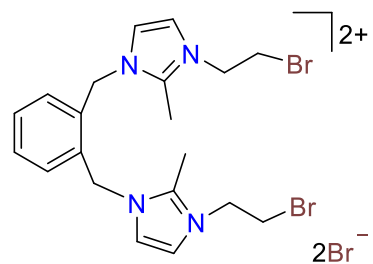
**2.11·Br<sub>2</sub>**



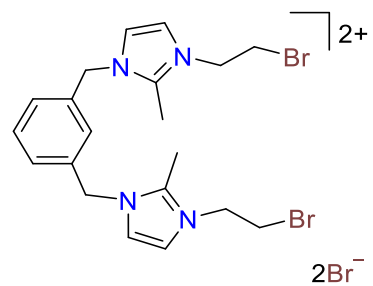
**2.12·Br<sub>2</sub>**



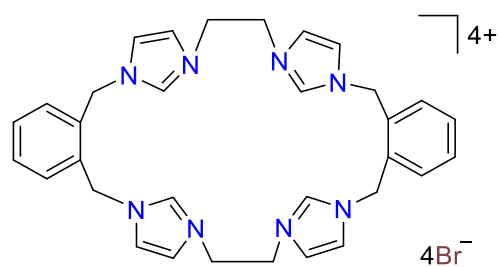
**2.13·Br<sub>2</sub>**



**2.14·Br<sub>2</sub>**

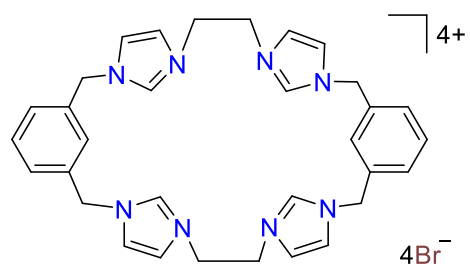


**2.15·Br<sub>4</sub>**

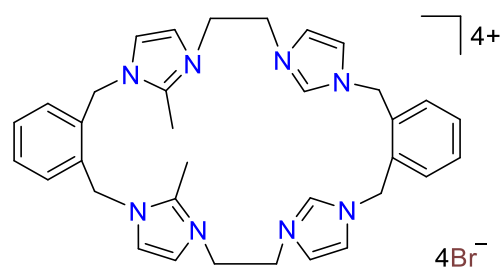


---

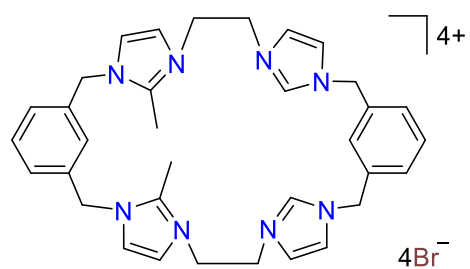
**2.16·Br<sub>4</sub>**



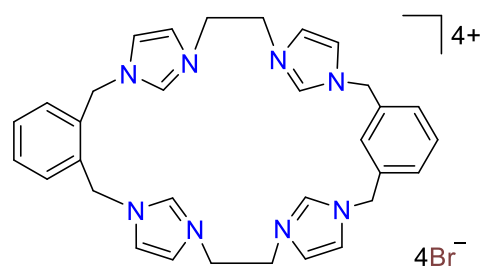
**2.17·Br<sub>4</sub>**



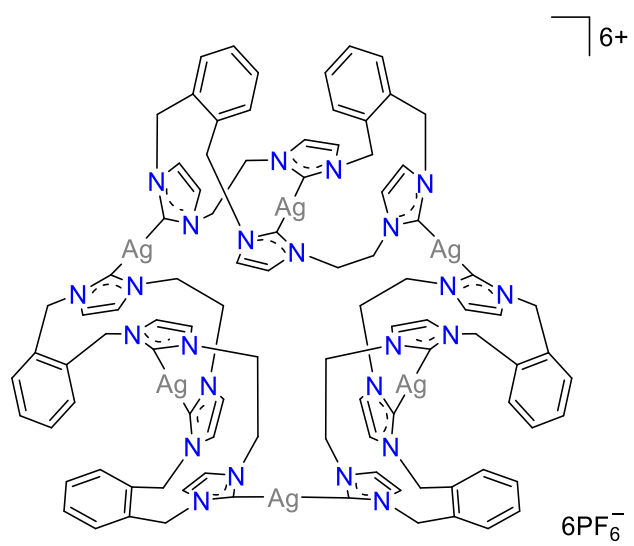
**2.18·Br<sub>4</sub>**



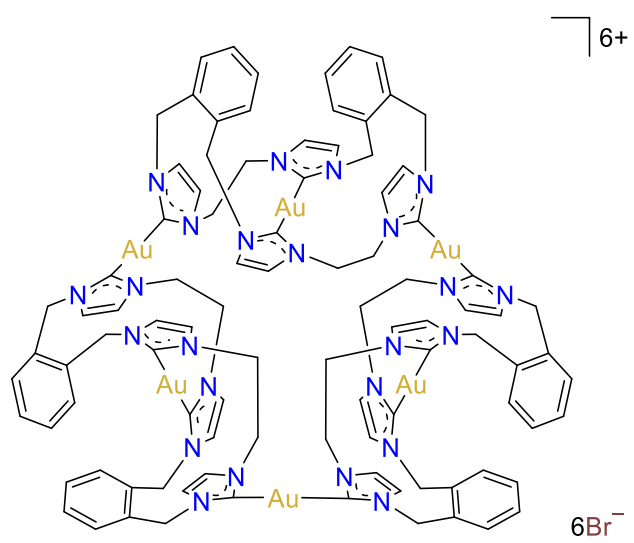
**2.19·Br<sub>4</sub>**



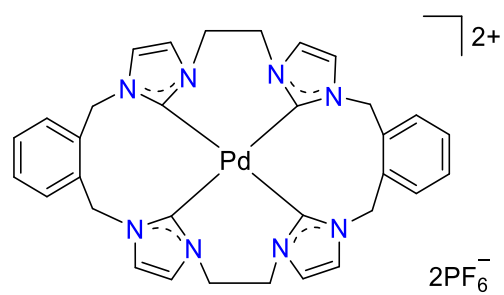
**2.20·(PF<sub>6</sub>)<sub>6</sub>**



**2.21·Br<sub>6</sub>**

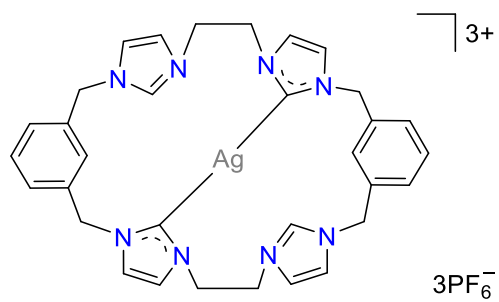


**2.22·(PF<sub>6</sub>)<sub>2</sub>**

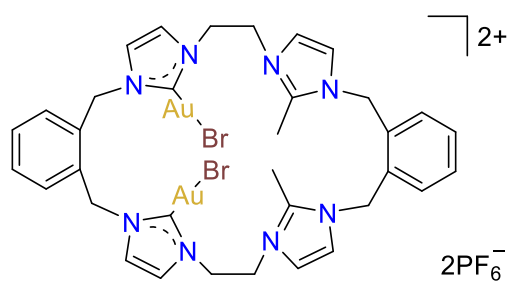


---

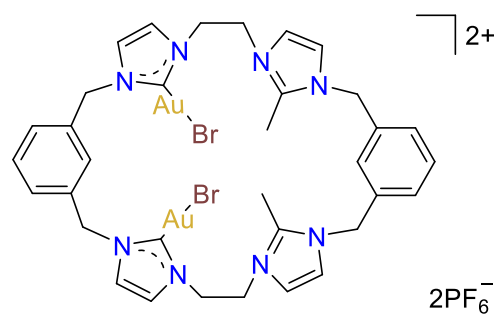
**2.23**·(PF<sub>6</sub>)<sub>3</sub>



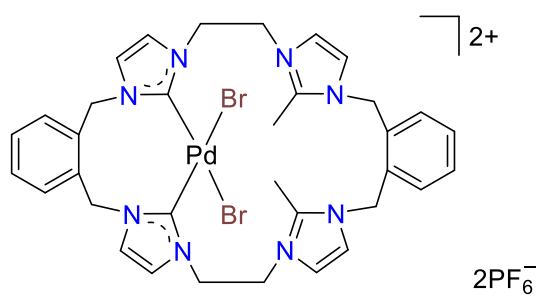
**2.24**·(PF<sub>6</sub>)<sub>2</sub>



**2.25**·(PF<sub>6</sub>)<sub>2</sub>



**2.26**·(PF<sub>6</sub>)<sub>2</sub>



---

## Chapter 3

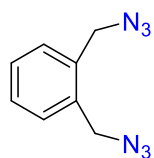
---

Compound Number

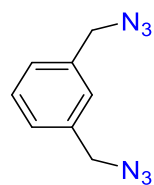
Structure

---

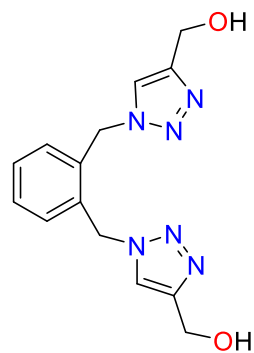
3.15



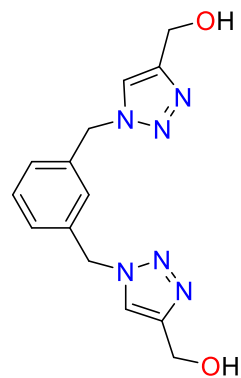
3.16



3.17

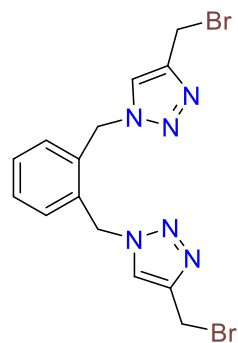


3.18

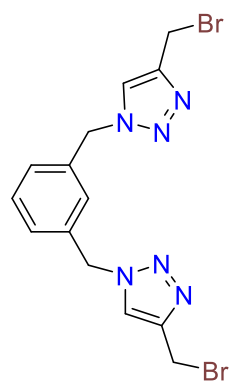


---

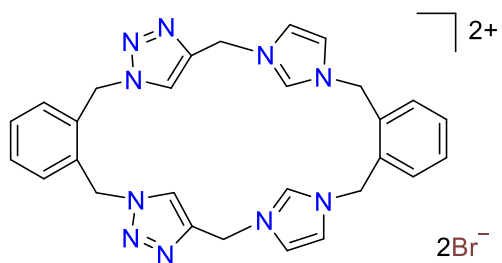
3.19



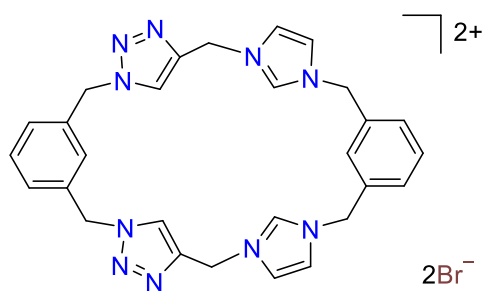
3.20



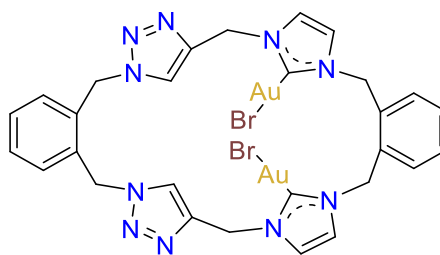
3.21·Br<sub>2</sub>



3.22·Br<sub>2</sub>



3.23

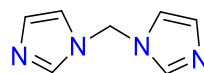


## Chapter 4

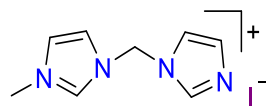
Compound Number

Structure

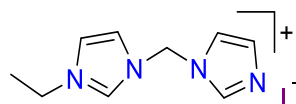
4.4



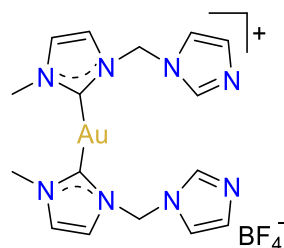
4.5·I



4.6·I

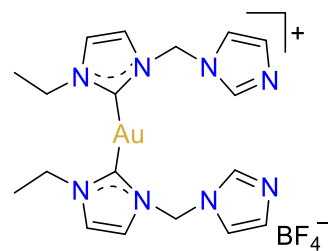


4.7·BF<sub>4</sub>

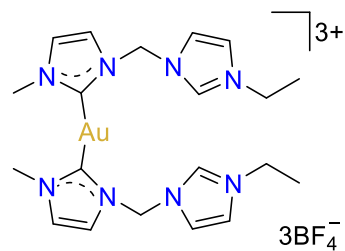


---

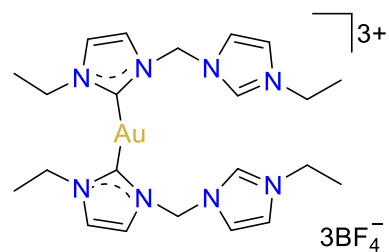
**4.8·BF<sub>4</sub>**



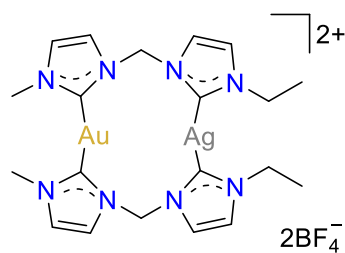
**4.9·(BF<sub>4</sub>)<sub>3</sub>**



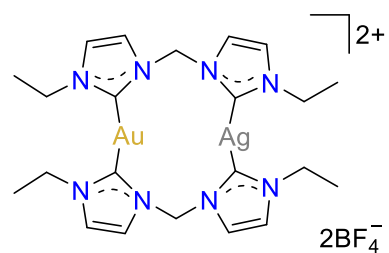
**4.10·(BF<sub>4</sub>)<sub>3</sub>**



**4.11·(BF<sub>4</sub>)<sub>2</sub>**



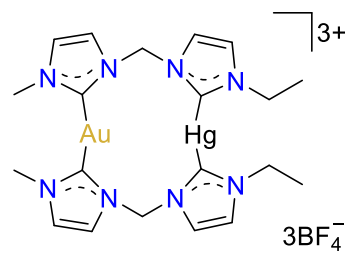
**4.12·(BF<sub>4</sub>)<sub>2</sub>**



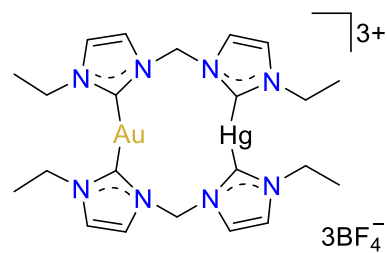


---

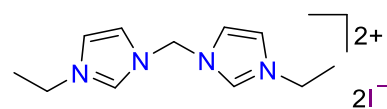
**4.13·(BF<sub>4</sub>)<sub>3</sub>**



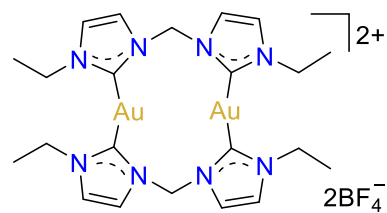
**4.14·(BF<sub>4</sub>)<sub>3</sub>**



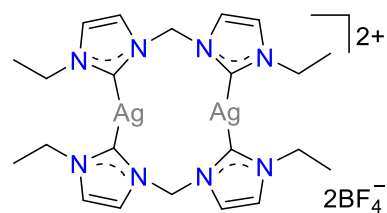
**4.16·I<sub>2</sub>**



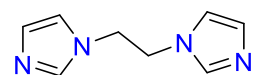
**4.17·(BF<sub>4</sub>)<sub>2</sub>**



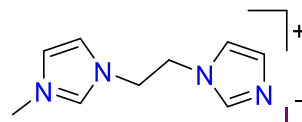
**4.18·(BF<sub>4</sub>)<sub>2</sub>**



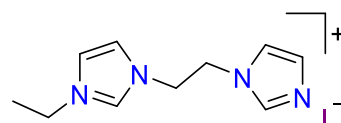
4.19



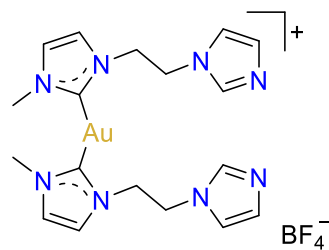
4.20·I



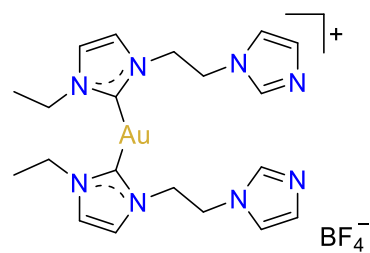
4.21·I



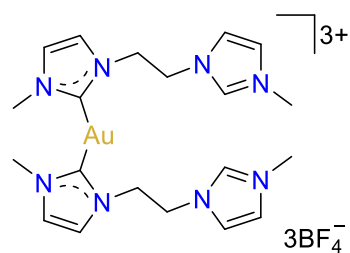
4.22·BF<sub>4</sub>



4.23·BF<sub>4</sub>

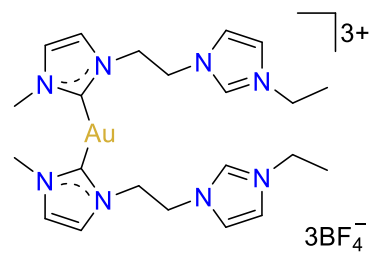


4.24·(BF<sub>4</sub>)<sub>3</sub>

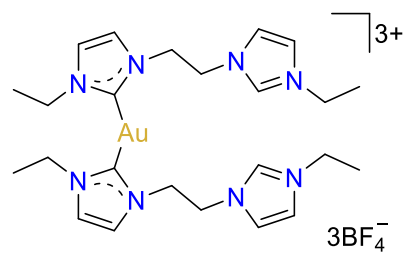


---

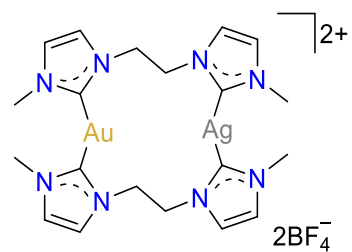
**4.25·(BF<sub>4</sub>)<sub>3</sub>**



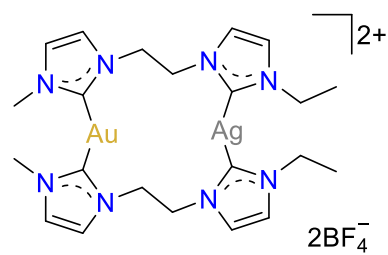
**4.26·(BF<sub>4</sub>)<sub>3</sub>**



**4.27·(BF<sub>4</sub>)<sub>2</sub>**



**4.28·(BF<sub>4</sub>)<sub>2</sub>**



## ABBREVIATIONS

<i>A. baumannii</i>	<b>A</b>	<i>Acinetobacter baumannii</i>
aNHC		Abnormal <i>N</i> -heterocyclic carbene
Ar		Aromatic
ATP		Adenosine triphosphate
	<b>B</b>	
br		Broad
Bu		Butyl
<sup>t</sup> Bu		Tertbutyl
<sup>t</sup> BuOH		<i>Tert</i> -butanol
Bn		Benzyl
	<b>C</b>	
calcd		Calculated
cat.		Catalyst
COD		1,5-Cyclooctadiene
COSY		Correlation spectroscopy
Cp*		Cyclopentadienyl
CuAAC		Cu(I)-catalyzed azide-alkyne cycloaddition
	<b>D</b>	
Dipp		2,6-Diisopropylphenyl
DMF		<i>N,N</i> -Dimethylformamide
DMSO		Dimethyl sulfoxide
DNA		Deoxyribonucleic acid
	<b>E</b>	
<i>E. coli</i>		<i>Escherichia coli</i>
<i>E. faecium</i>		<i>Enterococcus faecium</i>
eq.		equivalent
ESI		electrospray ion
Et		Ethyl
Et <sub>3</sub> OBF <sub>4</sub>		Triethyloxonium tetrafluoroborate
	<b>G</b>	
GTP		Guanosine triphosphate

HMBC

HOMO

HSQC

imi

LUMO

Me

Me<sub>3</sub>OBF<sub>4</sub>

Mes

MIC

NHC

NMR

NOESY

OAc

*P. aeruginosa*

Ph

ppt

ppy

<sup>t</sup>PrOH

RNA

RT

*S. aureus*

*S. epidermidis*

## H

Heteronuclear multiple bond correlation spectroscopy

Highest occupied molecular orbital

Heteronuclear single quantum correlation spectroscopy

## I

Imidazole

## L

Lowest unoccupied molecular orbital

## M

Methyl group

Trimethyloxonium tetrafluoroborate

Mesityl

Minimum inhibit concentration

## N

*N*-heterocyclic carbene

Nuclear magnetic resonance

Nuclear Overhauser effect spectroscopy

## O

Acetate

## P

*Pseudomonas aeruginosa*

Phenyl

Precipitate

Phenyl pyridine

Isopropanol

## R

Ribonucleic acid

Room temperature

## S

*Staphylococcus aureus*

*Staphylococcus epidermidis*

*S. mutans*

*Streptococcus mutans*

TBTA

THF

THT

trz

VOC

VT <sup>1</sup>H-NMR

## T

*Tris*(benzyltriazolylmethyl)amine

Tetrahydrofuran

Tetrahydrothiophene

1,2,3-Triazole

## V

Volatile organic compound

Variable temperature <sup>1</sup>H nuclear magnetic resonance

# CHAPTER 1 INTRODUCTION

## 1.1 *N*-Heterocyclic carbenes

### 1.1.1 Carbenes

Carbenes are neutral compounds featuring a divalent carbon with only six electrons in the valence shell. Singlet carbenes feature a lone pair of electrons in an  $sp^2$  hybridized orbital leaving an unhybridized  $p$ -orbital vacant, the non-bonding electrons in the triplet carbene occupy both the  $sp^2$  hybridized orbital and the unhybridized  $p$ -orbital (Figure 1.1).<sup>1-</sup>

3

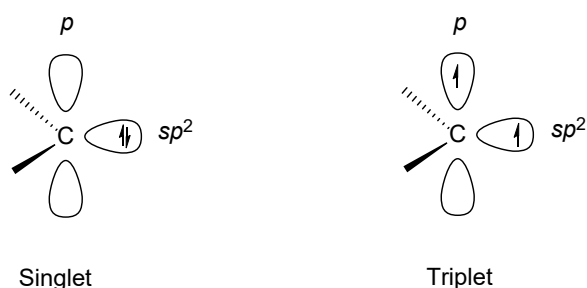


Figure 1.1 Electron configurations of singlet and triplet carbene.

Carbenes have played a significant role in organometallic chemistry. Carbenes were first introduced in this field with the synthesis of the tungsten carbonyl carbene complex **1.1** in 1964 (Figure 1.2).<sup>4</sup> Since this report, the organometallic chemistry of carbene metal complexes has been extensively studied and these compounds have been found a range of different applications.<sup>5-9</sup>

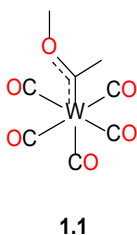
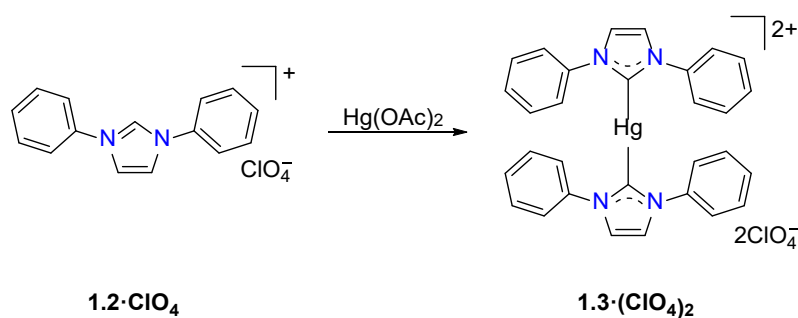


Figure 1.2 First reported tungsten carbonyl carbene complex.

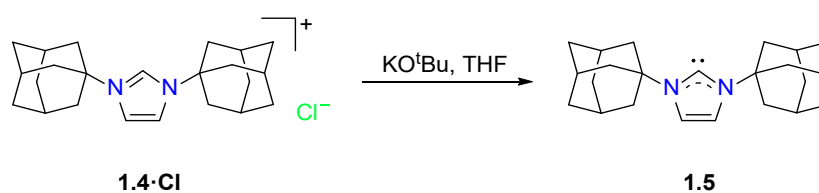
### 1.1.2 *N*-Heterocyclic carbenes (NHCs)

*N*-Heterocyclic carbenes (NHCs) are derived from azoles such as imidazole, benzimidazole and triazole and have been extensively studied since their first report in 1962.<sup>10</sup> In 1968 a Hg(II) complex of an NHC ligand **1.3**·(ClO<sub>4</sub>)<sub>2</sub> was reported by Wanzlick and co-workers and this is the first example of an NHC metal complex (Scheme 1.1).<sup>11</sup>



Scheme 1.1 Synthetic scheme for the preparation of the first NHC-Hg(II) complex **1.3**·(ClO<sub>4</sub>)<sub>2</sub>.

Arduengo and co-workers reported the first stable free NHC **1.5** (Scheme 1.2) in 1991. After the first report, numerous research studies have described the preparation of NHC from the corresponding azolium e.g. imidazolium and benzimidazolium precursors (Figure 1.3).<sup>5-9</sup>



Scheme 1.2 Synthesis of the first isolated free *N*-heterocyclic carbene (NHC).



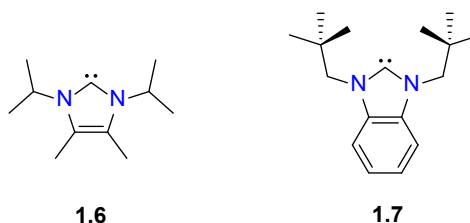
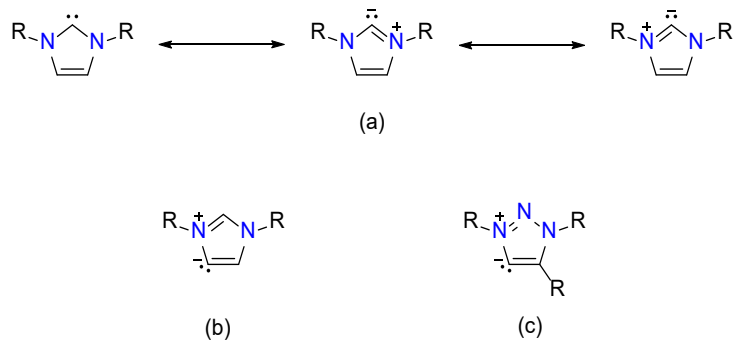


Figure 1.3 Selected examples of free NHC derived from azolium precursors.

For NHCs, the carbene exists in the singlet electronic state, where a pair of electrons occupy the  $sp^2$  orbital.<sup>1</sup> In the case of imidazolylidene, the carbene is located on the C2 position of the imidazolylidene ring and resonance structures with all neutral formal charges can be written (Scheme 1.3).<sup>2, 12-13</sup> Although less common, the carbene can also be located on the C4 or C5 position of the imidazolylidene ring or C5 position of the 1,2,4-triazolylidene ring. This class of carbenes is collectively known as an abnormal NHCs (aNHCs) and aNHCs are obliged to carry both positive and negative charges. The ring system is, therefore, mesoionic and resonance structures with all neutral formal charges cannot be written (Scheme 1.3).<sup>2, 12-13</sup>



Scheme 1.3 (a) The resonance structures of imidazolylidene and (b) The electron structure of abnormal *N*-heterocyclic carbene (aNHC) derived from imidazole and (c) The electron structure of aNHC derived from 1,2,3-triazole.

Although both the normal and abnormal NHC types are relatively reactive due to the lone pair located on the carbene, these carbenes are relatively stable compared to other carbene types because of electronic effects. Multiple researchers have found that the electronegative

nitrogen atom(s) in the NHC ring systems cause the withdrawal of  $\sigma$ -electrons from the carbene carbon atom via the inductive effect which decreases the energy of the highest occupied molecular orbital (HOMO) and this results in the lone electron pair located in the  $sp^2$  orbital being stabilized (Figure 1.4). On the other hand, there also exists a  $\pi$ -electron donating effect where the nitrogen lone pair electrons are donated into the unoccupied  $p$ -orbital of the carbene carbon increasing the energy of lowest unoccupied molecular orbitals (LUMO) and also stabilizing the singlet carbene (Figure 1.4).<sup>1, 3, 14-19</sup> Furthermore, there is a thermodynamic stabilization of the NHCs via cyclic 6  $\pi$ -electron delocalization.<sup>3, 20</sup> The combination of the  $\sigma$ -inductive and  $\pi$ -donating effect, results in an increase HOMO and LUMO energy gap and the singlet electronic state is favoured. These electronic effects also cause NHCs to be strong  $\sigma$ -donors and weak  $\pi$ -acceptors when forming metal complexes.

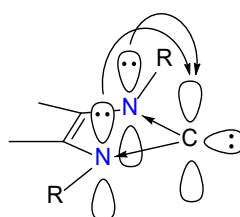


Figure 1.4 Schematic representation of the  $\sigma$ -withdrawing and  $\pi$ -donating electronic effects of the nitrogen atoms flanking the carbene centre in an NHC (imidazolydene) ring system.

## 1.2 Imidazolium linked macrocycles

### 1.2.1 Synthesis of imidazolium linked macrocycle

Due to their potential for acting as receptors to a range of anions including halides and other biologically relevant anionic species and their capacities to be utilized as precursors for the preparation of NHC metal complexes, numerous examples of imidazolium linked macrocyclic compounds in which the cyclic ring incorporates multiple imidazolium units (Figure 1.5) have been prepared and their properties investigated.

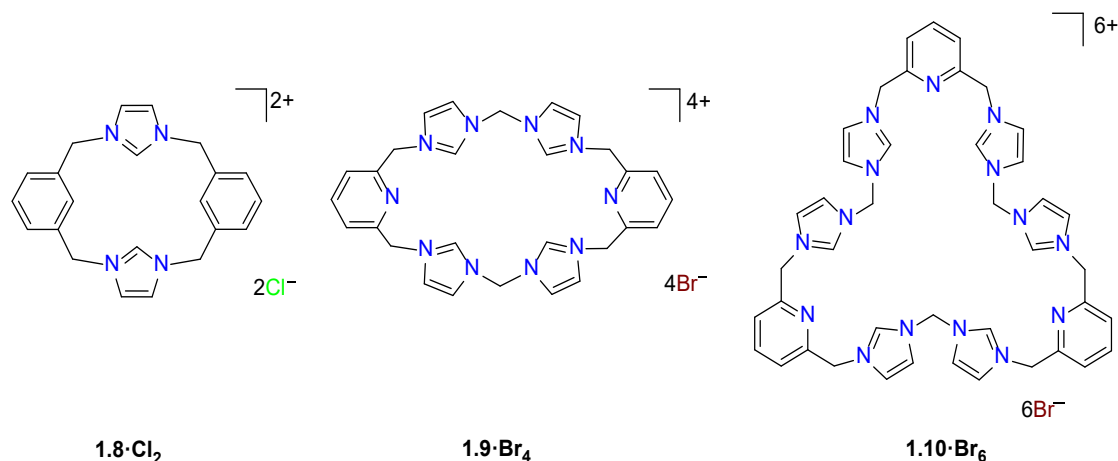
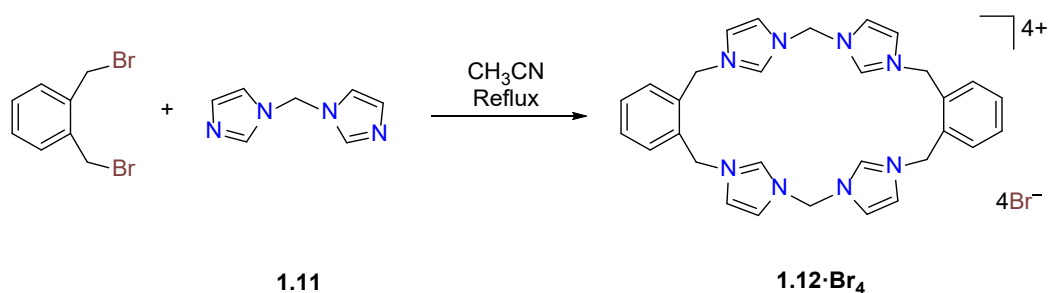


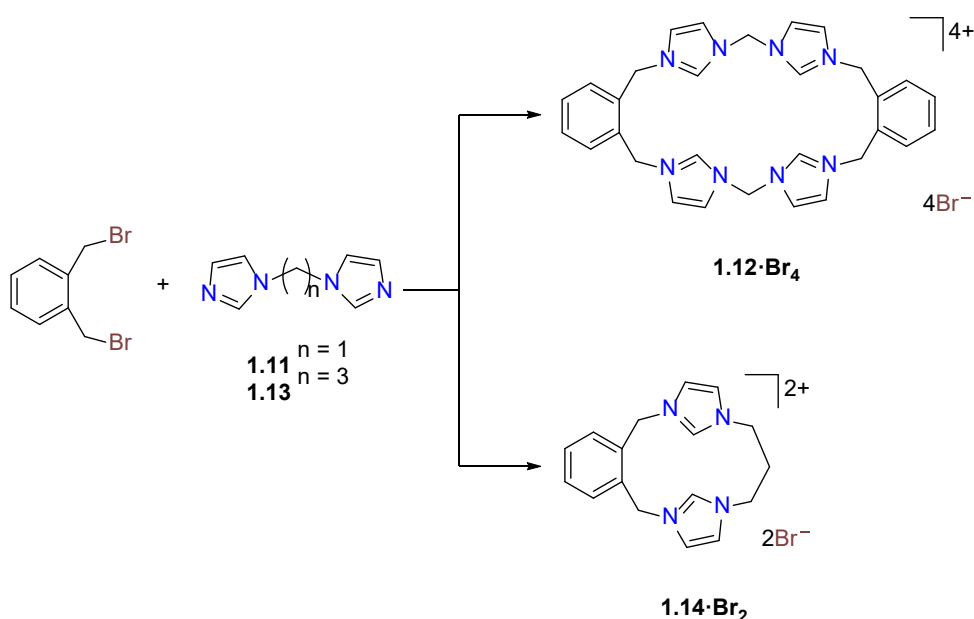
Figure 1.5 Selected examples of imidazolium linked cyclophanes and macrocycles.

The preparation of imidazolium linked macrocyclic compounds which have been previously reported includes direct macrocyclization,<sup>21-26</sup> stepwise macrocyclization<sup>27-29</sup> and anion template-directed<sup>30-33</sup> processes. One of the most straightforward approaches is direct macrocyclization, where the desired compounds are prepared by reacting equal quantities of a *bis*-imidazole precursor and a dihaloalkane under high dilution conditions. For example, the *tetra*-imidazolium linked macrocycle **1.12·Br<sub>4</sub>** was prepared by reacting an equimolar mixture of methylene linked *bis*-imidazole species **1.11** and  $\alpha,\alpha'$ -dibromo-*o*-xylene (Scheme 1.4).<sup>21</sup> Similarly, the *tetra*- and hexaimidazolium linked macrocyclic compounds **1.9·Br<sub>4</sub>** and **1.10·Br<sub>6</sub>** were also synthesized by a reaction of equal quantities of alkyl bridged *bis*-imidazole units and 2,6-*bis*-(bromomethyl)pyridine (Figure 1.5).<sup>22</sup>



Scheme 1.4 Direct macrocyclization synthesis of *tetra*-imidazolium macrocycle **1.12·Br<sub>4</sub>**.

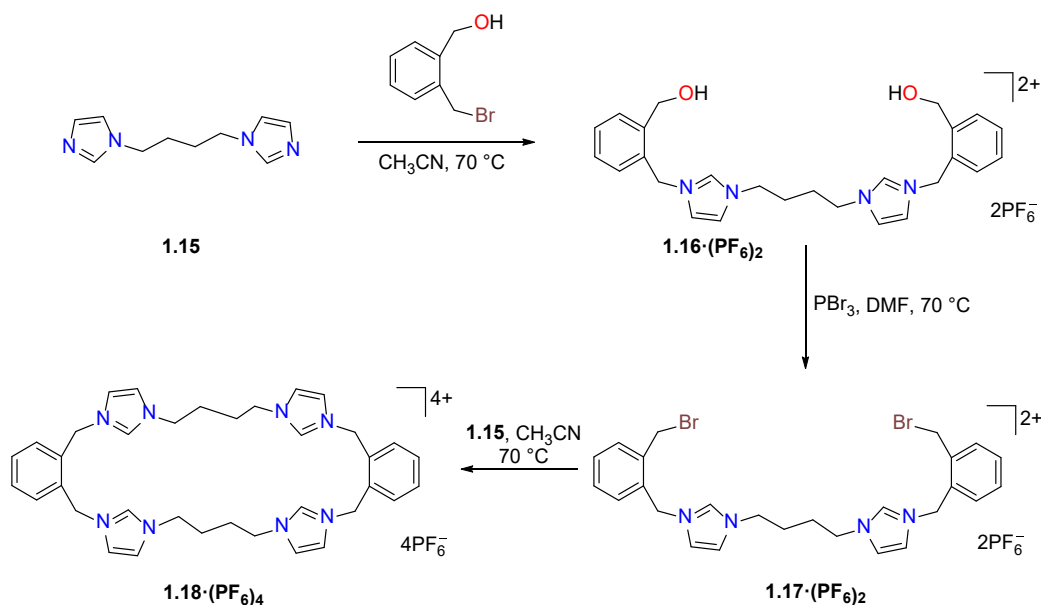
Unfortunately, however, the straightforward direct macrocyclization approach can be limited as a result of unintended reactivity between the precursor compounds, which can produce complex reaction mixtures and poor yields of the desired products. For example, the reaction of  $\alpha,\alpha'$ -dibromo-*o*-xylene and methylene linked *bis*-imidazole precursor **1.11** gave the desired *tetra*-imidazolium linked macrocycle **1.12·Br<sub>4</sub>** (Scheme 1.5).<sup>22</sup> However, using the same method by reacting  $\alpha,\alpha'$ -dibromo-*o*-xylene and propylene linked *bis*-imidazole species **1.13** a *bis*-imidazolium linked cyclophane compound **1.14·Br<sub>2</sub>** was produced instead of a *tetra*-imidazolium linked macrocycle (Scheme 1.5).<sup>34-35</sup> In this study, it was suggested that as the linker size increased, **1.13** has more flexibility compared with the *bis*-imidazolium **1.11** and the *bis*-imidazole cyclophane **1.14·Br<sub>2</sub>**, was formed.<sup>35</sup>



Scheme 1.5 Undesirable cyclophane **1.14·Br<sub>2</sub>** was generated as the chain length increased.

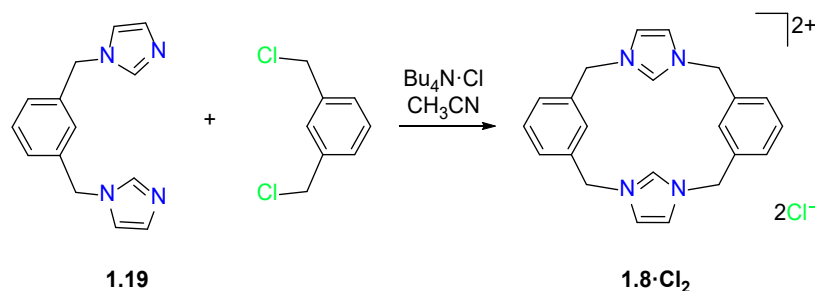
To overcome this problem, stepwise macrocyclization approaches have been used for the synthesis of the *tetra*-imidazolium linked macrocycles. For example, compound **1.18·(PF<sub>6</sub>)<sub>4</sub>** (Scheme 1.6) was prepared by the reaction of bromomethyl benzyl alcohol with the *bis*-imidazole precursor **1.15** to obtain **1.16·(PF<sub>6</sub>)<sub>2</sub>**. The hydroxyl group of **1.16·(PF<sub>6</sub>)<sub>2</sub>** was then converted to an alkyl bromide **1.17·(PF<sub>6</sub>)<sub>2</sub>** using PBr<sub>3</sub> and this intermediate

**1.17**·(PF<sub>6</sub>)<sub>2</sub> was then reacted with **1.15** to obtain the *tetra*-imidazolium linked macrocycle **1.18**·(PF<sub>6</sub>)<sub>4</sub>.<sup>35</sup>



Scheme 1.6 Stepwise synthesis of the *tetra*-imidazolium linked macrocycle **1.18**·(PF<sub>6</sub>)<sub>4</sub>.

Interestingly, a number of imidazolium linked macrocyclic compounds have been prepared using anion template-directed synthetic methods.<sup>31-33</sup> For example, a series of imidazolium linked cyclophanes were prepared via an anion directed ‘3 + 1’ macrocyclization method. Here, *bis*-(imidazolylmethyl)benzene species **1.19** and  $\alpha,\alpha'$ -dichloro-*m*-xylene were reacted in the presence of Bu<sub>4</sub>N·Cl as a source of Cl<sup>-</sup> as the templating agent. By using this method, the yield of the desired cyclophane compounds **1.8**·Cl<sub>2</sub> was very good at 83% (Scheme 1.7).<sup>36</sup> The same methodology was also used to prepare a series of similar *bis*-imidazolium linked cyclophanes (Figure 1.6)<sup>37</sup>. It was found that the halide anion templating reagent accelerated the reaction rate in the ring closure step as a result of hydrogen bonding between halide and the imidazolium units which allowed the formation of the desired macrocyclic product.<sup>30, 38-39</sup>



Scheme 1.7 Anion template-directed synthesis of *bis*-imidazolium linked macrocycle by using  $\text{Bu}_4\text{N}^+\text{Cl}^-$ .

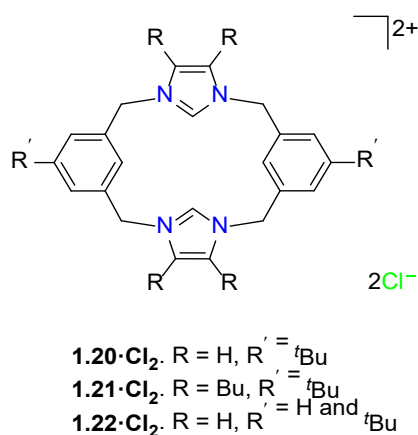


Figure 1.6 Imidazolium linked macrocycle prepared by an anion-based template-directed synthesis.

### 1.2.2 Imidazolium linked macrocycles as anion sensors

Due to the positive charge, the C2 position proton of the imidazolium ring is weakly acidic with a  $\text{p}K_{\text{a}}$  value in the range of 21 – 23.<sup>40-41</sup> As a result of the weak acidity of the C2-H, hydrogen bonding between this proton and anions such as halides,<sup>24, 27, 30, 37, 42-43</sup> acetate,<sup>24, 43</sup> dihydrogenphosphate<sup>26, 36</sup> and other biological anionic species often occurs and this provides the basis for the application of imidazolium linked macrocyclic compounds as anion sensors (Figure 1.7).<sup>36, 44-49</sup>

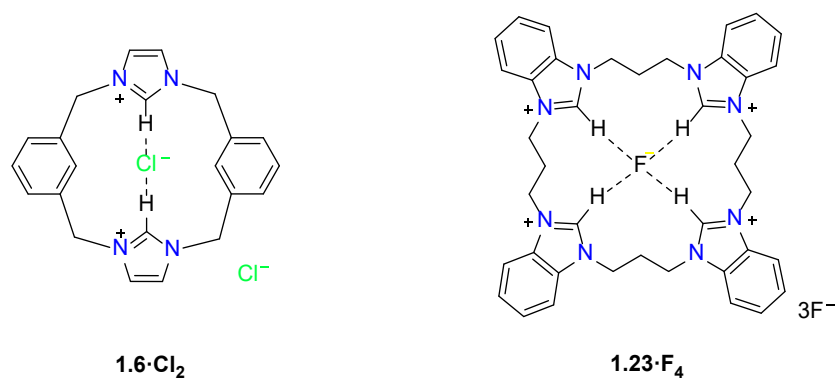


Figure 1.7 Hydrogen bonding between the hydrogen atom located at the C2 position with the anions chloride and fluoride for (a) an imidazolium linked cyclophane and (b) a benzimidazolium linked macrocycle.

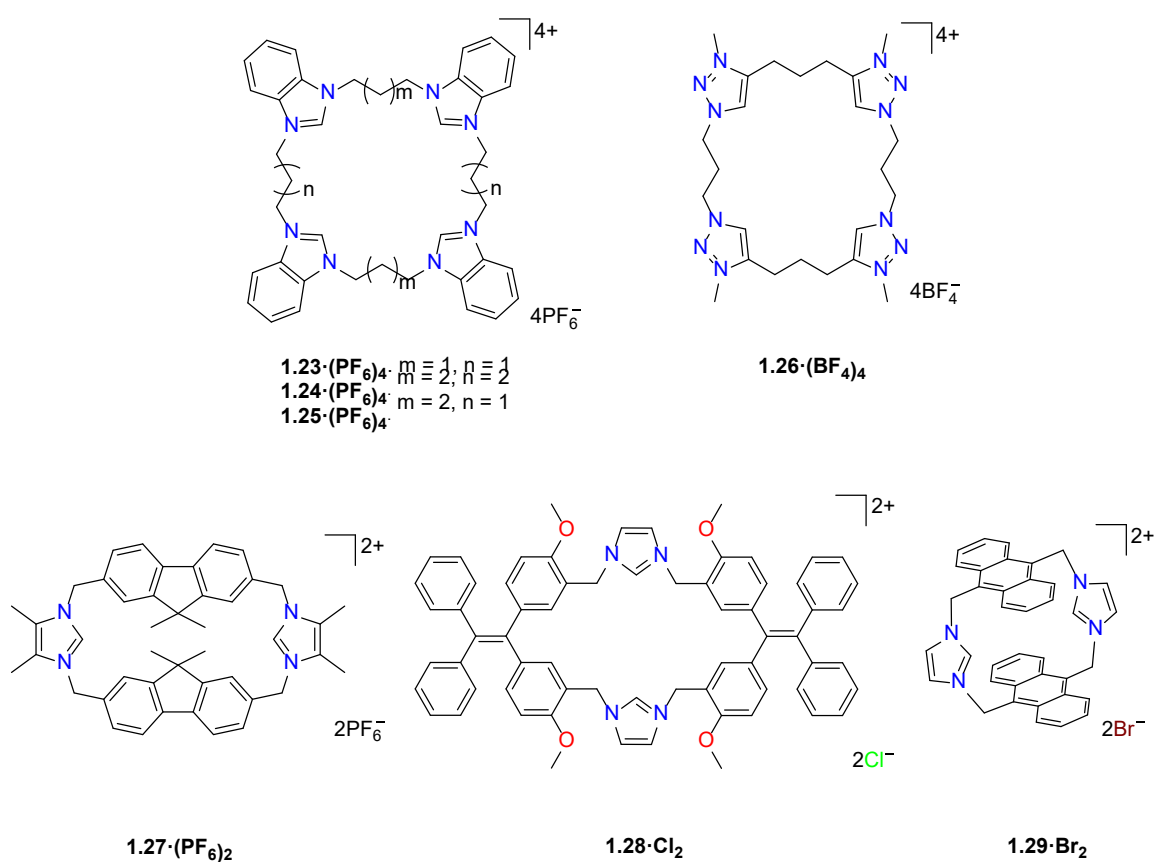
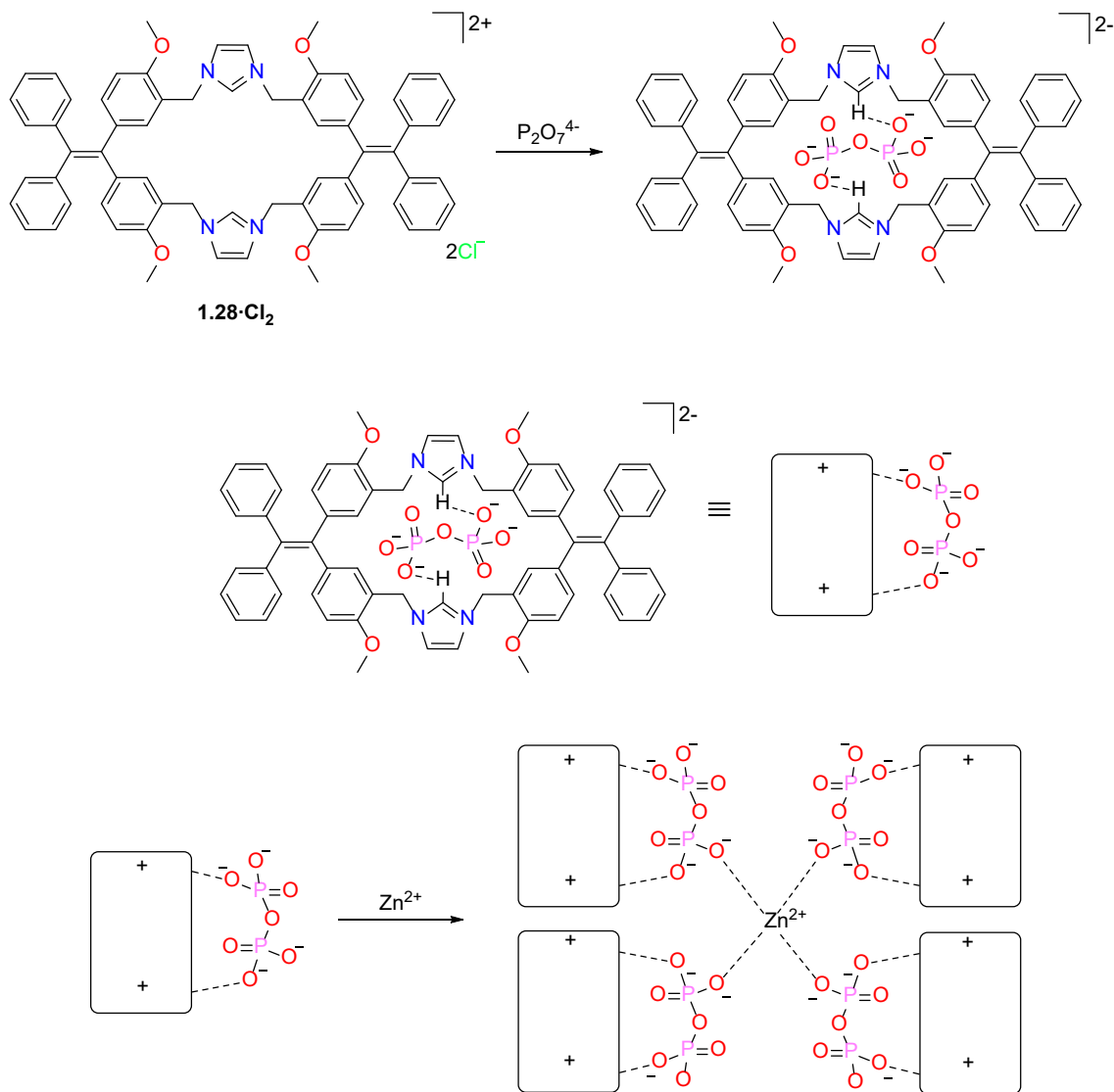


Figure 1.8 Selected examples of imidazolium and triazolium linked cyclophanes and macrocycles.

The hydrogen bonding interaction of the C2-H with anions can be readily detected using  $^1\text{H}$ -NMR spectroscopy. As the concentration of halide anions increases, the C2-H is progressively deshielded and shifts downfield. From the changes in the chemical shift, the binding constant  $K_a$  for the binding interaction can subsequently be calculated. For

example, a number of *tetra*-imidazolium linked macrocycles (Figure 1.8) have been shown to selectively recognize different anions. Monitoring the imidazolium C2-H proton resonance of receptor **1.23**·(PF<sub>6</sub>)<sub>4</sub> by <sup>1</sup>H-NMR spectroscopy, the receptor showed a downfield shift of the C2-H signal from 9.3 – 10.5 ppm after addition of F<sup>-</sup> anions (Bu<sub>4</sub>N·F). When other halide anions including Cl<sup>-</sup>, Br<sup>-</sup> and I<sup>-</sup> were added, a similar but smaller change in the C2-H chemical shift was observed. In addition, the receptors **1.24**·(PF<sub>6</sub>)<sub>4</sub> and **1.25**·(PF<sub>6</sub>)<sub>4</sub> showed a selectivity trend of F<sup>-</sup> > Cl<sup>-</sup> > Br<sup>-</sup> > I<sup>-</sup> and the K<sub>a</sub> value between **1.25**·(PF<sub>6</sub>)<sub>4</sub> and chloride, bromide and iodide were determined to be 1100, 1050, and 560 M<sup>-1</sup> respectively. Interestingly, these imidazolium receptors also interacted with the benzoate anion with a 1 : 2 stoichiometry.<sup>27</sup> In a second example, the *tetra*-1,2,3-triazolium linked macrocycle **1.26**·(BF<sub>4</sub>)<sub>4</sub> (Figure 1.8) also showed a pronounced binding interaction with halide anions (F<sup>-</sup>, Cl<sup>-</sup>, Br<sup>-</sup> and I<sup>-</sup>) through C-H···X<sup>-</sup> hydrogen bonding interactions and the K<sub>a</sub> values were determined to be within the range 226 – 463 M<sup>-1</sup> for these anions.<sup>29</sup> In addition, these interactions are strongly influenced by electrostatic interactions and the cavity size of the macrocycle and the *tetra*-triazolium linked macrocycle interacted strongly with sulfate anions (K<sub>a</sub> > 10<sup>4</sup> M<sup>-1</sup>).<sup>29</sup> Imidazolium linked cyclophane and macrocyclic compounds have also been shown to be useful for sensing other anions. For example, the dicationic *bis*-imidazolium cyclophane **1.27**·(PF<sub>6</sub>)<sub>2</sub> (Figure 1.8) was able to selectively sense anions such as H<sub>2</sub>PO<sub>4</sub><sup>-</sup> and HP<sub>2</sub>O<sub>7</sub><sup>3-</sup>. In this study, the addition of the HP<sub>2</sub>O<sub>7</sub><sup>3-</sup> to a solution of **1.27**·(PF<sub>6</sub>)<sub>2</sub> caused the chemical shift of the C2-H proton to move downfield by 0.9 ppm indicating a hydrogen bonding interaction between these protons and HP<sub>2</sub>O<sub>7</sub><sup>3-</sup>.<sup>26</sup> Luminescent imidazolium-linked cyclophanes and macrocycles have also received considerable attention and the tetraphenylethylene (TPE) cyclophane **1.28**·Cl<sub>2</sub> (Scheme 1.8) was shown to act as a sensor for P<sub>2</sub>O<sub>7</sub><sup>4-</sup> anions as a result of the optimal cavity size for this anion.<sup>50</sup> In addition, in the presence of Zn(II) cations, a coordination complex formed (Scheme 1.8) which displayed strong fluorescence.<sup>50</sup>





Scheme 1.8 Suggested mechanism of **1.28·Cl<sub>2</sub>** sensing  $\text{P}_2\text{O}_7^{4-}$  anion in the presence of  $\text{Zn}^{2+}$ .

Furthermore, imidazolium linked cyclophanes not only have the capacity for sensing inorganic anions but also have been prepared to selectively sense biological anions such as ATP, ADP, GTP, DNA and RNA. First reported by Ramaiah and co-workers, the imidazolium linked cyclophane **1.29·Br<sub>2</sub>** (Figure 1.8) underwent a sequence-selective interaction with DNA, which resulted in the formation of a sandwich-type excimer that emitted at 570 nm. However, this type of cyclophane did not interact with micelles and proteins in buffer solution, showing it was selective for DNA recognition.<sup>51</sup>

## 1.3 Metal complexes of NHC ligands

### 1.3.1 NHC metal complexes derived from imidazolium linked macrocycles

Imidazolium linked cyclophanes and macrocyclic compounds can also be utilized as precursors for the synthesis of the NHC metal complexes. In recent years, numerous examples of NHC linked cyclophane and macrocyclic metal complexes featuring metal centres such as gold<sup>52-58</sup>, silver<sup>55-59</sup>, palladium<sup>57, 59</sup>, copper<sup>55</sup>, iron<sup>56, 60-61</sup>, and nickel<sup>57, 62</sup> have been prepared (Figure 1.9).<sup>63</sup> In addition, the imidazolium linked macrocycle can also be used in the preparation of heterobimetallic NHC metal complexes (Figure 1.9).

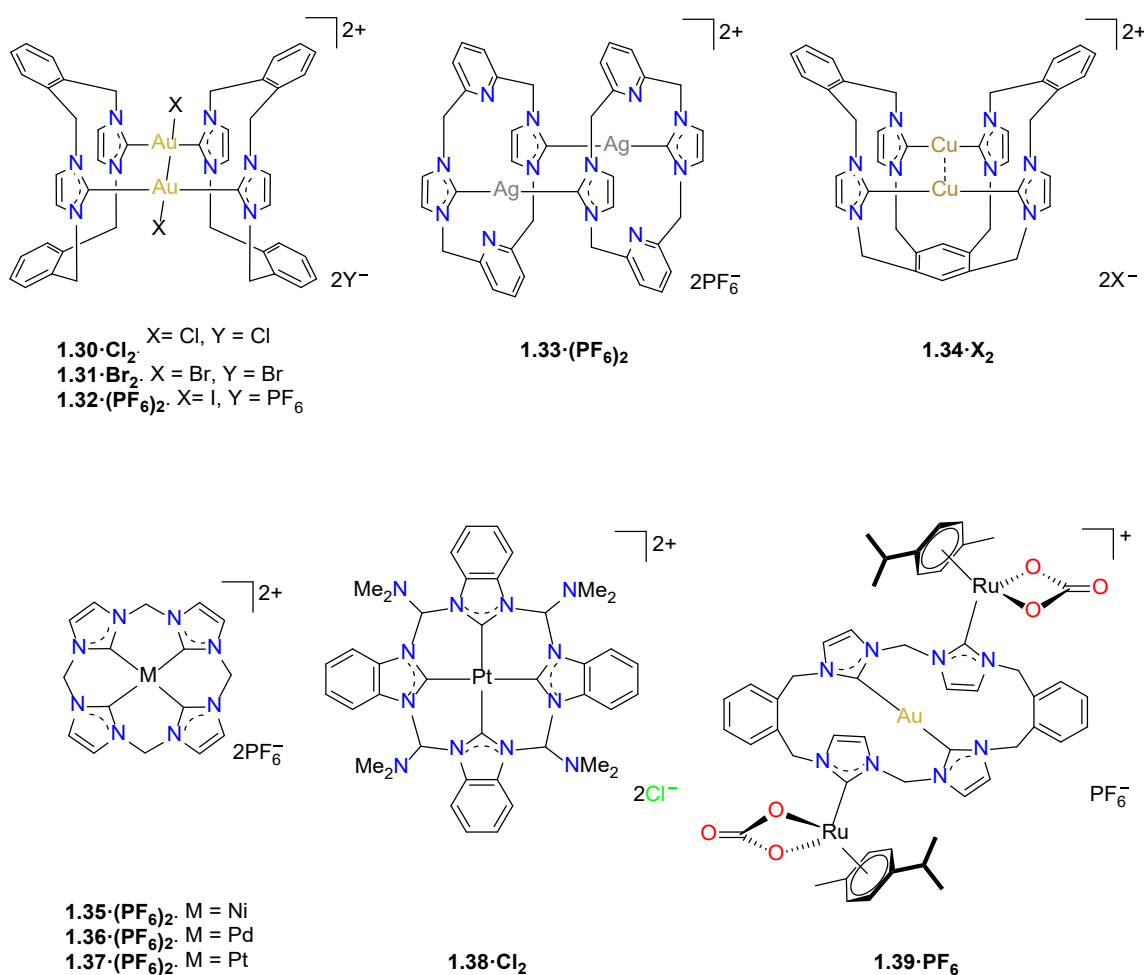
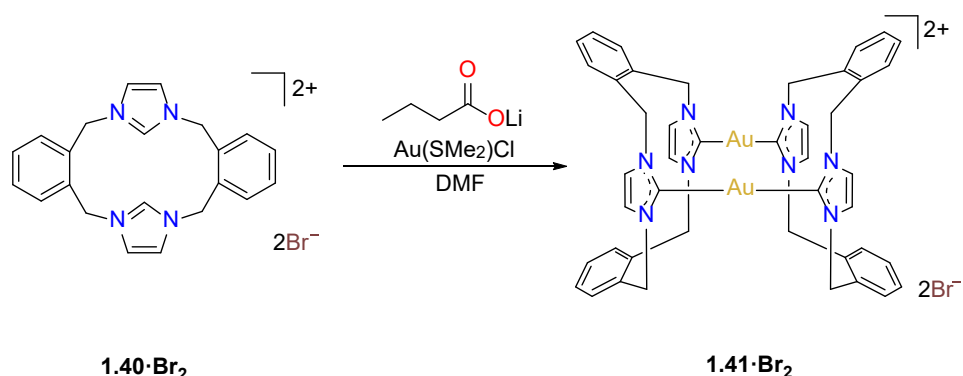


Figure 1.9 Selected examples of NHC metal complexes derived from NHC linked cyclophane and macrocyclic ligands.

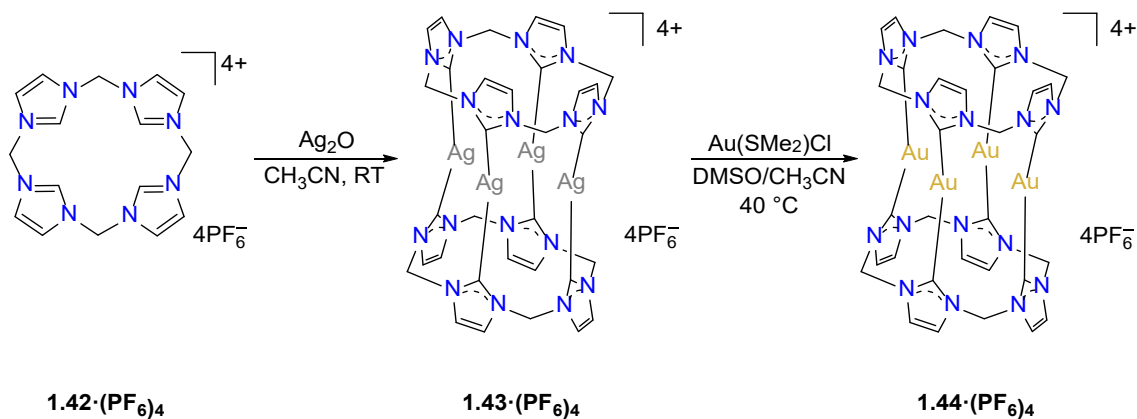
### 1.3.1.1 Gold complexes

Gold complexes derived from NHC linked cyclophane and macrocyclic ligand systems are conventionally prepared by reactions of imidazolium ligand precursors and a Au(I) source such as (THT)AuCl or Au(SMe<sub>2</sub>)Cl in the presence of a weak base.<sup>58</sup> For example, the dinuclear Au(I) complex **1.41·Br<sub>2</sub>** was prepared by the reaction of the imidazolium linked cyclophane ligand **1.40·Br<sub>2</sub>** with Au(SMe<sub>2</sub>)Cl in the presence of lithium butyrate as a base (Scheme 1.9).<sup>54</sup>



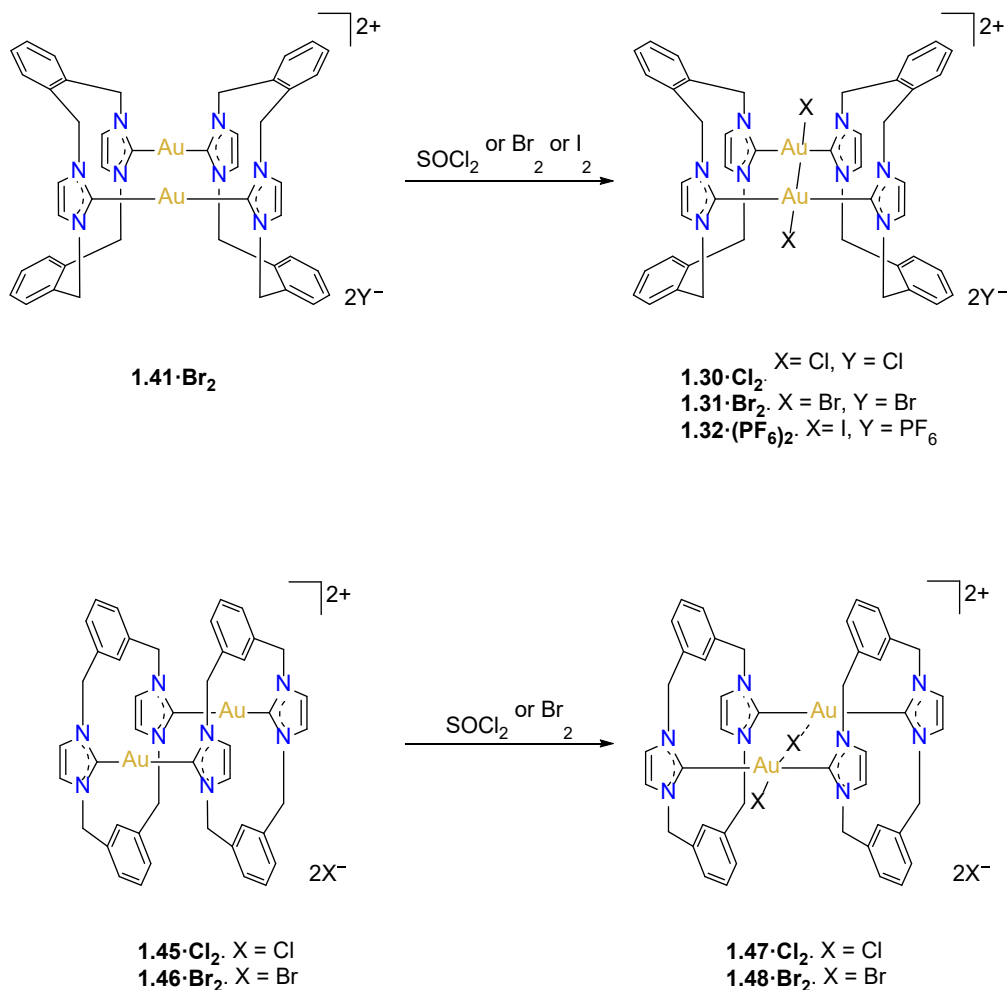
Scheme 1.9 Synthesis of dinuclear Au(I) complex **1.41·Br<sub>2</sub>** derived from the imidazolium-linked cyclophane precursor **1.40·Br<sub>2</sub>**.

In a second approach, transmetalation via Ag<sub>2</sub>O was used to synthesize Au(I) complexes of NHC-linked macrocyclic ligands. In one example, the imidazolium linked macrocycle **1.42·(PF<sub>6</sub>)<sub>4</sub>** was first reacted with Ag<sub>2</sub>O to obtain the tetranuclear Ag(I) complex **1.43·(PF<sub>6</sub>)<sub>4</sub>**. The Au(I) complex **1.44·(PF<sub>6</sub>)<sub>4</sub>** was then prepared by a reaction of **1.43·(PF<sub>6</sub>)<sub>4</sub>** and Au(SMe<sub>2</sub>)Cl (Scheme 1.10).<sup>57</sup>



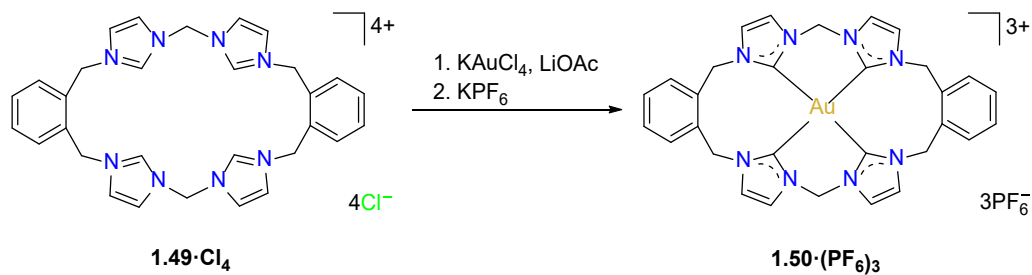
Scheme 1.10 Synthesis of Au(I) complex **1.44·(PF<sub>6</sub>)<sub>4</sub>** via transmetalation from the Ag(I) complex intermediate **1.43·(PF<sub>6</sub>)<sub>4</sub>**.

Furthermore, complexes of NHC linked cyclophane ligands featuring either Au(II) or Au(III) can also be prepared by oxidative addition of halogens or halogen equivalents to Au(I) complexes or by the reaction of  $\text{KAuCl}_4$  with imidazolium linked pro-ligands. For example, the dinuclear Au(II) complexes **1.30 Cl<sub>2</sub>**, **1.31 Br<sub>2</sub>** and **1.32 (PF<sub>6</sub>)<sub>2</sub>** (Scheme 1.10) were prepared by oxidation of the corresponding Au(I) complexes **1.41·Br<sub>2</sub>** with  $\text{SOCl}_2$ ,  $\text{Br}_2$  or  $\text{I}_2$ .<sup>53</sup> Using a similar method, the mixed valence gold complexes **1.47 Cl<sub>2</sub>** and **1.48 Br<sub>2</sub>** featuring both Au(I) and Au(III) centres were also prepared.<sup>53</sup>



Scheme 1.11 Preparation of Au(II) and Au(I)/Au(III) mixed valence complexes via oxidative addition of halogens and halogen equivalents to Au(I)-NHC precursor complexes.

Although sometimes problematic due to the reduction of Au(III) centre to Au(I),<sup>52, 64-67</sup> it is possible to synthesize Au(III) complexes of NHC linked macrocyclic ligands by reaction of the pro-ligands and Au(III) sources such as  $\text{KAuCl}_4$  or  $\text{HAuCl}_4$ .<sup>52, 56</sup> For example, the Au(III) complex **1.50**· $(\text{PF}_6)_3$  was prepared by reaction of *tetra*-imidazolium linked macrocycle **1.49**· $\text{Cl}_4$  and  $\text{KAuCl}_4$  in presence of lithium acetate as a mild base (Scheme 1.12).<sup>52</sup> Using a similar synthetic strategy, a square planar Au(III) complex **1.51**· $(\text{CF}_3\text{SO}_3)_3$  was also prepared (Figure 1.10).<sup>56</sup>



Scheme 1.12 Synthesis of the Au(III) complex **1.50·(PF<sub>6</sub>)<sub>3</sub>** from the *tetra*-imidazolium linked macrocycle **1.49·Cl<sub>4</sub>**.

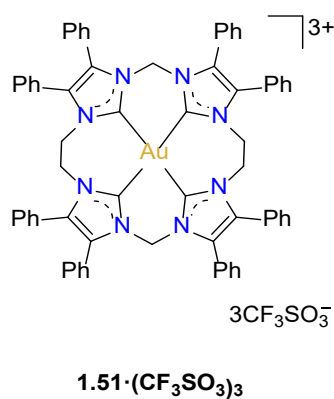
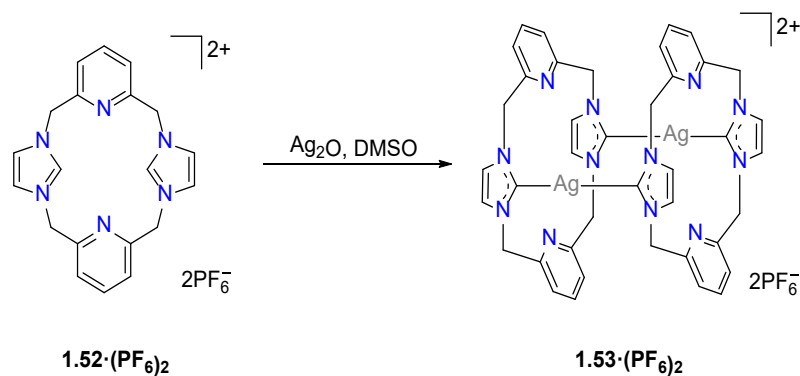


Figure 1.10 Structure of Au(III) complex **1.51·(CF<sub>3</sub>SO<sub>3</sub>)<sub>3</sub>**.

### 1.3.1.2 Silver complexes

As previously described, silver(I) complexes of NHC ligands have been demonstrated to be highly useful as transmetallation reagents in the synthesis of a variety of metal complexes.<sup>21, 68-69</sup> The synthesis of Ag(I) complexes of a NHC linked cyclophane ligands were first reported until 2001.<sup>58, 70</sup> In this initial study, the Ag(I) complex **1.53·(PF<sub>6</sub>)<sub>2</sub>** was prepared where two units of *bis*-NHC linked cyclophane ligands were bridged by two silver(I) centres (Scheme 1.13).<sup>70</sup>



Scheme 1.13 Synthesis of the first Ag(I) complex **1.53**·(PF<sub>6</sub>)<sub>2</sub> of the NHC linked macrocycle.

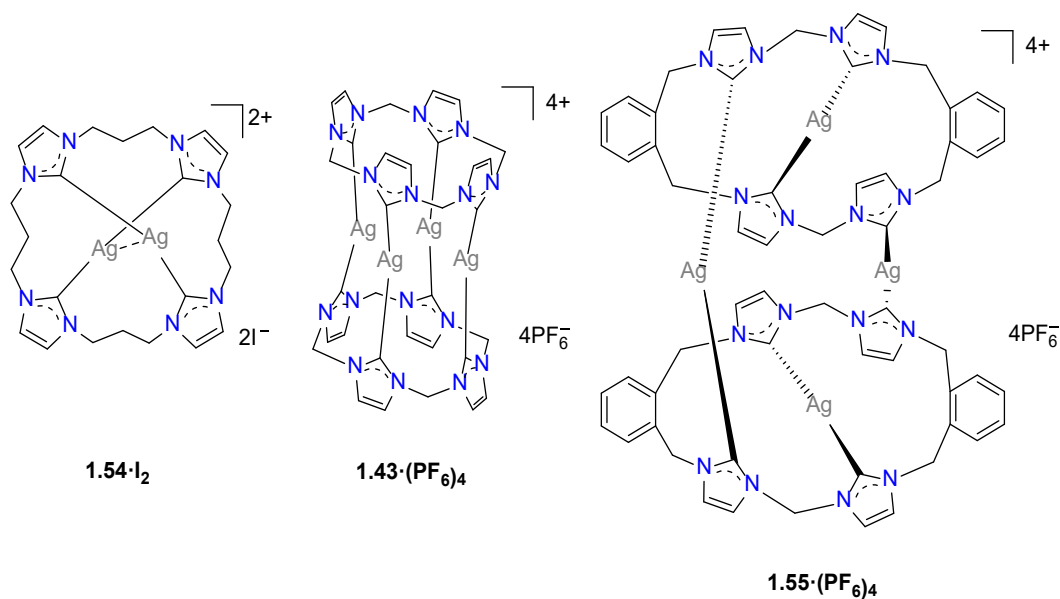
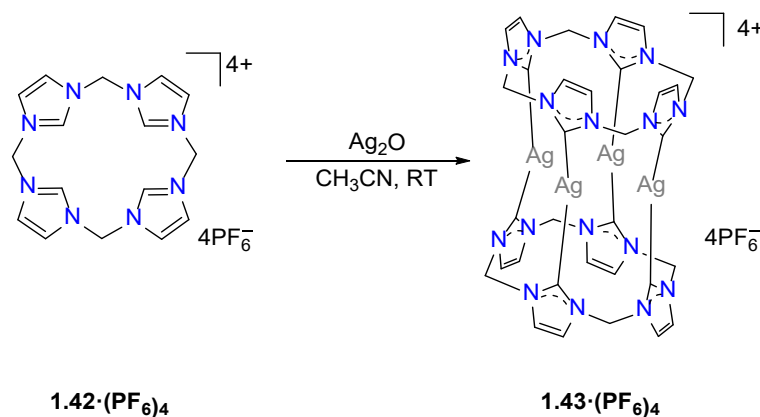


Figure 1.11 Selected Ag(I) complexes of NHC linked macrocyclic ligand. (a) **1.54**·I<sub>2</sub> and (b) **1.43**·(PF<sub>6</sub>)<sub>4</sub> and (c) **1.55**·(PF<sub>6</sub>)<sub>4</sub>.

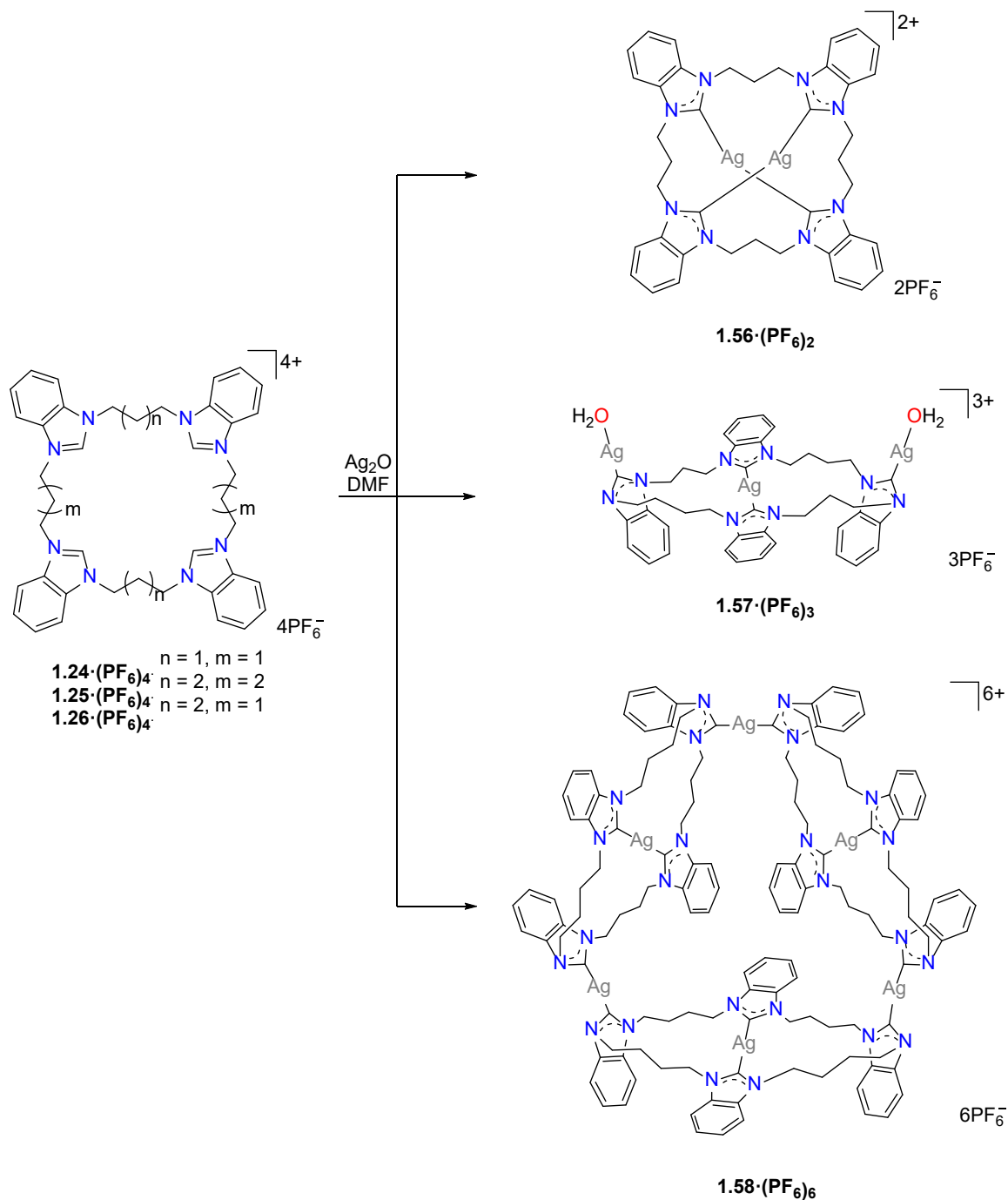
Since the first report, a large number of Ag(I) complexes of NHC linked macrocycles have been reported (Figure 1.11).<sup>21-22, 35, 56, 68-69, 71-75</sup> For example, a sandwich like tetranuclear Ag(I) complex **1.43**·(PF<sub>6</sub>)<sub>4</sub> featuring two methylene linked *tetra*-imidazolylidene ligands was prepared by reaction of the *tetra*-imidazolium macrocycle **1.42**·(PF<sub>6</sub>)<sub>4</sub> and Ag<sub>2</sub>O (Scheme 1.14). The Ag(I) complex **1.43**·(PF<sub>6</sub>)<sub>4</sub> was utilized as a precursor complex for the preparation of Au(I), Ni(II), Pd(II) and Pt(II) complexes of this ligand.<sup>57</sup>



Scheme 1.14 Synthesis of tetranuclear Ag(I) complexes **1.43·(PF<sub>6</sub>)<sub>4</sub>** derived from the *tetra*-imidazolium macrocycle **1.42·(PF<sub>6</sub>)<sub>4</sub>**.

In a second interesting example, a series of Ag(I) complexes **1.56·(PF<sub>6</sub>)<sub>2</sub>**, **1.57·(PF<sub>6</sub>)<sub>3</sub>** and **1.58·(PF<sub>6</sub>)<sub>6</sub>** were prepared from the *tetra*-benzimidazolium salts **1.24·(PF<sub>6</sub>)<sub>4</sub>**, **1.25·(PF<sub>6</sub>)<sub>4</sub>** and **1.26·(PF<sub>6</sub>)<sub>4</sub>** (Scheme 1.15). It was shown in this study that the Ag(I) can bind with poly-NHC linked macrocyclic ligands of this type with either box-like, cylinder-like or cage-like structures and the structures of these complexes depend on the coordination behaviour of the *tetra*-benzimidazolylidene ligands as a result of the linker lengths and the ring sizes. Here, as the alkyl linker length increased, the macrocyclic cavity ring size and the flexibility of the macrocycle increased leading to a variety of Ag(I) complexes structures.<sup>68</sup>



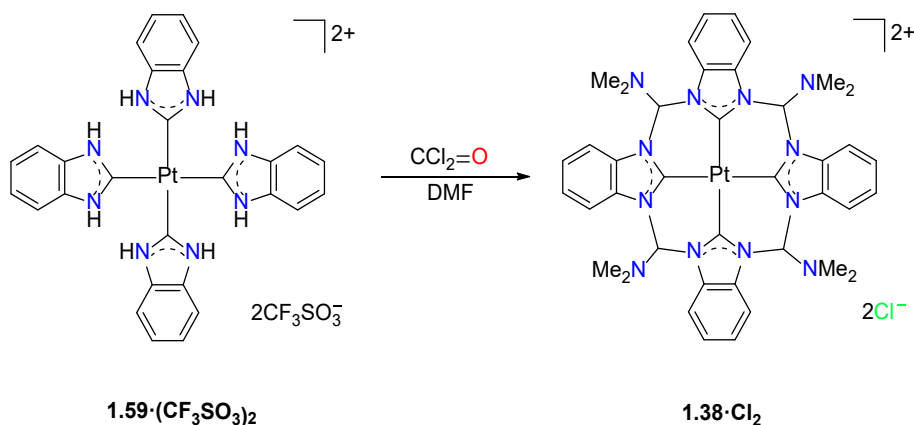


Scheme 1.15 Synthesis of macrocyclic Ag(I) complexes **1.56**·(PF<sub>6</sub>)<sub>2</sub>, **1.57**·(PF<sub>6</sub>)<sub>3</sub> and **1.58**·(PF<sub>6</sub>)<sub>6</sub>.

### 1.3.1.3 Template directed synthesis of the of NHC linked macrocycle metal complexes

Metal complexes of NHC linked macrocyclic ligands have also been prepared by template-controlled syntheses where a non-macrocyclic metal NHC complex is initially prepared followed by macrocyclization of the ligand.<sup>76-78</sup> Reported by Hahn and co-workers, the Pt(II) complex **1.38**·Cl<sub>2</sub> was prepared by a template controlled approach

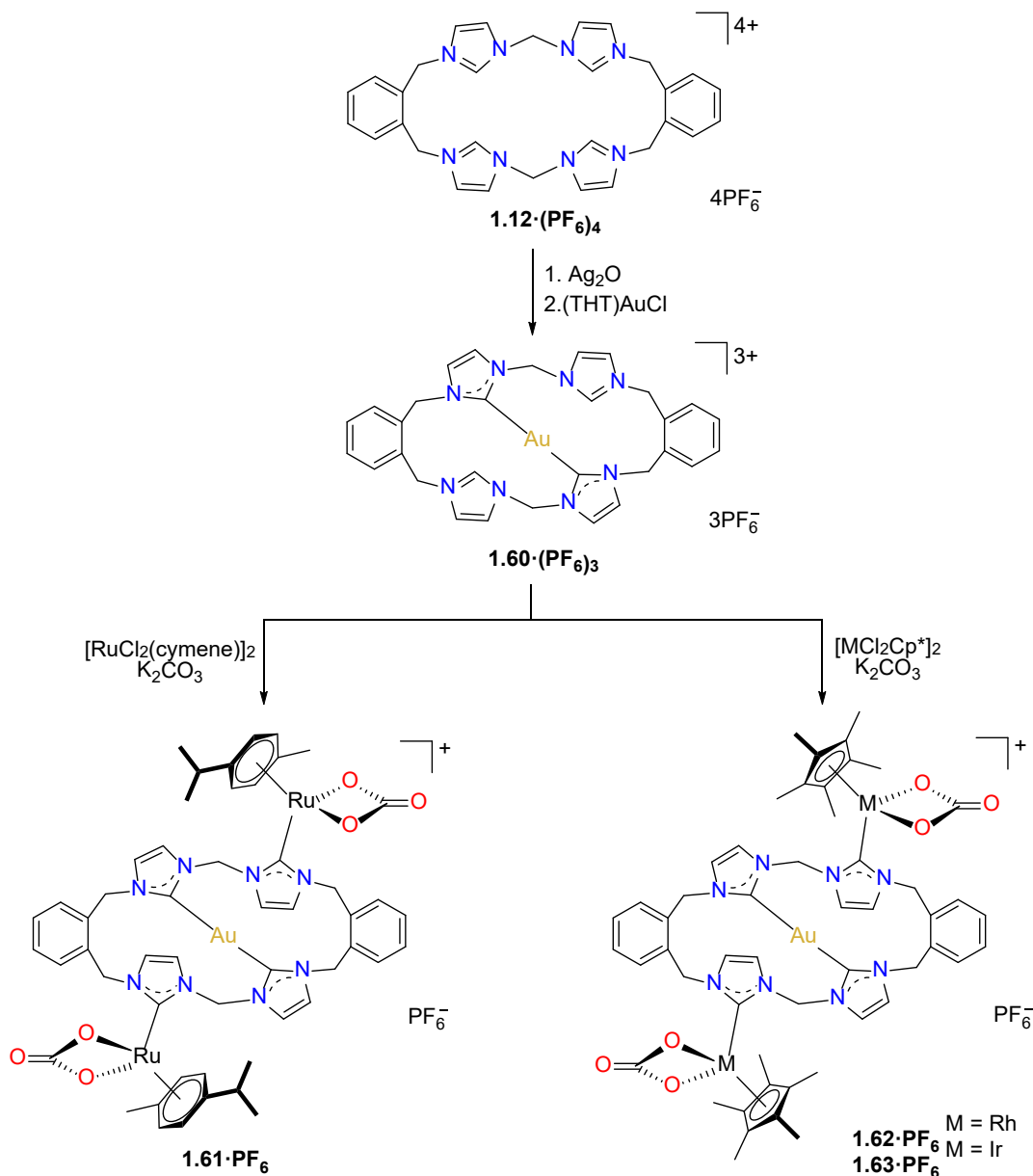
(Scheme 1.16). The synthesis of complex **1.38·Cl<sub>2</sub>** was achieved by treatment of the *tetra*-NHC Pt(II) complex **1.59·(CF<sub>3</sub>SO<sub>3</sub>)<sub>2</sub>** with phosgene to achieve macrocyclization of the ligand and formation of the Pt(II) complex in a moderate yield (~60%)<sup>76</sup> Employing a similar methodology, a dicarbene Pt(II) macrocyclic complex was also prepared.<sup>77</sup>



Scheme 1.16 Template-controlled synthesis of Pt(II) complex **1.38·Cl<sub>2</sub>** of a *tetra*-benzimidazolyldiene macrocyclic ligand.

#### 1.3.1.4 Synthesis of heterobimetallic complexes of NHC linked macrocyclic ligands

Although less common, heterobimetallic complexes of NHC linked macrocyclic ligands have also been reported. For example, the binuclear heterobimetallic complexes of the metals Rh(III)-Au(I), Ir(III)-Au(I) and Ru(II)-Au(I) were prepared by stepwise metallation of a *tetra*-imidazolium linked macrocycle.<sup>63</sup> In this study, the imidazolium linked macrocycle pro-ligand was first reacted with (THT)AuCl to obtain the monometallic Au(I) complex (Scheme 1.17). The Au(I) was then reacted with the second metal sources yielding the heterobimetallic complexes **1.61·PF<sub>6</sub>**, **1.62·PF<sub>6</sub>** and **1.63·PF<sub>6</sub>**. Due to the rigid structure of the *tetra*-imidazolium pro-ligand system **1.12·(PF<sub>6</sub>)<sub>4</sub>**, only one Au(I) atom coordinated to the ligand via two of the imidazole groups in complex **1.60·(PF<sub>6</sub>)<sub>3</sub>**, leaving the second pair of imidazolium unreacted. As a result, the unreacted imidazolium moieties could be coordinated to a second metal yielding a series of heterobimetallic complexes.<sup>63</sup>



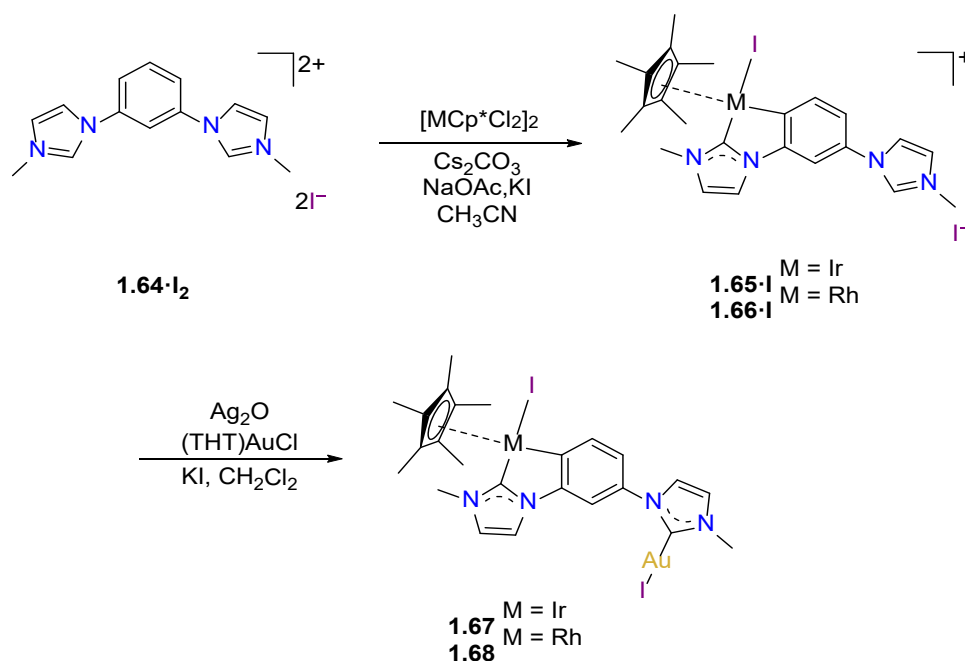
Scheme 1.17 Stepwise synthesis of the mononuclear Au(I) complex **1.60**·(PF<sub>6</sub>)<sub>3</sub> and heterobimetallic complexes **1.61**·PF<sub>6</sub>, **1.62**·PF<sub>6</sub> and **1.63**·PF<sub>6</sub>.

## 1.4 Heterobimetallic complex of NHC ligands

### 1.4.1 Synthesis of heterobimetallic metal complexes

Although a very large number of homobimetallic complexes of bidentate NHC ligands are known, heterobimetallic complexes which are defined as a metal complex featuring two different metals are much less common.<sup>79</sup> Heterobimetallic complexes have been prepared from NHC ligands using different strategies including stepwise metal

incorporation,<sup>63, 80-87</sup> one-pot metallation<sup>83-84</sup> and post synthetic modification and metallation<sup>88-90</sup>. In the stepwise synthetic method for the synthesis of heterobimetallic complexes of the NHC ligands, generally, one of the NHC units is bound to the first metal forming a mononuclear complex bearing an unreacted pre-carbene unit. The unreacted pre-carbene unit is then bound to a second metal as an NHC group to form the heterobimetallic complex. For example, Ir(III)-Au(I) **1.67** and Rh(III)-Au(I) complexes **1.68** were prepared by a reaction of the pro-ligands **1.64**·I<sub>2</sub> with Ir or Rh precursors in the presence of a base yielding the mononuclear complexes **1.65**·I and **1.66**·I (Scheme 1.18). These precursor complexes were then metallated with (THT)AuCl via a transmetalation reaction using Ag<sub>2</sub>O to produce the Ir(III)-Au(I) and Rh(III)-Au(I) heterobimetallic complexes **1.67** and **1.68** (Scheme 1.18).<sup>91</sup>



Scheme 1.18 Synthesis of Ir(III)-Au(I) **1.67** and Rh(III)-Au(I) **1.68** heterobimetallic complexes using a stepwise synthetic procedure.

Despite a wide range of studies on the synthesis of heterobimetallic complexes using stepwise synthetic approaches,<sup>63, 80-86</sup> the metallation of poly-NHC ligands in a site-selective manner remains a challenge due to the difficulty of selectively deprotonating the

pre-carbene units.<sup>92-93</sup> Due to the differences of basicity between different azolium groups, asymmetrical ligand systems featuring different azolium groups (e.g. imidazolium combined with triazolium) have been utilized to allow selective deprotonation and metallation. Using an asymmetrical ligand system featuring imidazolium and 1,2,3-triazolium groups, the Pd(II)-Rh(I) heterobimetallic complex **1.69** (Figure 1.12) was prepared using a stepwise synthetic approach.<sup>82</sup>

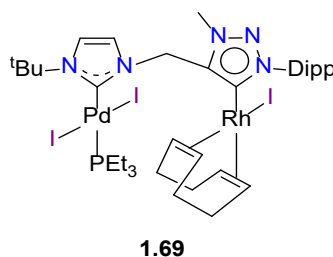
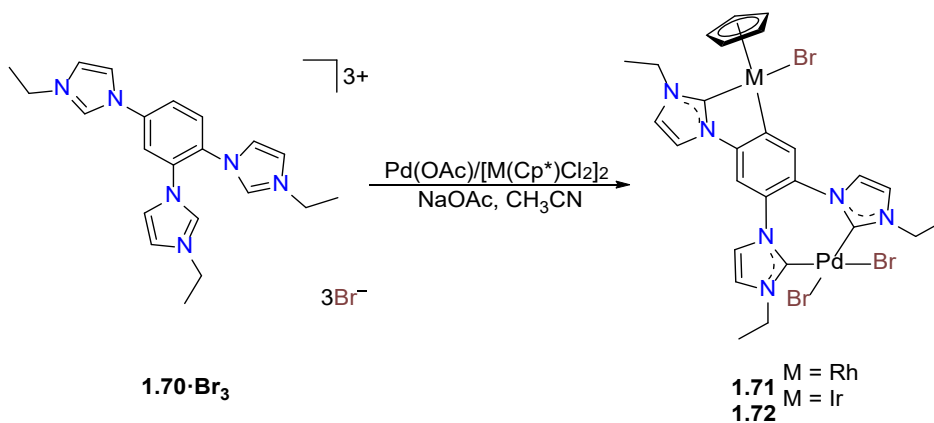


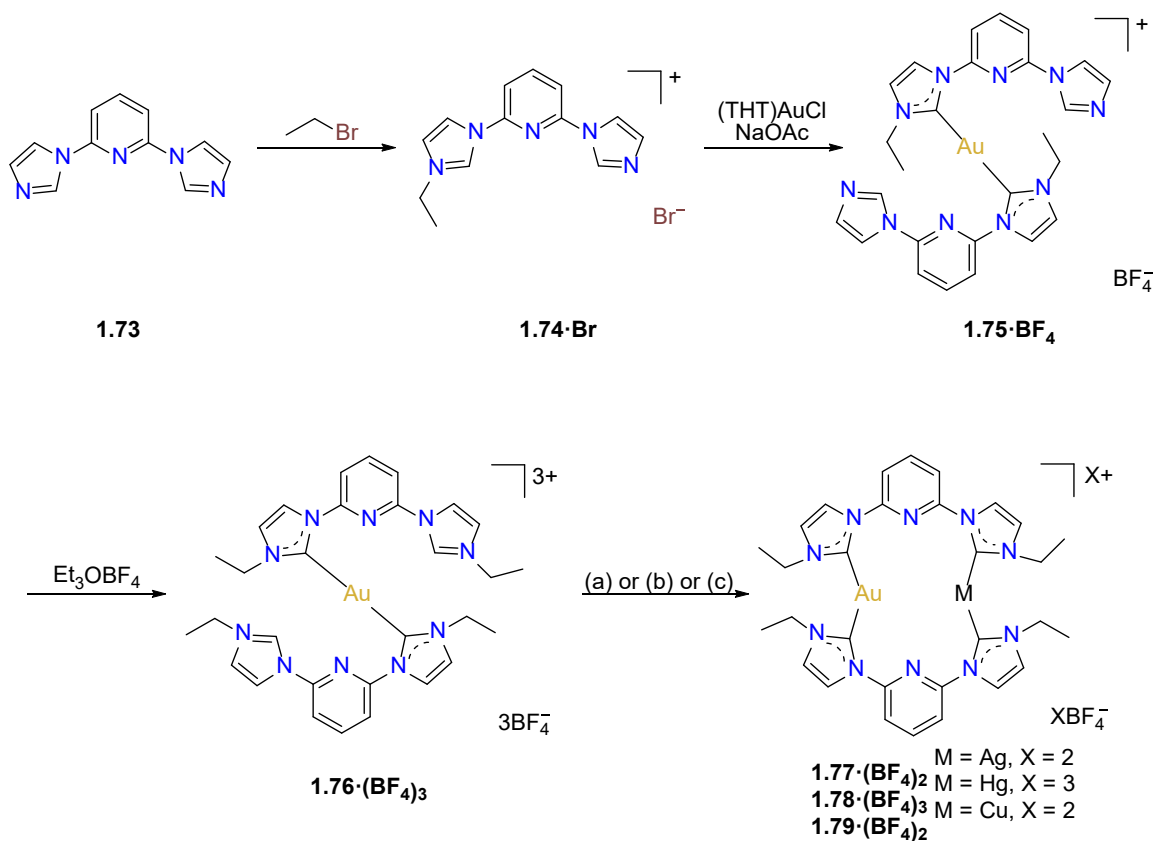
Figure 1.12 The Pd(II)-Rh(I) heterobimetallic complex **1.69** prepared from a pro-ligand featuring imidazolium and 1,2,3-triazolium groups.

An alternative approach for the synthesis of heterobimetallic complexes is one-pot metallation, in which the pro-ligand is treated with two or more metal sources in one pot. For example, the Pd(II)-Rh(III) complex **1.71** and the Pd(II)-Ir(III) complex **1.72** (Scheme 1.19) were synthesized using a one-pot metallation approach from a *tris*-imidazolium pro-ligand **1.70·Br<sub>3</sub>** and the metal sources Pd(OAc)<sub>2</sub> and [Rh(Cp<sup>\*</sup>)(Cl<sub>2</sub>)]<sub>2</sub> or [Ir(Cp<sup>\*</sup>)(Cl<sub>2</sub>)]<sub>2</sub> in the presence of base.<sup>83</sup> However, it was noted by the authors that the imidazolium groups in the 1 and 2 position of the benzene linker were expected to chelate with Pd(II) while the Rh(III) metal centre was expected to bind with the imidazolium group at position 4 of the aromatic ring of the ligand and to *ortho*-metallate with the central phenyl group.<sup>94-95</sup> Therefore, the different reactivities of Pd(II) and Rh(III) or Ir(III) results in the formation of the heterobimetallic complexes in this case.



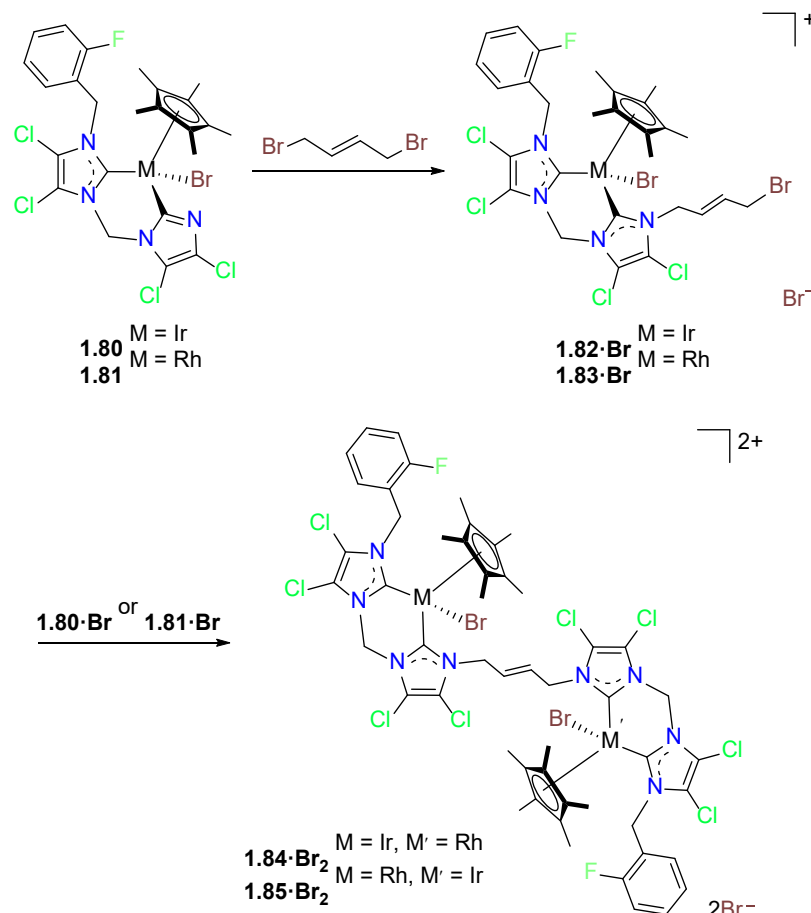
Scheme 1.19 Synthesis of Pd(II)-Rh(III) **1.71** and Pd(II)-Ir(III) **1.72** complexes via a one-pot synthetic approach.

In a third synthetic approach, heterobimetallic complexes can also be prepared using a post synthetic modification and metallation approach.<sup>88-90</sup> For example, a number of heterobimetallic complexes of *bis*-imidazolyliene ligands including Au(I)-Ag(I), Au(I)-Hg(II) and Au(I)-Cu(I) complexes have been synthesized using this method. Here an asymmetrical pro-ligand **1.74·Br** featuring a combination of imidazole and imidazolium units was initially synthesized and then reacted with (THT)AuCl to obtain a mononuclear Au(I) complex **1.75·BF<sub>4</sub>** bearing an imidazolium group. This compound could then be metallated with a second transition metal source e.g. Ag(I), Hg(II) and Cu(I) to prepare the heterobimetallic complexes **1.77·(BF<sub>4</sub>)<sub>2</sub>**, **1.78·(BF<sub>4</sub>)<sub>3</sub>** and **1.79·(BF<sub>4</sub>)<sub>2</sub>** (Scheme 1.20).<sup>88</sup>



Scheme 1.20 Synthesis of Au(I)-Ag(I), Au(I)-Hg(II) and Au(I)-Cu(I) heterobimetallic complexes **1.77·(BF<sub>4</sub>)<sub>2</sub>**, **1.78·(BF<sub>4</sub>)<sub>3</sub>** and **1.79·(BF<sub>4</sub>)<sub>2</sub>** using a post synthetic modification and metallation method. Conditions (a) Ag<sub>2</sub>O, DMF, RT and (b) Hg(OAc)<sub>2</sub>, CH<sub>3</sub>CN, reflux and (c) Cu(CH<sub>3</sub>CN)<sub>4</sub>BF<sub>4</sub>, K<sub>2</sub>CO<sub>3</sub>, CH<sub>3</sub>CN, RT.

Recently, the preparation of a series of heterobimetallic NHC complexes using a post synthetic modification method was described.<sup>89</sup> The Ir(III) complex **1.80** or Rh(III) complex **1.81** were first synthesized and then these complexes were alkylated with 1,4-dibromobut-2-ene yielding the precursor complex **1.82·Br** and **1.83·Br**. These complexes were then used to alkylate a second unsubstituted complex (e.g. **1.80** or **1.81**) yielding the heterobimetallic complexes **1.84·Br<sub>2</sub>** and **1.85·Br<sub>2</sub>** (Scheme 1.21).<sup>89</sup>



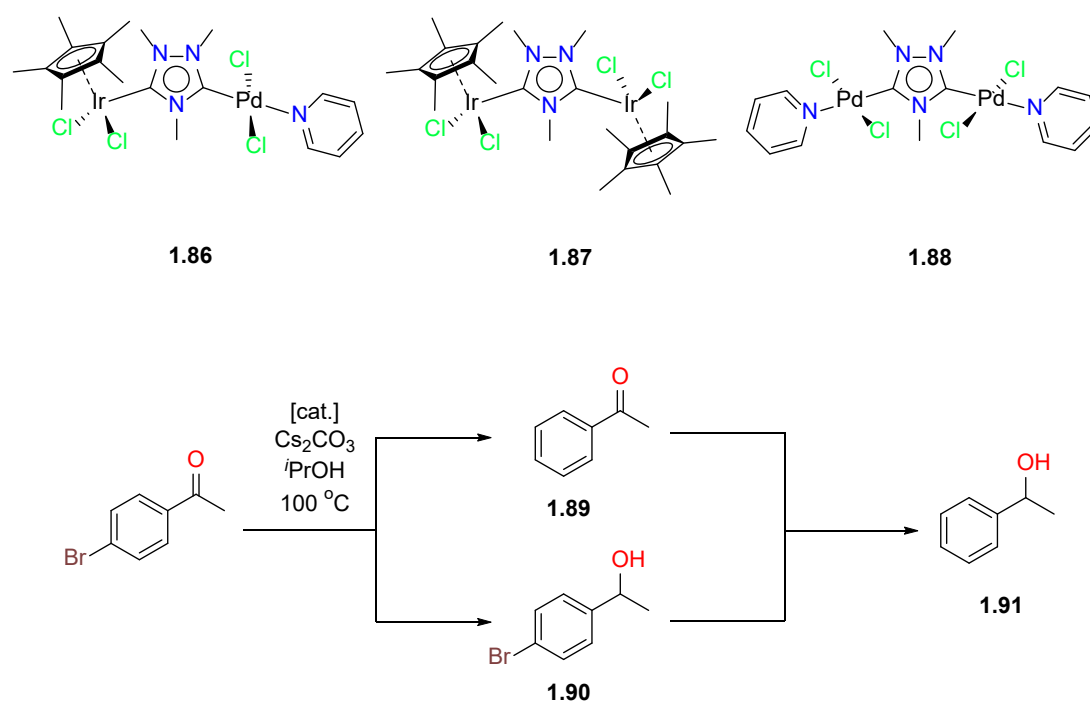
Scheme 1.21 Synthesis of heterobimetallic NHC complexes **1.84·Br<sub>2</sub>** and **1.85·Br<sub>2</sub>** using post synthetic modification metallation method.

## 1.4.2 Catalytic activities

Heterobimetallic complexes are of great interest as they offer the potential to act as catalysts for multiple catalytic transformations in one-pot. This class of reactions is known as “tandem reactions” and involves the use of one homogeneous catalyst in two or more different catalytic processes.<sup>85-86, 96-100</sup> In addition, heterobimetallic complex catalysts can have synergistic effects where the different metal centres catalyse different reactions and their combination in a single molecule results in an improvement in reactivity and/or selectivity compared with a combination of the corresponding homobimetallic complexes.<sup>85-86, 96, 98, 101-102</sup> For example, the Ir(III)-Pd(II) heterobimetallic complex **1.86** (Scheme 1.22) was catalytically active in the tandem dehalogenation/transfer hydrogenation of haloacetophenones.<sup>101</sup> In this study, when the Ir(III) homobimetallic



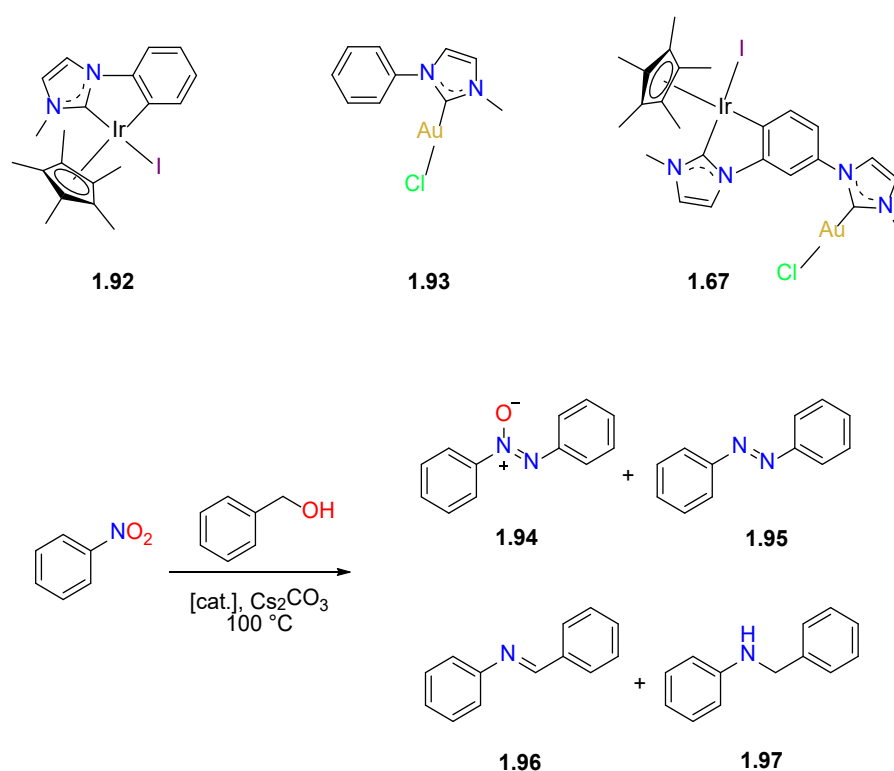
complex **1.87** was evaluated as the catalyst, the undesired compound **1.90** was generated with a yield of 89%. Similarly, when the Pd(II) homobimetallic complex was used, only compound **1.89** was obtained with a yield of 95%. However, when the Ir(III) complex **1.87** and Pd(II) complex **1.88** were combined in the reaction medium the desired compound **1.91** was obtained with a low yield of 25%. By sharp contrast, when the Ir(III)-Pd(II) heterobimetallic complex **1.90** was used as the catalyst in this tandem dehalogenation/transfer hydrogenation of haloacetophenones reaction, the target compound **1.91** was obtained with a very high yield of 99%. Heterobimetallic complex **1.86**, therefore, showed synergistic activity in the tandem reaction compared with a mixture of the Ir(III) and Pd(II) homobimetallic complexes.<sup>101</sup>



Scheme 1.22 Structures of Ir(III)-Pd(II) heterobimetallic complex **1.86**, homobimetallic complexes **1.87** and **1.88** and the catalytic dehalogenation/transfer hydrogenation of haloacetophenones reactions.<sup>101</sup>

In a second study, the Ir(III)-Au(I) heterobimetallic complex **1.67** was catalytically active in the coupling reaction of nitrobenzene and benzylic alcohol (Scheme 1.23). As in the previous example, complex **1.67** was found to be more catalytically active than a

mixture of the corresponding Ir(III) and Au(I) monometallic complexes **1.92** and **1.93**. The monometallic Ir(III) complex **1.92** could only produce moderate amounts of imine species **1.96** and the monometallic Au(I) complex resulted in the formation of a mixture of compounds **1.94** and **1.95**. Interestingly, using a mixture of the Ir(III) complex **1.92** and the Au(I) complex **1.93** produced the desired product in a poor yield of 18%. However, when the Ir(III)-Au(I) heterobimetallic complex **1.67** was used as the catalyst the desired product **1.97** was obtained in a very good yield of 82%.<sup>91</sup>



Scheme 1.23 Structures of Ir(III)-Au(I) heterobimetallic complex **1.67** and the monometallic complexes **1.92** and **1.93** and the reaction of nitrobenzene and benzylic alcohol producing compounds **1.94** – **1.97** depending on the conditions.

### 1.4.3 Metallophilicity and photophysical properties

Since early studies in the 1980s, aurophilic interactions in which two closed shell Au(I) atoms form weak bonding interactions with the metal...metal distance being less than the sum of the van der Waals radii have been extensively studied.<sup>103-111</sup> Although much less common, metallophilic interactions of this type between copper and silver (cuprophilic and

argentophilic interactions) have also been investigated.<sup>110, 112</sup> In the past decade, numerous studies have revealed that homo- and heterobimetallic complexes can also display interesting luminescent properties as a result of these metallophilic interactions.<sup>88, 105-107, 109, 113-114</sup> First observed by Schmidbaur and co-workers, a series of Au complexes exhibited close Au...Au contacts. Confirmed by X-ray crystal structure analysis, the Au complex **1.98·Cl** exhibited short Au...Au distance of 3.18 Å (Figure 1.13),<sup>107</sup> while complex **1.99·(CH<sub>3</sub>OBF<sub>3</sub>)<sub>2</sub>** has an average Au...Au distance of 3.003 Å (Figure 1.13),<sup>105</sup> which were significantly smaller than the distance causing by van der Waals radii for Au atoms (3.80 Å).<sup>115-116</sup> After the first report of aurophilic interactions, several studies revealed that a similar interaction can also be observed for silver and copper metal complexes (i.e. argentophilic and cuprophilic interactions). For example, the Ag atoms in the synthesized trinuclear NHC-Ag(I) complex **1.100·(CF<sub>3</sub>SO<sub>3</sub>)<sub>3</sub>** were found interacting with each other with a short Ag...Ag distance of 2.7599(3) Å, which indicates the existence of argentophilic interaction (Figure 1.13).<sup>110</sup> Reported in the same research article, the NHC-Cu(I) complex **1.101·(CF<sub>3</sub>SO<sub>3</sub>)<sub>3</sub>** also has a similar property (Figure 1.13).<sup>110</sup>

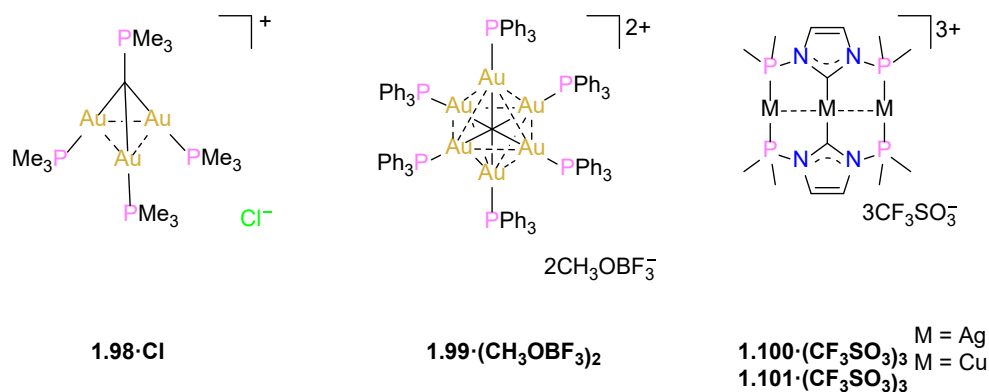
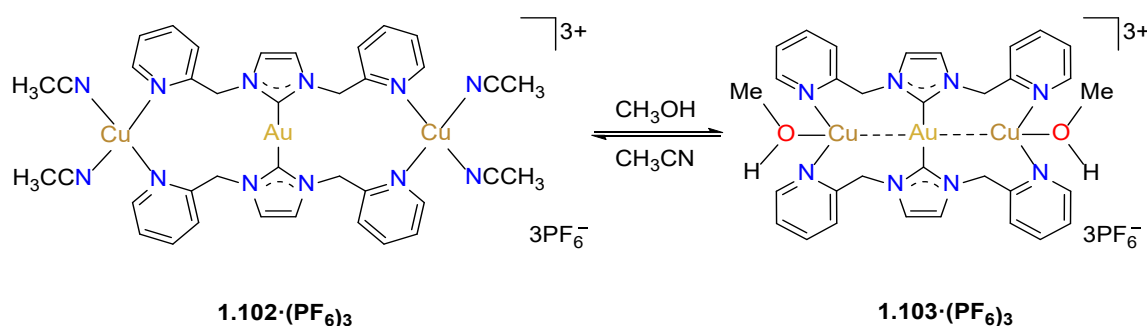


Figure 1.13 Selected examples of coinage metal complexes which display metallophilic interactions.

In addition, it has been noted by numerous researchers that metallophilic interactions are not only observed in homobimetallic systems but heterobimetallic complexes can also show similar metallophilic properties.<sup>88, 113, 117-120</sup> For example, a Au(I)-

Cu(I) heterobimetallic complex **1.102**·(PF<sub>6</sub>)<sub>3</sub> was reported which is luminescent and was evaluated as a volatile organic compound (VOC) sensor. Due to the short M···M (metallophilic) interaction, complex **1.102**·(PF<sub>6</sub>)<sub>3</sub> exhibited blue luminescence ( $\lambda_{\text{max}} = 462$  nm) in the solid state, with the Au(I)-Cu(I) distance being 4.59 Å. When exposed to methanol vapour, ligand exchange between coordinating molecules of CH<sub>3</sub>CN and methanol occurred resulting in a shortening of the M···M interaction between the Au(I) and Cu(I) atoms to 2.79 Å and emission at 520 nm. Here the change in the luminescence colour for compound **1.102**·(PF<sub>6</sub>)<sub>3</sub> was attributed to the change in the gold-copper interaction as a result of ligand exchange between acetonitrile and methanol. (Scheme 1.24).<sup>113</sup>



Scheme 1.24 Ligand exchange reaction where the coordinated acetonitrile molecules for compound **1.102**·(PF<sub>6</sub>)<sub>3</sub> are exchanged with methanol yielding compound **1.103**·(PF<sub>6</sub>)<sub>3</sub> resulting in a change in the Au-Cu distances of 2.79 Å.

In a second example, the dinuclear Au(I)-Ag(I) **1.77**·(BF<sub>4</sub>)<sub>2</sub>, and Au(I)-Hg(II) **1.78**·(BF<sub>4</sub>)<sub>3</sub> heterobimetallic complexes (Figure 1.14) are photoluminescent potentially as a result of the short metal-metal interaction between the metal centres, with the Au(I)-Ag(I) and Au(I)-Hg(II) metal-metal distances being 3.2897 Å and 3.2135 Å respectively. The complexes exhibited photoluminescent properties with emission maxima at 461 nm ( $\lambda_{\text{ex}} = 353$  nm) and 447 nm ( $\lambda_{\text{ex}} = 350$  nm) in a crystalline solid state for the Au(I)-Ag(I) complex **1.77**·(BF<sub>4</sub>)<sub>2</sub>, and the Au(I)-Hg(II) **1.78**·(BF<sub>4</sub>)<sub>3</sub> complex respectively.<sup>88</sup>

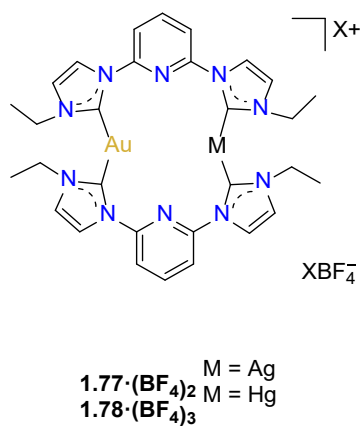


Figure 1.14 Au(I)-Ag(I), Au(I)-Hg(II) heterobimetallic complexes **1.77**·(BF<sub>4</sub>)<sub>3</sub> and **1.78**·(BF<sub>4</sub>)<sub>3</sub> of the same pyrido-linked *bis*-imidazolylidene ligand system which are photoluminescent in the solid state.

## 1.5 Biological applications of metal complexes of NHC ligands

### 1.5.1 Antimicrobial activities of silver (I) and gold(I) NHC complexes

As silver is relatively non-toxic to humans, silver-containing compounds have been widely used for pharmaceutical purposes. In the early 1800s, silver nitrate was used as a treatment to prevent infection for severe burns.<sup>121-123</sup> Later, the use of silver related compounds for antibiotic applications decreased with the discovery of penicillin. However, the resistance of bacteria to antibiotics resulting from the wide use of penicillin and its derivatives has led to the resurgence of the application of silver-based compounds as antibacterial agents, for example, silver sulfadiazine **1.104** (Figure 1.15) is used clinically to prevent infection in burns.<sup>124</sup> Although the mechanism of the antimicrobial activity for this silver based compound is not yet fully understood, it is suggested that the release of Ag(I) into the bacterial cell can cause disruption of the cell function resulting in the cell death.<sup>125</sup> To allow the active Ag(I) centre to cross the cell membrane and disrupt the cell function, a prolonged release of Ag(I) ion is required and as a result of this, a type of compound featuring ligands which can strongly coordinate to the active Ag(I) centre can offer a prolonged release of Ag(I) ion.<sup>123</sup> Due to the strong  $\sigma$ -donating and weak  $\pi$ -accepting properties<sup>1, 126</sup>, NHC ligands form relatively stable complexes with silver and

offer a potential for the development of novel silver-based antibacterial agents.<sup>123</sup> Thus, the antimicrobial activities of NHC-Ag(I) complexes have been of significant recent interest.<sup>127-137</sup> Youngs and co-workers have been particularly active in the field and these researchers have evaluated the antimicrobial properties of a range of NHC-Ag(I) complexes.<sup>73, 123, 128, 138-145</sup> For example, two NHC-Ag(I) coordination polymers **1.105**·(OH)<sub>n</sub> and **1.106**·(OH)<sub>n</sub> derived from the pincer type *bis*-imidazolium pro-ligands (Figure 1.15) were reported to have good antimicrobial activity against both Gram-positive bacteria (*S. aureus*) and Gram-negative bacteria (*E. coli* and *P. aeruginosa*).<sup>138</sup> Soon after the first report of **1.105**·(OH)<sub>n</sub> and **1.106**·(OH)<sub>n</sub>, the antimicrobial activity of a molecular NHC-Ag(I) complex of an NHC linked cyclophane ligand was also reported by this research group.<sup>73</sup> In this study, the Ag(I) complex **1.107**·(OH)<sub>2</sub> (Figure 1.15) exhibited good antimicrobial activities when it was encapsulation into nanofibers composed of the polymer Tecophilic. As a result of the incorporation of the silver complex into a nanofiber, this complex could deliver the active Ag(I) ions to bacteria for a longer period of time when compared to AgNO<sub>3</sub> and displayed prolonged activity.<sup>73</sup> In another example, the dinuclear Ag(I) complex **1.108** demonstrated antimicrobial activity against Gram-positive and Gram-negative bacteria (Figure 1.15).<sup>146</sup> In this study, complex **1.108** was tested against Gram-positive (*S. mutans* and *S. epidermidis*) and Gram-negative bacteria (*P. aeruginosa* and *E. coli*) which are human pathogens and are resistant to antibiotics. This complex was active with a low minimum inhibitory concentration (MIC) value of 4 µg/mL for the Gram-positive and 8 µg/mL for the Gram-negative bacteria strain respectively. Compared with clinically used antibiotics such as streptomycin, ciprofloxacin and chloramphenicol, which have a significantly higher MIC value of up to 128 µg/mL for the Gram-negative bacteria, the Ag(I) complex **1.108** demonstrated stronger antimicrobial activity. Interestingly, the dinuclear Au(I) complexes **1.109** of the same NHC ligand also displayed a comparable antimicrobial activity against Gram-positive and Gram-negative bacteria.<sup>146</sup>

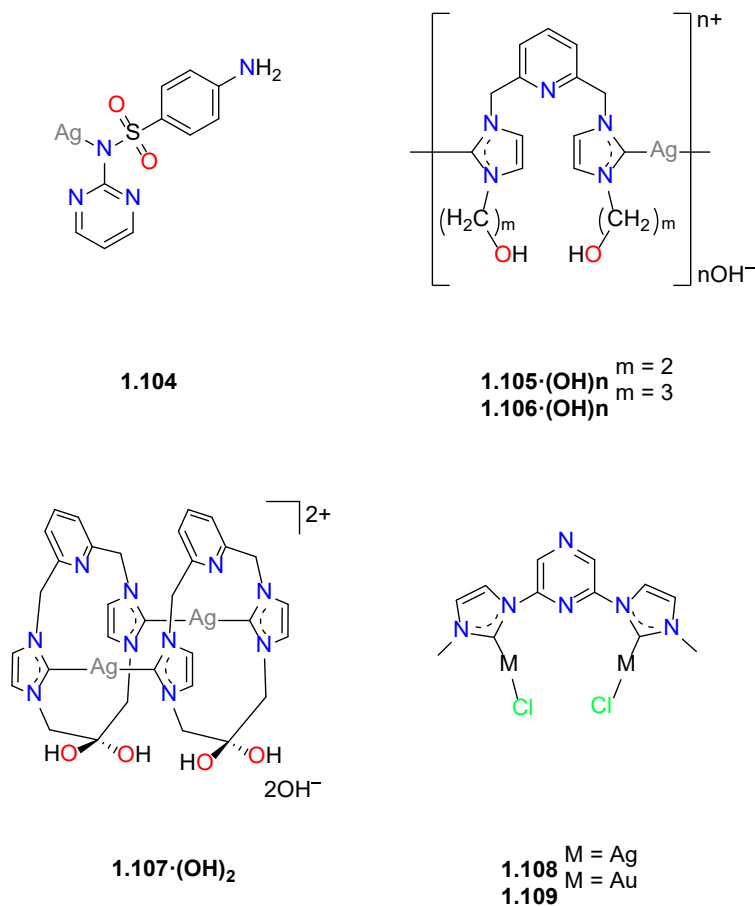


Figure 1.15 Selected silver complexes with antimicrobial activity.

Although these results are promising, the majority of the Ag(I)-NHC complexes evaluated to date only display moderate antimicrobial activity against both the Gram-positive and Gram-negative bacterial strains. In an effort to achieve a better antimicrobial activity, a series of Ag(I)-NHC complexes which have a higher capacity to cross the lipid cell membrane as a result of increased lipophilicity were designed and synthesized.<sup>147-150</sup> For example, the complexes **1.110** and **1.111** (Figure 1.16) demonstrated a higher antimicrobial activity against both Gram-positive (*S. aureus*) and Gram-negative (*E. coli*) bacteria strains, when compared to complex **1.112** (Figure 1.16). As noted by the authors, complexes **1.110** and **1.111** are more lipophilic than **1.112**, which allows the complexes to cross the cell membrane.<sup>147</sup>

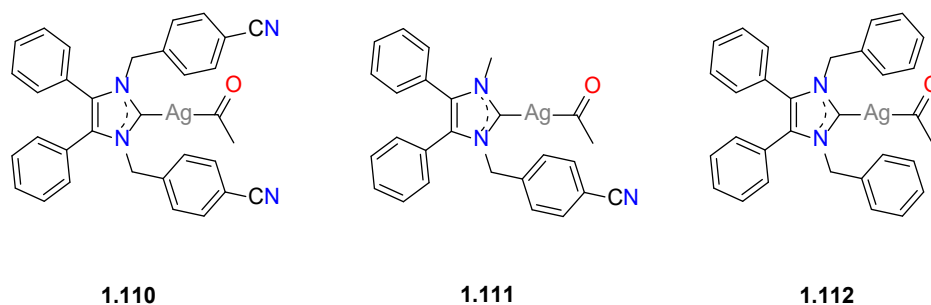


Figure 1.16 Silver complexes of NHC ligands **1.110**, **1.111** and **1.112** with improved antibacterial activity as a result of increased lipophilicity.

### 1.5.2 Biological applications of heterobimetallic NHC complexes

As another important biological application, the cytotoxic properties of homo- and heterobimetallic NHC metal complexes have been comprehensively studied.<sup>92, 151-153</sup> For example, homobimetallic complex **1.41**·Br<sub>2</sub> of NHC linked cyclophane ligand (Scheme 1.9)<sup>154</sup> was synthesised and this complex displayed a capacity to target mitochondria of cancer cells.<sup>154</sup> Complex **1.41**·Br<sub>2</sub> was shown to induce mitochondrial membrane permeabilization (MMP) in mitochondria isolated from rat liver. Based on these results the authors concluded that the complex has the potential to act as an antimitochondrial anticancer reagent. In a second example, the synthesized homobimetallic Au(I) complex **1.113** and Ag(I) complex **1.114** (Figure 1.17) were evaluated as potential anticancer agents.<sup>152</sup> These complexes were tested against six cancer lines including prostate, breast, lung, cervix, colon and a murine breast tumour line. The results showed that these complexes displayed excellent cytotoxicity against those cell lines which is comparable to currently available anticancer agent cisplatin.<sup>152</sup>

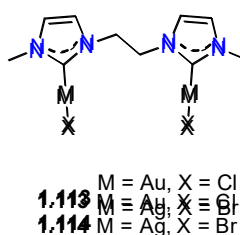


Figure 1.17 Structures of homobimetallic complexes **1.113** and **1.114**.



Interestingly, heterobimetallic complexes of NHC ligands have also been evaluated as potential anticancer agents.<sup>92, 153</sup> For example, a series heterobimetallic complexes of the metals Au(I)-Cu(II) **1.115**, Au(I)-Ru(I) **1.116·PF<sub>6</sub>** and **1.117·PF<sub>6</sub>** (Figure 1.17) were synthesised and found to be cytotoxic against ovarian carcinoma cell lines A2780 and SKOV-3 and human lung cancer cells A549.<sup>153</sup> The Au(I)-Ru(I) complex **1.116·PF<sub>6</sub>** showed low levels of cytotoxicity, while the Au(I)-Cu(I) complex **1.115** was highly cytotoxic, and this complex was comparable in activity to cisplatin against the SKOV-3 cell line. In addition, the heterobimetallic complex **1.117·PF<sub>6</sub>** was selectively cytotoxic against A2780 cells.<sup>153</sup>

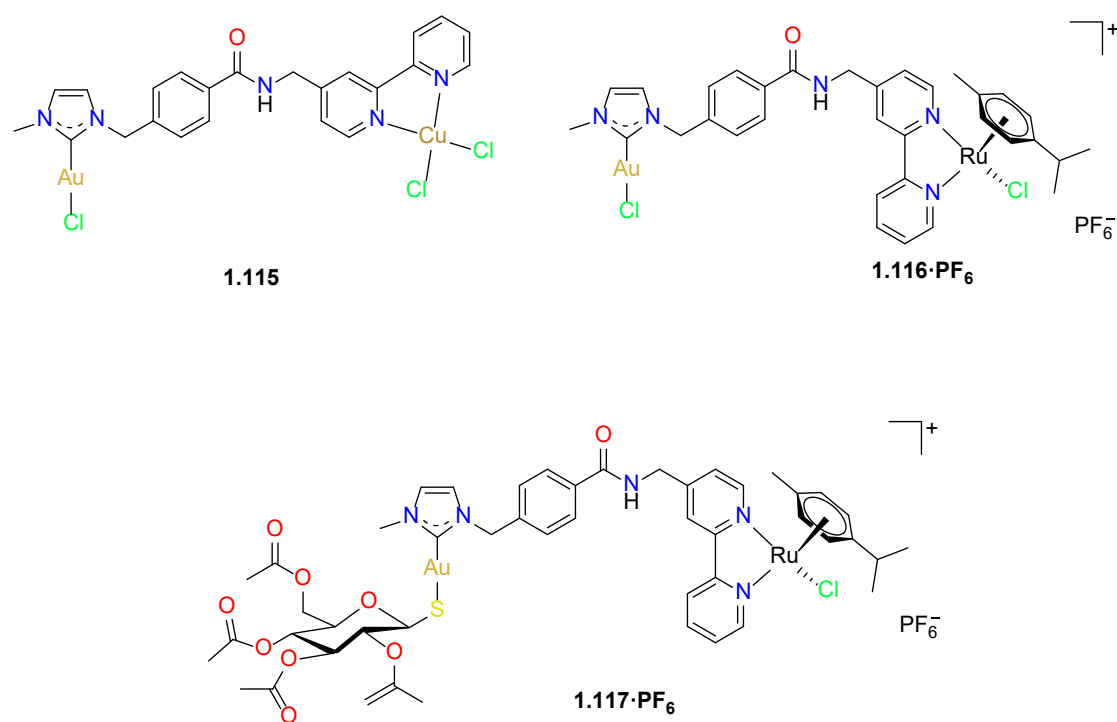


Figure 1.18 Structures of heterobimetallic complexes **1.115**, **1.116·PF<sub>6</sub>** and **1.117·PF<sub>6</sub>**.

In a second study, a family of heterobimetallic Ru(II)-Au(I) complexes (Figure 1.18) were prepared and evaluated for their cytotoxicity against Hep3B cancer cell lines. Complex **1.118·(PF<sub>6</sub>)<sub>2</sub>** was also tested against the parasites *Leishmania infantum* and *Plasmodium falciparum*. Studies showed that the complexes decomposed in biological media and were slowly transformed into the corresponding Ru(II) complexes with the release of Au(I) cations, resulting in the cytotoxicity against the cancer cells.<sup>92</sup>

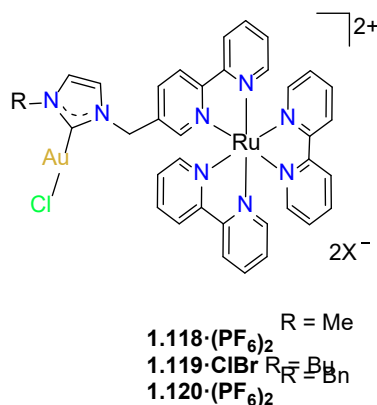


Figure 1.19 Structures of heterobimetallic Au(I)-Ru(II) complexes **1.118**·(PF<sub>6</sub>)<sub>2</sub>, **1.119**·(PF<sub>6</sub>)<sub>2</sub> and **1.120**·(PF<sub>6</sub>)<sub>2</sub> with cytotoxicity.

## 1.6 Research overview

Imidazolium linked macrocycles have attracted significant recent attention because of their capacity to recognise halides,<sup>24, 27, 30, 37, 42-43</sup> acetate,<sup>24, 43</sup> dihydrogenphosphate<sup>26, 36</sup> and other biological anionic species and act as anion receptor.<sup>155-157</sup> In addition, imidazolium linked macrocycles have also been utilized as precursors for NHC metal complexes with multiple potential applications.<sup>60, 73, 158</sup> As such, we became interested in developing new strategies for the synthesis of compounds of this type. In chapter 2 of this thesis, the aim of this section was the development of new strategies for the synthesis of symmetrical and asymmetrical tetra-imidazolium linked macrocycle and investigations of their anion binding properties. In addition, the preparation of NHC metal complexes of the tetra-imidazolium linked macrocycle pro-ligands was a key goal. A modular stepwise synthetic approach is described for the preparation of *tetra*-imidazolium macrocycles. A series of three *bis*-(imidazolylmethyl)benzene precursors were initially alkylated with 1,2-dibromoethane to produce the corresponding *bis*-bromoethylimidazolium bromide salts. In the second step, the *bis*-bromoethylimidazolium bromide salts were reacted with selected *bis*-(imidazolylmethyl)benzene molecules to generate a series of two symmetrical and three asymmetrical *tetra*-imidazolium macrocycles. These *tetra*-imidazolium salts were found to

act as receptors for anions and  $^1\text{H}$ -NMR titration studies were used to determine the association constants between two of the macrocycles and the halide anions ( $\text{Cl}^-$ ,  $\text{Br}^-$  and  $\text{I}^-$ ). The *tetra*-imidazolium salts also serve as precursors for NHC ligands and a series of silver(I), gold(I) and palladium(II) NHC complexes were synthesized. Varied structures were obtained, which depended on the chosen macrocyclic ligand and metal ion and in the case of the coinage metals Ag(I) and Au(I), mono, di and hexanuclear complexes were formed.

The anion binding properties of a range of 1,2,3-triazolium linked macrocycles have been studied and some compounds demonstrated their potential for developing novel sensors for biologically and environmentally important anions.<sup>28-29, 159-164</sup> In addition, compounds of this type can also be utilized for the synthesis of ‘abnormal’ NHC metal complexes for a range of applications including biological applications and developing novel catalysts.<sup>165-166</sup> Thus, we became interested in the synthesis of macrocycles incorporating 1,2,3-triazolium and imidazolium groups using modular stepwise macrocyclization method. In Chapter 3, the aim of this section was an investigation of the modular stepwise synthesis strategy for asymmetrical azolium (imidazolium and triazolium) linked macrocycles and their anion binding behaviours. A modular stepwise synthesis strategy related to that undertaken in Chapter 2, was therefore, used to prepare asymmetrical macrocyclic compounds bearing both imidazolium and 1,2,3-triazole groups. Two macrocycles containing 1,2,3-triazole and imidazolium groups were prepared. The synthesis was initiated with the preparation of an alcohol substituted 1,2,3-triazole species using copper(I)-catalyzed azide-alkyne cycloaddition (CuAAC) reaction. In the second step, the alcohol group was converted to an alkyl bromide and these precursors were then reacted with selected *bis*-(imidazolylmethyl)benzene molecules (*ortho*- or *meta*-) to generate the macrocycles. Using  $^1\text{H}$ -NMR titration studies the anion binding properties of the prepared macrocycles were evaluated and the association constants between these

compounds and halides ( $\text{Cl}^-$ ,  $\text{Br}^-$  and  $\text{I}^-$ ) were also determined. In addition, the prepared macrocycles also act as NHC pro-ligands and the dinuclear Au(I) complex of one of the macrocycles was also prepared.

As previously described, heterobimetallic complexes of NHC ligands is of great interest for studies of metallophilic interactions<sup>119-120, 167</sup> and the development of novel catalysts,<sup>85, 91, 96-101, 168-169</sup> in addition to biological applications such as anti-cancer drugs and antimicrobial medicines.<sup>92, 123, 170-173</sup> Therefore, we became interested in developing new strategies for the synthesis of compounds of this type to investigate their potential applications. In Chapter 4, the aim of this section was the development of new heterobimetallic complexes of NHC ligands and studies of their photophysical properties and antimicrobial properties. A series of heterobimetallic complexes of *bis*-NHC ligands were prepared using post synthetic modification and metallation approach. In this synthetic pathway, a series of two alkylene (methylene or ethylene) linked *bis*-imidazole precursor were first mono-alkylated to obtain the asymmetric imidazolium salts bearing pendant imidazole units. These compounds were then metallated yielding the corresponding monometallic Au(I)-NHC complexes. These complexes were further alkylated with either methyl or ethyl groups using the appropriate oxonium salts to obtain monometallic Au(I) precursor complexes bearing pendent imidazolium groups. These complexes were then metallated using a different metal source to prepare heterobimetallic complexes such as the Au(I)-Ag(II) and Au(I)-Hg(II) compounds. This method provides a straightforward approach to introduce two different metals selectively to *bis*-imidazolium pro-ligands and it avoids the formation of undesirable homobimetallic complexes as side products.

In addition to the heterobimetallic complexes, homobimetallic  $\text{Ag}_2$  and  $\text{Au}_2$  complexes were also synthesized for comparative studies. Variable temperature  $^1\text{H}$ -NMR studies were undertaken to analyse the conformational isomers of the prepared homo- and heterobimetallic complexes. The  $^1\text{H}$ -NMR spectra for the homo- and heterobimetallic

complexes of the methylene linked *bis*-NHC ligands are consistent with the complexes being relatively rigid in solution with interconversion between structural isomers occurring on a slow to intermediate rate on the NMR timescale. In addition, the X-ray crystallographic characterisation of one heterobimetallic complex showed that for this compound the distance between the Ag(I) and Au(I) atoms was 3.205(6) Å and is consistent with a metallophilic interaction. Photophysical studies were also undertaken, and these studies showed that the bimetallic complexes were non-emissive in the solution phase at room temperature due to the loss of metallophilic interaction resulting from fluxional behaviour of these molecules. Antimicrobial studies reveal the heterobimetallic Au(I)-Ag(I) complexes display good antimicrobial activity against two Gram-positive bacteria strain (*A. baumannii* and *E. coli*) with MIC value in the range of 4 – 16 µg·mL<sup>-1</sup> and two Gram-negative bacterial strains (*E. faecium* and *S. aureus*) with MIC value in the range of 8 – 32 µg·mL<sup>-1</sup>.

## 1.7 References

1. Bourissou, D.; Guerret, O.; Gabbaï, F. P.; Bertrand, G., *Chem. Rev.* **2000**, *100* (1), 39-92.
2. Moss, G. P.; Smith, P. A. S.; Tavernier, D., *Pure. Appl. Chem.* **1995**, *67* (8-9), 1307-1375.
3. Díez-González, S.; Nolan, S. P., *Coord. Chem. Rev.* **2007**, *251* (5), 874-883.
4. Fischer, E. O.; Maasböl, A., *Angew. Chem. Int. Ed. Engl.* **1964**, *3* (8), 580-581.
5. de Frémont, P.; Marion, N.; Nolan, S. P., *Coord. Chem. Rev.* **2009**, *253* (7), 862-892.
6. Bazinet, P.; Ong, T.-G.; O'Brien, J. S.; Lavoie, N.; Bell, E.; Yap, G. P. A.; Korobkov, I.; Richeson, D. S., *Organometallics* **2007**, *26* (11), 2885-2895.
7. Hahn, F. E.; Wittenbecher, L.; Boese, R.; Bläser, D., *Chem. Eur. J.* **1999**, *5* (6), 1931-1935.
8. Denk, M. K.; Thadani, A.; Hatano, K.; Lough, A. J., *Angew. Chem. Int. Ed.* **1997**, *36* (23), 2607-2609.
9. Kuhn, N.; Kratz, T., *Synthesis* **1993**, *1993* (06), 561-562.
10. Wanzlick, H. W., *Angew. Chem. Int. Ed.* **1962**, *1* (2), 75-80.
11. Wanzlick, H. W.; Schönherr, H. J., *Angew. Chem. Int. Ed.* **1968**, *7* (2), 141-142.
12. Crabtree, R. H., *Coord. Chem. Rev.* **2013**, *257* (3), 755-766.
13. Guisado-Barrios, G.; Bouffard, J.; Donnadieu, B.; Bertrand, G., *Angew. Chem. Int. Ed.* **2010**, *49* (28), 4759-4762.
14. Herrmann, W. A.; Köcher, C., *Angew. Chem. Int. Ed. Engl.* **1997**, *36* (20), 2162-2187.
15. Nelson, D. J.; Nolan, S. P., *Chem. Soc. Rev.* **2013**, *42* (16), 6723-6753.
16. Nesterov, V.; Reiter, D.; Bag, P.; Frisch, P.; Holzner, R.; Porzelt, A.; Inoue, S., *Chem. Rev.* **2018**, *118* (19), 9678-9842.
17. Heinemann, C.; Müller, T.; Apeloig, Y.; Schwarz, H., *J. Am. Chem. Soc.* **1996**, *118* (8), 2023-2038.
18. Collins, M. S.; Rosen, E. L.; Lynch, V. M.; Bielawski, C. W., *Organometallics* **2010**, *29* (13), 3047-3053.
19. Boehme, C.; Frenking, G., *J. Am. Chem. Soc.* **1996**, *118* (8), 2039-2046.
20. Arduengo, A. J.; Goerlich, J. R.; Marshall, W. J., *J. Am. Chem. Soc.* **1995**, *117* (44), 11027-11028.

21. Schulte to Brinke, C.; Pape, T.; Hahn, F. E., *Dalton Trans.* **2013**, 42 (20), 7330-7337.
22. Hahn, F. E.; Radloff, C.; Pape, T.; Hepp, A., *Chem. Eur. J.* **2008**, 14 (35), 10900-10904.
23. Bass, H. M.; Cramer, S. A.; Price, J. L.; Jenkins, D. M., *Organometallics* **2010**, 29 (15), 3235-3238.
24. Toure, M.; Charles, L.; Chendo, C.; Viel, S.; Chuzel, O.; Parrain, J.-L., *Chem. Eur. J.* **2016**, 22 (26), 8937-8942.
25. Altmann, P. J.; Jandl, C.; Pöthig, A., *Dalton Trans.* **2015**, 44 (25), 11278-11281.
26. Sabater, P.; Zapata, F.; Caballero, A.; Alkorta, I.; Ramirez de Arellano, C.; Elguero, J.; Molina, P., *ChemistrySelect* **2018**, 3 (13), 3855-3859.
27. Wong, W. W. H.; Vickers, M. S.; Cowley, A. R.; Paul, R. L.; Beer, P. D., *Org. Biomol. Chem.* **2005**, 3 (23), 4201-4208.
28. Mesquida, N.; Dinarès, I.; Ibáñez, A.; Alcalde, E., *Org. Biomol. Chem.* **2013**, 11 (37), 6385-6396.
29. White, N. G.; Carvalho, S.; Félix, V.; Beer, P. D., *Org. Biomol. Chem.* **2012**, 10 (34), 6951-6959.
30. Ramos, S.; Alcalde, E.; Doddi, G.; Mencarelli, P.; Pérez-García, L., *J. Org. Chem.* **2002**, 67 (24), 8463-8468.
31. Evans, N. H.; Beer, P. D., *Angew. Chem. Int. Ed.* **2014**, 53 (44), 11716-11754.
32. Gimeno, N.; Vilar, R., *Coord. Chem. Rev.* **2006**, 250 (23), 3161-3189.
33. Vilar, R., *Angew. Chem. Int. Ed.* **2003**, 42 (13), 1460-1477.
34. Barnard, P. J.; Wedlock, L. E.; Baker, M. V.; Berners-Price, S. J.; Joyce, D. A.; Skelton, B. W.; Steer, J. H., *Angew. Chem. Int. Ed.* **2006**, 45 (36), 5966-5970.
35. Schulte to Brinke, C.; Ekkehardt Hahn, F., *Dalton Trans.* **2015**, 44 (32), 14315-14322.
36. Alcalde, E.; Mesquida, N.; Pérez-García, L.; Alvarez-Rúa, C.; García-Granda, S.; García-Rodríguez, E., *Chem. Commun.* **1999**, (3), 295-296.
37. Alcalde, E.; Mesquida, N.; Vilaseca, M.; Alvarez-RÚA, C.; García-Granda, S., *Supramol. Chem.* **2007**, 19 (7), 501-509.
38. D'Acerno, C.; Doddi, G.; Ercolani, G.; Mencarelli, P., *Chem. Eur. J.* **2000**, 6 (19), 3540-3546.
39. Doddi, G.; Ercolani, G.; Franconeri, S.; Mencarelli, P., *J. Org. Chem.* **2001**, 66 (14), 4950-4953.

40. Melaimi, M.; Soleilhavoup, M.; Bertrand, G., *Angew. Chem. Int. Ed.* **2010**, *49* (47), 8810-8849.
41. Magill, A. M.; Yates, B. F., *Aust. J. Chem.* **2004**, *57* (12), 1205-1210.
42. Vickers, M. S.; Martindale, K. S.; Beer, P. D., *J. Mater. Chem.* **2005**, *15* (27-28), 2784-2790.
43. Chellappan, K.; Singh, N. J.; Hwang, I.-C.; Lee, J. W.; Kim, K. S., *Angew. Chem. Int. Ed.* **2005**, *44* (19), 2899-2903.
44. Xu, Z.; Kim, S. K.; Yoon, J., *Chem. Soc. Rev.* **2010**, *39* (5), 1457-1466.
45. Yuan, Y.; Gao, G.; Jiang, Z.-L.; You, J.-S.; Zhou, Z.-Y.; Yuan, D.-Q.; Xie, R.-G., *Tetrahedron* **2002**, *58* (44), 8993-8999.
46. Sato, K.; Onitake, T.; Arai, S., *Heterocycles* **2003**, *60* (4), 779-784.
47. Yoon, J.; Kim, S. K.; Singh, N. J.; Kim, K. S., *Chem. Soc. Rev.* **2006**, *35* (4), 355-360.
48. Gong, H.-Y.; Rambo, B. M.; Karnas, E.; Lynch, V. M.; Sessler, J. L., *Nat. Chem.* **2010**, *2*, 406.
49. Wei, J.; Jin, T.-T.; Yang, J.-X.; Jiang, X.-M.; Liu, L.-J.; Zhan, T.-G.; Zhang, K.-D., *Tetrahedron Lett.* **2020**, *61* (2), 151389.
50. Wang, J.-H.; Xiong, J.-B.; Zhang, X.; Song, S.; Zhu, Z.-H.; Zheng, Y.-S., *RSC Adv.* **2015**, *5* (74), 60096-60100.
51. Neelakandan, P. P.; Ramaiah, D., *Angew. Chem. Int. Ed.* **2008**, *47* (44), 8407-8411.
52. Mageed, A. H.; Skelton, B. W.; Baker, M. V., *Dalton Trans.* **2017**, *46* (24), 7844-7856.
53. Mageed, A. H.; Skelton, B. W.; Sobolev, A. N.; Baker, M. V., *Eur. J. Inorg. Chem.* **2018**, *2018* (1), 109-120.
54. Barnard, P. J.; Baker, M. V.; Berners-Price, S. J.; Skelton, B. W.; White, A. H., *Dalton Trans.* **2004**, (7), 1038-1047.
55. Nomiya, K.; Morozumi, S.; Yanagawa, Y.; Hasegawa, M.; Kurose, K.; Taguchi, K.; Sakamoto, R.; Mihara, K.; Kasuga, N. C., *Inorg. Chem.* **2018**, *57* (18), 11322-11332.
56. Lu, Z.; Cramer, S. A.; Jenkins, D. M., *Chem. Sci.* **2012**, *3* (10), 3081-3087.
57. Altmann, P. J.; Weiss, D. T.; Jandl, C.; Kühn, F. E., *Chem. Asian J.* **2016**, *11* (10), 1597-1605.
58. Lu, T.; Yang, C.-F.; Steren, C. A.; Fei, F.; Chen, X.-T.; Xue, Z.-L., *New J. Chem.* **2018**, *42* (6), 4700-4713.
59. Thapa, R.; Kilyanek, S. M., *Dalton Trans.* **2019**, *48* (33), 12577-12590.



60. Meyer, S.; Klawitter, I.; Demeshko, S.; Bill, E.; Meyer, F., *Angew. Chem. Int. Ed.* **2013**, 52 (3), 901-905.
61. Anneser, M. R.; Haslinger, S.; Pöthig, A.; Cokoja, M.; Basset, J.-M.; Kühn, F. E., *Inorg. Chem.* **2015**, 54 (8), 3797-3804.
62. Fei, F.; Lu, T.; Yang, C.-F.; Chen, X.-T.; Xue, Z.-L., *Eur. J. Inorg. Chem.* **2018**, 2018 (14), 1595-1602.
63. Schulte to Brinke, C.; Hahn, F. E., *Eur. J. Inorg. Chem.* **2015**, 2015 (20), 3227-3231.
64. Garcia Santos, I.; Hagenbach, A.; Abram, U., *Dalton Trans.* **2004**, (4), 677-682.
65. Zhu, S.; Liang, R.; Jiang, H., *Tetrahedron* **2012**, 68 (38), 7949-7955.
66. Baron, M.; Tubaro, C.; Basato, M.; Biffis, A.; Natile, M. M.; Graiff, C., *Organometallics* **2011**, 30 (17), 4607-4615.
67. Khanye, S. D.; Báthori, N. B.; Smith, G. S.; Chibale, K., *Dalton Trans.* **2010**, 39 (10), 2697-2700.
68. Fei, F.; Lu, T.; Chen, X.-T.; Xue, Z.-L., *New J. Chem.* **2017**, 41 (22), 13442-13453.
69. Andrew, R. E.; Storey, C. M.; Chaplin, A. B., *Dalton Trans.* **2016**, 45 (21), 8937-8944.
70. Garrison, J. C.; Simons, R. S.; Talley, J. M.; Wesdemiotis, C.; Tessier, C. A.; Youngs, W. J., *Organometallics* **2001**, 20 (7), 1276-1278.
71. McKie, R.; Murphy, J. A.; Park, S. R.; Spicer, M. D.; Zhou, S.-z., *Angew. Chem. Int. Ed.* **2007**, 46 (34), 6525-6528.
72. Garrison, J. C.; Simons, R. S.; Tessier, C. A.; Youngs, W. J., *J. Org. Chem.* **2003**, 68 (1), 1-4.
73. Melaiye, A.; Sun, Z.; Hindi, K.; Milsted, A.; Ely, D.; Reneker, D. H.; Tessier, C. A.; Youngs, W. J., *J. Am. Chem. Soc.* **2005**, 127 (7), 2285-2291.
74. Radloff, C.; Gong, H.-Y.; Schulte to Brinke, C.; Pape, T.; Lynch, V. M.; Sessler, J. L.; Hahn, F. E., *Eur. J. Inorg. Chem.* **2010**, 16 (44), 13077-13081.
75. Biffis, A.; Cipani, M.; Tubaro, C.; Basato, M.; Costante, M.; Bressan, E.; Venzo, A.; Graiff, C., *New J. Chem.* **2013**, 37 (12), 4176-4184.
76. Hahn, F. E.; Langenhahn, V.; Lügger, T.; Pape, T.; Le Van, D., *Angew. Chem. Int. Ed.* **2005**, 44 (24), 3759-3763.
77. Flores-Figueroa, A.; Pape, T.; Feldmann, K.-O.; Hahn, F. E., *Chem. Commun.* **2010**, 46 (2), 324-326.
78. Blase, V.; Pape, T.; Hahn, F. E., *J. Org. Chem.* **2011**, 696 (21), 3337-3342.

79. Muller, P., *Glossary of terms used in physical organic chemistry (IUPAC Recommendations 1994)*. 2009; Vol. 66.
80. Zamora, M. T.; Ferguson, M. J.; McDonald, R.; Cowie, M., *Dalton Trans.* **2009**, (35), 7269-7287.
81. Zamora, M. T.; Ferguson, M. J.; Cowie, M., *Organometallics* **2012**, *31* (15), 5384-5395.
82. Zamora, M. T.; Ferguson, M. J.; McDonald, R.; Cowie, M., *Organometallics* **2012**, *31* (15), 5463-5477.
83. Maity, R.; Koppetz, H.; Hepp, A.; Hahn, F. E., *J. Am. Chem. Soc.* **2013**, *135* (13), 4966-4969.
84. Maity, R.; Schulte to Brinke, C.; Hahn, F. E., *Dalton Trans.* **2013**, *42* (36), 12857-12860.
85. Majumder, A.; Naskar, R.; Roy, P.; Maity, R., *Eur. J. Inorg. Chem.* **2019**, *2019* (13), 1810-1815.
86. Böhmer, M.; Guisado-Barrios, G.; Kampert, F.; Roelfes, F.; Tan, T. T. Y.; Peris, E.; Hahn, F. E., *Organometallics* **2019**, *38* (9), 2120-2131.
87. Simler, T.; Möbius, K.; Müller, K.; Feuerstein, T. J.; Gamer, M. T.; Lebedkin, S.; Kappes, M. M.; Roesky, P. W., *Organometallics* **2019**, *38* (19), 3649-3661.
88. Pell, T. P.; Wilson, D. J. D.; Skelton, B. W.; Dutton, J. L.; Barnard, P. J., *Inorg. Chem.* **2016**, *55* (14), 6882-6891.
89. Aznarez, F.; Gao, W.-X.; Lin, Y.-J.; Hahn, F. E.; Jin, G.-X., *Dalton Trans.* **2018**, *47* (28), 9442-9452.
90. Longhi, A.; Baron, M.; Rancan, M.; Bottaro, G.; Armelao, L.; Sgarbossa, P.; Tubaro, C., *Molecules* **2019**, *24* (12).
91. Böhmer, M.; Kampert, F.; Tan, T. T. Y.; Guisado-Barrios, G.; Peris, E.; Hahn, F. E., *Organometallics* **2018**, *37* (21), 4092-4099.
92. Boselli, L.; Carraz, M.; Mazères, S.; Paloque, L.; González, G.; Benoit-Vical, F.; Valentin, A.; Hemmert, C.; Gornitzka, H., *Organometallics* **2015**, *34* (6), 1046-1055.
93. Bente, S.; Kampert, F.; Tan, T. T. Y.; Hahn, F. E., *Chem. Commun.* **2018**, *54* (91), 12887-12890.
94. Maity, R.; Rit, A.; Schulte to Brinke, C.; Daniliuc, C. G.; Hahn, F. E., *Chem. Commun.* **2013**, *49* (10), 1011-1013.
95. Rit, A.; Pape, T.; Hepp, A.; Hahn, F. E., *Organometallics* **2011**, *30* (2), 334-347.
96. Mata, J. A.; Hahn, F. E.; Peris, E., *Chem. Sci.* **2014**, *5* (5), 1723-1732.
97. Ajamian, A.; Gleason, J. L., *Angew. Chem. Int. Ed.* **2004**, *43* (29), 3754-3760.

98. Sabater, S.; Mata, J. A.; Peris, E., *Nat. Commun.* **2013**, *4*, 2553.
99. Bitzer, M. J.; Kühn, F. E.; Baratta, W., *J. Catal.* **2016**, *338*, 222-226.
100. Pardatscher, L.; Bitzer, M. J.; Jandl, C.; Kück, J. W.; Reich, R. M.; Kühn, F. E.; Baratta, W., *Dalton Trans.* **2019**, *48* (1), 79-89.
101. Gonell, S.; Poyatos, M.; Mata, J. A.; Peris, E., *Organometallics* **2012**, *31* (15), 5606-5614.
102. Zanardi, A.; Mata, J. A.; Peris, E., *J. Am. Chem. Soc.* **2009**, *131* (40), 14531-14537.
103. Pyykkö, P., *Chem. Rev.* **1997**, *97* (3), 597-636.
104. Schmidbaur, H.; Schier, A., *Angew. Chem. Int. Ed.* **2015**, *54* (3), 746-784.
105. Scherbaum, F.; Grohmann, A.; Huber, B.; Krüger, C.; Schmidbaur, H., *Angew. Chem. Int. Ed.* **1988**, *27* (11), 1544-1546.
106. Scherbaum, F.; Huber, B.; Müller, G.; Schmidbaur, H., *Angew. Chem. Int. Ed.* **1988**, *27* (11), 1542-1544.
107. Schmidbaur, H.; Scherbaum, F.; Huber, B.; Müller, G., *Angew. Chem. Int. Ed.* **1988**, *27* (3), 419-421.
108. Gu, W.-W.; Chen, W.-J.; Yan, C.-G., *Supramol. Chem.* **2015**, *27* (5-6), 407-413.
109. Ray, L.; Shaikh, M. M.; Ghosh, P., *Inorg. Chem.* **2008**, *47* (1), 230-240.
110. Ai, P.; Danopoulos, A. A.; Braunstein, P.; Monakhov, K. Y., *Chem. Commun.* **2014**, *50* (1), 103-105.
111. White-Morris, R. L.; Olmstead, M. M.; Balch, A. L., *J. Am. Chem. Soc.* **2003**, *125* (4), 1033-1040.
112. Harisomayajula, N. V. S.; Makovetskyi, S.; Tsai, Y.-C., *Chem. Eur. J.* **2019**, *25* (38), 8936-8954.
113. Strasser, C. E.; Catalano, V. J., *J. Am. Chem. Soc.* **2010**, *132* (29), 10009-10011.
114. Laguna, A.; Lasanta, T.; López-de-Luzuriaga, J. M.; Monge, M.; Naumov, P.; Olmos, M. E., *J. Am. Chem. Soc.* **2010**, *132* (2), 456-457.
115. Schmidbaur, H.; Schier, A., *Chemical Society Reviews* **2012**, *41* (1), 370-412.
116. Bondi, A., *J. Phys. Chem.* **1964**, *68* (3), 441-451.
117. Catalano, V. J.; Horner, S. J., *Inorg. Chem.* **2003**, *42* (25), 8430-8438.
118. Catalano, V. J.; Malwitz, M. A.; Etogo, A. O., *Inorg. Chem.* **2004**, *43* (18), 5714-5724.
119. Catalano, V. J.; Moore, A. L., *Inorg. Chem.* **2005**, *44* (19), 6558-6566.
120. Strasser, C. E.; Catalano, V. J., *Inorg. Chem.* **2011**, *50* (21), 11228-11234.
121. Russell, A. D.; Hugo, W. B., 7 Antimicrobial Activity and Action of Silver. In *Prog. Med. Chem.*, Ellis, G. P.; Luscombe, D. K., Eds. Elsevier: 1994; Vol. 31, pp 351-370.

122. Klasen, H. J., *Burns* **2000**, 26 (2), 117-130.
123. Johnson, N. A.; Southerland, M. R.; Youngs, W. J., *Molecules* **2017**, 22 (8).
124. Fox, C. L., Jr., *Arch. Surg.* **1968**, 96 (2), 184-188.
125. Hartinger, C. G.; Dyson, P. J., *Chem. Soc. Rev.* **2009**, 38 (2), 391-401.
126. Hopkinson, M. N.; Richter, C.; Schedler, M.; Glorius, F., *Nature* **2014**, 510 (7506), 485-496.
127. Kascatan-Nebioglu, A.; Melaiye, A.; Hindi, K.; Durmus, S.; Panzner, M. J.; Hogue, L. A.; Mallett, R. J.; Hovis, C. E.; Coughenour, M.; Crosby, S. D.; Milsted, A.; Ely, D. L.; Tessier, C. A.; Cannon, C. L.; Youngs, W. J., *J. Med. Chem.* **2006**, 49 (23), 6811-6818.
128. Hindi, K. M.; Siciliano, T. J.; Durmus, S.; Panzner, M. J.; Medvetz, D. A.; Reddy, D. V.; Hogue, L. A.; Hovis, C. E.; Hilliard, J. K.; Mallet, R. J.; Tessier, C. A.; Cannon, C. L.; Youngs, W. J., *J. Med. Chem.* **2008**, 51 (6), 1577-1583.
129. Wright, B. D.; Shah, P. N.; McDonald, L. J.; Shaeffer, M. L.; Wagers, P. O.; Panzner, M. J.; Smolen, J.; Tagaev, J.; Tessier, C. A.; Cannon, C. L.; Youngs, W. J., *Dalton Trans.* **2012**, 41 (21), 6500-6506.
130. Panzner, M. J.; Deeraksa, A.; Smith, A.; Wright, B. D.; Hindi, K. M.; Kascatan-Nebioglu, A.; Torres, A. G.; Judy, B. M.; Hovis, C. E.; Hilliard, J. K.; Mallett, R. J.; Cope, E.; Estes, D. M.; Cannon, C. L.; Leid, J. G.; Youngs, W. J., *Eur. J. Inorg. Chem.* **2009**, 2009 (13), 1739-1745.
131. Patil, S.; Dietrich, K.; Deally, A.; Gleeson, B.; Müller-Bunz, H.; Paradisi, F.; Tacke, M., *Helv. Chim. Acta.* **2010**, 93 (12), 2347-2364.
132. Patil, S.; Claffey, J.; Deally, A.; Hogan, M.; Gleeson, B.; Menéndez Méndez, L. M.; Müller-Bunz, H.; Paradisi, F.; Tacke, M., *Eur. J. Inorg. Chem.* **2010**, 2010 (7), 1020-1031.
133. Napoli, M.; Saturnino, C.; Cianciulli, E. I.; Varcamonti, M.; Zanfardino, A.; Tommonaro, G.; Longo, P., *J. Organomet. Chem.* **2013**, 725, 46-53.
134. Haque, R. A.; Asekunowo, P. O.; Razali, M. R.; Mohamad, F., *Heteroatom Chem.* **2014**, 25 (3), 194-204.
135. Gök, Y.; Akkoç, S.; Albayrak, S.; Akkurt, M.; Tahir, M. N., *Appl. Organomet. Chem.* **2014**, 28 (4), 244-251.
136. Kaloğlu, M.; Kaloğlu, N.; Özdemir, İ.; Günal, S.; Özdemir, İ., *Bioorg. Med. Chem.* **2016**, 24 (16), 3649-3656.
137. Günal, S.; Kaloğlu, N.; Özdemir, İ.; Demir, S.; Özdemir, İ., *Inorg. Chem. Commun.* **2012**, 21, 142-146.
138. Melaiye, A.; Simons, R. S.; Milsted, A.; Pingitore, F.; Wesdemiotis, C.; Tessier, C. A.; Youngs, W. J., *J. Med. Chem.* **2004**, 47 (4), 973-977.

139. Hindi, K. M.; Panzner, M. J.; Tessier, C. A.; Cannon, C. L.; Youngs, W. J., *Chem. Rev.* **2009**, *109* (8), 3859-3884.
140. Knapp, A. R.; Panzner, M. J.; Medvetz, D. A.; Wright, B. D.; Tessier, C. A.; Youngs, W. J., *Inorg. Chim. Acta.* **2010**, *364* (1), 125-131.
141. Cannon, C. L.; Hogue, L. A.; Vajravelu, R. K.; Capps, G. H.; Ibricevic, A.; Hindi, K. M.; Kascatan-Nebioglu, A.; Walter, M. J.; Brody, S. L.; Youngs, W. J., *Antimicrob. Agents Chemother.* **2009**, *53* (8), 3285.
142. Panzner, M. J.; Hindi, K. M.; Wright, B. D.; Taylor, J. B.; Han, D. S.; Youngs, W. J.; Cannon, C. L., *Dalton Trans.* **2009**, (35), 7308-7313.
143. Dileepan, A. G. B.; Ganesh Kumar, A.; Mathumidha, R.; Rajaram, R.; Rajam, S., *Chem. Pap.* **2018**, *72* (12), 3017-3031.
144. Karataş Mert, O.; Günal, S.; Mansur, A.; Alıcı, B.; Çetinkaya, E., Synthesis and antimicrobial properties of cycloheptyl substituted benzimidazolium salts and their silver(I) carbene complexes. In *Heterocycl. Commun.*, 2016; Vol. 22, p 357.
145. Sarı, Y.; Akkoç, S.; Gök, Y.; Sifniotis, V.; Özdemir, İ.; Günal, S.; Kayser, V., *J. Enzym. Inhib. Med. Ch.* **2016**, *31* (6), 1527-1530.
146. Roymahapatra, G.; M. Mandal, S.; F. Porto, W.; Samanta, T.; Giri, S.; Dinda, J.; L. Franco, O.; K. Chattaraj, P., *Curr. Med. Chem.* **2012**, *19* (24), 4184-4193.
147. Patil, S.; Deally, A.; Gleeson, B.; Müller-Bunz, H.; Paradisi, F.; Tacke, M., *Metallomics* **2011**, *3* (1), 74-88.
148. Tacke, M., *J. Organomet. Chem.* **2015**, *782*, 17-21.
149. Sharkey, A. M.; Gara, P. J.; Gordon, V. S.; Hackenberg, F.; Healy, C.; Paradisi, F.; Patil, S.; Schaible, B.; Tacke, M., *Antibiotics* **2012**, *1* (1).
150. Browne, N.; Hackenberg, F.; Streciwilk, W.; Tacke, M.; Kavanagh, K., *BioMetals* **2014**, *27* (4), 745-752.
151. Karaca, Ö.; Meier-Menches, S. M.; Casini, A.; Kühn, F. E., *Chem. Commun.* **2017**, *53* (59), 8249-8260.
152. Sanchez, O.; González, S.; Fernández, M.; Higuera-Padilla, A. R.; Leon, Y.; Coll, D.; Vidal, A.; Taylor, P.; Urdanibia, I.; Goite, M. C.; Castro, W., *Inorganica Chimica Acta* **2015**, *437*, 143-151.
153. Bertrand, B.; Citta, A.; Franken, I. L.; Picquet, M.; Folda, A.; Scalcon, V.; Rigobello, M. P.; Le Gendre, P.; Casini, A.; Bodio, E., *J Biol Inorg Chem.* **2015**, *20* (6), 1005-1020.
154. Barnard, P. J.; Baker, M. V.; Berners-Price, S. J.; Day, D. A., *J. Inorg. Biochem.* **2004**, *98* (10), 1642-1647.

155. Beer, P. D.; Gale, P. A., *Angew. Chem. int. Ed.* **2001**, *40* (3), 486-516.
156. Gale, P. A., *Coord. Chem. Rev.* **2003**, *240* (1), 191-221.
157. Martínez-Máñez, R.; Sancenón, F., *Chem. Rev.* **2003**, *103* (11), 4419-4476.
158. Sakamoto, R.; Morozumi, S.; Yanagawa, Y.; Toyama, M.; Takayama, A.; Kasuga, N. C.; Nomiya, K., *J. Inorg. Biochem.* **2016**, *163*, 110-117.
159. Safarnejad Shad, M.; Santhini, P. V.; Dehaen, W., *Beilstein J. Org. Chem.* **2019**, *15*, 2142-2155.
160. Zapata, F.; Gonzalez, L.; Caballero, A.; Alkorta, I.; Elguero, J.; Molina, P., *Chem. Eur. J.* **2015**, *21* (27), 9797-9808.
161. Aizpurua, J. M.; Fratila, R. M.; Monasterio, Z.; Pérez-Esnaola, N.; Andreieff, E.; Irastorza, A.; Sagartzazu-Aizpurua, M., *New J. Chem.* **2014**, *38* (2), 474-480.
162. Chhatra, R. K.; Kumar, A.; Pandey, P. S., *J. Org. Chem.* **2011**, *76* (21), 9086-9089.
163. Kumar, A.; Pandey, P. S., *Org. Lett.* **2008**, *10* (2), 165-168.
164. Kilah, N. L.; Wise, M. D.; Serpell, C. J.; Thompson, A. L.; White, N. G.; Christensen, K. E.; Beer, P. D., *J. Am. Chem. Soc.* **2010**, *132* (34), 11893-11895.
165. Karmis, R. E.; Carrara, S.; Baxter, A. A.; Hogan, C. F.; Hulett, M. D.; Barnard, P. J., *Dalton Trans.* **2019**, *48* (27), 9998-10010.
166. Hollering, M.; Albrecht, M.; Kühn, F. E., *Organometallics* **2016**, *35* (17), 2980-2986.
167. Kaub, C.; Lebedkin, S.; Li, A.; Kruppa, S. V.; Strebert, P. H.; Kappes, M. M.; Riehn, C.; Roesky, P. W., *Chem. Eur. J.* **2018**, *24* (23), 6094-6104.
168. Zanardi, A.; Mata, J. A.; Peris, E., *J. Am. Chem. Soc.* **2009**, *131* (40), 14531-14537.
169. Pezük, L. G.; Şen, B.; Hahn, F. E.; Türkmen, H., *Organometallics* **2019**, *38* (2), 593-601.
170. Bertrand, B.; Citta, A.; Franken, I. L.; Picquet, M.; Folda, A.; Scalcon, V.; Rigobello, M. P.; Le Gendre, P.; Casini, A.; Bodio, E., *J. Biol. Inorg. Chem.* **2015**, *20* (6), 1005-1020.
171. Hussaini, S. Y.; Haque, R. A.; Razali, M. R., *J. Org. Chem.* **2019**, *882*, 96-111.
172. Tan, S. J.; Yan, Y. K.; Lee, P. P. F.; Lim, K. H., *Future Med. Chem.* **2010**, *2* (10), 1591-1608.
173. Mora, M.; Gimeno, M. C.; Visbal, R., *Chem. Soc. Rev.* **2019**, *48* (2), 447-462.

# CHAPTER 2    STEPWISE SYNTHESIS OF *TETRA*- IMIDAZOLIUM MACROCYCLES AND THEIR *N*- HETEROCYCLIC CARBENE METAL COMPLEXES<sup>‡</sup>

## 2.1    Introduction

Imidazolium linked macrocycles have attracted significant recent attention because of their capacity to act as anion receptors and to function as pro-ligands for the synthesis of *N*-heterocyclic carbene (NHC) metal complexes. Due to the importance of negatively charged anionic species in biology, the preparation of receptor molecules designed to recognise and sense anions is an area of great research interest.<sup>1-4</sup> Imidazolium groups are now well recognised for their favourable features for the generation of anion receptors, which result both from electrostatic and hydrogen bonding interactions.<sup>4-10</sup> For example, a series of *tetra*-imidazolium linked macrocyclic compounds e.g. **2.1**·(PF<sub>6</sub>)<sub>4</sub> (Figure 2.1) were shown to bind to biologically relevant anions such as chloride and hydrogen sulphate.<sup>5, 11</sup> Additionally, compounds of this type (e.g. **1.29**·Br<sub>2</sub>) have been used as selective luminescent sensors for nucleic acids and nucleotide derivatives such as DNA, RNA, ATP and GTP and to sense and image RNA in living cells, as a result of strong hydrogen bonding interactions.<sup>12-15</sup>

A range of imidazolium linked macrocyclic compounds have been previously reported and both direct macrocyclization<sup>16-20</sup> and stepwise macrocyclization<sup>21</sup> processes have been previously described for the synthesis of compounds of this type. For example, the imidazolium linked macrocycle **2.1**·(PF<sub>6</sub>)<sub>4</sub> was prepared using the direct macrocyclization approach.<sup>22</sup> Meanwhile, stepwise macrocyclization can also be used for the synthesis of polyimidazolium linked macrocyclic compounds<sup>23</sup> and the synthesis of the

---

<sup>‡</sup> This work has been published as Li, Z.; Wiratpruk, N.; Barnard, P. J., *Frontiers in Chemistry* **2019**, 7, 270.

*tetra*-imidazolium macrocycle **2.2**·(PF<sub>6</sub>)<sub>4</sub> was achieved via sequential alkylation of *bis*-imidazolium precursors.<sup>5</sup>

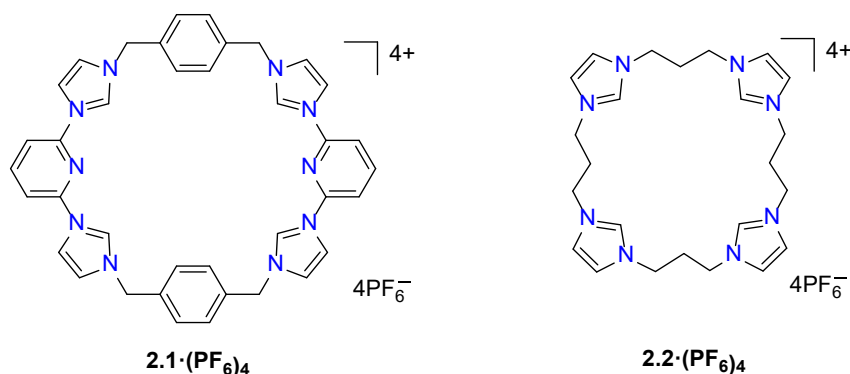


Figure 2.1 Polyimidazolium linked macrocyclic compounds (a) **2.1**·(PF<sub>6</sub>)<sub>4</sub> was prepared by direct macrocyclization and (b) **2.2**·(PF<sub>6</sub>)<sub>4</sub> prepared by stepwise macrocyclization.

Polyimidazolium linked macrocycles have also been utilized as precursors for NHC metal complexes. A large number of NHC metal complexes such as Au(I), Ag(I), Pt(II), Pd(II), Ni(II) and Fe(IV) complexes of polyimidazolium linked macrocycle pro-ligands have been previously reported.<sup>16-17,24-40</sup> For example, a series of Au(I) complexes of related cyclophane-based NHC ligand systems were synthesized and were shown to be selectively toxic to cancer cells as a result of an antimitochondrial mechanism.<sup>27-28</sup> In addition to Au(I) complexes, the synthesis of Ag(I)-NHC complexes of cyclophane ligands **1.107**·(OH)<sub>2</sub> which has antimicrobial activity has also been reported.<sup>24-25</sup> Furthermore, macrocyclic *tetra*-NHC ligands have been shown to act as tetradentate ligands for square-planar metals such as Pd(II), Ni(II), and Pt(II) (Figure 2.2).<sup>32</sup> Interestingly, a square-planar Pt(II) complex **1.38**·Cl<sub>2</sub> was prepared by metal-template reaction.<sup>26</sup> Additionally, Meyer and more recently Kühn have also extended the application of macrocyclic *tetra*-NHC ligands to the synthesis of Fe complexes.<sup>40-41</sup> For example, the complex **2.6**·(CF<sub>3</sub>SO<sub>3</sub>)<sub>2</sub> (Figure 2.2) provides fascinating models of reactive intermediates that are generated in the catalytic cycles of a range of heme and non-heme iron enzymes.<sup>40</sup>



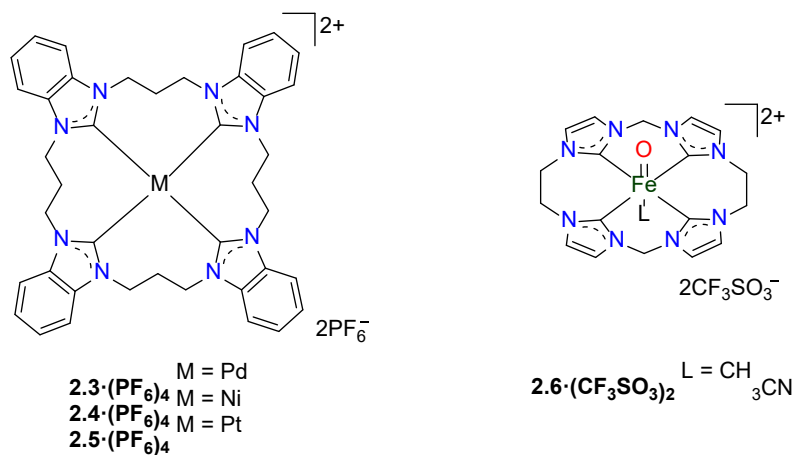


Figure 2.2 Selected metal complexes derived from macrocyclic imidazolium pro-ligands.

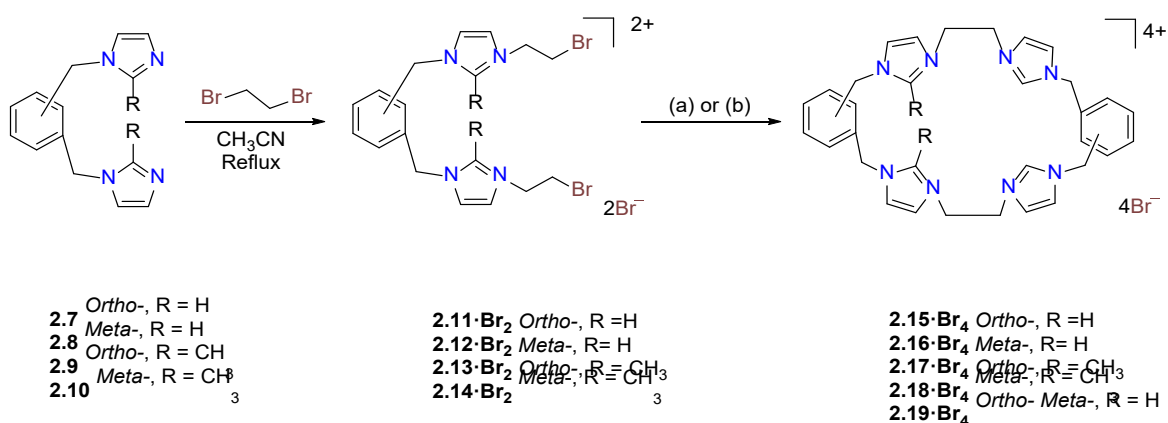
As imidazolium linked macrocycles offer the potential for the generation of novel sensors for biologically significant anions and as precursors for NHC metal complexes of metals that are well known for their biological properties, we became interested in developing new strategies for the synthesis of compounds of this type. In this chapter, we report a novel modular stepwise synthetic approach for the synthesis of *tetra*-imidazolium macrocycles. This approach involves the initial synthesis of *bis*-bromoethylimidazolium precursors, which could then be utilized for the formation of either symmetrical or asymmetrical *tetra*-imidazolium macrocycles. These *tetra*-imidazolium salts bind anions in solution and association constants between two of the macrocycles and the halide anions chloride, bromide and iodide were determined for two macrocycles. A range of Ag(I), Au(I) and Pd(II) NHC complexes were also prepared from these pro-ligands.

## 2.2 Results and discussion

### 2.2.1 Synthesis of *tetra*-imidazolium macrocycles

The *ortho*-phenylene linked *tetra*-imidazolium macrocycle **2.15·Br<sub>4</sub>** was prepared via a stepwise macrocyclization procedure. Initially, 1,2-*bis*-(imidazolylmethyl)benzene **2.7**<sup>42</sup> was alkylated with an excess of 1,2-dibromoethane (30 equivalents) to obtain the *bis*-bromoethylimidazolium bromide salt **2.11·Br<sub>2</sub>** in a moderate yield (Scheme 2.1). The <sup>1</sup>H-

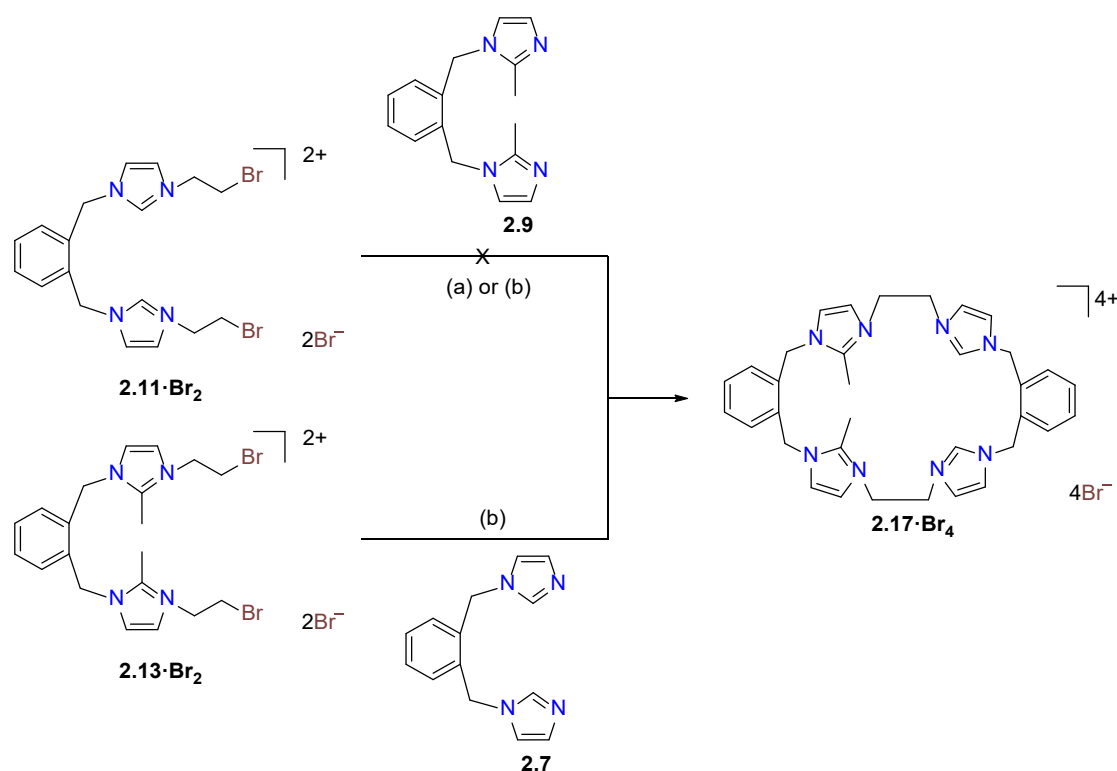
NMR spectrum of **2.11·Br<sub>2</sub>** shows a singlet signal for the imidazolium C2-H proton at 9.50 ppm, while the ethylene group protons resonate as two upfield shifted triplet signals at 4.00 and 4.68 ppm. The macrocycle **2.15·Br<sub>4</sub>**, was prepared by heating an equimolar mixture of **2.11·Br<sub>2</sub>** and **2.7** in a solvent system consisting of a 1:4 mixture of DMF and acetonitrile under high dilution conditions (Scheme 2.1) and was isolated in a moderate yield of 29.7%. Compound **2.15·Br<sub>4</sub>** gave a simple <sup>1</sup>H-NMR spectrum consistent with its high symmetry (point group *D*<sub>2h</sub>) with downfield shifted signals for the imidazolium protons which resonated at 9.45 (C2-H) and 7.98 and 7.88 ppm (C4-H/C5-H). The protons of the ethylene linker groups resonated as a singlet signal at 4.81 ppm. A similar method was adopted for the synthesis of the *meta*-phenylene linked macrocycle **2.16·Br<sub>4</sub>** from a mixture of **2.8** and **2.12·Br<sub>2</sub>** (Scheme 2.1).



Scheme 2.1 Synthesis of *tetra*-imidazolium macrocyclic compounds **2.15·Br<sub>4</sub>**, **2.16·Br<sub>4</sub>**, **2.17·Br<sub>4</sub>**, **2.18·Br<sub>4</sub>** and **2.19·Br<sub>4</sub>**. (a) DMF/CH<sub>3</sub>CN 1:4, 110 °C. (b) Bu<sub>4</sub>N<sup>+</sup>·Br<sup>-</sup>, DMF/CH<sub>3</sub>CN 1:4, 110 °C.

With the successful synthesis of the symmetrical macrocycles **2.15·Br<sub>4</sub>** and **2.16·Br<sub>4</sub>**, we were interested in further exploring the versatility of our stepwise synthetic methodology with the synthesis of asymmetric *tetra*-imidazolium salts. In initial studies, the reaction of either **2.9** with **2.11·Br<sub>2</sub>** or **2.7** with **2.13·Br<sub>2</sub>** (Scheme 2.1) under high dilution condition did not successfully produce the desired asymmetrical *tetra*-imidazolium salts. Additionally, attempts to use *tetra*-*n*-butylammonium bromide (Bu<sub>4</sub>N<sup>+</sup>·Br<sup>-</sup>) as a templation reagent in the reaction of **2.9** with **2.11·Br<sub>4</sub>** also did not give the desired product

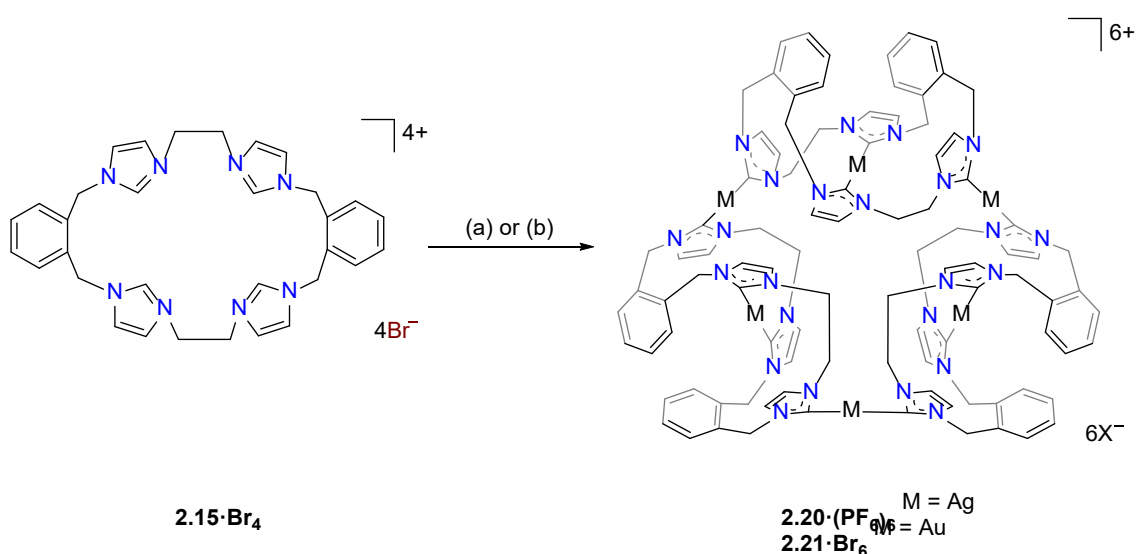
(Scheme 2.2). This lack of reactivity may be the result of the methyl groups blocking the C2 position of the imidazole ring, preventing the formation of hydrogen bonding between the *bis*-imidazole and the halide template reagent. By contrast, the reaction of compound **2.7** with **2.13·Br<sub>2</sub>** under high dilution conditions in presence of Bu<sub>4</sub>N·Br gave the desired product **2.17·Br<sub>4</sub>** in a low yield (Scheme 2.2). The <sup>1</sup>H-NMR spectrum of **2.17·Br<sub>4</sub>** showed the imidazolium C2-H proton as singlet signal at 9.76 ppm and the methyl group on the imidazolium C2 carbon resonated as a singlet signal at 2.64 ppm. In addition, consistent with the lower symmetry structure, the benzylic proton resonates as two singlet signals at 5.47 and 5.52 ppm. The asymmetrical pro-ligands **2.18·Br<sub>4</sub>** and **2.19·Br<sub>4</sub>** were prepared in a similar manner from the reaction of either **2.8** and **2.14·Br<sub>2</sub>** or **2.8** and **2.11·Br<sub>2</sub>** respectively in presence of Bu<sub>4</sub>N·Br. Again, the <sup>1</sup>H-NMR spectrum for **2.19·Br<sub>4</sub>** is consistent with the lower symmetry structure, with the C2-H protons resonating as two singlet signals at 8.99 and 9.13 ppm.



Scheme 2.2 Various attempts to synthesize asymmetrical *tetra*-imidazolium macrocycle **2.17·Br<sub>4</sub>**. Conditions (a) DMF/CH<sub>3</sub>CN1:4, 110 °C and (b) Bu<sub>4</sub>N·Br, DMF/CH<sub>3</sub>CN1:4, 110 °C.

## 2.2.2 Synthesis of Ag(I), Au(I) and Pd(II) complexes

The Ag(I) complex **2.20**·(PF<sub>6</sub>)<sub>6</sub> was prepared by the reaction of pro-ligand **2.15**·Br<sub>4</sub> with Ag<sub>2</sub>O in DMF with the exclusion of light (Scheme 2.3) and the product was isolated as a white crystalline solid with a yield of 21%. The <sup>1</sup>H-NMR spectrum of **2.20**·(PF<sub>6</sub>)<sub>6</sub> showed no imidazolium C2-H proton signal, indicating that the C2 carbon is deprotonated and coordinated to the metal centre as a carbene. The ortho-substituted phenyl-linker group protons resonate as two sets of doublets (5.68 and 6.94 ppm) and triplet (7.17 and 7.52 ppm) signals, consistent with a more complex magnetic environment for the Ag(I) complex when compared to the pro-ligand. The <sup>13</sup>C-NMR spectrum for **2.20**·(PF<sub>6</sub>)<sub>6</sub> revealed a downfield shifted signal at 186.31 ppm, for which <sup>107</sup>Ag-<sup>13</sup>C (d, <sup>1</sup>J = 182.32 Hz) and <sup>109</sup>Ag-<sup>13</sup>C (d, <sup>1</sup>J = 209.99 Hz) couplings were observed, which is also consistent with coordination of the C2 carbon to Ag(I) (Figure 2.3). The high-resolution mass spectrum for **2.20**·(PF<sub>6</sub>)<sub>6</sub> (Figure 2.4) produced two of peaks consistent with a hexanuclear structure with the general formula [Ag<sub>6</sub>L<sub>3</sub>]<sup>6+</sup> (where L is the macrocyclic *tetra*-carbene ligand). The base peak was observed at m/z = 372.0334 in addition to a peak at m/z = 889.0490, which corresponds to the formula [C<sub>96</sub>H<sub>96</sub>N<sub>24</sub>Ag<sub>6</sub>]<sup>6+</sup> (calculated = 372.0419) and the formula [C<sub>96</sub>H<sub>96</sub>N<sub>24</sub>Ag<sub>6</sub>]<sup>3+</sup> (calculated = 889.0485) respectively



Scheme 2.3 Synthesis of the Ag(I) and Au(I) complexes **2.20**·(PF<sub>6</sub>)<sub>6</sub> and **2.21**·Br<sub>6</sub> derived from pro-ligand **2.15**·Br<sub>4</sub>. (a) Ag<sub>2</sub>O, DMF, 50 °C, 3 d. (b) (THT)AuCl, NaOAc, DMF, 110 °C, 1 h.

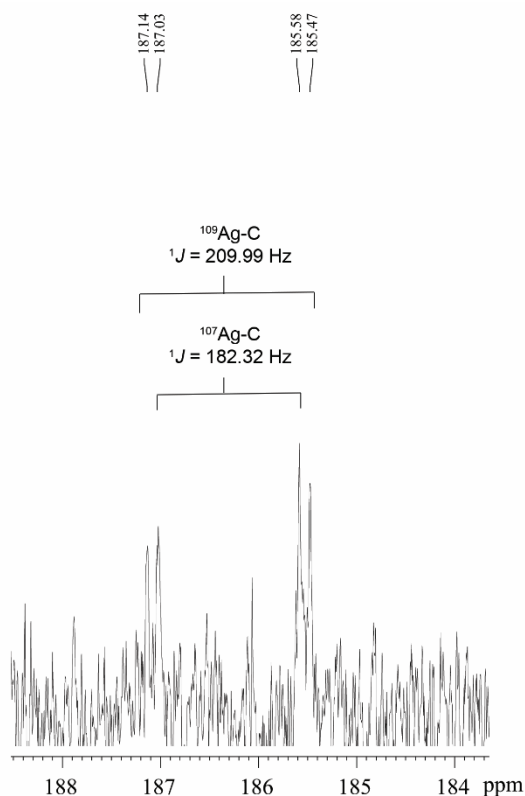


Figure 2.3  $^{107}\text{Ag}-^{13}\text{C}$  (d,  $^1J = 182.32 \text{ Hz}$ ) and  $^{109}\text{Ag}-^{13}\text{C}$  (d,  $^1J = 209.99 \text{ Hz}$ ) couplings in  $^{13}\text{C}$ -NMR spectrum of hexanucler Ag(I) complex **2.20**·(**PF**<sub>6</sub>)<sub>6</sub> suggesting the coordination of the C2 carbon to Ag(I).

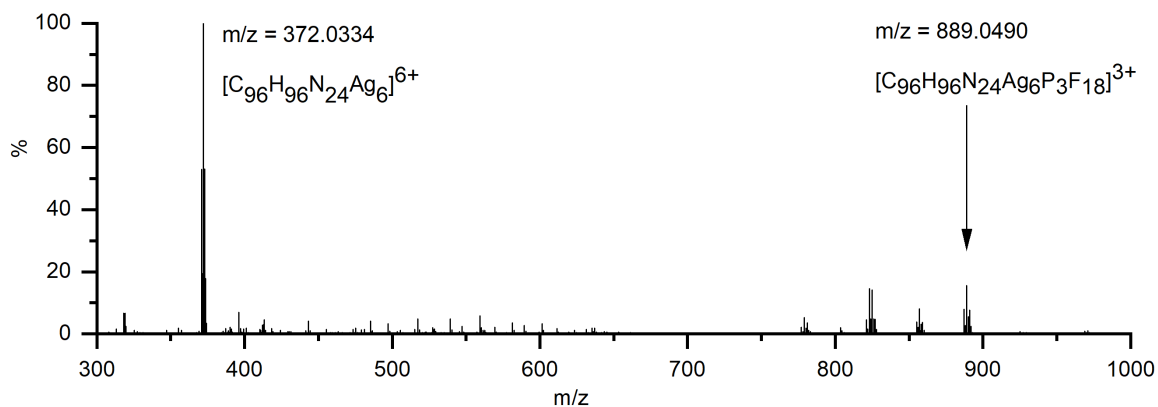
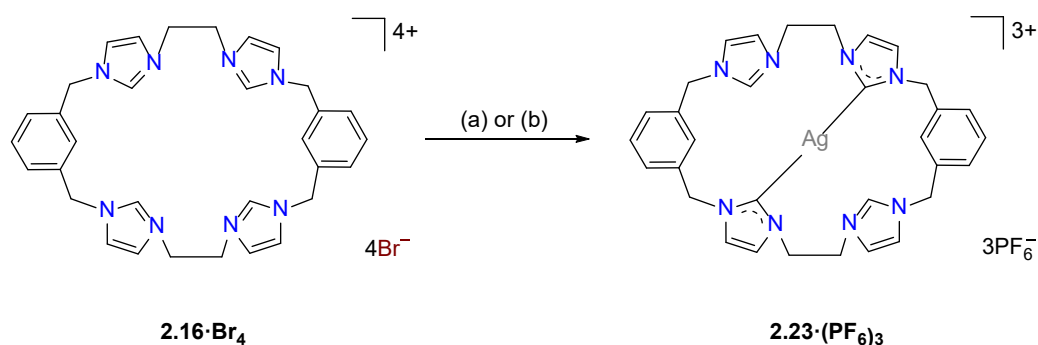


Figure 2.4 High-resolution mass spectrum for hexanucler Ag(I) complex **2.20**·(**PF**<sub>6</sub>)<sub>6</sub>.

Using a similar approach, the Ag(I) complex **2.23**·(**PF**<sub>6</sub>)<sub>3</sub> was prepared from the pro-ligand **2.16**·**Br**<sub>4</sub>, however for this compound, the  $^1\text{H}$ -NMR spectrum showed a signal at 8.37 ppm, consistent with the C2-H proton being present in the complex. However, the  $^{13}\text{C}$ -NMR spectrum of **2.23**·(**PF**<sub>6</sub>)<sub>3</sub> showed a downfield shifted signal at 180.4 ppm that displays  $^{107}\text{Ag}-^{13}\text{C}$  (d,  $^1J = 183.58 \text{ Hz}$ ) and  $^{109}\text{Ag}-^{13}\text{C}$  (d,  $^1J = 211.24 \text{ Hz}$ ) couplings,

indicating coordination of the imidazole C2 carbon to Ag(I) (Figure 2.5). These NMR results are consistent with a mononuclear complex, where two of the imidazole units are coordinated to the metal, while the other two remain uncoordinated imidazolium units (Scheme 2.4). To further study this result, a different synthetic method was investigated where the pro-ligand **2.16**·(**PF<sub>6</sub>**)<sub>4</sub> was reacted with AgNO<sub>3</sub> in present of NH<sub>4</sub>OH.<sup>43</sup> However, the same mononuclear Ag(I) complex **2.23**·(**PF<sub>6</sub>**)<sub>3</sub> was obtained (Scheme 2.4) which is in contrast to the previous reported polynuclear Ag(I) complexes in the literature.<sup>43</sup> As discussed in Chapter 1, the coordination modes of the macrocyclic NHC-Ag(I) complexes can be a result of the variable chain length of the alkyl linker on the macrocycle.<sup>44</sup> In this case, the *meta*- substitution of both phenyl rings increased the ring size of the *tetra*-imidazolium pro-ligand by two atoms. The formation of the mononuclear Ag(I) complex **2.23**·(**PF<sub>6</sub>**)<sub>3</sub> may be, therefore, a result of the changing of ring size.<sup>44</sup>



Scheme 2.4 Synthesis of Ag(I) complex **2.23**·(**PF<sub>6</sub>**)<sub>3</sub> from the pro-ligand **2.16**·**Br**<sub>4</sub>. (a) Ag<sub>2</sub>O, DMF, 70 °C, 3 d. (b) AgNO<sub>3</sub>, NH<sub>4</sub>OH, CH<sub>3</sub>CN, RT, overnight.

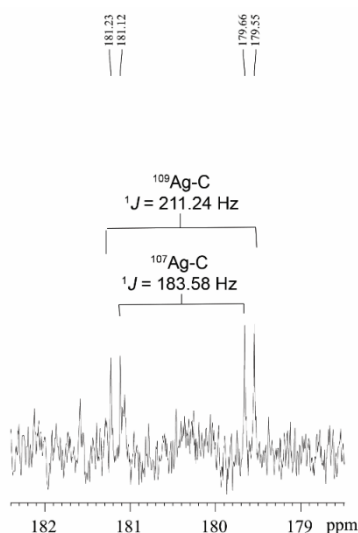
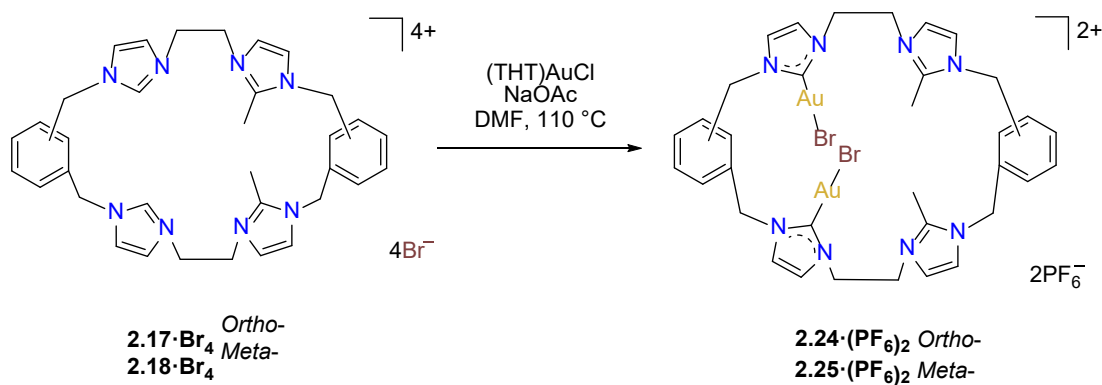


Figure 2.5  $^{107}\text{Ag}-^{13}\text{C}$  (d,  $^1J = 183.58 \text{ Hz}$ ) and  $^{109}\text{Ag}-^{13}\text{C}$  (d,  $^1J = 211.24 \text{ Hz}$ ) couplings in  $^{13}\text{C}$ -NMR spectrum of Ag(I) complex **2.23**·( $\text{PF}_6$ )<sub>3</sub> suggesting the coordination of the C2 carbon to Ag(I).

The hexanuclear Au(I) complex **2.21**· $\text{Br}_6$  was prepared by the reaction of **2.15**· $\text{Br}_4$  with (THT)AuCl in the presence of the mild base sodium acetate (Scheme 2.3) and the complex was obtained as an off-white solid in 54.2% yield. The same approach was used in an attempt to prepare the Au(I) complex of pro-ligand **2.16**· $\text{Br}_4$ , however, no complex could be isolated from the reaction mixture. In the next set of reactions, the pro-ligand **2.17**· $\text{Br}_4$  (with both normal and C2-blocked imidazolium groups) was reacted with (THT)AuCl in the presence of sodium acetate. It was anticipated that this ligand might produce a complex displaying both ‘normal’ and ‘abnormal’ NHC coordination modes, however, the dinuclear Au(I) complex **2.24**·( $\text{PF}_6$ )<sub>2</sub> was obtained, which displayed only the ‘normal’ NHC coordination mode (Scheme 2.5). Using the same method, a dinuclear Au(I) complex **2.24**·( $\text{PF}_6$ )<sub>2</sub> derived from **2.18**·( $\text{PF}_6$ )<sub>4</sub> was also prepared. The high-resolution mass spectrum for **2.24**·( $\text{PF}_6$ )<sub>2</sub> (Figure 2.5) showed a peak at  $m/z = 556.0369$ , which corresponds to the dinuclear Au(I) complex  $[\text{C}_{34}\text{H}_{38}\text{N}_8\text{Au}_2\text{Br}_2]^+$  (calculated = 556.0433) (Figure 2.5). Consultation of the literature suggested that the formation of ‘normal’ NHC complexes **2.24**·( $\text{PF}_6$ )<sub>2</sub> and **2.25**·( $\text{PF}_6$ )<sub>2</sub> may be a result of a lower  $\text{p}K_a$  value (ca. 24.90) for the C2-H proton on the imidazolium ring compared to the C4-H on the imidazolium ring (ca. 32.97).<sup>45-46</sup> As a result of the lower  $\text{p}K_a$  value of the C2-H, the deprotonation and

coordination to the metal centre are more favourable on C2 position of the imidazolium units than the C4 position of the C2 methyl blocked imidazolium units. Therefore, these complexes only displayed the ‘normal’ NHC coordination mode with those C2 methyl blocked imidazolium units uncoordinated.



Scheme 2.5 Synthesis of dinuclear Au(I) complex **2.24·(PF<sub>6</sub>)<sub>2</sub>** and **2.25·(PF<sub>6</sub>)<sub>2</sub>** derived from **2.17·Br<sub>4</sub>** and **2.18·Br<sub>4</sub>**.

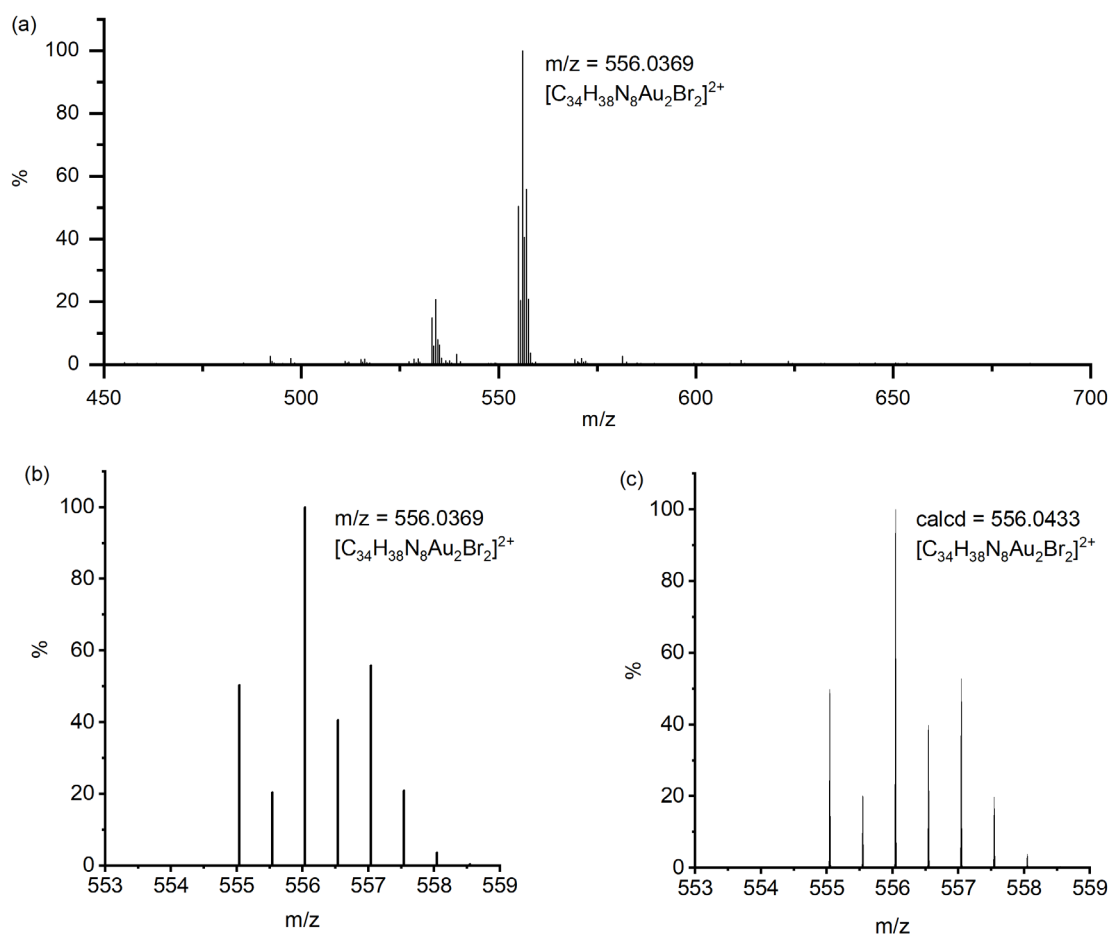


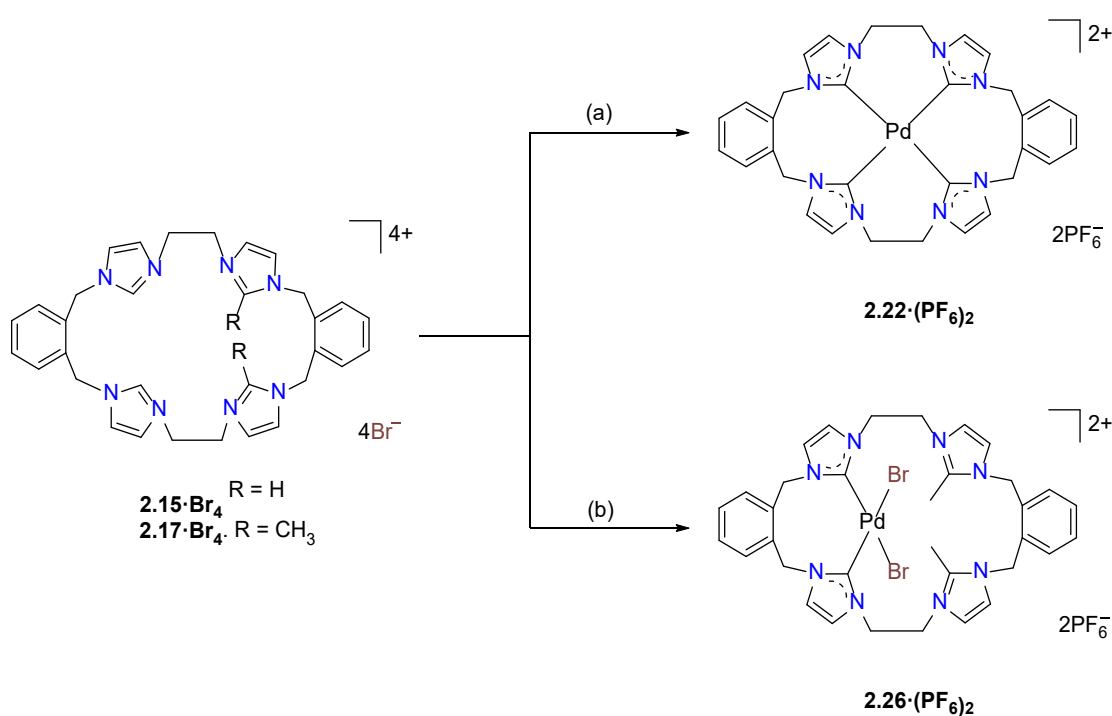
Figure 2.6 (a) High-resolution mass spectrum Au(I) complex **2.24·(PF<sub>6</sub>)<sub>2</sub>** and (b) expanded spectrum for the base peak for **2.24·(PF<sub>6</sub>)<sub>2</sub>** and (c) theoretical mass spectrum for  $[\text{C}_{34}\text{H}_{38}\text{N}_8\text{Au}_2\text{Br}_2]^{2+}$ .



Due to their potential to act as tetradentate ligands with metals that adopt square-planar coordination geometries, the Pd(II) complex of pro-ligand **2.15·Br<sub>4</sub>** was prepared. A range of approaches have been previously employed for the preparation of Pd(II)-NHC complexes, including *in situ* deprotonation and metallation<sup>32, 42</sup> and transmetallation via an intermediate Ag(I) complex.<sup>17, 47</sup> In this work the former *in situ* deprotonation and metallation approach was initially investigated by reacting **2.15·(PF<sub>6</sub>)<sub>4</sub>** with Pd(OAc)<sub>2</sub> in DMSO, however the desired Pd(II) complex could not be isolated. As described previously, a hexanuclear Ag(I) complex could be prepared from the pro-ligand **2.15·(PF<sub>6</sub>)<sub>4</sub>** and in a second attempt to synthesise the Pd(II) complex, pro-ligand **2.15·Br<sub>4</sub>** was first reacted with Ag<sub>2</sub>O to form the Ag(I) complex *in situ* followed by addition of K<sub>2</sub>PdCl<sub>4</sub> (Scheme 2.6). <sup>1</sup>H-NMR analysis of Pd(II) complex **2.22·(PF<sub>6</sub>)<sub>2</sub>** showed a relatively simple spectrum with the C4/5 protons of the NHC groups resonating as two sets of doublets at 7.48 and 7.83 ppm. The benzylic protons resonate as two sets of doublet signals at 5.20 and 6.44 ppm as an AX pattern, which is consistent with a rigid molecular structure in solution. Furthermore, the <sup>13</sup>C-NMR spectrum showed a downfield shifted signal at 167.41 ppm, which corresponds to the NHC carbene carbon coordinated to the Pd(II) metal centre.

The Ag(I) transmetallation approach did not successfully produce a Pd(II) complex of pro-ligand **2.17·Br<sub>4</sub>**. In this attempt, Ag<sub>2</sub>CO<sub>3</sub> was used instead of Ag<sub>2</sub>O to avoid the undesirable oxidative cleavage of the C2-blocking methyl group by Ag<sub>2</sub>O followed by subsequent formation of the nNHC-Ag(I) complex which has been observed previously.<sup>48</sup> In a second synthetic attempt, the pro-ligand **2.17·Br<sub>4</sub>** was reacted with K<sub>2</sub>PdCl<sub>4</sub> in the presence of NaOAc in DMSO (Scheme 2.6). The <sup>1</sup>H-NMR spectrum of the crude product showed no peak for the C2-H proton for the ‘unblocked’ imidazole units indicating that these groups are coordinated to the metal centre. The C4/5 protons of the C2 ‘blocked’ imidazolium group were observed at 7.34 and 7.66 ppm suggesting that the C2 blocked

imidazolium unit did not coordinate to the metal. Furthermore, the benzylic proton signals at 5.24 and 5.26 ppm and the ethylene linker signal at 4.61 – 4.70 ppm also indicated an asymmetrical structure for the metal complex. The crystal structure for **2.26**·(**PF**<sub>6</sub>)<sub>2</sub> in Figure 2.9 showed that the Pd(II) complex **2.26**·(**PF**<sub>6</sub>)<sub>2</sub> was successfully synthesized. Unfortunately, various attempts to purify this compound using recrystallization in different solvents or vapour diffusion of diethyl ether into a solution of crude **2.26**·(**PF**<sub>6</sub>)<sub>2</sub> in acetonitrile was unsuccessful and it was not possible to separate this complex as pure product.



Scheme 2.6 Synthesis of Pd(II) complex **2.22**·(**PF**<sub>6</sub>)<sub>2</sub> and **2.26**·(**PF**<sub>6</sub>)<sub>2</sub>. (a) **2.15**·Br<sub>4</sub>, Ag<sub>2</sub>O, K<sub>2</sub>PdCl<sub>4</sub>, DMF, 85 °C. (b) **2.17**·Br<sub>4</sub>, K<sub>2</sub>PdCl<sub>4</sub>, NaOAc, DMSO, 85°C, overnight.

### 2.2.3 Structural studies

Compounds **2.11**·Br<sub>2</sub>, **2.15**·Br<sub>4</sub>, **2.16**·Br<sub>3</sub>PF<sub>6</sub>, **2.17**·Br<sub>4</sub>, **2.21**·Br<sub>2</sub>(PF<sub>6</sub>)<sub>4</sub> and **2.26**·(**PF**<sub>6</sub>)<sub>2</sub> were characterised by X-ray crystallography. A representation of the precursor compound **2.11**·Br<sub>2</sub> is shown in Figure 2.6 while representations of the *tetra*-imidazolium macrocycles **2.15**·Br<sub>4</sub>, **2.16**·Br<sub>3</sub>PF<sub>6</sub> and **2.17**·Br<sub>4</sub> are shown in Figure 2.7. In all cases, these

imidazolium salts display hydrogen bonding interactions between various hydrogens on the cationic imidazolium units and the bromide counter anions. For example, the shortest C2 $\cdots$ Br distances for **2.11**·Br<sub>2</sub>, **2.15**·Br<sub>4</sub>, **2.16**·Br<sub>3</sub>PF<sub>6</sub> and **2.17**·Br<sub>4</sub> are 3.4496(3), 3.42219(5) Å, 3.4822(4) Å, and 3.6552 (5) Å respectively, which fall within a typical range of C-H $\cdots$ Br distance caused by hydrogen bonding.<sup>49</sup>

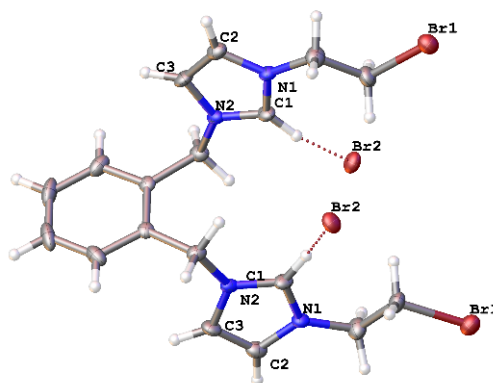


Figure 2.7 Representation of the X-ray crystal structure of **2.11**·Br<sub>2</sub>. Atomic displacement ellipsoids are shown at the 50% probability level.

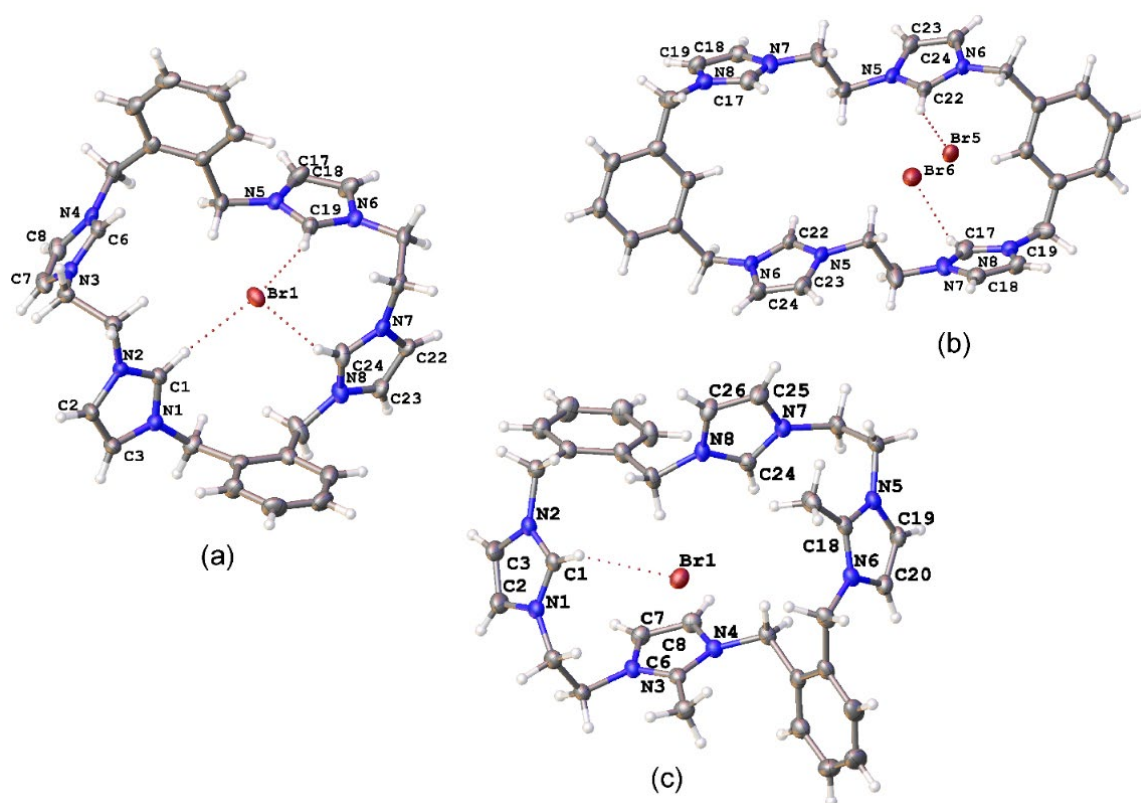


Figure 2.8 Representations of the X-ray crystal structures of (a) **2.15·Br<sub>4</sub>** and (b) **2.16·Br<sub>3</sub>PF<sub>6</sub>** and (c) **2.17·Br<sub>4</sub>**. Only counter ions involved in hydrogen bonding are included for clarity. Atomic displacement ellipsoids are shown at the 50% probability level.

Two representations of the X-ray crystal structure for the Au(I) complex **2.21·Br<sub>2</sub>(PF<sub>6</sub>)<sub>4</sub>** are shown in Figure 2.8. This remarkable structure reveals that the Au(I) complex adopts a cyclic hexanuclear supramolecular assembly with the overall formula [Au<sub>6</sub>L<sub>3</sub>]<sup>6+</sup>. In the cation, each of the Au(I) centres adopt linear two-coordinate geometries, and they can be divided into two distinct groups of three atoms each. For the first group, each Au(I) atom (Au1, Au4 and Au5) is bound to two NHC units on opposite sides of each of the three ligand molecules. While each of the Au(I) atoms in the second group (Au2, Au3 and Au6) are coordinated to NHC donors from adjacent ligand molecules, resulting in the formation of a metallo-macrocyclic. In each case, the ligand molecules are bowl shaped to accommodate the two Au(I) coordination modes. Interestingly, the metallo-macrocyclic is arrayed around an encapsulated central bromide counterion. This bromide ion displays interactions with Au(I) atoms Au1, Au4 and Au5 with the distances being 3.19488(5),

3.24731(5) and 3.23064(4) Å respectively. Previously, a hexanuclear Ag(I) complex was reported for a *tetra*-carbene ligand linked by aliphatic butyl chains.<sup>32</sup>

A representation of the X-ray crystal structure for the Pd(II) **2.26**·(PF<sub>6</sub>)<sub>2</sub> is shown in Figure 2.9 The molecular structure shows that the ligand is coordinated to the metal centre through the ‘normal’ NHC groups, with the C2 ‘blocked’ groups present as cationic imidazolium units. The Pd(II) centre is four-coordinate, with the two-remaining sites being occupied by bromide ions.

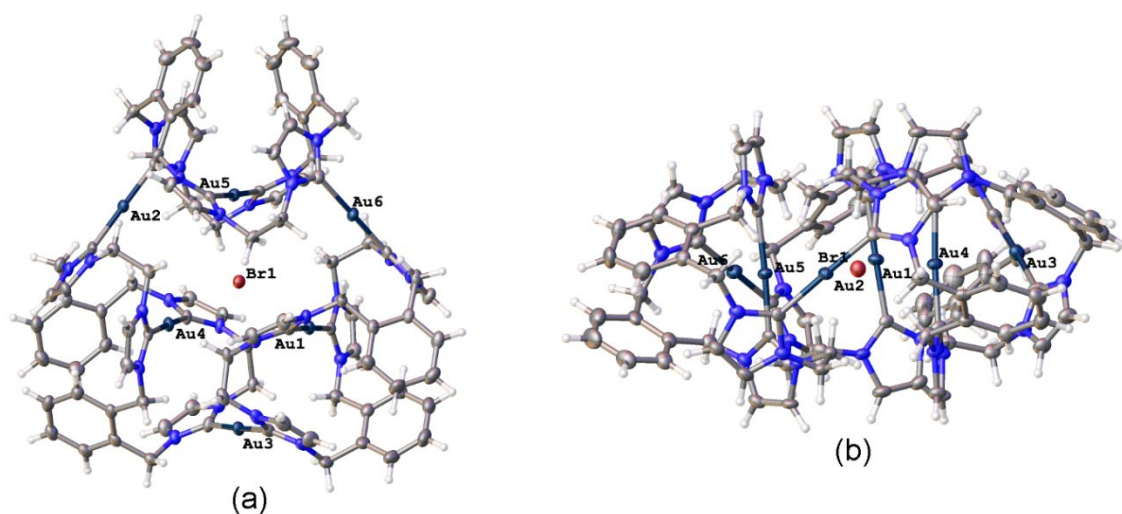


Figure 2.9 Two representations of the X-ray crystal structures of **2.21**·Br<sub>2</sub>(PF<sub>6</sub>)<sub>4</sub> (a) top view and (b) edge view. Hydrogen atoms are excluded and only the encapsulated bromide counterion included for clarity. Atomic displacement ellipsoids are shown at the 50% probability level.

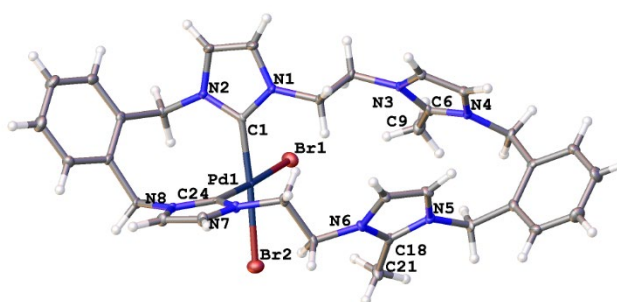


Figure 2.10 Representations of the X-ray crystal structures of the Pd(II) complex **2.26**·(PF<sub>6</sub>)<sub>2</sub>. Atomic displacement ellipsoids are shown at the 50% probability level.

#### 2.2.4 Anion binding studies

Due to the tetracationic charge of the imidazolium linked macrocycles prepared in this work, the propensity of **2.15**·(PF<sub>6</sub>)<sub>4</sub> and **2.16**·(PF<sub>6</sub>)<sub>4</sub> to bind to the halide anions F<sup>-</sup>, Cl<sup>-</sup>, Br<sup>-</sup> and I<sup>-</sup> (as their *tetra*-*n*-butylammonium halide salts) was evaluated using <sup>1</sup>H-NMR titration experiments. In initial studies, it was found that the addition of Bu<sub>4</sub>N·F to **2.15**·(PF<sub>6</sub>)<sub>4</sub> in d<sub>6</sub>-DMSO caused an immediate colour change to pale yellow. <sup>1</sup>H-NMR analysis of the reaction showed that the colour change occurred concurrently with a significant broadening and downfield shift of the imidazolium C2-H signal. In addition, the appearance of new unidentified <sup>1</sup>H NMR signals was observed which were consistent with decomposition of the macrocyclic receptor. As such this anion was not studied further.

Addition of increasing equivalents of Bu<sub>4</sub>N·Cl (0.25 - 14.0 eq.) to a solution of **2.15**·(PF<sub>6</sub>)<sub>4</sub> in d<sub>6</sub>-DMSO caused a significant downfield shift of the resonance corresponding to the imidazolium C2-H signal from 8.96 ppm to 9.64 ppm. In addition, the benzylic proton signal was also shifted downfield from 5.34 ppm to 5.76 ppm. Unfortunately, this study was hampered by the gradual precipitation of the imidazolium salt at higher Cl<sup>-</sup> concentrations. In a similar manner, the addition of increasing equivalents of Bu<sub>4</sub>N·Br and Bu<sub>4</sub>N·I to **2.16**·(PF<sub>6</sub>)<sub>4</sub> caused downfield shifts in the imidazolium C2-H signal, although to a lesser extent than that seen for Bu<sub>4</sub>N·Cl, however for these anions no precipitation of the macrocycle was seen. Figure 2.10 shows the <sup>1</sup>H-NMR titration between **2.15**·(PF<sub>6</sub>)<sub>4</sub> and Bu<sub>4</sub>N·Br, while Figure 2.11(a) shows the change in the imidazolium C2-H chemical shift for **2.15**·(PF<sub>6</sub>)<sub>4</sub> in response to increasing equivalents of the added halide anions (black solid lines). Similar results were seen for the macrocyclic receptor **2.16**·(PF<sub>6</sub>)<sub>4</sub> and the plot of experimental titration data is shown in Figure 2.11(b). Jobs plot analysis was then used to evaluate the stoichiometry of the interactions between the macrocyclic receptors and the anions Cl<sup>-</sup>, Br<sup>-</sup> and I<sup>-</sup>. The results of these studies showed

that maxima occurred at close to  $\chi = 0.5$  indicating 1:1 stoichiometry for both receptor **2.15**<sup>4+</sup> and **2.16**<sup>4+</sup> with these anions.

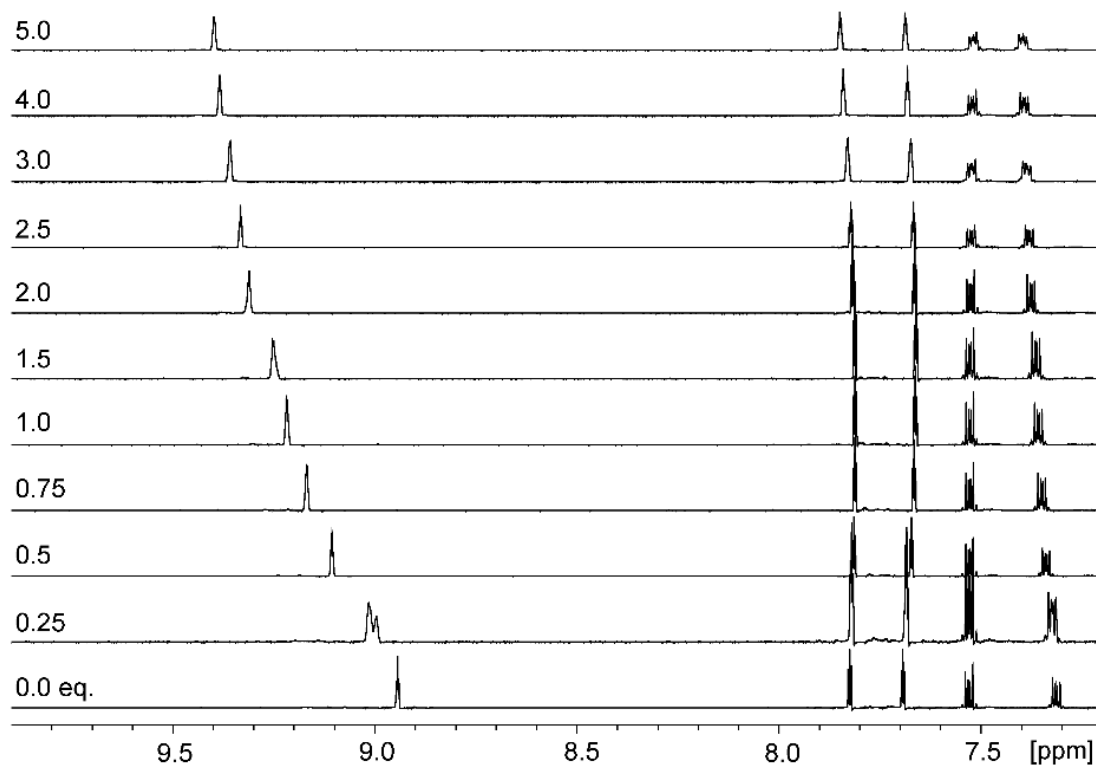


Figure 2.11 <sup>1</sup>H-NMR titration of **2.15**·(PF<sub>6</sub>)<sub>4</sub> in d<sub>6</sub>-DMSO in the presence of increasing concentrations of Bu<sub>4</sub>N·Br.

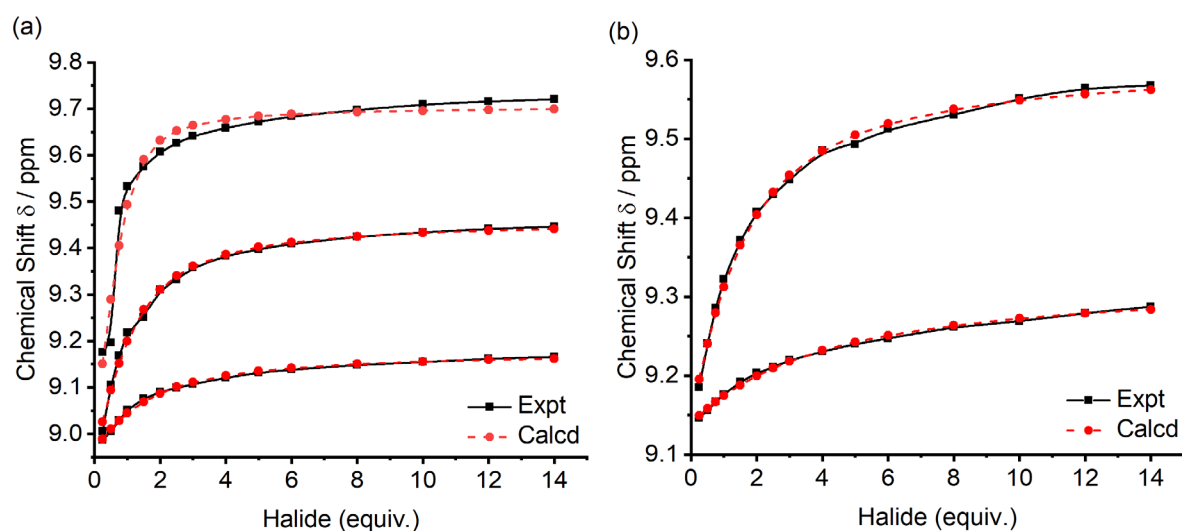


Figure 2.12 Experimental titration data (black solid line, squares) and fitted binding isotherms (red dashed line, circles) for the addition of either Bu<sub>4</sub>N·Cl, Bu<sub>4</sub>N·Br or Bu<sub>4</sub>N·I to a solution of (a) **2.15**·(PF<sub>6</sub>)<sub>4</sub> and (b) **2.16**·(PF<sub>6</sub>)<sub>4</sub> in d<sub>6</sub>-DMSO.

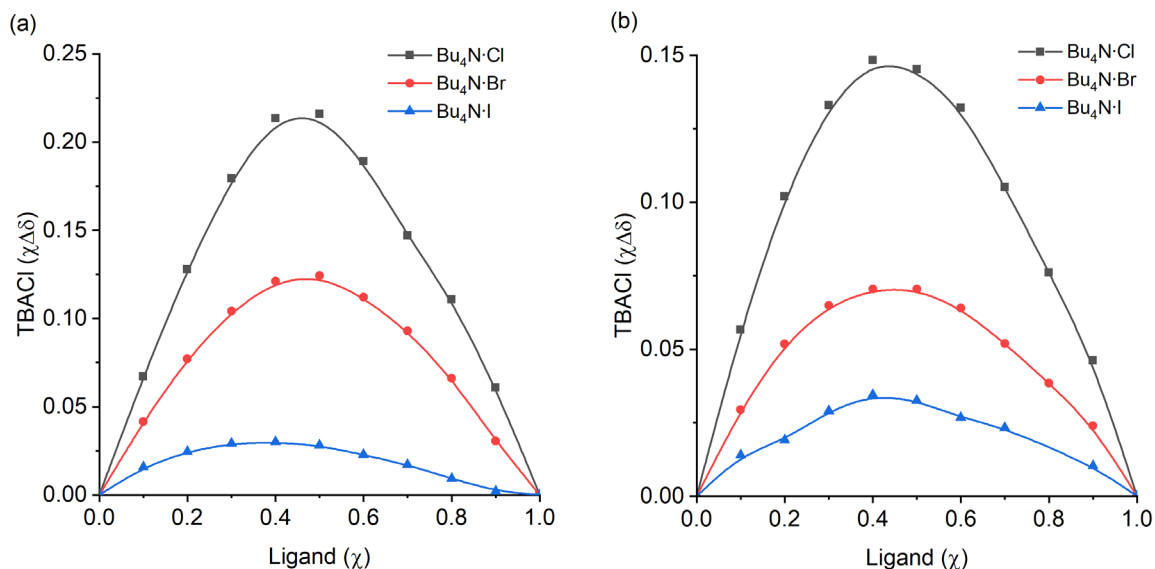


Figure 2.13 Jobs plot based on the  $^1\text{H}$ -NMR titration of (a) **2.15**·(**PF**<sub>6</sub>)<sub>4</sub> with Bu<sub>4</sub>N·Cl, Bu<sub>4</sub>N·Br and Bu<sub>4</sub>N·I and (b) **2.16**·(**PF**<sub>6</sub>)<sub>4</sub> with Bu<sub>4</sub>N·Cl, Bu<sub>4</sub>N·Br and Bu<sub>4</sub>N·I.

Binding (association) constants  $K_a$  ( $\text{M}^{-1}$ ) for the *tetra*-imidazolium macrocycles **2.15**·(**PF**<sub>6</sub>)<sub>4</sub> and **2.16**·(**PF**<sub>6</sub>)<sub>4</sub> were determined by analysis of the  $^1\text{H}$ -NMR titration data using the computer program HypNMR 2018.<sup>50-51</sup> The fitted binding isotherms are shown in Figure 2.11 (red dashed lines) and the calculated binding constants are given in Table 2.1. The values obtained for the compounds studied in this work are similar in magnitude to those reported previously for related compounds. For example, Beer and co-workers reported association constants of 420(23), 241(3) and 120(1)  $\text{M}^{-1}$  for a *tetra*-imidazolium macrocycle in  $d_6$ -DMSO solution with the anions Cl<sup>−</sup>, Br<sup>−</sup> and I<sup>−</sup> respectively.<sup>11</sup>

Table 2.1 Association constants of the *tetra*-imidazolium macrocycles **2.15**·(**PF**<sub>6</sub>)<sub>4</sub> and **2.16**·(**PF**<sub>6</sub>)<sub>4</sub> with Cl<sup>−</sup>, Br<sup>−</sup> and I<sup>−</sup>.

	<b>2.15</b> ·( <b>PF</b> <sub>6</sub> ) <sub>4</sub>	<b>2.16</b> ·( <b>PF</b> <sub>6</sub> ) <sub>4</sub>
Cl <sup>−</sup>	501(12) <sup>a</sup>	ppt <sup>b</sup>
Br <sup>−</sup>	126(15)	63(6)
I <sup>−</sup>	63(6)	20(2)

<sup>a</sup>Precipitate forms after 4 equivalents of Bu<sub>4</sub>N·Cl added; <sup>b</sup>precipitate forms rapidly and measurement of the association constant not possible.



## 2.3 Conclusion

In conclusion, in this chapter, a novel stepwise synthetic strategy was reported that allows for the synthesis of both symmetrical and asymmetrical *tetra*-imidazolium linked macrocyclic compounds. The synthetic strategy is modular as initially a range of *bis*-bromoethylimidazolium bromide precursors were synthesised, which when combined with chosen *bis*(imidazolylmethyl)benzene molecules produced a range of *tetra*-imidazolium linked macrocycles. These *tetra*-imidazolium salts are of significant interest as they bind anions in solution and offer the potential for the development of sensors for biologically relevant anions. Using  $^1\text{H}$ -NMR titration studies, the association constants between **2.15**·(PF<sub>6</sub>)<sub>4</sub> and **2.16**·(PF<sub>6</sub>)<sub>4</sub> and the halide anions Cl<sup>-</sup>, Br<sup>-</sup>, and I<sup>-</sup> were determined and these ranged between 501 – 20 M<sup>-1</sup>. Imidazolium salts are precursors for NHC ligands and the Ag(I), Au(I) and Pd(II) NHC complexes derived from these *tetra*-imidazolium linked macrocycles were prepared. The Ag(I) complexes **2.20**<sup>6+</sup> and the analogous Au(I) complex **2.21**<sup>6+</sup> adopted intriguing hexanuclear structures with the general formula [M<sub>6</sub>L<sub>3</sub>]<sup>6+</sup>.

## 2.4 Experimental

### 2.4.1 $^1\text{H}$ -NMR titration studies

A solution of the title compound (10 mg) in d<sub>6</sub>-DMSO (600 μL) and a 1.5 M solution of Bu<sub>4</sub>N·X (X=Cl, Br and I) in d<sub>6</sub>-DMSO were prepared respectively. To the solution of the title compound, increasing equivalents (0.25 – 14.0 eq.) of 1.5 M Bu<sub>4</sub>N·X solution was added and the resultant solution was thoroughly mixed. The  $^1\text{H}$ -NMR spectrum was recorded ~2 minutes after each addition at 302 K.

### 2.4.2 Jobs plot analysis

A solution of the title compound (10 mg/mL) in d<sub>6</sub>-DMSO and a 0.050 M solution of Bu<sub>4</sub>N·X (X=Cl, Br and I) in d<sub>6</sub>-DMSO were prepared respectively. A varied fraction of

title compound solution and Bu<sub>4</sub>N·X solution was added and diluted with d<sub>6</sub>-DMSO to 600  $\mu$ L to maintain the total concentration of substance at 10 mM. The resultant solution was thoroughly mixed and <sup>1</sup>H-NMR spectrum was recorded at 302 K.

### 2.4.3 Synthesis

**2.7.** This compound was prepared according to a literature procedure.<sup>42</sup> A solution of  $\alpha,\alpha'$ -dibromo-*o*-xylene (3.00 g, 11.30 mmol) and imidazole (12.38 g, 181.8 mmol) in methanol (100 mL) was stirred at reflux for 27 h followed by evaporation *in vacuo* to obtain a yellow oil. To the resultant residue, a solution of 1.4 M K<sub>2</sub>CO<sub>3</sub> in aqueous (200 mL) was added and the mixture was stirred overnight. The precipitate was collected and recrystallised in methanol (15 mL) yielding a white solid. Yield: 1.56 g, 57.6%. <sup>1</sup>H-NMR (500.02 MHz, d<sub>6</sub>-DMSO):  $\delta$  = 7.71 (s, 2H, *H*<sub>imi</sub>), 7.29 – 7.32 (m, 2H, *ArH*), 7.09 (t, <sup>3</sup>*J*<sub>H-H</sub> = 1.0 Hz 2H, *H*<sub>imi</sub>), 6.96 – 6.98 (m, 2H, *ArH*), 6.95 (t, <sup>3</sup>*J*<sub>H-H</sub> = 1.0 Hz 2H, *H*<sub>imi</sub>), 5.33 (s, 4H, *CH*<sub>2</sub>). <sup>13</sup>C-NMR (125.74 MHz, d<sub>6</sub>-DMSO):  $\delta$  = 138.18 (*C*<sub>q</sub>), 135.73 (*C*<sub>imi</sub>), 129.29 (*C*<sub>imi</sub>), 128.72 (*C*<sub>Ar</sub>), 128.45 (*C*<sub>Ar</sub>), 120.23 (*C*<sub>imi</sub>), 46.92 (*CH*<sub>2</sub>). HRESI-MS<sup>+</sup>: [C<sub>14</sub>H<sub>15</sub>N<sub>4</sub>]<sup>+</sup> *m/z* = 239.1285, calcd = 239.1291.

**2.8.** This compound was prepared in the same method as **2.7** according to a literature procedure<sup>42</sup> by using  $\alpha,\alpha'$ -dibromo-*m*-xylene (4.00 g, 15.15 mmol) and imidazole (16.50 g, 242.26 mmol) in methanol (120 mL). Yield: 2.60 g, 72.0%. <sup>1</sup>H-NMR (500.02 MHz, d<sub>6</sub>-DMSO):  $\delta$  = 7.74 (s, 2H, *H*<sub>imi</sub>), 7.34 (t, <sup>3</sup>*J*<sub>H-H</sub> = 7.5 Hz, 1H, *ArH*), 7.21 (s, 1H, *ArH*), 7.15 – 7.16 (m, 4H, *ArH*, *H*<sub>imi</sub>), 6.91 (s, 2H, *H*<sub>imi</sub>), 5.18 (s, 4H, *CH*<sub>2</sub>). <sup>13</sup>C-NMR (125.74 MHz, d<sub>6</sub>-DMSO):  $\delta$  = 138.75 (*C*<sub>q</sub>), 137.87 (*C*<sub>imi</sub>), 129.58 (*C*<sub>Ar</sub>), 129.21 (*C*<sub>imi</sub>), 127.29 (*C*<sub>Ar</sub>), 127.09 (*C*<sub>Ar</sub>), 199.99 (*C*<sub>imi</sub>), 49.75 (*CH*<sub>2</sub>). HRESI-MS<sup>+</sup>: [C<sub>14</sub>H<sub>15</sub>N<sub>4</sub>]<sup>+</sup> *m/z* = 239.1240, calcd = 238.12, [C<sub>14</sub>H<sub>15</sub>N<sub>4</sub>]<sup>+</sup> *m/z* = 239.1240, calcd = 239.1291.

**2.9.** This compound was prepared in the same method as **2.7** according to a literature procedure<sup>42</sup> by using  $\alpha,\alpha'$ -dibromo-*o*-xylene (2.0 g, 8.44 mmol) and 2-methylimidazole (11.09 g, 135.04 mmol) in methanol (100 mL). A solution of 0.5 M K<sub>2</sub>CO<sub>3</sub> in aqueous (100 mL) was used in this workup. Yield: 1.36 g, 67.3%. <sup>1</sup>H-NMR (500.02 MHz, d<sub>6</sub>-DMSO):  $\delta$  = 7.25 (dd, <sup>3</sup>J<sub>H-H</sub> = 5.7 Hz, <sup>4</sup>J<sub>H-H</sub> = 3.4 Hz, 2H, ArH), 7.02 (d, <sup>3</sup>J<sub>H-H</sub> = 1.2 Hz, 2H, H<sub>imi</sub>), 6.84 (d, <sup>3</sup>J<sub>H-H</sub> = 1.2 Hz, 2H, H<sub>imi</sub>), 6.54 (dd, <sup>3</sup>J<sub>H-H</sub> = 5.6 Hz, <sup>4</sup>J<sub>H-H</sub> = 3.5 Hz, 2H, ArH), 5.24 (s, 4H, CH<sub>2</sub>), 2.19 (s, 6H, CH<sub>3</sub>). <sup>13</sup>C-NMR (125.74 MHz, d<sub>6</sub>-DMSO):  $\delta$  = 144.83 (C<sub>q</sub>), 135.22 (C<sub>q</sub>), 128.27 (C<sub>Ar</sub>), 127.26 (C<sub>Ar</sub>), 126.44 (C<sub>imi</sub>), 120.86 (C<sub>imi</sub>), 46.31 (CH<sub>2</sub>), 13.04 (CH<sub>3</sub>). HRESI-MS<sup>+</sup>: [C<sub>14</sub>H<sub>15</sub>N<sub>4</sub>]<sup>+</sup> m/z = 267.1593, calcd = 267.1604.

**2.10.** Sodium hydride (1.14 g, 47.35 mmol) was added to a solution of 2-methylimidazole (3.11 g, 37.88 mmol) in DMF (50 mL) cooled to 0 °C and the resultant mixture was stirred at RT for 1 h and  $\alpha,\alpha'$ -dibromo-*m*-xylene (5.00 g, 18.94 mmol) was then added. Stirring was continued at RT for 12 h and the mixture was then diluted with water (100 mL). The mixture was then extracted with CH<sub>2</sub>Cl<sub>2</sub> (5 × 10 mL) and the combined organic extracts were washed with water (5 × 50 mL) and then brine (20 mL). The organic layer was dried with MgSO<sub>4</sub> and the solvent was evaporated *in vacuo* yielding a yellow oil. Yield: 2.18 g, 43.2%. <sup>1</sup>H-NMR (500.02 MHz, d<sub>6</sub>-DMSO):  $\delta$  = 7.33 (t, <sup>3</sup>J<sub>H-H</sub> = 7.5 Hz, 1H, ArH), 7.08 (d, <sup>3</sup>J<sub>H-H</sub> = 1.0 Hz, 2H, H<sub>imi</sub>), 7.02 (d, <sup>3</sup>J<sub>H-H</sub> = 8.0 Hz, 2H, ArH), 6.96 (s, 1H, ArH), 6.76 (d, <sup>3</sup>J<sub>H-H</sub> = 1.5 Hz, 2H, H<sub>imi</sub>), 5.12 (s, 4H, CH<sub>2</sub>), 2.19 (s, 6H, CH<sub>3</sub>). <sup>13</sup>C-NMR (125.74 MHz, d<sub>6</sub>-DMSO):  $\delta$  = 144.36 (C<sub>q</sub>), 138.55 (C<sub>q</sub>), 129.64 (C<sub>Ar</sub>), 126.96 (C<sub>imi</sub>), 126.59 (C<sub>Ar</sub>), 126.07 (C<sub>Ar</sub>), 120.70 (C<sub>imi</sub>), 48.94 (CH<sub>2</sub>), 13.18 (CH<sub>3</sub>). HRESI-MS<sup>+</sup>: [C<sub>14</sub>H<sub>15</sub>N<sub>4</sub>]<sup>+</sup> m/z = 267.1543, calcd = 267.1604.

**2.11·Br<sub>2</sub>.** To a solution of 1,2-dibromoethane (21.69 mL, 251.7 mmol) in acetonitrile (50 mL) stirred at 110 °C, was added dropwise a solution of **2.7** (2.0 g, 8.39 mmol) in

acetonitrile (100 mL) over a period of 3 h. The resultant mixture was stirred at the same temperature for 12 h and then filtered whilst still hot. The filtrate was then evaporated *in vacuo* and the resulting solid was recrystallised from hot ethanol (20 mL) yielding a white crystalline solid. Yield: 2.19 g, 41.2%. <sup>1</sup>H-NMR (500.02 MHz, d<sub>6</sub>-DMSO): δ = 9.50 (s, 2H, *H*<sub>imi</sub>), 7.98 (t, <sup>3</sup>*J*<sub>H-H</sub> = 1.8 Hz, 2H, *H*<sub>imi</sub>), 7.88 (t, <sup>3</sup>*J*<sub>H-H</sub> = 1.8 Hz, 2H, *H*<sub>imi</sub>), 7.49 (dd, <sup>3</sup>*J*<sub>H-H</sub> = 5.8 Hz, <sup>4</sup>*J*<sub>H-H</sub> = 3.5 Hz, 2H, *ArH*), 7.30 (dd, <sup>3</sup>*J*<sub>H-H</sub> = 5.5 Hz, <sup>4</sup>*J*<sub>H-H</sub> = 3.5 Hz, 2H, *ArH*), 5.75 (s, 4H, *CH*<sub>2</sub>), 4.69 (t, <sup>3</sup>*J*<sub>H-H</sub> = 6.0 Hz, 4H, *CH*<sub>2</sub>), 4.01 (t, <sup>3</sup>*J*<sub>H-H</sub> = 6.0 Hz, 4H, *CH*<sub>2</sub>). <sup>13</sup>C-NMR (125.74 MHz, d<sub>6</sub>-DMSO): δ = 137.56 (*C*<sub>imi</sub>), 133.38 (*C*<sub>q</sub>), 130.10 (*C*<sub>Ar</sub>), 129.83 (*C*<sub>Ar</sub>), 123.42 (*C*<sub>imi</sub>), 123.38 (*C*<sub>imi</sub>), 50.76 (*CH*<sub>2</sub>), 49.61 (*CH*<sub>2</sub>), 32.90 (*CH*<sub>2</sub>). HRESI-MS<sup>+</sup>: [C<sub>18</sub>H<sub>22</sub>N<sub>4</sub>Br<sub>2</sub>]<sup>2+</sup> *m/z* = 227.0094, calcd = 227.0090, [C<sub>18</sub>H<sub>22</sub>N<sub>4</sub>Br<sub>3</sub>]<sup>+</sup> *m/z* = 532.9367, calcd = 532.9369.

**2.12·Br<sub>2</sub>**. This compound was prepared using the same method as described for **2.11·Br<sub>2</sub>** from 1,2-dibromoethane (10.80 mL, 125.90 mmol) and **2.8** (1.00 g, 4.20 mmol). The crude product was purified by a trituration with diethyl ether (3 × 10 mL) yielding a light brown oil. Yield: 0.62 g, 24.0%. <sup>1</sup>H-NMR (500.02 MHz, d<sub>6</sub>-DMSO): δ = 9.63 (s, 2H, *H*<sub>imi</sub>), 7.95 – 7.97 (m, 4H, *H*<sub>imi</sub>), 7.65 (s, 1H, *ArH*), 7.44 – 7.50 (m, 3H, *ArH*), 5.56 (s, 4H, *CH*<sub>2</sub>), 4.69 (t, <sup>3</sup>*J*<sub>H-H</sub> = 5.9 Hz, 4H, *CH*<sub>2</sub>), 4.01 (t, <sup>3</sup>*J*<sub>H-H</sub> = 5.9 Hz, 4H, *CH*<sub>2</sub>). <sup>13</sup>C-NMR (125.74 MHz, d<sub>6</sub>-DMSO): δ = 137.31 (*C*<sub>imi</sub>), 136.02 (*C*<sub>q</sub>), 130.19 (*C*<sub>Ar</sub>), 129.08 (*C*<sub>Ar</sub>), 128.90 (*C*<sub>Ar</sub>), 123.36 (*C*<sub>imi</sub>), 123.16 (*C*<sub>imi</sub>), 52.05 (*CH*<sub>2</sub>), 50.76 (*CH*<sub>2</sub>), 32.90 (*CH*<sub>2</sub>). HRESI-MS<sup>+</sup>: [C<sub>18</sub>H<sub>22</sub>N<sub>4</sub>Br<sub>2</sub>]<sup>2+</sup> *m/z* = 227.0102, calcd = 227.0090.

**2.13·Br<sub>2</sub>**. This compound was prepared using the same method as described for **2.11·Br<sub>2</sub>** from 1,2-dibromoethane (4.85 mL, 56.31 mmol) and **2.9** (0.50 g, 1.88 mmol). The crude product was recrystallised from ethanol yielding a white solid. Yield: 0.62 g, 51.6%. <sup>1</sup>H-NMR (500.02 MHz, d<sub>6</sub>-DMSO): δ = 7.90 (d, <sup>3</sup>*J*<sub>H-H</sub> = 2.1 Hz, 2H, *H*<sub>imi</sub>), 7.68 (d, <sup>3</sup>*J*<sub>H-H</sub> = 2.1

Hz, 2H,  $H_{\text{imi}}$ ), 7.40 (dd,  $^3J_{\text{H-H}} = 5.5$  Hz,  $^4J_{\text{H-H}} = 3.4$  Hz, 2H, ArH), 6.82 (dd,  $^3J_{\text{H-H}} = 5.7$  Hz,  $^4J_{\text{H-H}} = 3.5$  Hz, 2H, ArH), 5.67 (s, 4H,  $\text{CH}_2$ ), 4.68 (t,  $^3J_{\text{H-H}} = 5.9$  Hz, 4H,  $\text{CH}_2$ ), 4.00 (t,  $^3J_{\text{H-H}} = 5.9$  Hz, 4H,  $\text{CH}_2$ ), 2.69 (s, 6H,  $\text{CH}_3$ ).  $^{13}\text{C}$ -NMR (125.74 MHz,  $\text{d}_6$ -DMSO):  $\delta = 146.15$  ( $\text{C}_q$ ), 132.62 ( $\text{C}_q$ ), 129.28 ( $\text{C}_{\text{Ar}}$ ), 126.95 ( $\text{C}_{\text{Ar}}$ ), 122.65 ( $\text{C}_{\text{imi}}$ ), 122.43 ( $\text{C}_{\text{imi}}$ ), 49.29 ( $\text{CH}_2$ ), 48.85 ( $\text{CH}_2$ ), 31.96 ( $\text{CH}_2$ ), 10.70 ( $\text{CH}_3$ ). HRESI-MS $^+$ :  $[\text{C}_{20}\text{H}_{26}\text{N}_4\text{Br}_2]^{2+}$   $m/z = 241.0306$ , calcd = 241.0246.

**2.14·Br<sub>2</sub>**. This compound was prepared using the same method as described for **2.11·Br<sub>2</sub>** from 1,2-dibromoethane (8.15 mL, 94.61 mmol) and **2.10** (0.84 g, 3.15 mmol). The crude product was recrystallised from ethanol yielding a white solid. Yield: 0.76 g, 37.5%.  $^1\text{H}$ -NMR (500.02 MHz,  $\text{d}_6$ -DMSO):  $\delta = 7.81$  (s, 2H,  $H_{\text{imi}}$ ), 7.79 (s, 2H,  $H_{\text{imi}}$ ), 7.46 (t,  $^3J_{\text{H-H}} = 7.8$  Hz, 1H, ArH), 7.33 (s, 1H, ArH), 7.27 (d,  $^3J_{\text{H-H}} = 7.7$  Hz, 2H, ArH), 5.47 (s, 4H,  $\text{CH}_2$ ), 4.62 (t,  $^3J_{\text{H-H}} = 6.0$  Hz, 4H,  $\text{CH}_2$ ), 3.93 (t,  $^3J_{\text{H-H}} = 5.9$  Hz, 4H,  $\text{CH}_2$ ), 2.67 (s, 6H,  $\text{CH}_3$ ).  $^{13}\text{C}$ -NMR (125.74 MHz,  $\text{d}_6$ -DMSO):  $\delta = 145.47$  ( $\text{C}_q$ ), 135.76 ( $\text{C}_q$ ), 130.32 ( $\text{C}_{\text{Ar}}$ ), 128.15 ( $\text{C}_{\text{Ar}}$ ), 127.59 ( $\text{C}_{\text{Ar}}$ ), 122.40 ( $\text{C}_{\text{imi}}$ ), 122.35 ( $\text{C}_{\text{imi}}$ ), 50.88 ( $\text{CH}_2$ ), 49.17 ( $\text{CH}_2$ ), 31.78 ( $\text{CH}_2$ ), 10.37 ( $\text{CH}_3$ ). HRESI-MS $^+$ :  $[\text{C}_{20}\text{H}_{26}\text{N}_4\text{Br}_2]^{2+}$   $m/z = 241.0294$ , calcd = 241.0246,  $[\text{C}_{20}\text{H}_{26}\text{N}_4\text{Br}_3]^+$   $m/z = 560.9702$ , calcd = 560.9682.

**2.15·Br<sub>4</sub>**. Solutions of **2.7** (0.31 g, 1.30 mmol) in acetonitrile (100 mL) and **2.11·Br<sub>2</sub>** (0.80 g, 1.30 mmol) in DMF (100 mL) were added simultaneously dropwise to 150 mL of acetonitrile heated at 110 °C over a period of 3 h. The mixture was then stirred at the same temperature for a further 5 d during which time a precipitate formed. The precipitate was collected and washed with acetonitrile (3  $\times$  5 mL) and recrystallised from a mixture of methanol and isopropanol yielding a white crystalline solid. Yield: 0.33 g, 29.7%.  $^1\text{H}$ -NMR (500.02 MHz,  $\text{d}_6$ -DMSO):  $\delta = 9.45$  (s, 4H,  $H_{\text{imi}}$ ), 7.90 (t,  $^3J_{\text{H-H}} = 1.5$  Hz, 4H,  $H_{\text{imi}}$ ), 7.77 (t,  $^3J_{\text{H-H}} = 1.5$  Hz, 4H,  $H_{\text{imi}}$ ), 7.52 (dd,  $^3J_{\text{H-H}} = 5.8$  Hz,  $^4J_{\text{H-H}} = 3.0$  Hz, 4H, ArH), 7.40 (dd,  $^3J_{\text{H-H}}$

$_{\text{H}} = 5.5 \text{ Hz}$ ,  $^4J_{\text{H-H}} = 3.5 \text{ Hz}$ , 4H, ArH), 5.68 (s, 8H, CH<sub>2</sub>), 4.81 (s, 8H, CH<sub>2</sub>). <sup>13</sup>C-NMR (125.74 MHz, d<sub>6</sub>-DMSO):  $\delta = 136.75$  (C<sub>imi</sub>), 133.13 (C<sub>q</sub>), 131.04 (C<sub>Ar</sub>), 130.38 (C<sub>Ar</sub>), 123.66 (C<sub>imi</sub>), 123.51 (C<sub>imi</sub>), 49.95 (CH<sub>2</sub>). HRESI-MS<sup>+</sup>: [C<sub>32</sub>H<sub>36</sub>N<sub>8</sub>]<sup>4+</sup>  $m/z = 133.0655$ , calcd = 133.0760, [C<sub>32</sub>H<sub>36</sub>N<sub>8</sub>P<sub>3</sub>F<sub>18</sub>]<sup>+</sup>  $m/z = 967.2020$ , calcd = 967.1967.

**2.16·Br<sub>4</sub>**. This compound was prepared using the same method as described for **2.15·Br<sub>4</sub>** from **2.8** (0.24 g, 1.01 mmol) and **2.12·Br<sub>2</sub>** (0.62 g, 1.01 mmol). Yield: 0.16 g, 18.0%. <sup>1</sup>H-NMR (500.02 MHz, d<sub>6</sub>-DMSO):  $\delta = 9.53$  (s, 4H, H<sub>imi</sub>) 7.83 (t,  $^3J_{\text{H-H}} = 1.7 \text{ Hz}$ , 4H, H<sub>imi</sub>), 7.80 (t,  $^3J_{\text{H-H}} = 1.7 \text{ Hz}$ , 4H, H<sub>imi</sub>), 7.51 (s, 2H, ArH), 7.36 (t,  $^3J_{\text{H-H}} = 7.7 \text{ Hz}$ , 4H, ArH), 7.26 – 7.28 (m, 4H, ArH), 5.45 (s, 8H, CH<sub>2</sub>), 4.84 (s, 8H, CH<sub>2</sub>). <sup>13</sup>C-NMR (125.74 MHz, d<sub>6</sub>-DMSO):  $\delta = 137.50$  (C<sub>imi</sub>), 135.80 (C<sub>q</sub>), 130.70 (C<sub>Ar</sub>), 128.92 (C<sub>Ar</sub>), 128.87 (C<sub>Ar</sub>), 128.39 (C<sub>imi</sub>), 52.21 (CH<sub>2</sub>), 48.83 (CH<sub>2</sub>). HRESI-MS<sup>+</sup>: [C<sub>32</sub>H<sub>36</sub>N<sub>8</sub>]<sup>4+</sup>  $m/z = 133.0686$ , calcd = 133.0760, [C<sub>32</sub>H<sub>36</sub>N<sub>8</sub>P<sub>2</sub>F<sub>12</sub>]<sup>2+</sup>  $m/z = 411.1099$ , calcd = 411.1163, [C<sub>32</sub>H<sub>36</sub>N<sub>8</sub>P<sub>3</sub>F<sub>18</sub>]<sup>+</sup>  $m/z = 967.1990$ , calcd = 967.1967.

**2.17·Br<sub>4</sub>**. Solutions of **2.7** (0.19 g, 0.80 mmol) in acetonitrile (50 mL) and **2.13·Br<sub>2</sub>** (0.50 g, 0.80 mmol) in DMF (50 mL) were added simultaneously dropwise to a solution of Bu<sub>4</sub>N·Br (1.55 g, 4.80 mmol) in acetonitrile (150 mL) heated at 110 °C over a period of 3 h. The mixture was stirred at the same temperature for a further 5 d during which time a precipitate formed. The precipitate was collected and washed with acetonitrile (3 × 5 mL) and then recrystallised from a mixture of methanol and diethyl ether yielding a white crystalline solid. Yield: 0.10g, 7.5%. <sup>1</sup>H-NMR (500.02 MHz, d<sub>6</sub>-DMSO):  $\delta = 9.76$  (s, 2H, H<sub>imi</sub>), 8.00 (s, 2H, H<sub>imi</sub>), 7.65 (s, 2H, H<sub>imi</sub>), 7.49 – 7.53 (m, 10H, ArH, H<sub>imi</sub>), 7.23 (dd,  $^3J_{\text{H-H}} = 5.4 \text{ Hz}$ ,  $^4J_{\text{H-H}} = 3.6 \text{ Hz}$ , 4H, ArH), 5.52 (s, 4H, CH<sub>2</sub>), 5.47 (s, 4H, CH<sub>2</sub>), 4.81 – 4.83 (m, 4H, CH<sub>2</sub>), 4.70 – 4.72 (m, 4H, CH<sub>2</sub>), 2.64 (s, 6H, CH<sub>3</sub>). <sup>13</sup>C-NMR (125.74 MHz, d<sub>6</sub>-DMSO):  $\delta = 145.98$  (C<sub>q</sub>), 137.44 (C<sub>imi</sub>), 132.92 (C<sub>q</sub>), 132.34 (C<sub>q</sub>), 131.15 (C<sub>Ar</sub>), 130.47 (C<sub>Ar</sub>), 129.97 (C<sub>Ar</sub>), 129.56 (C<sub>Ar</sub>), 123.98 (C<sub>imi</sub>), 123.42 (C<sub>imi</sub>), 122.83 (C<sub>imi</sub>), 122.67 (C<sub>imi</sub>),

49.48 (CH<sub>2</sub>), 49.38 (CH<sub>2</sub>), 49.19 (CH<sub>2</sub>), 47.90 (CH<sub>2</sub>), 10.02 (CH<sub>3</sub>). HRESI-MS<sup>+</sup>: [C<sub>32</sub>H<sub>36</sub>N<sub>8</sub>P<sub>2</sub>F<sub>12</sub>]<sup>2+</sup> m/z = 425.1335, calcd = 425.1324, [C<sub>34</sub>H<sub>40</sub>N<sub>8</sub>P<sub>3</sub>F<sub>18</sub>]<sup>+</sup> m/z = 995.2323, calcd 995.2296.

**2.18·Br<sub>4</sub>**. This compound was prepared using the same method described for **2.17·Br<sub>4</sub>** from **2.8** (0.11g, 0.47 mmol) and **2.14·Br<sub>2</sub>** (0.30 g, 0.47 mmol). The crude product was recrystallised from methanol yielding a white crystalline solid. Yield: 0.068 g, 16.5%. <sup>1</sup>H-NMR (500.023 MHz, d<sub>6</sub>-DMSO): δ = 9.53 (s, 2H, *H*<sub>imi</sub>), 7.80-7.84 (m, 4H, *H*<sub>imi</sub>), 7.62 (d, <sup>3</sup>*J*<sub>H-H</sub> = 2.2 Hz, 2H, *H*<sub>imi</sub>), 7.48 (d, <sup>3</sup>*J*<sub>H-H</sub> = 2.2 Hz, 2H, *H*<sub>imi</sub>), 7.46 (s, 1H, *ArH*), 7.40 (t, <sup>3</sup>*J*<sub>H-H</sub> = 7.7 Hz, 1H, *ArH*), 7.34 (s, 1H, *ArH*), 7.24 – 7.30 (m, 3H, *ArH*), 7.12 (dd, <sup>3</sup>*J*<sub>H-H</sub> = 7.7 Hz, <sup>4</sup>*J*<sub>H-H</sub> = 1.3 Hz, 2H, *ArH*), 5.42 (s, 4H, CH<sub>2</sub>), 5.38 (s, 4H, CH<sub>2</sub>), 4.74 (s, 8H, CH<sub>2</sub>), 2.63 (s, 6H, CH<sub>3</sub>). <sup>13</sup>C-NMR (125.74 MHz, d<sub>6</sub>-DMSO): δ = 145.85 (C<sub>q</sub>), 137.61 (C<sub>imi</sub>), 135.54 (C<sub>q</sub>), 135.39 (C<sub>q</sub>), 128.47 (C<sub>Ar</sub>), 128.04 (C<sub>Ar</sub>), 123.50 (C<sub>imi</sub>), 123.41 (C<sub>imi</sub>), 122.30 (C<sub>imi</sub>), 122.23 (C<sub>imi</sub>), 52.19 (CH<sub>2</sub>), 50.92 (CH<sub>2</sub>), 48.33 (CH<sub>2</sub>), 47.73 (CH<sub>2</sub>), 10.49 (CH<sub>3</sub>). HRESI-MS<sup>+</sup>: [C<sub>32</sub>H<sub>36</sub>N<sub>8</sub>Br<sub>2</sub>]<sup>2+</sup> m/z = 360.0861, calcd = 360.0865.

**2.19·(PF<sub>6</sub>)<sub>4</sub>** This compound was prepared using the same method described for **2.17·Br<sub>4</sub>** from **2.8** and **2.11·Br<sub>2</sub>** (0.52 g, 0.85 mmol) and Bu<sub>4</sub>N<sup>+</sup>Br<sup>-</sup> (1.37 g, 4.25 mmol). The crude product was then dried *in vacuo* and re-dissolved in water (5 mL) and then filtered through a plug of celite. To this solution, a solution of KPF<sub>6</sub> saturated in aqueous (3 mL) was added to obtain a white precipitate. The precipitate was washed with isopropanol (5 mL) and recrystallised by vapour diffusion of acetonitrile/diethyl ether to obtain a white crystalline. Yield: 0.15 g, 16.0%. <sup>1</sup>H-NMR (500.023 MHz, d<sub>6</sub>-DMSO): δ = 9.13 (s, 2H, *H*<sub>imi</sub>), 8.99 (s, 2H, *H*<sub>imi</sub>), 7.84 (t, <sup>3</sup>*J*<sub>H-H</sub> = 1.8 Hz, 2H, *H*<sub>imi</sub>), 7.72 (t, <sup>3</sup>*J*<sub>H-H</sub> = 1.8 Hz, 2H, *H*<sub>imi</sub>), 7.71 (t, <sup>3</sup>*J*<sub>H-H</sub> = 1.8 Hz, 2H, *H*<sub>imi</sub>), 7.65 (t, <sup>3</sup>*J*<sub>H-H</sub> = 1.8 Hz, 2H, *H*<sub>imi</sub>), 7.39 – 7.43 (m, 3H, *ArH*), 7.11 (s, 1H, *ArH*), 7.02 (dd, <sup>3</sup>*J*<sub>H-H</sub> = 7.7 Hz, <sup>4</sup>*J*<sub>H-H</sub> = 1.1 Hz, 2H, *ArH*), 6.92 – 6.96 (m, 2H, *ArH*),

5.37 (s, 4H, CH<sub>2</sub>), 5.36 (s, 4H, CH<sub>2</sub>), 4.72 - 4.80 (m, 8H, CH<sub>2</sub>). <sup>13</sup>C-NMR (125.74 MHz, d<sub>6</sub>-DMSO): δ = 137.40 (C<sub>imi</sub>), 137.28 (C<sub>imi</sub>), 135.56 (C<sub>q</sub>), 132.55 (C<sub>q</sub>), 130.16 (C<sub>Ar</sub>), 130.04 (C<sub>Ar</sub>), 129.30 (C<sub>Ar</sub>), 127.75 (C<sub>Ar</sub>), 127.35 (C<sub>Ar</sub>), 123.99 (C<sub>imi</sub>), 123.74 (C<sub>imi</sub>), 123.72 (C<sub>imi</sub>), 123.57 (C<sub>imi</sub>), 52.14 (CH<sub>2</sub>), 49.50 (CH<sub>2</sub>), 49.20 (CH<sub>2</sub>). HRESI-MS<sup>+</sup>: [C<sub>32</sub>H<sub>36</sub>N<sub>8</sub>]<sup>4+</sup> m/z = 133.0750, calcd = 133.0760, [C<sub>32</sub>H<sub>36</sub>N<sub>8</sub>P<sub>2</sub>F<sub>12</sub>]<sup>2+</sup> m/z = 411.1158, calcd = 411.1168, [C<sub>32</sub>H<sub>36</sub>N<sub>8</sub>P<sub>3</sub>F<sub>18</sub>]<sup>+</sup> m/z = 967.1985, calcd = 967.1983.

**2.20·(PF<sub>6</sub>)<sub>6</sub>.** A slurry of **2.15·Br<sub>4</sub>** (0.10 g, 0.12 mmol) and Ag<sub>2</sub>O (0.11 g, 0.47 mmol) was stirred at 50 °C for 3 d with the exclusion of light. Diethyl ether (~50 mL) was then added to the mixture and a grey precipitate formed which was collected and dissolved in hot water (5 mL). The solution was clarified by filtration through syringe filter and a saturated solution of KPF<sub>6</sub> (2 mL) was added to obtain an off-white precipitate. The solid collected and washed with hot isopropanol (2 mL) and then recrystallised from a mixture of acetonitrile and diethyl ether to obtain a white crystalline solid. Yield: 0.026 g, 21.4%. <sup>1</sup>H-NMR (500.02 MHz, d<sub>6</sub>-DMSO): δ = 7.70 (s, 6H, H<sub>imi</sub>), 7.68 (s, 6H, H<sub>imi</sub>), 7.52 (d, <sup>3</sup>J<sub>H-H</sub> = 7.5 Hz, 6H, ArH), 7.17 (t<sub>app</sub>, J = 7.5 Hz, 6H, ArH), 7.09 (s, 6H, H<sub>imi</sub>), 6.94 (t<sub>app</sub>, J = 7.5 Hz, 6H, ArH), 6.76 (s, 6H, H<sub>imi</sub>), 5.75 (d, <sup>2</sup>J<sub>H-H</sub> = 15.0 Hz, 12H, CH<sub>2</sub>), 5.68 (d, <sup>3</sup>J<sub>H-H</sub> = 7.5 Hz, 6H, ArH), 5.60 (d, <sup>2</sup>J<sub>H-H</sub> = 17.0 Hz, 6H, CH<sub>2</sub>), 4.98 (d, <sup>2</sup>J<sub>H-H</sub> = 14.5 Hz, 6H, CH<sub>2</sub>), 4.65 (t, <sup>3</sup>J<sub>H-H</sub> = 12.5 Hz, 6H, CH<sub>2</sub>), 4.52 (t, <sup>3</sup>J<sub>H-H</sub> = 12.5 Hz, 6H, CH<sub>2</sub>), 4.21 (d, <sup>3</sup>J<sub>H-H</sub> = 12.0 Hz, 6H, CH<sub>2</sub>), 2.48 (s, 6H, CH<sub>2</sub>). <sup>13</sup>C-NMR (125.74 MHz, d<sub>6</sub>-DMSO): δ = 186.31 (d, <sup>1</sup>J = 182.32 Hz, <sup>107</sup>Ag-C<sub>carbene</sub>), 186.31 (d, <sup>1</sup>J = 209.99 Hz, <sup>109</sup>Ag-C<sub>carbene</sub>), 178.75 (d, <sup>1</sup>J = 182.32 Hz, <sup>107</sup>Ag-C<sub>carbene</sub>), 178.75 (d, <sup>1</sup>J = 209.99 Hz, <sup>109</sup>Ag-C<sub>carbene</sub>), 135.80 (C<sub>q</sub>), 131.60 (C<sub>q</sub>), 130.88 (C<sub>Ar</sub>), 129.41 (C<sub>Ar</sub>), 128.14 (C<sub>Ar</sub>), 124.63 (C<sub>Ar</sub>), 123.90 (C<sub>imi</sub>), 123.78 (C<sub>imi</sub>), 121.75 (C<sub>imi</sub>), 55.37 (CH<sub>2</sub>), 52.58 (CH<sub>2</sub>), 51.66 (CH<sub>2</sub>), 51.24 (CH<sub>2</sub>), 50.50 (CH<sub>2</sub>). HRESI-MS<sup>+</sup>: [C<sub>96</sub>H<sub>96</sub>N<sub>24</sub>Ag<sub>6</sub>]<sup>6+</sup> m/z = 372.0334, calcd = 372.0419, [C<sub>96</sub>H<sub>96</sub>N<sub>24</sub>Ag<sub>6</sub>P<sub>3</sub>F<sub>18</sub>]<sup>3+</sup> m/z = 889.0490, calcd = 889.0485.



**2.21·Br<sub>6</sub>.** A slurry of **2.15·Br<sub>4</sub>** (0.10 g, 0.12 mmol) and (THT)AuCl (0.083 g, 0.26 mmol) in DMF (10 mL) was stirred at 110 °C for 0.5 h. To this mixture NaOAc (0.050 g, 0.59 mmol) was added and the solution was stirred at the same temperature for 1 h. The resultant mixture was cooled to RT and then diethyl ether (50 mL) was added to obtain a white precipitate. The precipitate was collected and recrystallised from hot methanol (~5 mL). Yield: 0.048 g, 54.2%. <sup>1</sup>H-NMR (500.02 MHz, d<sub>6</sub>-DMSO): δ = 7.83 (s, 6H, *H<sub>imi</sub>*), 7.72 (s, 6H, *H<sub>imi</sub>*), 7.57 (d, <sup>3</sup>*J<sub>H-H</sub>* = 7.5 Hz, 6H, *ArH*), 7.21 (t<sub>app</sub>, *J* = 7.5 Hz, 6H, *ArH*) 7.11 (s, 6H, *H<sub>imi</sub>*), 6.93 (t<sub>app</sub>, *J* = 7.5 Hz, 6H, *ArH*) 6.84 (s, 6H, *H<sub>imi</sub>*), 6.07 (d, <sup>2</sup>*J<sub>H-H</sub>* = 16.5 Hz, 6H, *CH<sub>2</sub>*), 5.74 – 5.78 (m, 12H, *ArH*, *CH<sub>2</sub>*), 5.66 (d, <sup>3</sup>*J<sub>H-H</sub>* = 16.5 Hz, 6H, *CH<sub>2</sub>*), 5.06 (d, <sup>3</sup>*J<sub>H-H</sub>* = 14.0 Hz, 12H, *CH<sub>2</sub>*), 4.49 (t, <sup>3</sup>*J<sub>H-H</sub>* = 12.8 Hz, 6H, *CH<sub>2</sub>*), 4.37 (d, <sup>3</sup>*J<sub>H-H</sub>* = 12.5 Hz, 6H, *CH<sub>2</sub>*), 2.33 (d, <sup>3</sup>*J<sub>H-H</sub>* = 12.5 Hz, 6H, *CH<sub>2</sub>*). <sup>13</sup>C-NMR (125.74 MHz, d<sub>6</sub>-DMSO): δ = 186.31 (*C<sub>carbene</sub>*), 181.48 (*C<sub>carbene</sub>*), 135.84 (*C<sub>q</sub>*), 131.37 (*C<sub>q</sub>*), 131.02 (*C<sub>Ar</sub>*), 129.62 (*C<sub>Ar</sub>*), 127.99 (*C<sub>Ar</sub>*), 124.59 (*C<sub>Ar</sub>*), 123.95 (*C<sub>imi</sub>*), 123.64 (*C<sub>imi</sub>*), 121.86 (*C<sub>imi</sub>*), 51.89 (*CH<sub>2</sub>*), 51.27 (*CH<sub>2</sub>*), 50.22 (*CH<sub>2</sub>*). HRESI-MS<sup>+</sup>: [C<sub>96</sub>H<sub>96</sub>N<sub>24</sub>Au<sub>6</sub>]<sup>6+</sup> *m/z* = 461.1022, calcd = 461.1035.

**2.22·(PF<sub>6</sub>)<sub>2</sub>.** A slurry of **2.15·Br<sub>4</sub>** (0.050 g, 0.059 mmol) and Ag<sub>2</sub>O (0.030 g, 0.13 mmol) in DMF (5 mL) was stirred at 50 °C for 12 h with the exclusion of light. To this mixture K<sub>2</sub>PdCl<sub>4</sub> (0.019 g, 0.059 mmol) was added and stirring was continued for a further stirred for 12 h at 80 °C. The reaction mixture was clarified by centrifugation and diethyl ether (30 mL) was added to the supernatant yielding a grey precipitate. The precipitate was collected and re-dissolved in hot water (5 mL) and the solution filtered through a syringe filter. To the filtrate, a saturated solution of KPF<sub>6</sub> (2 mL) was added to obtain an off-white precipitate. The precipitate was dried *in vacuo* and then recrystallised from a mixture of acetonitrile and diethyl ether to obtain a white crystalline solid. Yield: 0.0052 g, 9.6%. <sup>1</sup>H-NMR (500.02 MHz, d<sub>6</sub>-DMSO): δ = 7.87 – 7.92 (m, 4H, *ArH*), 7.83 (d, <sup>3</sup>*J<sub>H-H</sub>* = 2.0 Hz, 4H, *H<sub>imi</sub>*), 7.48 (d, <sup>3</sup>*J<sub>H-H</sub>* = 2.0 Hz, 4H, *H<sub>imi</sub>*), 7.42 – 7.47 (m, 4H, *ArH*), 6.44 (d, <sup>3</sup>*J<sub>H-H</sub>* = 15.0 Hz, 4H,

$CH_2$ ), 5.20 (d,  $^3J_{H-H} = 14.7$  Hz, 4H,  $CH_2$ ), 4.98 – 5.06 (m, 4H,  $CH_2$ ), 4.54 – 4.61 (m, 4H,  $CH_2$ ).  $^{13}C$ -NMR (125.74 MHz,  $d_6$ -DMSO):  $\delta = 167.41$  ( $C_{carbene}$ ), 135.56 ( $C_q$ ), 131.73 ( $C_{Ar}$ ), 129.83 ( $C_{Ar}$ ), 124.96 ( $C_{imi}$ ), 122.68 ( $C_{imi}$ ), 50.79 ( $CH_2$ ), 47.39 ( $CH_2$ ). HRESI-MS $^+$ :  $[C_{32}H_{32}N_8Pd]^{2+}$   $m/z = 317.0889$ , calcd = 317.0887.

**2.23·(PF<sub>6</sub>)<sub>3</sub>.** This compound was prepared using the same method as described for **2.20·(PF<sub>6</sub>)<sub>6</sub>** from **2.16·Br<sub>4</sub>** (0.050 g, 0.059 mmol) and Ag<sub>2</sub>O (0.057 g, 0.24 mmol). Yield: 0.0050 g, 6.2 %.  $^1H$ -NMR (500.02 MHz, CD<sub>3</sub>CN):  $\delta = 8.37$  (t,  $J = 1.5$  Hz, 2H,  $H_{imi}$ ), 7.45 – 7.53 (m, 12H,  $ArH$ ,  $H_{imi}$ ), 7.21 (t,  $^3J_{H-H} = 1.8$  Hz, 2H,  $H_{imi}$ ), 6.98 (s, 2H,  $ArH$ ), 6.95 (t,  $^3J_{H-H} = 1.9$  Hz, 2H,  $H_{imi}$ ) 5.31 (s, 4H,  $CH_2$ ), 5.08 (s, 4H,  $CH_2$ ), 4.60 (d,  $^3J_{H-H} = 4.3$  Hz, 4H,  $CH_2$ ), 4.55 (d,  $^3J_{H-H} = 4.7$  Hz, 4H,  $CH_2$ ).  $^{13}C$ -NMR (125.74 MHz, CD<sub>3</sub>CN):  $\delta = 180.39$  (d,  $^1J = 183.58$  Hz,  $^{107}Ag-C_{carbene}$ ), 180.39 (d,  $^1J = 211.24$  Hz,  $^{109}Ag-C_{carbene}$ ), 138.62 ( $C_q$ ), 136.79 ( $C_q$ ), 136.18 ( $C_{imi}$ ), 130.86 ( $C_{Ar}$ ), 129.82 ( $C_{imi}$ ), 129.48 ( $C_{imi}$ ), 126.74 ( $C_{Ar}$ ), 125.47 ( $C_{Ar}$ ), 125.42 ( $C_{Ar}$ ), 124.47 ( $C_{imi}$ ), 124.12 ( $C_{imi}$ ), 122.39 ( $C_{Ar}$ ), 122.35 ( $C_{Ar}$ ), 55.33 ( $CH_2$ ), 53.45 ( $CH_2$ ), 52.73 ( $CH_2$ ), 50.96 ( $CH_2$ ). HRESI-MS $^+$ :  $[C_{32}H_{34}N_8Ag]^{3+}$   $m/z = 213.0643$ , calcd = 213.0646,  $[C_{32}H_{34}N_8AgPF_6]^{2+}$   $m/z = 391.2845$ , calcd = 391.0794,  $[C_{32}H_{34}N_8AgP_2F_{12}]^+$   $m/z = 927.1228$ , calcd = 927.1235.

**2.24·(PF<sub>6</sub>)<sub>2</sub>.** This compound was prepared using the same method as described for **2.21·Br<sub>6</sub>** from **2.17·Br<sub>4</sub>** (0.050 g, 0.057 mmol), (THT)AuCl (0.040 g, 0.13 mmol) and NaOAc (0.019 g, 0.23 mmol). For exchange of the bromide anion to hexafluorophosphate the crude product was dissolved in water (3 mL) and the solution filtered through celite. To this solution, a saturated solution of KPF<sub>6</sub> (2 mL) was added to obtain a white precipitate which was then recrystallised from a mixture of acetonitrile and diethyl ether yielding a white crystalline solid. Yield: 0.020 g, 29.9%.  $^1H$ -NMR (500.02 MHz, CD<sub>3</sub>CN):  $\delta = 7.55 - 7.57$  (m, 1H,  $ArH$ ), 7.46 – 7.48 (m, 1H,  $ArH$ ), 7.44 (d,  $^3J_{H-H} = 2.0$  Hz, 1H,  $H_{imi}$ ), 7.41 -7.42 (m,

1H, ArH), 7.38 (s, 1H,  $H_{\text{imi}}$ ), 7.23 (d,  $^3J_{\text{H-H}} = 2.1$  Hz, 1H,  $H_{\text{imi}}$ ), 7.21-7.22 (m, 1H, ArH), 7.15 (d,  $^3J_{\text{H-H}} = 1.9$  Hz, 1H,  $H_{\text{imi}}$ ), 5.53 (s, 2H,  $\text{CH}_2$ ), 5.49 (s, 2H,  $\text{CH}_2$ ), 4.66 – 4.67 (m, 2H,  $\text{CH}_2$ ), 4.57 – 4.59 (m, 2H,  $\text{CH}_2$ ), 2.54 (s, 3H,  $\text{CH}_3$ ).  $^{13}\text{C}$ -NMR (125.74 MHz,  $\text{CD}_3\text{CN}$ ):  $\delta =$  145.20 ( $C_{\text{carbene}}$ ), 133.61 ( $C_{\text{q}}$ ), 130.51 ( $C_{\text{Ar}}$ ), 130.43 ( $C_{\text{Ar}}$ ), 130.22 ( $C_{\text{Ar}}$ ), 129.75 ( $C_{\text{Ar}}$ ), 122.74 ( $C_{\text{imi}}$ ), 122.50 ( $C_{\text{imi}}$ ), 122.24 ( $C_{\text{imi}}$ ), 122.05 ( $C_{\text{imi}}$ ), 51.84 ( $\text{CH}_2$ ), 50.05 ( $\text{CH}_2$ ), 49.69 ( $\text{CH}_2$ ), 48.48 ( $\text{CH}_2$ ), 10.36 ( $\text{CH}_3$ ). HRESI-MS $^+$ :  $[\text{C}_{34}\text{H}_{38}\text{N}_8\text{Au}_2\text{Br}_2]^{2+}$   $m/z = 556.0369$ , calcd = 556.0443.

**2.25·(PF<sub>6</sub>)<sub>2</sub>.** This compound was prepared using the same method as that described for **2.21·Br<sub>6</sub>** from **2.18·Br<sub>4</sub>** (0.030 g, 0.034 mmol), (THT)AuCl (0.024 g, 0.075 mmol) and NaOAc (0.11 g, 0.14 mmol). For exchange of the bromide anion to hexafluorophosphate, the crude product was dissolved in water (3 mL) and the solution filtered through Celite. To this solution, a saturated solution of KPF<sub>6</sub> (2 mL) was added to obtain a white precipitate which was then recrystallized from a mixture of acetonitrile and diethyl ether yielding a white crystalline solid. Yield: 0.0070 g, 1.5 %.  $^1\text{H}$ -NMR (500.02 MHz,  $d_6$ -DMSO):  $\delta =$  7.71 (d,  $^3J_{\text{H-H}} = 1.9$  Hz, 2H,  $H_{\text{imi}}$ ), 7.62 (d,  $^3J_{\text{H-H}} = 1.9$  Hz, 2H,  $H_{\text{imi}}$ ), 7.56 (d,  $^3J_{\text{H-H}} = 1.9$  Hz, 2H,  $H_{\text{imi}}$ ), 7.39 -7.43 (m, 3H, ArH,  $H_{\text{imi}}$ ), 7.28 – 7.38 (m, 3H, ArH), 7.14 – 7.19 (m, 1 H, ArH), 7.07 – 7.14 (m, 1H, ArH), 6.56 – 6.69 (m, 2H, ArH), 5.31 (s, 4H,  $\text{CH}_2$ ), 5.06 (s, 4H,  $\text{CH}_2$ ), 4.67 (s, 4H,  $\text{CH}_2$ ), 4.66 (s, 4H,  $\text{CH}_2$ ), 2.40 (s, 6H,  $\text{CH}_3$ ).  $^{13}\text{C}$ -NMR (125.74 MHz,  $d_6$ -DMSO):  $\delta =$  172.52 ( $C_{\text{carbene}}$ ), 144.61 ( $C_{\text{q}}$ ), 136.79 ( $C_{\text{q}}$ ), 134.11 ( $C_{\text{q}}$ ), 130.12 ( $C_{\text{Ar}}$ ), 127.96 ( $C_{\text{Ar}}$ ), 125.29 ( $C_{\text{Ar}}$ ), 123.45 ( $C_{\text{imi}}$ ), 122.28 ( $C_{\text{imi}}$ ), 121.98 ( $C_{\text{imi}}$ ), 121.91 ( $C_{\text{imi}}$ ), 52.82 ( $\text{CH}_2$ ), 50.44 ( $\text{CH}_2$ ), 49.84 ( $\text{CH}_2$ ), 48.11 ( $\text{CH}_2$ ), 9.19 ( $\text{CH}_3$ ). HRESI-MS $^+$ :  $[\text{C}_{34}\text{H}_{38}\text{N}_8\text{Au}_2\text{Br}_2]^{2+}$   $m/z = 556.0422$ , calcd = 556.0443.

**2.26·(PF<sub>6</sub>)<sub>2</sub>.** To a solution of **2.17·Br<sub>4</sub>** (0.050 g, 0.057 mmol) and K<sub>2</sub>PdCl<sub>4</sub> (0.019 g, 0.057 mmol) in DMSO (5 mL) at 85 °C, NaOAc (0.019 g, 0.23 mmol) was added and the reaction

mixture was stirred same temperature for 12 h. The resultant mixture was then diluted with acetone (5 mL) followed by adding diethyl ether (20 mL) to form a precipitate. The crude precipitate was collected and then redissolved in water and filtered through a plug of Celite followed by addition of a saturated solution of  $\text{KPF}_6$  (3 mL). The resultant precipitate was collected and washed with isopropanol (5 mL) and diethyl ether ( $2 \times 5$  mL) and then recrystallised from a mixture of acetonitrile and diethyl ether yielding the product as a pale yellow solid. NMR analysis showed this material to be impure and the  $^1\text{H}$ -NMR spectrum is reported for the impure material.  $^1\text{H}$ -NMR (500.02 MHz,  $\text{CD}_3\text{CN}$ ):  $\delta = 7.66$  (s, 2H,  $H_{\text{imi}}$ ), 7.55 – 7.57 (m, 4H,  $\text{ArH}$ ), 7.35 -7.40 (m, 2h,  $\text{ArH}$ ), 7.34 (s, 2H,  $H_{\text{imi}}$ ), 7.22 – 7.24 (m, 2H,  $H_{\text{imi}}$ ), 7.03 (s, 2H,  $H_{\text{imi}}$ ), 7.02 (s, 2H,  $H_{\text{imi}}$ ), 5.26 (s, 4H,  $\text{CH}_2$ ), 5.24 (s, 4H,  $\text{CH}_2$ ), 4.61 – 4.70 (m, 8H,  $\text{CH}_2$ ), 2.57 (s, 6H,  $\text{CH}_3$ ). A crystal suitable for single crystal X-ray diffraction analysis of **2.26**·( $\text{PF}_6$ )<sub>2</sub> was grown from diffusion of diethyl ether into an acetonitrile solution of **2.26**·( $\text{PF}_6$ )<sub>2</sub>.

## 2.5 References

1. Beer, P. D.; Gale, P. A., *Angew. Chem. int. Ed.* **2001**, *40*, 486-516.
2. Gale, P. A., *Coord. Chem. Rev.* **2003**, *240*, 191-221.
3. Martínez-Máñez, R.; Sancenón, F., *Chem. Rev.* **2003**, *103*, 4419-4476.
4. Wei, J.; Jin, T.-T.; Yang, J.-X.; Jiang, X.-M.; Liu, L.-J.; Zhan, T.-G.; Zhang, K.-D., *Tetrahedron Lett.* **2020**, *61*, 151389.
5. Wong, W. W. H.; Vickers, M. S.; Cowley, A. R.; Paul, R. L.; Beer, P. D., *Org. Biomol. Chem.* **2005**, *3*, 4201-4208.
6. Chellappan, K.; Singh, N. J.; Hwang, I.; Lee, J. W.; Kim, K. S., *Angew. Chem. Int. Ed.* **2005**, *44*, 2899-2903.
7. Yoon, J.; Kim, S. K.; Singh, N. J.; Kim, K. S., *Chem. Soc. Rev.* **2006**, *35*, 355-360.
8. Alcalde, E.; Mesquida, N.; Perez-Garcia, L.; Alvarez-Rua, C.; Garcia-Granda, S.; Garcia-Rodriguez, E., *Chem. Commun.* **1999**, *0*, 295-296.
9. Xu, Z.; Kim, S. K.; Yoon, J., *Chem. Soc. Rev.* **2010**, *39*, 1457-1466.
10. Alcalde, E.; Mesquida, N.; Vilaseca, M.; Alvarez-RÚA, C.; GarcÍA-Granda, S., *Supramol. Chem.* **2007**, *19*, 501-509.
11. Serpell, C. J.; Cookson, J.; Thompson, A. L.; Beer, P. D., *Chem. Sci.* **2011**, *2*, 494-500.
12. Neelakandan, P. P.; Ramaiah, D., *Angew. Chem. Int. Ed.* **2008**, *47*, 8407-8411.
13. Ahmed, N.; Shirinfar, B.; Youn, I. S.; Bist, A.; Suresh, V.; Kim, K. S., *Chem. Commun.* **2012**, *48*, 2662-2664.
14. Shirinfar, B.; Ahmed, N.; Park, Y. S.; Cho, G.; Youn, I. S.; Han, J.; Nam, H. G.; Kim, K. S., *J. Am. Chem. Soc.* **2013**, *135*, 90-93.
15. Ahmed, N.; Shirinfar, B.; Geronimo, I.; Kim, K. S., *Org. Lett.* **2011**, *13*, 5476-5479.
16. Hahn, F. E.; Radloff, C.; Pape, T.; Hepp, A., *Chem. Eur. J.* **2008**, *14*, 10900-10904.
17. Schulte to Brinke, C.; Pape, T.; Hahn, F. E., *Dalton Trans.* **2013**, *42*, 7330-7337.
18. Bass, H. M.; Cramer, S. A.; Price, J. L.; Jenkins, D. M., *Organometallics* **2010**, *29*, 3235-3238.
19. Toure, M.; Charles, L.; Chendo, C.; Viel, S.; Chuzel, O.; Parrain, J.-L., *Chem. Eur. J.* **2016**, *22*, 8937-8942.
20. Altmann, P. J.; Jandl, C.; Pöthig, A., *Dalton Transactions* **2015**, *44*, 11278-11281.
21. Mesquida, N.; Dinarès, I.; Ibáñez, A.; Alcalde, E., *Org. Biomol. Chem.* **2013**, *11*, 6385-6396.

22. Gong, H.-Y.; Rambo, B. M.; Karnas, E.; Lynch, V. M.; Sessler, J. L., *Nat. Chem.* **2010**, *2*, 406-409.
23. Schulte to Brinke, C.; Hahn, F. E., *Dalton Trans.* **2015**, *44*, 14315-14322.
24. Melaiye, A.; Sun, Z.; Hindi, K.; Milsted, A.; Ely, D.; Reneker, D. H.; Tessier, C. A.; Youngs, W. J., *J. Am. Chem. Soc.* **2005**, *127*, 2285-2291.
25. Sakamoto, R.; Morozumi, S.; Yanagawa, Y.; Toyama, M.; Takayama, A.; Kasuga, N. C.; Nomiya, K., *J. Inorg. Biochem.* **2016**, *163*, 110-117.
26. Hahn, F. E.; Langenhahn, V.; Lügger, T.; Pape, T.; Le Van, D., *Angew. Chem. Int. Ed.* **2005**, *44*, 3759-3763.
27. Barnard, P. J.; Baker, M. V.; Berners-Price, S. J.; Day, D. A., *J. Inorg. Biochem.* **2004**, *98*, 1642-1647.
28. Barnard, P. J.; Wedlock, L. E.; Baker, M. V.; Berners-Price, S. J.; Joyce, D. A.; Skelton, B. W.; Steer, J. H., *Angew. Chem. Int. Ed.* **2006**, *45*, 5966-5970.
29. Mageed, A. H.; Skelton, B. W.; Baker, M. V., *Dalton Trans.* **2017**, *46*, 7844-7856.
30. Mageed, A. H.; Skelton, B. W.; Sobolev, A. N.; Baker, M. V., *Eur. J. Inorg. Chem.* **2018**, *2018*, 109-120.
31. Altmann, P. J.; Weiss, D. T.; Jandl, C.; Kühn, F. E., *Chem. Asian J.* **2016**, *11*, 1597-1605.
32. Fei, F.; Lu, T.; Chen, X.; Xue, Z., *New J. Chem.* **2017**, *41*, 13442-13453.
33. Lu, T.; Yang, C.; Steren, C. A.; Fei, F.; Chen, X.; Xue, Z., *New J. Chem.* **2018**, *42*, 4700-4713.
34. Lu, T.; Yang, C.; Zhang, L.; Fei, F.; Chen, X.; Xue, Z., *Inorg. Chem.* **2017**, *56*, 11917-11928.
35. McKie, R.; Murphy, J. A.; Park, S. R.; Spicer, M. D.; Zhou, S. Z., *Angew. Chem. Int. Ed.* **2007**, *46*, 6525-6528.
36. Nomiya, K.; Morozumi, S.; Yanagawa, Y.; Hasegawa, M.; Kurose, K.; Taguchi, K.; Sakamoto, R.; Mihara, K.; Kasuga, N. C., *Inorg. Chem.* **2018**, *57*, 11322-11332.
37. Shah, P. N.; Lin, L. Y.; Smolen, J. A.; Tagaev, J. A.; Gunsten, S. P.; Han, D. S.; Heo, G. S.; Li, Y.; Zhang, F.; Zhang, S.; Wright, B. D.; Panzner, M. J.; Youngs, W. J.; Brody, S. L.; Wooley, K. L.; Cannon, C. L., *ACS Nano* **2013**, *7*, 4977-4987.
38. Aweda, T. A.; Ikotun, O.; Mastren, T.; Cannon, C. L.; Wright, B.; Youngs, W. J.; Cutler, C.; Guthrie, J.; Lapi, S. E., *Med. Chem. Commun.* **2013**, *4*, 1015-1017.
39. Pöthig, A.; Ahmed, S.; Winther-Larsen, H. C.; Guan, S.; Altmann, P. J.; Kudermann, J.; Santos Andresen, A. M.; Gjøslen, T.; Høgmoe Åstrand, O. A., *Front. Chem.* **2018**, *6*.

40. Meyer, S.; Klawitter, I.; Demeshko, S.; Bill, E.; Meyer, F., *Angew. Chem. Int. Ed.* **2013**, *52*, 901-905.
41. Anneser, M. R.; Haslinger, S.; Pöthig, A.; Cokoja, M.; Basset, J.-M.; Kühn, F. E., *Inorg. Chem.* **2015**, *54*, 3797-3804.
42. Baker, M. V.; Skelton, B. W.; White, A. H.; Williams, C. C., *Dalton Trans.* **2001**, *0*, 111-120.
43. Radloff, C.; Gong, H.-Y.; Schulte to Brinke, C.; Pape, T.; Lynch, V. M.; Sessler, J. L.; Hahn, F. E., *Eur. J. Inorg. Chem.* **2010**, *16*, 13077-13081.
44. Fei, F.; Lu, T.; Chen, X.-T.; Xue, Z.-L., *New J. Chem.* **2017**, *41*, 13442-13453.
45. Melaimi, M.; Soleilhavoup, M.; Bertrand, G., *Angew. Chem. Int. Ed.* **2010**, *49*, 8810-8849.
46. Magill, A. M.; Yates, B. F., *Aust. J. Chem.* **2004**, *57*, 1205-1210.
47. Andrew, R. E.; Storey, C. M.; Chaplin, A. B., *Dalton Trans.* **2016**, *45*, 8937-8944.
48. Chianese, A. R.; Zeglis, B. M.; Crabtree, R. H., *Chem. Commun.* **2004**, *0*, 2176-2177.
49. Yuan, Y.; Gao, G.; Jiang, Z.; You, J.; Zhou, Z.; Yuan, D.; Xie, R., *Tetrahedron* **2002**, *58*, 8993-8999.
50. Frassinetti, C.; Alderighi, L.; Gans, P.; Sabatini, A.; Vacca, A.; Ghelli, S., *Anal Bioanal Chem* **2003**, *376*, 1041-1052.
51. Frassinetti, C.; Ghelli, S.; Gans, P.; Sabatini, A.; Moruzzi, M. S.; Vacca, A., *Anal. Biochem.* **1995**, *231*, 374-382.

# CHAPTER 3 SYNTHESIS OF MACROCYCLES

## INCORPORATING 1,2,3-TRIAZOLE AND IMIDAZOLIUM

### UNITS AND THEIR METAL COMPLEXES

#### 3.1 Introduction

The synthesis of 1,2,3-triazolium salts is of significant interest because of their capacity to act as anion receptors<sup>1</sup> and to be utilized as pro-ligands for the synthesis of abnormal *N*-heterocyclic carbene (aNHC) metal complexes.<sup>2</sup> Due to the critical role of negatively charged anionic species in environmental and biological processes, the preparation of receptor molecules designed to recognize and sense anions is an area of great research interest.<sup>1, 3-4</sup> Although less well studied, 1,2,3-triazolium groups have also been recognised for their properties as anion receptors, which result both from electrostatic and hydrogen bonding interactions and a range of 1,2,3-triazolium linked anion binding cyclophane and macrocycle salts have been evaluated.<sup>1, 5-11</sup> For example, the *tris*-1,2,3-triazolium salts<sup>12</sup> **3.1·Cl<sub>3</sub>** and the *bis*-triazolium linked cyclophane<sup>6</sup> **3.2·Cl<sub>2</sub>** (Figure 3.1) exhibit selective binding of chloride anions.<sup>6, 12</sup> Interestingly, in the case of **3.2·Cl<sub>2</sub>**, it was noted that the presence of the 1,2,3-triazolium groups decreases the ability of anion recognition when compared with the *bis*-imidazolium analogue.<sup>6</sup> Furthermore, the *tetra*-triazolium linked macrocycle **3.3·(BF<sub>4</sub>)<sub>2</sub>SO<sub>4</sub>** (Figure 3.1) displayed a very high binding affinity for the sulfate anion with an association constant of  $K_a > 10^{-4} \text{ M}^{-1}$ .<sup>11</sup>



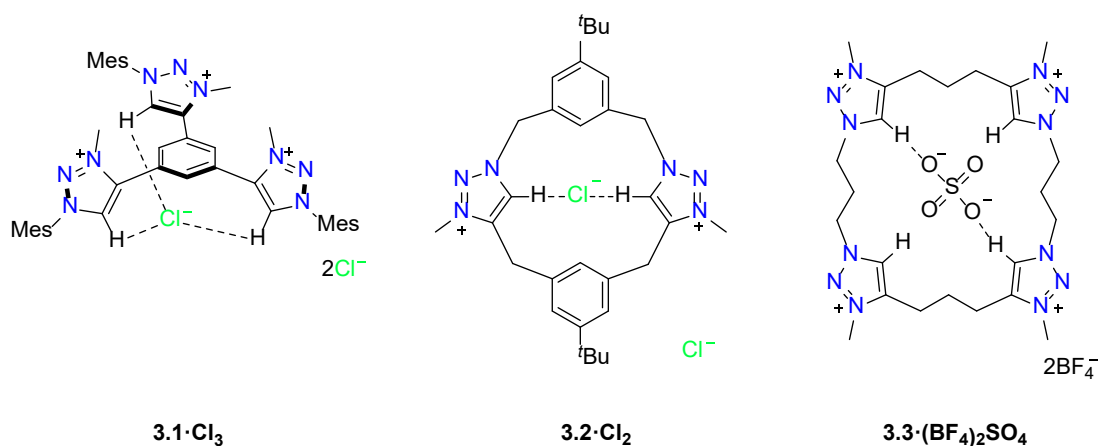
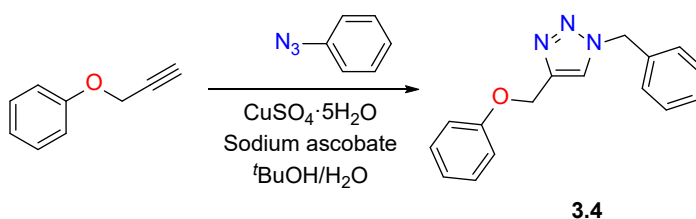


Figure 3.1 Selected examples of 1,2,3-triazolium compounds that act as anion receptors.

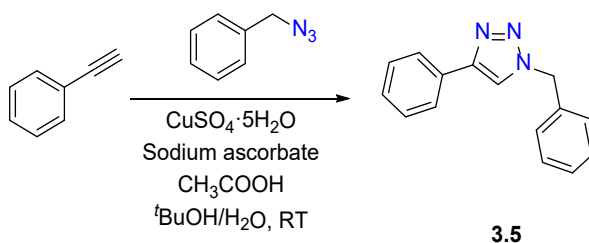
The best known ‘click’ chemical reaction is the copper(I)-catalyzed azide-alkyne cycloaddition (CuAAC) and this process is commonly used for the preparation of 1,2,3-triazole derivatives.<sup>12-21</sup> For example, using the CuAAC reaction the 1,2,3-triazole species **3.4** was prepared by the reaction of phenyl propargyl ether and benzylazide in the presence of a Cu(I) catalyst (Scheme 3.1). It was noted by the authors that a mixture of 1,4- and 1,5-substituted products is obtained for this reaction at elevated temperatures in the absence of a Cu(I) catalyst. In contrast, only the 1,4-substituted 1,2,3-triazole species is produced in the presence of Cu(I) and in the reaction shown in Scheme 3.1, the Cu(I) catalyst is generated *in situ* by the reduction of Cu(II) using sodium ascorbate.<sup>18</sup>



Scheme 3.1 Synthesis of the 1,2,3-triazole **3.4** using copper catalysed azide-alkyne cycloaddition reaction between phenyl propargyl ether and benzyl azide.

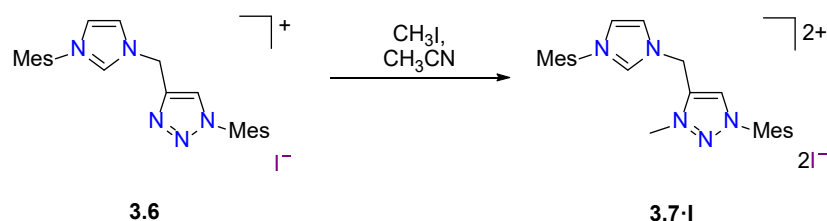
Using a similar synthetic approach, **3.5** was prepared by the reaction of phenylacetylene with benzylazide using the CuAAC reaction (Scheme 3.2).<sup>19</sup> Interestingly, when the

reaction was performed in the absence of acetic acid, the desired 1,2,3-triazole product was produced with a low yield of 21%. However, the addition of the acetic acid to the reaction mixture resulted in acceleration of the reaction as a result of dissociation of Cu(I) and protonation of position 5 of the 1,2,3-triazole ring.<sup>19</sup>



Scheme 3.2 Synthesis of **3.5** via a CuAAC reaction in the presence of acetic acid.

Due to their potential to be utilized for the development of anion receptors and pro-ligands for the synthesis of aNHC metal complexes, a range of synthetic methods for the preparation of 1,2,3-triazolium compounds have been reported.<sup>6, 11-13, 22-27</sup> For example, **3.7·I** was synthesized by the alkylation of **3.6** with  $\text{CH}_3\text{I}$  (Scheme 3.3).<sup>23</sup>

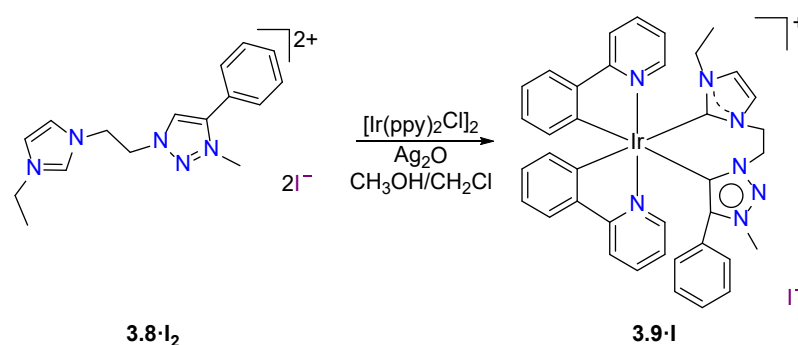


Scheme 3.3 Synthesis of 1,2,3-triazolium-imidazolium salt **3.7·I** using  $\text{CH}_3\text{I}$ .

1,2,3-triazoles can also be alkylated with oxonium salts and for example, the *tris*-(1,2,3-triazolyl)benzene precursor was methylated using  $\text{Me}_3\text{OBF}_4$  yielding the 1,2,3-triazolium salt **3.1·(BF<sub>4</sub>)<sub>3</sub>** (Figure 3.1).<sup>12</sup> In the same research article, the *tris*-triazolium salt **3.1·(BF<sub>4</sub>)<sub>3</sub>** was shown to be a selective receptor for chloride anions through strong hydrogen bonding interactions.<sup>12</sup> Using a similar synthetic approach, the *bis*-1,2,3-triazolium linked

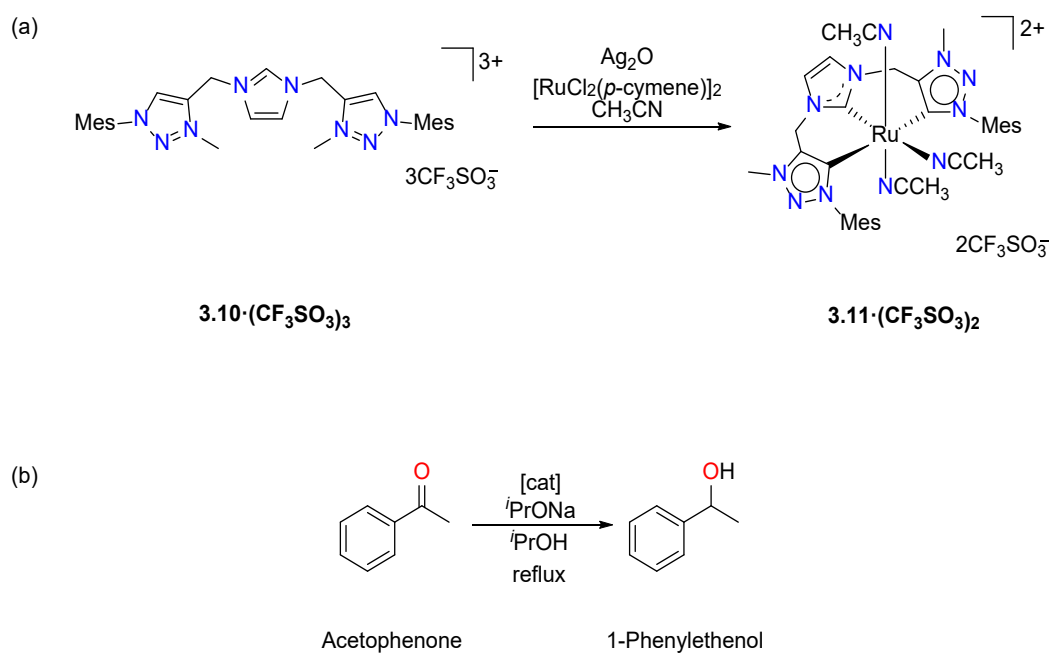
cyclophane **3.2·Cl<sub>2</sub>** and the *tetra*-1,2,3-triazolium-linked macrocycle **3.3·(BF<sub>4</sub>)<sub>4</sub>** (Figure 3.1) were also prepared using Me<sub>3</sub>OBF<sub>4</sub>.<sup>6, 11</sup>

1,2,3-triazolium salts have also been utilized as precursors for aNHC metal complexes and a range of metal complexes of this type have been previously synthesized.<sup>12-13, 28-32</sup> For example, the Ir(III) complex with both a normal NHC and an abnormal NHC derived from a 1,2,3-triazolium salt was prepared using a silver transmetallation method (Scheme 3.4).<sup>30</sup> In this study, the 1,2,3-triazolium pro-ligand **3.8·I<sub>2</sub>** was treated with Ag<sub>2</sub>O and [Ir(ppy)<sub>2</sub>Cl]<sub>2</sub> in one pot yielding complex **3.9·I** which features both normal and abnormal NHC donors. In addition, the authors noted that this complex was luminescent and has the potential to be a cell imaging reagent for microscopy studies.<sup>30</sup>



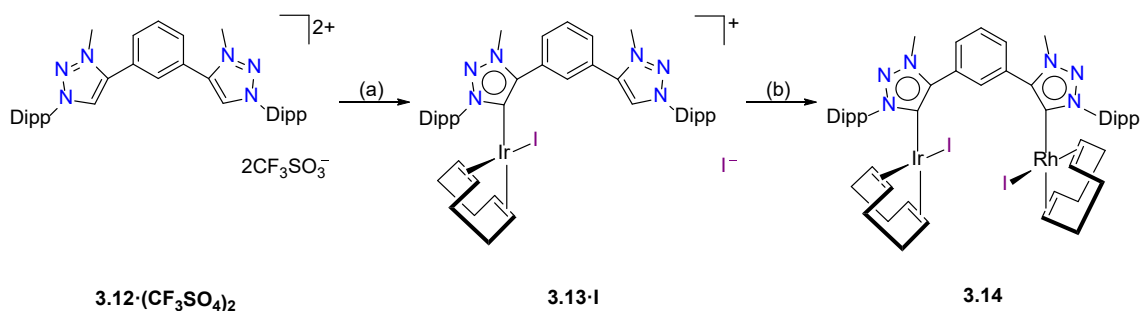
Scheme 3.4 Synthesis of Ir(III) complex **3.9·I** with a dual imidazole- and 1,2,3-triazole-based NHC ligand.

In a second example, a catalytically active Ru(II) complex **3.11·(CF<sub>3</sub>SO<sub>3</sub>)<sub>2</sub>** with a tridentate ligand system with imidazole- and 1,2,3-triazole-based NHC donors (Scheme 3.5 a) was prepared in a similar manner.<sup>28</sup> This complex was found to be catalytically active for transfer hydrogenation of acetophenone (Scheme 3.5 b) and the desired product 1-phenylethanol was produced in the presence of complex **3.11·(CF<sub>3</sub>SO<sub>3</sub>)<sub>2</sub>** as the catalyst (0.5 mol %) with 98% conversion in 80 minutes.<sup>28</sup>



Scheme 3.5 (a) Synthesis of Ru(II) complex **3.11**·(CF<sub>3</sub>SO<sub>3</sub>)<sub>2</sub> and (b) transfer hydrogenation of acetophenone reaction catalysed using **3.11**·(CF<sub>3</sub>SO<sub>3</sub>)<sub>2</sub>.

Interestingly, 1,2,3-triazolium groups have also been utilized for the synthesis of heterobimetallic complexes.<sup>22, 33</sup> Here the Ir(I)-Rh(I) heterobimetallic complex **3.14** (Scheme 3.6) was prepared by the reaction of **3.12**·(CF<sub>3</sub>SO<sub>3</sub>)<sub>2</sub> with [Ir(μ-OMe)(COD)]<sub>2</sub> yielding the monometallic complex **3.13-I**, and this complex was then further reacted with [Rh(μ-OMe)(COD)]<sub>2</sub> yielding the heterobimetallic complex **3.14** (Scheme 3.6).<sup>33</sup>



Scheme 3.6 Synthesis of the Ir(I)-Rh(I) heterobimetallic complex **3.14**. (a) [Ir(μ-OMe)(COD)]<sub>2</sub>, KI and (b) [Rh(μ-OMe)(COD)]<sub>2</sub>, KI.

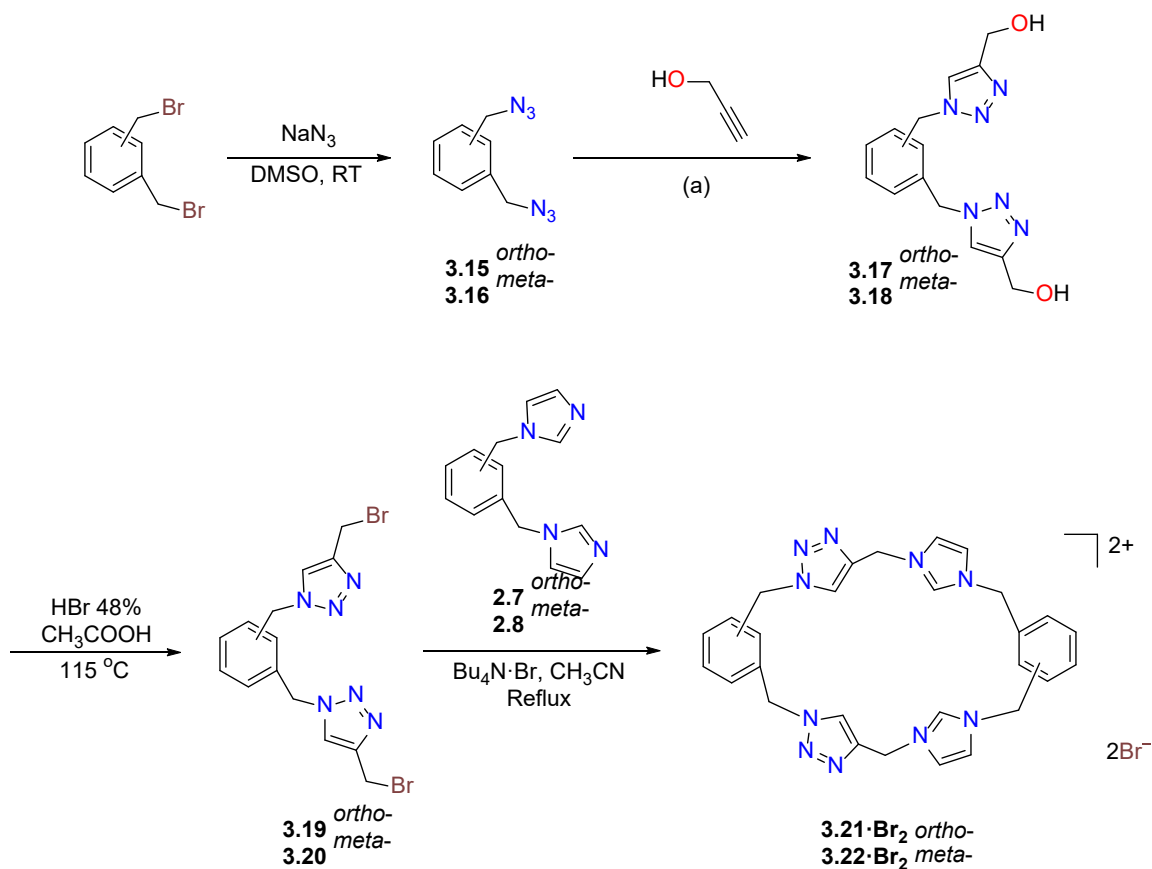
The anion binding properties of compounds of this type offer the potential for developing novel sensors for biologically and environmentally important anions.<sup>1, 5-11</sup> In addition, compounds of this type can also serve as precursors for abnormal NHC metal complexes for a range of applications including for the development of novel catalysts.<sup>28, 30</sup> Therefore, we were interested in the synthesis of macrocycles containing 1,2,3-triazolium and imidazolium groups using a stepwise macrocyclization method. As described in Chapter 2, modular stepwise synthetic approaches can be used to selectively prepare both symmetrical and asymmetrical macrocyclic compounds. In this chapter, the synthesis of novel macrocycles containing both imidazolium and 1,2,3-triazolium groups using a stepwise synthetic approach is described. In addition, the anion binding properties of the synthesized macrocycles was also evaluated. The synthesis of the corresponding metal complexes is also discussed.

## 3.2 Results and discussion

### 3.2.1 Synthesis of macrocycles containing 1,2,3-triazole and imidazolium groups

A stepwise macrocyclization method was developed to prepare macrocycles containing 1,2,3-triazole and imidazolium groups. The synthesis of the precursor compounds **3.21·Br<sub>2</sub>** and **3.22·Br<sub>2</sub>** (Scheme 3.7) involved a reaction of either  $\alpha,\alpha'$ -dibromo-*o*-xylene or  $\alpha,\alpha'$ -dibromo-*m*-xylene and sodium azide yielding 1,2-*bis*(azidomethyl)benzene **3.15** and 1,3-*bis*(azidomethyl)benzene **3.16** respectively. CuAAC conditions were then used to combine **3.15** and **3.16** with propargyl alcohol in the presence of copper sulfate and sodium ascorbate yielding the *bis*-1,2,3-triazolyl species **3.17** and **3.18**. The alcohol was then converted to a bromide group using HBr in acetic acid to obtain **3.19** and **3.20** (Scheme 3.7). The macrocyclic compounds **3.21·Br<sub>2</sub>** and **3.22·Br<sub>2</sub>** were then

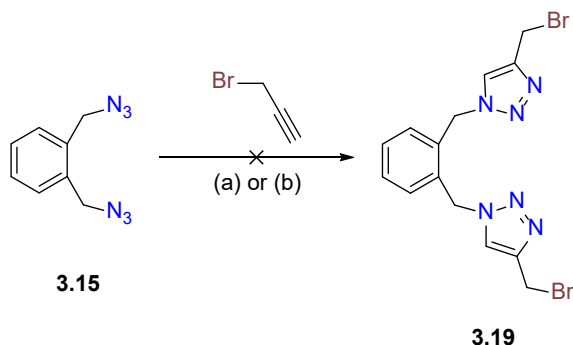
prepared by reaction of **3.19** and **2.7** or **3.20** and **2.8** in the presence of  $\text{Bu}_4\text{N}^+\text{Br}^-$  (Scheme 3.7).



Scheme 3.7 General synthetic route for the preparation of 1,2,3-triazole-imidazolium linked macrocycle **3.21·Br<sub>2</sub>** and **3.22·Br<sub>2</sub>**. Condition (a)  $\text{CuSO}_4\cdot 5\text{H}_2\text{O}$ , sodium ascorbate,  $\text{CH}_3\text{COOH}$ ,  $\text{BuOH}/\text{H}_2\text{O}$  1:1, RT.

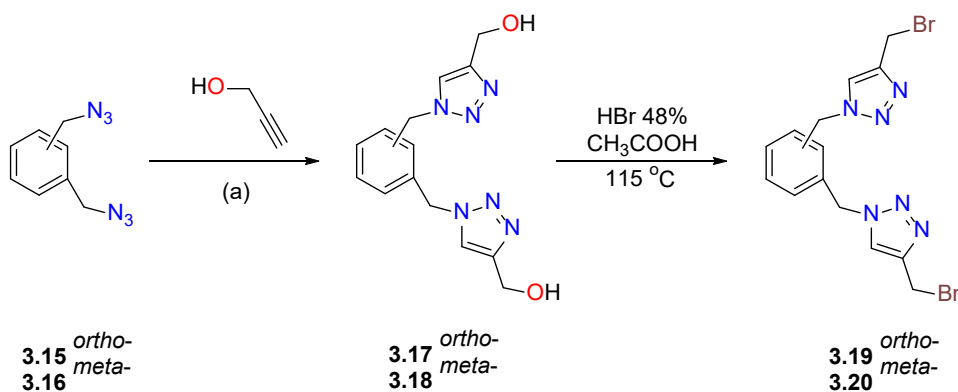
In an initial attempt to perform the ‘click reaction’, **3.15** was reacted with two equivalents of propargyl bromide in the presence of  $\text{CuI}$  and *tris*(benzyltriazolylmethyl)amine (TBTA). Unfortunately, however this reaction was unsuccessful in producing the desired product (Scheme 3.8). Consultation of the literature suggested that the *in situ* generation of the  $\text{Cu(I)}$  catalyst could be achieved by reducing copper sulfate with sodium ascorbate.<sup>18, 34</sup> Furthermore, published results suggest that the addition of acetic acid can also accelerate the reaction rate and provide a better yield of the 1,2,3-triazole.<sup>19</sup> Hence, **3.15** and propargyl bromide were reacted in the presence of cupric

sulfate and sodium ascorbate with acetic acid. Unfortunately, however this attempt was also unsuccessful in yielding the desired product.



Scheme 3.8 Attempts to synthesis **3.19** via CuAAC catalysed reaction of **3.15** with propargyl bromide. Conditions (a) CuI, TBTA, <sup>t</sup>BuOH/H<sub>2</sub>O 1:1, RT and (b) CuSO<sub>4</sub>·5H<sub>2</sub>O, sodium ascorbate, CH<sub>3</sub>COOH, <sup>t</sup>BuOH/H<sub>2</sub>O 1:1, RT.

Alternatively, it was envisaged that the desired bromomethyl substituted 1,2,3-triazole species could be prepared in two steps.<sup>35</sup> In this approach, the *bis*-alcohol compounds **3.17** and **3.18** were prepared and these were then converted to alkyl bromides using HBr in glacial acetic acid yielding compounds **3.19** and **3.20** (Scheme 3.9).



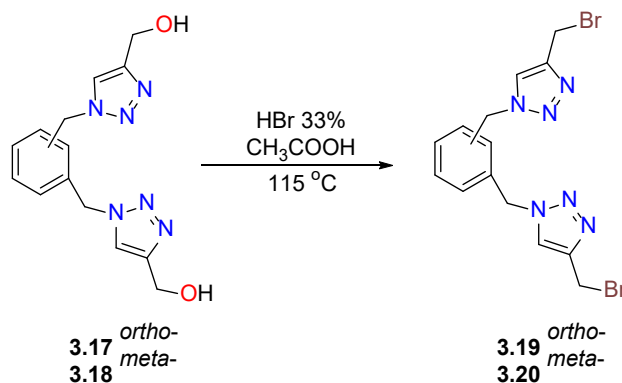
Scheme 3.9 Synthesis of bromomethyl substituted 1,2,3-triazole species **3.19** and **3.20** via stepwise method. Condition (a) CuSO<sub>4</sub>·5H<sub>2</sub>O, sodium ascorbate, CH<sub>3</sub>COOH, <sup>t</sup>BuOH/H<sub>2</sub>O 1:1, RT.

In detail, compounds **3.17** and **3.18** were prepared by the reaction of **3.15** or **3.16** with two equivalents of propargyl alcohol in presence of Cu(I) which was generated *in situ* from copper sulfate and sodium ascorbate (Scheme 3.9). The <sup>1</sup>H-NMR spectra exhibited new

downfield shifted signals at 7.99 ppm for **3.17** and 8.00 ppm for **3.18** suggesting the formation of the 1,2,3-triazole ring. In addition, signals corresponding to the methylene groups (4.52 ppm and 4.05 ppm) and the hydroxyl groups (5.19 and 5.16 ppm) were observed for **3.17** and **3.18** respectively, indicating the formation of the hydroxymethyl species. Furthermore, high-resolution mass spectra exhibited signals for the molecular ions in each case, for example in the case of **3.19** the base peak was observed at  $m/z = 301.1402$ , which corresponds to the formula of  $[C_{14}H_{17}N_6O_2]^+$  (calcd = 301.1408) (protonated cation).

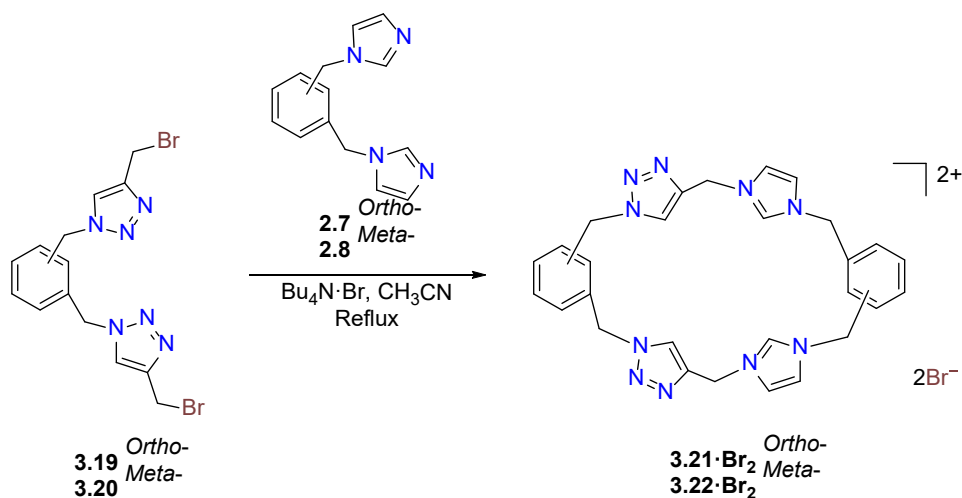
With the successful synthesis of **3.17** and **3.18**, attempts were made to brominate **3.17** to obtain the dibromo- species **3.19** (Scheme 3.10). After consultation of the literature, it was thought that the hydroxyl group could be converted to an alkylbromide using either *N*-bromosuccinimide (NBS) or a hydrobromic acid solution.<sup>36-38</sup> In early attempts to form **3.19** using either NBS in the presence of  $PPh_3$  or a 45% aqueous solution of HBr no product was isolated due to purification problems. Compounds **3.17** and **3.18** were successfully brominated in good yield using a 33% solution of HBr in acetic acid yielding **3.19** and **3.20** respectively (Scheme 3.10). The formation of these compounds was confirmed using  $^1H$ -NMR spectroscopy and in each case a downfield shift of the methylene group proton singlet signals was observed with these groups resonating at 4.57 and 4.73 ppm for **3.19** and **3.20** respectively. In addition, the high-resolution mass spectrum for **3.19** exhibited a peak at  $m/z = 448.9528$  corresponding to the formula  $[C_{14}H_{14}N_6Br_2Na]^+$  (calcd = 448.9518) which is the  $[M+Na]^+$  species. Meanwhile, the high-resolution mass spectrum for **3.20** showed a base peak at  $m/z = 426.9704$  which corresponds to the molecular fragment  $[C_{14}H_{15}N_6Br_2]^+$  (calcd = 426.9699) which corresponds to the protonated cation.





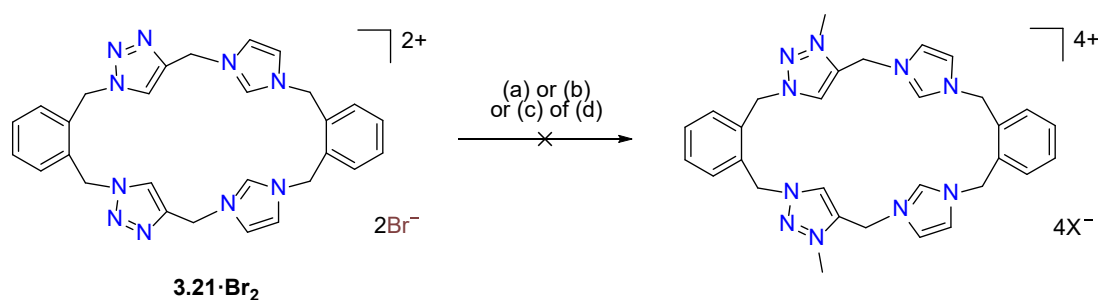
Scheme 3.10 Synthesis of **3.19** and **3.20** using a solution of HBr 33% in acetic acid.

The *ortho*- and *meta*- macrocyclic compounds **3.21·Br<sub>2</sub>** and **3.22·Br<sub>2</sub>** containing 1,2,3-triazole and imidazolium groups were prepared by reacting equal quantities of either **3.19** and **2.7** or **3.20** and **2.8** under high dilution condition in the presence of the templating reagent BuN<sub>4</sub>·Br (5.0 eq.). The <sup>1</sup>H-NMR spectra for **3.21·Br<sub>2</sub>** and **3.22·Br<sub>2</sub>** showed a signal for the C2-H imidazolium protons at 9.04 and 9.32 ppm while the 1,2,3-triazole C-H protons signal resonated at 8.15 and 8.33 ppm for **3.21·Br<sub>2</sub>** and **3.22·Br<sub>2</sub>** respectively. Consistent with the presence of the differentazole rings, the protons of benzylic groups resonate as two individual singlet signals at 5.53 and 5.72 ppm for **3.21·Br<sub>2</sub>** and 5.53 and 5.61 ppm for **3.22·Br<sub>2</sub>**.



Scheme 3.11 Synthesis of the *ortho*- and *meta*-substituted macrocyclic compounds **3.21·Br<sub>2</sub>** and **3.22·Br<sub>2</sub>**.

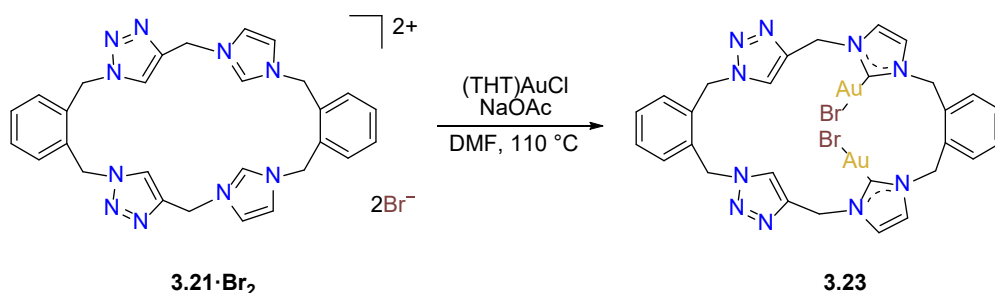
To prepare the macrocycles featuring both 1,2,3-triazolium and imidazolium units, attempts were made to alkylate the 1,2,3-triazole group of macrocycle **3.21**·Br<sub>2</sub> with reagents such as CH<sub>3</sub>I, Me<sub>3</sub>OBF<sub>4</sub> and CH<sub>3</sub>OSO<sub>2</sub>CF<sub>3</sub> (Scheme 3.12). In the case of the reaction of **3.21**·Br<sub>2</sub> with CH<sub>3</sub>I at reflux in acetonitrile or in a sealed tube unreacted **3.21**·Br<sub>2</sub> and small amounts of unidentified products were obtained. These unidentified materials may be the result of either partial alkylation of 1,2,3-triazole units yielding the mono-alkylation species or slow decomposition of macrocyclic precursor.<sup>11</sup> The behaviours of these compound are consistent with a related *tetra*-1,2,3-triazole macrocycle reported by Beer and co-workers.<sup>11</sup> When **3.21**·Br<sub>2</sub> was reacted with trifluoromethanesulfonate, decomposition of the starting material was observed and no product could be isolated. Similarly, the reaction of **3.21**·Br<sub>2</sub> with Me<sub>3</sub>OBF<sub>4</sub> at reflux in acetonitrile did not produce the desired product. The difficulties encountered in the alkylation of **3.21**·Br<sub>2</sub> may be the result of the constrained macrocyclic structure of this compound causing alkylation to be less favourable. In addition, the imidazolium groups in the macrocycle carry positive charges which may decrease the nucleophilicity of the nitrogen atom on the 1,2,3-triazole ring. Consequently, the alkylation of the 1,2,3-triazole groups for **3.21**·Br<sub>2</sub> could not be achieved.



Scheme 3.12 Attempted alkylation of **3.21**·Br<sub>2</sub> using different alkylating reagents. Conditions (a) CH<sub>3</sub>I, CH<sub>3</sub>CN, reflux and (b) CH<sub>3</sub>I, CH<sub>3</sub>CN, sealed, 120 °C and (c) CH<sub>3</sub>OSO<sub>2</sub>CF<sub>3</sub>, CH<sub>3</sub>CN, RT and (d) Me<sub>3</sub>OBF<sub>4</sub>, CH<sub>3</sub>CN, reflux.

### 3.2.2 Synthesis of the metal complexes of macrocycle **3.21·Br<sub>2</sub>**

To further investigate the properties of these macrocycles, the Au(I) complex **3.23** was prepared by the reaction of **3.21·Br<sub>2</sub>** and (THT)AuCl (2.0 eq.) in the presence of NaOAc (Scheme 3.13). The formation of **3.23** was confirmed by <sup>1</sup>H-NMR and <sup>13</sup>C-NMR spectra and high-resolution mass spectrometry. The <sup>1</sup>H-NMR spectra for **3.23** showed the absence of signal of imidazolium C2-H protons while the triazole proton signal resonated at 8.07 ppm, which is consistent with the deprotonation and coordination of C2 carbon of the imidazolium group only (Figure 3.2). In addition, the downfield shift of C2 carbon signal at 170.71 ppm also suggests the formation of the coordinated carbene. Furthermore, the coordination and the spectrum exhibited a peak at *m/z* = 977.0832 which corresponds to the formula [C<sub>28</sub>H<sub>26</sub>N<sub>10</sub>Au<sub>2</sub>Br]<sup>+</sup> (calcd = 977.0830). In addition, the isotopic pattern is consistent with the formulation of the complex as shown by the theoretical spectrum for this ion (Figure 3.3 b). Unfortunately, however due to the low yield (12.6%) of the macrocyclic pro-ligand **3.22·Br<sub>2</sub>**, the preparation of Au(I) complex from this compound was not undertaken.



Scheme 3.13 Synthesis of the dinuclear Au(I) complex **3.23** from pro-ligand **3.21·Br<sub>2</sub>**.

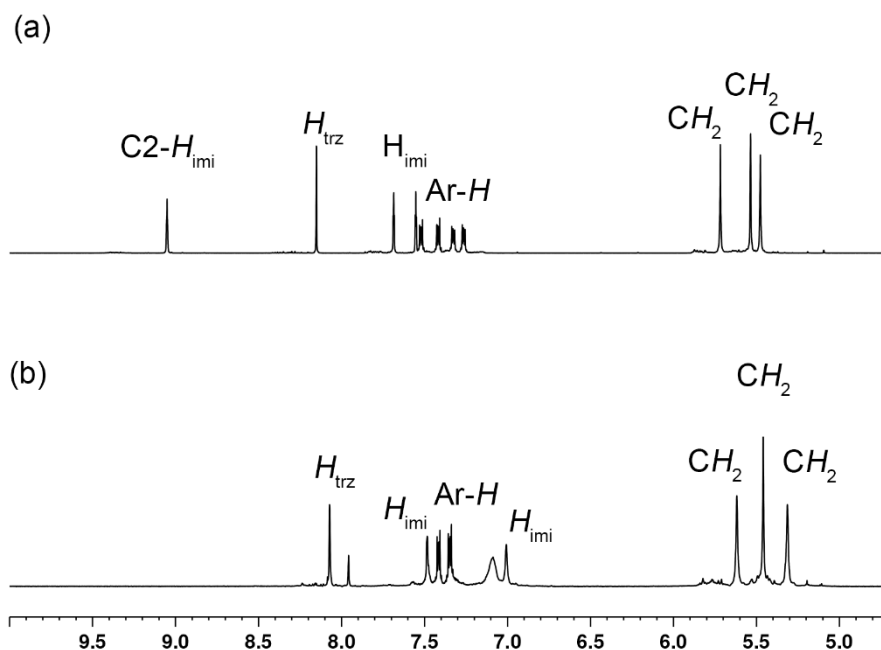


Figure 3.2 Stacked  $^1\text{H}$ -NMR spectra of (a) pro-ligand **3.21**· $\text{Br}_2$  and (b) dinuclear Au(I) complex **3.23**.

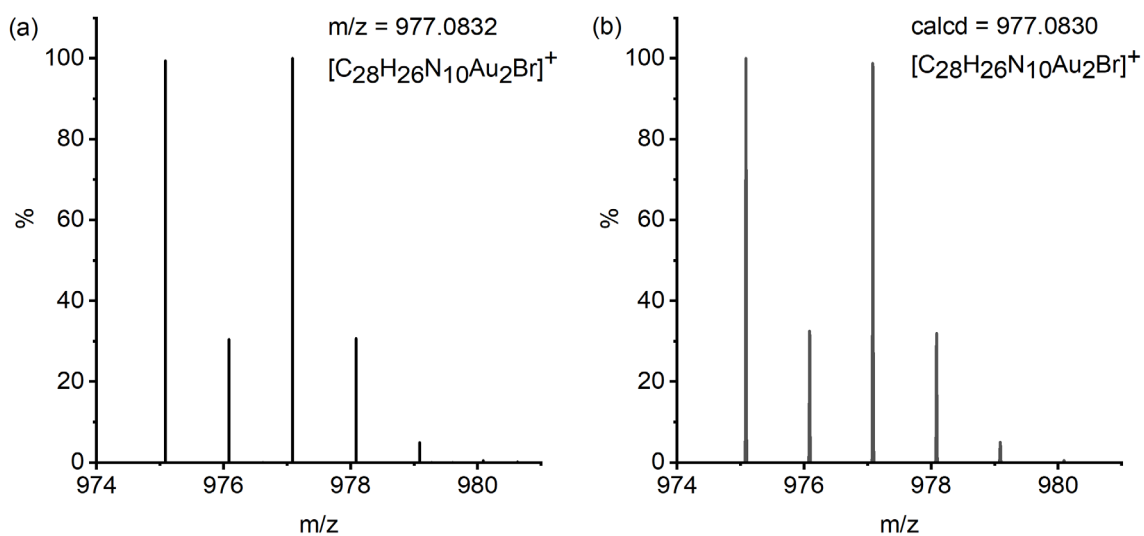


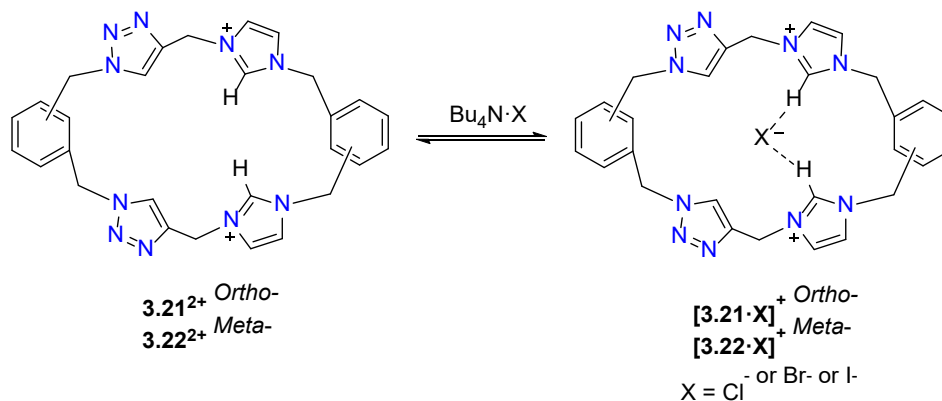
Figure 3.3 (a) Base peak from the high-resolution mass spectrum of complex **3.23** and (b) Theoretical mass spectrum for  $[\text{C}_{28}\text{H}_{26}\text{N}_{10}\text{Au}_2\text{Br}]^+$ .

### 3.2.3 Anion binding studies

Due to the dicationic charge of the imidazolium linked macrocycles, the propensity of **3.21**·( $\text{PF}_6$ )<sub>2</sub> and **3.22**·( $\text{PF}_6$ )<sub>2</sub> to bind the halide anions  $\text{F}^-$ ,  $\text{Cl}^-$ ,  $\text{Br}^-$  and  $\text{I}^-$  (as their *tetra*-*n*-butylammonium halide salts) was investigated using  $^1\text{H}$ -NMR titration experiments. In

early studies, the addition of Bu<sub>4</sub>N·F into the solutions of **3.21**·(PF<sub>6</sub>)<sub>2</sub> and **3.22**·(PF<sub>6</sub>)<sub>2</sub> in d<sub>6</sub>-DMSO caused a rapid colour change to yellow. Additionally, the <sup>1</sup>H-NMR spectra of these receptors showed that the colour change occurred simultaneously with significant broadening and downfield shift of the C2-H imidazolium proton signals (Figure A.61). Furthermore, the appearance of new unidentified <sup>1</sup>H-NMR signals were observed suggesting the decomposition of the macrocyclic receptor. Consequently, the anion binding studies between receptors and F<sup>-</sup> were not undertaken.

Addition of increasing equivalents (0.25 – 14.0 eq.) of Bu<sub>4</sub>N·Cl to solutions of **3.21**·(PF<sub>6</sub>)<sub>2</sub> and **3.22**·(PF<sub>6</sub>)<sub>2</sub> in d<sub>6</sub>-DMSO resulted in significant downfield shift of the C2-H imidazolium proton signal from 9.01 to 9.40 ppm and 9.32 to 9.91 ppm for **3.21**·(PF<sub>6</sub>)<sub>2</sub> and **3.22**·(PF<sub>6</sub>)<sub>2</sub> respectively. In addition, the benzylic proton signals also shifted downfield from 5.52 to 5.56 and 5.71 to 5.75 for **3.21**·(PF<sub>6</sub>)<sub>2</sub> and 5.52 to 5.63 and 5.60 to 5.63 for **3.22**·(PF<sub>6</sub>)<sub>2</sub>. In contrast to the downfield shift of C2-H imidazolium proton signals, little or no changes were observed in the chemical shifts for the C4/5-H proton of the 1,2,3-triazole units for each macrocycle, which is consistent with this group not being involved in the anion binding interaction.<sup>6, 11</sup> This is likely to be the result of the C4/5-H protons on the 1,2,3-triazole units being less acidic than the imidazolium C2-H proton. Using a similar method, the addition of increasing equivalents of Bu<sub>4</sub>N·Br and Bu<sub>4</sub>N·I resulted in downfield signal shifts in the imidazolium C2-H proton signals. However, these anions (especially I<sup>-</sup>) interact with receptors **3.21**<sup>2+</sup> and **3.22**<sup>2+</sup> more weakly than Cl<sup>-</sup>. The experimental titration data for **3.21**·(PF<sub>6</sub>)<sub>2</sub> and **3.22**·(PF<sub>6</sub>)<sub>2</sub> with halides is shown in Figure 3.5. Jobs plot experiments were used to analyse the stoichiometry of the interactions between the macrocyclic receptors and the halide anions Cl<sup>-</sup>, Br<sup>-</sup> and I<sup>-</sup> and these experiments exhibited maxima at  $\chi = 0.5$  (Figure 3.4) suggesting 1:1 stoichiometry for both **3.21**<sup>2+</sup> and **3.22**<sup>2+</sup> with the halide anions (Scheme 3.14).



Scheme 3.14 Receptor **3.21**<sup>2+</sup> and **3.22**<sup>2+</sup> interact with halide such as Cl<sup>-</sup>, Br<sup>-</sup> and I<sup>-</sup> in a 1:1 stoichiometry.

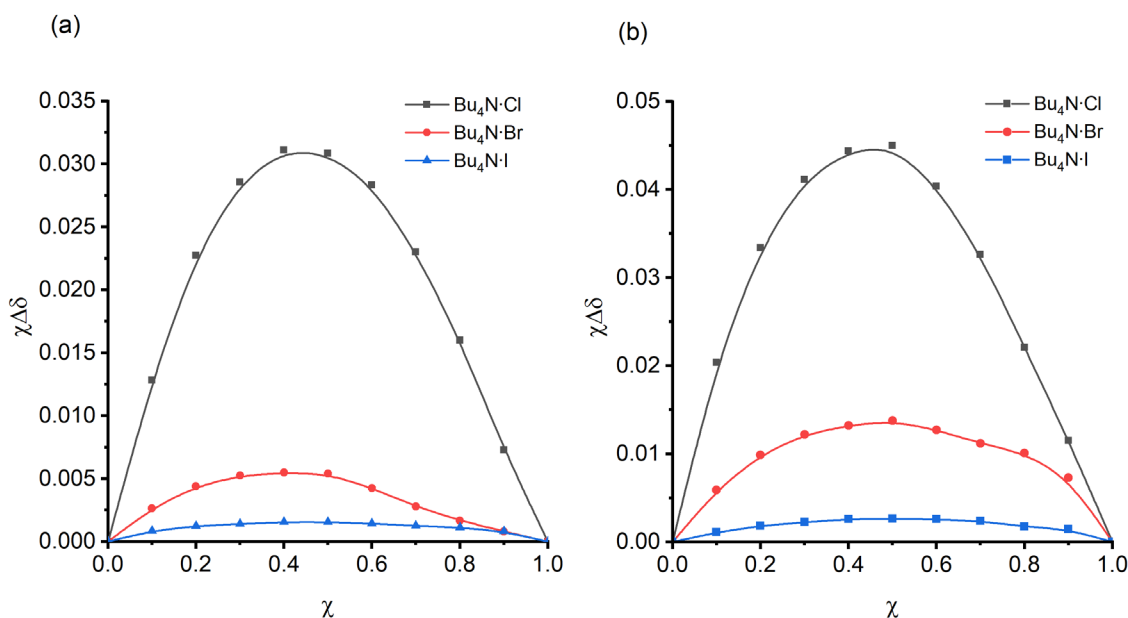


Figure 3.4 Job plots based on the <sup>1</sup>H-NMR titration of (a) **3.21**·(PF<sub>6</sub>)<sub>2</sub> with Bu<sub>4</sub>N·Cl, Bu<sub>4</sub>N·Br and Bu<sub>4</sub>N·I and (b) **3.22**·(PF<sub>6</sub>)<sub>2</sub> with Bu<sub>4</sub>N·Cl, Bu<sub>4</sub>N·Br and Bu<sub>4</sub>N·I in d<sub>6</sub>-DMSO solution.

Using the computer program HypNMR 2018,<sup>39-40</sup> the association (binding) constants  $K_a$  (M<sup>-1</sup>) between the macrocycle receptors **3.21**·(PF<sub>6</sub>)<sub>2</sub> and **3.22**·(PF<sub>6</sub>)<sub>2</sub> and the halides (Cl<sup>-</sup>, Br<sup>-</sup> and I<sup>-</sup>) were calculated based on the <sup>1</sup>H-NMR titration data. The stacked <sup>1</sup>H-NMR spectra are shown in Figure A.62 to Figure A.67 in Appendix and the fitted binding curves are shown in Figure 3.5 (red dashed lines) and the calculated association constants are provided in Table 3.1. The calculated data for the macrocycle receptors

**3.21·(PF<sub>6</sub>)<sub>2</sub>** and **3.22·(PF<sub>6</sub>)<sub>2</sub>** showed a selective trend of Cl<sup>-</sup> > Br<sup>-</sup> > I<sup>-</sup> (Figure 3.5 and Table 3.1) and are significantly lower than those reported previously for related imidazolium macrocyclic receptors.<sup>41-42</sup> For example, Beer and co-worker reported the association values between the *tetra*-imidazolium macrocycle **1.23·(PF<sub>6</sub>)<sub>4</sub>** and Cl<sup>-</sup>, Br<sup>-</sup> and I<sup>-</sup> were 1100, 1050 and 560 M<sup>-1</sup> respectively.<sup>41</sup> In an addition example, the association constants values for receptors **2.15·(PF<sub>6</sub>)<sub>4</sub>** prepared in chapter 2 were 501, 126 and 63 M<sup>-1</sup> for Cl<sup>-</sup>, Br<sup>-</sup> and I<sup>-</sup> which are also significantly higher than the values for receptors **3.21·(PF<sub>6</sub>)<sub>2</sub>** and **3.22·(PF<sub>6</sub>)<sub>2</sub>** (Table 3.1).<sup>42</sup> These results suggest that the macrocycle receptors **3.21·(PF<sub>6</sub>)<sub>2</sub>** and **3.22·(PF<sub>6</sub>)<sub>2</sub>** only weakly interact with halide anions (i.e. Cl<sup>-</sup>, Br<sup>-</sup> and I<sup>-</sup>). The weak binding between the receptors and the halides likely result from a weaker electrostatic interaction between the macrocycles and the anions.<sup>11</sup> Compound **3.21·(PF<sub>6</sub>)<sub>2</sub>** and **3.22·(PF<sub>6</sub>)<sub>2</sub>** feature a di-positive charge on the two imidazolium groups while the 1,2,3-triazole groups in these compounds are electronically neutral. As a result, the macrocycle **3.21·(PF<sub>6</sub>)<sub>2</sub>** and **3.22·(PF<sub>6</sub>)<sub>2</sub>** carry a lower overall charged compared to the *tetra*-imidazolium macrocycles **2.15·(PF<sub>6</sub>)<sub>4</sub>** and **2.16·(PF<sub>6</sub>)<sub>4</sub>** reported in chapter 2. In addition, the smaller cavity size of these macrocycles, which is due to the linker lengths may also be responsible for the weak interaction between these receptors and halides. Interestingly, the *meta*-substituted macrocycle **3.21·(PF<sub>6</sub>)<sub>2</sub>** exhibits a slightly stronger binding to the halide anions when compared to the *ortho*-substituted macrocycle **3.22·(PF<sub>6</sub>)<sub>2</sub>**.

Table 3.1 Association constants of the 1,2,3-triazole *bis*-imidazolium macrocycles **3.21**·(PF<sub>6</sub>)<sub>2</sub> and **3.22**·(PF<sub>6</sub>)<sub>2</sub> and the halide anions Cl<sup>-</sup>, Br<sup>-</sup> and I<sup>-</sup> (added as their tetrabutylammonium salts).

	<b>3.21</b> ·(PF <sub>6</sub> ) <sub>2</sub>	<b>3.22</b> ·(PF <sub>6</sub> ) <sub>2</sub>
Cl <sup>-</sup>	24.10	29.65
Br <sup>-</sup>	16.90	18.37
I <sup>-</sup>	9.62	6.78

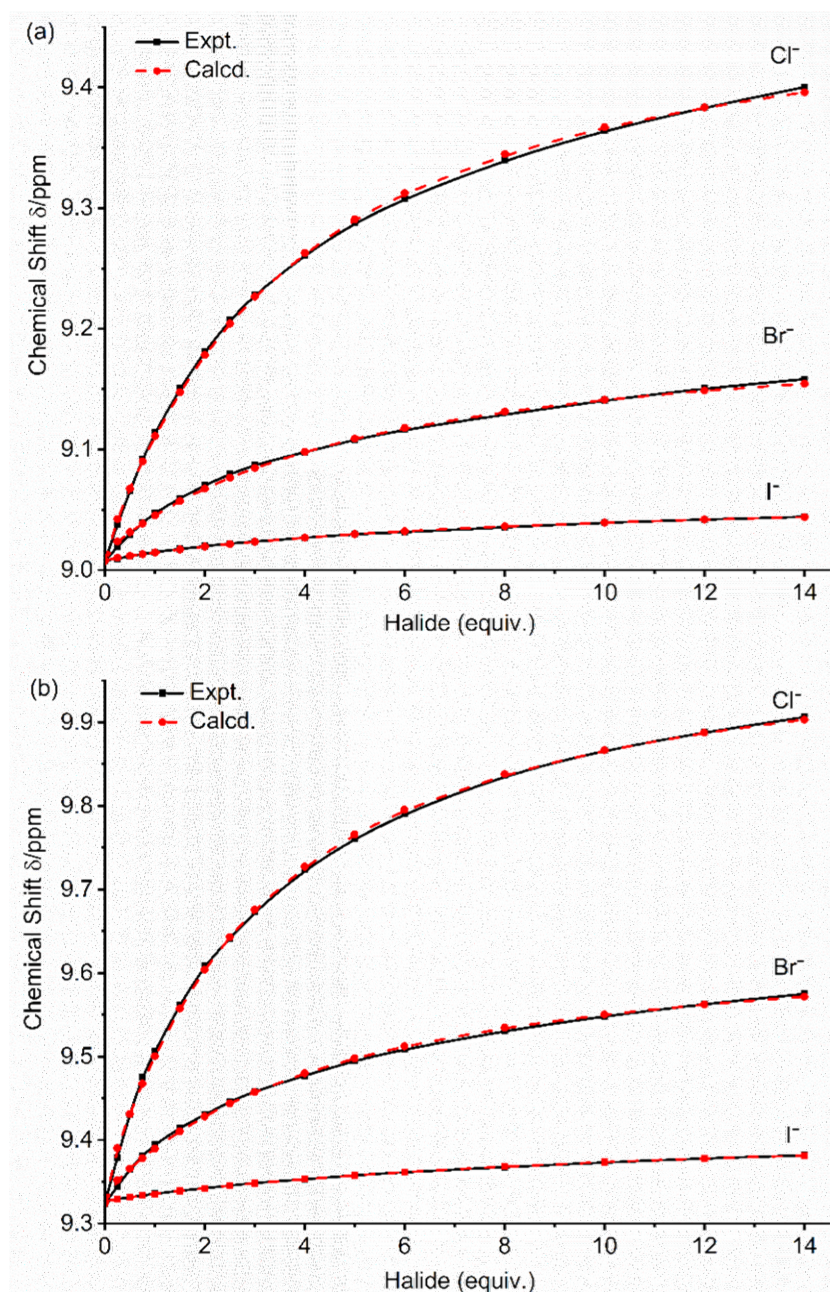


Figure 3.5 Experimental titration data (black solid line, squares) and calculated binding isotherms (red dashed line, circles) for the addition of Cl<sup>-</sup>, Br<sup>-</sup> or I<sup>-</sup> (as Bu<sub>4</sub>N<sup>+</sup> salts) to a solutions of (a) **3.21**·(PF<sub>6</sub>)<sub>2</sub> and (b) **3.22**·(PF<sub>6</sub>)<sub>2</sub> in d<sub>6</sub>-DMSO.



### 3.3 Conclusion

In this chapter, a series of two macrocycles that incorporated 1,2,3-triazole and imidazolium groups were synthesized using a modular stepwise method. In this synthetic strategy, the *bis*-(bromomethyl)-1,2,3-triazole precursors were first prepared using copper(I)-catalyzed azide-alkyne cycloaddition (CuAAC) reaction. These precursors were then reacted with either *ortho*- or *meta*-substituted *bis*(imidazolylmethyl)benzene. Although a number of studies have reported the synthesis of symmetrical imidazolium linked macrocycle<sup>41, 43-44</sup> and 1,2,3-triazolium linked macrocycles<sup>3, 8, 11</sup>, this is the first time asymmetrical macrocycles which carry different azole groups i.e. imidazolium and 1,2,3-triazole have been prepared. However, despite several attempts to alkylate the 1,2,3-triazole groups to obtain 1,2,3-triazolium units, these were unsuccessful. This lack of success may be due to the positive charge associated with the imidazolium group decreasing nucleophilicity of the 1,2,3-triazole nitrogen atoms. Using <sup>1</sup>H-NMR titration studies and the HypNMR2018 computer program,<sup>39-40</sup> the association constants between **3.21**·(PF<sub>6</sub>)<sub>2</sub> and **3.22**·(PF<sub>6</sub>)<sub>2</sub> and the halide anions (Cl<sup>-</sup>, Br<sup>-</sup> and I<sup>-</sup>) were determined to be in the range of 29.7 – 6.8 M<sup>-1</sup>. These results revealed that this type of macrocyclic receptor only weakly associate with halide anions and this may be due to the lower di-positive charge carried by these molecules. In addition, the low affinity for anions shown by these receptors compared with the previously reported relevant macrocycles suggests that they will not be useful as anion receptors.<sup>41</sup> Imidazolium salts are also precursors for the preparation on NHC metal complexes and a dinuclear Au(I)-NHC complex from the receptor **3.21**·Br<sub>2</sub> was also prepared. The Au(I) atoms were found to coordinate to the carbene (i.e. imidazolylidene) and the 1,2,3-triazole groups were not coordinated.

### 3.4 Experimental

#### 3.4.1 <sup>1</sup>H-NMR titration studies

A solution of the title compound (5 mg) in d<sub>6</sub>-DMSO (500 μL) and a 0.79 M solution of Bu<sub>4</sub>N·X (X=Cl, Br and I) in d<sub>6</sub>-DMSO were prepared respectively. To the solution of the title compound, increasing equivalents (0.25 – 14.0 eq.) of 0.79 M Bu<sub>4</sub>N·X solution was added, and the resultant solution was thoroughly mixed. The <sup>1</sup>H-NMR spectrum was recorded ~2 minutes after each addition at 300 K.

#### 3.4.2 Jobs plot analysis

A solution of the title compound (50 mg/mL) in d<sub>6</sub>-DMSO and a 0.020 M solution of Bu<sub>4</sub>N·X (X=Cl, Br and I) in d<sub>6</sub>-DMSO were prepared respectively. A varied fraction of title compound solution and Bu<sub>4</sub>N·X solution was added and diluted with d<sub>6</sub>-DMSO to 500 μL to maintain the total concentration of substance at 10 mM. The resultant solution was thoroughly mixed and the <sup>1</sup>H-NMR spectrum was recorded at 300 K.

#### 3.4.3 Synthesis

**3.15.** A mixture of α,α'-dibromo-*o*-xylene (2.00 g, 7.58 mmol) and NaN<sub>3</sub> (1.23 g, 18.94 mmol) in DMSO (50 mL) was stirred at RT for 3 d. The resultant mixture was diluted with water (100 mL) and extracted with diethyl ether (3 × 50 mL). The combined organic layer was washed with water (50 mL) and brine (50 mL) and was dried with MgSO<sub>4</sub>. The solvent was evaporated *in vacuo* yielding a yellow oil. Yield: 1.30 g, 91.1 %. <sup>1</sup>H-NMR (500.02 MHz, d<sub>6</sub>-DMSO): δ = 7.44 – 7.49 (m, 2H, ArH), 7.39 - 7.44 (m, 2H, ArH), 4.56 (s, 4H, CH<sub>2</sub>). <sup>13</sup>C-NMR (125.74 MHz, d<sub>6</sub>-DMSO): δ = 134.61 (C<sub>q</sub>), 130.52 (C<sub>Ar</sub>), 129.19 (C<sub>Ar</sub>), 51.43 (CH<sub>2</sub>). ESI-MS<sup>+</sup>: [C<sub>8</sub>H<sub>8</sub>N<sub>6</sub>Na]<sup>+</sup> m/z = 211.13, calcd = 211.07.

**3.16.** This compound was prepared using the same method as described for **3.15** from  $\alpha,\alpha'$ -dibromo-*m*-xylene (2.00 g, 7.58 mmol) and NaN<sub>3</sub> (1.23 g, 18.94 mmol). Yield 1.35 g, 94.7 %. (500.02 MHz, d<sub>6</sub>-DMSO):  $\delta$  = 7.42 – 7.47 (m, 1H, ArH), 7.34 - 7.40 (m, 3H, ArH), 4.49 (s, 4H, CH<sub>2</sub>). <sup>13</sup>C-NMR (125.74 MHz, d<sub>6</sub>-DMSO):  $\delta$  = 136.68 (C<sub>q</sub>), 129.59 (C<sub>Ar</sub>), 128.74 (C<sub>Ar</sub>), 128.61 (C<sub>Ar</sub>), 53.38 (CH<sub>2</sub>). ESI-MS<sup>+</sup>: [C<sub>8</sub>H<sub>8</sub>N<sub>6</sub>Na]<sup>+</sup> m/z = 211.13, calcd = 211.07.

**3.17.** A mixture of **3.15** (0.20 g, 1.06 mmol), propargyl alcohol (0.12 mL, 2.12 mmol), CuSO<sub>4</sub>·5H<sub>2</sub>O (0.016 g, 0.064 mmol), sodium ascorbate (0.025 g, 0.128 mmol) and acetic acid (0.073 mL, 1.28 mmol) in 1:1 water/isopropanol (5 mL) was stirred in 30 °C overnight. The resultant solid was collected and re-dissolved in hot methanol (30 mL) followed by filtration through a plug of silica gel. The solvent was evaporation *in vacuo* yielding a white solid. Yield: 0.17 g, 53.7%. <sup>1</sup>H-NMR: (500.02 MHz d<sub>6</sub>-DMSO):  $\delta$  = 7.99 (s, 2H, H<sub>trz</sub>), 7.33 – 7.36 (m, 2H, ArH), 7.11 – 7.15 (m, 2H, ArH), 5.80 (s, 4H, CH<sub>2</sub>), 5.19 (t, <sup>3</sup>J<sub>H-H</sub> = 5.6 Hz, 2H, CH<sub>2</sub>OH), 4.52 (d, <sup>3</sup>J<sub>H-H</sub> = 5.2 Hz, 2H, CH<sub>2</sub>OH). <sup>13</sup>C-NMR (125.74 MHz, d<sub>6</sub>-DMSO):  $\delta$  = 148.98 (C<sub>q</sub>), 134.81 (C<sub>q</sub>), 129.50 (C<sub>Ar</sub>), 129.22 (C<sub>Ar</sub>), 55.50 (CH<sub>2</sub>), 50.21 (CH<sub>2</sub>OH). ESI-MS<sup>+</sup>: [C<sub>14</sub>H<sub>16</sub>N<sub>6</sub>O<sub>2</sub>Na]<sup>+</sup> m/z = 323.20, calcd = 323.12

**3.18.** This compound was prepared using the same method as described for **3.17** from **3.16** (0.65 g, 3.45 mmol), propargyl alcohol (0.39 mL, 6.90 mmol), CuSO<sub>4</sub>·5H<sub>2</sub>O (0.051 g, 0.21 mmol), sodium ascorbate (0.083 g, 0.42 mmol) and acetic acid (0.24 mL, 4.20 mmol) in 1:1 water/isopropanol (10 mL). Yield: 0.45 g, 43.4%. <sup>1</sup>H-NMR: (500.02 MHz d<sub>6</sub>-DMSO):  $\delta$  = 8.00 (s, 2H, H<sub>trz</sub>), 7.38 (t, <sup>3</sup>J<sub>H-H</sub> = 6.8 Hz, 1H, ArH), 7.33 (s, 1H, ArH), 7.25 (d, <sup>3</sup>J<sub>H-H</sub> = 6.8 Hz, 2H, ArH), 5.56 (s, 4H, CH<sub>2</sub>), 5.16 (t, <sup>3</sup>J<sub>H-H</sub> = 4.8 Hz, 2H, CH<sub>2</sub>OH), 4.50 (d, <sup>3</sup>J<sub>H-H</sub> = 4.1 Hz, 4H, CH<sub>2</sub>OH). <sup>13</sup>C-NMR (125.74 MHz, d<sub>6</sub>-DMSO):  $\delta$  = 148.7 (C<sub>q</sub>), 137.22 (C<sub>q</sub>),

129.68 ( $C_{Ar}$ ), 128.17 ( $C_{Ar}$ ), 128.02 ( $C_{Ar}$ ), 123.32 ( $C_{trz}$ ), 55.51 ( $CH_2$ ), 52.92 ( $CH_2OH$ ).  
HRESI-MS<sup>+</sup>:  $[C_{14}H_{17}N_6O_2]^+$   $m/z = 301.1402$ , calcd = 301.1408.

**3.19.** A mixture of **3.17** (0.20 g, 0.67 mmol) and hydrobromic acid 33% w.t in acetic acid (25 mL, 142.8 mmol) was stirred at 105 °C for overnight. The resultant mixture was cooled to RT followed by addition of NaOH (5 M) to pH = 8. The mixture was then extracted with dichloromethane (3 × 20 mL) and the combined organic layer was washed with water (2 × 5 mL) and brine (5 mL). The organic layer was dried with Na<sub>2</sub>SO<sub>4</sub> followed by evaporation of solvent *in vacuo* yielding an off-white powder. Yield: 0.25 g, 88.1%. <sup>1</sup>H-NMR: (500.02 MHz d<sub>6</sub>-DMSO): δ = 8.21 (s, 2H,  $H_{trz}$ ), 7.35 – 7.38 (m, 2H,  $ArH$ ), 7.12 – 7.15 (m, 2H,  $ArH$ ), 5.81 (s, 4H,  $CH_2$ ), 4.57 (s, 4H,  $CH_2$ ). <sup>13</sup>C-NMR (125.74 MHz, d<sub>6</sub>-DMSO): δ = 144.40 ( $C_q$ ), 134.52 ( $C_q$ ), 129.63 ( $C_{Ar}$ ), 129.44 ( $C_{Ar}$ ), 125.03 ( $C_{trz}$ ), 50.39 ( $CH_2$ ), 23.77 ( $CH_2$ ). HRESI-MS<sup>+</sup>:  $[C_{14}H_{14}N_6Br_2Na]^+$   $m/z = 448.9528$ , calcd = 448.9518,  $[C_{14}H_{15}N_6Br_2]^+$   $m/z = 426.9717$ , calcd = 426.9699.

**3.20.** This compound was prepared using the same method as described for **3.19** from **3.18** (0.20 g, 0.67 mmol) and hydrobromic acid 33% w.t in acetic acid (25 mL, 142.8 mmol). Yield: 0.26 g, 91.6%. <sup>1</sup>H-NMR (500.02 MHz d<sub>6</sub>-DMSO): 8.24 (s, 2H,  $H_{trz}$ ), 7.39 (t, <sup>3</sup> $J_{H-H} = 7.5$  Hz, 1H,  $ArH$ ), 7.33 (s, 1H,  $ArH$ ), 7.26 (dd, <sup>3</sup> $J_{H-H} = 7.8$  Hz, <sup>4</sup> $J_{H-H} = 1.5$  Hz, 2H,  $ArH$ ), 5.59 (s, 4H,  $CH_2$ ), 4.73 (s, 4H,  $CH_2$ ). <sup>13</sup>C-NMR (125.74 MHz, d<sub>6</sub>-DMSO): 144.30 ( $C_q$ ), 136.93 ( $C_q$ ), 129.83 ( $C_{Ar}$ ), 128.33 ( $C_{Ar}$ ), 128.12 ( $C_{Ar}$ ), 124.82 ( $C_{trz}$ ), 53.07 ( $CH_2$ ), 23.84 ( $CH_2$ ). HRESI-MS<sup>+</sup>:  $[C_{14}H_{15}N_6Br_2]^+$   $m/z = 426.9704$ , calcd = 426.9699.

**3.21·Br<sub>2</sub>.** A mixture of **3.19** (0.050 g, 0.12 mmol), **2.7** (0.011 g, 0.12 mmol) and Bu<sub>4</sub>N·Br (0.19 g, 0.60 mmol) in acetonitrile was stirred at reflux for 5 d. The resultant mixture was

filtered while hot and the organic filtrate was dried in vacuo yielding a colourless residue. The resultant residue was washed with acetonitrile ( $3 \times 15$  mL) yielding a white solid followed by recrystallization from a mixture of methanol and diethyl ether yielding a white solid. The solid was re-dissolved in water (2 mL) and then filtered through a plug of Celite. To this solution, a solution of  $\text{KPF}_6$  saturated in aqueous (1 mL) was added to obtain a white precipitate. The precipitate was washed with isopropanol (5 mL) and recrystallised from a mixture of acetonitrile and diethyl ether to obtain a white crystalline. Yield: 0.026 g, 27.3%.  $^1\text{H-NMR}$ : (500.02 MHz  $\text{d}_6$ -DMSO):  $\delta$  = 9.04 (s, 2H,  $H_{\text{imi}}$ ), 8.15 (s, 2H,  $H_{\text{trz}}$ ), 7.96 (t,  $^3J_{\text{H-H}} = 1.5$  Hz, 2H,  $H_{\text{imi}}$ ), 7.55 (t,  $^3J_{\text{H-H}} = 1.5$  Hz, 2H,  $H_{\text{imi}}$ ), 7.51 – 7.54 (m, 2H,  $\text{ArH}$ ), 7.40 – 7.45 (m, 2H,  $\text{ArH}$ ), 7.30 – 7.35 (m, 2H,  $\text{ArH}$ ), 7.25 – 7.29 (m, 2H,  $\text{ArH}$ ), 5.72 (s, 4H,  $\text{CH}_2$ ), 5.53 (s, 4H,  $\text{CH}_2$ ), 5.47 (s, 4H,  $\text{CH}_2$ ).  $^{13}\text{C-NMR}$  (125.74 MHz,  $\text{d}_6$ -DMSO):  $\delta$  = 140.48 ( $\text{C}_q$ ), 137.33 ( $\text{C}_q$ ), 134.23 ( $\text{C}_q$ ), 133.16 ( $\text{C}_{\text{imi}}$ ), 130.51 ( $\text{C}_{\text{Ar}}$ ), 130.35 ( $\text{C}_{\text{Ar}}$ ), 130.14 ( $\text{C}_{\text{Ar}}$ ), 129.47 ( $\text{C}_{\text{Ar}}$ ), 126.02 ( $\text{C}_{\text{trz}}$ ), 123.80 ( $\text{C}_{\text{imi}}$ ), 122.78 ( $\text{C}_{\text{imi}}$ ), 50.90 ( $\text{CH}_2$ ), 50.25 ( $\text{CH}_2$ ), 49.06 ( $\text{CH}_2$ ). ESI- $\text{MS}^+$ :  $[\text{C}_{28}\text{H}_{28}\text{N}_{10}]^{2+}$   $m/z$  = 252.00, calcd = 252.12,  $[\text{C}_{28}\text{H}_{28}\text{N}_{10}\text{PF}_6]^+$   $m/z$  = 649.20, calcd = 649.21.

**3.22·Br<sub>2</sub>**. This compound was prepared using the same method as described for **3.21·Br<sub>2</sub>** from **3.20** (0.050 g, 0.12 mmol) and **2.8** (0.011 g, 0.12 mmol) and  $\text{Bu}_4\text{N}^+\cdot\text{Br}^-$  (0.19 g, 0.60 mmol). Yield: 0.012 g, 12.6%.  $^1\text{H-NMR}$  (500.02 MHz  $\text{d}_6$ -DMSO):  $\delta$  = 9.32 (s, 2H  $H_{\text{imi}}$ ), 8.33 (s, 2H,  $H_{\text{trz}}$ ), 7.73 (s, 2H,  $H_{\text{imi}}$ ), 7.57 (s, 2H,  $H_{\text{imi}}$ ), 7.48 – 7.55 (m, 6H,  $\text{ArH}$ ). 7.41 – 7.44 (m, 2H,  $\text{ArH}$ ), 7.05 (s, 2H,  $\text{ArH}$ ), 5.61 (s, 2H,  $\text{CH}_2$ ), 5.53 (s, 2H,  $\text{CH}_2$ ), 5.43 (s, 2H,  $\text{CH}_2$ ).  $^{13}\text{C-NMR}$  (125.74 MHz,  $\text{d}_6$ -DMSO):  $\delta$  = 140.79 ( $\text{C}_q$ ), 136.88 ( $\text{C}_q$ ), 136.78 ( $\text{C}_{\text{imi}}$ ), 136.02 ( $\text{C}_q$ ), 130.36 ( $\text{C}_{\text{Ar}}$ ), 130.00 ( $\text{C}_{\text{Ar}}$ ), 129.71 ( $\text{C}_{\text{Ar}}$ ), 128.99 ( $\text{C}_{\text{Ar}}$ ), 128.91 ( $\text{C}_{\text{Ar}}$ ), 128.04 ( $\text{C}_{\text{Ar}}$ ), 125.33 ( $\text{C}_{\text{trz}}$ ), 123.19 ( $\text{C}_{\text{imi}}$ ), 123.11 ( $\text{C}_{\text{imi}}$ ), 53.16 ( $\text{CH}_2$ ), 52.29 ( $\text{CH}_2$ ), 44.21 ( $\text{CH}_2$ ). ESI- $\text{MS}^+$ :  $[\text{C}_{28}\text{H}_{28}\text{N}_{10}\text{PF}_6]^+$   $m/z$  = 649.31, calcd = 649.21.

**3.23.** A mixture of **3.21·Br<sub>2</sub>** (0.050g, 0.075 mmol) and (THT)AuCl (0.048 g, 0.15 mmol) in DMF (10 mL) was stirred at 110 °C for 0.5 h. To the resultant mixture, NaOAc (0.025g, 3.00 mmol) was added and the mixture was further stirred at the same temperature for 2 h. The reaction mixture was then cooled to RT followed by addition of excess amount of diethyl ether. The precipitate was collected and washed diethyl ether (3 × 5 mL) followed by recrystallization in a mixture of acetonitrile and diethyl ether. Yield: 0.042 g, 56.7%. <sup>1</sup>H-NMR (500.02 MHz d<sub>6</sub>-DMSO): δ = 8.07 (s, 2H, *H<sub>trz</sub>*), 7.48 (s, 2H, *H<sub>imi</sub>*), 7.40 – 7.42 (m, 2H, *ArH*), 7.33 – 7.36 (m, 2H, *ArH*), 7.04 – 7.15 (m<sub>br</sub> 4H, *ArH*), 7.00 (s, 2H, *H<sub>imi</sub>*), 5.62 (s, 4H, *CH<sub>2</sub>*), 5.46 (s, 4H, *CH<sub>2</sub>*), 5.31 (s, 4H, *CH<sub>2</sub>*). <sup>13</sup>C-NMR (125.74 MHz, d<sub>6</sub>-DMSO): δ = 170.71 (*C<sub>carbene</sub>*), 143.51 (*C<sub>q</sub>*), 134.50 (*C<sub>q</sub>*), 134.28(*C<sub>q</sub>*), 129.57 (*C<sub>Ar</sub>*), 129.24 (*C<sub>Ar</sub>*), 129.06 (*C<sub>Ar</sub>*), 124. 86 (*C<sub>trz</sub>*), 123.67 (*C<sub>imi</sub>*), 121.36 (*C<sub>imi</sub>*), 52.43 (*CH<sub>2</sub>*), 50.91 (*CH<sub>2</sub>*), 46.59 (*CH<sub>2</sub>*). HRESI-MS<sup>+</sup>: [C<sub>28</sub>H<sub>26</sub>N<sub>10</sub>Au<sub>2</sub>Br]<sup>+</sup> m/z = 977.0832, calcd = 977.0830.

### 3.5 References

1. Safarnejad Shad, M.; Santhini, P. V.; Dehaen, W., *Beilstein J. Org. Chem.* **2019**, *15*, 2142-2155.
2. Guisado-Barrios, G.; Soleilhavoup, M.; Bertrand, G., *Acc. Chem. Res.* **2018**, *51*, 3236-3244.
3. Hua, Y.; Flood, A. H., *Chem. Soc. Rev.* **2010**, *39*, 1262-1271.
4. Steed, J. W., *Chem. Soc. Rev.* **2009**, *38*, 506-519.
5. Zapata, F.; Gonzalez, L.; Caballero, A.; Alkorta, I.; Elguero, J.; Molina, P., *Chem. Eur. J.* **2015**, *21*, 9797-9808.
6. Mesquida, N.; Dinarès, I.; Ibáñez, A.; Alcalde, E., *Org. Biomol. Chem.* **2013**, *11*, 6385-6396.
7. Aizpurua, J. M.; Fratila, R. M.; Monasterio, Z.; Pérez-Esnaola, N.; Andreieff, E.; Irastorza, A.; Sagartzazu-Aizpurua, M., *New J. Chem.* **2014**, *38*, 474-480.
8. Chhatra, R. K.; Kumar, A.; Pandey, P. S., *J. Org. Chem.* **2011**, *76*, 9086-9089.
9. Kumar, A.; Pandey, P. S., *Org. Lett.* **2008**, *10*, 165-168.
10. Kilah, N. L.; Wise, M. D.; Serpell, C. J.; Thompson, A. L.; White, N. G.; Christensen, K. E.; Beer, P. D., *J. Am. Chem. Soc.* **2010**, *132*, 11893-11895.
11. White, N. G.; Carvalho, S.; Félix, V.; Beer, P. D., *Org. Biomol. Chem.* **2012**, *10*, 6951-6959.
12. Al-Shnani, F.; Guisado-Barrios, G.; Sainz, D.; Peris, E., *Organometallics* **2019**, *38*, 697-701.
13. Zhang, P.; Yamamoto, T.; Suginome, M., *ChemCatChem* **2019**, *11*, 424-429.
14. Shao, C.; Cheng, G.; Su, D.; Xu, J.; Wang, X.; Hu, Y., *Adv. Synth. Catal.* **2010**, *352*, 1587-1592.
15. Andreeva, O. V.; Belenok, M. G.; Saifina, L. F.; Shulaeva, M. M.; Dobrynin, A. B.; Sharipova, R. R.; Voloshina, A. D.; Saifina, A. F.; Gubaidullin, A. T.; Khairutdinov, B. I.; Zuev, Y. F.; Semenov, V. E.; Kataev, V. E., *Tetrahedron Lett.* **2019**, *60*, 151276.
16. Tripolszky, A.; Németh, K.; Szabó, T. P.; Bálint, E., *Molecules* **2019**, *24*.
17. Miller, R. G.; Vázquez-Hernández, M.; Prochnow, P.; Bandow, J. E.; Metzler-Nolte, N., *Inorg. Chem.* **2019**, *58*, 9404-9413.
18. Rostovtsev, V. V.; Green, L. G.; Fokin, V. V.; Sharpless, K. B., *Angew. Chem. Int. Ed.* **2002**, *41*, 2596-2599.
19. Shao, C.; Wang, X.; Xu, J.; Zhao, J.; Zhang, Q.; Hu, Y., *J. Org. Chem.* **2010**, *75*, 7002-7005.

20. Saehlim, N.; Kasemsuk, T.; Sirion, U.; Saeeng, R., *J. Org. Chem.* **2018**, *83*, 13233-13242.
21. Spiteri, C.; Moses, J. E., *Angew. Chem. Int. Ed.* **2010**, *49*, 31-33.
22. Zamora, M. T.; Ferguson, M. J.; McDonald, R.; Cowie, M., *Organometallics* **2012**, *31*, 5463-5477.
23. Mendoza-Espinosa, D.; Alvarez-Hernández, A.; Angeles-Beltrán, D.; Negrón-Silva, G. E.; Suárez-Castillo, O. R.; Vásquez-Pérez, J. M., *Inorg. Chem.* **2017**, *56*, 2092-2099.
24. Mathew, P.; Neels, A.; Albrecht, M., *J. Am. Chem. Soc.* **2008**, *130*, 13534-13535.
25. Telegina, L. N.; Kelbysheva, E. S.; Strelkova, T. V.; Ezernitskaya, M. G.; Borisov, Y. A.; Smol'yakov, A. F.; Peregudov, A. S.; Rodionov, A. N.; Ikonnikov, N. S.; Loim, N. M., *Eur. J. Org. Chem.* **2016**, *2016*, 5897-5906.
26. Kilpin, K. J.; Crot, S.; Riedel, T.; Kitchen, J. A.; Dyson, P. J., *Dalton Trans.* **2014**, *43*, 1443-1448.
27. Wei, Y.; Petronilho, A.; Mueller-Bunz, H.; Albrecht, M., *Organometallics* **2014**, *33*, 5834-5844.
28. Hollering, M.; Albrecht, M.; Kühn, F. E., *Organometallics* **2016**, *35*, 2980-2986.
29. Saravanakumar, R.; Ramkumar, V.; Sankararaman, S., *Organometallics* **2011**, *30*, 1689-1694.
30. Karmis, R. E.; Carrara, S.; Baxter, A. A.; Hogan, C. F.; Hulett, M. D.; Barnard, P. J., *Dalton Trans.* **2019**, *48*, 9998-10010.
31. Wright, J. R.; Young, P. C.; Lucas, N. T.; Lee, A.-L.; Crowley, J. D., *Organometallics* **2013**, *32*, 7065-7076.
32. Wang, H.; Zhang, B.; Yan, X.; Guo, S., *Dalton Trans.* **2018**, *47*, 528-537.
33. Zamora, M. T.; Ferguson, M. J.; Cowie, M., *Organometallics* **2012**, *31*, 5384-5395.
34. Huang, J.; Cai, J.; Feng, H.; Liu, Z.; Fu, X.; Miao, Q., *Tetrahedron* **2013**, *69*, 5460-5467.
35. Schulte to Brinke, C.; Ekkehardt Hahn, F., *Dalton Trans.* **2015**, *44*, 14315-14322.
36. Ito, M.; Matsunaga, N.; Yamada, M.; Hitaka, T.; Yamamoto, S. Preparation of pyrrole derivatives as androgen receptor antagonists for treatment of cancer. WO 2007/145349 A2, December 12, 2007.
37. Rasheed, O. K.; Bawn, C.; Davies, D.; Raftery, J.; Vitorica-Yrzebal, I.; Pritchard, R.; Zhou, H.; Quayle, P., *Eur. J. Org. Chem.* **2017**, *2017*, 5252-5261.
38. Xue, F.; Fang, J.; Delker, S. L.; Li, H.; Martásek, P.; Roman, L. J.; Poulos, T. L.; Silverman, R. B., *J. Med. Chem.* **2011**, *54*, 2039-2048.



39. Frassinetti, C.; Alderighi, L.; Gans, P.; Sabatini, A.; Vacca, A.; Ghelli, S., *Anal. Bioanal. Chem.* **2003**, 376, 1041-1052.
40. Frassinetti, C.; Ghelli, S.; Gans, P.; Sabatini, A.; Moruzzi, M. S.; Vacca, A., *Anal. Biochem.* **1995**, 231, 374-382.
41. Wong, W. W. H.; Vickers, M. S.; Cowley, A. R.; Paul, R. L.; Beer, P. D., *Org. Biomol. Chem.* **2005**, 3, 4201-4208.
42. Li, Z.; Wiratpruk, N.; Barnard, P. J., *Frontiers in Chemistry* **2019**, 7, 270.
43. Sabater, P.; Zapata, F.; Caballero, A.; Alkorta, I.; Ramirez de Arellano, C.; Elguero, J.; Molina, P., *ChemistrySelect* **2018**, 3, 3855-3859.
44. Evans, N. H.; Beer, P. D., *Angew. Chem. Int. Ed.* **2014**, 53, 11716-11754.

# CHAPTER 4 HETEROBIMETALLIC *N*-HETEROCYCLIC CARBENE COMPLEXES

## 4.1 Introduction

The synthesis of heterobimetallic complexes of *N*-heterocyclic carbene (NHC) ligands is of great interest for various applications including studies of metallophilic interactions<sup>1-3</sup> and the development of novel catalysts,<sup>4-13</sup> in addition to potential medicinal inorganic chemical applications including as anti-cancer and antimicrobial agents.<sup>14-19</sup>

Since the first characterisation of aurophilic interactions in the 1980s,<sup>20-23</sup> many compounds displaying these weak bonding interactions and to a lesser extent argentophilic<sup>24</sup> and cuprophilic<sup>24</sup> interactions have been reported. Interestingly, compounds displaying aurophilic interactions have in some cases been found to exhibit photoluminescent properties.<sup>2-3, 25-29</sup> In addition, similar luminescence has also been observed for heterobimetallic complexes of the coinage metals and other isoelectronic metals that also display metallophilic interactions including Au(I)-Ag(I), Au(I)-Hg(II) and Au(I)-Cu(I).<sup>1-3, 25, 27</sup> For example, the Au(I)-Cu(I) complex **1.106**·(**PF<sub>6</sub>**)<sub>3</sub> (Figure 1.15) is luminescent and has been investigated as a sensor for volatile organic compounds (VOC). This compound supports a short Au(I)-Cu(I) interaction of 4.59 Å and this shortens to 2.79 Å as a result of ligand exchange between acetonitrile and methanol at the Cu(I) centre.<sup>27</sup> In addition, the Au(I)-Ag(I) heterobimetallic complex **4.1**·(**BF<sub>4</sub>**)<sub>2</sub> (Figure 4.1) of a picolyl-substituted NHC ligand was found to be luminescent at both room temperature and 77 K.<sup>1</sup> Interestingly, a polymeric Au(I)-Ag(I) heterometallic complex **4.2**·(**BF<sub>4</sub>**)<sub>m</sub> (Figure 4.1) was also reported by the same research group.<sup>30</sup>

Heterobimetallic complexes of NHC ligands have been extensively investigated as catalysts for multiple catalytic transformations in one-pot reactions. These reactions, known

as “tandem reactions”, involve the use of one catalyst in two or more different chemical processes.<sup>4-10</sup> Heterobimetallic complexes are of particular interest as they can display synergistic effects, where the different metal centres catalyse different reactions with improved yields and selectivity when compared with a combination of the corresponding homobimetallic complexes.<sup>4-6, 8, 11-12, 31</sup> For example, the Ir(III)-Pd(II) heterobimetallic complex **4.3** (Figure 4.1) was catalytically active in the Suzuki–Miyaura coupling/transfer hydrogenation of *p*-bromoacetophenone in isopropanol.<sup>31</sup>

The biological properties of metal complexes of NHC ligands have also been of significant recent interest and Au(I) and Ag(I) complexes have been shown to possess anticancer<sup>15, 32-37</sup> and antimicrobial activities.<sup>16-17, 19, 38-43</sup>

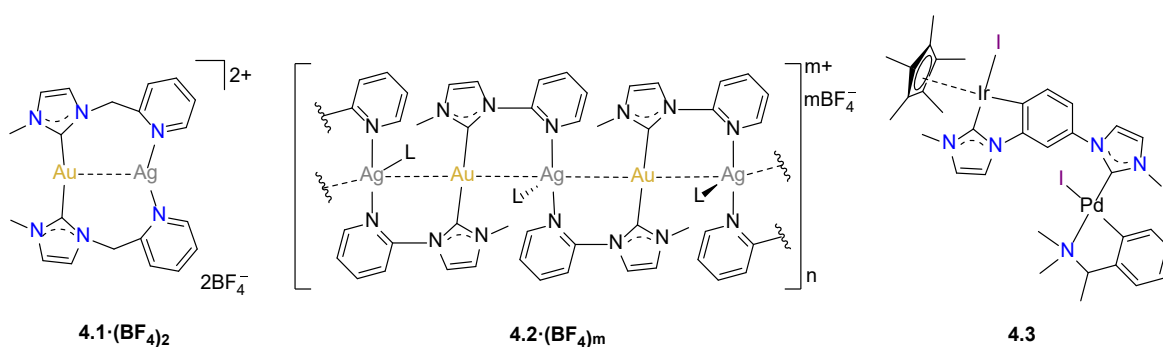


Figure 4.1 Structures of selected heterobimetallic complexes of NHC ligands.

A range of synthetic strategies has been developed for the synthesis of heterobimetallic complexes of NHC ligands. These methods include one-pot metalation with two metals,<sup>44-45</sup> stepwise metal incorporation<sup>5, 31, 45-51</sup> and post synthetic modification and metallation.<sup>25, 50, 52-54</sup> The Ir(III)-Pd(II) heterobimetallic complex **1.72** (Scheme 1.19) was prepared using a one-pot metallation,<sup>44</sup> while complex **1.67** was prepared by stepwise incorporation of the two metals.<sup>4</sup> However, the metallation method of poly-NHC ligands in a site-selective manner is often limited because the selective deprotonation of the different NHC groups is often not possible. In an alternative approach, different azolium groups (e.g.

imidazolium and triazolium) can be incorporated, thereby producing an asymmetrical ligand system which can be selective deprotonated and metallated.<sup>49</sup> Interestingly, heterobimetallic complexes can also be prepared by using post synthetic modification metallation methods.<sup>25, 52-53</sup> For example, the heterobimetallic complexes **1.77**·(**BF<sub>4</sub>**)<sub>2</sub> was prepared using this approach. In the synthesis, the precursor Au(I) complex featuring imidazole units was first prepared followed by alkylation and metallation with a second metal source to generate the desired heterobimetallic complexes.<sup>25</sup>

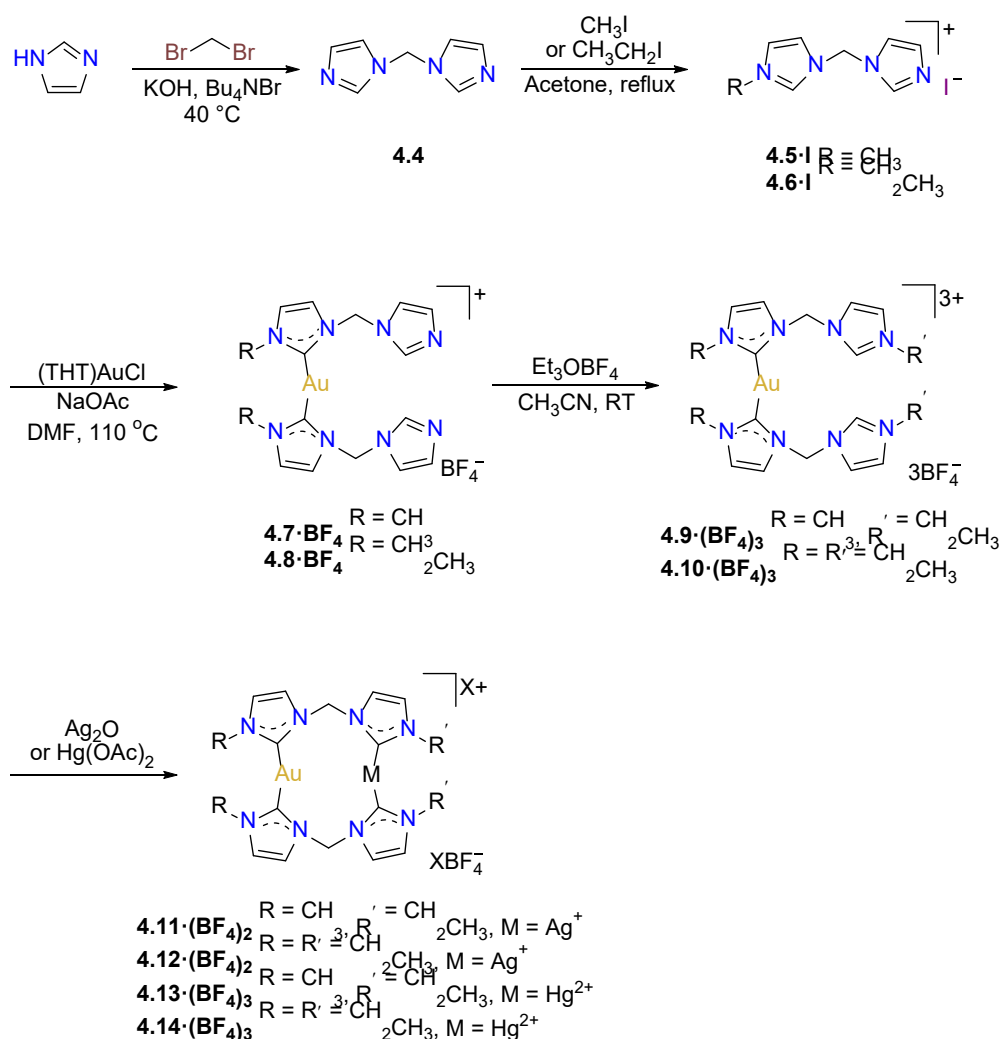
In this chapter, the synthesis of a series of heterobimetallic Au(I)-Ag(I) and Au(I)-Hg(II) complexes of symmetrical and asymmetrical NHC ligands derived from methylene and ethylene linked *bis*-imidazolium precursors is described. To allow for a comparative investigation of the photophysical and antimicrobial properties of these compounds, the Au(I) and Ag(I) homobimetallic complexes of these ligand systems were also prepared.

## 4.2 Results and discussion

### 4.2.1 Synthesis of methylene linked imidazolium salt pro-ligands and corresponding metal complexes

As heterobimetallic NHC complexes are of interest for various applications including for the development of novel catalysts, luminescent materials and as potential medicinal inorganic compounds, we became interested in the synthesis of novel heterobimetallic NHC complexes. The synthetic scheme for the preparation of the desired heterobimetallic complexes is shown in Scheme 4.1. The synthesis was initiated by the reaction of imidazole and dibromomethane yielding the methylene linked *bis*-imidazole **4.4**. This compound was then mono-alkylated with either iodomethane or iodoethane, to obtain the mono-imidazolium salts **4.5**·**I** and **4.6**·**I**. The mono-alkylated species **4.5**·**I** and **4.6**·**I** were then metallated with (THT)AuCl in the presence of NaOAc to obtain the

monometallic Au(I)-NHC complexes **4.7·BF<sub>4</sub>** and **4.8·BF<sub>4</sub>** respectively. These monometallic Au(I) complexes were then further alkylated with a triethyloxonium tetrafluoroborate (Et<sub>3</sub>OBF<sub>4</sub>) followed by metallation with a second metal source, either Ag<sub>2</sub>O or Hg(OAc)<sub>2</sub> to obtain the desired heterobimetallic NHC complexes **4.11·(BF<sub>4</sub>)<sub>2</sub>**, **4.12·(BF<sub>4</sub>)<sub>2</sub>**, **4.13·(BF<sub>4</sub>)<sub>3</sub>**, and **4.14·(BF<sub>4</sub>)<sub>3</sub>**.

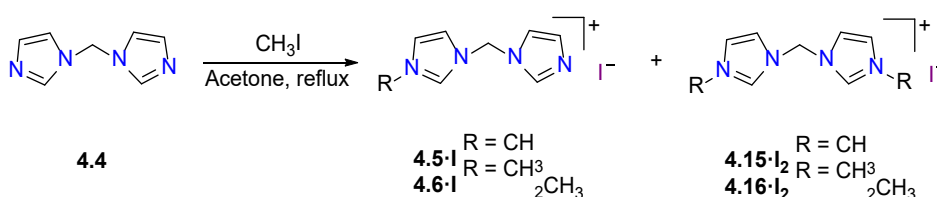


Scheme 4.1 General synthetic route for the preparation of the heterobimetallic NHC complexes **4.11·(BF<sub>4</sub>)<sub>2</sub>**, **4.12·(BF<sub>4</sub>)<sub>2</sub>**, **4.13·(BF<sub>4</sub>)<sub>3</sub>**, and **4.14·(BF<sub>4</sub>)<sub>3</sub>** using post synthetic modification metallation method.

#### 4.2.1.1 Synthesis of the mono-alkylated pro-ligand

Compound **4.4** was mono-alkylated to obtain the required monoalkylated synthetic precursors, **4.5-I** and **4.6-I**. Multiple unsuccessful attempts were made to mono-alkylate compound **4.4** and these initial studies were hampered because mixtures of the mono- and

di-substituted imidazolium salts were generated necessitating difficult purification procedures, which resulted in poor yields of the desired mono-imidazolium salts. It was later found that slow addition of either iodomethane or iodoethane into a solution of **4.4** in acetone over a period of 1 hour gave the best yield of the monoalkylated products (Scheme 4.2). Although generation of the di-substituted imidazolium salts **4.15·I<sub>2</sub>** and **4.16·I<sub>2</sub>** was unavoidable, the yields of the reactions were improved to 46.0% for **4.5·I** and 22.3% for **4.6·I** respectively. In addition, due to the precipitation of the *bis*-imidazolium **4.15·I<sub>2</sub>** and **4.16·I<sub>2</sub>** from the reaction mixture where acetone was used as the solvent, the monoalkylated imidazolium salt **4.15·I<sub>2</sub>** and **4.16·I<sub>2</sub>** could be easily isolated from the reactions. The <sup>1</sup>H-NMR spectrum of **4.5·I** exhibited five signals for the imidazole and imidazolium groups at 7.00, 7.49, 7.74, 7.95 and 8.00 ppm with one downfield shifted signal at 9.34 ppm consistent with the asymmetrical structure. A similar <sup>1</sup>H-NMR spectrum obtained for **4.6·I** is also consistent with the monoalkylated formulation.

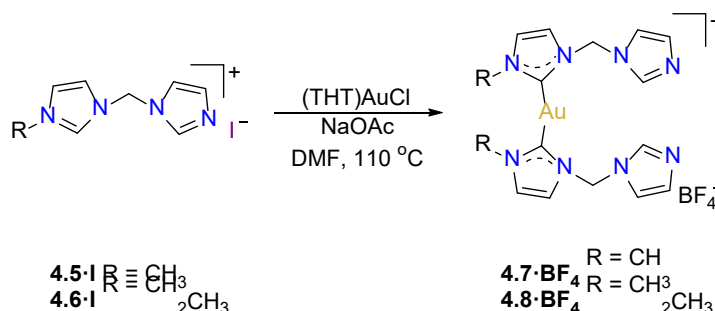


Scheme 4.2 Alkylation of *bis*-imidazole **4.4** to obtain mono-imidazolium salts **4.5·I** and **4.6·I**.

#### 4.2.1.2 Synthesis of gold(I) monometallic and heterobimetallic complexes

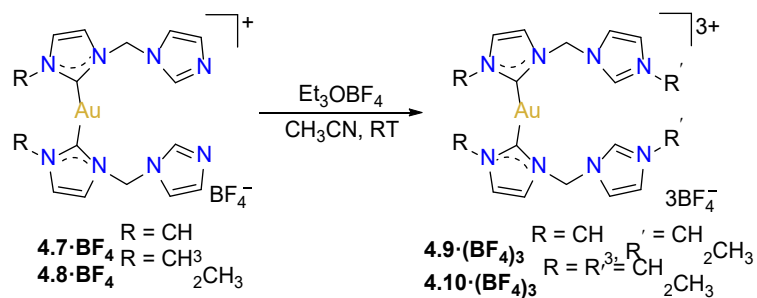
To synthesize the heterobimetallic NHC complexes **4.11·(BF<sub>4</sub>)<sub>2</sub>**, **4.12·(BF<sub>4</sub>)<sub>2</sub>**, **4.13·(BF<sub>4</sub>)<sub>3</sub>**, and **4.14·(BF<sub>4</sub>)<sub>3</sub>**, the Au(I) monometallic precursor complexes **4.7·BF<sub>4</sub>** and **4.8·BF<sub>4</sub>** were prepared by the reaction of two equivalents of **4.5·I** or **4.6·I** and one equivalent of (THT)AuCl in the presence of NaOAc as a weak base to deprotonate the imidazolium salt *in situ* (Scheme 4.3). The <sup>1</sup>H-NMR spectra for **4.7·BF<sub>4</sub>** and **4.8·BF<sub>4</sub>** showed no imidazolium C2-H proton signal, indicating that the C2 carbon of the imidazolium group had been deprotonated and coordinated to the metal centre as a carbene.

In addition, the  $^{13}\text{C}$ -NMR spectra showed downfield signals at 183.65 ppm for the carbene carbon atom for both **4.7·BF<sub>4</sub>** and **4.8·BF<sub>4</sub>**.



Scheme 4.3 Synthesis of the monometallic Au(I) complexes **4.7·BF<sub>4</sub>**, and **4.8·BF<sub>4</sub>** derived from pro-ligands **4.5·I** and **4.6·I**.

To allow the introduction of the second metal ion, the monometallic Au(I) complexes **4.7·BF<sub>4</sub>** and **4.8·BF<sub>4</sub>** were alkylated using Et<sub>3</sub>OBF<sub>4</sub> in acetonitrile at RT to produce the complexes **4.9·(BF<sub>4</sub>)<sub>3</sub>** and **4.10·(BF<sub>4</sub>)<sub>3</sub>** which carries imidazolium group (Scheme 4.4). The formation of the alkylated complexes **4.9·(BF<sub>4</sub>)<sub>3</sub>** and **4.10·(BF<sub>4</sub>)<sub>3</sub>** were confirmed by the downfield signal of the imidazolium C2-H proton, which resonated at 9.44 ppm and 9.42 ppm for **4.9·(BF<sub>4</sub>)<sub>3</sub>** and **4.10·(BF<sub>4</sub>)<sub>3</sub>** respectively and the appearance of a new set of ethyl group signals (Figure 4.2). Furthermore, the high-resolution mass spectrum for **4.9·(BF<sub>4</sub>)<sub>3</sub>** produced a series of peaks consistent with a tricationic structure with the general formula [AuL<sub>2</sub>]<sup>3+</sup>. For example, the peak observed at m/z = 753.2326 corresponds to the formula [C<sub>20</sub>H<sub>30</sub>N<sub>8</sub>AuB<sub>2</sub>F<sub>8</sub>]<sup>+</sup> which is [AuL<sub>2</sub>·(BF<sub>4</sub>)<sub>2</sub>]<sup>+</sup> (calculated = 752.2312).



Scheme 4.4 Alkylation of monometallic Au(I) complexes **4.7**·**BF**<sub>4</sub> and **4.8**·**BF**<sub>4</sub> yielding Au(I) complexes **4.9**·(**BF**<sub>4</sub>)<sub>3</sub> and **4.10**·(**BF**<sub>4</sub>)<sub>3</sub>.

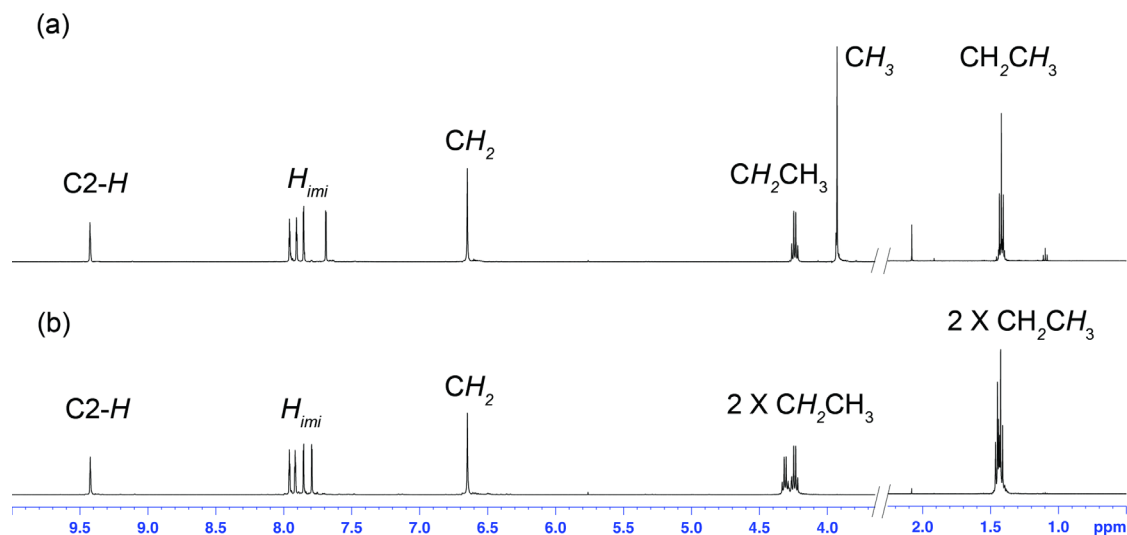


Figure 4.2 <sup>1</sup>H-NMR spectra of monometallic Au(I) complexes (a) **4.9**·(**BF**<sub>4</sub>)<sub>3</sub> and (b) **4.10**·(**BF**<sub>4</sub>)<sub>3</sub>.

A representation of the X-ray crystal structure for complex **4.9**·(**BF**<sub>4</sub>)<sub>3</sub> is shown in Figure 4.3. The structure of this complex shows the gold(I) centre is bound to two NHC ligands with a linear two-coordinate geometry with the average of the C-Au(I) distances and the C-Au-C angles being 1.99 Å and 174.5° respectively. The structure also shows that in each case the two NHC units are bound to uncoordinated imidazolium units formed by the alkylation of complex **4.7**·**BF**<sub>4</sub> with ethyl groups.



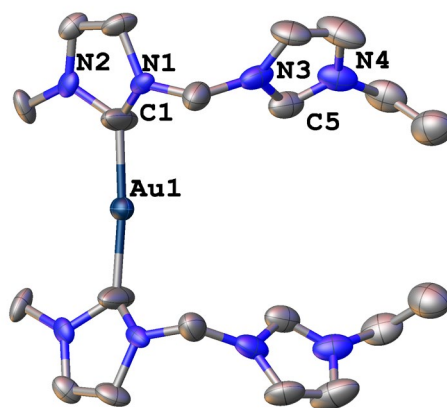
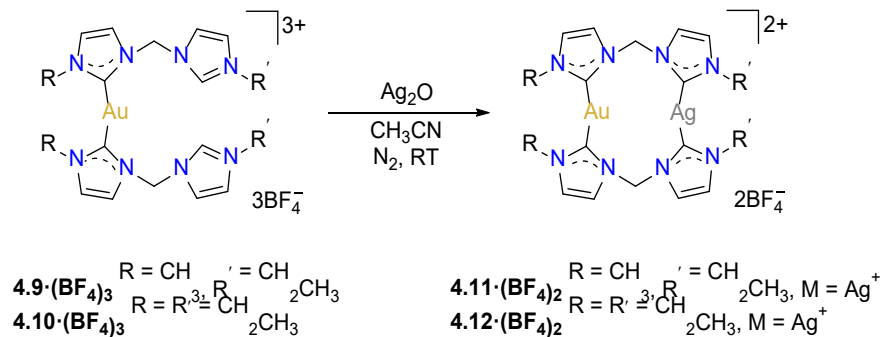


Figure 4.3 Representation of the X-ray crystal structure of the Au(I) complex **4.9·(BF<sub>4</sub>)<sub>3</sub>**. Atomic displacement ellipsoids are shown at the 50% probability level.

In order to prepare heterobimetallic Au(I)-Ag(I) complexes, the precursor Au(I) complexes **4.9·(BF<sub>4</sub>)<sub>3</sub>** and **4.10·(BF<sub>4</sub>)<sub>3</sub>** were reacted with Ag<sub>2</sub>O in acetonitrile in the absence of light (Scheme 4.5) and the heterobimetallic complexes **4.11·(BF<sub>4</sub>)<sub>2</sub>** and **4.12·(BF<sub>4</sub>)<sub>2</sub>** were obtained in moderate yields (56.4% and 36.7% respectively).



Scheme 4.5 Synthesis of Au(I)-Ag(I) heterobimetallic NHC complexes **4.11·(BF<sub>4</sub>)<sub>2</sub>** and **4.12·(BF<sub>4</sub>)<sub>2</sub>** derived from *bis*-imidazolylidene ligands.

The high-resolution mass spectrum for **4.11·(BF<sub>4</sub>)<sub>2</sub>** (Figure 4.4) shows a peak at  $m/z = 771.1180$  corresponding to  $[\text{C}_{20}\text{H}_{28}\text{N}_8\text{AuAgBF}_4]^+$  which is  $[\text{AuAgL}_2\text{·BF}_4]^+$  (calculated = 771.1177), while the base peak at  $m/z = 342.0577$  corresponds to the dicationic species  $[\text{C}_{20}\text{H}_{28}\text{N}_8\text{AuAg}]^{2+}$  (calculated = 342.0571). In the case of Au(I)-Ag(I) heterobimetallic complex **4.12·(BF<sub>4</sub>)<sub>2</sub>**, the mass spectrum exhibited a base peak at  $m/z = 365.0906$

(calculated = 365.0708) corresponding to the  $[\text{C}_{22}\text{H}_{32}\text{N}_8\text{AuAg}]^{2+}$  species. In contrast to **4.11**·(**BF**<sub>4</sub>)<sub>2</sub>, the monocationic fragment  $[\text{AuAgL}_2\cdot\text{BF}_4]^+$  was not observed (Figure 4.4). The high-resolution mass spectra of the complexes **4.11**·(**BF**<sub>4</sub>)<sub>2</sub> and **4.12**·(**BF**<sub>4</sub>)<sub>2</sub> and the theoretical spectra are shown in Figure 4.4

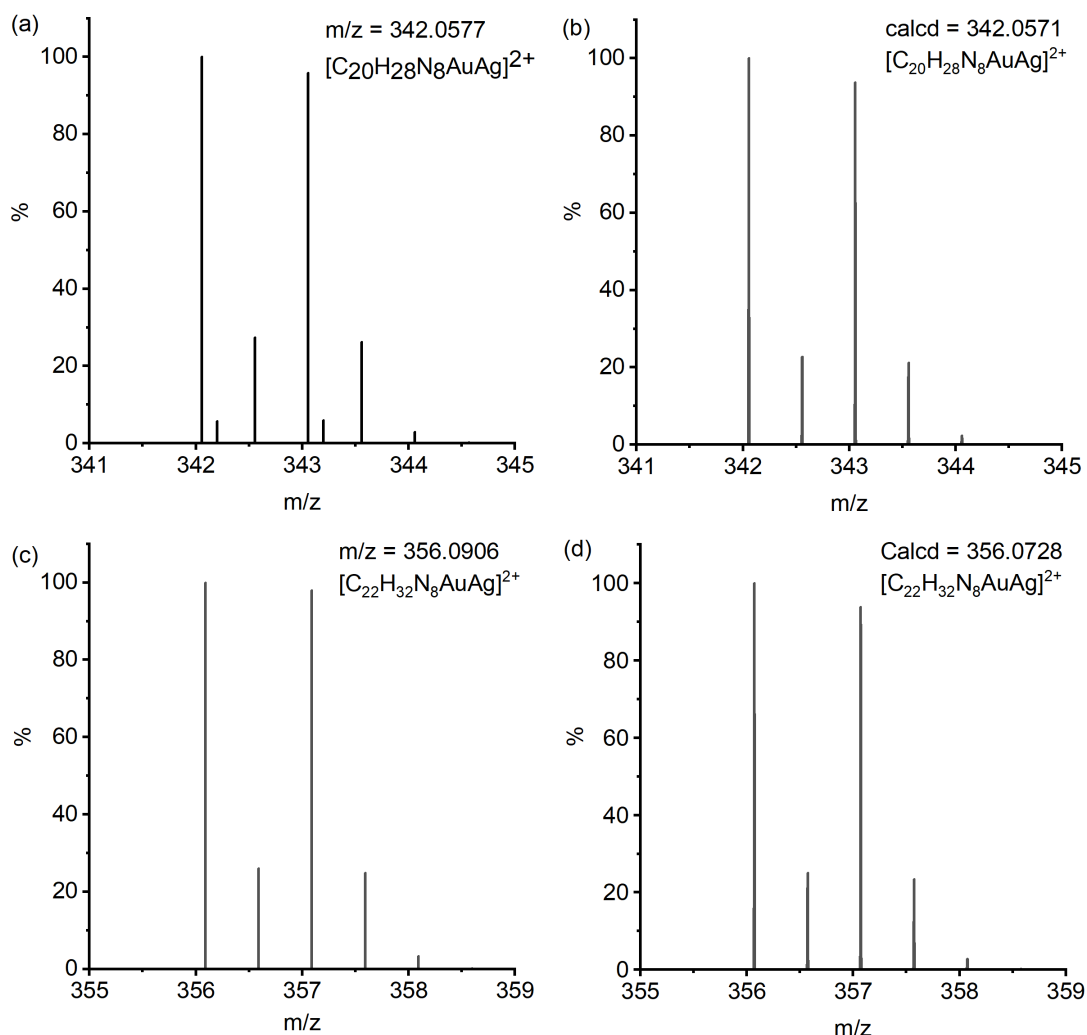


Figure 4.4 (a) High-resolution mass spectrum of Au(I)-Ag(I) heterobimetallic complex **4.11**·(**BF**<sub>4</sub>)<sub>2</sub> and (b) theoretical mass spectrum for isotopic distribution for  $[\text{C}_{20}\text{H}_{28}\text{N}_8\text{AuAg}]^{2+}$  corresponding to **4.11**<sup>2+</sup> and (c) High-resolution mass spectra for complex **4.12**·(**BF**<sub>4</sub>)<sub>2</sub> and (d) Theoretical mass spectrum for isotopic distribution for  $[\text{C}_{22}\text{H}_{32}\text{N}_8\text{AuAg}]^{2+}$  corresponding to **4.12**<sup>2+</sup>.

The <sup>1</sup>H-NMR spectrum of the **4.11**·(**BF**<sub>4</sub>)<sub>2</sub> at 298 K shows a broad AX pattern for the methylene protons. However, three methyl group signals were observed at 3.84, 3.85 and 3.87 ppm while peaks corresponding to the ethyl groups were observed at 4.20 (quartet) and 4.26 ppm (quartet) and in the range 1.39 – 1.48 ppm (multiplet). This complexity is

consistent with different conformational isomers in solution. To analyse the structures and the conformational isomers for the synthesized complexes, variable temperature  $^1\text{H}$ -NMR experiments were performed and the results will be discussed in the next section.

A representation of the X-ray crystal structure for the Au(I)-Ag(I) heterobimetallic complex **4.12**·( $\text{BF}_4$ )<sub>2</sub> is shown in Figure 4.6. This structure reveals that the complex is dicationic and composed of dinuclear  $[\text{AuAgL}_2]^{2+}$  cations, with a gold(I) atom and silver(I) atom being bridged by a pair of methylene linked *bis*-imidazolylidene ligands. Each dinuclear cation is accompanied by two tetrafluoroborate anions. In each case, the metal centres adopt linear two-coordinate geometries with the linearity being slightly distorted and the C-M-C bond angles being ( $174.6(2)^\circ$  for C-Au-C and  $171.0(3)^\circ$  for C-Ag-C respectively), possibly due to a metallophilic interaction. In addition, the ligand molecules adopted a folded structure with both of the methylene groups orientated in the same direction with respect to the plane defined by the four carbene carbon atoms (i.e. up-up). Furthermore, the Au...Ag distance ( $3.205(6)$  Å) is comparable to literature values which fall in the range of  $3.03 - 3.29$  Å for heterobimetallic Au-Ag complexes<sup>1, 25, 55</sup> and are in agreement with a metallophilic interaction.<sup>1, 25, 55</sup> Previously reported bimetallic NHC complexes of the metals Ag(I) and Au(I) (Figure 4.5) showed metal...metal distances of  $3.3314(5)$  Å for Ag(I) and  $3.2999(4)$  Å for Au(I), which is comparable to the value reported in this work and also suggestive of a weak metallophilic interaction in complex **4.12**·( $\text{BF}_4$ )<sub>2</sub>.<sup>34</sup>

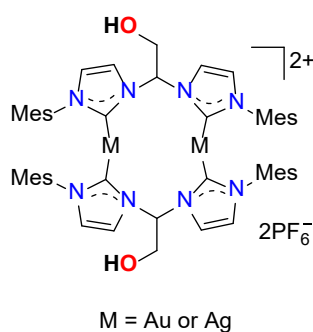


Figure 4.5 Homobimetallic complexes reported with similar structural behaviour.

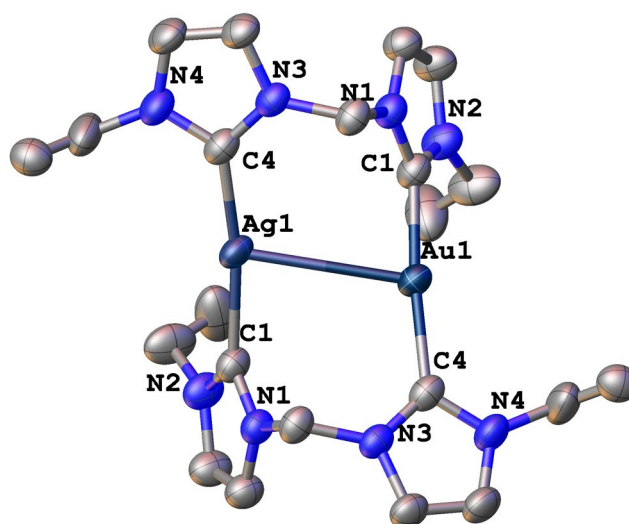
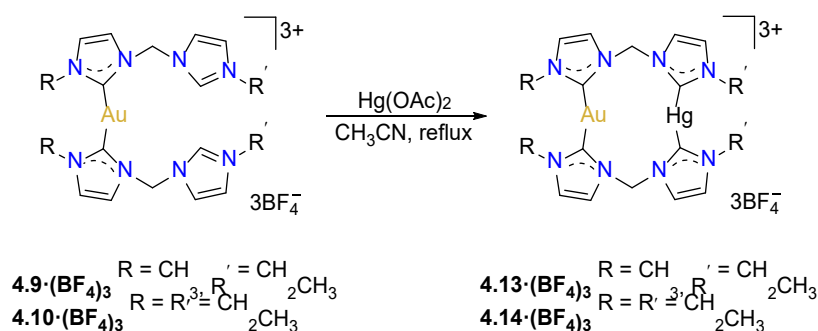


Figure 4.6 Representation of the X-ray crystal structure of Au(I)-Ag(I) heterobimetallic complex **4.12·(BF<sub>4</sub>)<sub>2</sub>**. Atomic displacement ellipsoids are shown at the 50% probability level.

In addition to the synthesis of Au(I)-Ag(I) heterobimetallic complexes, Hg(II) which is isoelectronic with Au(I) ( $5d^{10}$  electron configuration), was also of interest in this work. The heterobimetallic Au(I)-Hg(II) complexes were prepared by treating the precursor Au(I) complexes **4.9·(BF<sub>4</sub>)<sub>3</sub>** and **4.10·(BF<sub>4</sub>)<sub>3</sub>** with Hg(OAc)<sub>2</sub> in acetonitrile. Due to the compounds being purified by recrystallisation using vapour diffusion, the complexes **4.13·(BF<sub>4</sub>)<sub>3</sub>** and **4.14·(BF<sub>4</sub>)<sub>3</sub>** were obtained in a moderate yield (20.2% and 67.1% respectively).



Scheme 4.6 Synthesis of NHC Au(I)-Hg(II) heterobimetallic complexes **4.13·(BF<sub>4</sub>)<sub>3</sub>** and **4.14·(BF<sub>4</sub>)<sub>3</sub>**.

The formation of the Au(I)-Hg(II) heterobimetallic complexes **4.13**·(BF<sub>4</sub>)<sub>3</sub> and **4.14**·(BF<sub>4</sub>)<sub>3</sub> was confirmed using NMR and high-resolution mass spectral studies (Figure 4.7). The mass spectra for **4.13**·(BF<sub>4</sub>)<sub>3</sub> and **4.14**·(BF<sub>4</sub>)<sub>3</sub> showed a peak at  $m/z = 951.1853$  and  $m/z = 979.1355$  indicating monocationic species [AuHgL<sub>2</sub>·(BF<sub>4</sub>)<sub>2</sub>]<sup>+</sup> which corresponds to the formula [C<sub>20</sub>H<sub>28</sub>N<sub>8</sub>AuHgB<sub>2</sub>F<sub>8</sub>]<sup>+</sup> and [C<sub>22</sub>H<sub>32</sub>N<sub>8</sub>AuHgB<sub>2</sub>F<sub>8</sub>]<sup>+</sup> for **4.13**·(BF<sub>4</sub>)<sub>3</sub> and **4.14**·(BF<sub>4</sub>)<sub>3</sub> respectively. In addition, the isotopic patterns are consistent with the formulation of the complexes and the theoretical spectra of these species are shown in Figure 4.7.

The <sup>1</sup>H-NMR of **4.13**·(BF<sub>4</sub>)<sub>3</sub> at room temperature showed a broadened AX pattern for the methylene group protons. In addition and similarly to the Au(I)-Ag(I) complex **4.11**·(BF<sub>4</sub>)<sub>2</sub>, two methyl proton signals which resonated at 3.88 and 4.00 ppm and corresponding ethyl proton signals, which were observed as multiplets also suggest different possible conformational structures for this complex in solution at room temperature and this will be further discussed in the variable temperature <sup>1</sup>H-NMR experiments section.

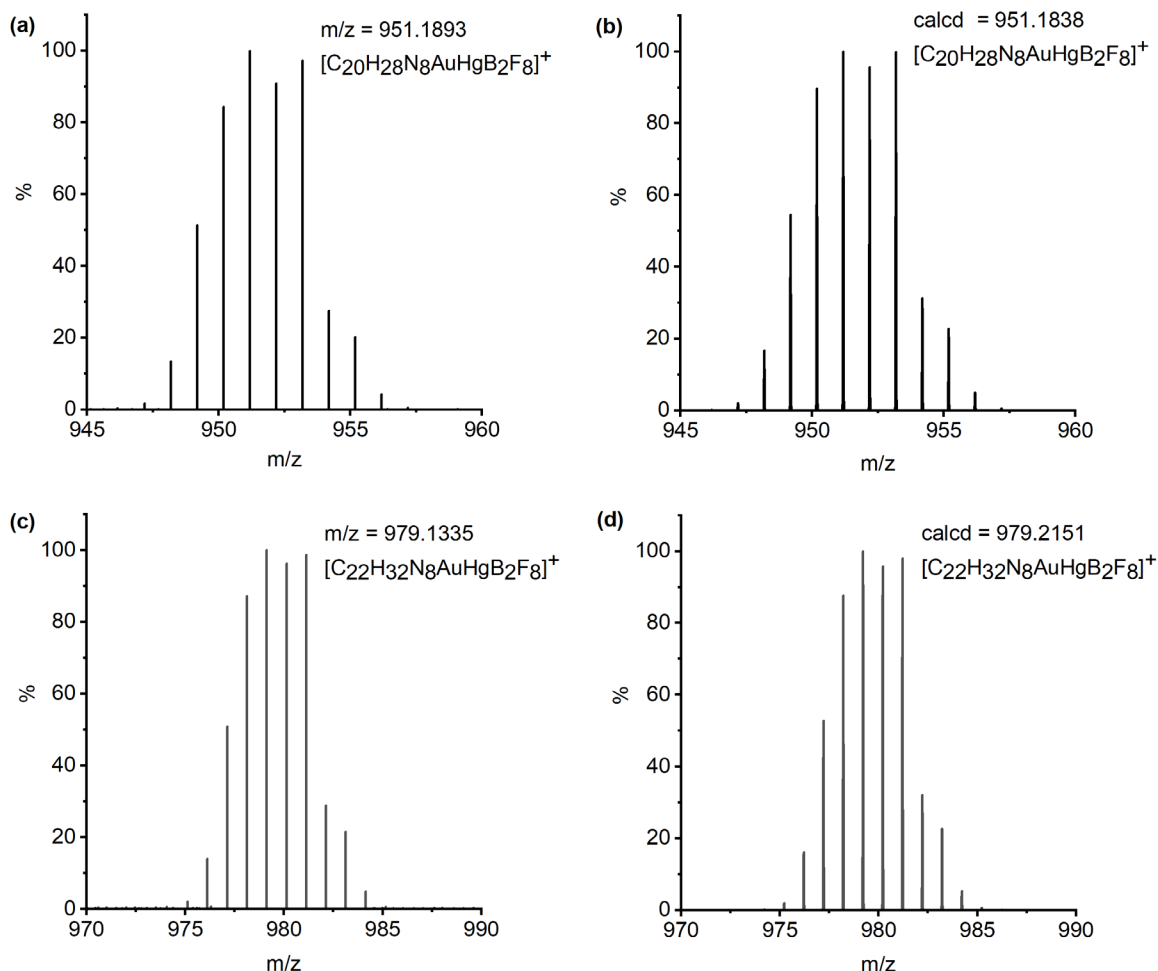
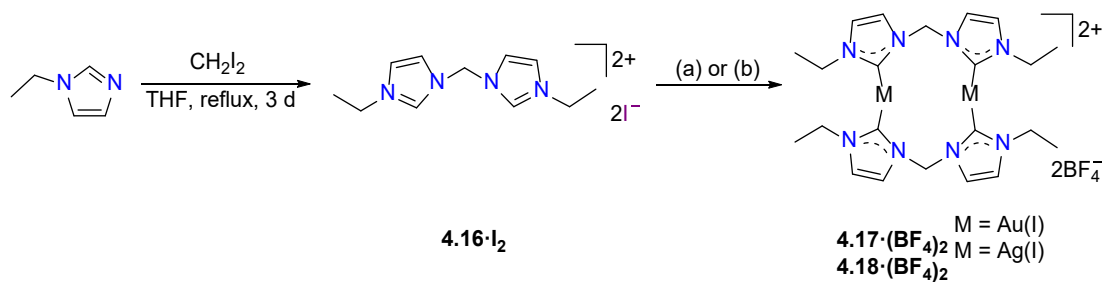


Figure 4.7 (a) High-resolution mass spectrum of Au(I)-Hg(II) heterobimetallic complex **4.13**·(**BF**<sub>4</sub>)<sub>3</sub> and (b) Theoretical mass spectrum showing isotopic distribution for  $[\text{C}_{20}\text{H}_{28}\text{N}_8\text{AuHgB}_2\text{F}_8]^+$  corresponding to **4.13**·(**BF**<sub>4</sub>)<sub>2</sub><sup>+</sup> and (c) high-resolution mass spectrum of **4.14**·(**BF**<sub>4</sub>)<sub>3</sub> and (d) Theoretical mass spectrum showing isotopic distribution for  $[\text{C}_{22}\text{H}_{32}\text{N}_8\text{AuHgB}_2\text{F}_8]^+$  corresponding to **4.14**·(**BF**<sub>4</sub>)<sub>2</sub><sup>+</sup>.

#### 4.2.2 Synthesis of homobimetallic complexes

The symmetrical *bis*-imidazolium salt **4.16**·**I**<sub>2</sub> was synthesized by a reaction of *N*-ethylimidazole and diiodomethane in THF (Scheme 4.7). The homobimetallic Au(I) complex **4.17**·(**BF**<sub>4</sub>)<sub>2</sub> was prepared from the *bis*-imidazolium salt **4.16**·**I**<sub>2</sub> and (THT)AuCl while the homobimetallic Ag(I) complex was synthesized from by the reaction of **4.16**·**I**<sub>2</sub> and Ag<sub>2</sub>O (Scheme 4.7).



Scheme 4.7 Synthesis of *bis*-imidazolium salt **4.16·I<sub>2</sub>** and the corresponding Au(I)<sub>2</sub> and Ag(I)<sub>2</sub> homobimetallic complexes **4.17·(BF<sub>4</sub>)<sub>2</sub>** and **4.18·(BF<sub>4</sub>)<sub>2</sub>**. Conditions (a) (THT)AuCl, NaOAc, DMF, 110 °C, 3 h and (b) Ag<sub>2</sub>O, H<sub>2</sub>O, RT, 0.5 h.

The formation of the homobimetallic complexes **4.17·(BF<sub>4</sub>)<sub>2</sub>** and **4.18·(BF<sub>4</sub>)<sub>2</sub>** was confirmed by NMR spectroscopy. The <sup>1</sup>H-NMR spectra for **4.17·(BF<sub>4</sub>)<sub>2</sub>** and **4.18·(BF<sub>4</sub>)<sub>2</sub>** showed no imidazolium C2-H proton signal, indicating coordination of the carbene carbon to the metal centre. In addition, the <sup>13</sup>C-NMR spectra showed downfield signals at 183.65 and 206.98 ppm for carbene carbon atom for **4.17·(BF<sub>4</sub>)<sub>2</sub>** and **4.18·(BF<sub>4</sub>)<sub>2</sub>** respectively. In addition, the <sup>1</sup>H-NMR spectra showed only two signals for the imidazole ring protons at 7.88 and 7.65 ppm for **4.17·(BF<sub>4</sub>)<sub>2</sub>** and 7.89 and 7.71 for **4.18·(BF<sub>4</sub>)<sub>2</sub>** suggesting a symmetrical structure which is in contrast to the heterobimetallic complexes **4.11·(BF<sub>4</sub>)<sub>2</sub>** and **4.12·(BF<sub>4</sub>)<sub>2</sub>**.

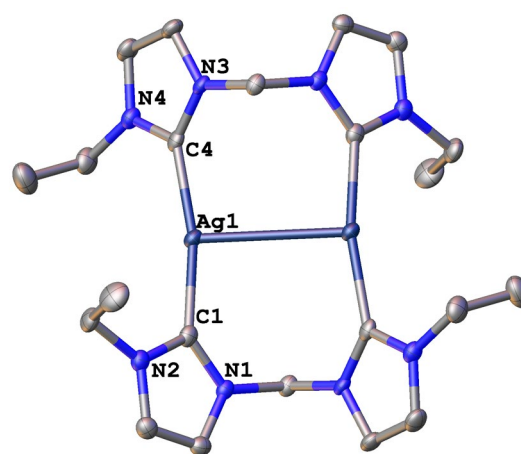


Figure 4.8 Representation of the X-ray crystal structure of Ag(I)<sub>2</sub> homobimetallic complex **4.18·(BF<sub>4</sub>)<sub>2</sub>**. Atomic displacement ellipsoids are shown at the 50% probability level.

The structure of the homobimetallic Ag(I)<sub>2</sub> complex **4.18**·(BF<sub>4</sub>)<sub>2</sub> is shown in Figure 4.8 and the Ag(I) centres adopted linear two-coordinate geometries with the average of the C<sub>carbene</sub>-Ag bond distances being 2.09 Å. In addition, the C-Ag-C bond angles (167.40(11)°) are significantly distorted from linearity, suggesting the possibility of an argentophilic interaction.<sup>23, 26</sup> Consistent with this, the Ag...Ag distance is 3.2458(3) Å which is slightly shorter than the sum of the van der Waals radii for silver (3.44 Å)<sup>56</sup> and consistent with the literature value for the argentophilic interaction (3.358(5) Å).<sup>56</sup> In contrast to the heterobimetallic complex **4.12**·(BF<sub>4</sub>)<sub>2</sub>, the homobimetallic complex **4.18**·(BF<sub>4</sub>)<sub>2</sub> adopted a structure where the methylene groups are orientated on opposite sides with respect to a plane described by the carbene carbon atoms (up-down).

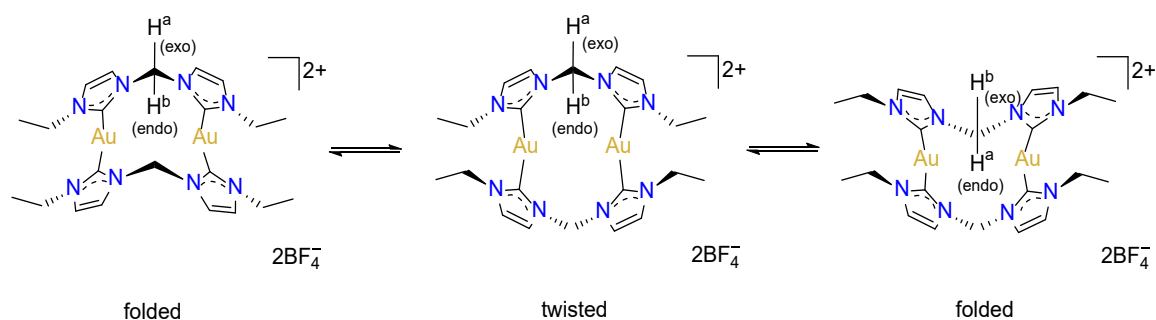
#### 4.2.3 Variable temperature <sup>1</sup>H-NMR studies

As noted in the previous section <sup>1</sup>H-NMR studies were consistent with certain complexes adopting different conformational forms in solution at room temperature. To further investigate the conformational isomeric forms of the complexes **4.11**·(BF<sub>4</sub>)<sub>2</sub>, **4.12**·(BF<sub>4</sub>)<sub>2</sub>, **4.13**·(BF<sub>4</sub>)<sub>3</sub>, **4.14**·(BF<sub>4</sub>)<sub>3</sub>, and **4.17**·(BF<sub>4</sub>)<sub>2</sub> variable temperature <sup>1</sup>H-NMR (VT <sup>1</sup>H-NMR) experiments were performed between the temperatures 233 K to 343 K and the stacked spectra for the complexes **4.17**·(BF<sub>4</sub>)<sub>2</sub>, **4.12**·(BF<sub>4</sub>)<sub>2</sub> and **4.11**·(BF<sub>4</sub>)<sub>2</sub> in CD<sub>3</sub>CN solution are shown in Figure 4.9, Figure 4.10 and Figure 4.11 respectively while the stacked spectra for the complexes **4.14**·(BF<sub>4</sub>)<sub>3</sub> and **4.13**·(BF<sub>4</sub>)<sub>3</sub> in CD<sub>3</sub>CN solution are showed in Figure A.115 and Figure A.114 in Appendix.

For complex **4.17**·(BF<sub>4</sub>)<sub>2</sub>, then VT <sup>1</sup>H-NMR spectra are shown in Figure 4.9. At low temperature, (243 K), the spectrum for complex **4.17**·(BF<sub>4</sub>)<sub>2</sub> exhibits two doublet signals for the methylene protons at 6.08 and 6.89 ppm as an AX pattern suggesting a folded conformational structure where the two protons on each methylene group are in non-



equivalent environments (exo and endo) and the interconversion between the folded and twisted conformational isomers is slow on the NMR timescale (Scheme 4.8). When the temperature was increased to 303 K these signals began broadening and could not be resolved at 343 K. In addition, the CH<sub>2</sub> unit of the ethyl group resonates as a multiplet at 243 K and simplifies to a quartet at 303 K. These can be explained by an inversion process between two folded forms of **4.17**·(**BF**<sub>4</sub>)<sub>2</sub> (Scheme 4.8). At low temperature interconversion of these conformational isomers is slow but as the temperature is increased the rate increases until fast exchange is reached at 343 K. Interestingly, some small visible signals at 7.35 and 7.59 ppm and 6.77 ppm were observed at 243 K and these signals are no longer resolved at 303 K. This result is consistent with a small amount of a twisted conformational isomeric form of the complex (Scheme 4.8). These observations are also consistent with previously reported VT NMR studies for closely reported compounds.<sup>32, 57</sup>



Scheme 4.8 Conformational structures for complex **4.17**·(**BF**<sub>4</sub>)<sub>2</sub> caused by ring inversion.

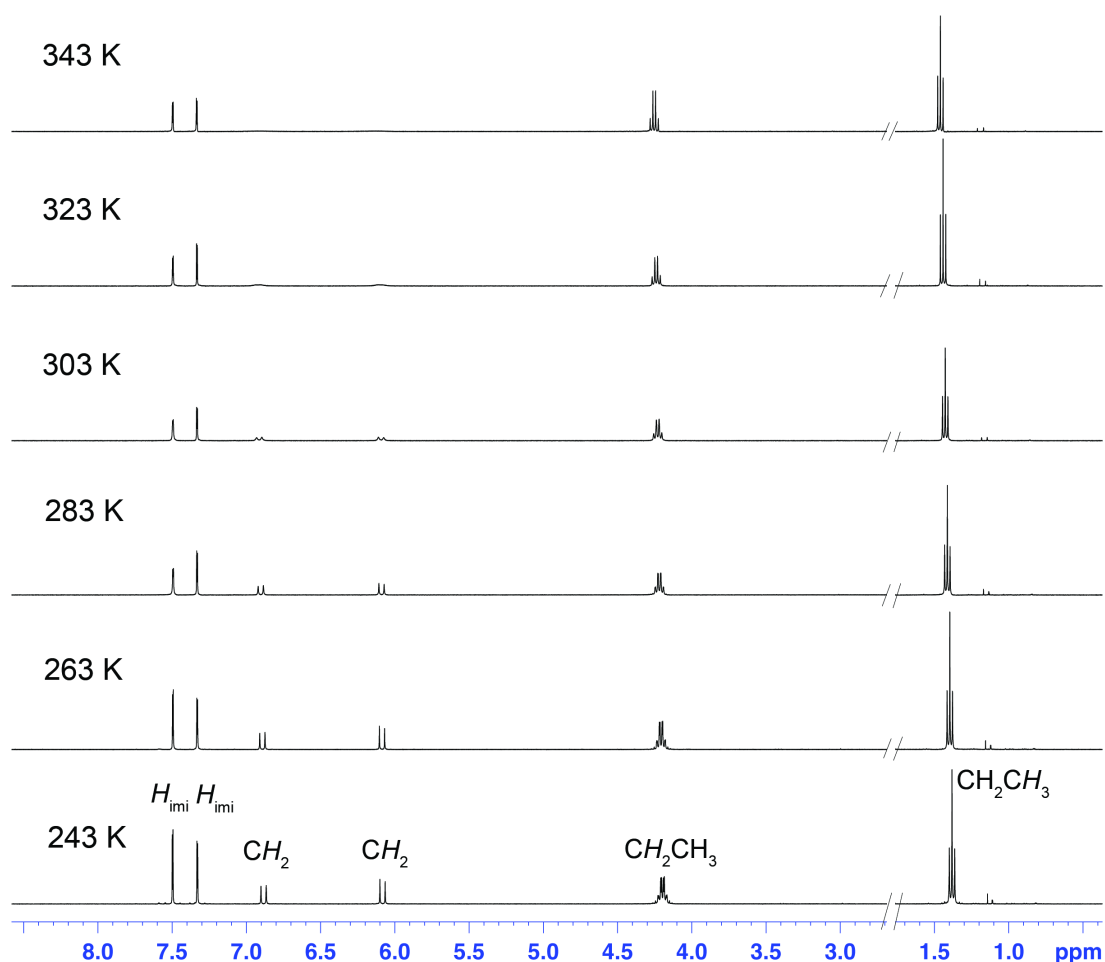
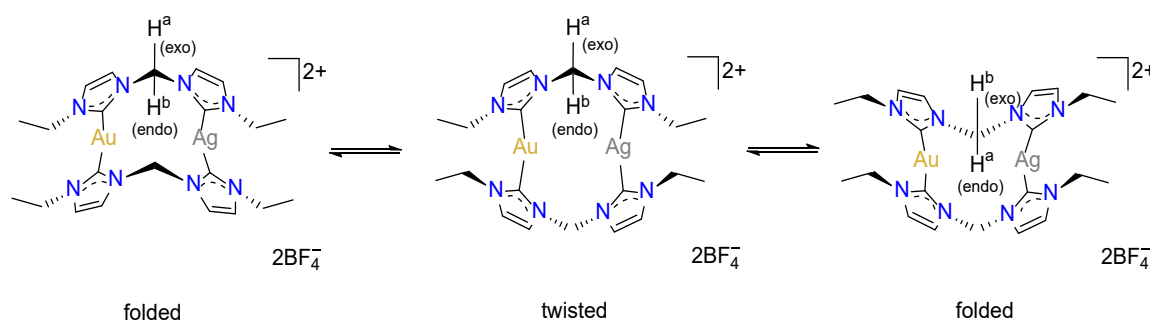


Figure 4.9 Stacked  $^1\text{H}$ -NMR Spectra for  $\text{Au(I)}_2$  homobimetallic complex **4.17**·( $\text{BF}_4$ ) $_2$ .

A VT  $^1\text{H}$ -NMR study was then undertaken for the  $\text{Au(I)}$ - $\text{Ag(I)}$  heterobimetallic complex **4.12**·( $\text{BF}_4$ ) $_2$  and the stacked spectra are shown in Figure 4.10. At low temperature (233 K), the spectrum for **4.12**·( $\text{BF}_4$ ) $_2$  shows two sets of quartets at 4.14 and 4.20 ppm and two sets of overlapping triplets at 1.36 and 1.39 ppm for the ethyl group protons, while the protons on the imidazole rings resonate at 7.30, 7.34, 7.49 and 7.54 ppm. In addition, the methylene group protons resonate as an AX pattern. As was the case with **4.17**·( $\text{BF}_4$ ) $_2$  the methylene proton signal indicate a folded conformational isomer with two non-equivalent (exo and endo) protons on each methylene group and the inversion between two different conformational structures (folded and twisted) being slow on the NMR timescale (Scheme 4.9). As the temperature was increased to 263 K the methylene proton signals broadened

and underwent coalescence at 323 K, consistent with the inversion process between the two possible folded forms of **4.12**·(**BF**<sub>4</sub>)<sub>2</sub> (Scheme 4.9) occurring with an intermediate rate on the NMR timescale. At 343 K, the methylene proton signal was apparent as a broad singlet signal, suggesting that the interconversion process between the folded and twisted structures was fast with respect to the NMR timescale. Once again, a series of less intense signals were observed at 6.09, 6.87 and 7.74 ppm at 243 K, and these signals were no longer resolved when the solution was warmed to 303 K, which is also consistent with the small amount of the twisted conformational structure of the molecular cation existing at the low temperature and the exchange of these conformational structures (folded and twisted) account for the disappearance of the less intense signals (Scheme 4.9).

A VT <sup>1</sup>H-NMR study was also conducted on the Au(I)-Hg(II) heterobimetallic complex **4.14**·(**BF**<sub>4</sub>)<sub>3</sub> and the stacked spectra are shown in Figure A.115 in Appendix. In a similar manner to **4.12**·(**BF**<sub>4</sub>)<sub>2</sub>, coalescence of the proton signals for the methylene group occurred at 343 K, which is consistent with ring inversion between two folded structures, while two sets of ethyl group signals are expected as the compound symmetry is decreased due to the presence of different metal atoms (i.e. Au and Hg).



Scheme 4.9 Conformational structures for complex **4.12**·(**BF**<sub>4</sub>)<sub>2</sub> caused by ring inversion.

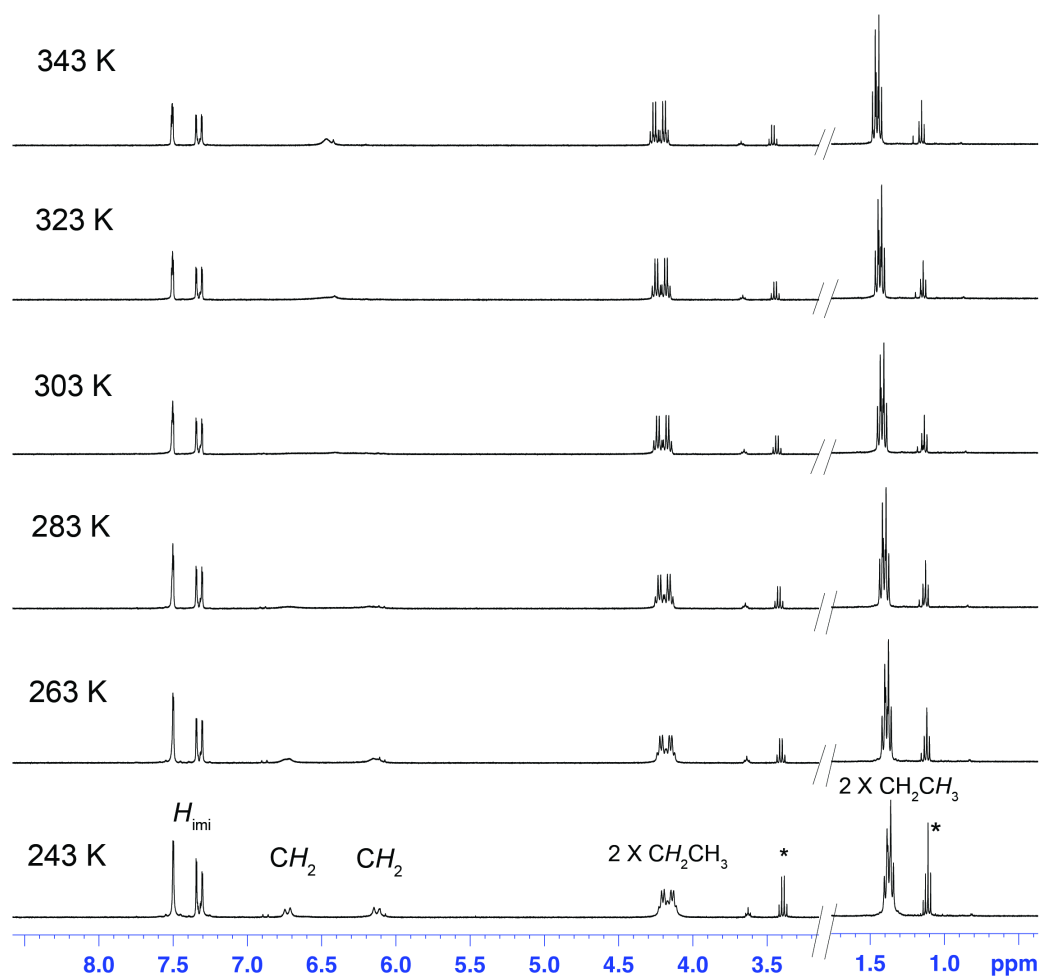
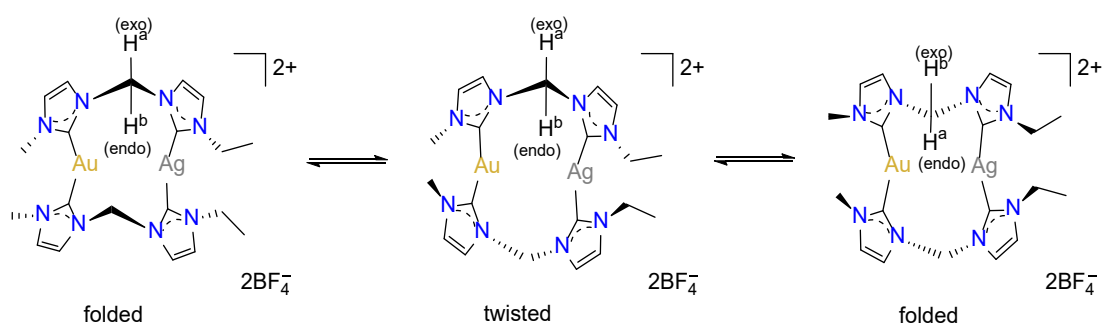


Figure 4.10 Stacked  $^1\text{H}$ -NMR Spectra for **4.12**·( $\text{BF}_4$ ) $_2$ . \*Trace amount of diethyl ether was found in the sample.

The lowest symmetry compound is **4.11**·( $\text{BF}_4$ ) $_2$ , for which the ligand is asymmetrical (methyl and ethyl groups) and the complex contains both Au and Ag metal atoms. The results of a VT  $^1\text{H}$ -NMR study are shown in Figure 4.11. At the low temperature (243 K), a broad AX pattern is observed for the methylene group protons and these signals broadened at 283 K and eventually coalesced at 303 K, consistent with the proton environments being non-equivalent (exo and endo) at low temperature (Scheme 4.10), in a similar manner to the VT  $^1\text{H}$ -NMR results for complexes **4.12**·( $\text{BF}_4$ ) $_2$  and **4.17**·( $\text{BF}_4$ ) $_2$ . The broadening and eventual coalescence of this signal also suggests that at the low temperature the inversion of the structure is slow on NMR timescale and the rate of the process increases as the temperature is increased to 323 K. In addition, low intensity signals are apparent at

6.88 and 6.92 ppm at 243 K and these are no longer resolved as the temperature is raised to 283 K. These signals are consistent with there being a small amount of the twisted conformational structure (Scheme 4.10) in solution at low temperature (243 K). Interestingly, the imidazole ring protons resonate within the range of 7.20 – 7.60 ppm as multiplet signals and the pattern observed for these protons did not change significantly as the temperature was raised. In addition, two quartet and two singlet signals were observed for the wingtip ethyl and methyl groups. This increased complexity can be rationalised when the crystal structure for compound **4.11**·(**BF<sub>4</sub>**)<sub>2</sub> (Figure 4.6) is carefully studied. It is apparent here that the complex is distorted and that this distortion gives rise to result in two distinct imidazole environments for each of the NHC units coordinated to the Ag(I) and Au(I) atoms. This leads to the two different methyl and ethyl wingtip group signals being different. To complete the series a VT <sup>1</sup>H-NMR study was conducted for the Au(I)-Hg(II) heterobimetallic complex **4.13**·(**BF<sub>4</sub>**)<sub>3</sub>. The results of this study are shown in Appendix section A 4.2 and these spectra showed that this complex undergoes a more complex process compared to the Au(I)-Ag(I) analogue complex and this process is not yet fully understood. The stacked <sup>1</sup>H-NMR spectra for **4.13**·(**BF<sub>4</sub>**)<sub>3</sub> is shown in Appendix Figure A.114.<sup>34</sup>



Scheme 4.10 Conformational structures for complex **4.11**·(**BF<sub>4</sub>**)<sub>2</sub> caused by ring inversion.

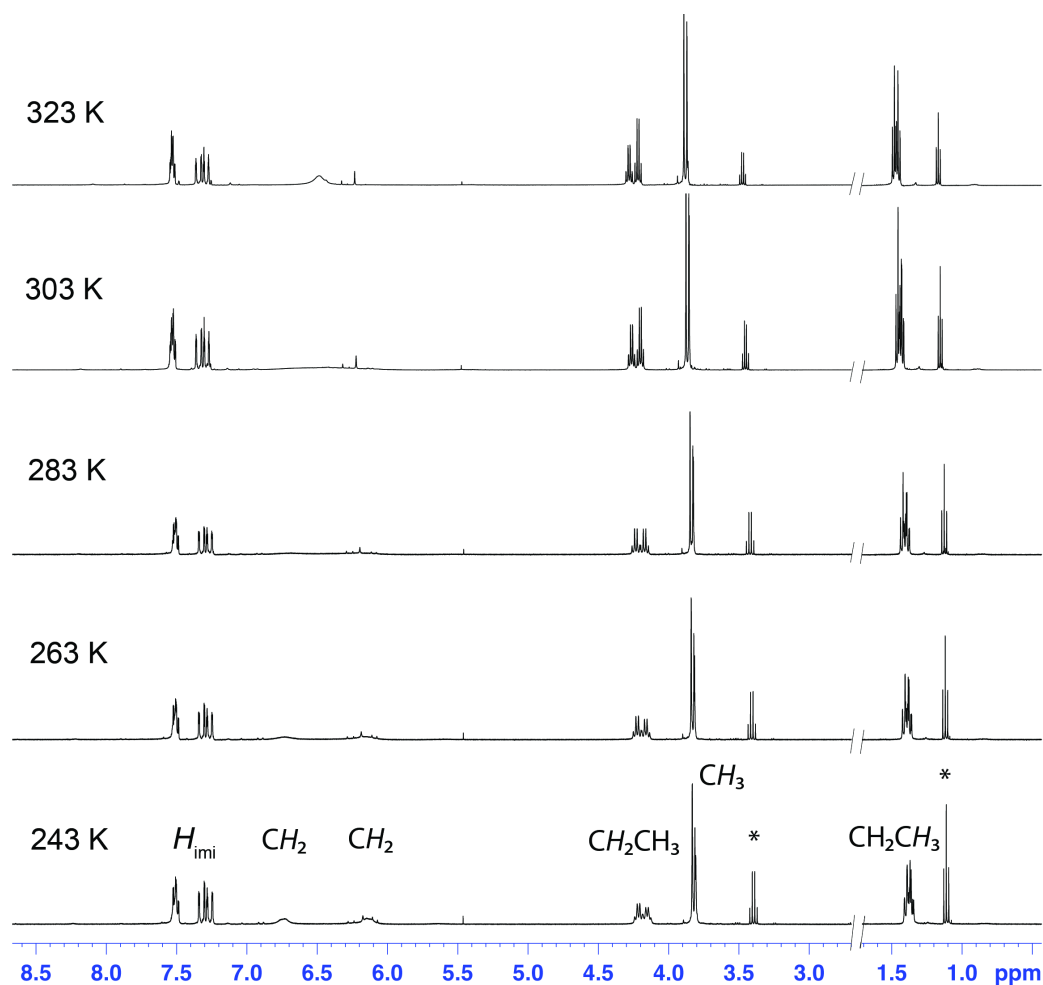
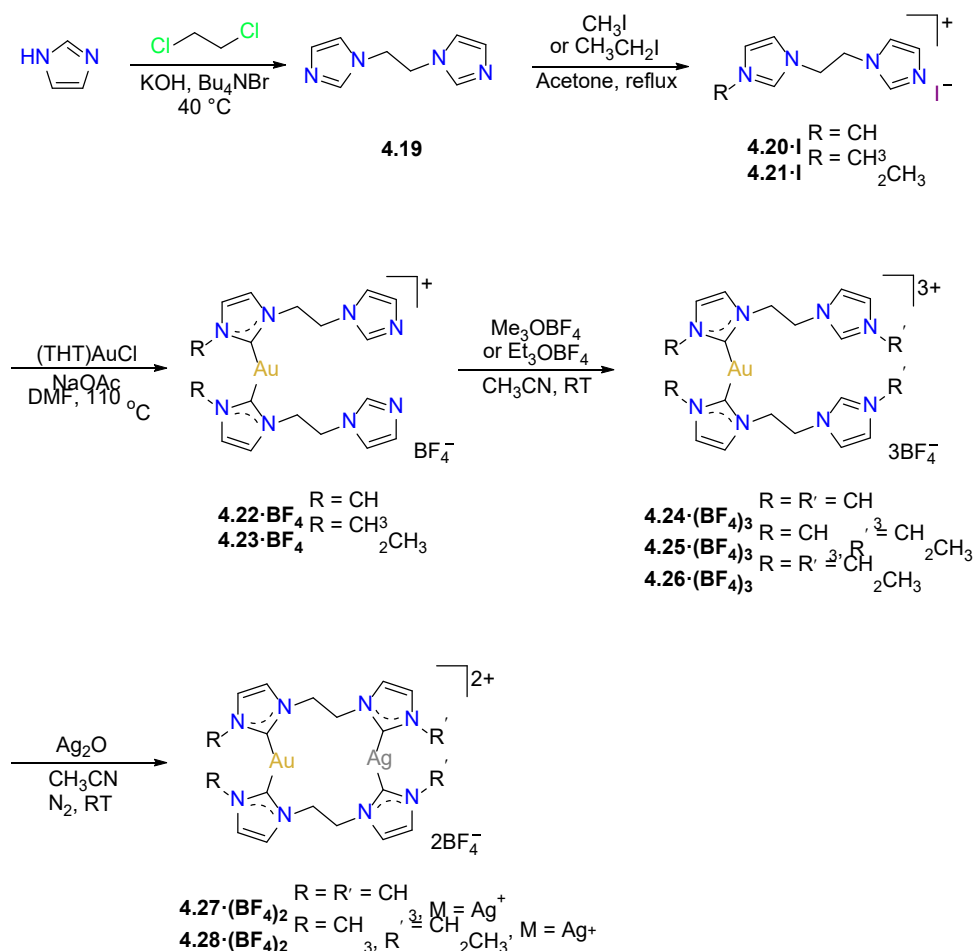


Figure 4.11 Stacked  $^1\text{H}$ -NMR Spectra for **4.11**·( $\text{BF}_4$ ) $_2$ . \*Trace amount of diethyl ether was found in the sample.

Overall, the results of the VT  $^1\text{H}$ -NMR study suggest that all of these complexes underwent a ring interconversion process between folded and twisted conformational structures. At low temperature interconversion of these conformational isomers is slow but as the temperature is increased the rate increases and became fast exchange. In addition, the results also suggest that symmetry of the structure decreased when hetero- metal atoms or different wingtip groups were introduced which results in the increased complexity of the spectra. Furthermore, the distorted structure of complex **4.11**·( $\text{BF}_4$ ) $_2$  leads to two distinct imidazole environments for each of the NHC units coordinated to the Ag(I) and Au(I) atom in addition to two different methyl and ethyl group signals wingtip group being different.

#### 4.2.4 Heterobimetallic complexes of ethylene linked *bis*-NHC ligands

To further explore the properties of heterobimetallic complexes of NHC ligands derived from *bis*-imidazolium pro-ligands, a series of heterobimetallic complexes were prepared from ethylene linked *bis*-imidazolium pro-ligands (Scheme 4.11). The synthesis (Scheme 4.11) was begun with the reaction of imidazole and 1,2-dichloroethane to obtain the 1,2-diimidazolylethane **4.19**. Compound **4.19** was then mono-alkylated with either CH<sub>3</sub>I or CH<sub>3</sub>CH<sub>2</sub>I yielding the mono-imidazolium species **4.20·I** and **4.21·I**, which were then metallated with (THT)AuCl yielding the Au(I) complexes **4.22·BF<sub>4</sub>** and **4.23·BF<sub>4</sub>**. These complexes were then alkylated with either Me<sub>3</sub>OBF<sub>4</sub> or Et<sub>3</sub>OBF<sub>4</sub> yielding complexes **4.24·(BF<sub>4</sub>)<sub>3</sub>**, **4.25·(BF<sub>4</sub>)<sub>3</sub>** and **4.26·(BF<sub>4</sub>)<sub>3</sub>**, which were then reacted with a second metal to obtain the heterobimetallic complexes **4.27·(BF<sub>4</sub>)<sub>2</sub>** and **4.28·(BF<sub>4</sub>)<sub>2</sub>**.



Scheme 4.11 Synthetic reaction scheme for the preparation of heterobimetallic complexes **4.27·(BF<sub>4</sub>)<sub>2</sub>** and **4.28·(BF<sub>4</sub>)<sub>2</sub>**.

The formation of compounds **4.19**, **4.20·I** and **4.21·I** was confirmed by NMR spectroscopy and mass spectrometry and **4.20·I** was also characterised using X-ray crystallography. A representation of the X-ray crystal structure of compound **4.20·I** is shown in Figure 4.12 and this structure shows only one of the imidazole units is alkylated with a methyl group.

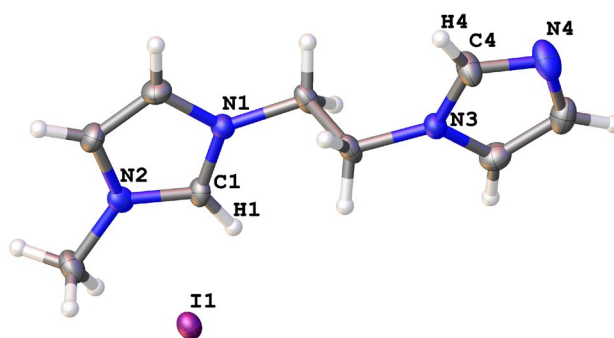


Figure 4.12 Representation of the X-ray crystal structure of **4.20·I**. Atomic displacement ellipsoids are shown at the 50% probability level.

$^1\text{H}$  and  $^{13}\text{C}$ -NMR studies were used to confirm the structures of the metal complexes **4.22·BF<sub>4</sub>** – **4.28·(BF<sub>4</sub>)<sub>2</sub>**. In all cases, the C2 proton signals of the pro-ligands were absent from the  $^1\text{H}$  NMR spectra of the metal complexes and the downfield shift for carbenic carbon signals (183.77, 183.01 for compounds **4.22·BF<sub>4</sub>**, **4.23·BF<sub>4</sub>**, 183.01, 183.32 and 183.34 for compounds **4.24·(BF<sub>4</sub>)<sub>3</sub>**, **4.25·(BF<sub>4</sub>)<sub>3</sub>** and **4.26·(BF<sub>4</sub>)<sub>3</sub>**, 184.55 and 183.93 ppm for **4.28·(BF<sub>4</sub>)<sub>2</sub>** respectively) were observed. Furthermore, the successful alkylations were confirmed by the downfield shift of C2-H imidazolium signals (8.87, 9.03 and 8.87 for **4.24·(BF<sub>4</sub>)<sub>3</sub>**, **4.25·(BF<sub>4</sub>)<sub>3</sub>** and **4.26·(BF<sub>4</sub>)<sub>3</sub>** respectively) in addition to the wingtip group signals (3.81 for **4.24·(BF<sub>4</sub>)<sub>3</sub>**, 4.13 and 1.31 for **4.25·(BF<sub>4</sub>)<sub>3</sub>** and 1.29 for **4.26·(BF<sub>4</sub>)<sub>3</sub>** respectively). The structure of the monometallic complex **4.23·BF<sub>4</sub>** was also confirmed by X-ray crystallography and a representation of the crystal structure for this compound is shown in Figure 4.13. The structure for **4.23·BF<sub>4</sub>** shows that the Au(I) centre adopts a linear two coordinate geometry with the Au(I) centre coordinated to two NHC groups with the



bond lengths being 2.026(7) and 2.029(7) Å, with a C-Au-C angle of 175.12°. The crystal structure of the same complex grown from a mixture of acetonitrile and THF is shown in Figure 4.13 and as expected shows that the Au(I) centre adopts the same coordination geometry as that described for the previous structure of this compound. Interestingly however, this X-ray crystal structure also shows that a sodium atom was coordinating to four unalkylated imidazole groups from two units of the Au(I) complex **4.23**·BF<sub>4</sub>. In addition, an acetonitrile molecule was also coordinated to the sodium atom giving a trigonal bipyramidal coordination geometry about the sodium metal centre. The sodium atoms in this structure are likely to have originated from the NaOAc used in the synthesis of the Au(I) complex.

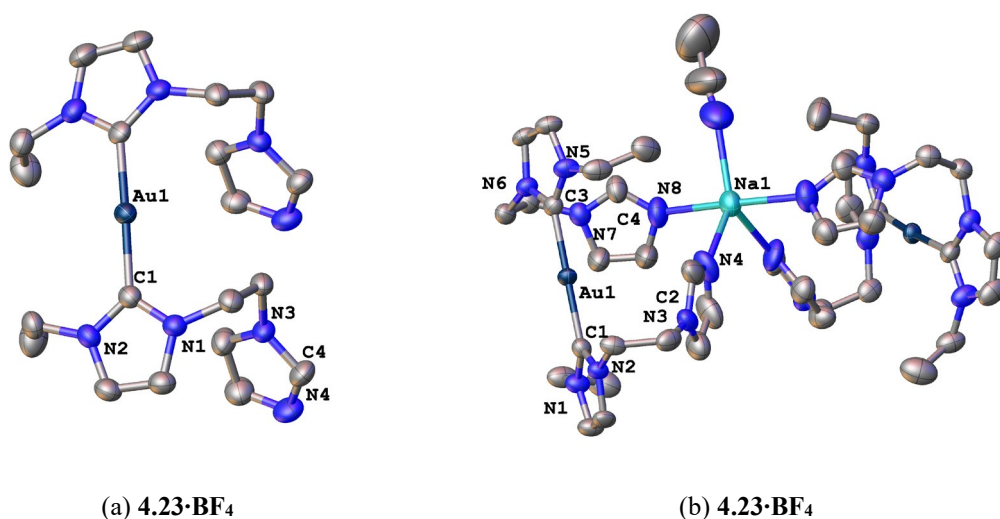


Figure 4.13 Representation of two X-ray crystal structures of the mononuclear Au(I) complexes. (a) Structure of **4.23**·BF<sub>4</sub> grown from a mixture of acetonitrile and diethyl ether (b) Structure of **4.23**·BF<sub>4</sub> grown from a mixture of acetonitrile and THF. Anions are omitted for clarity. Atomic displacement ellipsoids are shown at the 50% probability level.

Formation of the heterobimetallic complex **4.27**·(BF<sub>4</sub>)<sub>2</sub> was confirmed by <sup>1</sup>H-NMR and a high-resolution mass spectrum of the crude product. Unfortunately, despite several attempts to purify this heterobimetallic complex this compound could not be obtained in the pure form. However, the analogous complex **4.28**·(BF<sub>4</sub>)<sub>2</sub> (Scheme 4.11) was successfully purified and characterised. The <sup>1</sup>H-NMR spectrum of **4.28**·(BF<sub>4</sub>)<sub>2</sub> showed

signals for imidazole ring protons at 7.03, 7.09, 7.14 and 7.16 ppm indicating a lower symmetry structure resulting from the different imidazole wingtip groups (i.e. methyl and ethyl group). In addition, the protons on the ethylene linker resonated as two sets of triplets at 4.66 and 4.73 ppm which is also consistent with the asymmetrical structure. In contrast to the corresponding methylene linked complex **4.11**·(BF<sub>4</sub>)<sub>2</sub>, the spectrum for **4.28**·(BF<sub>4</sub>)<sub>2</sub> suggests a more conformationally labile structure due to the increasing flexibility imparted by the ethylene linker when compared to the methylene linker (Figure 4.14).

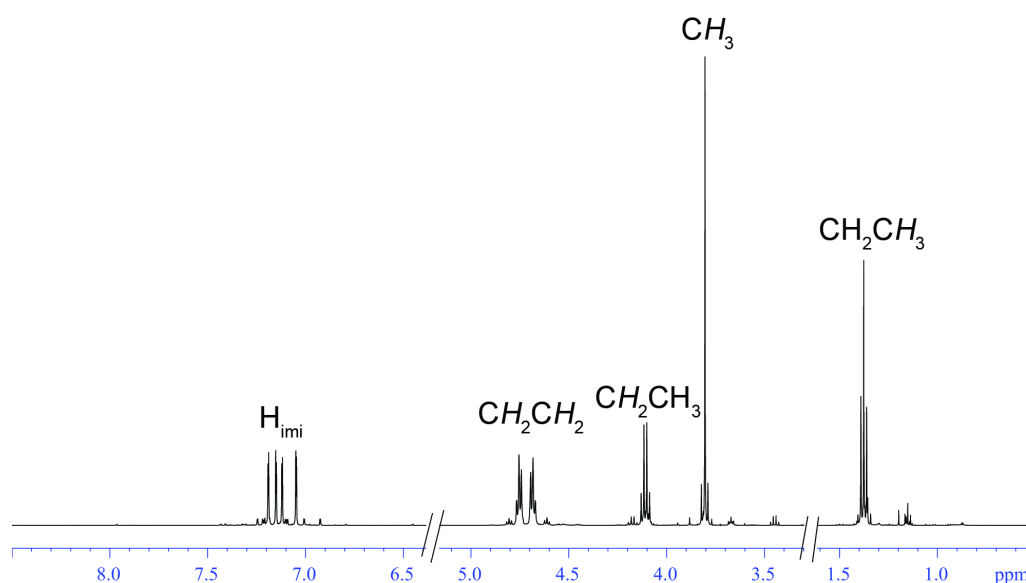


Figure 4.14 <sup>1</sup>H-NMR spectra of complex **4.28**·(BF<sub>4</sub>)<sub>2</sub>.

The high-resolution mass spectrum for **4.28**·(BF<sub>4</sub>)<sub>2</sub> (Figure 4.15) produced a series of peaks consistent with the heterobimetallic dinuclear structure with the general formula [AuAgL<sub>2</sub>]<sup>2+</sup> (where L is the ethylene linked *bis*-NHC ligand). For example, a peak observed at *m/z* = 356.0726, corresponds to the formula [C<sub>22</sub>H<sub>32</sub>N<sub>8</sub>AuAg]<sup>2+</sup> (calculated = 356.0728), while the peak at *m/z* = 799.1485 is in agreement with the formula [C<sub>22</sub>H<sub>32</sub>N<sub>8</sub>AuAgBF<sub>4</sub>]<sup>+</sup> (calculated = 799.1490).

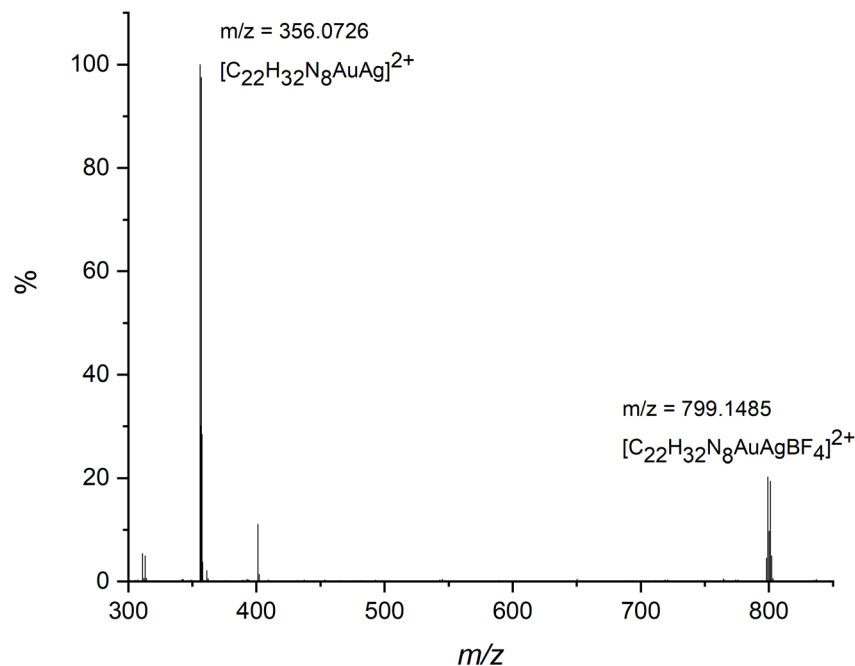


Figure 4.15 High-resolution mass spectrum of Au(I)-Ag(I) heterobimetallic complex **4.28·(BF<sub>4</sub>)<sub>2</sub>**.

Interestingly, the heterobimetallic complex **4.28·(BF<sub>4</sub>)<sub>2</sub>** showed limited stability in solution. The <sup>1</sup>H-NMR spectrum of the freshly prepared sample of this compound dissolved in d<sub>3</sub>-CD<sub>3</sub>CN is shown in Figure 4.16 and the expected number of signals for the title compound are observed. Spectra were then recorded after 24 h, 3 months and 4 months (Figure 4.16) and these showed extra signals compared with the freshly prepared sample. In addition, over the course of the NMR time course, a white solid slowly precipitated from solution. The NMR spectra recorded at later time points (3-months and 4-months) did not show evidence of the pro-ligand indicating that simple decomposition back to the starting materials was not occurring. Meanwhile, crystals were obtained using diffusion of diethyl ether into an aged acetonitrile solution of **4.28·(BF<sub>4</sub>)<sub>2</sub>**. The poor-quality X-ray crystal structure (Figure 4.17) suggests that a polymerization process is occurring with a coordination polymer being formed. These observations are also consistent with previously reported studies for Au(I)-Ag(I) heterobimetallic complexes of NHC ligands.<sup>30, 55</sup>

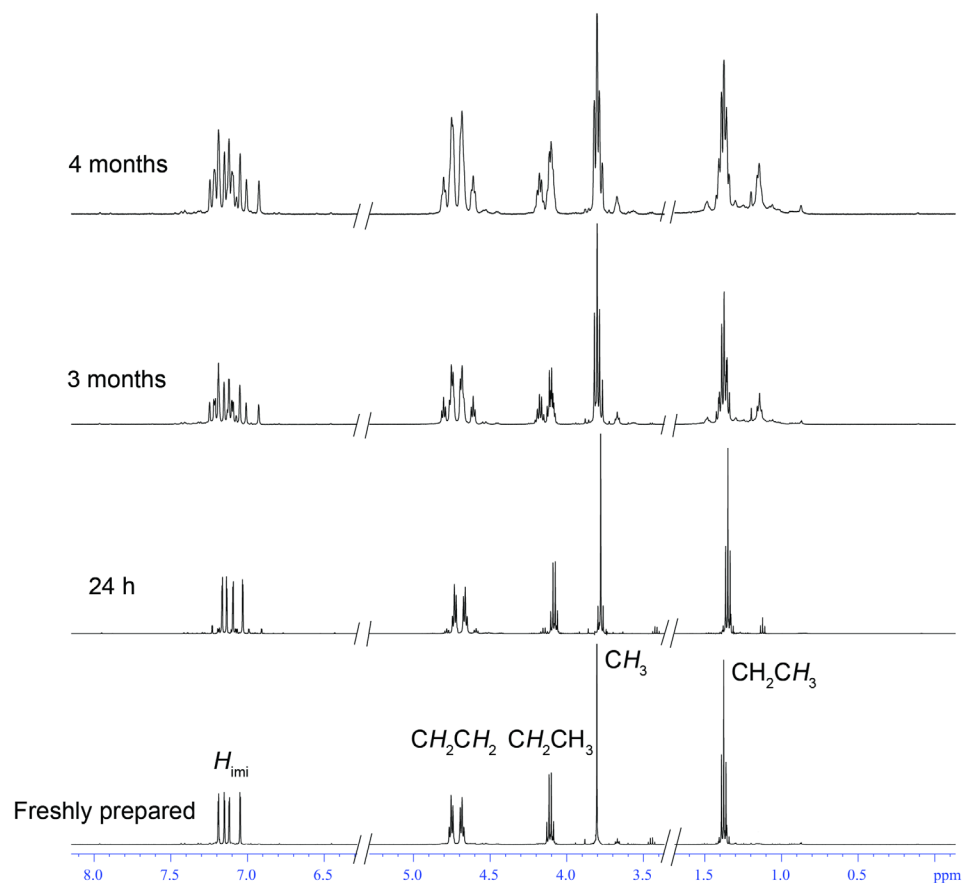


Figure 4.16 Timecourse experiment showing the slow decomposition of compound **4.28**·(**BF**<sub>4</sub>)<sub>2</sub> over a period of 4 months in d<sub>3</sub>-CD<sub>3</sub>CN.

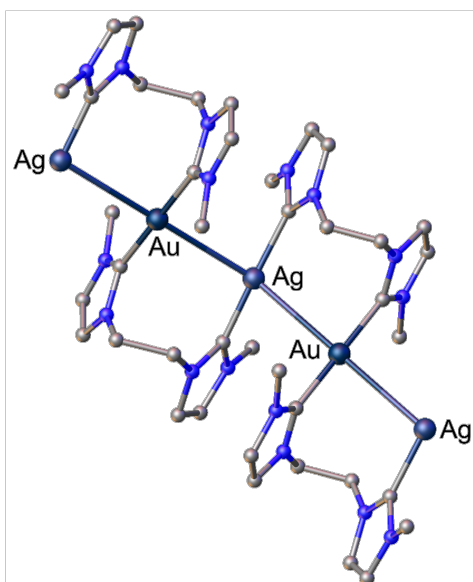


Figure 4.17 Crystal structure of **4.28**·(**BF**<sub>4</sub>)<sub>2</sub> showing the formation of a coordination polymer.

#### 4.2.5 Photophysical studies

Numerous previous studies have shown that bimetallic complexes of the coinage metals exhibiting metallophilic interactions (e.g. aurophilic, argentophilic and cuprophilic interactions) display interesting photophysical properties such as luminescence.<sup>27, 30</sup> As such, we were interested to explore the photophysical properties of the homo- and heterobimetallic complexes prepared in this chapter. The UV-visible absorption spectra for the symmetrical *bis*-imidazolium pro-ligand **4.16·I<sub>2</sub>** and the homobimetallic Au(I)<sub>2</sub> complex **4.17·(BF<sub>4</sub>)<sub>2</sub>** and the Ag(I)<sub>2</sub> complex **4.18·(BF<sub>4</sub>)<sub>2</sub>**, in addition to the heterobimetallic complexes **4.11·(BF<sub>4</sub>)<sub>2</sub>**, **4.12·(BF<sub>4</sub>)<sub>2</sub>**, **4.13·(BF<sub>4</sub>)<sub>3</sub>** and **4.14·(BF<sub>4</sub>)<sub>3</sub>** are shown in Figure 4.18 and the UV-visible absorption data are summarized in Table 4.1. The pro-ligand **4.16·I<sub>2</sub>** displayed two intense absorption bands at 208 and 246 nm while the homobimetallic complexes display a strong absorption band at 228 nm for **4.18·(BF<sub>4</sub>)<sub>2</sub>** and 252 nm for **4.17·(BF<sub>4</sub>)<sub>2</sub>**. However, the heterobimetallic complexes **4.11·(BF<sub>4</sub>)<sub>2</sub>**, **4.12·(BF<sub>4</sub>)<sub>2</sub>**, **4.13·(BF<sub>4</sub>)<sub>3</sub>** and **4.14·(BF<sub>4</sub>)<sub>3</sub>** displayed a prominent absorption band in the region of 235 – 237 nm with a less intense shoulder in the region 254 – 263 nm. Luminescence studies showed that none of these homo- or heterobimetallic complexes were emissive at room temperature in solution and this may be due to the loss of metallophilic interaction resulting from fluxional behaviour in solution.<sup>25</sup>

Table 4.1 Spectroscopic properties of **4.11·(BF<sub>4</sub>)<sub>2</sub>**, **4.12·(BF<sub>4</sub>)<sub>2</sub>**, **4.13·(BF<sub>4</sub>)<sub>3</sub>**, **4.14·(BF<sub>4</sub>)<sub>3</sub>**, **4.16·I<sub>2</sub>**, **4.17·(BF<sub>4</sub>)<sub>2</sub>**, and **4.18·(BF<sub>4</sub>)<sub>2</sub>**.

	UV-vis $\lambda_{\text{max}}$ /nm ( $\epsilon/\text{M}^{-1}\cdot\text{cm}^{-1}$ )
<b>4.16·I<sub>2</sub></b>	208 (40703), 246 (25796)
<b>4.11·(BF<sub>4</sub>)<sub>2</sub></b>	237 (23969), 254 (17109)
<b>4.10·(BF<sub>4</sub>)<sub>2</sub></b>	235 (18439), 251 (12240)
<b>4.12·(BF<sub>4</sub>)<sub>3</sub></b>	237(14961), 261(13773)
<b>4.13·(BF<sub>4</sub>)<sub>3</sub></b>	237 (22057), 263 (12961)
<b>4.17·(BF<sub>4</sub>)<sub>2</sub></b>	211(16240), 228 (210847), 240 (27589), 252 (32228)
<b>4.18·(BF<sub>4</sub>)<sub>2</sub></b>	228 (32828), 258 (9879)

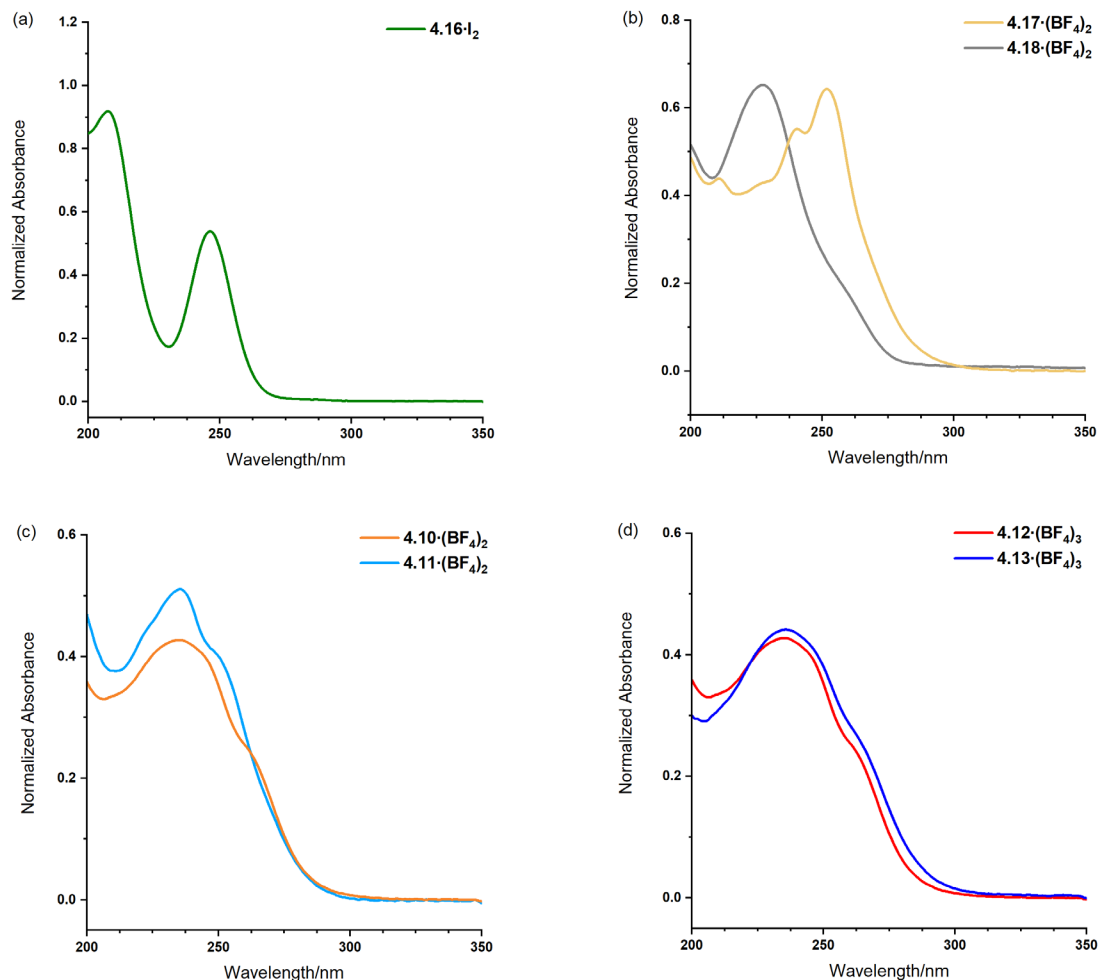


Figure 4.18 Absorbance spectra of (a) *bis*-imidazolium pro-ligand **4.16·I<sub>2</sub>** and (b) homobimetallic complexes **4.17·(BF<sub>4</sub>)<sub>2</sub>** and **4.18·(BF<sub>4</sub>)<sub>2</sub>** and (c) Au(I)-Ag(I) heterobimetallic complexes **4.10·(BF<sub>4</sub>)<sub>2</sub>** and **4.11·(BF<sub>4</sub>)<sub>2</sub>** and (d) Au(I)-Hg(II) heterobimetallic complexes **4.12·(BF<sub>4</sub>)<sub>3</sub>** and **4.13·(BF<sub>4</sub>)<sub>3</sub>**. All the spectra were recorded at  $2.0 \times 10^{-5}$  M from acetonitrile solutions.

#### 4.2.6 Antimicrobial studies

Many previous studies have demonstrated that Ag(I) and a lesser extent Au(I) complexes of NHC ligands have antimicrobial activity and may have potential medicinal applications for the treatment of bacterial infections. However, the antimicrobial activity of heterobimetallic NHC complexes has not yet been explored. As such, we were interested to investigate the antimicrobial properties of the synthesized homo- and heterobimetallic complexes reported in this chapter. The antimicrobial activities of the compounds **4.11·(BF<sub>4</sub>)<sub>2</sub>**, **4.12·(BF<sub>4</sub>)<sub>2</sub>**, **4.16·I<sub>2</sub>**, **4.17·(BF<sub>4</sub>)<sub>2</sub>** and **4.18·(BF<sub>4</sub>)<sub>2</sub>** were tested against the two Gram-negative bacterial strains *A. baumannii* and *E. coli* and two Gram-positive bacterial

strains *E. faecium* and *S. aureus* and the minimum inhibitory concentration (MIC) of the compounds are summarized in Table 4.2. The *bis*-imidazolium pro-ligand **4.16·I<sub>2</sub>** was inactive with the MIC >256 µg·mL<sup>-1</sup> suggesting the pro-ligand is non-toxic to either Gram-negative or Gram-positive bacteria. However, the Ag(I)<sub>2</sub> homobimetallic complex **4.18·(BF<sub>4</sub>)<sub>2</sub>** was highly active with a MIC value in a range of 8 – 32 µg·mL<sup>-1</sup> for both the Gram-negative and Gram-positive bacteria strain which is in consistent with previously reported for the Ag(I)<sub>2</sub> homobimetallic complexes **1.108** (Figure 1.15).<sup>42</sup> Meanwhile, the Au(I) homobimetallic complex **4.17·(BF<sub>4</sub>)<sub>2</sub>** was inactive against those bacterial strain with MIC >256 µg·mL<sup>-1</sup>. The low activity of this compound is in contrast to the antimicrobial activity of the homobimetallic Au(I)<sub>2</sub> complex **1.109** (Figure 1.15) which showed a MIC of 16 µg·mL<sup>-1</sup> for *E. coli*.<sup>42</sup> The heterobimetallic complexes **4.11·(BF<sub>4</sub>)<sub>2</sub>** and **4.12·(BF<sub>4</sub>)<sub>2</sub>** were also tested for their antimicrobial efficacy again the same bacterial strains. Interestingly, the both **4.11·(BF<sub>4</sub>)<sub>2</sub>** and **4.12·(BF<sub>4</sub>)<sub>2</sub>** were the most active of the compounds tested and they displayed the same low MIC values of 4 - 8 µg·mL<sup>-1</sup> and 16 µg·mL<sup>-1</sup> for the Gram-negative bacteria *A. baumannii* and *E. coli* respectively. Although being less effective, these heterobimetallic complexes also display moderate toxicity against the Gram-positive bacteria *E. faecium* and *S. aureus*. In addition, the MIC values for the heterobimetallic complexes showed the antibacterial efficacy were slightly higher compared with the Ag(I)<sub>2</sub> homobimetallic complex **4.18·(BF<sub>4</sub>)<sub>2</sub>**. To date the antimicrobial mechanism of action for Ag(I) and Au(I) complexes of NHC ligands has not been elucidated, the antimicrobial process may be the result of the metal inhibiting the cell division of the bacteria or the damage caused by the metal attaching to the cells receptors.<sup>19, 42, 58-60</sup> The MIC values of **4.11·(BF<sub>4</sub>)<sub>2</sub>**, **4.12·(BF<sub>4</sub>)<sub>2</sub>** and **4.18·(BF<sub>4</sub>)<sub>2</sub>** revealed these complexes displayed moderate antimicrobial activities against Gram-negative and Gram-positive bacterial strain which are comparable to the currently available antibiotics for the Gram-negative or Gram-positive infection treatment and highlight the potential broad-spectrum application for this type of

metalloidrug. For example, as one of the top WHO priority pathogens,<sup>61</sup> carbapenem-resistant *A. baumannii* and *E. coli* infections can be treated with colistin, which has a MIC of  $\leq 4 \mu\text{g}\cdot\text{mL}^{-1}$  against sensitive strains.<sup>61</sup> In addition, multi-drug resistant infections caused by Gram-positive bacteria, vancomycin has long been the last-line treatment and has a MIC for susceptible strains of *S. aureus* and *Enterococcus spp* of  $\leq 2 \mu\text{g}\cdot\text{mL}^{-1}$  and  $\leq 4 \mu\text{g}\cdot\text{mL}^{-1}$ , respectively.<sup>62-63</sup>

Table 4.2 Minimum inhibitory concentrations (MIC) for **4.16·I<sub>2</sub>**, the homobimetallic complexes **4.17·(BF<sub>4</sub>)<sub>2</sub>** and **4.18·(BF<sub>4</sub>)<sub>2</sub>** and Au(I)-Ag(I) heterobimetallic complexes **4.11·(BF<sub>4</sub>)<sub>2</sub>** and **4.12·(BF<sub>4</sub>)<sub>2</sub>**.

	Gram-negative		Gram-positive	
	<i>A. baumannii</i> ( $\mu\text{g}\cdot\text{mL}^{-1}$ )	<i>E. coli</i> ( $\mu\text{g}\cdot\text{mL}^{-1}$ )	<i>E. faecium</i> ( $\mu\text{g}\cdot\text{mL}^{-1}$ )	<i>S. aureus</i> ( $\mu\text{g}\cdot\text{mL}^{-1}$ )
<b>4.16·I<sub>2</sub></b>	>256	>256	>256	>256
<b>4.17·(BF<sub>4</sub>)<sub>2</sub></b>	>256	>256	>256	>256
<b>4.18·(BF<sub>4</sub>)<sub>2</sub></b>	8	16 - 32	16	32
<b>4.11·(BF<sub>4</sub>)<sub>2</sub></b>	4 - 8	16	8 - 16	16 - 32
<b>4.12·(BF<sub>4</sub>)<sub>2</sub></b>	4 - 8	16	8 - 16	16 - 32

### 4.3 Conclusion

A series of five heterobimetallic transition metal complexes of NHC ligands derived from *bis*-imidazolium salts were prepared using a post synthetic modification and metallation method. Initially, a series of monometallic Au(I) complexes featuring unalkylated imidazole units were prepared. These complexes were then further alkylated with either methyl or ethyl groups and in the final step, the precursor Au(I) complexes were treated with a second metal source (e.g. Ag or Hg) yielding the desired heterobimetallic complexes. Meanwhile, the Au(I)<sub>2</sub> and Ag(I)<sub>2</sub> homobimetallic complexes were synthesized using direct metallation method for comparative studies. An X-ray crystal structure study on complexes **4.12·(BF<sub>4</sub>)<sub>2</sub>** and **4.18·(BF<sub>4</sub>)<sub>2</sub>** revealed short Au(I)⋯Ag(I) and Ag(I)⋯Ag(I) distances of 3.205(6) Å and 3.2458(3) Å respectively, which are consistent with



metallophilic interactions. A series of VT  $^1\text{H}$ -NMR studies reveal that both homo- and heterobimetallic complexes of the methylene linked *bis*-NHC ligands are rigid on the NMR timescale in solution at low temperature. In addition, the ring interconversion of the complexes between folded and twisted conformational isomers were observed and this process was slow on NMR timescale at low temperature and the rate of this process increased at elevated temperatures. Furthermore, the introduction of heteroatoms (i.e. Ag or Hg) or different wingtip groups resulted in lower symmetry structures and increased the complexity of the spectra. The distorted structure of complex **4.11**·(**BF**<sub>4</sub>)<sub>2</sub> contribute to two distinct imidazole environments for each of the NHC units coordinated to the Ag(I) and Au(I) atom in addition to two different methyl and ethyl wingtip group signals being different. UV-visible absorption studies showed that the bimetallic complexes are non-emissive and non-luminescent in solution phase possibly as a result of the loss of metallophilic interaction resulting from fluxional behaviour in the solvent. Antimicrobial studies were conducted and the results showed that Au(I)-Ag(I) heterobimetallic complexes showed good MIC values against both Gram-positive and Gram-negative bacteria strains in comparison to the Au(I)<sub>2</sub> and Ag(I)<sub>2</sub> homobimetallic complexes and the pro-ligands. In addition, the Au(I)-Ag(I) heterobimetallic complexes **4.12**·(**BF**<sub>4</sub>)<sub>2</sub> and **4.12**·(**BF**<sub>4</sub>)<sub>2</sub> displayed lower MIC values against Gram-negative bacteria strain and Gram-positive bacteria strain compared with the Au(I)<sub>2</sub> and Ag(I)<sub>2</sub> homobimetallic complexes suggesting these novel Au(I)-Ag(I) heterobimetallic complexes are most toxic to Gram-negative bacteria strain. Although being less active to Gram-positive bacteria strain, the results also suggest that the Au(I)-Ag(I) heterobimetallic complexes are more toxic to the Gram-positive bacteria strain compared to the Au(I)<sub>2</sub> and Ag(I)<sub>2</sub> homobimetallic complexes. To our best knowledge, this is the first report of the antimicrobial activity of Au(I)-Ag(I) heterobimetallic complexes.

## 4.4 Experimental

### 4.4.1 Synthesis

**4.4.** A mixture of imidazole (10.00 g, 146.89 mmol), finely powdered KOH (9.88 g, 176.26 mmol) and *tetra-n*-butylammonium bromide (1.42 g, 4.41 mmol) was stirred at RT for 1 h followed by addition of dibromomethane (5.10 mL, 73.44 mmol). The resultant mixture was further stirred at 40 °C for 24 h followed by addition of finely powdered KOH (4.94 g, 88.13 mmol) and dibromomethane (5.10 mL, 73.44 mmol). This mixture was then further reacted under the same condition for 24 h followed by trituration with chloroform (5 × 20 mL) and gravity filtration. The filtrate was then concentrated to 20 mL *in vacuo* followed by addition of hexane (5 mL) to obtain a pale yellow crystalline. Yield: 1.45 g, 13.3 %. <sup>1</sup>H-NMR (500.023 MHz, d<sub>6</sub>-DMSO): δ = 7.93 (s, 2H, *H*<sub>imi</sub>), 7.40 (s, 2H, *H*<sub>imi</sub>), 6.91 (s, 2H, *H*<sub>imi</sub>), 6.22 (s, 2H, CH<sub>2</sub>). <sup>13</sup>C-NMR (125.74 MHz, d<sub>6</sub>-DMSO): δ = 137.76 (*C*<sub>imi</sub>), 129.61 (*C*<sub>imi</sub>), 119.57 (*C*<sub>imi</sub>), 55.27 (CH<sub>2</sub>). ESI-MS<sup>+</sup>: [C<sub>7</sub>H<sub>9</sub>N<sub>4</sub>]<sup>+</sup> *m/z* = 149.19, calcd = 149.18

**4.5-I.** To a solution of **4.4** (0.50 g, 3.37 mmol) in acetone (35 mL) at reflux, a solution of iodomethane (0.21 mL, 3.37 mmol) in acetone (15 mL) was added dropwise over a period of 1.5 h. The resultant mixture was further stirred under the same condition for 4 h followed by gravity filtration. The solvent was evaporated *in vacuo* yielding a yellow residue which was further washed with dichloromethane (5 × 10 mL). The resultant residue was then dried *in vacuo* overnight yielding an off-white solid. Yield: 0.45 g, 46.0%. <sup>1</sup>H-NMR (500.023 MHz, d<sub>6</sub>-DMSO): δ = 9.34 (s, 1H, *H*<sub>imi</sub>), 8.02 (s, 1H, *H*<sub>imi</sub>), 7.95 (t, <sup>3</sup>*J*<sub>H-H</sub> = 2.0 Hz, 1H, *H*<sub>imi</sub>), 7.74 (t, <sup>3</sup>*J*<sub>H-H</sub> = 2.0 Hz, 1H, *H*<sub>imi</sub>), 7.49 (t, <sup>3</sup>*J*<sub>H-H</sub> = 1.0 Hz, 1H, *H*<sub>imi</sub>), 7.00 (d, <sup>3</sup>*J*<sub>H-H</sub> = 1.0 Hz, 1H, *H*<sub>imi</sub>), 6.48 (s, 2H, CH<sub>2</sub>), 3.88 (s, 3H, CH<sub>3</sub>). <sup>13</sup>C-NMR (125.74 MHz, d<sub>6</sub>-DMSO): δ = 138.28 (*C*<sub>imi</sub>), 137.47 (*C*<sub>imi</sub>), 130.19 (*C*<sub>imi</sub>), 124.79 (*C*<sub>imi</sub>), 122.08 (*C*<sub>imi</sub>), 119.79

(C<sub>imi</sub>), 57.26 (CH<sub>2</sub>), 36.65 (CH<sub>3</sub>). HRESI-MS<sup>+</sup>: [C<sub>8</sub>H<sub>11</sub>N<sub>4</sub>]<sup>+</sup> m/z = 163.0981, calcd = 163.0978.

**4.6·I.** This compound was prepared using the same method as described for **4.4·I** from **4.5** (0.50 g, 3.37 mmol) and iodoethane (0.27 mL, 3.37 mmol). Yield: 0.23 g, 22.3%. <sup>1</sup>H-NMR (500.023 MHz, d<sub>6</sub>-DMSO): δ = 9.39 (s, 1H, H<sub>imi</sub>), 8.00 (s, 1H, H<sub>imi</sub>), 7.94 (t, <sup>3</sup>J<sub>H-H</sub> = 2.0 Hz, 1H, H<sub>imi</sub>), 7.85 (t, <sup>3</sup>J<sub>H-H</sub> = 2.0 Hz, 1H, H<sub>imi</sub>), 7.47 (t, <sup>3</sup>J<sub>H-H</sub> = 2.0 Hz, 1H, H<sub>imi</sub>), 7.01 (s, 1H, H<sub>imi</sub>), 6.45 (s, 2H, CH<sub>2</sub>), 4.22 (q, <sup>3</sup>J<sub>H-H</sub> = 7.0 Hz, 2H, CH<sub>2</sub>CH<sub>3</sub>), 1.43 (t, <sup>3</sup>J<sub>H-H</sub> = 7.5 Hz, 3H, CH<sub>2</sub>CH<sub>3</sub>). <sup>13</sup>C-NMR (125.74 MHz, d<sub>6</sub>-DMSO): δ = 138.32 (C<sub>imi</sub>), 136.08 (C<sub>imi</sub>), 130.19 (C<sub>imi</sub>), 123.30 (C<sub>imi</sub>), 122.28 (C<sub>imi</sub>), 119.81 (C<sub>imi</sub>), 57.35 (CH<sub>2</sub>), 45.09 (CH<sub>2</sub>CH<sub>3</sub>), 15.24 (CH<sub>2</sub>CH<sub>3</sub>). HRESI-MS<sup>+</sup>: [C<sub>9</sub>H<sub>13</sub>N<sub>4</sub>]<sup>+</sup> m/z = 177.1137, calcd = 177.1135.

**4.7·BF<sub>4</sub>.** A mixture of **4.5·I** (0.20 g, 0.69 mmol) and (THT)AuCl (0.12 g, 0.38 mmol) in DMF (5 mL) was stirred at 110 °C for 0.5 h. To the resultant mixture, NaOAc (0.11 g, 1.38 mmol) was added and the mixture was further stirred under the same condition for 3 h followed by filtration through a plug of Celite. To the filtrate, diethyl ether (30 mL) was added to obtain a white precipitate. The solid was re-dissolved in water (2 mL) and a saturation solution of KBF<sub>4</sub> in water (20 mL) was added. The solvent was evaporated *in vacuo* and the residue was recrystallised from a mixture of acetonitrile and diethyl ether to obtain a white solid. 0.11 g, 52.4%. <sup>1</sup>H-NMR (500.023 MHz, d<sub>6</sub>-DMSO): δ = 8.03 (s, 2H, H<sub>imi</sub>), 7.83 (d, <sup>3</sup>J<sub>H-H</sub> = 2.0 Hz, 2H, H<sub>imi</sub>), 7.59 (d, <sup>3</sup>J<sub>H-H</sub> = 2.0 Hz, 2H, H<sub>imi</sub>), 7.45 (t, <sup>3</sup>J<sub>H-H</sub> = 1.0 Hz, 2H, H<sub>imi</sub>), 6.97 (d, <sup>3</sup>J<sub>H-H</sub> = 1.0 Hz, 2H, H<sub>imi</sub>), 6.49 (s, 4H, CH<sub>2</sub>), 3.92 (s, 6H, CH<sub>3</sub>). <sup>13</sup>C-NMR (125.74 MHz, d<sub>6</sub>-DMSO): δ = 183.65 (C<sub>carbene</sub>), 137.95 (C<sub>imi</sub>), 130.10 (C<sub>imi</sub>), 124.76 (C<sub>imi</sub>), 122.30 (C<sub>imi</sub>), 119.49 (C<sub>imi</sub>), 59.23 (CH<sub>2</sub>), 38.44 (CH<sub>3</sub>). HRESI-MS<sup>+</sup>: [C<sub>16</sub>H<sub>20</sub>N<sub>8</sub>Au]<sup>+</sup> m/z = 521.1483, calcd = 521.1471.

**4.8•BF<sub>4</sub>**. This compound was prepared using the same method as described for **4.6•BF<sub>4</sub>** from **4.6•I** (0.20 g, 0.66 mmol), (THT)AuCl (0.12 g, 0.36 mmol) and NaOAc (0.11 g, 1.31 mmol). Yield: 0.093 g, 44.5%. <sup>1</sup>H-NMR (500.023 MHz, d<sub>6</sub>-DMSO): δ = 8.03 (s, 2H, *H*<sub>imi</sub>), 7.83 (d, <sup>3</sup>*J*<sub>H-H</sub> = 2.0 Hz, 2H, *H*<sub>imi</sub>), 7.59 (d, <sup>3</sup>*J*<sub>H-H</sub> = 2.0 Hz, 2H, *H*<sub>imi</sub>), 7.45 (t, <sup>3</sup>*J*<sub>H-H</sub> = 1.0 Hz, 2H, *H*<sub>imi</sub>), 6.97 (d, <sup>3</sup>*J*<sub>H-H</sub> = 1.0 Hz, 2H, *H*<sub>imi</sub>), 6.49 (s, 4H, CH<sub>2</sub>), 3.92 (s, 6H, CH<sub>3</sub>). <sup>13</sup>C-NMR (125.74 MHz, d<sub>6</sub>-DMSO): δ = 183.65 (*C*<sub>carbene</sub>), 137.95 (*C*<sub>imi</sub>), 130.10 (*C*<sub>imi</sub>), 124.76 (*C*<sub>imi</sub>), 122.30 (*C*<sub>imi</sub>), 119.49 (*C*<sub>imi</sub>), 59.23 (CH<sub>2</sub>), 38.44 (CH<sub>3</sub>). HRESI-MS<sup>+</sup>: [C<sub>18</sub>H<sub>24</sub>N<sub>8</sub>Au]<sup>+</sup> *m/z* = 549.1787, calcd = 549.1784.

**4.9•(BF<sub>4</sub>)<sub>3</sub>**. In a N<sub>2</sub> filled glove box, a solution of **4.7•BF<sub>4</sub>** (0.080 g, 0.13 mmol) and Et<sub>3</sub>OBF<sub>4</sub> (0.063 g, 0.13 mmol) in acetonitrile (5 mL) was stirred at RT overnight. The reaction mixture was clarified by centrifugation followed by a filtration through syringe filter. The solvent was then evaporated *in vacuo* yielding a yellow residue. The residue was re-dissolved in minimum amount of a mixture of acetonitrile and dichloromethane (1:1) followed by dropwise addition of diethyl ether to obtain a pale yellow solid. Yield: 0.026 g, 23.5%. <sup>1</sup>H-NMR (500.023 MHz, d<sub>6</sub>-DMSO): δ = 9.44 (s, 2H, *H*<sub>imi</sub>), 7.96 (s, 2H, *H*<sub>imi</sub>), 7.90 (s, 2H, *H*<sub>imi</sub>), 7.86 (s, 2H, *H*<sub>imi</sub>), 7.69 (s, 2H, *H*<sub>imi</sub>), 6.66 (s, 4H, CH<sub>2</sub>), 4.24 (q, <sup>3</sup>*J*<sub>H-H</sub> = 6.5 Hz, 4H, CH<sub>2</sub>CH<sub>3</sub>), 3.93 (s, 6H, CH<sub>3</sub>), 1.42 (t, <sup>3</sup>*J*<sub>H-H</sub> = 6.3 Hz, 6H, CH<sub>2</sub>CH<sub>3</sub>). <sup>13</sup>C-NMR (125.74 MHz, d<sub>6</sub>-DMSO): δ = 184.52 (*C*<sub>carbene</sub>), 136.93 (*C*<sub>imi</sub>), 125.38 (*C*<sub>imi</sub>), 123.50 (*C*<sub>imi</sub>), 122.52 (*C*<sub>imi</sub>), 122.41 (*C*<sub>imi</sub>), 61.04 (CH<sub>2</sub>), 45.19 (CH<sub>2</sub>CH<sub>3</sub>), 38.52 (CH<sub>3</sub>), 15.38 (CH<sub>2</sub>CH<sub>3</sub>). HRESI-MS<sup>+</sup>: [C<sub>20</sub>H<sub>30</sub>N<sub>8</sub>AuB<sub>2</sub>F<sub>8</sub>]<sup>+</sup> *m/z* = 753.2326, calcd = 752.2312.

**4.10•(BF<sub>4</sub>)<sub>3</sub>**. This compound was prepared using the same method as described for **4.9•(BF<sub>4</sub>)<sub>3</sub>** from **4.8•BF<sub>4</sub>** (0.093 g, 0.15 mmol) and Et<sub>3</sub>OBF<sub>4</sub> (0.069 g, 0.37 mmol). Yield: 0.077 g, 60.0%. <sup>1</sup>H-NMR (500.023 MHz, d<sub>6</sub>-DMSO): δ = 9.42 (s, 2H, *H*<sub>imi</sub>), 7.96 (t, <sup>3</sup>*J*<sub>H-H</sub>

= 2.0 Hz, 2H,  $H_{\text{imi}}$ ), 7.92 (t,  $^3J_{\text{H-H}} = 2.0$  Hz, 2H,  $H_{\text{imi}}$ ), 7.84 (d,  $^3J_{\text{H-H}} = 2.0$  Hz, 2H,  $H_{\text{imi}}$ ), 7.79 (d,  $^3J_{\text{H-H}} = 2.0$  Hz, 2H,  $H_{\text{imi}}$ ), 6.65 (s, 4H,  $\text{CH}_2$ ), 4.31 (q,  $^3J_{\text{H-H}} = 7.0$  Hz, 4H,  $\text{CH}_2\text{CH}_3$ ), 4.24 (q,  $^3J_{\text{H-H}} = 7.0$  Hz, 4H,  $\text{CH}_2\text{CH}_3$ ), 1.40 – 1.47 (m, 12H,  $\text{CH}_2\text{CH}_3$ ).  $^{13}\text{C}$ -NMR (125.74 MHz,  $\text{d}_6$ -DMSO):  $\delta = 183.73$  ( $C_{\text{Carbene}}$ ), 136.97 ( $C_{\text{imi}}$ ), 123.97 ( $C_{\text{imi}}$ ), 123.49 ( $C_{\text{imi}}$ ), 122.64 ( $C_{\text{imi}}$ ), 122.37 ( $C_{\text{imi}}$ ), 61.22 ( $\text{CH}_2$ ), 46.71 ( $\text{CH}_2\text{CH}_3$ ), 45.19 ( $\text{CH}_2\text{CH}_3$ ), 17.05 ( $\text{CH}_2\text{CH}_3$ ), 15.38 ( $\text{CH}_2\text{CH}_3$ ). HRESI-MS $^+$ :  $[\text{C}_{20}\text{H}_{30}\text{N}_8\text{B}_2\text{F}_8]^+$   $m/z = 753.2326$ , calcd = 753.2312,  $[\text{C}_{20}\text{H}_{30}\text{N}_8\text{BF}_4]^{2+}$   $m/z = 333.1144$ , calcd = 333.1139.

**4.11·(BF<sub>4</sub>)<sub>2</sub>.** In a N<sub>2</sub> filled glove box, a mixture of **4.9·(BF<sub>4</sub>)<sub>3</sub>** (0.026 g, 0.031 mmol) and Ag<sub>2</sub>O (0.018 g, 0.078 mmol) in acetonitrile (5 mL) was stirred at RT for 3 d in absence of light. The reaction mixture was clarified by centrifugation followed by filtration through syringe filter. To the filtrate, diethyl ether (5 mL) was added to and a white precipitate was formed. The precipitate was collected and the crude product was recrystallised from a mixture of acetonitrile and diethyl ether yielding a white powder. Yield: 0.015 g, 56.4%.  $^1\text{H}$ -NMR (500.023 MHz,  $\text{d}_3$ -CD<sub>3</sub>CN):  $\delta = 7.50 - 7.58$  (m, 4H,  $H_{\text{imi}}$ ), 7.36 (t<sub>app</sub>,  $^3J_{\text{H-H}} = 2.0$  Hz, 1H,  $H_{\text{imi}}$ ), 7.32 (d,  $^3J_{\text{H-H}} = 1.5$  Hz, 1H,  $H_{\text{imi}}$ ), 7.30 (t<sub>app</sub>,  $^3J_{\text{H-H}} = 2.0$  Hz, 1H,  $H_{\text{imi}}$ ), 7.27 (t<sub>app</sub>,  $^3J_{\text{H-H}} = 1.5$  Hz, 1H,  $H_{\text{imi}}$ ), 6.00 – 7.00 (m<sub>br</sub>, 4H,  $\text{CH}_2$ ), 4.26 (q,  $^3J_{\text{H-H}} = 7.5$  Hz, 2H,  $\text{CH}_2\text{CH}_3$ ), 4.20 (q,  $^3J_{\text{H-H}} = 7.0$  Hz, 2H,  $\text{CH}_2\text{CH}_3$ ), 3.83 - 3.90 (m, 6H,  $\text{CH}_3$ ), 1.39 – 1.48 (m, 6H,  $\text{CH}_2\text{CH}_3$ ).  $^{13}\text{C}$ -NMR (125.74 MHz,  $\text{d}_3$ -CD<sub>3</sub>CN):  $\delta = 184.69$  ( $C_{\text{carbene}}$ ), 183.83 ( $C_{\text{carbene}}$ ), 125.55 ( $C_{\text{imi}}$ ), 124.77 ( $C_{\text{imi}}$ ), 123.97 ( $C_{\text{imi}}$ ), 123.24 ( $C_{\text{imi}}$ ), 122.49 ( $C_{\text{imi}}$ ), 122.45 ( $C_{\text{imi}}$ ), 122.35 ( $C_{\text{imi}}$ ), 122.24 ( $C_{\text{imi}}$ ), 64.47 ( $\text{CH}_2$ ), 64.44 ( $\text{CH}_2$ ), 48.23 ( $\text{CH}_2\text{CH}_3$ ), 47.79 ( $\text{CH}_2\text{CH}_3$ ), 39.69 ( $\text{CH}_3$ ), 39.08 ( $\text{CH}_3$ ), 17.31 ( $\text{CH}_2\text{CH}_3$ ), 17.13 ( $\text{CH}_2\text{CH}_3$ ). HRESI-MS $^+$ :  $[\text{C}_{20}\text{H}_{28}\text{N}_8\text{AuAgBF}_4]^+$   $m/z = 771.1180$ , calcd = 771.1177,  $[\text{C}_{20}\text{H}_{28}\text{N}_8\text{AuAg}]^{2+}$   $m/z = 342.0577$ , calcd = 342.0571.

**4.12·(BF<sub>4</sub>)<sub>2</sub>.** This compound was prepared using the same method as described for **4.11·(BF<sub>4</sub>)<sub>2</sub>** from **4.10·(BF<sub>4</sub>)<sub>3</sub>** (0.040 g, 0.046 mmol) and Ag<sub>2</sub>O (0.021 g, 0.093 mmol). Yield: 0.015 g, 36.7%. <sup>1</sup>H-NMR: (500.023 MHz, d<sub>3</sub>-CD<sub>3</sub>CN): δ = 7.53 (d, <sup>3</sup>J<sub>H-H</sub> = 1.5 Hz, 2H, *H*<sub>imi</sub>), 7.52 (d, <sup>3</sup>J<sub>H-H</sub> = 2.0 Hz, 2H, *H*<sub>imi</sub>), 7.36 (d, <sup>3</sup>J<sub>H-H</sub> = 2.0 Hz, 2H, *H*<sub>imi</sub>), 7.32 (d, <sup>3</sup>J<sub>H-H</sub> = 2.0 Hz, 2H, *H*<sub>imi</sub>), 6.50 – 7.00 (m, 2H, CH<sub>2</sub>), 6.00 – 6.50 (m, 2H, CH<sub>2</sub>), 4.25 (q, <sup>3</sup>J<sub>H-H</sub> = 7.5 Hz, 4H, CH<sub>2</sub>CH<sub>3</sub>), 4.19 (q, <sup>3</sup>J<sub>H-H</sub> = 7.5 Hz, 4H, CH<sub>2</sub>CH<sub>3</sub>), 1.45 (t, <sup>3</sup>J<sub>H-H</sub> = 7.5 Hz, 6H, CH<sub>2</sub>CH<sub>3</sub>), 1.42 (t, <sup>3</sup>J<sub>H-H</sub> = 7.5 Hz, 6H, CH<sub>2</sub>CH<sub>3</sub>). <sup>13</sup>C-NMR (125.74 MHz, d<sub>3</sub>-CD<sub>3</sub>CN): δ = 182.87 (*C*<sub>carbene</sub>), 122.89 (*C*<sub>imi</sub>), 122.27 (*C*<sub>imi</sub>), 121.50 (*C*<sub>imi</sub>), 121.43 (*C*<sub>imi</sub>), 63.63 (CH<sub>2</sub>), 47.29 (CH<sub>2</sub>CH<sub>3</sub>), 46.86 (CH<sub>2</sub>CH<sub>3</sub>), 16.31 (CH<sub>2</sub>CH<sub>3</sub>), 16.15 (CH<sub>2</sub>CH<sub>3</sub>). HRESI-MS<sup>+</sup>: [C<sub>22</sub>H<sub>32</sub>N<sub>8</sub>AuAgBF<sub>4</sub>]<sup>+</sup> *m/z* = 799.1537, calcd = 799.1490, [C<sub>22</sub>H<sub>32</sub>N<sub>8</sub>AuAg]<sup>2+</sup> *m/z* = 356.0906, calcd = 356.0728.

**4.13·(BF<sub>4</sub>)<sub>3</sub>.** A mixture of **4.9·(BF<sub>4</sub>)<sub>3</sub>** (0.060 g, 0.071 mmol) and Hg(OAc)<sub>2</sub> (0.025 g, 0.078 mmol) in acetonitrile (5 mL) was stirred at reflux for 3 d. The resultant mixture was filtered through a plug of Celite and the solvent was evaporated *in vacuo* yielding a colourless residue. The crude product was purified by a vapour diffusion of diethyl ether into an acetonitrile solution of the crude **4.9·(BF<sub>4</sub>)<sub>3</sub>** yielding a white solid. Yield: 0.015 g, 20.2%. <sup>1</sup>H-NMR: (500.023 MHz, d<sub>3</sub>-CD<sub>3</sub>CN): δ = 7.80 – 7.85 (m, 2H, *H*<sub>imi</sub>), 7.50 (d, <sup>3</sup>J<sub>H-H</sub> = 2.0 Hz, 1H, *H*<sub>imi</sub>), 7.62 (d, <sup>3</sup>J<sub>H-H</sub> = 2.0 Hz, 2H, *H*<sub>imi</sub>), 7.56 (t<sub>app</sub>, <sup>3</sup>J<sub>H-H</sub> = 1.7 Hz, 1H, *H*<sub>imi</sub>), 7.42 (d, <sup>3</sup>J<sub>H-H</sub> = 2.0 Hz, 1H, *H*<sub>imi</sub>), 7.36 (d, <sup>3</sup>J<sub>H-H</sub> = 2.0 Hz, 1H, *H*<sub>imi</sub>), 6.92 (d, <sup>3</sup>J<sub>H-H</sub> = 13.0 Hz, 2H, CH<sub>2</sub>), 6.36 (d, <sup>3</sup>J<sub>H-H</sub> = 13.0 Hz, 2H, CH<sub>2</sub>), 4.30 – 4.40 (m, 2H, CH<sub>2</sub>CH<sub>3</sub>), 4.26 (q, <sup>3</sup>J<sub>H-H</sub> = 7.3 Hz, 2H, CH<sub>2</sub>CH<sub>3</sub>), 4.00 (s, 3H, CH<sub>3</sub>), 3.88 (s, 3H, CH<sub>3</sub>), 1.43 – 1.53 (m, 6H, CH<sub>2</sub>CH<sub>3</sub>). <sup>13</sup>C-NMR (125.74 MHz, d<sub>3</sub>-CD<sub>3</sub>CN): δ = 182.90 (*C*<sub>carbene</sub>), 182.05 (*C*<sub>carbene</sub>), 176.06 (*C*<sub>carbene</sub>), 175.14 (*C*<sub>carbene</sub>), 127.39 (*C*<sub>imi</sub>), 127.35 (*C*<sub>imi</sub>), 126.05 (*C*<sub>imi</sub>), 125.32 (*C*<sub>imi</sub>), 125.28 (*C*<sub>imi</sub>), 124.78 (*C*<sub>imi</sub>), 124.40 (*C*<sub>imi</sub>), 122.99 (*C*<sub>imi</sub>), 63.36 (CH<sub>2</sub>), 63.26 (CH<sub>2</sub>), 48.52

(CH<sub>2</sub>CH<sub>3</sub>), 47.94 (CH<sub>2</sub>CH<sub>3</sub>), 39.61 (CH<sub>3</sub>), 39.17 (CH<sub>3</sub>), 17.05 (CH<sub>2</sub>CH<sub>3</sub>), 16.56 (CH<sub>2</sub>CH<sub>3</sub>).  
HRESI-MS<sup>+</sup>: [C<sub>20</sub>H<sub>28</sub>N<sub>8</sub>AuHgB<sub>2</sub>F<sub>8</sub>]<sup>+</sup> m/z = 951.1893, calcd = 951.1838.

**4.14·(BF<sub>4</sub>)<sub>2</sub>.** This compound was prepared using the same method as described for **4.13·(BF<sub>4</sub>)<sub>3</sub>** from **4.10·(BF<sub>4</sub>)<sub>3</sub>** (0.040 g, 0.046 mmol) and Hg(OAc)<sub>2</sub> (0.030 g, 0.092 mmol). Yield: 0.033 g, 67.1%. <sup>1</sup>H-NMR: (500.023 MHz, d<sub>3</sub>-CD<sub>3</sub>CN): δ = 7.83 (s, 2H, *H*<sub>imi</sub>), 7.64 (d, <sup>3</sup>*J*<sub>H-H</sub> = 2.0 Hz, 2H, *H*<sub>imi</sub>), 7.61 (d, <sup>3</sup>*J*<sub>H-H</sub> = 2.0 Hz, 2H, *H*<sub>imi</sub>), 7.43 (d, <sup>3</sup>*J*<sub>H-H</sub> = 2.0 Hz, 2H, *H*<sub>imi</sub>), 6.89 (d, <sup>3</sup>*J*<sub>H-H</sub> = 13.0 Hz, 2H, CH<sub>2</sub>), 6.35 (d, <sup>3</sup>*J*<sub>H-H</sub> = 14.0 Hz, 2H, CH<sub>2</sub>), 4.33 (q, <sup>3</sup>*J*<sub>H-H</sub> = 7.5 Hz, 4H, CH<sub>2</sub>CH<sub>3</sub>), 4.25 (q, <sup>3</sup>*J*<sub>H-H</sub> = 7.0 Hz, 4H, CH<sub>2</sub>CH<sub>3</sub>), 1.44 – 1.53 (m, 12H, CH<sub>2</sub>CH<sub>3</sub>). <sup>13</sup>C-NMR (125.74 MHz, d<sub>3</sub>-CD<sub>3</sub>CN): δ = 182.91 (*C*<sub>carbene</sub>), 174.97 (*C*<sub>carbene</sub>), 125.40 (*C*<sub>imi</sub>), 125.35 (*C*<sub>imi</sub>), 124.38 (*C*<sub>imi</sub>), 123.19 (*C*<sub>imi</sub>), 63.42 (CH<sub>2</sub>), 48.52 (CH<sub>2</sub>CH<sub>3</sub>), 47.98 (CH<sub>2</sub>CH<sub>3</sub>), 17.02 (CH<sub>2</sub>CH<sub>3</sub>), 16.48 (CH<sub>2</sub>CH<sub>3</sub>). HRESI-MS<sup>+</sup>: [C<sub>22</sub>H<sub>32</sub>N<sub>8</sub>AuHgB<sub>2</sub>F<sub>8</sub>]<sup>+</sup> m/z = 979.1335, calcd = 979.2151.

**4.16·I<sub>2</sub>.** This compound was prepared according to a literature procedure.<sup>64</sup> A solution of *N*-ethylimidazole (2.00 g, 20.80 mmol) and diiodomethane (0.93 mL, 11.44 mmol) in THF (20 mL) was stirred at reflux for 2 d. The resultant solid was collected and washed with THF (3 × 5 mL) and acetonitrile (5 mL) and dried *in vacuo* yielding an off-white solid. Yield: 1.78 g, 37.2%. <sup>1</sup>H-NMR (500.023 MHz, d<sub>6</sub>-DMSO): δ = 9.46 (s, 2H, *H*<sub>imi</sub>), 8.01 (t, <sup>3</sup>*J*<sub>H-H</sub> = 1.9 Hz, 2H, *H*<sub>imi</sub>), 7.93 (t, <sup>3</sup>*J*<sub>H-H</sub> = 1.7 Hz, 2H, *H*<sub>imi</sub>), 6.64 (s, 2H, CH<sub>2</sub>), 4.27 (q, <sup>3</sup>*J*<sub>H-H</sub> = 7.3 Hz, 4H, CH<sub>2</sub>CH<sub>3</sub>), 1.45 (t, <sup>3</sup>*J*<sub>H-H</sub> = 7.3 Hz, 6H, CH<sub>2</sub>CH<sub>3</sub>). <sup>13</sup>C-NMR (125.74 MHz, d<sub>6</sub>-DMSO): δ = 137.71 (*C*<sub>imi</sub>), 123.38 (*C*<sub>imi</sub>), 122.64 (*C*<sub>imi</sub>), 58.74 (CH<sub>2</sub>), 45.26 (CH<sub>2</sub>CH<sub>3</sub>), 15.21 (CH<sub>2</sub>CH<sub>3</sub>). ESI-MS<sup>+</sup>: [C<sub>11</sub>H<sub>18</sub>N<sub>4</sub>I]<sup>+</sup> m/z = 333.00, calcd = 333.06, [C<sub>11</sub>H<sub>18</sub>N<sub>4</sub>]<sup>2+</sup> m/z = 103.20, calcd = 103.57.

**4.17·(BF<sub>4</sub>)<sub>2</sub>.** This compound was prepared according to a literature procedure<sup>57</sup> from **4.16·I<sub>2</sub>** (0.10 g, 0.22 mmol), (THT)AuCl (0.070 g, 0.22 mmol), NaOAc (0.036 g, 0.44 mmol) and KBF<sub>4</sub> (0.041 g, 0.33 mmol). Yield: 0.072 g, 30.3%. <sup>1</sup>H-NMR (500.023 MHz, d<sub>6</sub>-DMSO): δ = 7.89 (d, *J* = 1.7 Hz, 4H, *H*<sub>imi</sub>), 7.71 (d, <sup>3</sup>*J*<sub>H-H</sub> = 1.8 Hz, 4H, *H*<sub>imi</sub>), 7.14 (d, <sup>3</sup>*J*<sub>H-H</sub> = 13.9 Hz, 2H, *CH*<sub>2</sub>), 6.35 (d, <sup>3</sup>*J*<sub>H-H</sub> = 14.0 Hz, 2H, *CH*<sub>2</sub>), 4.10 – 4.40 (m, 8H, *CH*<sub>2</sub>*CH*<sub>3</sub>), 1.40 (t, <sup>3</sup>*J*<sub>H-H</sub> = 7.3 Hz, 12H, *CH*<sub>2</sub>*CH*<sub>3</sub>). <sup>13</sup>C-NMR (125.74 MHz, d<sub>6</sub>-DMSO): δ = 182.76 (*C*<sub>carbene</sub>), 123.54 (*C*<sub>imi</sub>), 122.42 (*C*<sub>imi</sub>), 62.62 (*CH*<sub>2</sub>), 46.72 (*CH*<sub>2</sub>*CH*<sub>3</sub>), 17.14 (*CH*<sub>2</sub>*CH*<sub>3</sub>). ESI-MS<sup>+</sup>: [C<sub>22</sub>H<sub>32</sub>N<sub>8</sub>Au<sub>2</sub>BF<sub>4</sub>]<sup>+</sup> *m/z* = 889.20, calcd = 889.21, [C<sub>22</sub>H<sub>32</sub>N<sub>8</sub>Au<sub>2</sub>]<sup>2+</sup> *m/z* = 401.20, calcd = 401.10.

**4.18·(BF<sub>4</sub>)<sub>2</sub>.** This compound was prepared according to a literature procedure.<sup>64</sup> A mixture of **4.16·I<sub>2</sub>** (0.10 g, 0.22 mmol) and Ag<sub>2</sub>O (0.13 g, 0.55 mmol) in water (5 mL) was stirred in the absence of light at RT for 1 h. The resultant mixture was filtered through a plug of Celite and syringe filter. To the filtrate, a solution of KBF<sub>4</sub> saturated in water (10 mL) was added yielding a white precipitate. The resultant precipitate was washed with water (2 × 5 mL), isopropanol (5 mL) and diethyl ether (5 mL). and was dried in vacuo yielding a white solid. Yield: 0.050 g, 25.2%. <sup>1</sup>H-NMR (500.023 MHz, d<sub>6</sub>-DMSO): δ = 7.88 (d, <sup>3</sup>*J*<sub>H-H</sub> = 1.1 Hz, 4H, *H*<sub>imi</sub>), 7.65 (d, <sup>3</sup>*J*<sub>H-H</sub> = 1.1 Hz, 4H, *H*<sub>imi</sub>), 6.70 – 7.15 (m, 2H, *CH*<sub>2</sub>), 6.25 – 6.70 (m, 2H, *CH*<sub>2</sub>), 4.19 (q, <sup>3</sup>*J*<sub>H-H</sub> = 7.2 Hz, 8H, *CH*<sub>2</sub>*CH*<sub>3</sub>), 1.37 (t, <sup>3</sup>*J*<sub>H-H</sub> = 7.3 Hz, 12H, *CH*<sub>2</sub>*CH*<sub>3</sub>). <sup>13</sup>C-NMR (125.74 MHz, d<sub>6</sub>-DMSO): δ = 206.98 (*C*<sub>carbene</sub>), 123.13 (*C*<sub>imi</sub>), 122.36 (*C*<sub>imi</sub>), 47.11 (*CH*<sub>2</sub>), 31.36 (*CH*<sub>2</sub>*CH*<sub>3</sub>), 17.40 (*CH*<sub>2</sub>*CH*<sub>3</sub>). ESI-MS<sup>+</sup>: [C<sub>22</sub>H<sub>32</sub>N<sub>8</sub>Ag<sub>2</sub>BF<sub>4</sub>]<sup>+</sup> *m/z* = 711.20, calcd = 889.21, [C<sub>22</sub>H<sub>32</sub>N<sub>8</sub>Au<sub>2</sub>]<sup>2+</sup> *m/z* = 311.20, calcd = 311.04.

**4.19.** This compound was prepared using the same method as described for **4.4** using imidazole (5.44 g, 80.00 mmol), 1,2-dichloroethane (6.36 mL, 80.32 mmol), KOH (8.04 g,



143.28 mmol) and *tetra-n*-butylammonium bromide (0.76 g, 2.36 mmol). Yield: 2.44 g, 34.6 %. <sup>1</sup>H-NMR (500.023 MHz, d<sub>6</sub>-DMSO): δ = 7.37 (s, 2H, *H*<sub>imi</sub>), 7.00 (s, 2H, *H*<sub>imi</sub>), 6.85 (s, 2H, *H*<sub>imi</sub>), 4.32 (s, 4H, *CH*<sub>2</sub>). <sup>13</sup>C-NMR (125.74 MHz, d<sub>6</sub>-DMSO): δ = 137.80 (*C*<sub>imi</sub>), 129.03 (*C*<sub>imi</sub>), 119.56 (*C*<sub>imi</sub>), 47.09 (*CH*<sub>2</sub>). HRESI-MS<sup>+</sup>: [C<sub>8</sub>H<sub>11</sub>N<sub>4</sub>]<sup>+</sup> *m/z* = 163.0930, calcd = 163.0984.

**4.20•I.** This compound was prepared using the same method as described for **4.5•I** using **4.19** (0.50 g, 3.08 mmol) and iodomethane (0.19 mL, 3.08 mmol). The crude product was purified by recrystallization from a mixture of methanol and diethyl ether to obtain an off-white solid. Yield: 0.51 g, 54.4%. <sup>1</sup>H-NMR (500.023 MHz, d<sub>6</sub>-DMSO): δ = 8.93 (s, 1H, *H*<sub>imi</sub>), 7.67 (t, <sup>3</sup>*J*<sub>H-H</sub> = 1.6 Hz, 1H, *H*<sub>imi</sub>), 7.52 (s, 1H, *H*<sub>imi</sub>), 7.49 (t, <sup>3</sup>*J*<sub>H-H</sub> = 1.7 Hz, 1H, *H*<sub>imi</sub>), 7.11 (s, 1H, *H*<sub>imi</sub>), 6.92 (s, 1H, *H*<sub>imi</sub>), 4.57 (t, <sup>3</sup>*J*<sub>H-H</sub> = 6.1 Hz, 2H, *CH*<sub>2</sub>), 4.46 (t, <sup>3</sup>*J*<sub>H-H</sub> = 6.1 Hz, 2H, *CH*<sub>2</sub>), 3.82 (s, 3H, *CH*<sub>3</sub>). <sup>13</sup>C-NMR (125.74 MHz, d<sub>6</sub>-DMSO): δ = 137.87 (*C*<sub>imi</sub>), 137.27(*C*<sub>imi</sub>), 129.19 (*C*<sub>imi</sub>), 124.23(*C*<sub>imi</sub>), 122.76(*C*<sub>imi</sub>), 119.71(*C*<sub>imi</sub>), 49.87 (*CH*<sub>2</sub>), 46.09 (*CH*<sub>2</sub>), 36.35 (*CH*<sub>3</sub>). HRESI-MS<sup>+</sup>: [C<sub>9</sub>H<sub>13</sub>N<sub>4</sub>]<sup>+</sup> *m/z* = 177.1135, calcd = 177.1135.

**4.21•I.** This compound was prepared using the same method as described for **4.5•I** from **4.19** (0.25 g, 1.54 mmol) and iodoethane (0.13 mL, 1.54 mmol). The crude product was triturated with dichloromethane (3 × 10 mL) yielding a pale-yellow oil. Yield: 0.19 g, 38.7%. <sup>1</sup>H-NMR (500.023 MHz, d<sub>6</sub>-DMSO): δ = 8.95 (s, 1H, *H*<sub>imi</sub>), 7.79 (s, 1H, *H*<sub>imi</sub>), 7.54 (s, 1H, *H*<sub>imi</sub>), 7.47 (s, 1H, *H*<sub>imi</sub>), 7.08 (s, 1H, *H*<sub>imi</sub>), 6.90 (s, 1H, *H*<sub>imi</sub>), 4.57 (t, <sup>3</sup>*J*<sub>H-H</sub> = 5.3 Hz, 2H, *CH*<sub>2</sub>), 4.47 (t, <sup>3</sup>*J*<sub>H-H</sub> = 5.3 Hz, 2H, *CH*<sub>2</sub>), 4.17 (q, <sup>3</sup>*J*<sub>H-H</sub> = 7.6 Hz, 2H, *CH*<sub>2</sub>*CH*<sub>3</sub>), 1.37, (t, <sup>3</sup>*J*<sub>H-H</sub> = 7.3 Hz, 3H, *CH*<sub>2</sub>*CH*<sub>3</sub>). <sup>13</sup>C-NMR (125.74 MHz, d<sub>6</sub>-DMSO): δ = 137.87 (*C*<sub>imi</sub>), 136.43 (*C*<sub>imi</sub>), 129.40 (*C*<sub>imi</sub>), 122.90 (*C*<sub>imi</sub>), 122.81 (*C*<sub>imi</sub>), 119.61 (*C*<sub>imi</sub>), 44.99 (*CH*<sub>2</sub>), 46.02

(CH<sub>2</sub>), 44.77 (CH<sub>2</sub>CH<sub>3</sub>), 15.63 (CH<sub>2</sub>CH<sub>3</sub>). HRESI-MS<sup>+</sup>: [C<sub>10</sub>H<sub>15</sub>N<sub>4</sub>]<sup>+</sup> m/z = 191.1292, calcd = 191.1291.

**4.22·BF<sub>4</sub>**. This compound was prepared using the same method as described for **4.7·BF<sub>4</sub>** from **4.20·I** (0.20 g, 0.66 mmol), (THT)AuCl (0.11 g, 0.33 mmol) and NaOAc (0.11 g, 1.31 mmol). Yield 0.11 g, 51.0%. <sup>1</sup>H-NMR (500.023 MHz, d<sub>6</sub>-DMSO): δ = 7.49 (d, <sup>3</sup>J<sub>H-H</sub> = 1.8 Hz, 1H, *H*<sub>imi</sub>), 7.40 (d, <sup>3</sup>J<sub>H-H</sub> = 1.8 Hz, 1H, *H*<sub>imi</sub>), 7.39 (s, 1H, *H*<sub>imi</sub>), 6.99 (s, 1H, *H*<sub>imi</sub>), 6.84 (s, 1H, *H*<sub>imi</sub>), 4.49 – 4.54 (m, 2H, CH<sub>2</sub>), 4.42 – 4.47 (m, 2H, CH<sub>2</sub>), 3.76 (s, 1H, CH<sub>3</sub>). <sup>13</sup>C-NMR (125.74 MHz, d<sub>6</sub>-DMSO): δ = 183.77 (*C*<sub>carbene</sub>), 137.78 (*C*<sub>imi</sub>), 129.13 (*C*<sub>imi</sub>), 124.15 (*C*<sub>imi</sub>), 122.03 (*C*<sub>imi</sub>), 119.88 (*C*<sub>imi</sub>), 51.57 (CH<sub>2</sub>), 47.02 (CH<sub>2</sub>), 37.97 (CH<sub>3</sub>). HRESI-MS<sup>+</sup>: [C<sub>18</sub>H<sub>24</sub>N<sub>8</sub>Au]<sup>+</sup> m/z = 549.1780, calcd = 549.1784.

**4.23·BF<sub>4</sub>**. This compound was prepared using the same method as described for **4.7·BF<sub>4</sub>** from **4.21·I** (0.14 g, 0.44 mmol), (THT)AuCl (g, 0.24 mmol) and NaOAc (0.072 g, 0.88 mmol). Yield: 0.080 g, 56.6%. <sup>1</sup>H-NMR (500.023 MHz, d<sub>6</sub>-DMSO): δ = 7.58 (d, <sup>3</sup>J<sub>H-H</sub> = 1.9 Hz, 1H, *H*<sub>imi</sub>), 7.43 (d, <sup>3</sup>J<sub>H-H</sub> = 1.9 Hz, 1H, *H*<sub>imi</sub>), 7.35 (s, 1H, *H*<sub>imi</sub>), 6.92 (s, 1H, *H*<sub>imi</sub>), 6.83 (s, 1H, *H*<sub>imi</sub>), 4.48 – 4.53 (m, 2H, CH<sub>2</sub>), 4.42 – 4.47 (m, 2H, CH<sub>2</sub>), 4.12 (q, <sup>3</sup>J<sub>H-H</sub> = 7.3 Hz, 2H, CH<sub>2</sub>CH<sub>3</sub>), 1.35 (t, <sup>3</sup>J<sub>H-H</sub> = 7.3 Hz). <sup>13</sup>C-NMR (125.74 MHz, d<sub>6</sub>-DMSO): δ = 183.01 (*C*<sub>carbene</sub>), 137.69 (*C*<sub>imi</sub>), 129.07 (*C*<sub>imi</sub>), 122.64 (*C*<sub>imi</sub>), 122.07 (*C*<sub>imi</sub>), 119.80 (*C*<sub>imi</sub>), 51.77 (CH<sub>2</sub>), 47.01 (CH<sub>2</sub>), 45.99 (CH<sub>2</sub>CH<sub>3</sub>), 17.41 (CH<sub>2</sub>CH<sub>3</sub>). HRESI-MS<sup>+</sup>: [C<sub>20</sub>H<sub>28</sub>N<sub>8</sub>Au]<sup>+</sup> m/z = 577.2019, calcd = 577.2097.

**4.24·(BF<sub>4</sub>)<sub>3</sub>**. This compound was prepared using the same method as described for **4.9·(BF<sub>4</sub>)<sub>3</sub>** from **4.22·BF<sub>4</sub>** (0.15 g, 0.24 mmol) and Me<sub>3</sub>OBF<sub>4</sub> (0.089 g, 0.60 mmol). Yield: 0.13 g, 65.7%. <sup>1</sup>H-NMR (500.023 MHz, d<sub>6</sub>-DMSO): δ = 8.87 (s, 2H, *H*<sub>imi</sub>), 7.67 (t, <sup>3</sup>J<sub>H-H</sub> =

1.5 Hz, 2H,  $H_{\text{imi}}$ ), 7.59 (t,  $^3J_{\text{H-H}} = 1.5$  Hz, 2H,  $H_{\text{imi}}$ ), 7.57 (d,  $^3J_{\text{H-H}} = 1.5$  Hz, 2H,  $H_{\text{imi}}$ ), 7.47 (d,  $^3J_{\text{H-H}} = 2.0$  Hz, 2H,  $H_{\text{imi}}$ ), 4.61 – 4.66 (m, 4H,  $\text{CH}_2\text{CH}_2$ ), 3.81 (s, 3H,  $\text{CH}_3$ ), 3.76 (s, 3H,  $\text{CH}_3$ ).  $^{13}\text{C}$ -NMR (125.74 MHz,  $\text{d}_6$ -DMSO):  $\delta = 183.01$  ( $C_{\text{carbene}}$ ), 137.23 ( $C_{\text{imi}}$ ), 124.75 ( $C_{\text{imi}}$ ), 124.49 ( $C_{\text{imi}}$ ), 123.15 ( $C_{\text{imi}}$ ), 122.34 ( $C_{\text{imi}}$ ), 50.48 ( $\text{CH}_2$ ), 49.95 ( $\text{CH}_2$ ), 38.14 ( $\text{CH}_3$ ), 36.26 ( $\text{CH}_3$ ). HRESI-MS<sup>+</sup>:  $[\text{C}_{20}\text{H}_{30}\text{N}_8\text{AuB}_2\text{F}_8]^+$   $m/z = 753.2325$ , calcd = 753.2317,  $[\text{C}_{20}\text{H}_{30}\text{N}_8\text{AuBF}_4]^{2+}$   $m/z = 333.1143$ , calcd = 333.1139,  $[\text{C}_{20}\text{H}_{30}\text{N}_8\text{Au}]^{3+}$   $m/z = 193.0754$ , calcd 193.0747.

**4.25·(BF<sub>4</sub>)<sub>3</sub>.** This compound was prepared using the same method as described for **4.9·(BF<sub>4</sub>)<sub>3</sub>** from **4.22·BF<sub>4</sub>** (0.050 g, 0.079 mmol) and Et<sub>3</sub>OBF<sub>4</sub> (0.037 g, 0.019 mmol). Yield: 0.055 g, 80.6%.  $^1\text{H}$ -NMR (500.023 MHz,  $\text{d}_6$ -DMSO):  $\delta = 9.03$  (s, 2H,  $H_{\text{imi}}$ ), 7.80 (t,  $^3J_{\text{H-H}} = 1.6$  Hz, 2H,  $H_{\text{imi}}$ ), 7.75 (t,  $^3J_{\text{H-H}} = 1.6$  Hz, 2H,  $H_{\text{imi}}$ ), 7.59 (t,  $^3J_{\text{H-H}} = 1.8$  Hz, 2H,  $H_{\text{imi}}$ ), 7.51 (t,  $^3J_{\text{H-H}} = 1.8$  Hz, 2H,  $H_{\text{imi}}$ ), 4.64 – 4.72 (m, 8H,  $\text{CH}_2\text{CH}_2$ ) 4.13 (q,  $^3J_{\text{H-H}} = 7.3$  Hz, 4H,  $\text{CH}_2\text{CH}_3$ ), 3.81 (s, 6H,  $\text{CH}_3$ ), 1.31 (t,  $^3J_{\text{H-H}} = 7.3$  Hz, 6H,  $\text{CH}_2\text{CH}_3$ ).  $^{13}\text{C}$ -NMR (125.74 MHz,  $\text{d}_6$ -DMSO):  $\delta = 183.32$  ( $C_{\text{Car}}$ ), 136.43 ( $C_{\text{imi}}$ ), 124.76 ( $C_{\text{imi}}$ ), 123.30 ( $C_{\text{imi}}$ ), 123.08 ( $C_{\text{imi}}$ ), 122.32 ( $C_{\text{imi}}$ ), 50.57 ( $\text{CH}_2$ ), 50.02 ( $\text{CH}_2$ ), 44.70 ( $\text{CH}_2\text{CH}_3$ ), 38.19 ( $\text{CH}_3$ ), 15.86 ( $\text{CH}_2\text{CH}_3$ ). HRESI-MS<sup>+</sup>:  $[\text{C}_{22}\text{H}_{34}\text{N}_8\text{AuB}_2\text{F}_8]^+$   $m/z = 781.2635$ , calcd = 781.2625,  $[\text{C}_{22}\text{H}_{34}\text{N}_8\text{AuBF}_4]^{2+}$   $m/z = 347.1285$ , calcd = 347.1295,  $[\text{C}_{22}\text{H}_{34}\text{N}_8\text{Au}]^{3+}$   $m/z = 202.4178$ , calcd = 202.4185.

**4.26·(BF<sub>4</sub>)<sub>3</sub>.** This compound was prepared using the same method as described for **4.9·(BF<sub>4</sub>)<sub>3</sub>** from **4.23·BF<sub>4</sub>** (0.050g, 0.075 mmol) and Et<sub>3</sub>OBF<sub>4</sub> (0.036 g, 0.19 mmol). Yield: 0.031 g, 46.0%.  $^1\text{H}$ -NMR (500.023 MHz,  $\text{d}_6$ -DMSO):  $\delta = 8.87$  (s, 2H,  $H_{\text{imi}}$ ), 7.78 (s, 2H,  $H_{\text{imi}}$ ), 7.67 (d,  $^3J_{\text{H-H}} = 1.7$  Hz, 2H,  $H_{\text{imi}}$ ), 7.61 (s, 2H,  $H_{\text{imi}}$ ), 7.50 (d,  $^3J_{\text{H-H}} = 1.7$  Hz, 2H,  $H_{\text{imi}}$ ), 4.58 – 4.68 (m, 8H,  $\text{CH}_2\text{CH}_2$ ), 4.06 – 4.18 (m, 8H,  $\text{CH}_2\text{CH}_3$ ), 1.38 (t,  $^3J_{\text{H-H}} = 7.3$ , 6H,

CH<sub>2</sub>CH<sub>3</sub>), 1.29 (t, <sup>3</sup>J<sub>H-H</sub> = 7.3, 6H, CH<sub>2</sub>CH<sub>3</sub>). <sup>13</sup>C-NMR (125.74 MHz, d<sub>6</sub>-DMSO): δ = 182.34 (C<sub>carbene</sub>), 136.33 (C<sub>imi</sub>), 123.35 (C<sub>imi</sub>), 123.23 (C<sub>imi</sub>), 123.13 (C<sub>imi</sub>), 122/37 (C<sub>imi</sub>), 50.76 (CH<sub>2</sub>), 50.05 (CH<sub>2</sub>), 46.19 (CH<sub>2</sub>CH<sub>3</sub>), 44.70 (CH<sub>2</sub>CH<sub>3</sub>), 17.30 (CH<sub>2</sub>CH<sub>3</sub>), 15.76 (CH<sub>2</sub>CH<sub>3</sub>). ESI-MS<sup>+</sup>: [C<sub>24</sub>H<sub>38</sub>N<sub>8</sub>AuBF<sub>4</sub>]<sup>2+</sup> m/z = 361.20, calcd = 361.14, [C<sub>24</sub>H<sub>38</sub>N<sub>8</sub>Au]<sup>3+</sup> m/z = 211.60, calcd = 211.76.

**4.27·(BF<sub>4</sub>)<sub>2</sub>.** This compound was prepared using the same method as described for **4.11·(BF<sub>4</sub>)<sub>2</sub>** from **4.24·(BF<sub>4</sub>)<sub>3</sub>** (0.020 g, 0.024 mmol) and Ag<sub>2</sub>O (0.014 g, 0.024 mmol). The crude mixture was recrystallized from a mixture of acetonitrile and diethyl ether yielding an off-white solid. NMR analysis showed this material to be impure and the <sup>1</sup>H-NMR: (500.023 MHz, d<sub>3</sub>-CD<sub>3</sub>CN): δ = 7.13 – 7.14 (m, 6H, H<sub>imi</sub>), 7.08 (s, 2H, H<sub>imi</sub>), 4.75 (s, 4H, CH<sub>2</sub>), 4.68 (s, 4H, CH<sub>2</sub>), 3.82 (s, 6H, CH<sub>3</sub>), 3.79 (s, 6H, CH<sub>3</sub>). [C<sub>20</sub>H<sub>28</sub>N<sub>8</sub>AuAgBF<sub>4</sub>]<sup>+</sup> m/z = 771.1191, calcd = 771.1177, [C<sub>20</sub>H<sub>28</sub>N<sub>8</sub>AuAg]<sup>2+</sup> m/z = 342.0571, calcd = 342.0571.

**4.28·(BF<sub>4</sub>)<sub>2</sub>.** This compound was prepared using the same method as described for **4.11·(BF<sub>4</sub>)<sub>2</sub>** from **4.25·(BF<sub>4</sub>)<sub>3</sub>** (0.050 g, 0.058 mmol) and Ag<sub>2</sub>O (0.030 g, 0.13 mmol). Yield: 0.044 g, 86.1 %. <sup>1</sup>H-NMR (500.023 MHz, d<sub>3</sub>-CD<sub>3</sub>CN): δ = 7.16 (d, <sup>3</sup>J<sub>H-H</sub> = 1.8 Hz, 1H, H<sub>imi</sub>), 7.14 (d, <sup>3</sup>J<sub>H-H</sub> = 1.8 Hz, 1H, H<sub>imi</sub>), 7.09 (d, <sup>3</sup>J<sub>H-H</sub> = 1.8 Hz, 1H, H<sub>imi</sub>), 7.03 (d, <sup>3</sup>J<sub>H-H</sub> = 1.8 Hz, 1H, H<sub>imi</sub>), 4.73 (t, <sup>3</sup>J<sub>H-H</sub> = 6.1 Hz, 2H, CH<sub>2</sub>), 4.66 (t, <sup>3</sup>J<sub>H-H</sub> = 6.1 Hz, 2H, CH<sub>2</sub>), 4.08 (q, <sup>3</sup>J<sub>H-H</sub> = 7.4 Hz, 2H, CH<sub>2</sub>CH<sub>3</sub>), 3.78 (s, 3H, CH<sub>3</sub>), 1.35 (t, <sup>3</sup>J<sub>H-H</sub> = 7.3 Hz, 3H, CH<sub>2</sub>CH<sub>3</sub>). <sup>13</sup>C-NMR (125.74 MHz, d<sub>3</sub>-CD<sub>3</sub>CN): δ = 184.55 (C<sub>carbene</sub>), 183.93 (C<sub>carbene</sub>), 124.02 (C<sub>imi</sub>), 123.31 (C<sub>imi</sub>), 122.85 (C<sub>imi</sub>), 122.40 (C<sub>imi</sub>), 51.86 (CH<sub>2</sub>), 51.44 (CH<sub>2</sub>), 47.84 (CH<sub>2</sub>CH<sub>3</sub>), 37.76 (CH<sub>3</sub>), 17.62 (CH<sub>2</sub>CH<sub>3</sub>). HRESI-MS<sup>+</sup>: [C<sub>22</sub>H<sub>32</sub>N<sub>8</sub>AuAgBF<sub>4</sub>]<sup>+</sup> m/z = 799.1485, calcd = 799.1490, [C<sub>22</sub>H<sub>32</sub>N<sub>8</sub>AuAg]<sup>2+</sup> m/z = 356.0726, calcd = 356.0728.

#### **4.4.2 Photophysical studies**

UV-visible spectra were collected using an Agilent Cary Series UV-Vis spectrophotometer with a 1 cm path length quartz cuvette, a spectral bandwidth of 2.00 nm, signal averaging time of 0.10 s, data interval of 1.00 nm, scan rate of 600 nm/min and baseline/zero corrected. Anhydrous acetonitrile for the solutions were dried using  $\text{CaH}_2$  and were distilled in an atmosphere of  $\text{N}_2$ . The stock solution (0.2 mM) were by dissolving titled compound (1 mM) in acetonitrile (10.00 mL). A varied volume of stock solutions of titled compounds were diluted with acetonitrile to 5.00 mL and the UV-vis spectra of the solutions were recorded at 298 K.

#### **4.4.3 Antimicrobial studies**

The minimum inhibitory concentration (MIC) was determined using a broth microdilution method according to guidelines defined by the Clinical Laboratory Standards Institute. An inoculum of  $1 \times 10^5$  colony forming units per mL was used and the testing conducted using tryptic soy broth in 96-well plates. Plates were incubated at 37 °C for 20 h and growth assessed by measuring the absorbance at 600 nm. The screening was performed against a panel of Gram-positive and Gram-negative bacterial strains. The MIC value is defined as the lowest concentration of inhibitor where no bacterial growth is observed. Experiments were repeated with 3 biological replicates. Assays were performed by Emily R. R. Mackie (Soares da Costa Laboratory, Department of Biochemistry and Genetics, La Trobe University).

## 4.5 References

1. Catalano, V. J.; Moore, A. L., *Inorg. Chem.* **2005**, *44* (19), 6558-6566.
2. Strasser, C. E.; Catalano, V. J., *Inorg. Chem.* **2011**, *50* (21), 11228-11234.
3. Kaub, C.; Lebedkin, S.; Li, A.; Kruppa, S. V.; Strebert, P. H.; Kappes, M. M.; Riehn, C.; Roesky, P. W., *Chem. Eur. J.* **2018**, *24* (23), 6094-6104.
4. Böhmer, M.; Kampert, F.; Tan, T. T. Y.; Guisado-Barrios, G.; Peris, E.; Hahn, F. E., *Organometallics* **2018**, *37* (21), 4092-4099.
5. Majumder, A.; Naskar, R.; Roy, P.; Maity, R., *Eur. J. Inorg. Chem.* **2019**, *2019* (13), 1810-1815.
6. Mata, J. A.; Hahn, F. E.; Peris, E., *Chem. Sci.* **2014**, *5* (5), 1723-1732.
7. Ajamian, A.; Gleason, J. L., *Angew. Chem. Int. Ed.* **2004**, *43* (29), 3754-3760.
8. Sabater, S.; Mata, J. A.; Peris, E., *Nat. Commun.* **2013**, *4*, 2553.
9. Bitzer, M. J.; Kühn, F. E.; Baratta, W., *J. Catal.* **2016**, *338*, 222-226.
10. Pardatscher, L.; Bitzer, M. J.; Jandl, C.; Kück, J. W.; Reich, R. M.; Kühn, F. E.; Baratta, W., *Dalton Trans.* **2019**, *48* (1), 79-89.
11. Gonell, S.; Poyatos, M.; Mata, J. A.; Peris, E., *Organometallics* **2012**, *31* (15), 5606-5614.
12. Zanardi, A.; Mata, J. A.; Peris, E., *J. Am. Chem. Soc.* **2009**, *131* (40), 14531-14537.
13. Pezük, L. G.; Şen, B.; Hahn, F. E.; Türkmen, H., *Organometallics* **2019**, *38* (2), 593-601.
14. Boselli, L.; Carraz, M.; Mazères, S.; Paloque, L.; González, G.; Benoit-Vical, F.; Valentin, A.; Hemmert, C.; Gornitzka, H., *Organometallics* **2015**, *34* (6), 1046-1055.
15. Bertrand, B.; Citta, A.; Franken, I. L.; Picquet, M.; Folda, A.; Scalcon, V.; Rigobello, M. P.; Le Gendre, P.; Casini, A.; Bodio, E., *J. Biol. Inorg. Chem.* **2015**, *20* (6), 1005-1020.
16. Hussaini, S. Y.; Haque, R. A.; Razali, M. R., *J. Org. Chem.* **2019**, *882*, 96-111.
17. Tan, S. J.; Yan, Y. K.; Lee, P. P. F.; Lim, K. H., *Future Med. Chem.* **2010**, *2* (10), 1591-1608.
18. Mora, M.; Gimeno, M. C.; Visbal, R., *Chem. Soc. Rev.* **2019**, *48* (2), 447-462.
19. Johnson, N. A.; Southerland, M. R.; Youngs, W. J., *Molecules* **2017**, *22* (8).
20. Scherbaum, F.; Grohmann, A.; Huber, B.; Krüger, C.; Schmidbaur, H., *Angew. Chem. Int. Ed.* **1988**, *27* (11), 1544-1546.
21. Scherbaum, F.; Huber, B.; Müller, G.; Schmidbaur, H., *Angew. Chem. Int. Ed.* **1988**, *27* (11), 1542-1544.

22. Schmidbaur, H.; Scherbaum, F.; Huber, B.; Müller, G., *Angew. Chem. Int. Ed.* **1988**, 27 (3), 419-421.
23. Schmidbaur, H.; Schier, A., *Angew. Chem. Int. Ed.* **2015**, 54 (3), 746-784.
24. Ai, P.; Danopoulos, A. A.; Braunstein, P.; Monakhov, K. Y., *Chem. Commun.* **2014**, 50 (1), 103-105.
25. Pell, T. P.; Wilson, D. J. D.; Skelton, B. W.; Dutton, J. L.; Barnard, P. J., *Inorg. Chem.* **2016**, 55 (14), 6882-6891.
26. Ray, L.; Shaikh, M. M.; Ghosh, P., *Inorg. Chem.* **2008**, 47 (1), 230-240.
27. Strasser, C. E.; Catalano, V. J., *J. Am. Chem. Soc.* **2010**, 132 (29), 10009-10011.
28. Laguna, A.; Lasanta, T.; López-de-Luzuriaga, J. M.; Monge, M.; Naumov, P.; Olmos, M. E., *J. Am. Chem. Soc.* **2010**, 132 (2), 456-457.
29. Poblet, J.-M.; Bénard, M., *Chem. Commun.* **1998**, (11), 1179-1180.
30. Catalano, V. J.; Etogo, A. O., *J. Organomet. Chem.* **2005**, 690 (24), 6041-6050.
31. Böhmer, M.; Guisado-Barrios, G.; Kampert, F.; Roelfes, F.; Tan, T. T. Y.; Peris, E.; Hahn, F. E., *Organometallics* **2019**, 38 (9), 2120-2131.
32. Barnard, P. J.; Baker, M. V.; Berners-Price, S. J.; Skelton, B. W.; White, A. H., *Dalton Trans.* **2004**, (7), 1038-1047.
33. Barnard, P. J.; Wedlock, L. E.; Baker, M. V.; Berners-Price, S. J.; Joyce, D. A.; Skelton, B. W.; Steer, J. H., *Angew. Chem. Int. Ed.* **2006**, 45 (36), 5966-5970.
34. Rieb, J.; Dominelli, B.; Mayer, D.; Jandl, C.; Drechsel, J.; Heydenreuter, W.; Sieber, S. A.; Kühn, F. E., *Dalton Trans.* **2017**, 46 (8), 2722-2735.
35. Haque, R. A.; Ghddhayeb, M. Z.; Salman, A. W.; Budagumpi, S.; Khadeer Ahamed, M. B.; Abdul Majid, A. M. S., *Inorg. Chem. Commun.* **2012**, 22, 113-119.
36. Haque, R. A.; Hasanudin, N.; Iqbal, M. A.; Ahmad, A.; Hashim, S.; Abdul Majid, A.; Ahamed, M. B. K., *J. Coord. Chem.* **2013**, 66 (18), 3211-3228.
37. Hussaini, S. Y.; Haque, R. A.; Asekunowo, P. O.; Abdul Majid, A. M. S.; Taleb Agha, M.; Razali, M. R., *J. Organomet. Chem.* **2017**, 840, 56-62.
38. Aweda, T. A.; Ikotun, O.; Mastren, T.; Cannon, C. L.; Wright, B.; Youngs, W. J.; Cutler, C.; Guthrie, J.; Lapi, S. E., *MedChemComm* **2013**, 4 (6), 1015-1017.
39. Hindi, K. M.; Panzner, M. J.; Tessier, C. A.; Cannon, C. L.; Youngs, W. J., *Chem. Rev.* **2009**, 109 (8), 3859-3884.
40. Melaiye, A.; Sun, Z.; Hindi, K.; Milsted, A.; Ely, D.; Reneker, D. H.; Tessier, C. A.; Youngs, W. J., *J. Am. Chem. Soc.* **2005**, 127 (7), 2285-2291.
41. Schmidt, C.; Albrecht, L.; Balasupramaniam, S.; Misgeld, R.; Karge, B.; Brönstrup, M.; Prokop, A.; Baumann, K.; Reichl, S.; Ott, I., *Metallomics* **2019**, 11 (3), 533-545.

42. Roymahapatra, G.; Mandal, S.; Porto, W.; Samanta, T.; Giri, S.; Dinda, J.; L. Franco, O.; K. Chattaraj, P., *Curr. Med. Chem.* **2012**, *19* (24), 4184-4193.
43. Haque, R. A.; Asekunowo, P. O.; Razali, M. R.; Mohamad, F., *Heteroatom Chem.* **2014**, *25* (3), 194-204.
44. Maity, R.; Koppetz, H.; Hepp, A.; Hahn, F. E., *J. Am. Chem. Soc.* **2013**, *135* (13), 4966-4969.
45. Maity, R.; Schulte to Brinke, C.; Hahn, F. E., *Dalton Trans.* **2013**, *42* (36), 12857-12860.
46. Schulte to Brinke, C.; Hahn, F. E., *Eur. J. Inorg. Chem.* **2015**, *2015* (20), 3227-3231.
47. Zamora, M. T.; Ferguson, M. J.; McDonald, R.; Cowie, M., *Dalton Trans.* **2009**, (35), 7269-7287.
48. Zamora, M. T.; Ferguson, M. J.; Cowie, M., *Organometallics* **2012**, *31* (15), 5384-5395.
49. Zamora, M. T.; Ferguson, M. J.; McDonald, R.; Cowie, M., *Organometallics* **2012**, *31* (15), 5463-5477.
50. Bente, S.; Kampert, F.; Tan, T. T. Y.; Hahn, F. E., *Chem. Commun.* **2018**, *54* (91), 12887-12890.
51. Simler, T.; Möbius, K.; Müller, K.; Feuerstein, T. J.; Gamer, M. T.; Lebedkin, S.; Kappes, M. M.; Roesky, P. W., *Organometallics* **2019**, *38* (19), 3649-3661.
52. Aznarez, F.; Gao, W.-X.; Lin, Y.-J.; Hahn, F. E.; Jin, G.-X., *Dalton Trans.* **2018**, *47* (28), 9442-9452.
53. Longhi, A.; Baron, M.; Rancan, M.; Bottaro, G.; Armelao, L.; Sgarbossa, P.; Tubaro, C., *Molecules* **2019**, *24* (12).
54. Wang, W.; Zhao, L.; Lv, H.; Zhang, G.; Xia, C.; Hahn, F. E.; Li, F., *Angew. Chem. Int. Ed.* **2016**, *55* (27), 7665-7670.
55. Catalano, V. J.; Malwitz, M. A.; Etogo, A. O., *Inorg. Chem.* **2004**, *43* (18), 5714-5724.
56. Haziz, U. F. M.; Haque, R. A.; Amirul, A. A.; Aidda, O. N.; Razali, M. R., *J. Organomet. Chem.* **2019**, *899*, 120914.
57. Kobialka, S.; Müller-Tautges, C.; Schmidt, M. T. S.; Schnakenburg, G.; Hollóczki, O.; Kirchner, B.; Engeser, M., *Inorg. Chem.* **2015**, *54* (13), 6100-6111.
58. Li, W.-R.; Xie, X.-B.; Shi, Q.-S.; Zeng, H.-Y.; Ou-Yang, Y.-S.; Chen, Y.-B., *Appl. Microbiol. Biotechnol.* **2010**, *85* (4), 1115-1122.
59. Son-di, I.; Salopek-Son-di, B., *J. Colloid. Interface. Sci.* **2004**, *275* (1), 177-182.



60. Hartinger, C. G.; Dyson, P. J., *Chem. Soc. Rev.* **2009**, 38 (2), 391-401.
61. Satlin, M. J., *J. Clin. Microbiol.* **2019**, 57 (2), e01608-18.
62. Boneca, I. G.; Chiosis, G., *Expert Opin. Ther. Targets.* **2003**, 7 (3), 311-328.
63. NCCLS. *Performance Standards for Antimicrobial Susceptibility Testing* **2020**, 30, NCCLS publication no. M100.
64. Fernández, A.; López-Torres, M.; Fernández, J. J.; Vázquez-García, D.; Marcos, I., *J. Chem. Educ.* **2017**, 94 (10), 1552-1556.

## CHAPTER 5 CONCLUSION AND FUTURE WORK

### 5.1 Conclusion and future work

Chapter 2 of this thesis described a modular and stepwise method for the preparation of both symmetrical and asymmetrical *tetra*-imidazolium linked macrocycles. In this work, a series of four *bis*(imidazolylmethyl)benzene precursors were alkylated with 1,2-dibromoethane to produce the corresponding *bis*-bromoethylimidazolium synthetic intermediates. In the following step, these *bis*-bromoethylimidazolium compounds were reacted with selected *bis*(imidazolylmethyl)benzenes to produce a series of two symmetrical and three asymmetrical *tetra*-imidazolium macrocycles. This synthetic approach is useful when compared to other synthetic methodologies as the formation of undesirable side products is minimised during the macrocyclization process. In addition, the stepwise methodology also provides access to both symmetrical and asymmetrical *tetra*-imidazolium linked macrocycles bearing different linking groups (e.g. *ortho*- or *meta*-substituted phenyl units) or different imidazolium groups (i.e. 2-methyl imidazole).

Using the synthesised *tetra*-imidazolium macrocycles, a series of NHC metal complexes for the metals Au(I), Ag(I) and Pd(II) were also prepared. A variety of different metal complex structures were obtained depending on the chosen macrocyclic pro-ligands and the metal ion. The Au(I) and Ag(I) complexes of the symmetrical *ortho*-substituted pro-ligand adopted hexanuclear structures where six metal atoms combined with three macrocycle ligand molecules while the Ag(I) complex derived from the symmetrical *meta*-substituted pro-ligand was mononuclear, with two NHC groups coordinated to the metal ion. In contrast to the complexes of the symmetrical ligands, the Au(I) and Pd(II) complexes of the asymmetrical C2-blocked macrocyclic ligands adopted mononuclear structures with only the 'normal' NHC groups coordinated to the metal centre. This outcome may be the

result from a lower  $pK_a$  value for the C2-H on the imidazolium units when compared to the C4/5-H on the C2-blocked imidazolium group.<sup>1-2</sup>

Due to the positive charge, imidazolium groups have relatively high acidity of the C2 position proton with  $pK_a$  values in the range of 21 – 23.<sup>1-2</sup> As a result of the high acidity of the C2-H, hydrogen bonding occurs between C2-H and anions which provides the imidazolium linked macrocyclic compounds anion sensing properties. Using <sup>1</sup>H-NMR titration studies, the association constants ( $K_a$ ) between the macrocycles **2.15**·(PF6)<sub>4</sub> and **2.16**·(PF6)<sub>4</sub> and the halide anions Cl<sup>-</sup>, Br<sup>-</sup> and I<sup>-</sup> were determined to be in the range 20 – 501 M<sup>-1</sup> and these results demonstrated that the *tetra*-imidazolium receptors more strongly associated with the smaller more charge dense chloride anion with the selective trend Cl<sup>-</sup> > Br<sup>-</sup> > I<sup>-</sup> indicating that these macrocycles have moderate selectivity of sensing chloride. Furthermore, the good affinity for anions shown for these *tetra*-imidazolium macrocycles compared with the previously reported relevant macrocycles suggests that they may be useful in the development of anion receptors.<sup>3</sup>

In Chapter 3, the stepwise macrocyclization method described in Chapter 2 was extended to allow for the synthesis of macrocycles incorporating both 1,2,3-triazole and imidazolium units. In this work, the *ortho*- or *meta*-substituted *bis*-(bromomethyl)-1,2,3-triazole precursors were first prepared using copper(I)-catalyzed azide-alkyne cycloaddition (CuAAC) reactions. Several attempts were made to prepare the required *bis*-(bromomethyl)-1,2,3-triazole intermediates by the reaction of either the *ortho*- or *meta*-substituted *bis*-(azidomethyl)benzene precursors with propargyl bromide using ‘click’ reaction conditions however these attempts were unsuccessful. To circumvent this problem the *bis*-(bromomethyl)-1,2,3-triazole precursors were prepared using a two-step method in which the *bis*-(azidomethyl)benzene precursors were first reacted with propargyl alcohol via the CuAAC reaction. The formed alcohol substituted triazoles were then brominated yielding the desired *bis*-(bromomethyl)-1,2,3-triazole intermediates. These compounds

were then reacted with either *ortho*- or *meta*-substituted *bis*(imidazolylmethyl)benzene yielding two novel macrocycles incorporating 1,2,3-triazole and imidazolium groups. The synthesis of symmetrical imidazolium linked macrocycles<sup>4-6</sup> and 1,2,3-triazolium linked macrocycles<sup>7-9</sup> have been previously reported; however, this is the first time asymmetrical macrocycles incorporating both imidazolium and 1,2,3-triazole groups have been prepared. Unfortunately, however, the N3 nitrogen atom of the 1,2,3-triazole groups could not be alkylated using a range of different highly reactive alkylation reagents. The inability to alkylate this nitrogen atom may be due to a decreased nucleophilicity of this nitrogen atom as a result of the close proximity of the positively charged imidazolium groups. Attempts were made to prepare metal-NHC complexes of these macrocycles and a dinuclear Au(I) complex corresponding to the *ortho*-substituted macrocycle **3.21**·Br<sub>2</sub> was successfully synthesized. Using <sup>1</sup>H-NMR titration studies, the association constants between the macrocyclic compounds **3.21**·(PF<sub>6</sub>)<sub>2</sub> and **3.22**·(PF<sub>6</sub>)<sub>2</sub> and the halide anions Cl<sup>-</sup>, Br<sup>-</sup> and I<sup>-</sup> were determined and these were found to be within the range of 6.8 – 29.7 M<sup>-1</sup>. These results suggest that the macrocyclic receptors only weakly bound halide anions and this may be the result of the lower dipositive charge on these molecules when compared to the *tetra*-imidazolium macrocycles. Furthermore, the low affinity for anions demonstrated for these receptors compared with relevant macrocycles described previously suggests that these compounds will not be useful for the development of anion receptors for halide anions.<sup>5, 10</sup>

Overall, a series of novel symmetrical and asymmetrical macrocycles, which combined different azole groups e.g. imidazolium, 2-methylimidazolium and 1,2,3-triazole with either methylene or ethylene alkyl linkers were successfully prepared using modular stepwise synthetic methodology. In addition, the synthesized macrocyclic compounds were evaluated for their ability to act as receptors for halide anions. In future work, it may be of

interest to explore the use of this synthetic method for the synthesis of macrocycles that incorporate different azole groups such as pyrazole or 1,2,4-triazole.

Chapter 4 describes the synthesis, characterization and antimicrobial properties of a range of heterobimetallic metal-NHC complexes. A series of three Au(I)-Ag(I) and two Au(I)-Hg(II) complexes were prepared using a post synthetic modification and metallation approach where a range of imidazolium pro-ligands bearing pendant imidazole groups were prepared and then metallated with Au(I) yielding monometallic Au(I)-NHC complexes. These complexes were then alkylated with an oxonium salt (either trimethyloxonium or triethyloxonium tetrafluoroborate to obtain the corresponding Au(I) complexes with a pendant imidazolium group. In the final step, these complexes were treated with a second metal source (i.e. Ag(I) or Hg(II)) to obtain the heterobimetallic complexes. These studies represent the first examples of heterobimetallic complexes that feature asymmetrical *bis*-imidazolylidene ligands. Compared with previously described stepwise synthetic strategies for the preparation of heterobimetallic complexes, the synthetic approach reported here allowed for the incorporation of different metal centres selectively to both symmetrical and asymmetrical NHC ligands. In addition, this method avoids the formation of the undesirable homobimetallic metal complexes as byproducts. X-ray crystal structural studies revealed a short Au(I)⋯Ag(I) distance for complex **4.12**·(BF<sub>4</sub>)<sub>2</sub> (3.205(6) Å) which is consistent with the previously reported value 3.2897(4) Å<sup>11</sup> suggesting a metallophilic interaction between the Au and Ag atoms in this complex.<sup>11-13</sup> Metal complexes that support metallophilic interactions are known to possess interesting luminescent properties<sup>11-13</sup> and the luminescence can be utilized in a variety of applications such as for sensing volatile organic compounds (VOC).<sup>14</sup> The <sup>1</sup>H-NMR spectra for the homo-and heterobimetallic complexes of the methylene linked *bis*-NHC ligands are consistent with the complexes being relatively rigid in solution with interconversion between structural isomers occurring on a slow to intermediate rate on the NMR timescale. Variable temperature NMR studies showed both

the homobimetallic complex **4.17**·(**BF**<sub>4</sub>)<sub>2</sub> and the heterobimetallic complexes **4.11**·(**BF**<sub>4</sub>)<sub>2</sub>, **4.12**·(**BF**<sub>4</sub>)<sub>2</sub> and **4.13**·(**BF**<sub>4</sub>)<sub>3</sub> adopted folded conformational structures together with low concentrations of the twisted conformational isomers at low temperature (243 K). As the temperature was raised to 343 K, the spectra for the complexes were consistent with intermediate to fast interconversion of the conformational isomers on the NMR timescale. Electronic absorption and emission studies showed that the bimetallic complexes are non-luminescent in solution phase perhaps due to the loss of the metallophilic interactions as a result of the fluxional behaviour of these molecules in solution. However, previous studies have shown that conformationally labile heterobimetallic complexes can be luminescent at low temperature (77 K) in the solid state.<sup>11</sup> In the future, electronic emission studies could be conducted on the homo- and heterobimetallic complexes prepared here at low temperature (77 K). These studies would allow the photophysical property of these complexes resulting from metallophilic interactions to be explored. Silver complexes of NHC ligands are well known for their excellent antimicrobial properties.<sup>15-17</sup> With this in mind, the antimicrobial properties of the Au(I)-Ag(I) heterobimetallic complexes **4.11**·(**BF**<sub>4</sub>)<sub>2</sub> and **4.12**·(**BF**<sub>4</sub>)<sub>2</sub> were evaluated. These complexes displayed good minimum inhibitory concentrations (MIC) values in a range of 8 – 32 µg·mL<sup>-1</sup> for the Gram-positive bacteria strain while the MIC value for the Gram-negative bacteria strain fell in the range of 4 – 16 µg·mL<sup>-1</sup>. The MIC values show that the Au(I)-Ag(I) heterobimetallic complexes inhibited the growth of both the Gram-positive and Gram-negative bacterial strains while the pro-ligand **4.16**·**I**<sub>2</sub> has no antimicrobial activity. Similarly, the homobimetallic Ag(I) complex also displayed antimicrobial activity with a moderate MIC value (16 – 32 µg for Gram-positive and 8 – 32 for Gram-negative bacterial strain). In contrast to the heterobimetallic complexes and the homobimetallic Ag(I) complex, the homobimetallic Au(I) complex was inactive with the MIC >256 µg·mL<sup>-1</sup>. Previously a range of Ag(I) and some Au(I) complexes of NHC ligands have been shown to have antimicrobial activity,<sup>15,</sup>

<sup>18</sup> and the Au(I)-Ag(I) complexes prepared in this work provide the first example of antimicrobial active heterobimetallic complexes and their antimicrobial activities are comparable to the previously reported Ag(I) and Au(I) homobimetallic complexes.<sup>15, 18</sup> Overall, Chapter 4 described the further development of the post synthetic modification and metallation strategy for the synthesis of heterobimetallic complexes. In addition, the synthesized Au(I)-Ag(I) heterobimetallic complexes displayed good antimicrobial activity against both Gram-positive and Gram-negative bacterial strains and molecules of this type may offer a new direction for the development of antimicrobial agents. To improve the antimicrobial activities of heterobimetallic complexes it may be beneficial to develop new NHC ligand systems with higher lipophilicity to allow the complexes to cross the lipid membranes.<sup>19</sup> As such, the ligand system carrying lipophilic units i.e. benzyl, picolyl or benzimidazole groups should be investigated (e.g. Figure 5.1).

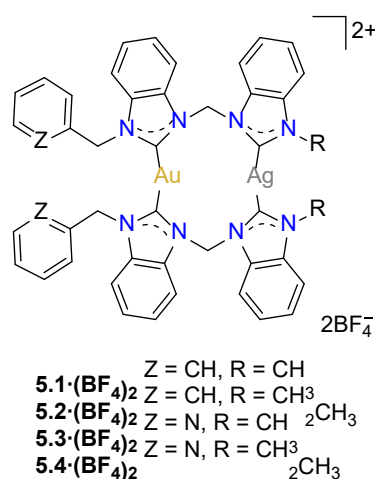
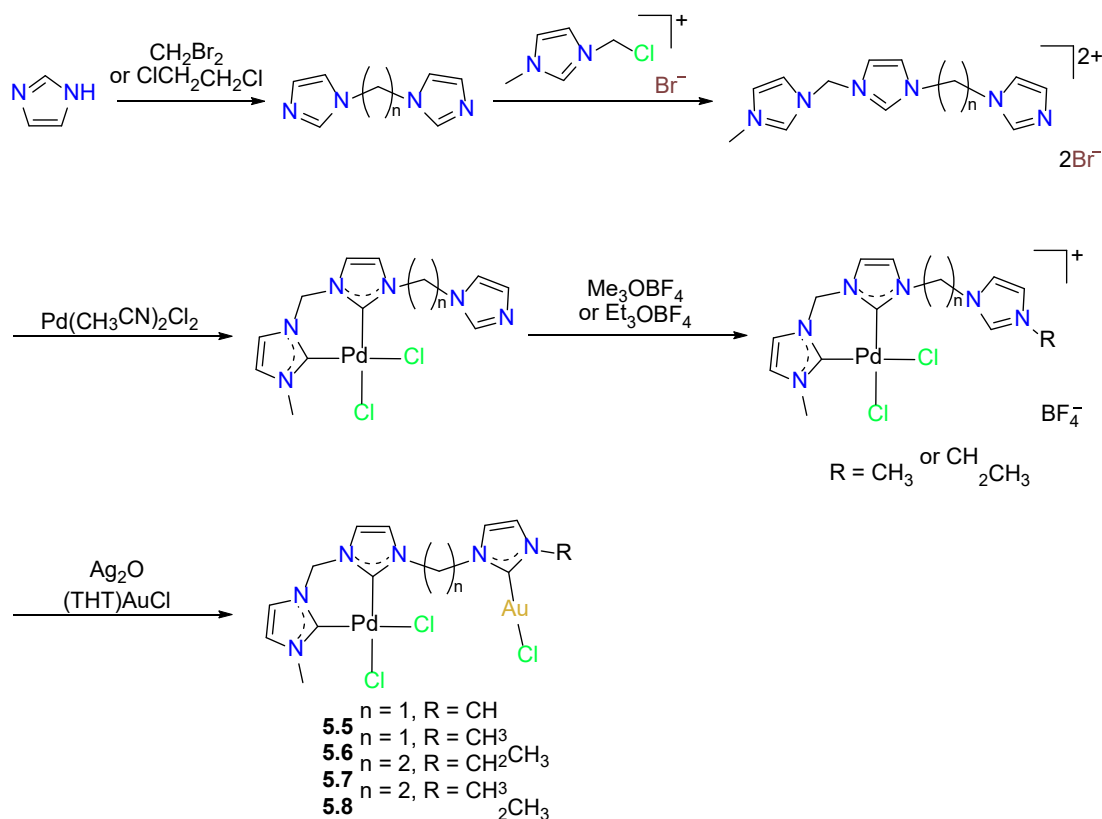


Figure 5.1 Lipophilic Au(I)-Ag(I) heterobimetallic complexes with increased lipophilicity for future antimicrobial studies.

Heterobimetallic complexes of NHC ligands have also been extensively investigated as catalysts for multiple catalytic transformations in one-pot reactions.<sup>20-26</sup> Thus, the synthesis of heterobimetallic NHC complexes using post synthetic modification and metallation method could be investigated for the preparation for the NHC heterobimetallic complexes with potential catalytic activity. For example, the synthesis of Pd(II)-Au(I) heterobimetallic

complexes of *tris*-NHC ligands could be prepared using the post synthetic modification and metallation method e.g. (Scheme 5.1) Molecules of this type are likely to have catalytic activity for the tandem processes e.g. the condensation of nitrobenzene with benzyl alcohol and imine reduction. The catalytic activities of complexes of this type for tandem hydroalkoxylation of alkynes and heck coupling reaction may also be investigated.



Scheme 5.1 Suggested synthetic route for the potential catalytically active heterobimetallic complexes for future catalytic studies.



## 5.2 References

1. Melaimi, M.; Soleilhavoup, M.; Bertrand, G., *Angew. Chem. Int. Ed.* **2010**, *49* (47), 8810-8849.
2. Magill, A. M.; Yates, B. F., *Aust. J. Chem.* **2004**, *57* (12), 1205-1210.
3. Serpell, C. J.; Cookson, J.; Thompson, A. L.; Beer, P. D., *Chem. Sci.* **2011**, *2* (3), 494-500.
4. Sabater, P.; Zapata, F.; Caballero, A.; Alkorta, I.; Ramirez de Arellano, C.; Elguero, J.; Molina, P., *ChemistrySelect* **2018**, *3* (13), 3855-3859.
5. Wong, W. W. H.; Vickers, M. S.; Cowley, A. R.; Paul, R. L.; Beer, P. D., *Org. Biomol. Chem.* **2005**, *3* (23), 4201-4208.
6. Evans, N. H.; Beer, P. D., *Angew. Chem. Int. Ed.* **2014**, *53* (44), 11716-11754.
7. Chhatra, R. K.; Kumar, A.; Pandey, P. S., *J. Org. Chem.* **2011**, *76* (21), 9086-9089.
8. White, N. G.; Carvalho, S.; Félix, V.; Beer, P. D., *Org. Biomol. Chem.* **2012**, *10* (34), 6951-6959.
9. Hua, Y.; Flood, A. H., *Chem. Soc. Rev.* **2010**, *39* (4), 1262-1271.
10. Li, Z.; Wiratpruk, N.; Barnard, P. J., *Frontiers in Chemistry* **2019**, *7*, 270.
11. Pell, T. P.; Wilson, D. J. D.; Skelton, B. W.; Dutton, J. L.; Barnard, P. J., *Inorg. Chem.* **2016**, *55* (14), 6882-6891.
12. Catalano, V. J.; Moore, A. L., *Inorg. Chem.* **2005**, *44* (19), 6558-6566.
13. Catalano, V. J.; Malwitz, M. A.; Etogo, A. O., *Inorg. Chem.* **2004**, *43* (18), 5714-5724.
14. Strasser, C. E.; Catalano, V. J., *J. Am. Chem. Soc.* **2010**, *132* (29), 10009-10011.
15. Roymahapatra, G.; Mandal, S.; Porto, W.; Samanta, T.; Giri, S.; Dinda, J.; L. Franco, O.; K. Chattaraj, P., *Curr. Med. Chem.* **2012**, *19* (24), 4184-4193.
16. Melaiye, A.; Simons, R. S.; Milsted, A.; Pingitore, F.; Wesdemiotis, C.; Tessier, C. A.; Youngs, W. J., *J. Med. Chem.* **2004**, *47* (4), 973-977.
17. Melaiye, A.; Sun, Z.; Hindi, K.; Milsted, A.; Ely, D.; Reneker, D. H.; Tessier, C. A.; Youngs, W. J., *J. Am. Chem. Soc.* **2005**, *127* (7), 2285-2291.
18. Johnson, N. A.; Southerland, M. R.; Youngs, W. J., *Molecules* **2017**, *22* (8).
19. Patil, S.; Deally, A.; Gleeson, B.; Müller-Bunz, H.; Paradisi, F.; Tacke, M., *Metallomics* **2011**, *3* (1), 74-88.
20. Majumder, A.; Naskar, R.; Roy, P.; Maity, R., *Eur. J. Inorg. Chem.* **2019**, *2019* (13), 1810-1815.

21. Böhmer, M.; Kampert, F.; Tan, T. T. Y.; Guisado-Barrios, G.; Peris, E.; Hahn, F. E., *Organometallics* **2018**, 37 (21), 4092-4099.
22. Mata, J. A.; Hahn, F. E.; Peris, E., *Chem. Sci.* **2014**, 5 (5), 1723-1732.
23. Ajamian, A.; Gleason, J. L., *Angew. Chem. Int. Ed.* **2004**, 43 (29), 3754-3760.
24. Sabater, S.; Mata, J. A.; Peris, E., *Nat. Commun.* **2013**, 4, 2553.
25. Bitzer, M. J.; Kühn, F. E.; Baratta, W., *J. Catal.* **2016**, 338, 222-226.
26. Pardatscher, L.; Bitzer, M. J.; Jandl, C.; Kück, J. W.; Reich, R. M.; Kühn, F. E.; Baratta, W., *Dalton Trans.* **2019**, 48 (1), 79-89.

## APPENDIX

### A.1 General details

All solvents and chemicals were purchased from Sigma-Aldrich, Chem Supply, Alfa Aesar and were used as received unless otherwise stated. Where necessary, solvents were further purified using an Innovative Technology Pure Solv solvent purification system. All experiments were performed under an atmosphere of N<sub>2</sub> unless otherwise stated. <sup>1</sup>H-NMR and <sup>13</sup>C-NMR spectra were recorded on either Bruker Advance 400 (400.13 MHz for <sup>1</sup>H and 100.61 for <sup>13</sup>C) or Bruker Advance 500 (500.02 MHz for <sup>1</sup>H and 125.74 MHz for <sup>13</sup>C) and spectra were referenced to solvent resonances. Where required, COSY, HSQC, HMBC and NOESY 2-dimensional experiments were used to assist assignments. Mass spectra were obtained using either Bruker Daltonics HCT ultra ion trap mass spectrometer fitted with a Bruker electrospray ion source or an Agilent 6530 Q-TOF LC/MS mass spectrometer fitted with an Agilent electrospray ion (ESI) source.

## A.2 Appendix for Chapter 2

### A.2.1 NMR Spectra for Chapter 2

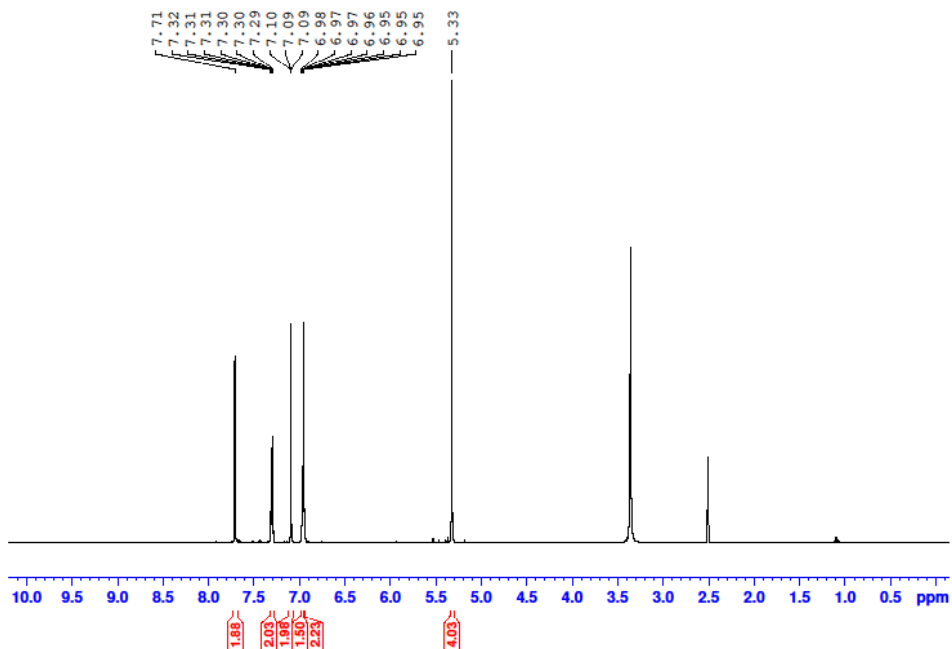


Figure A.1 <sup>1</sup>H-NMR spectrum of compound 2.7.

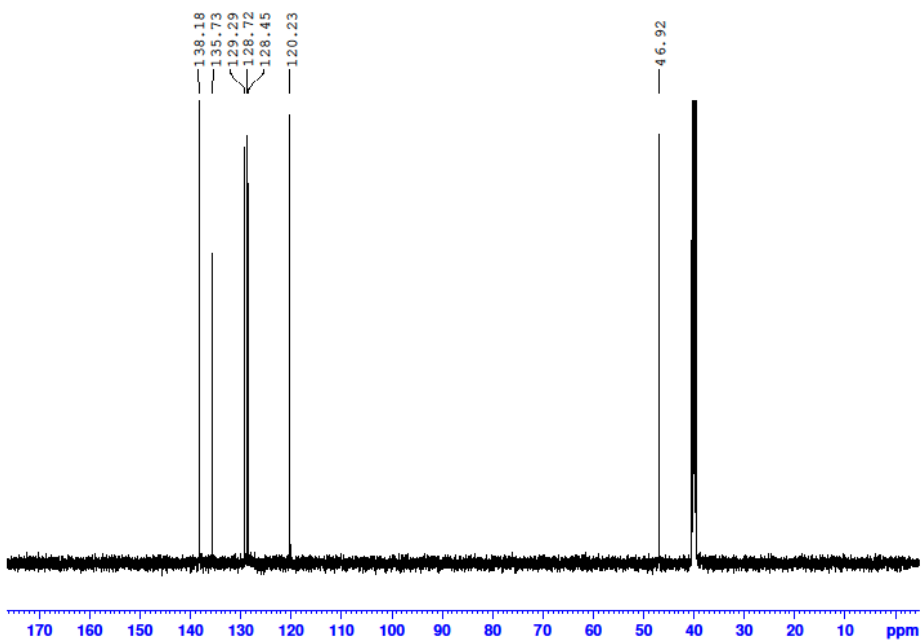


Figure A.2 <sup>13</sup>C-NMR spectrum of compound 2.7.

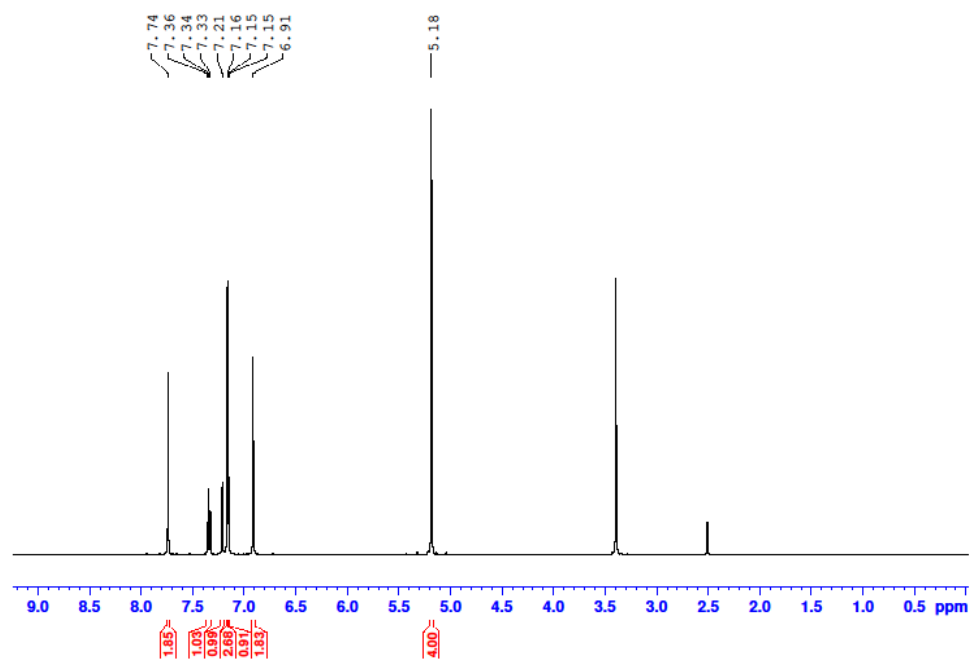


Figure A.3 <sup>1</sup>H-NMR spectrum of compound **2.8**.

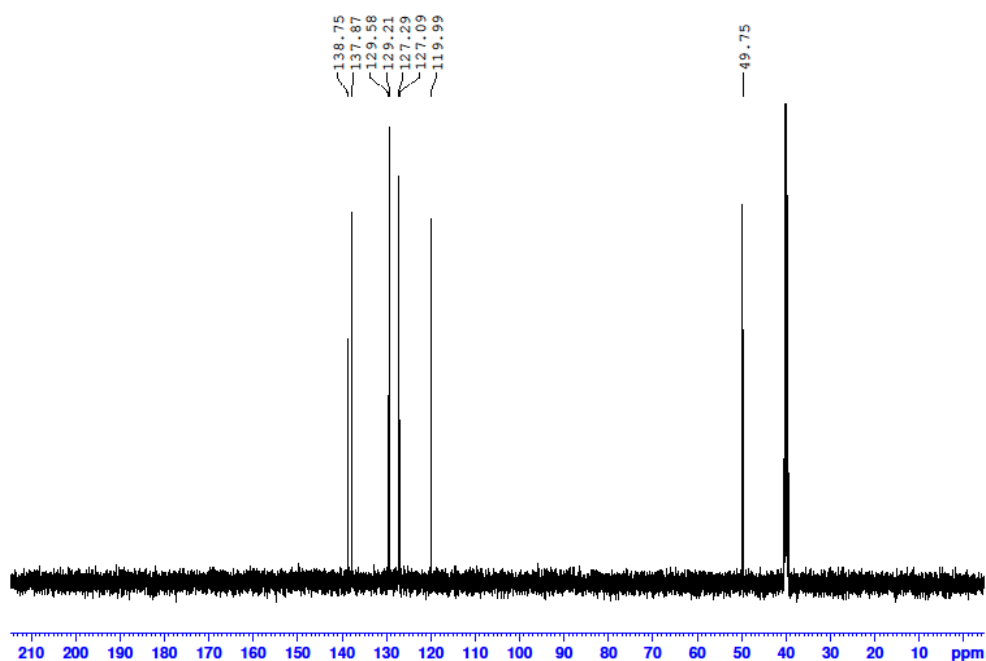


Figure A.4 <sup>13</sup>C-NMR spectrum of compound **2.8**.

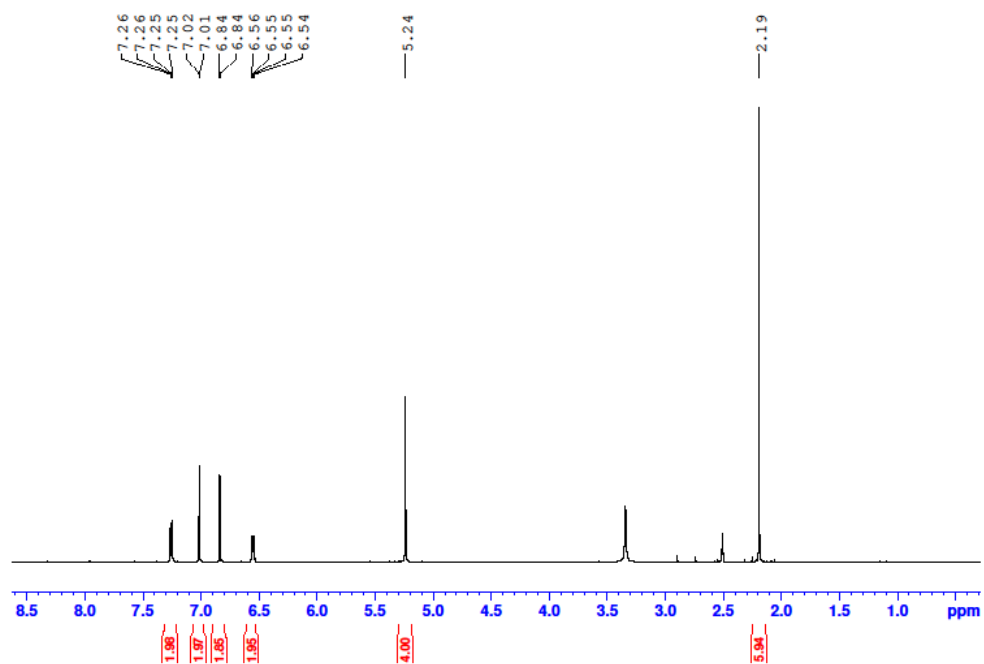


Figure A.5 <sup>1</sup>H-NMR spectrum of compound **2.9**.

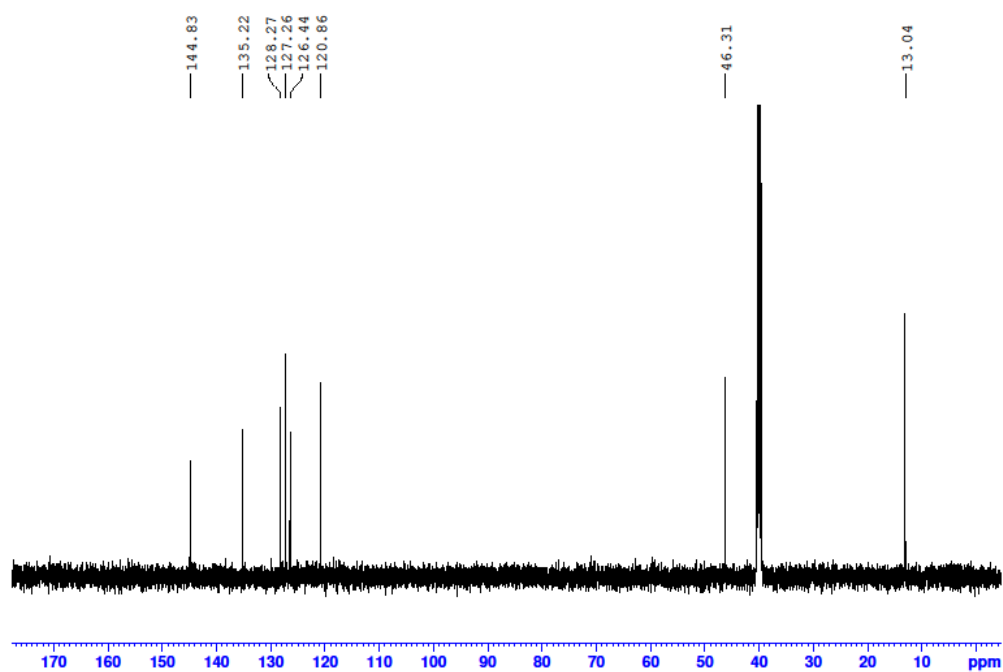


Figure A.6 <sup>13</sup>C-NMR spectrum of compound **2.9**.

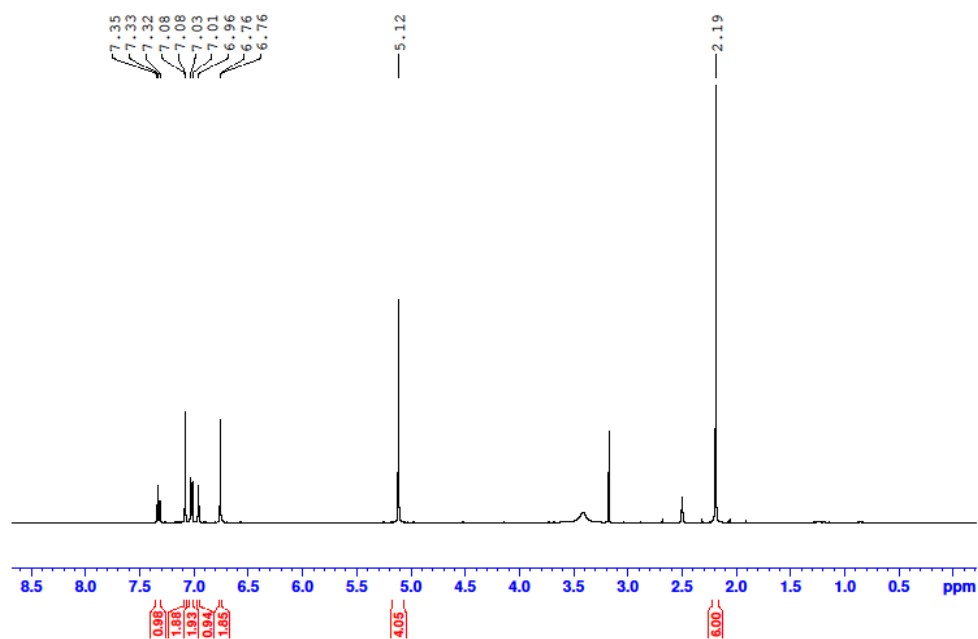


Figure A.7  $^1\text{H}$ -NMR spectrum of compound **2.10**.

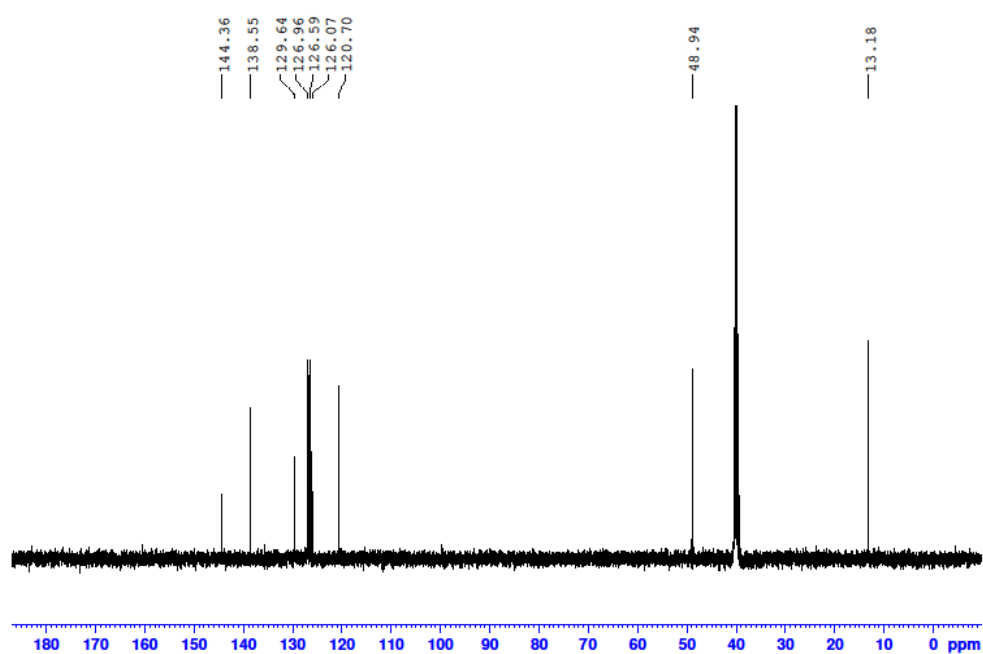


Figure A.8  $^{13}\text{C}$ -NMR spectrum of compound **2.10**.

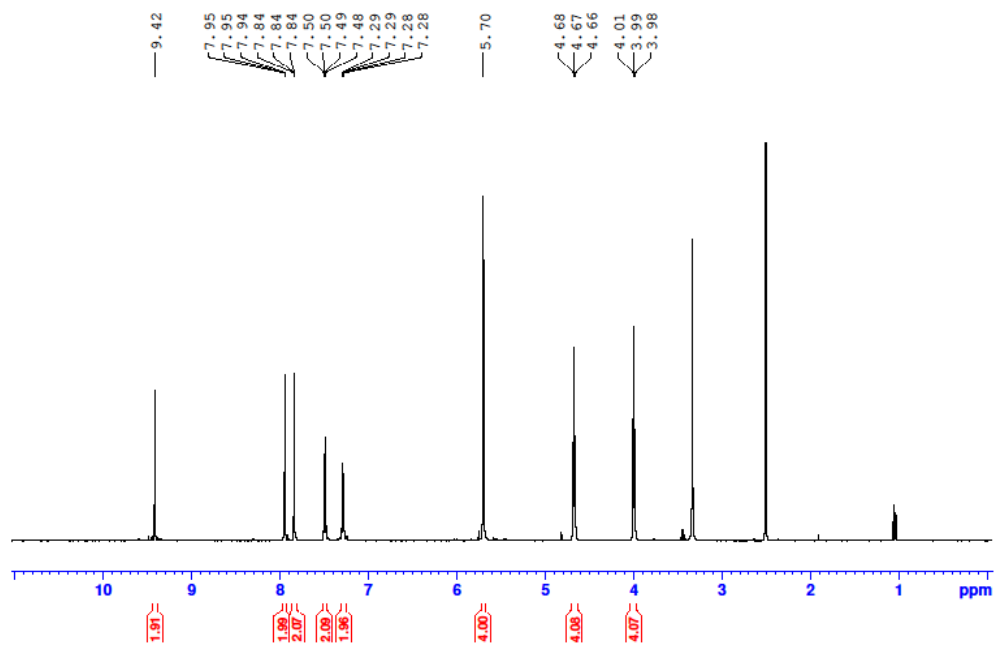


Figure A.9 <sup>1</sup>H-NMR spectrum of compound **2.11·Br<sub>2</sub>**.

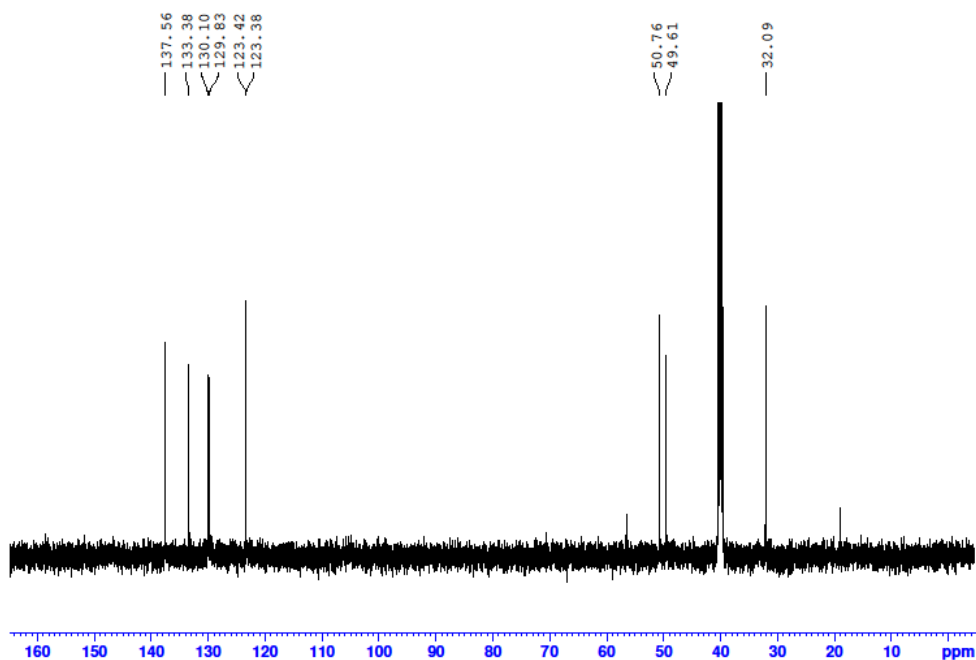


Figure A.10 <sup>13</sup>C-NMR spectrum of compound **2.11·Br<sub>2</sub>**.



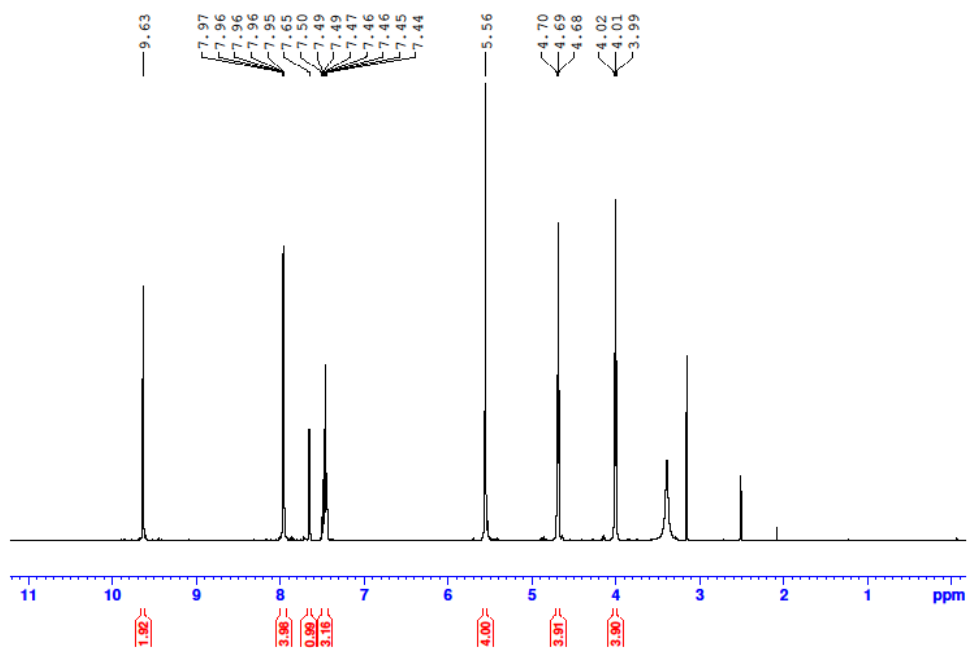


Figure A.11 <sup>1</sup>H-NMR spectrum of compound **2.12·Br<sub>2</sub>**.

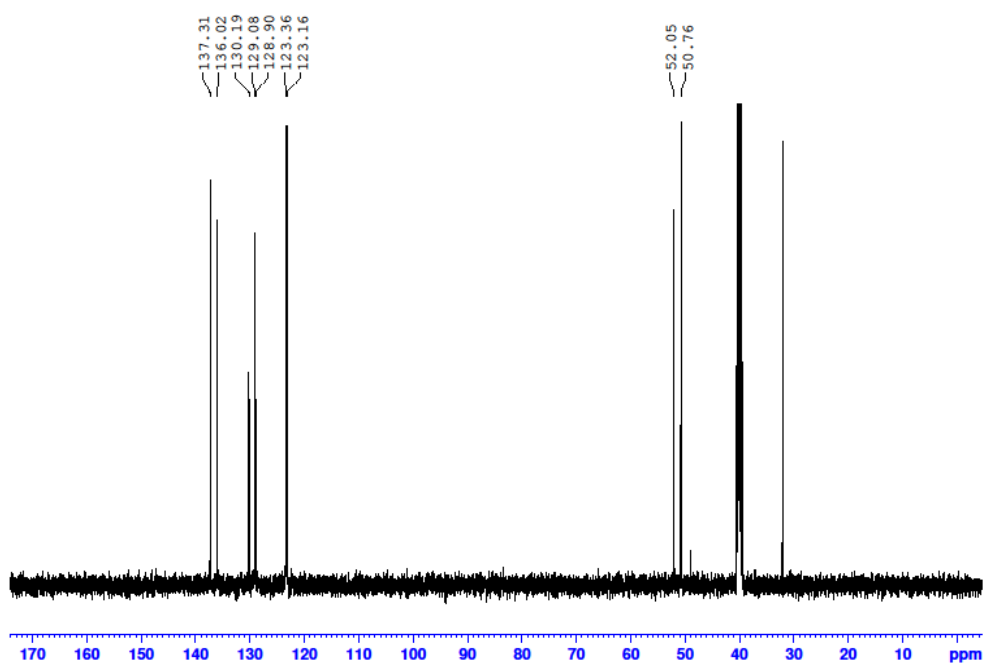


Figure A.12 <sup>13</sup>C-NMR spectrum of compound **2.12·Br<sub>2</sub>**.

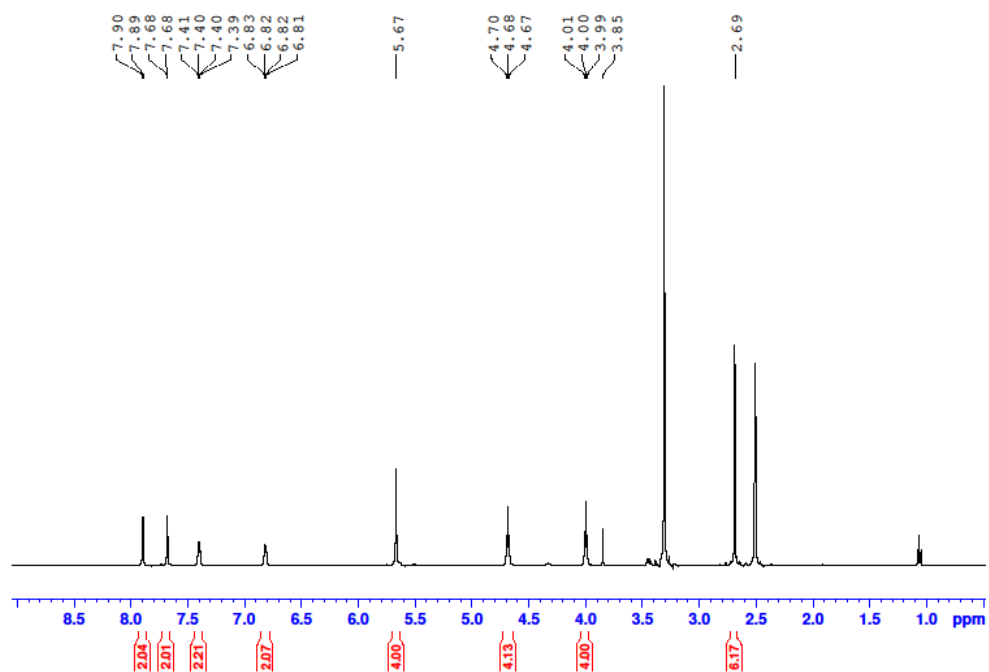


Figure A.13 <sup>1</sup>H-NMR spectrum of compound **2.13·Br<sub>2</sub>**.

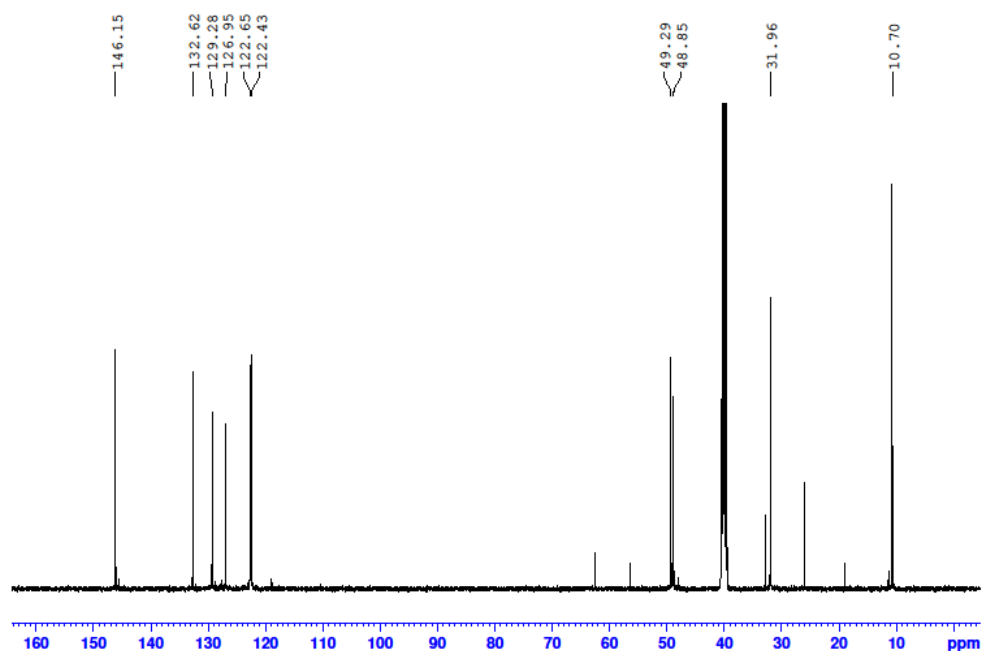


Figure A.14 <sup>13</sup>C-NMR spectrum of compound **2.13·Br<sub>2</sub>**.

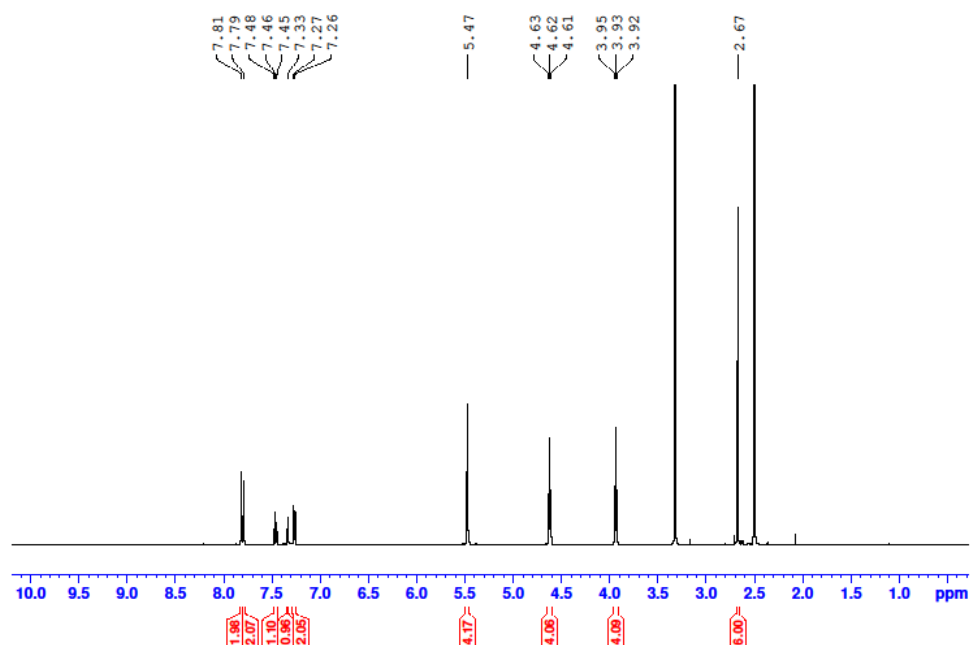


Figure A.15 <sup>1</sup>H-NMR spectrum of compound **2.14·Br<sub>2</sub>**.

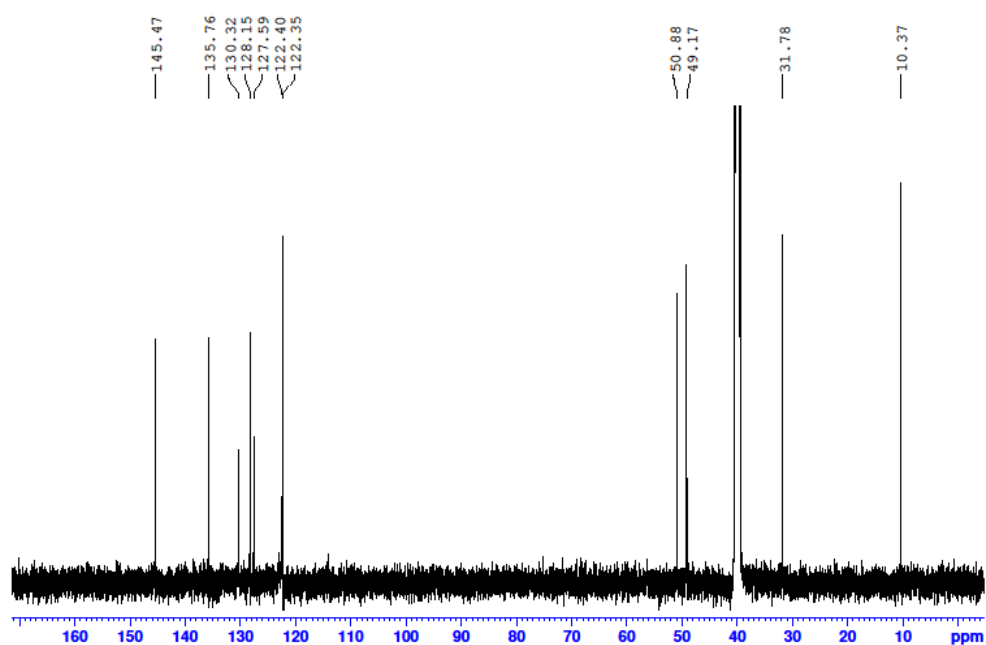


Figure A.16 <sup>13</sup>C-NMR spectrum of compound **2.14·Br<sub>2</sub>**.

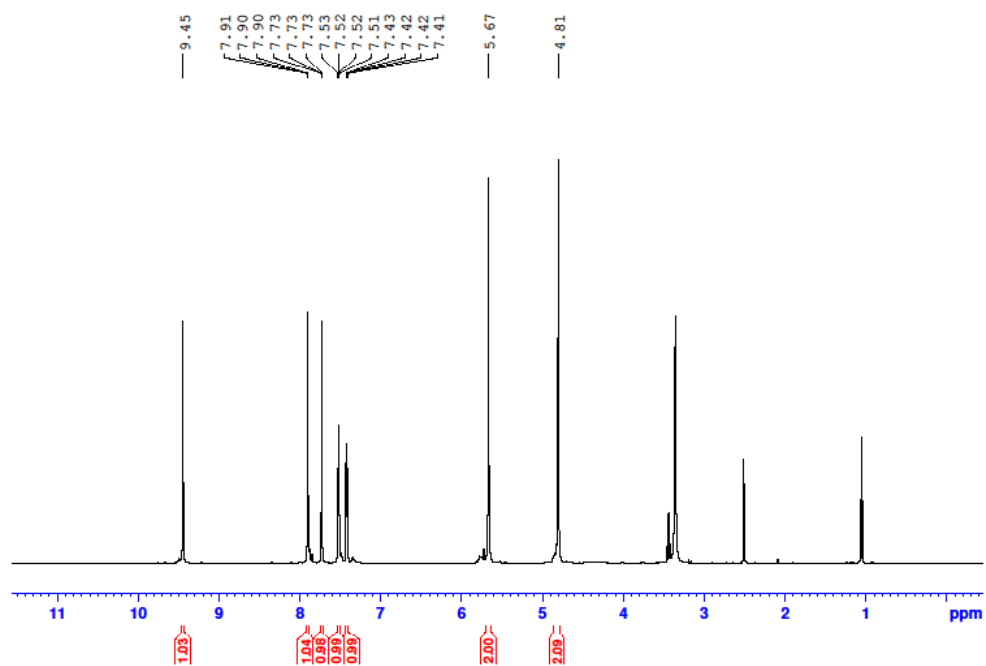


Figure A.17  $^1\text{H}$ -NMR spectrum of macrocycle **2.15·Br<sub>4</sub>**.

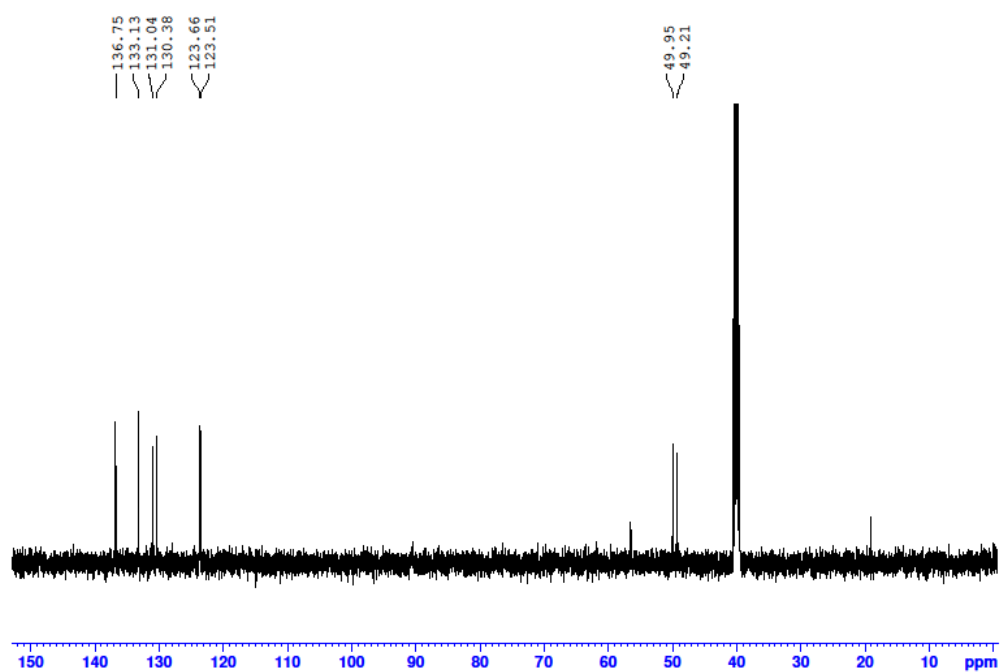


Figure A.18  $^{13}\text{C}$ -NMR spectrum of macrocycle **2.15·Br<sub>4</sub>**.

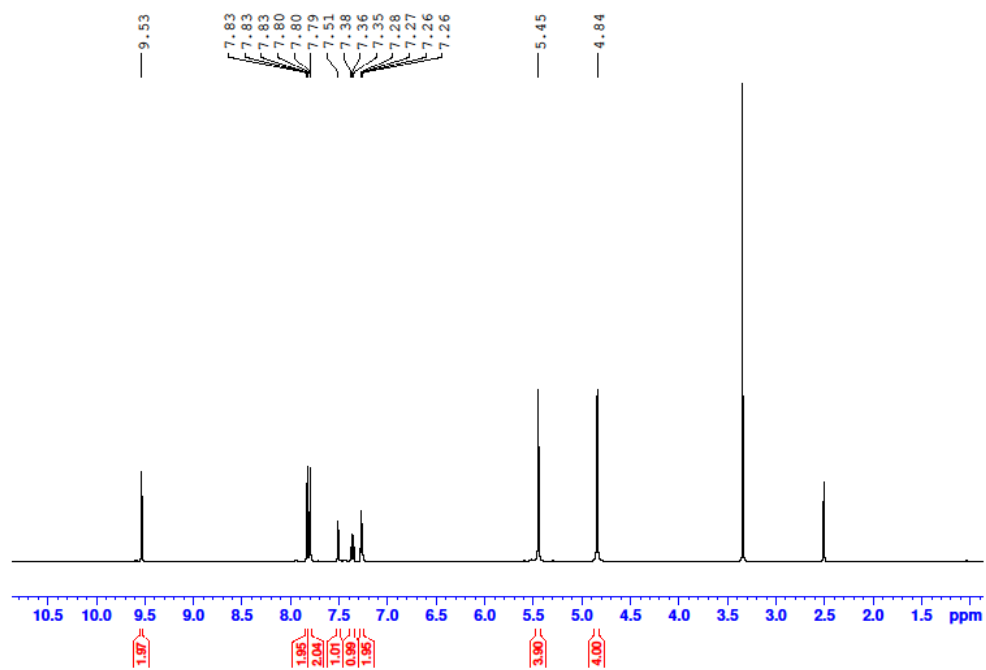


Figure A.19 <sup>1</sup>H-NMR spectrum of macrocycle **2.16·Br<sub>4</sub>**.

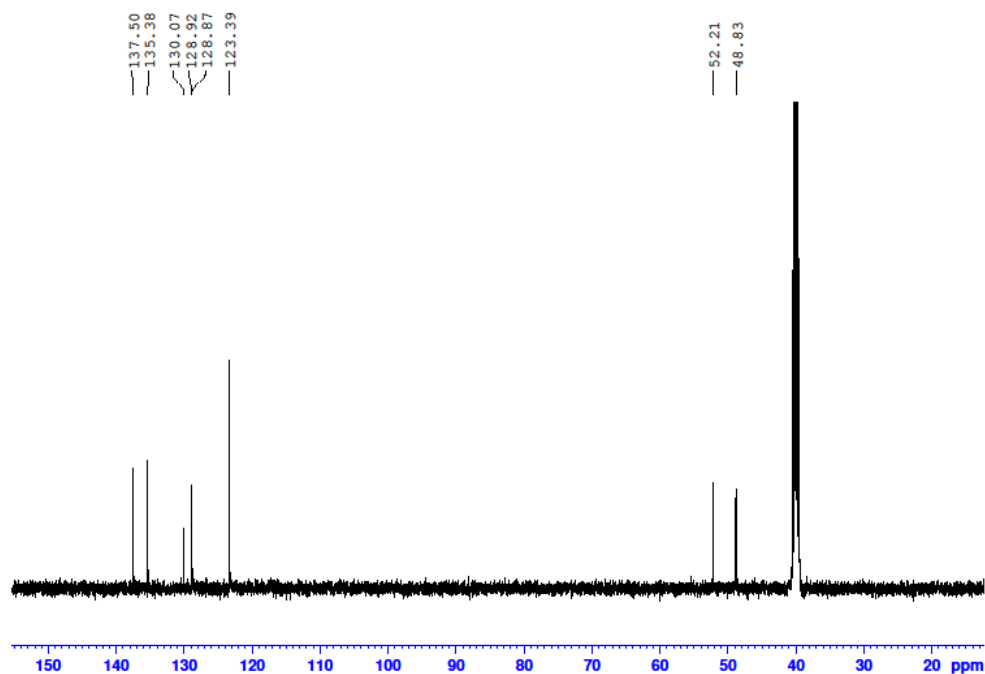


Figure A.20 <sup>13</sup>C-NMR spectrum of macrocycle **2.16·Br<sub>4</sub>**.

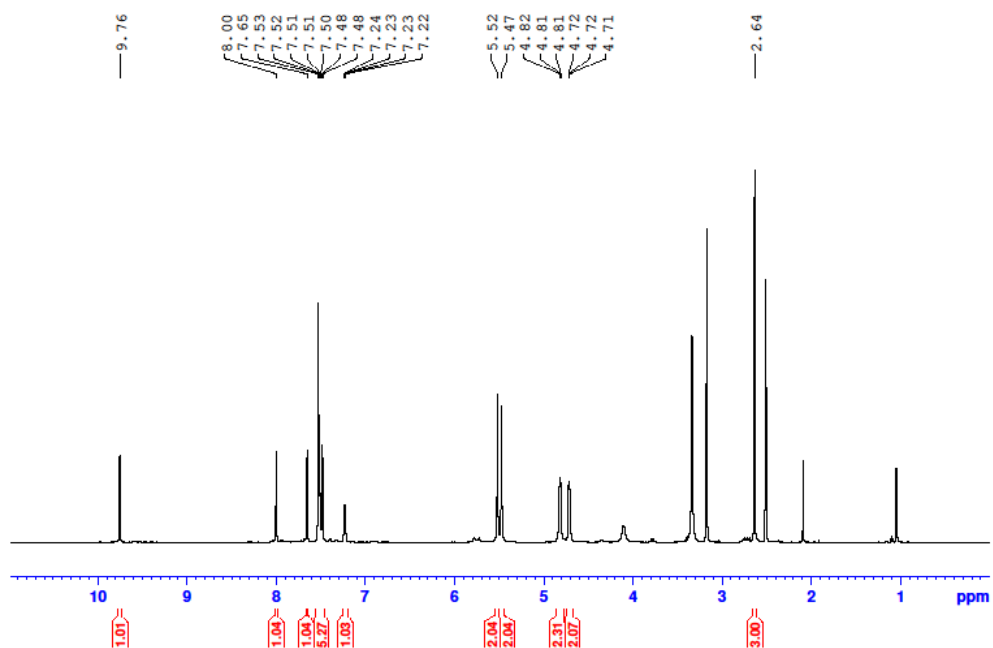


Figure A.21  $^1\text{H}$ -NMR spectrum of macrocycle **2.17·Br<sub>4</sub>**.

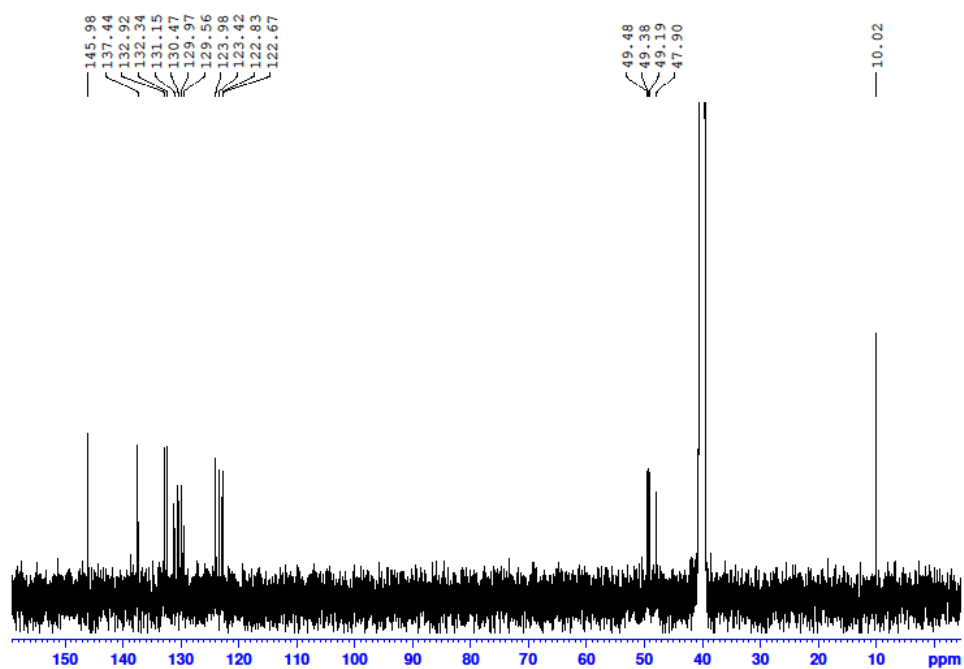


Figure A.22  $^{13}\text{C}$ -NMR spectrum of macrocycle **2.17·Br<sub>4</sub>**.

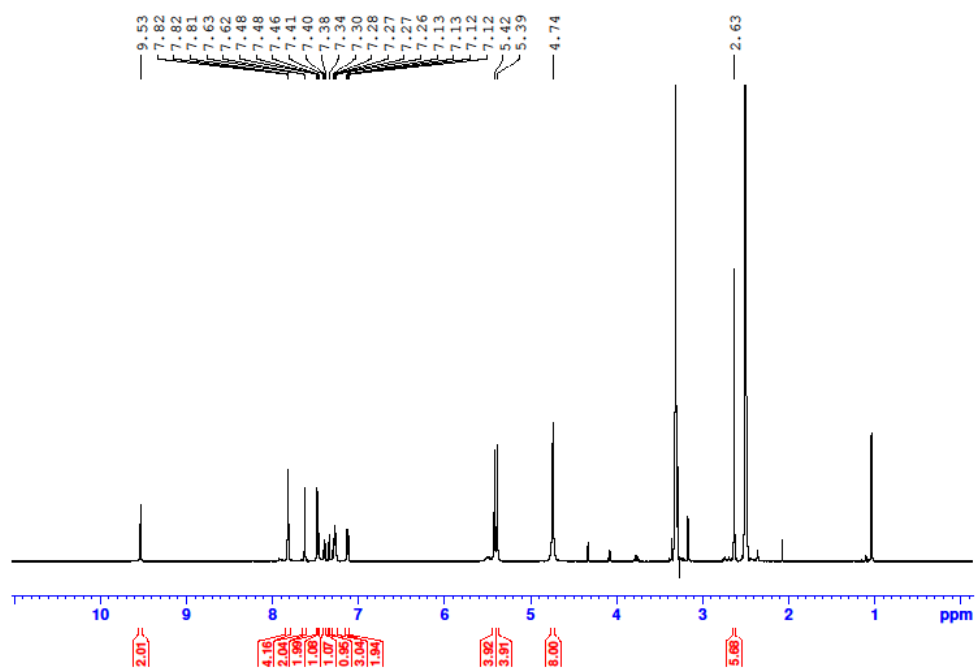


Figure A.23  $^1\text{H}$ -NMR spectrum of macrocycle **2.18·Br<sub>4</sub>**.

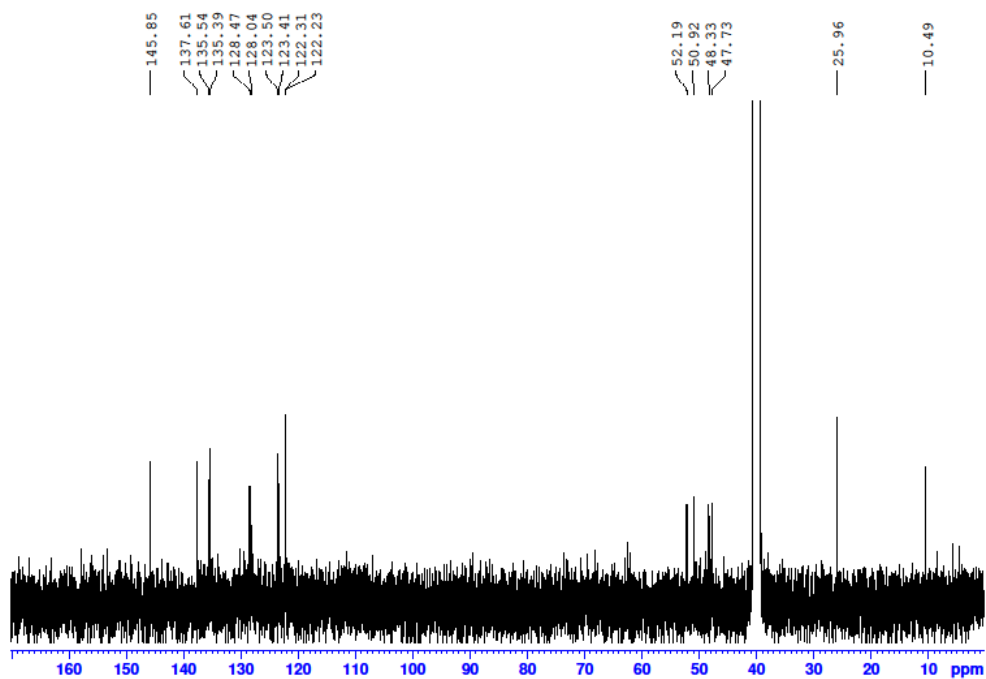


Figure A.24  $^{13}\text{C}$ -NMR spectrum of macrocycle **2.18·Br<sub>4</sub>**.

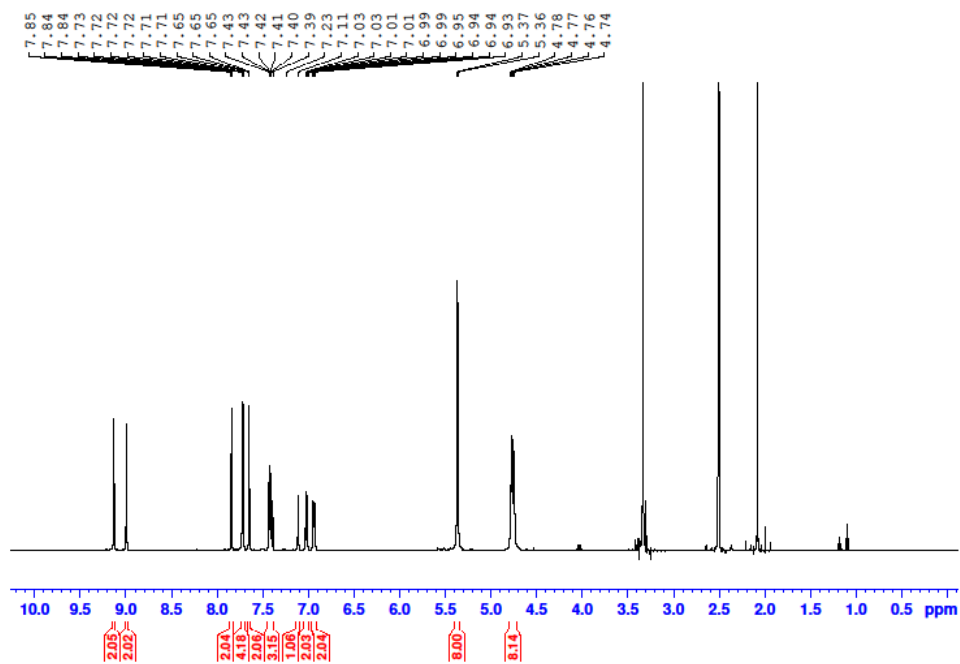


Figure A.25  $^1\text{H}$ -NMR spectrum of macrocycle **2.19·Br<sub>4</sub>**.

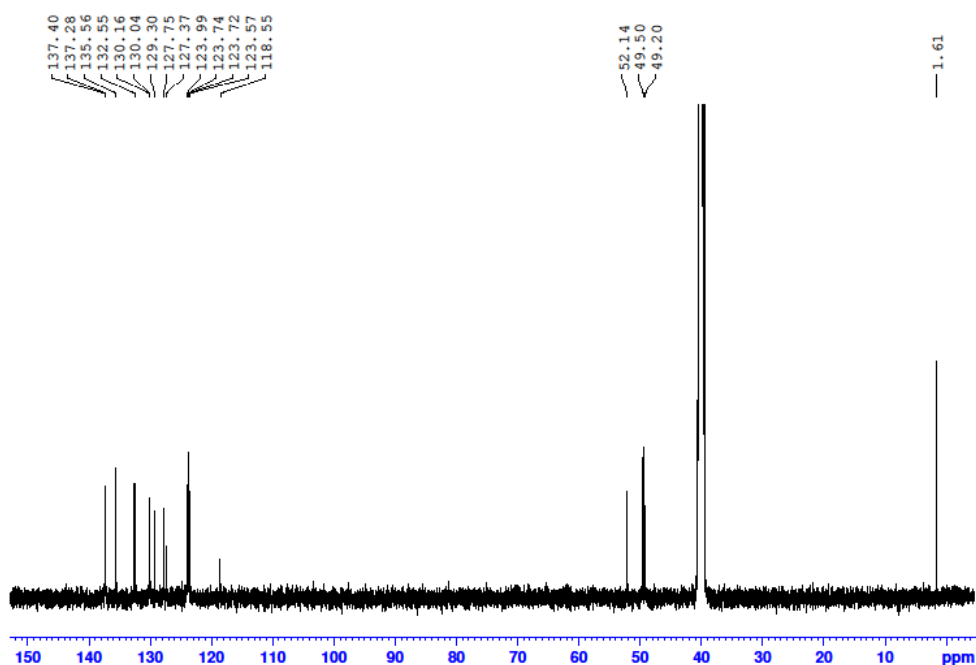


Figure A.26  $^{13}\text{C}$ -NMR spectrum of macrocycle **2.19·Br<sub>4</sub>**.



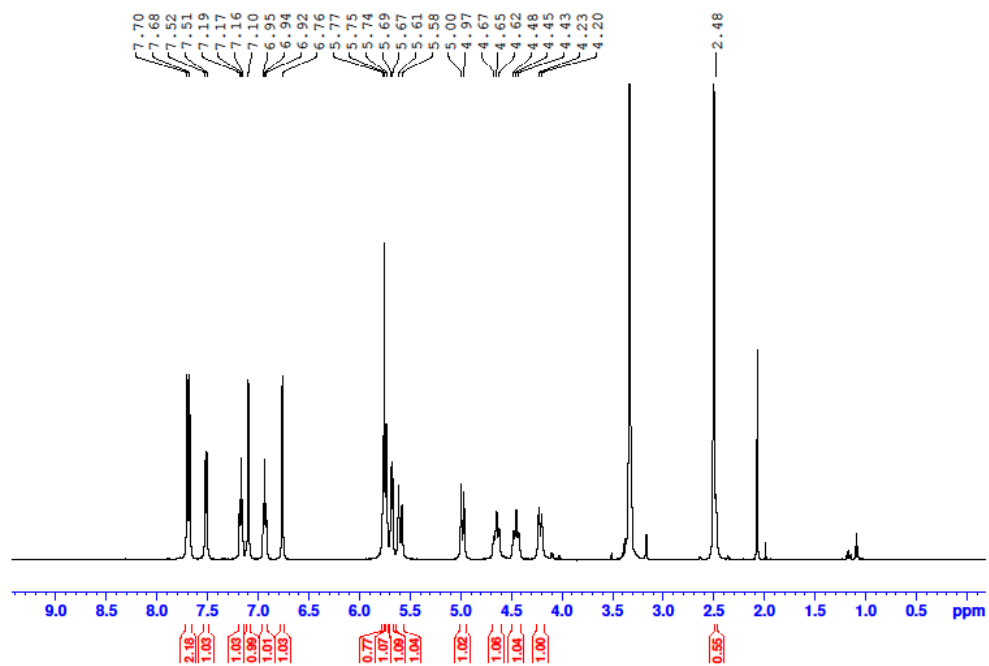


Figure A.27  $^1\text{H}$ -NMR spectrum of hexanuclear Ag(I) complex **2.20**·(PF<sub>6</sub>)<sub>6</sub>.

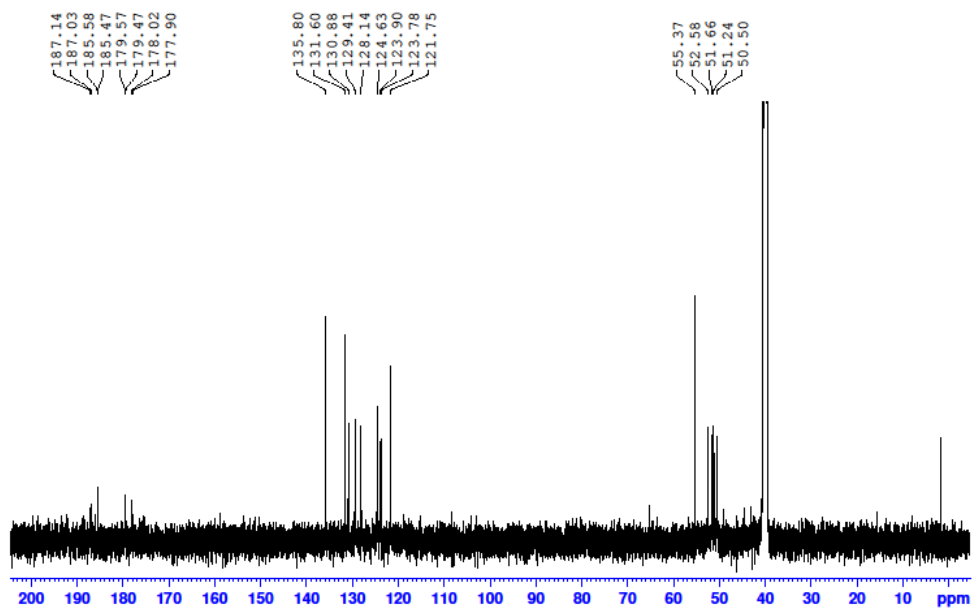


Figure A.28  $^{13}\text{C}$ -NMR spectrum of hexanuclear Ag(I) complex **2.20**·(PF<sub>6</sub>)<sub>6</sub>.

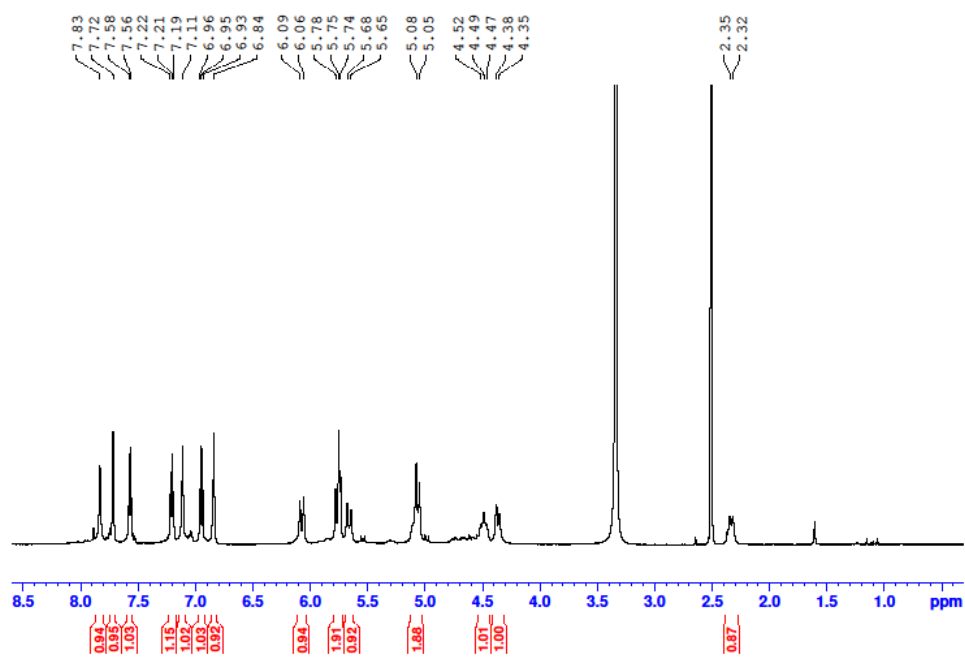


Figure A.29 <sup>1</sup>H-NMR spectrum of hexanuclear Au(I) complex **2.21·Br<sub>6</sub>**.

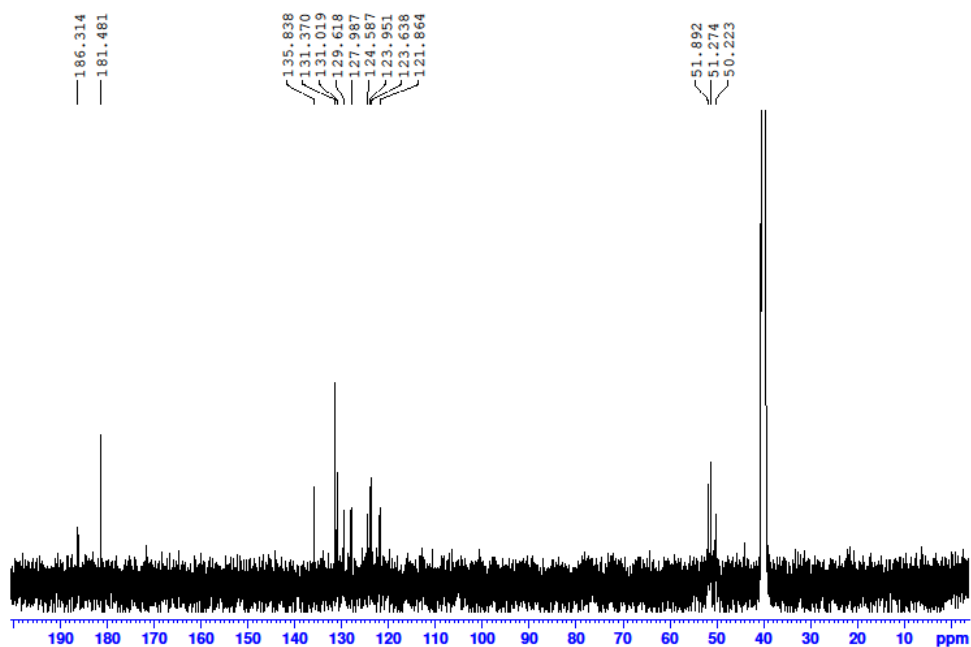


Figure A.30 <sup>13</sup>C-NMR spectrum of hexanuclear Au(I) complex **2.21·Br<sub>6</sub>**.

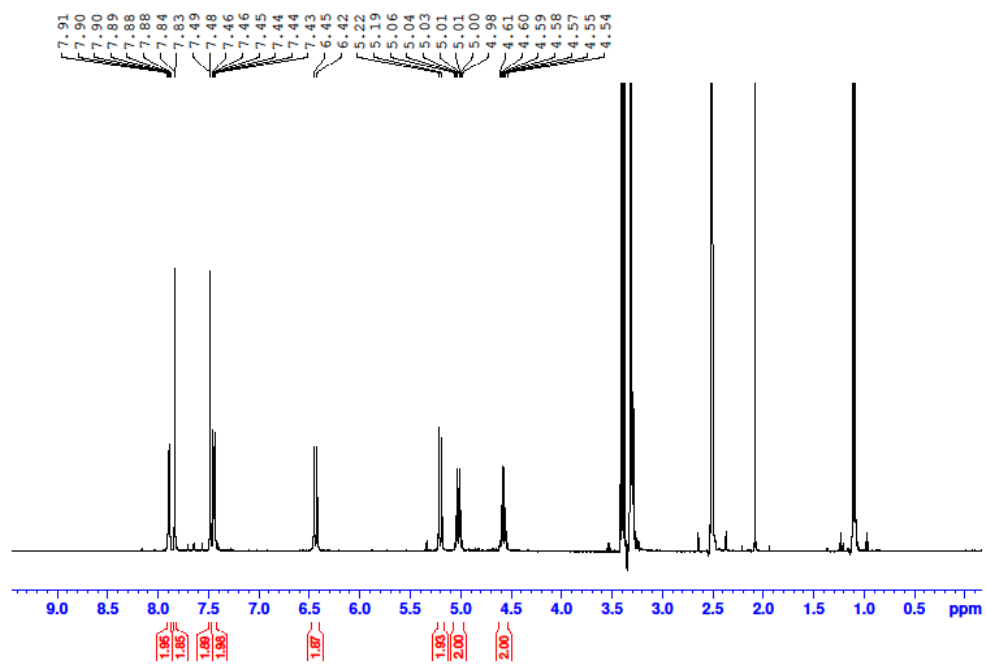


Figure A.31 <sup>1</sup>H-NMR spectrum of mononuclear Pd(II) complex **2.22**·(PF<sub>6</sub>)<sub>2</sub>.

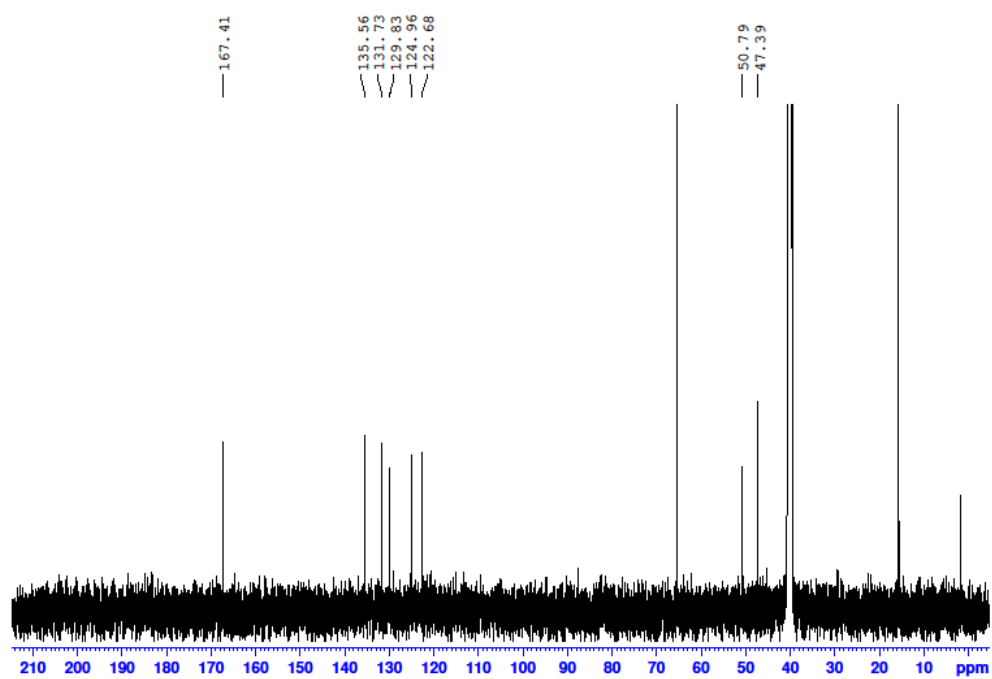


Figure A.32 <sup>13</sup>C-NMR spectrum of mononuclear Pd(II) complex **2.22**·(PF<sub>6</sub>)<sub>2</sub>.

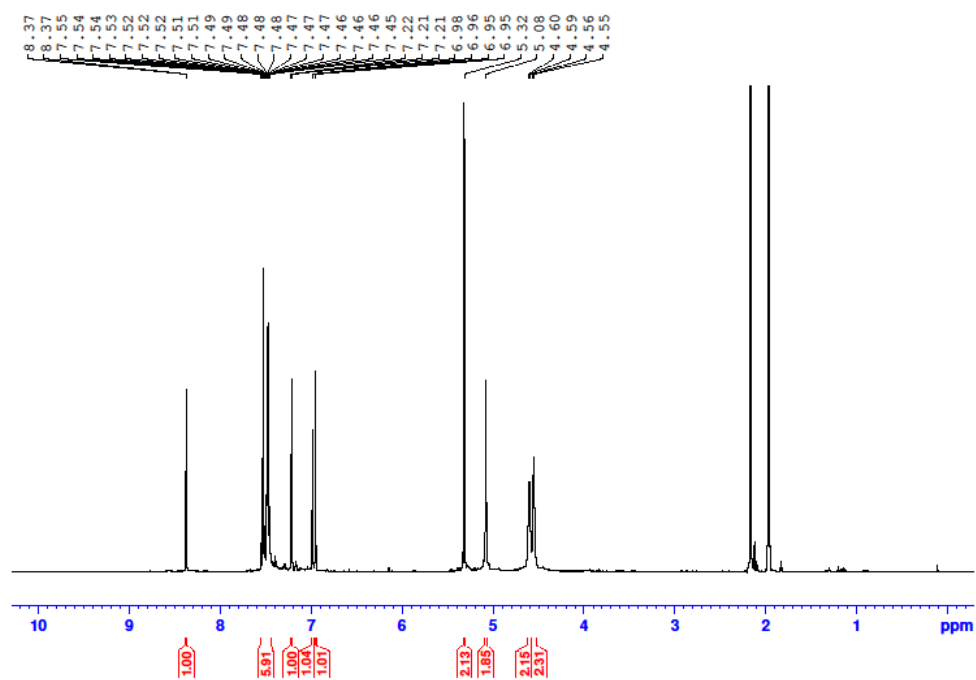


Figure A.33 <sup>1</sup>H-NMR spectrum of mononuclear Ag(I) complex **2.23**·(PF<sub>6</sub>)<sub>3</sub>

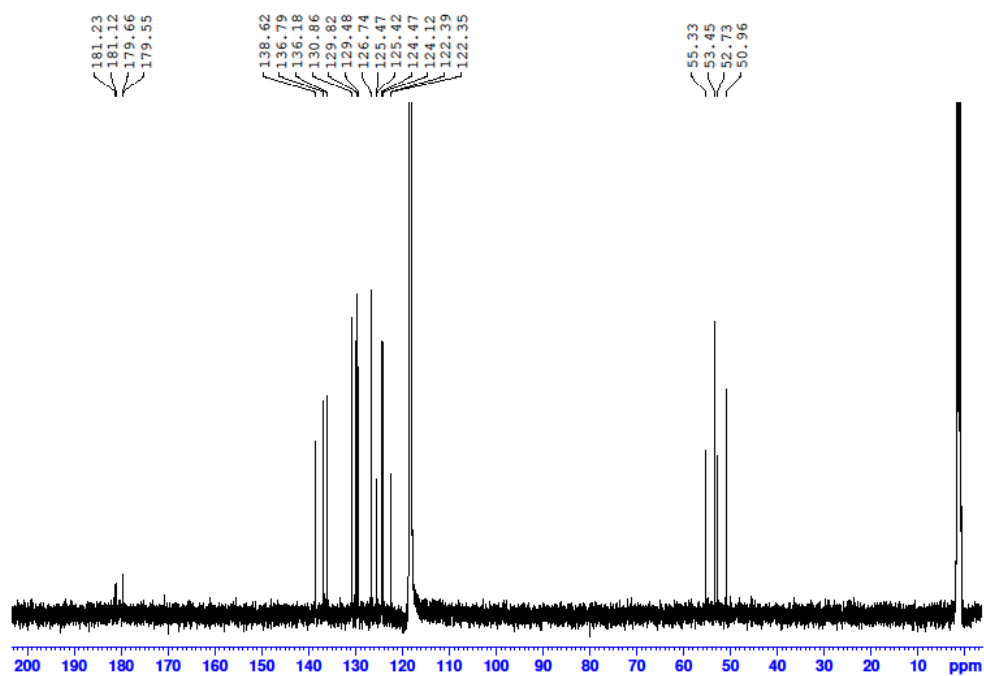


Figure A.34 <sup>13</sup>C-NMR spectrum of mononuclear Ag(I) complex **2.23**·(PF<sub>6</sub>)<sub>3</sub>.

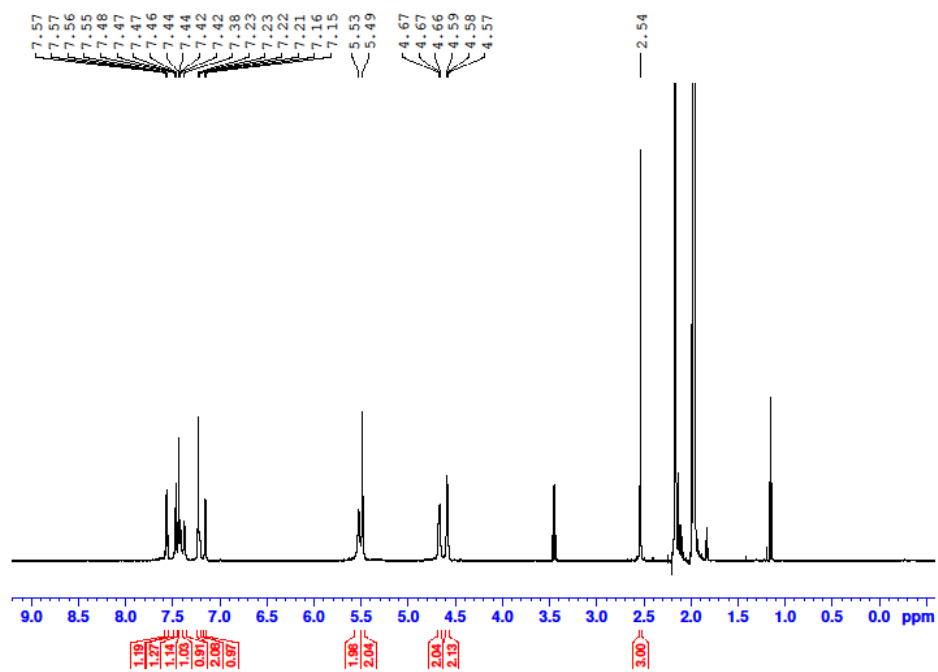


Figure A.35 <sup>1</sup>H-NMR spectrum of dinuclear Au(I) complex **2.24**·(PF<sub>6</sub>)<sub>2</sub>.

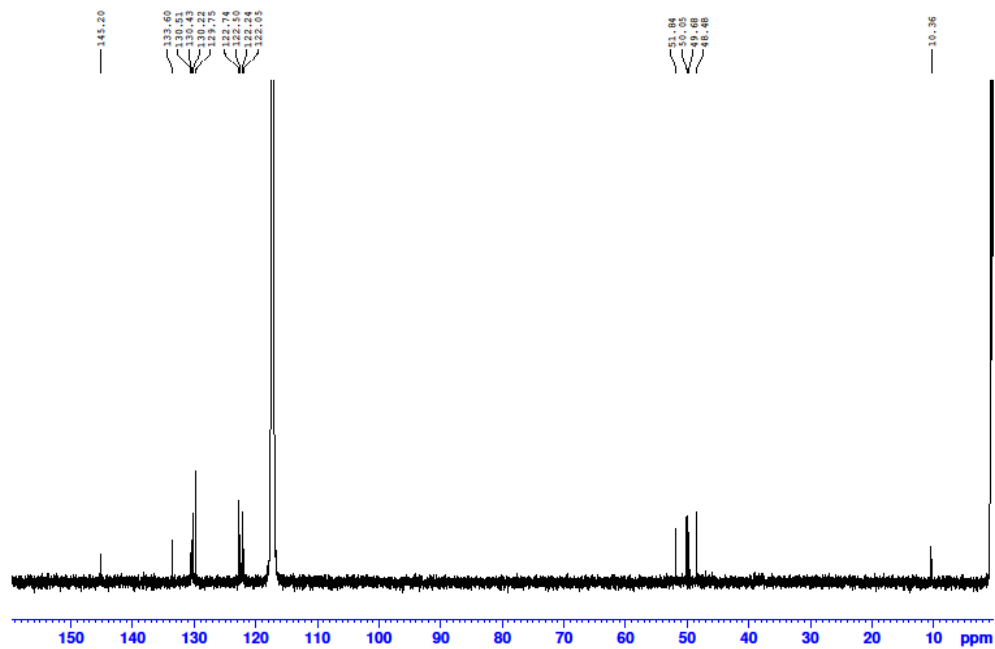


Figure A.36 <sup>13</sup>C-NMR spectrum of dinuclear Au(I) complex **2.24**·(PF<sub>6</sub>)<sub>2</sub>.

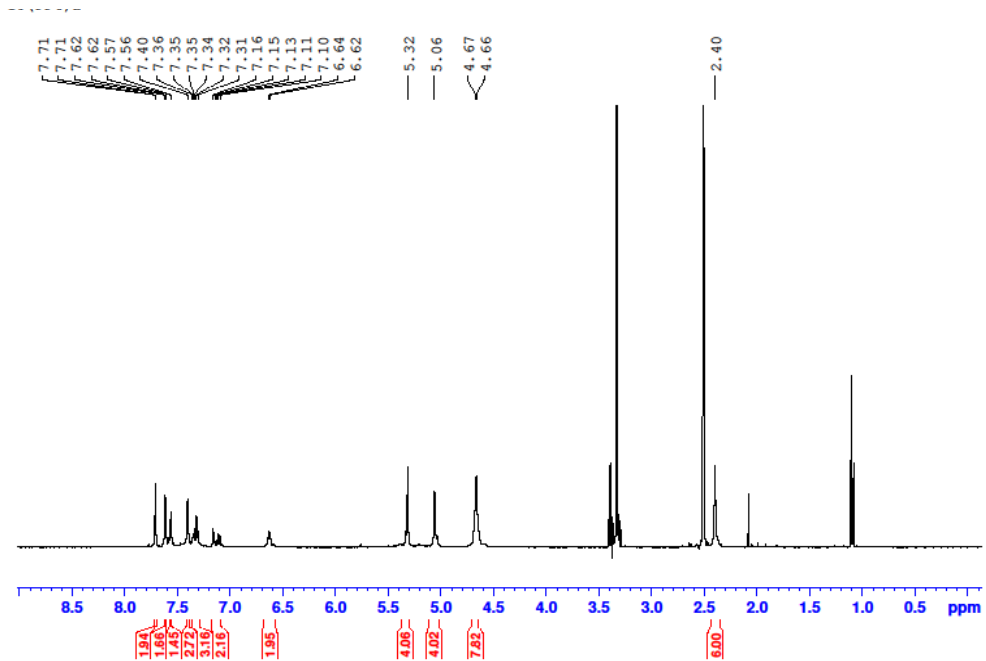


Figure A.37 <sup>1</sup>H-NMR spectrum of dinuclear Au(I) complex **2.25**·(PF<sub>6</sub>)<sub>2</sub>.

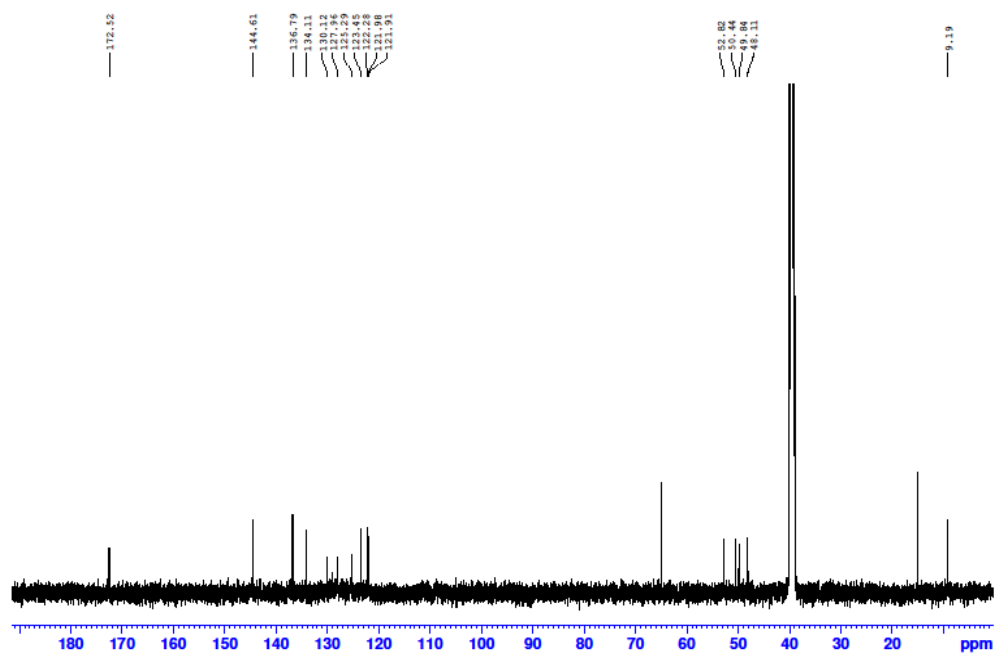


Figure A.38 <sup>13</sup>C-NMR spectrum of dinuclear Au(I) complex **2.25**·(PF<sub>6</sub>)<sub>2</sub>.

## A.2.2 $^1\text{H}$ -NMR titration spectra for Chapter 2

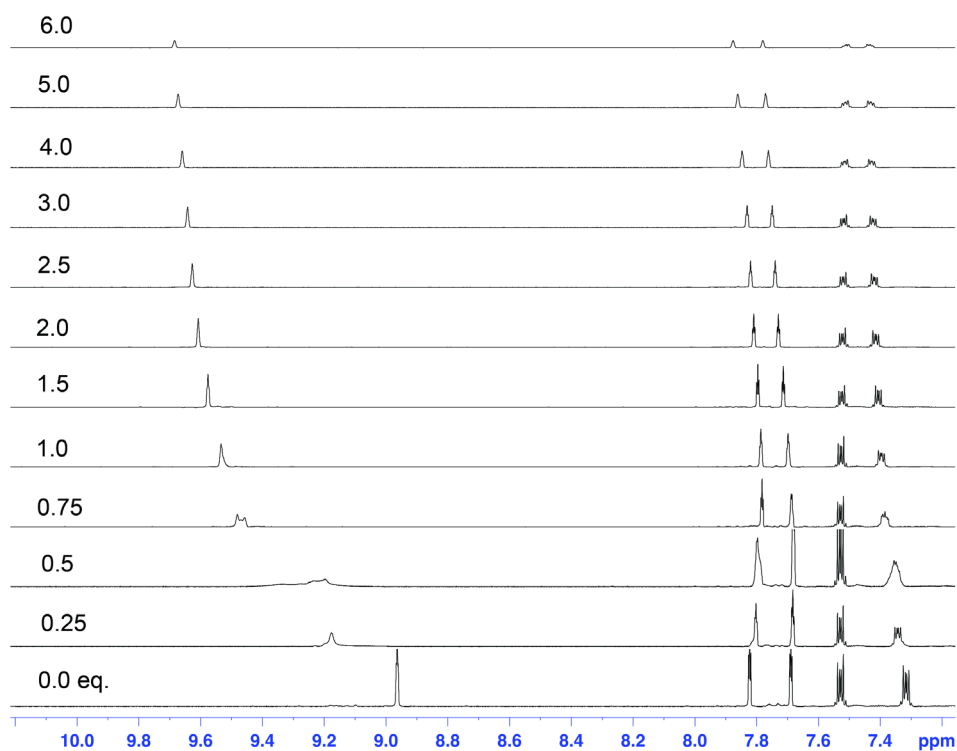


Figure A.39  $^1\text{H}$ -NMR titration of  $2.15 \cdot (\text{PF}_6)_4$  in  $\text{d}_6$ -DMSO in the presence of increasing concentrations of  $\text{BuN} \cdot \text{Cl}$ .

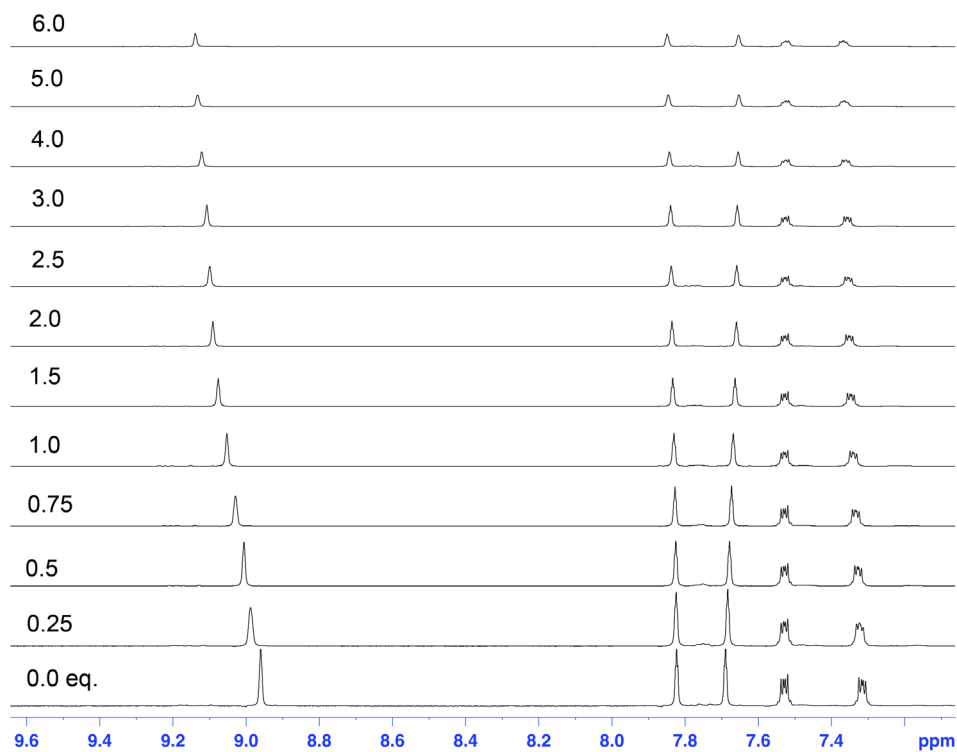


Figure A.40  $^1\text{H}$ -NMR titration of  $2.15 \cdot (\text{PF}_6)_4$  in  $\text{d}_6$ -DMSO in the presence of increasing concentrations of  $\text{BuN} \cdot \text{I}$ .

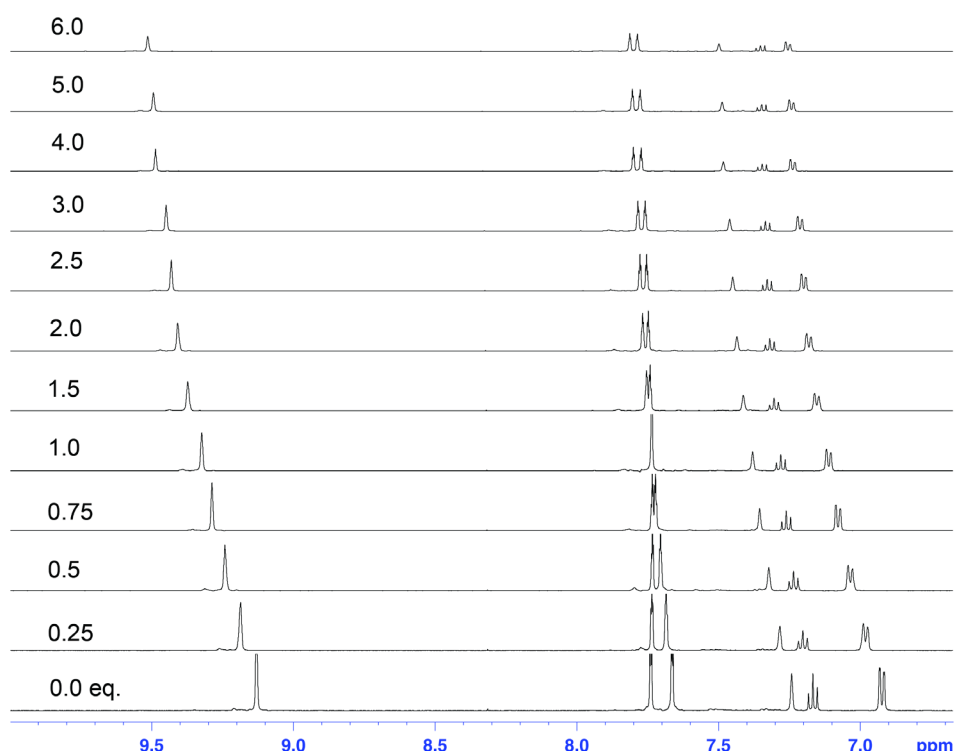


Figure A.41  $^1\text{H}$ -NMR titration of **2.16**•( $\text{PF}_6$ ) $_4$  in  $\text{d}_6$ -DMSO in the presence of increasing concentrations of  $\text{BuN}^+\text{Br}^-$ .

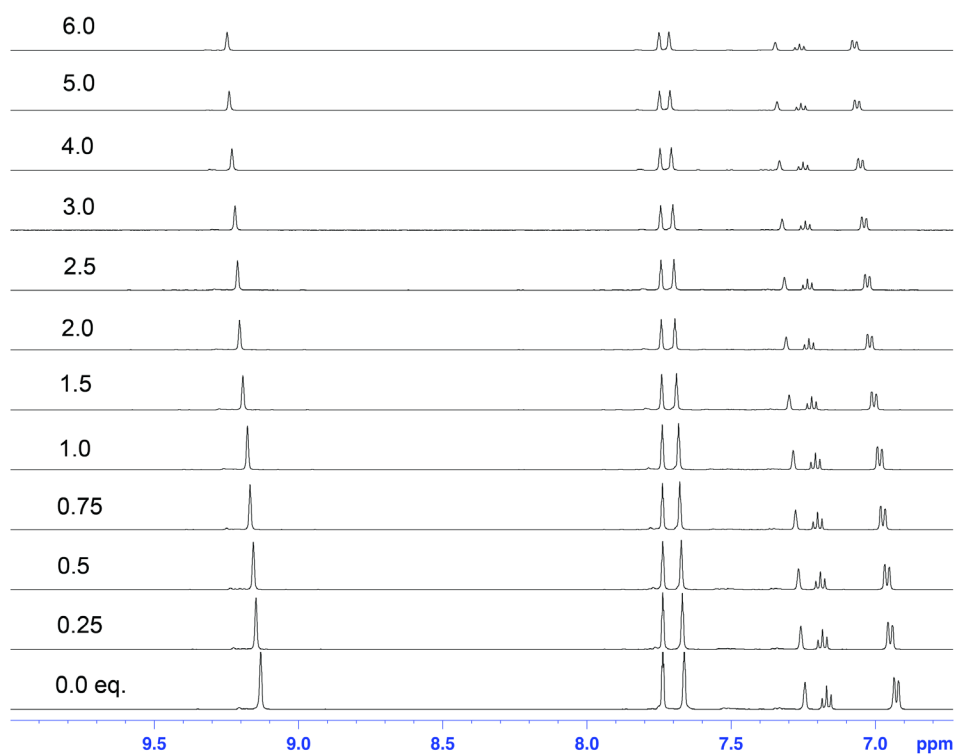


Figure A.42  $^1\text{H}$ -NMR titration of **2.16**•( $\text{PF}_6$ ) $_4$  in  $\text{d}_6$ -DMSO in the presence of increasing concentrations of  $\text{BuN}^+\text{I}^-$ .



## A.3 Appendix for Chapter 3

### A.3.1 NMR Spectra for Chapter 3

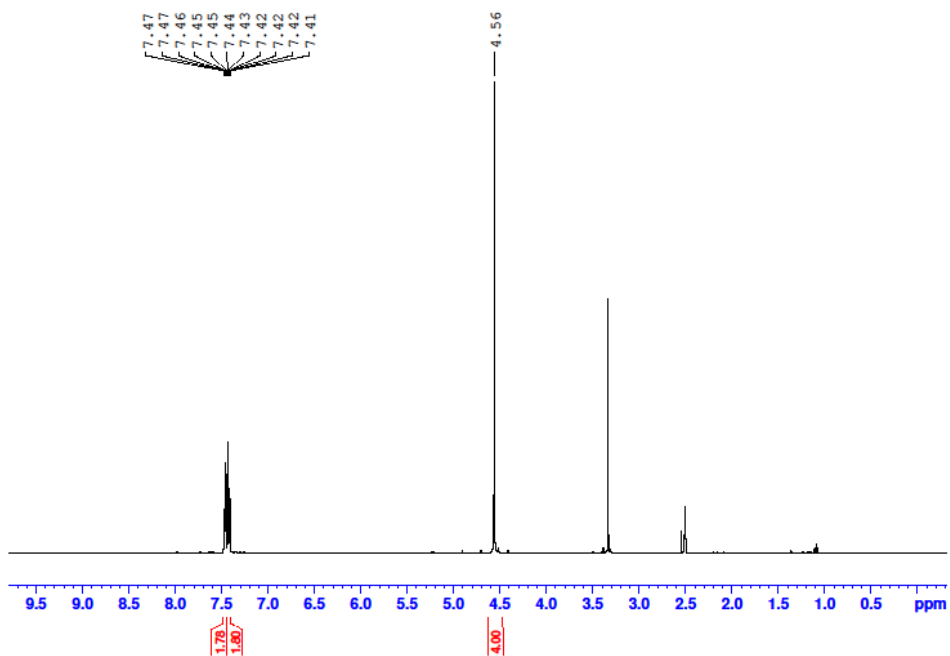


Figure A.43  $^1\text{H}$ -NMR spectrum of compound **3.15**.

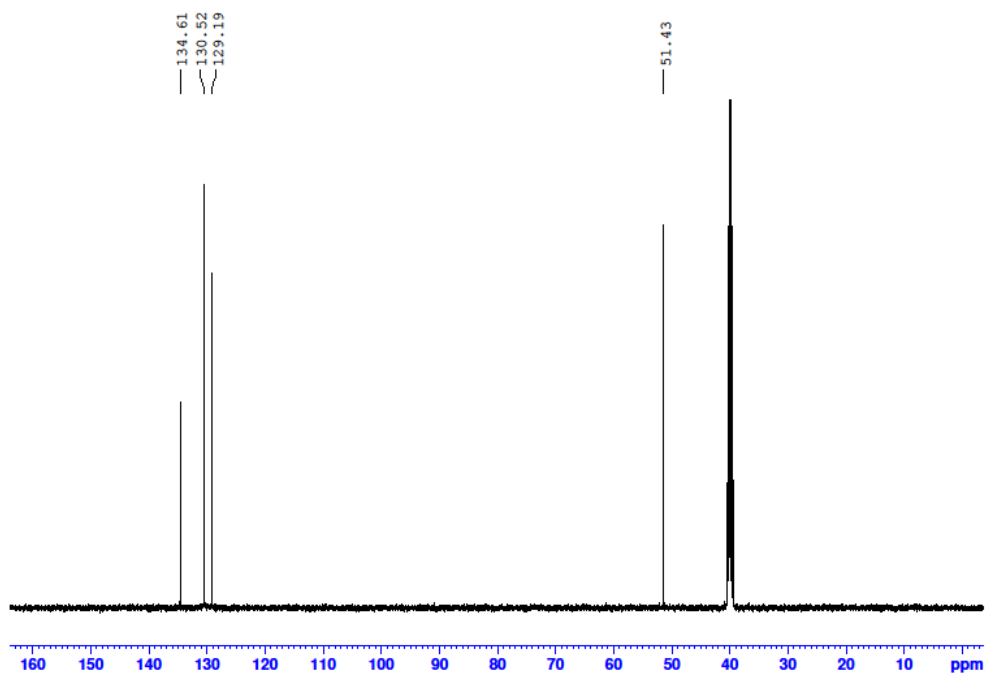


Figure A.44  $^{13}\text{C}$ -NMR spectrum of compound **3.15**.

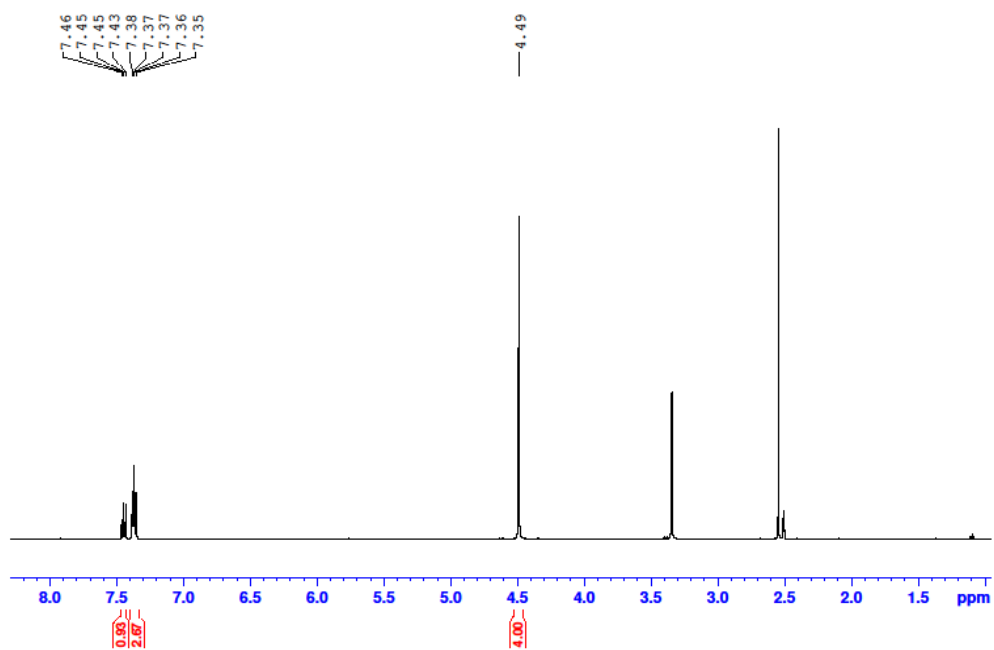


Figure A.45 <sup>1</sup>H-NMR spectrum of compound **3.16**.

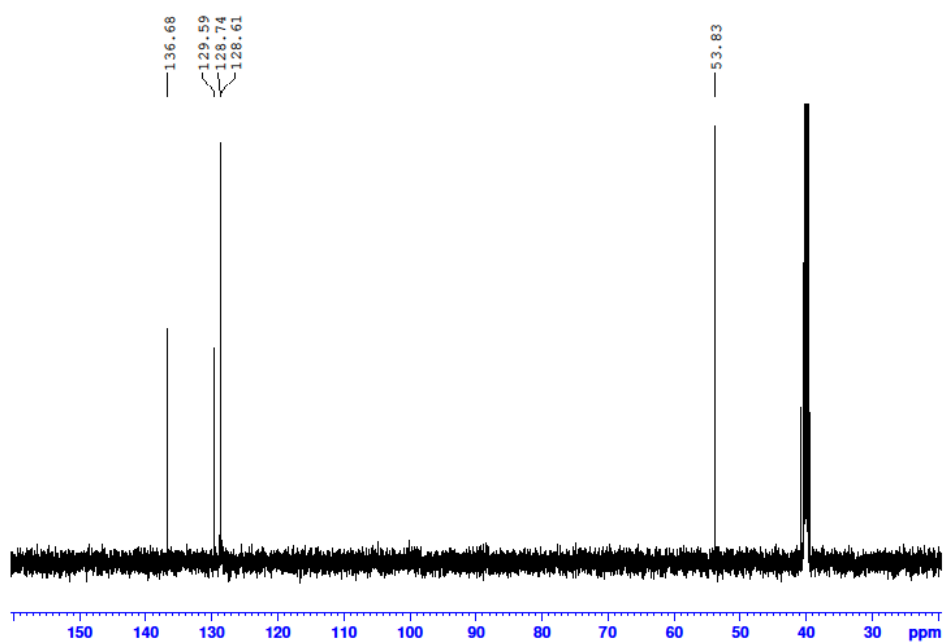


Figure A.46 <sup>13</sup>C-NMR spectrum of compound **3.16**.

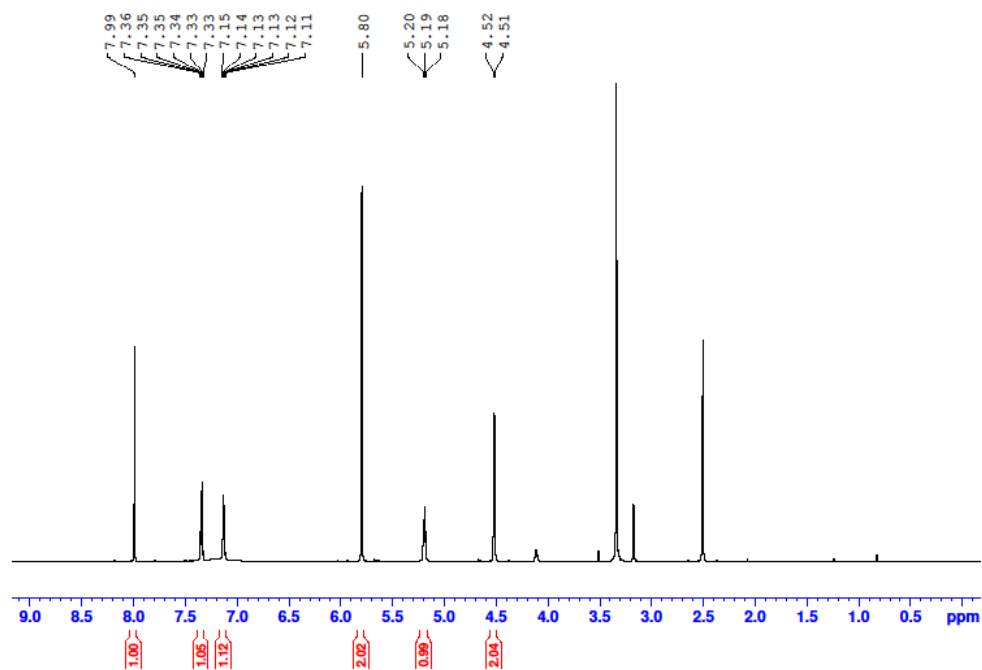


Figure A.47  $^1\text{H}$ -NMR spectrum of compound **3.17**.

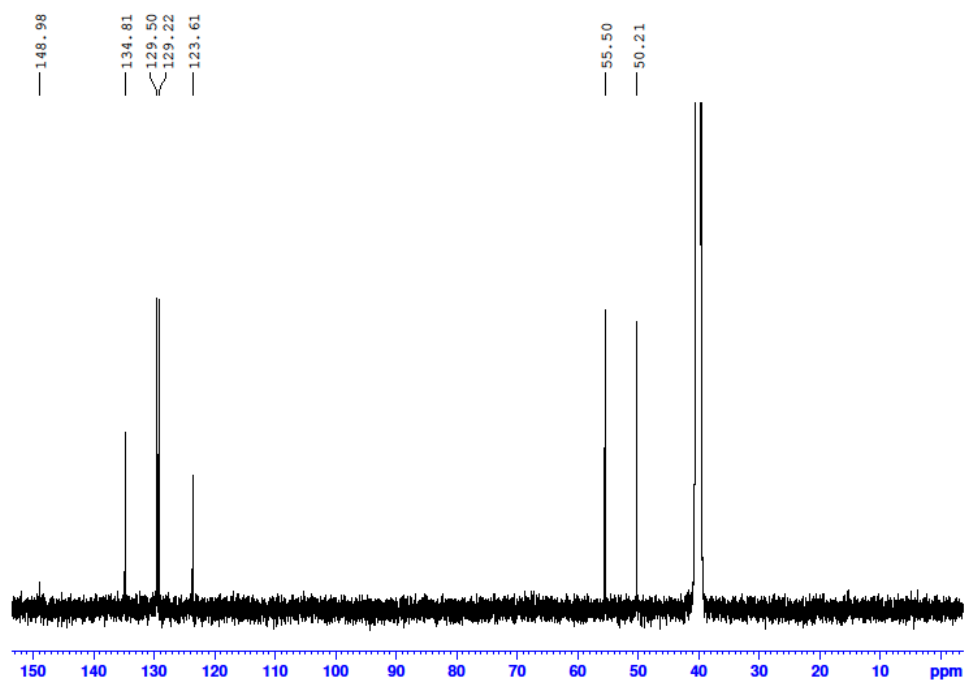


Figure A.48  $^{13}\text{C}$ -NMR spectrum of compound **3.17**.

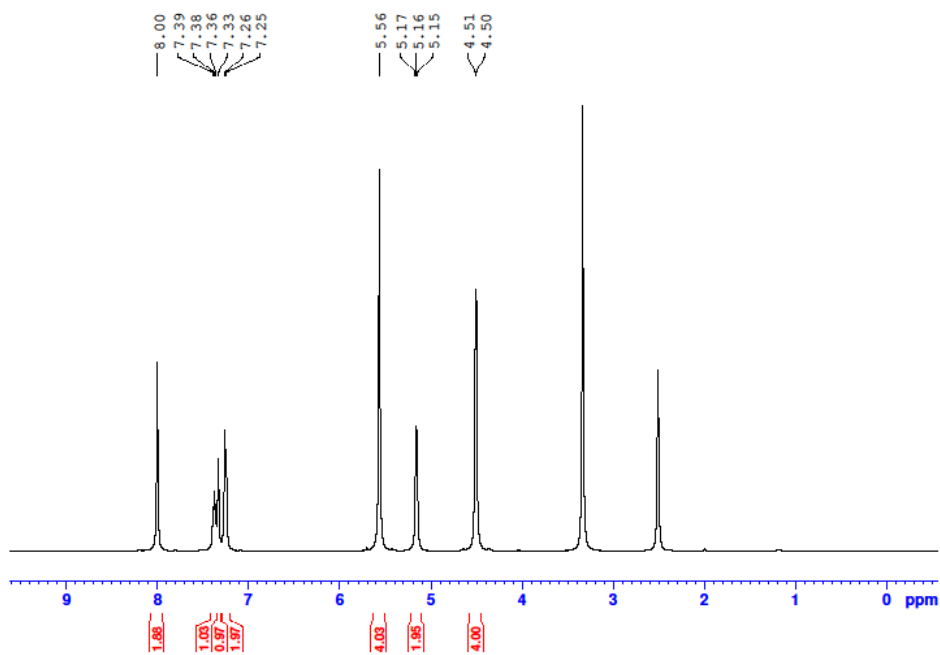


Figure A.49 <sup>1</sup>H-NMR spectrum of compound **3.18**.

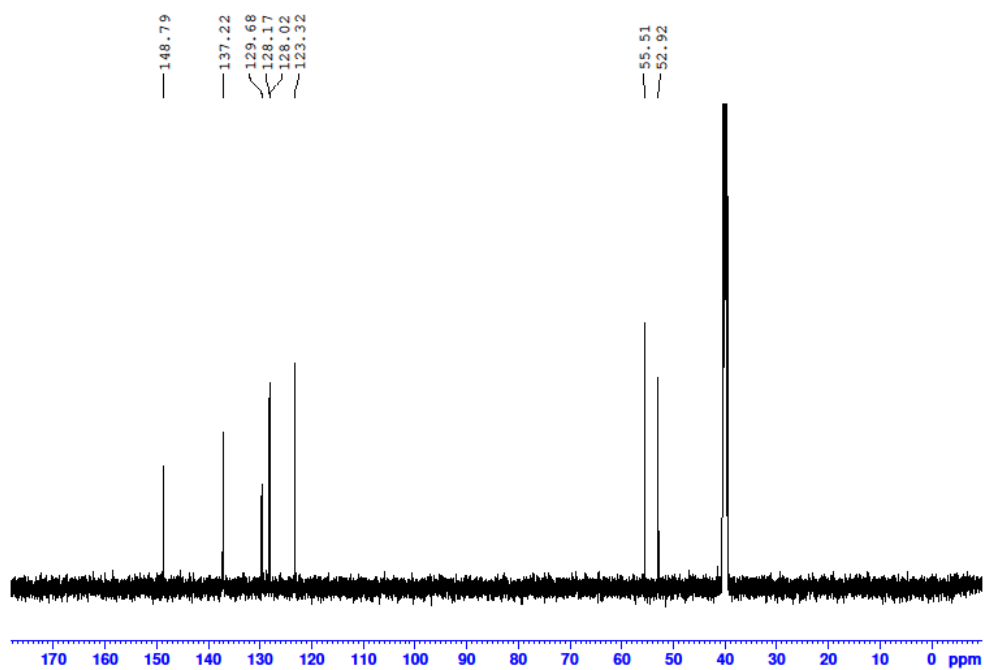


Figure A.50 <sup>13</sup>C-NMR spectrum of compound **3.18**.

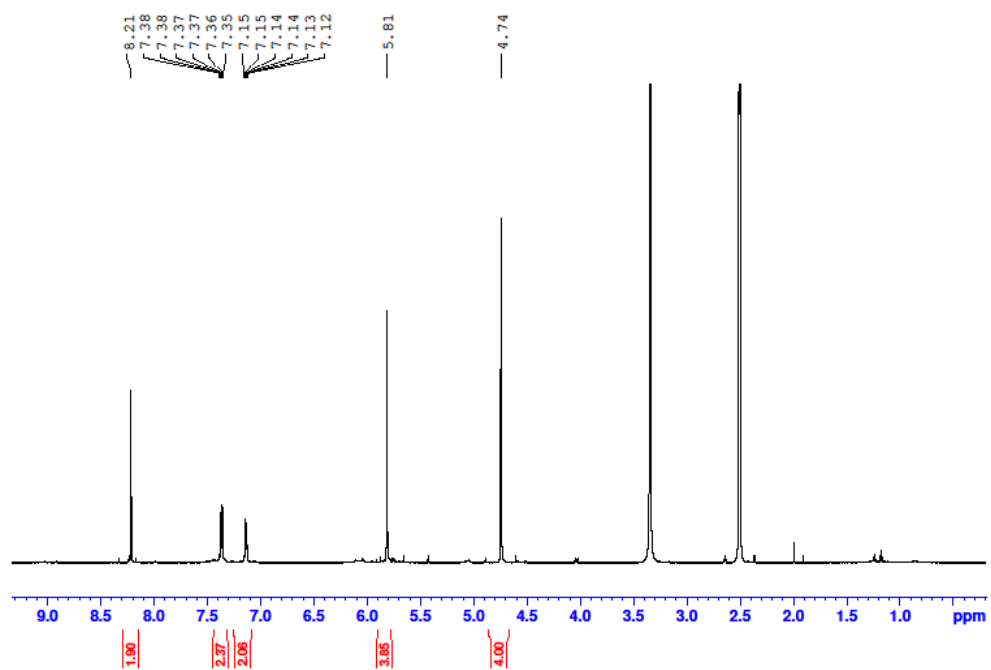


Figure A.51  $^1\text{H}$ -NMR spectrum of compound **3.19**.

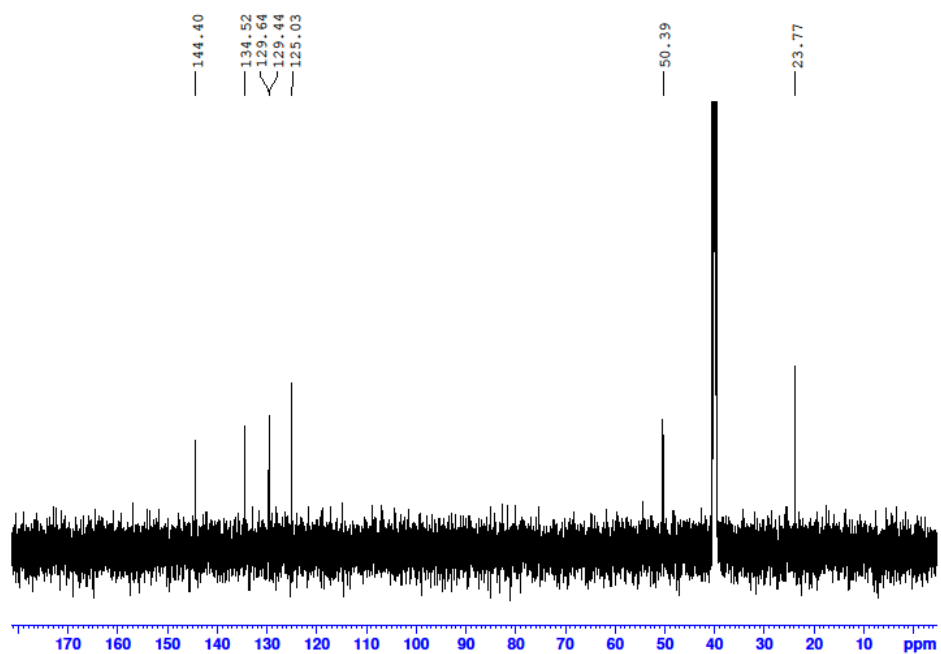


Figure A.52  $^{13}\text{C}$ -NMR spectrum of compound **3.19**.

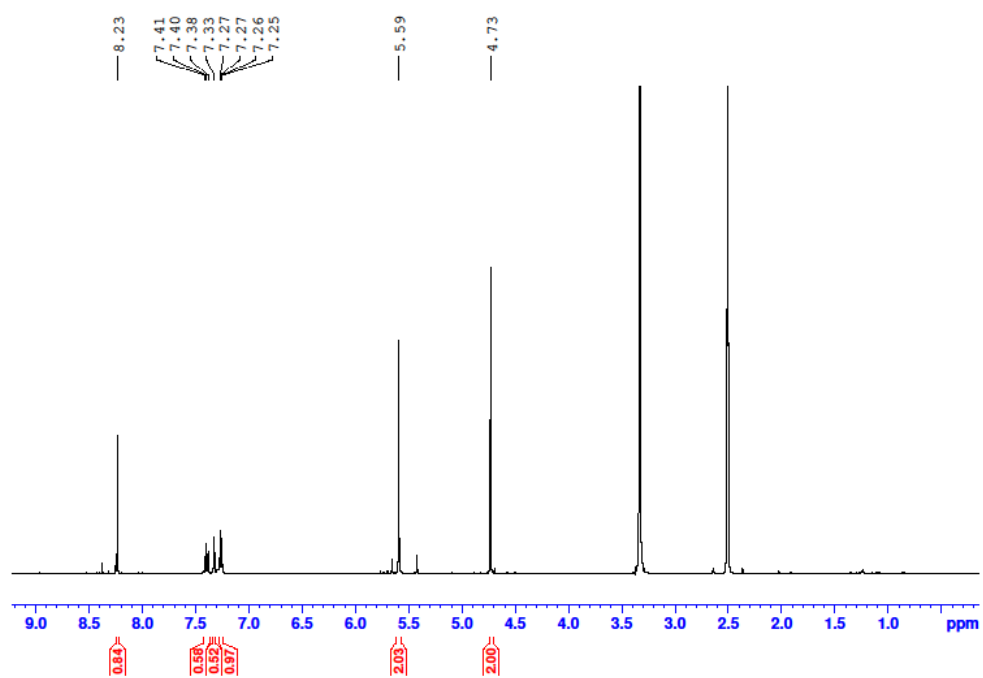


Figure A.53  $^1\text{H}$ -NMR spectrum of compound **3.20**.

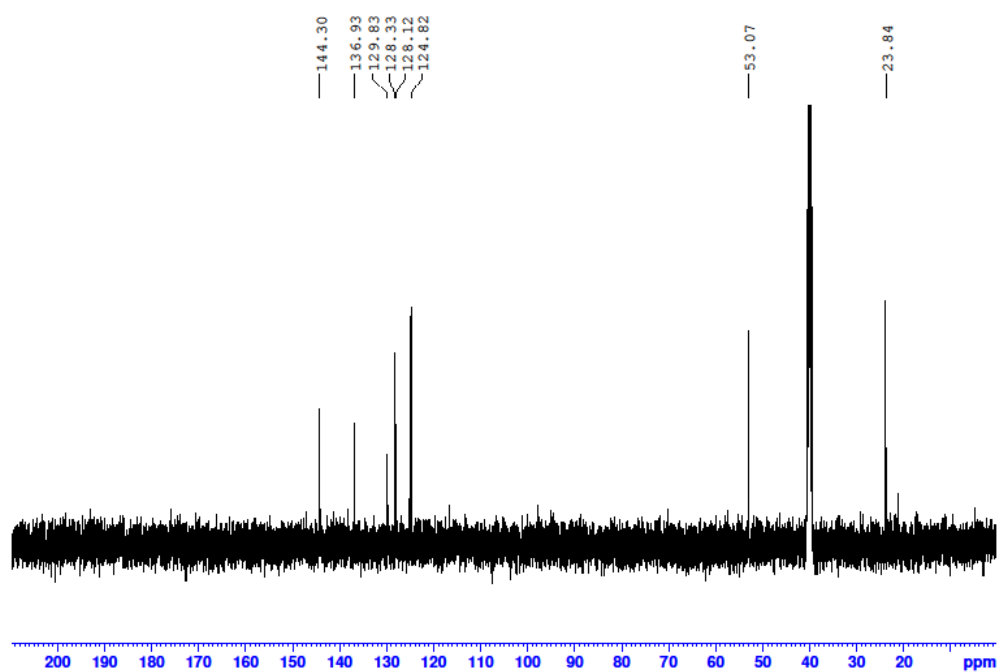


Figure A.54  $^{13}\text{C}$ -NMR spectrum of compound **3.20**.

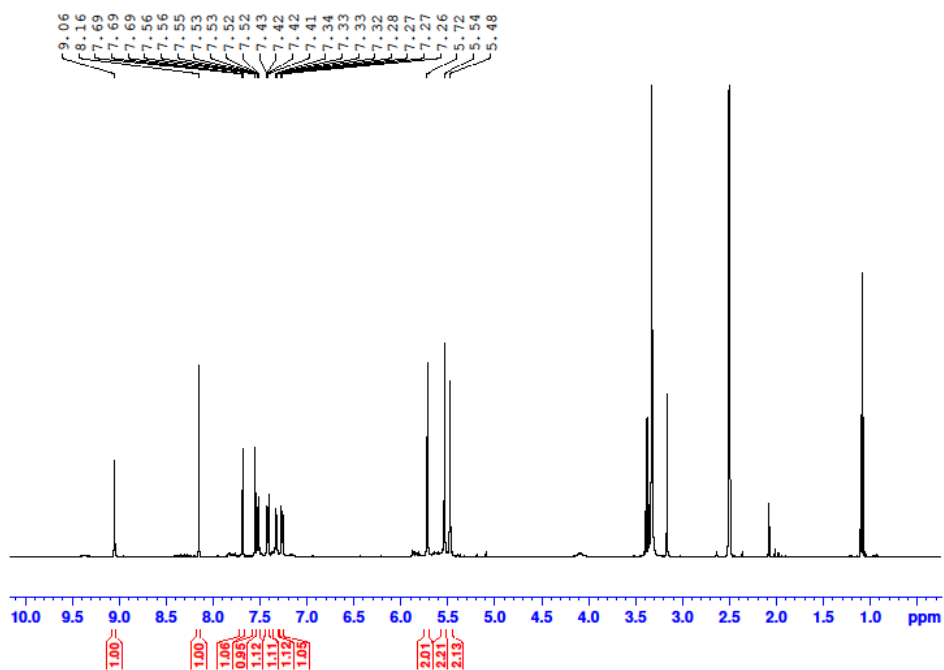


Figure A.55 <sup>1</sup>H-NMR spectrum of macrocycle **3.21·Br<sub>2</sub>**.

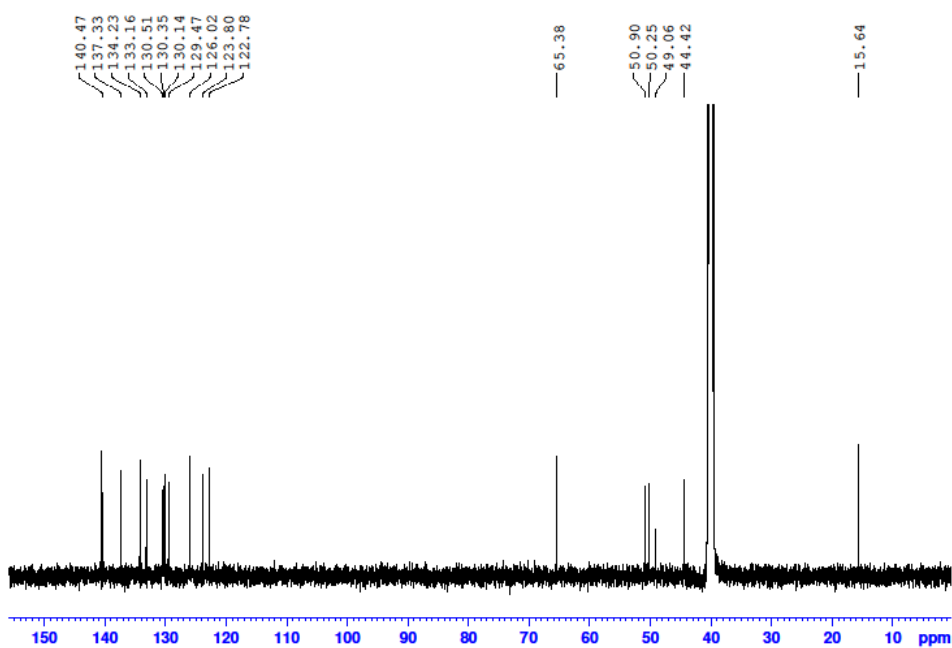


Figure A.56 <sup>13</sup>C-NMR spectrum of macrocycle **3.21·Br<sub>2</sub>**.

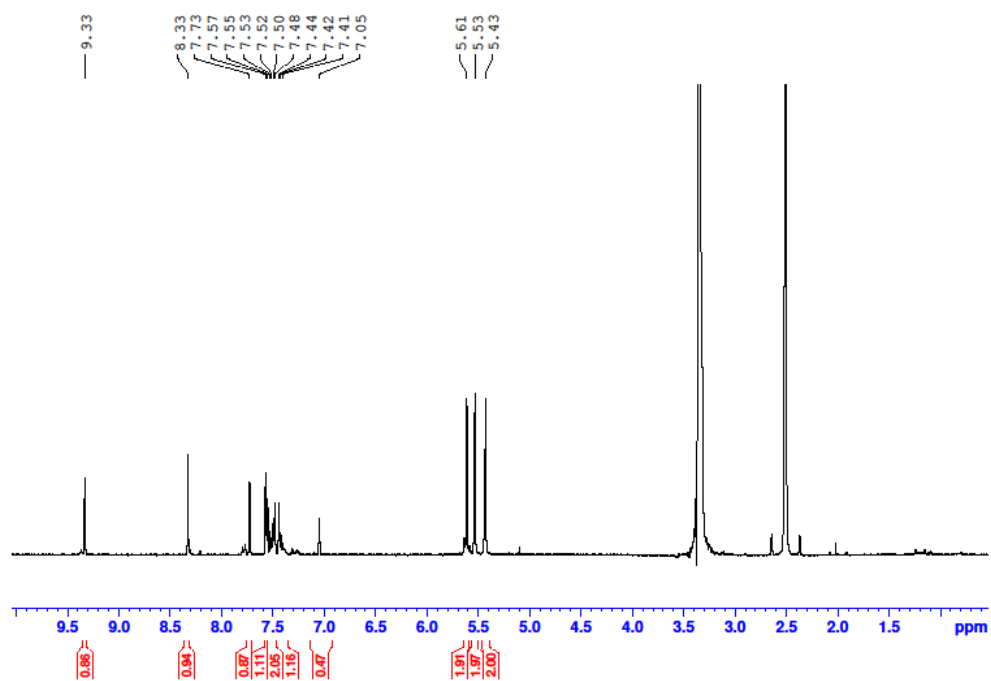


Figure A.57  $^1\text{H}$ -NMR spectrum of macrocycle **3.22·Br<sub>2</sub>**.

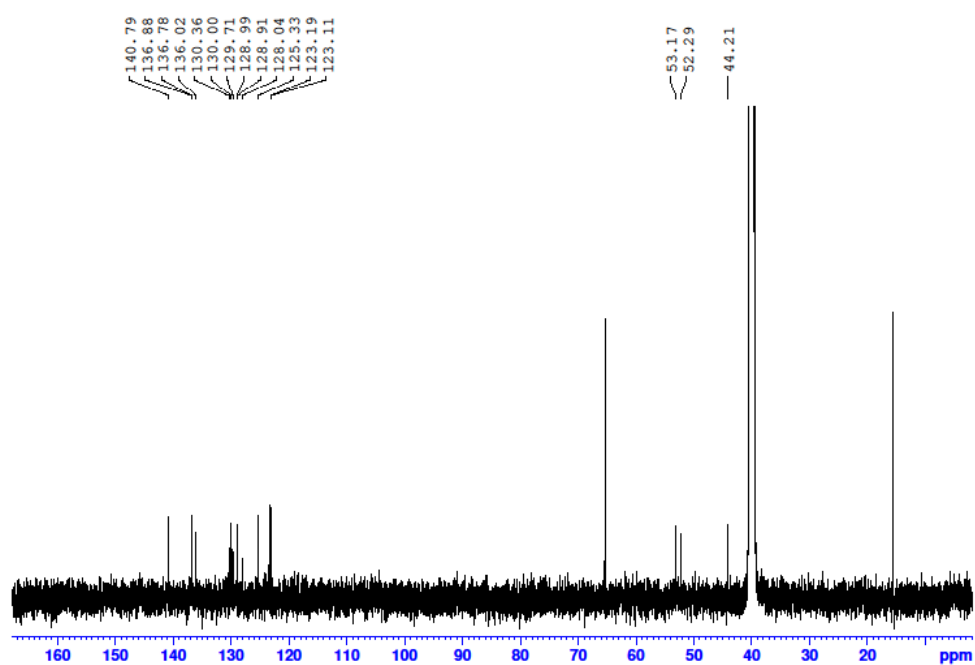


Figure A.58  $^{13}\text{C}$ -NMR spectrum of macrocycle **3.22·Br<sub>2</sub>**.



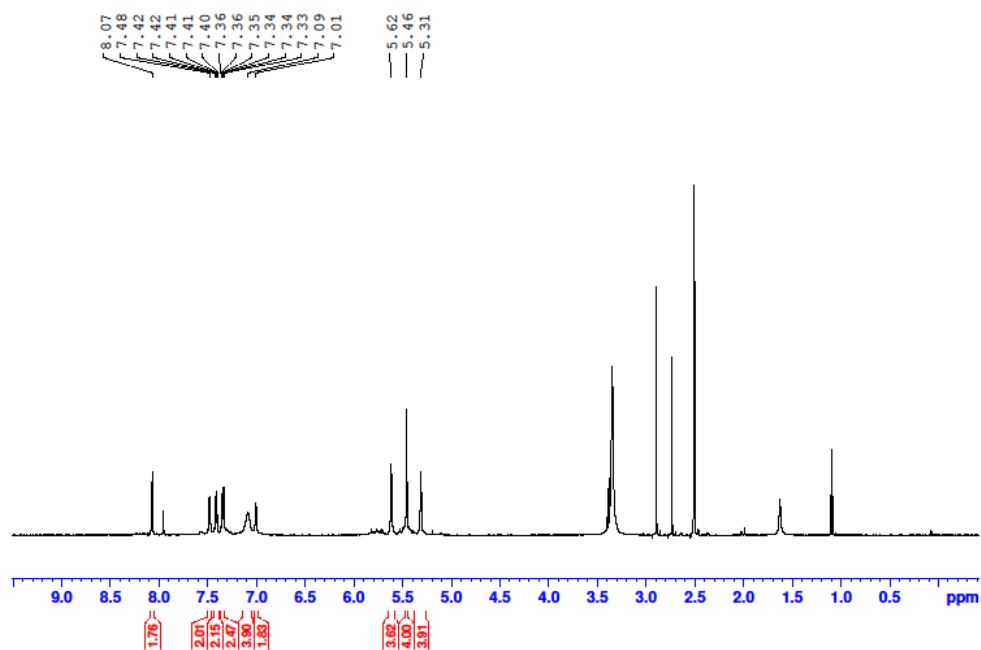


Figure A.59 <sup>1</sup>H-NMR spectrum of dinuclear Au(I) complex **3.23**.

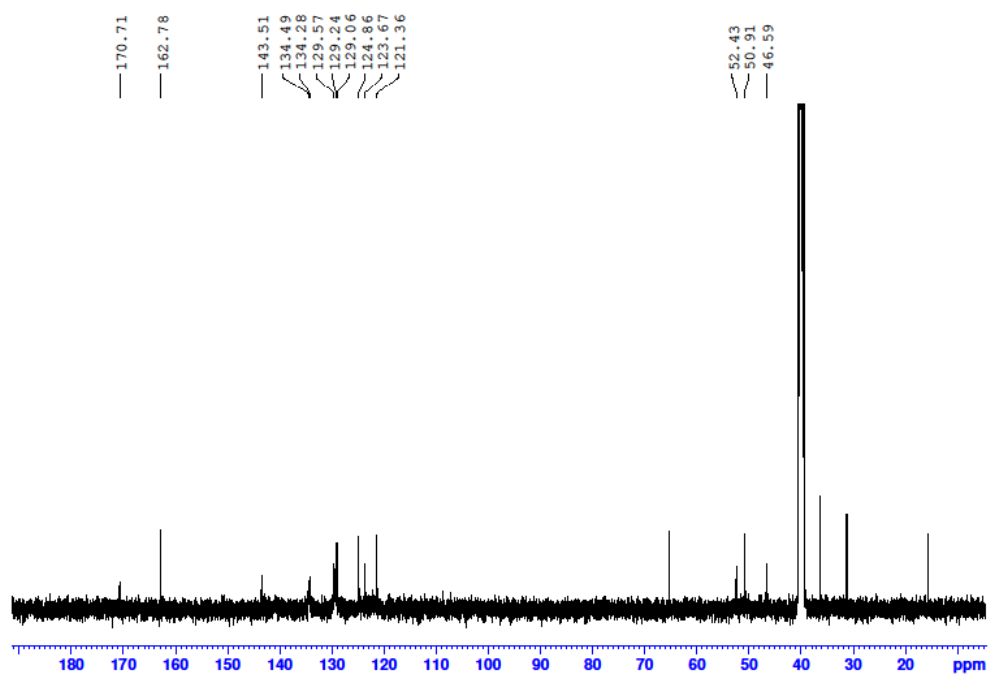


Figure A.60 <sup>13</sup>C-NMR spectrum of dinuclear Au(I) complex **3.23**.

### A.3.2 $^1\text{H}$ -NMR titration spectra

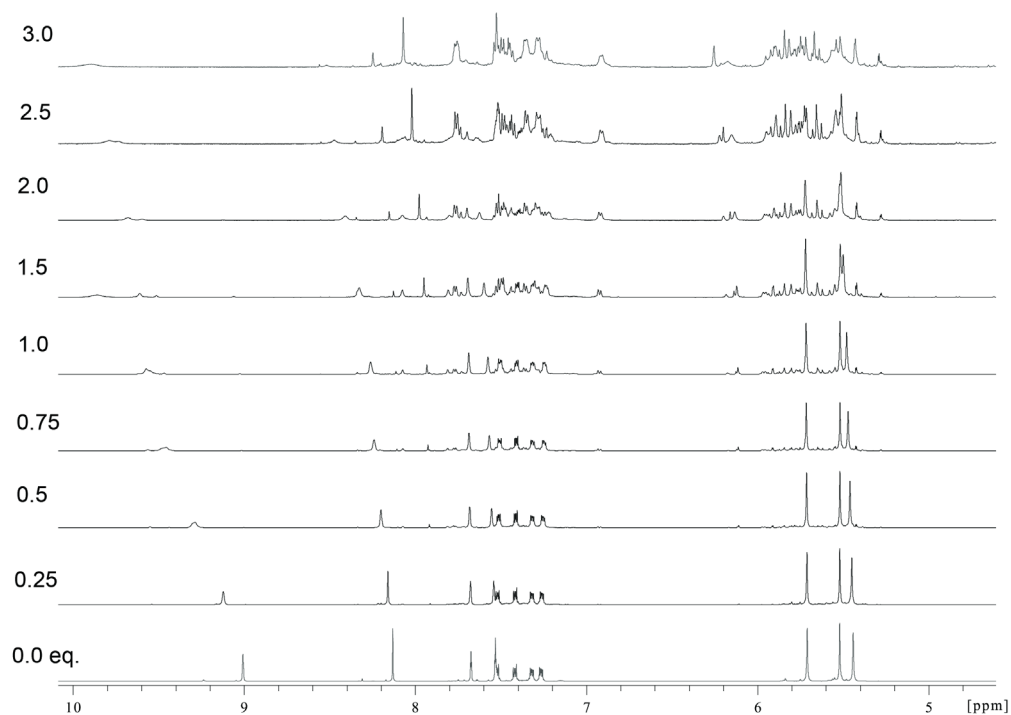


Figure A.61  $^1\text{H}$ -NMR titration of  $3.21 \cdot (\text{PF}_6)_2$  in  $\text{d}_6$ -DMSO in the presence of increasing concentrations of  $\text{BuN} \cdot \text{F}$ .

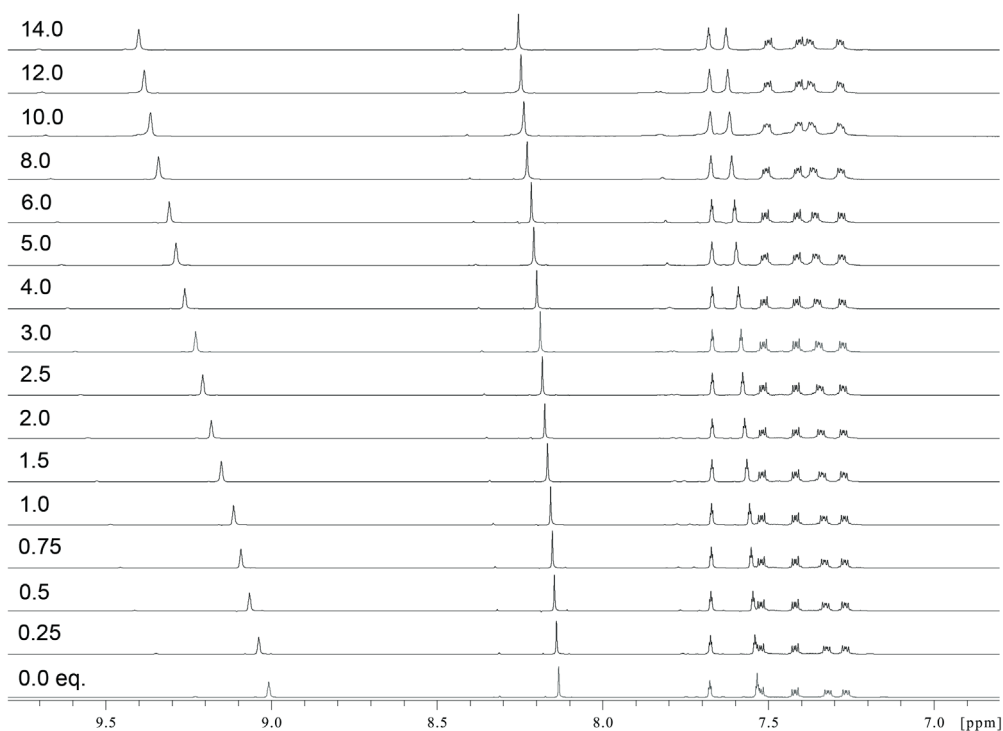


Figure A.62  $^1\text{H}$ -NMR titration of  $3.21 \cdot (\text{PF}_6)_2$  in  $\text{d}_6$ -DMSO in the presence of increasing concentrations of  $\text{BuN} \cdot \text{Cl}$ .

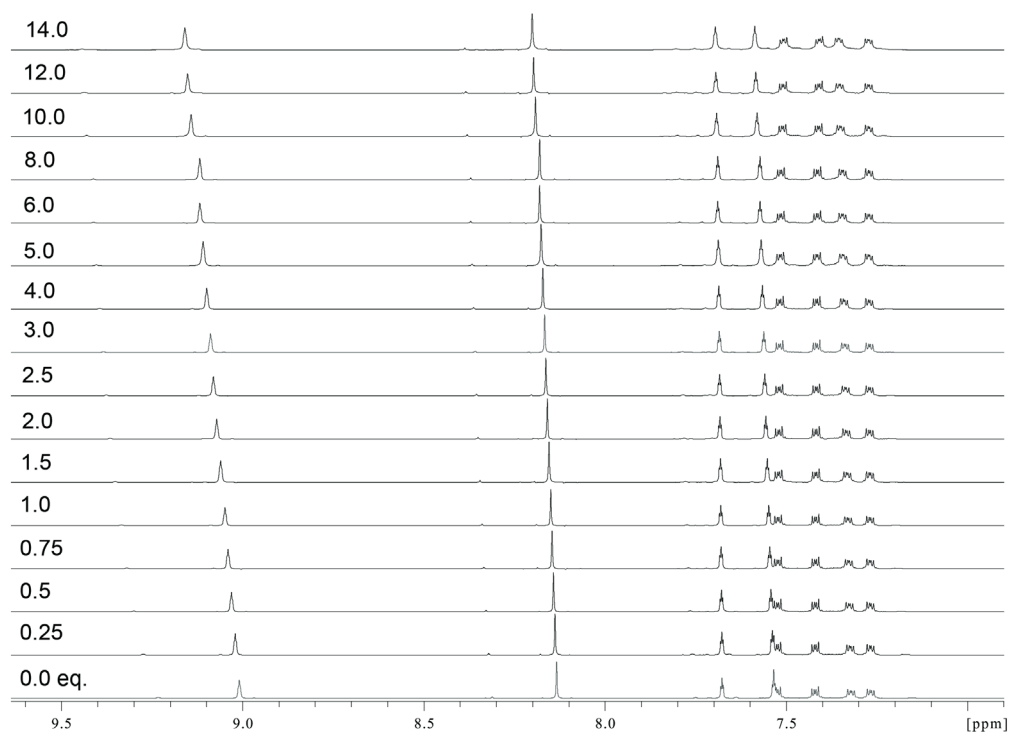


Figure A.63  $^1\text{H}$ -NMR titration of **3.21**·( $\text{PF}_6$ ) $_2$  in  $\text{d}_6$ -DMSO in the presence of increasing concentrations of  $\text{BuN}\cdot\text{Br}$ .

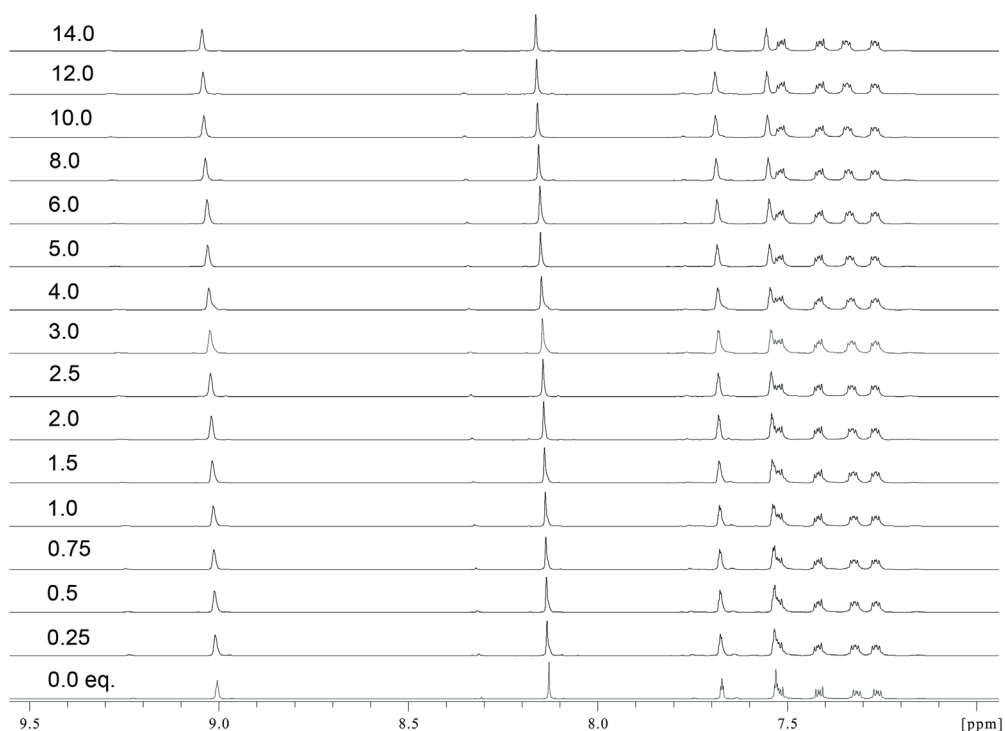


Figure A.64  $^1\text{H}$ -NMR titration of **3.21**·( $\text{PF}_6$ ) $_2$  in  $\text{d}_6$ -DMSO in the presence of increasing concentrations of  $\text{BuN}\cdot\text{I}$ .

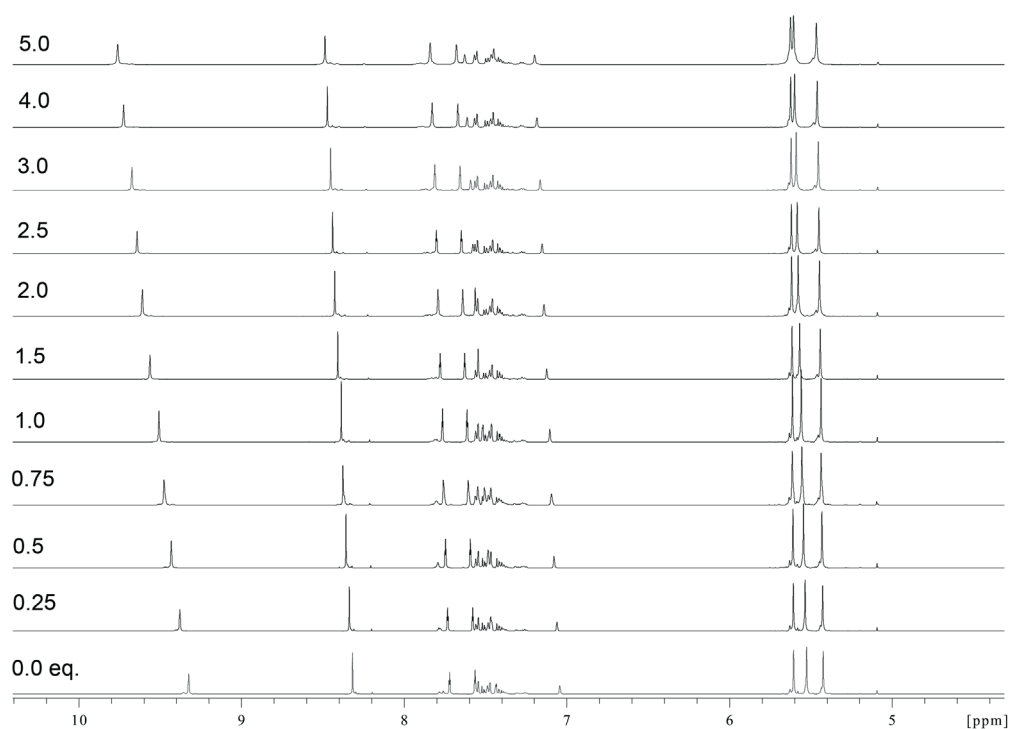


Figure A.65  $^1\text{H}$ -NMR titration of **3.22**·( $\text{PF}_6$ ) $_2$  in  $\text{d}_6$ -DMSO in the presence of increasing concentrations of  $\text{BuN}\cdot\text{Cl}$ .

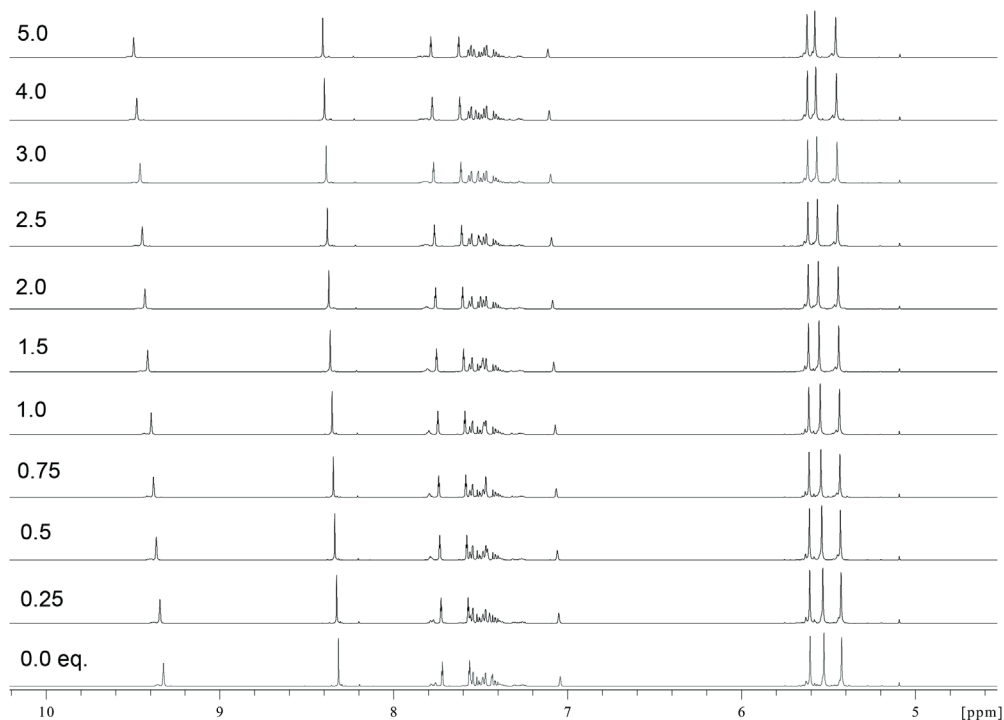


Figure A.66  $^1\text{H}$ -NMR titration of **3.22**·( $\text{PF}_6$ ) $_2$  in  $\text{d}_6$ -DMSO in the presence of increasing concentrations of  $\text{BuN}\cdot\text{Br}$ .

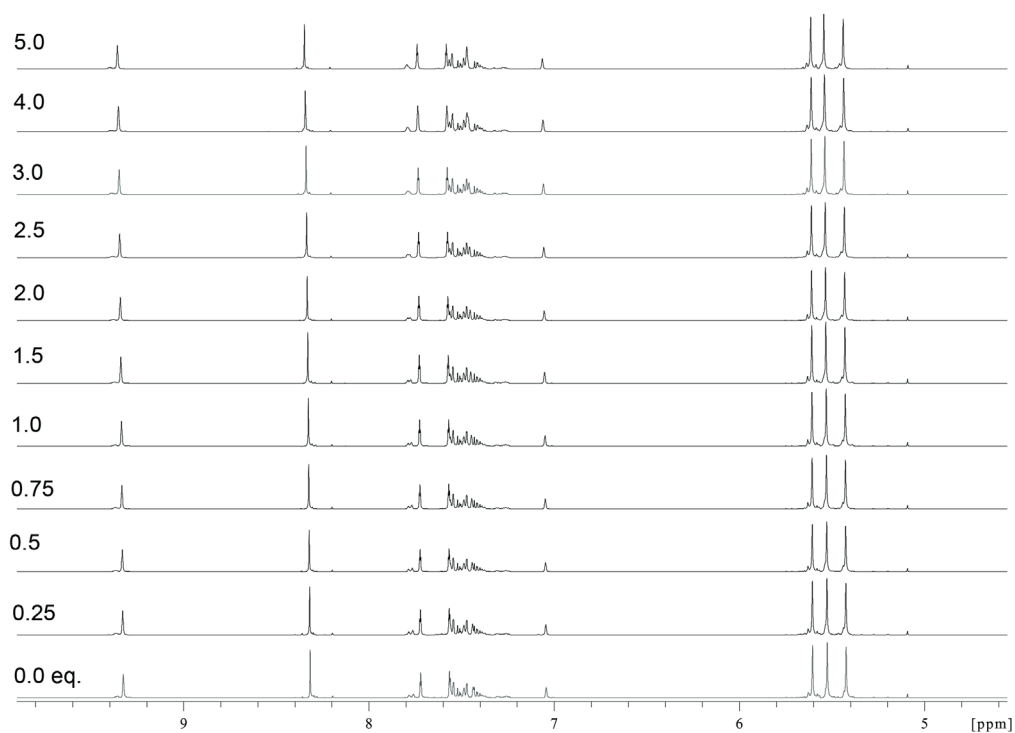


Figure A.67 <sup>1</sup>H-NMR titration of **3.22·(PF<sub>6</sub>)<sub>2</sub>** in d<sub>6</sub>-DMSO in the presence of increasing concentrations of BuN·I.

## A.4 Appendix for Chapter 4

### A.4.1 NMR Spectra for Chapter 4

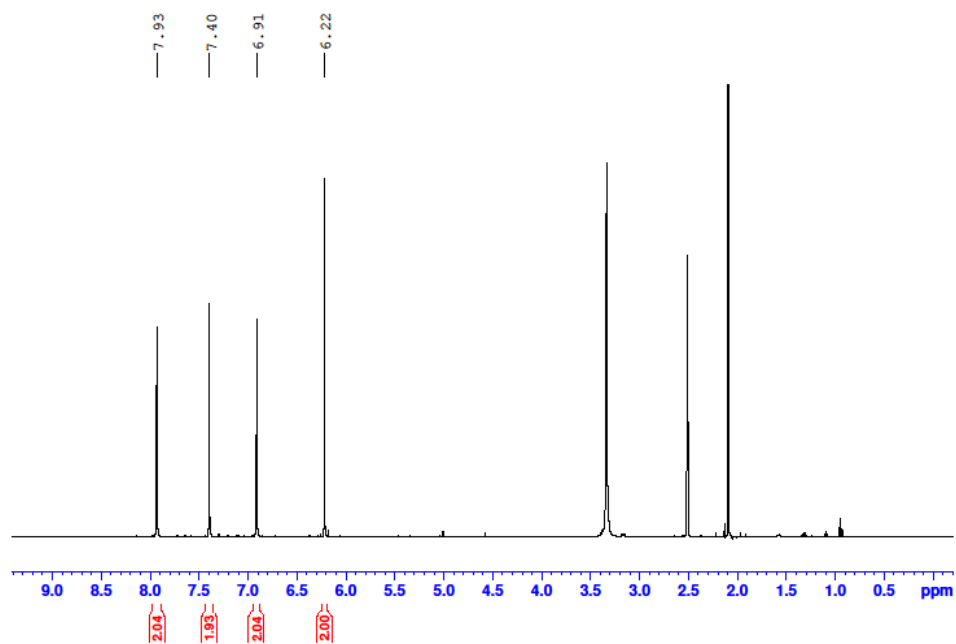


Figure A.68 <sup>1</sup>H-NMR spectrum of compound 4.4.

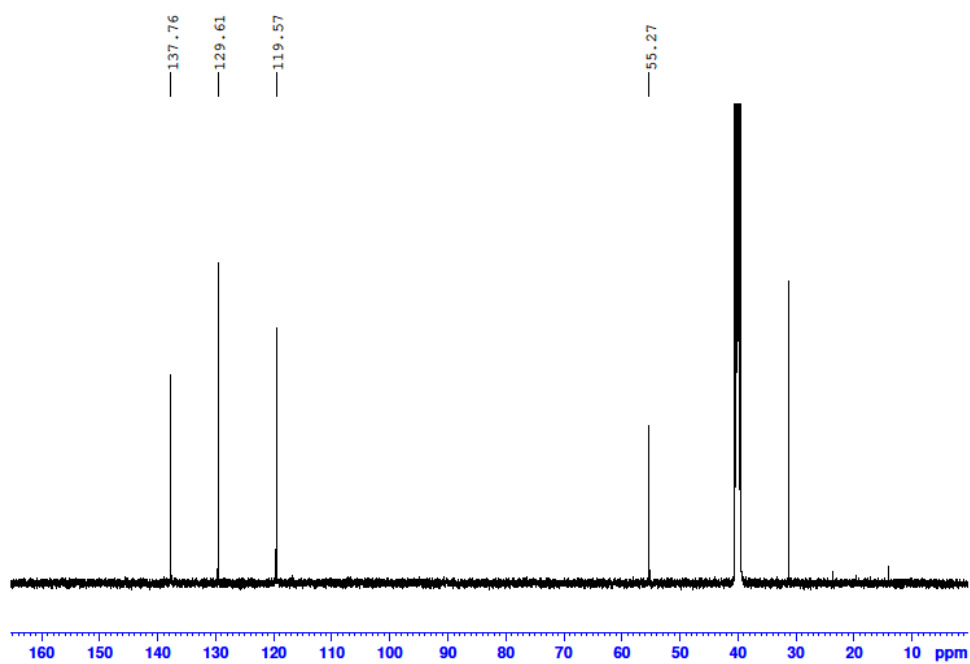


Figure A.69 <sup>13</sup>C-NMR spectrum of compound 4.4.

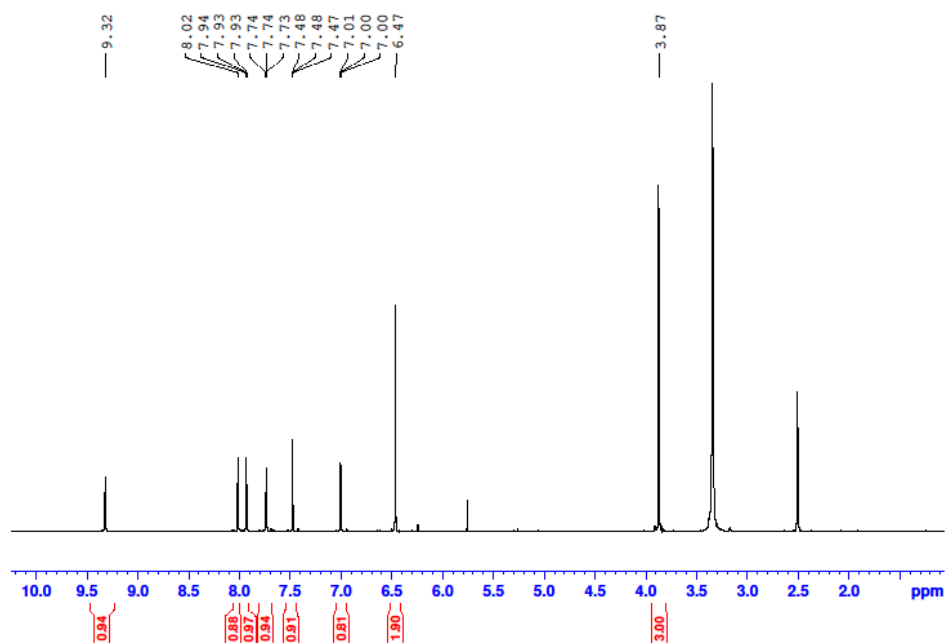


Figure A.70  $^1\text{H}$ -NMR spectrum of pro-ligand **4.5-I**.

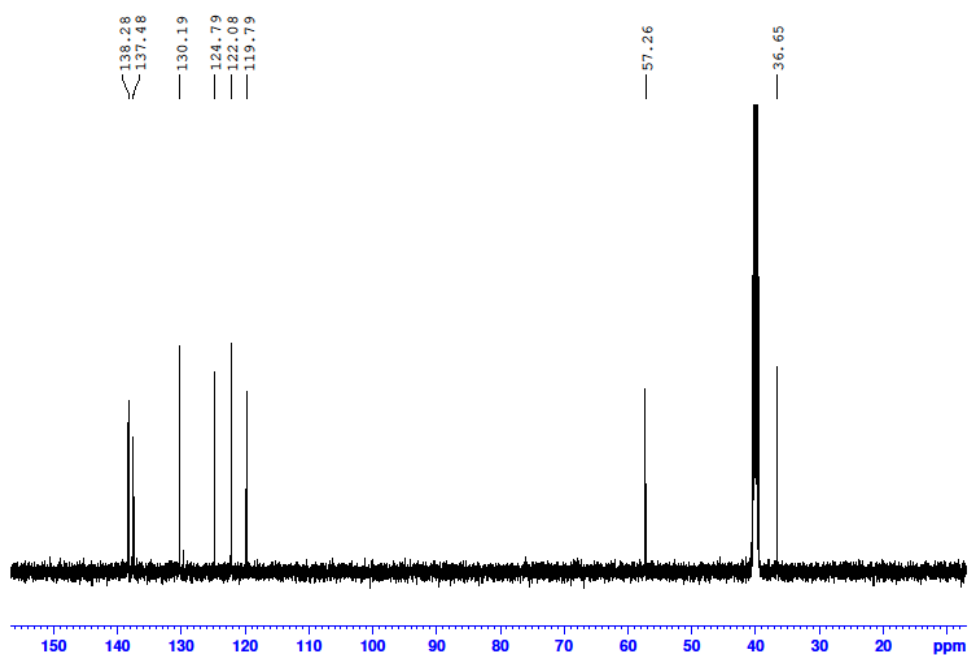


Figure A.71  $^{13}\text{C}$ -NMR spectrum of pro-ligand **4.5-I**.

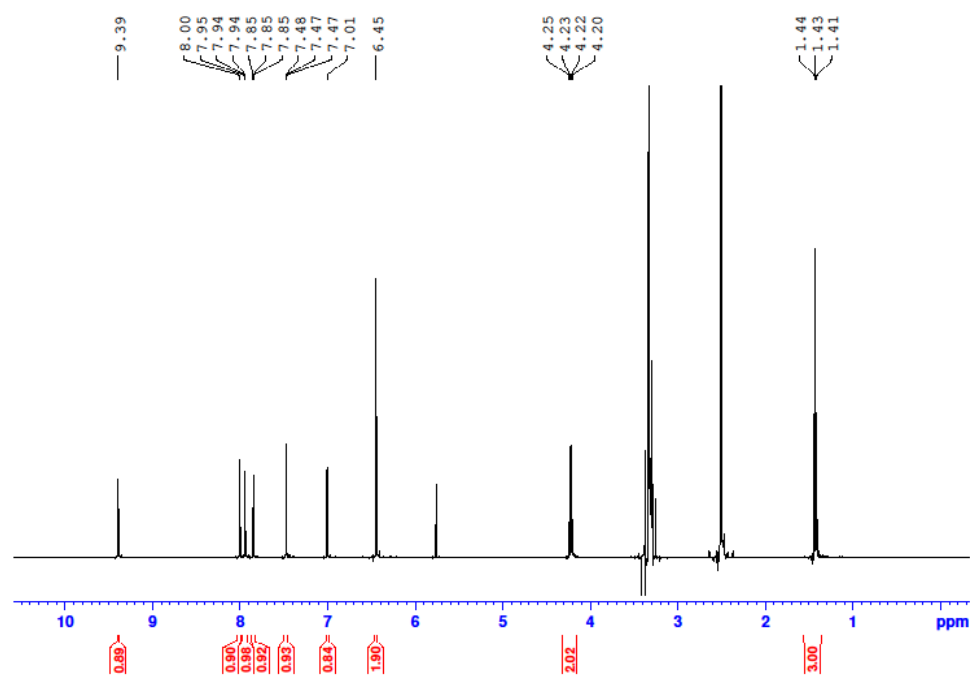


Figure A.72 <sup>1</sup>H-NMR spectrum of pro-ligand **4.6-I**.

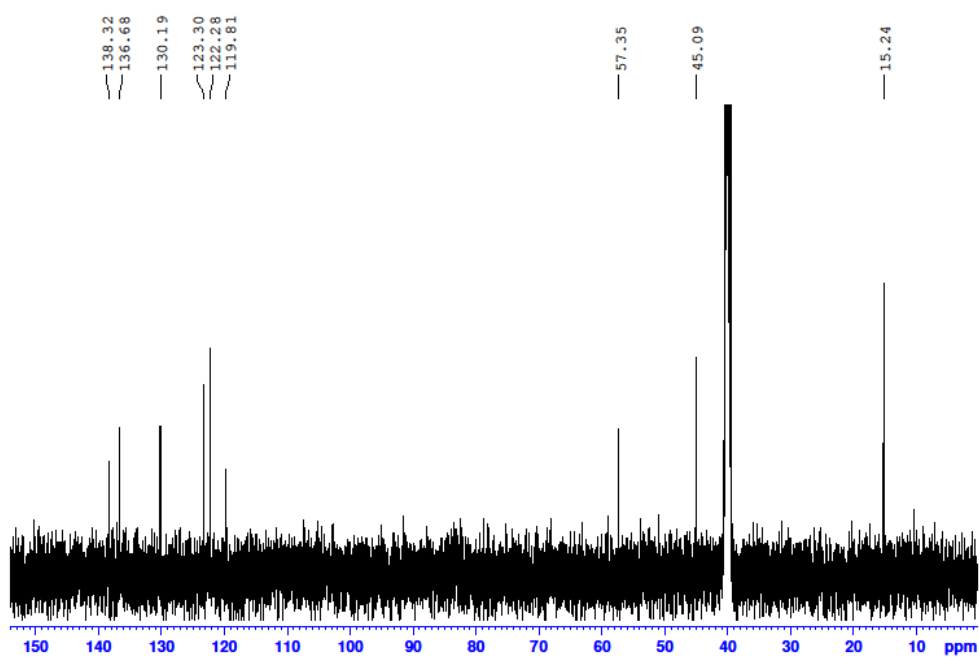


Figure A.73 <sup>13</sup>C-NMR spectrum of pro-ligand **4.6-I**.



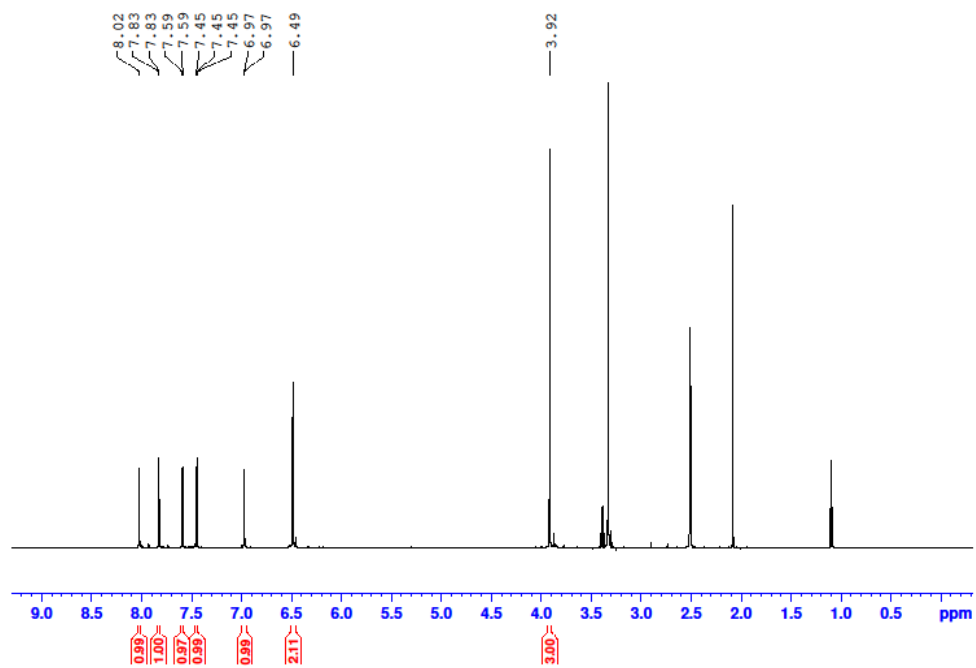


Figure A.74 <sup>1</sup>H-NMR spectrum of Au(I) monometallic complex **4.7·BF<sub>4</sub>**.

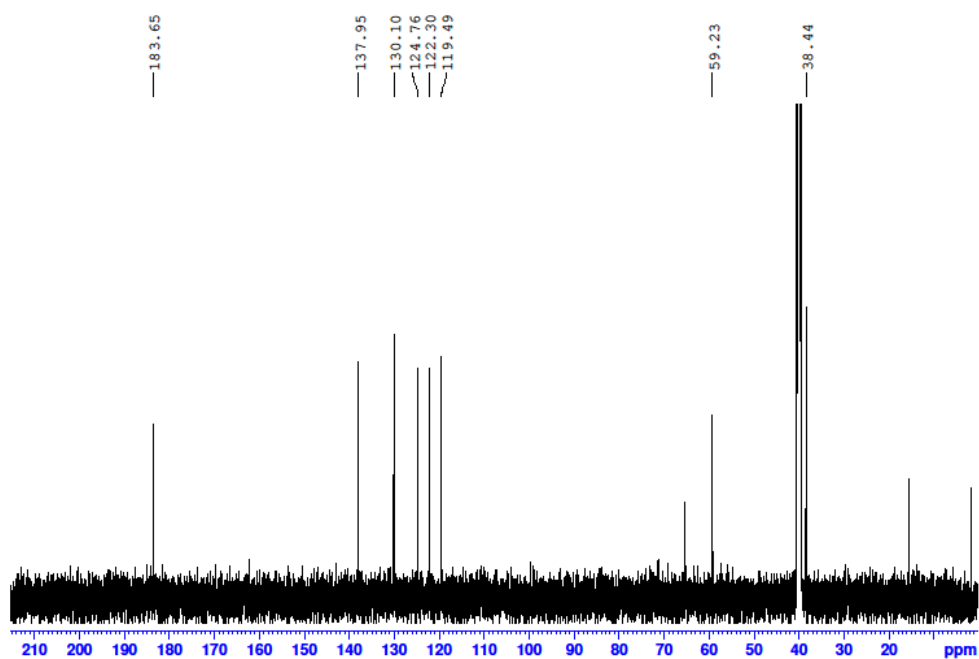


Figure A.75 <sup>13</sup>C-NMR spectrum of Au(I) monometallic complex **4.7·BF<sub>4</sub>**.

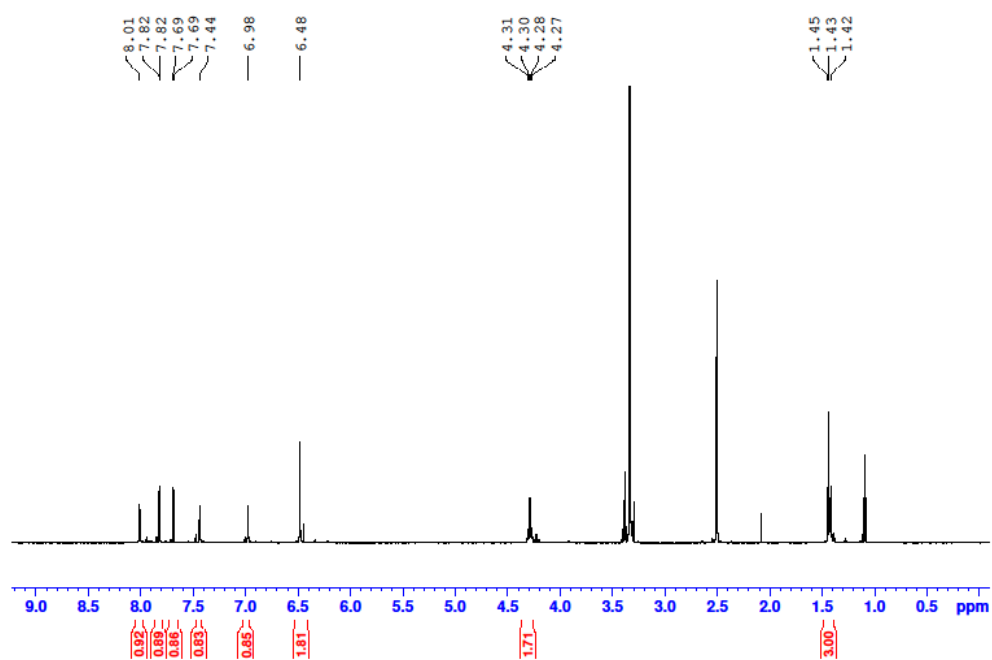


Figure A.76 <sup>1</sup>H-NMR spectrum of Au(I) monometallic complex **4.8·BF<sub>4</sub>**.

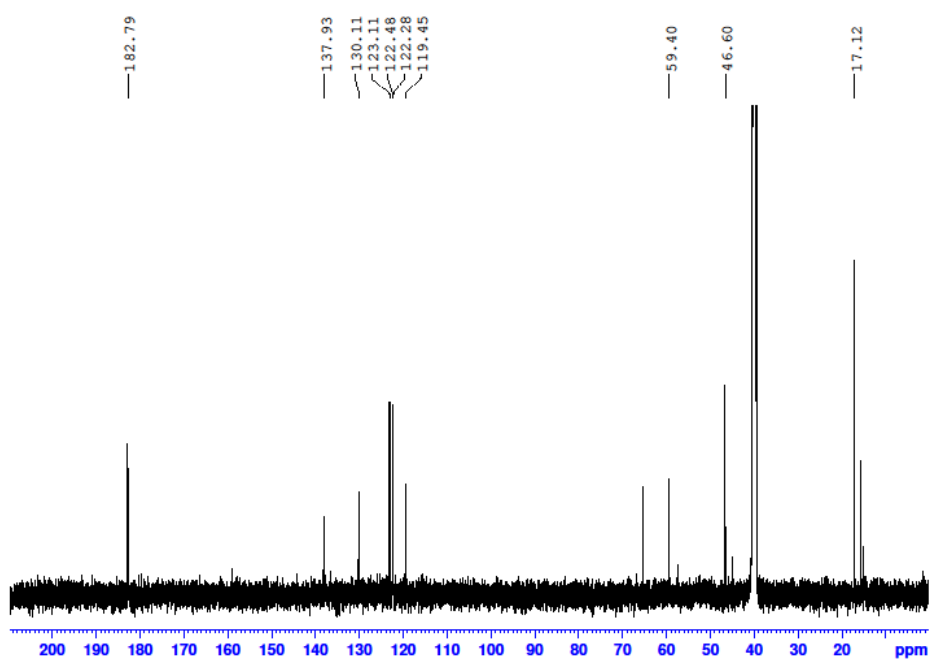


Figure A.77 <sup>13</sup>C-NMR spectrum of Au(I) monometallic complex **4.8·BF<sub>4</sub>**.

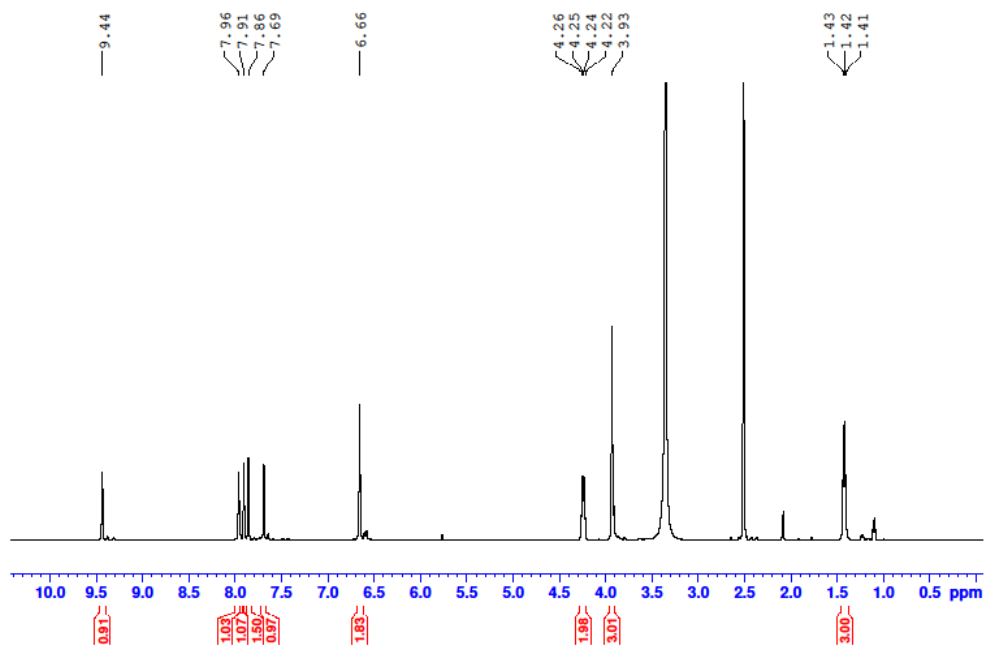


Figure A.78 <sup>1</sup>H-NMR spectrum of Au(I) monometallic complex **4.9**·(BF<sub>4</sub>)<sub>3</sub>.

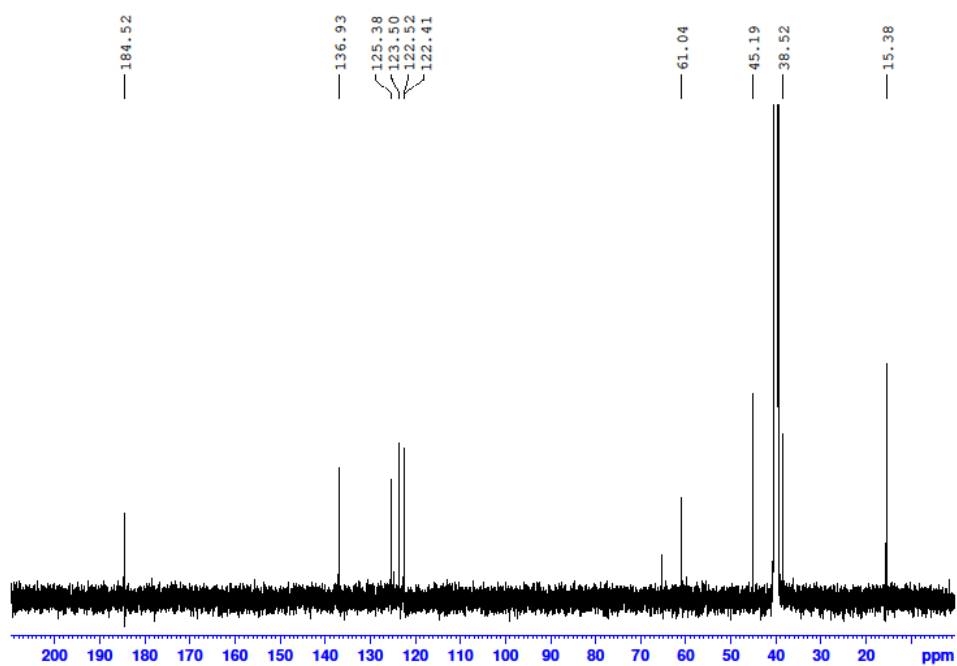


Figure A.79 <sup>13</sup>C-NMR spectrum of Au(I) monometallic complex **4.9**·(BF<sub>4</sub>)<sub>3</sub>.

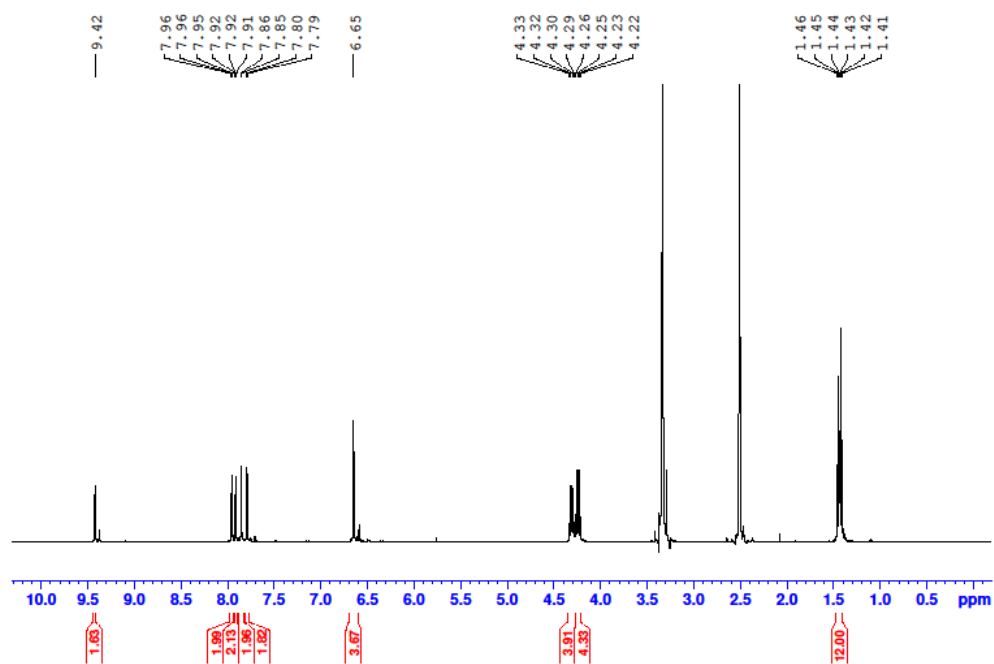


Figure A.80 <sup>1</sup>H-NMR spectrum of Au(I) monometallic complex **4.10**·(BF<sub>4</sub>)<sub>3</sub>.

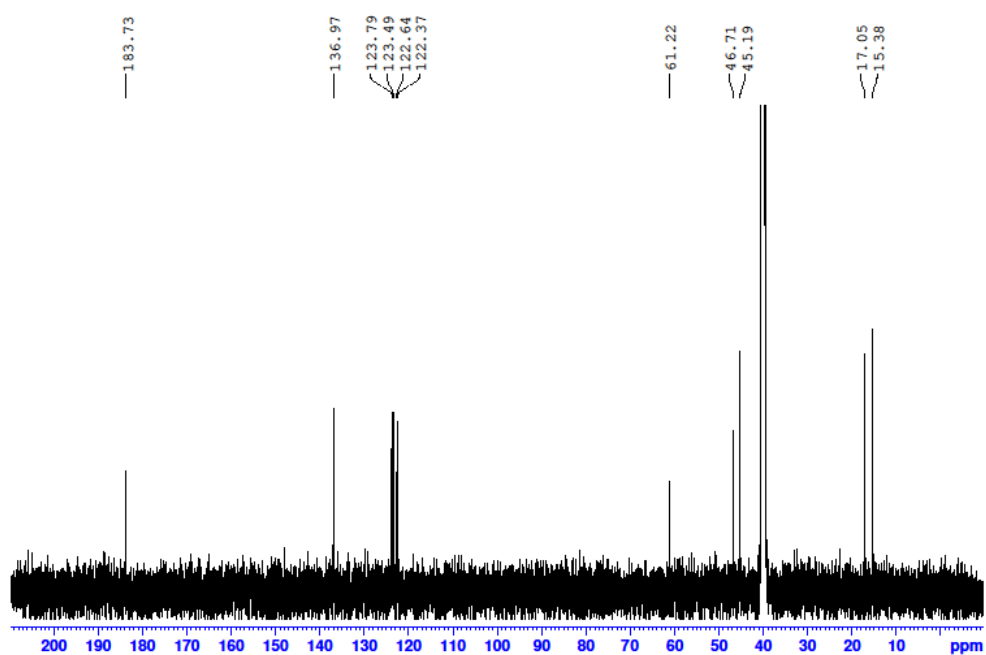


Figure A.81 <sup>13</sup>C-NMR spectrum of Au(I) monometallic complex **4.10**·(BF<sub>4</sub>)<sub>3</sub>.

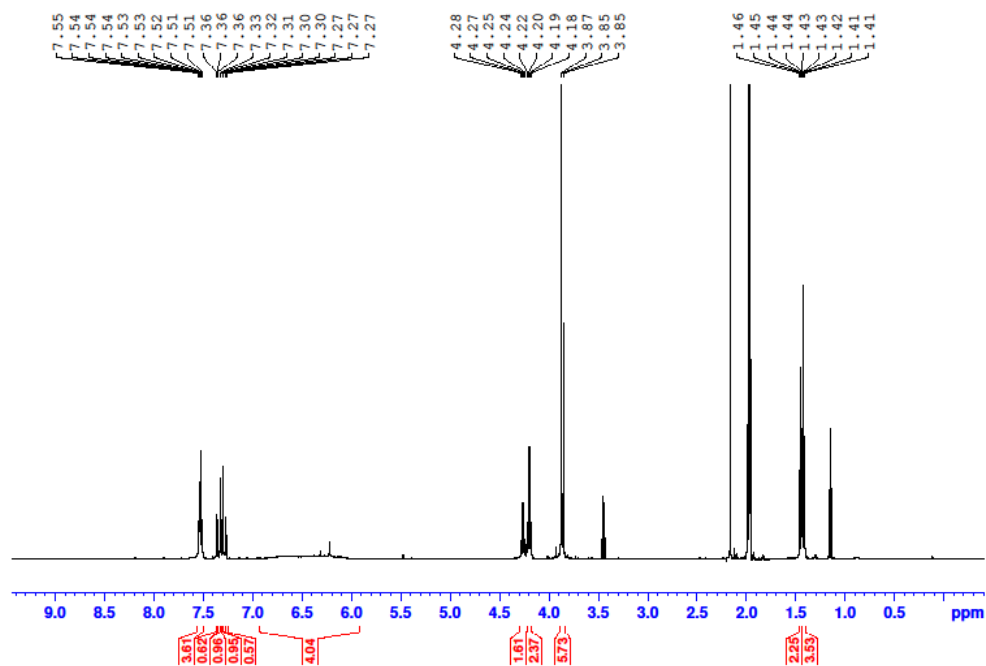


Figure A.82 <sup>1</sup>H-NMR spectrum of Au(I)-Ag(I) heterobimetallic complex **4.11**·(BF<sub>4</sub>)<sub>2</sub>.

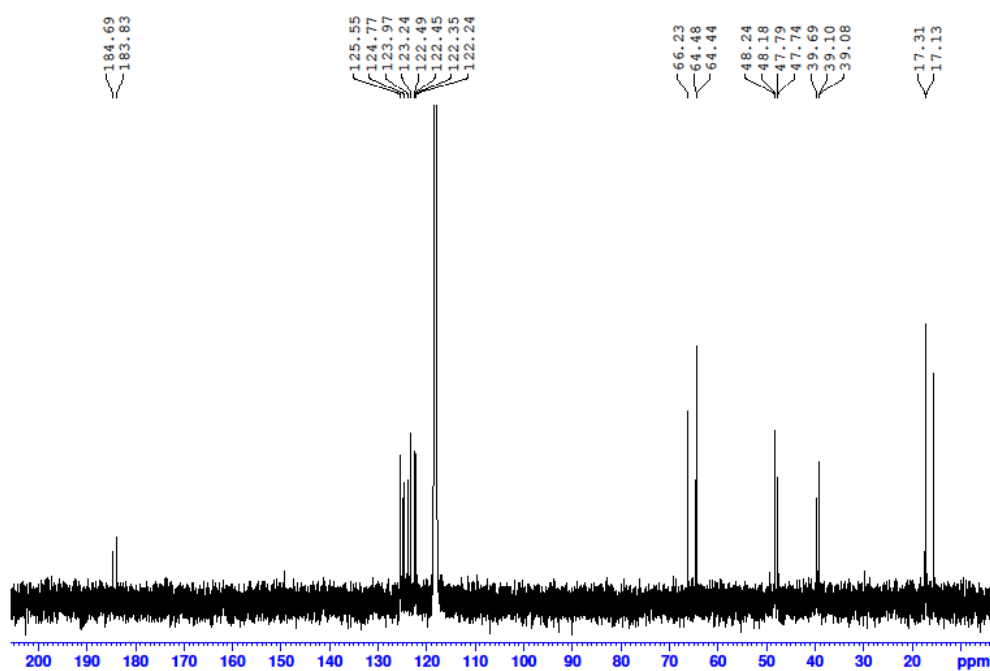


Figure A.83 <sup>13</sup>C-NMR spectrum of Au(I)-Ag(I) heterobimetallic complex **4.11**·(BF<sub>4</sub>)<sub>3</sub>.

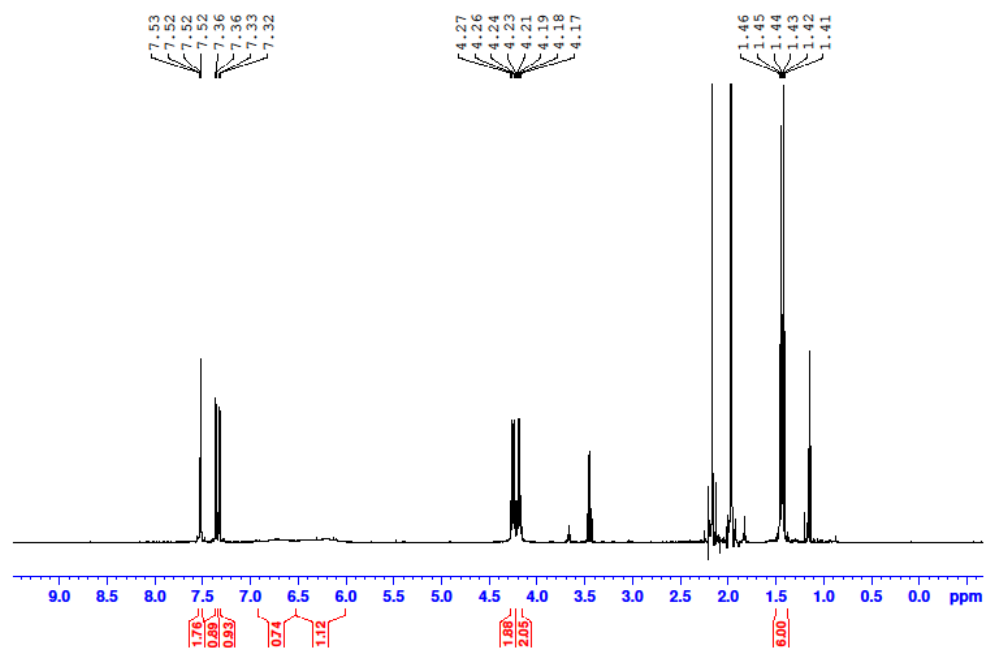


Figure A.84 <sup>1</sup>H-NMR spectrum of Au(I)-Ag(I) heterobimetallic complex **4.12**·(BF<sub>4</sub>)<sub>2</sub>.

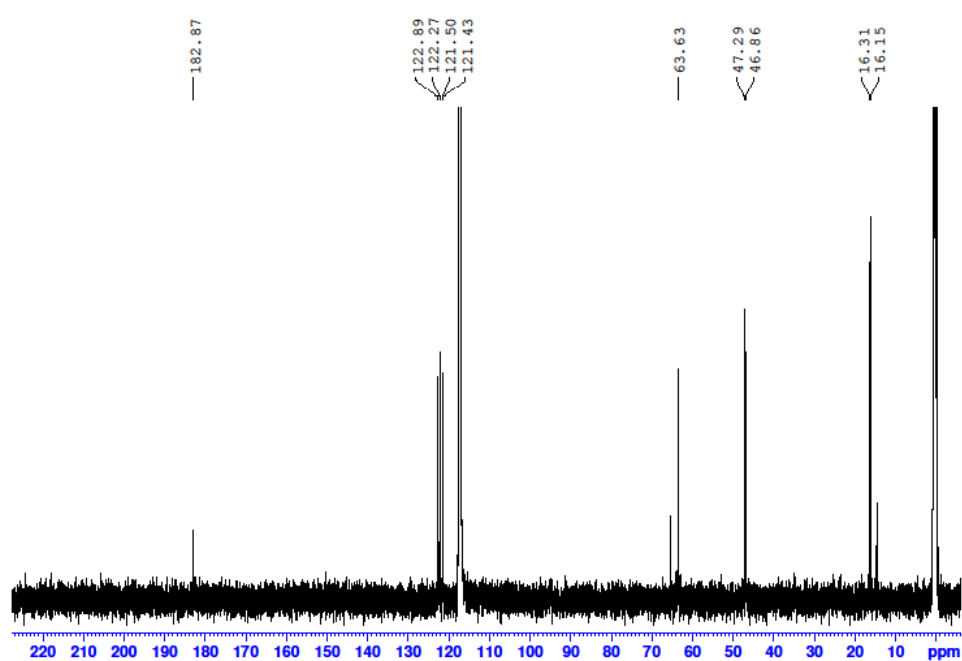


Figure A.85 <sup>13</sup>C-NMR spectrum of Au(I)-Ag(I) heterobimetallic complex **4.12**·(BF<sub>4</sub>)<sub>2</sub>.

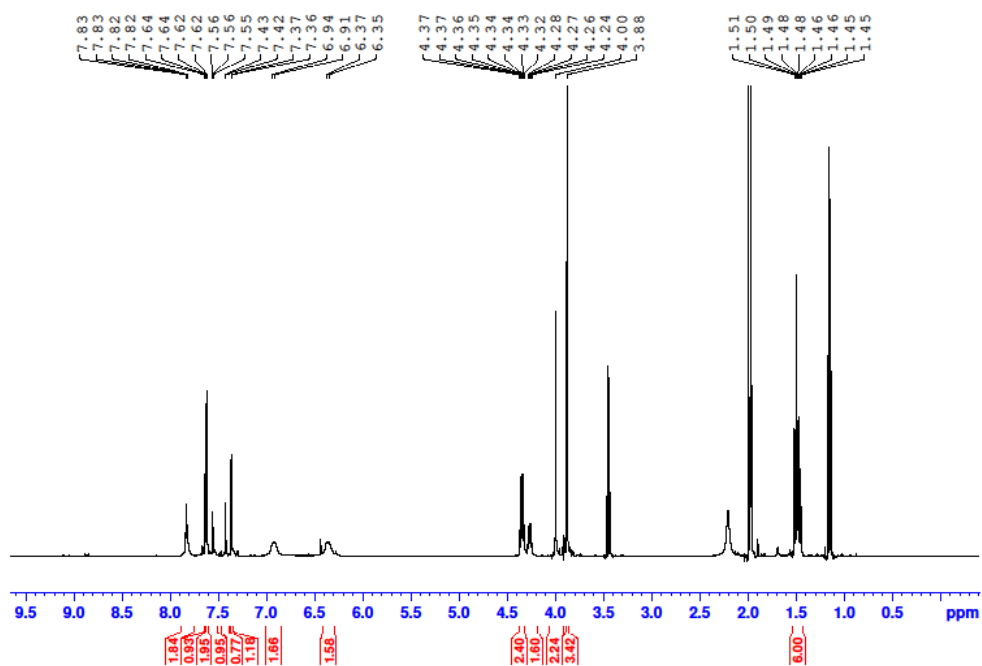


Figure A.86 <sup>1</sup>H-NMR spectrum of Au(I)-Hg(II) heterobimetallic complex **4.13**·(BF<sub>4</sub>)<sub>3</sub>.

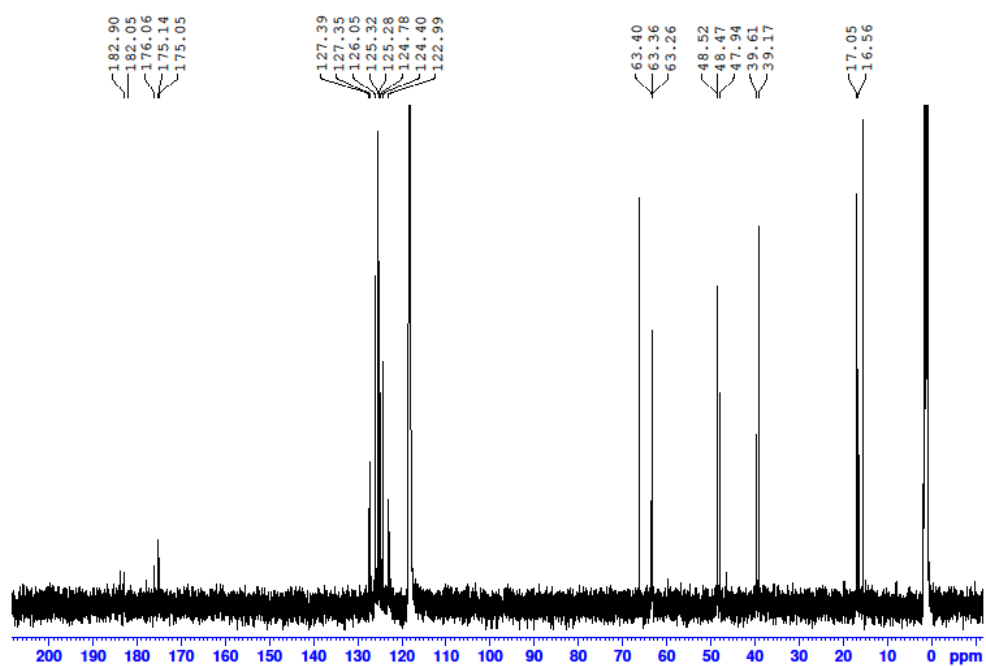


Figure A.87 <sup>13</sup>C-NMR spectrum of Au(I)-Hg(II) heterobimetallic complex **4.13**·(BF<sub>4</sub>)<sub>3</sub>.

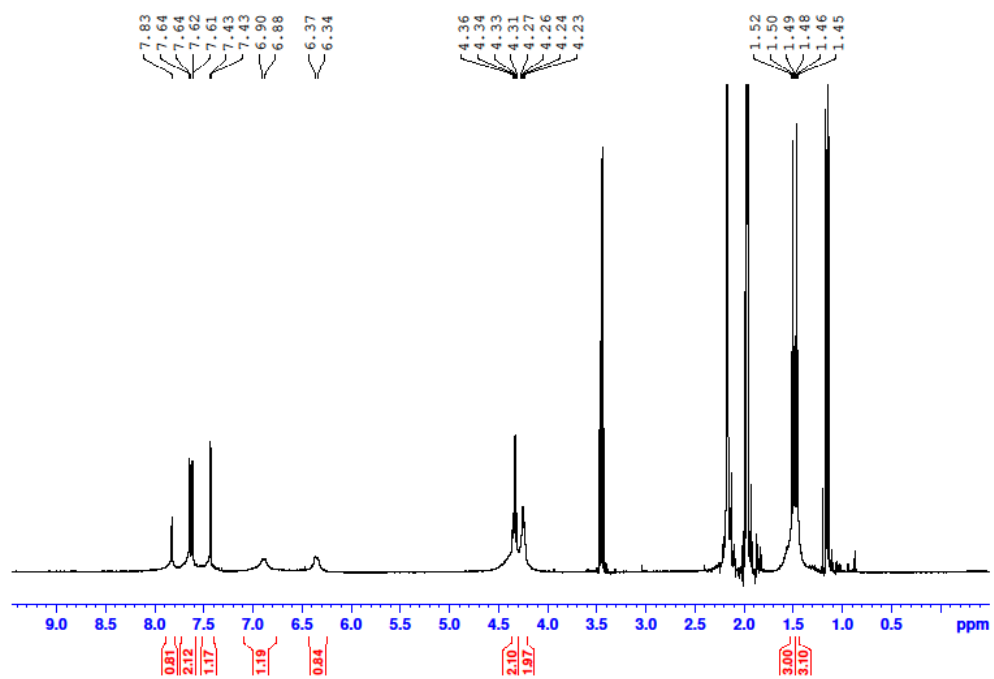


Figure A.88 <sup>1</sup>H-NMR spectrum of Au(I)-Hg(II) heterobimetallic complex **4.14**·(BF<sub>4</sub>)<sub>3</sub>.

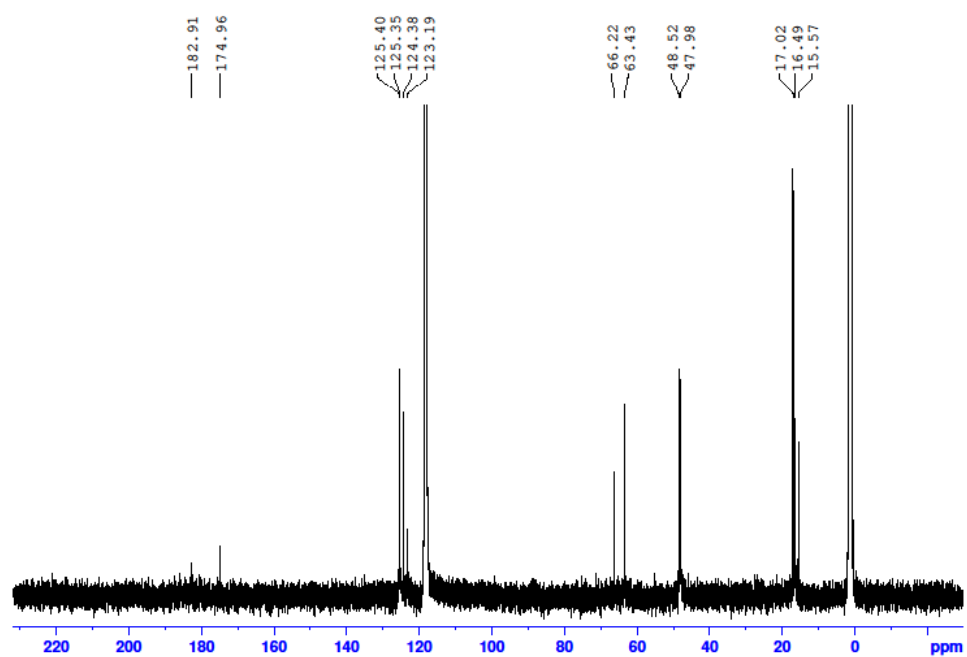


Figure A.89 <sup>13</sup>C-NMR spectrum of Au(I)-Hg(II) heterobimetallic complex **4.14**·(BF<sub>4</sub>)<sub>3</sub>.



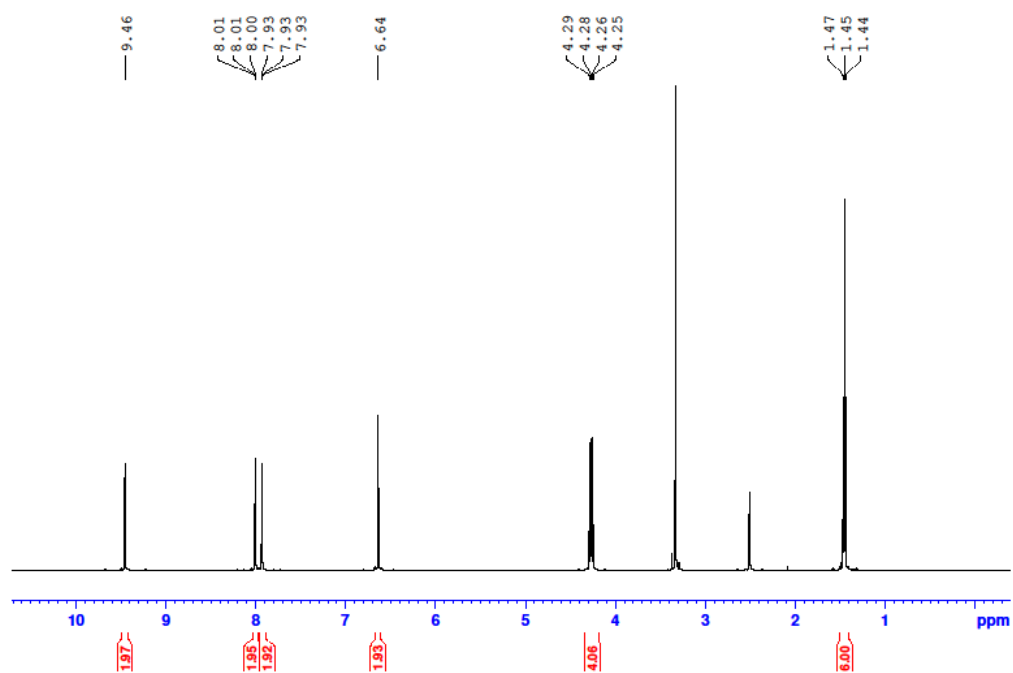


Figure A.90 <sup>1</sup>H-NMR spectrum of *bis*-imidazolium pro-ligand **4.16·I<sub>2</sub>**.

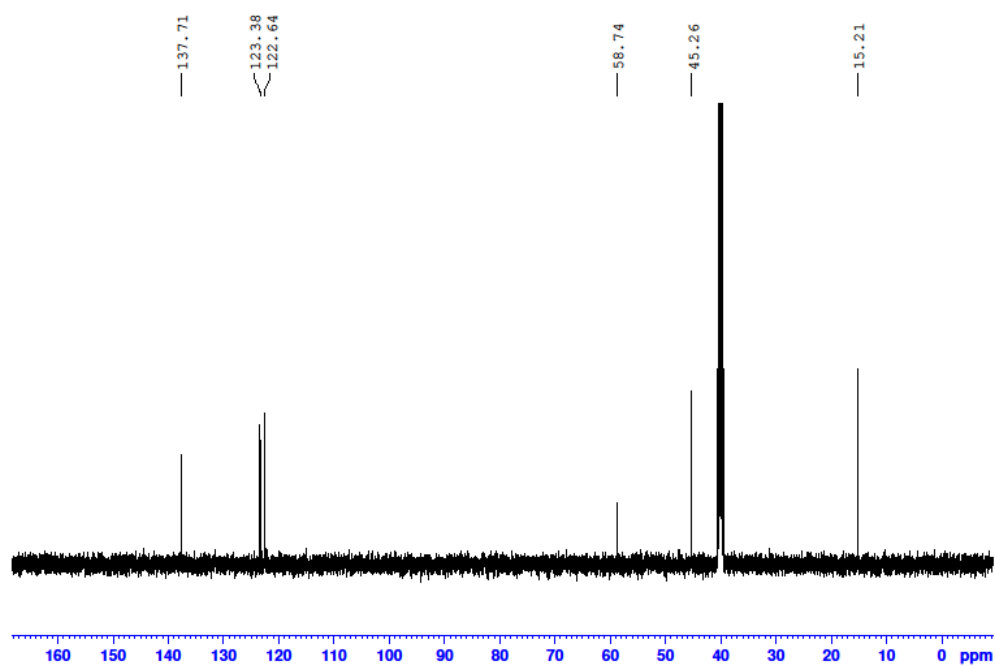


Figure A.91 <sup>13</sup>C-NMR spectrum of *bis*-imidazolium pro-ligand **4.16·I<sub>2</sub>**.

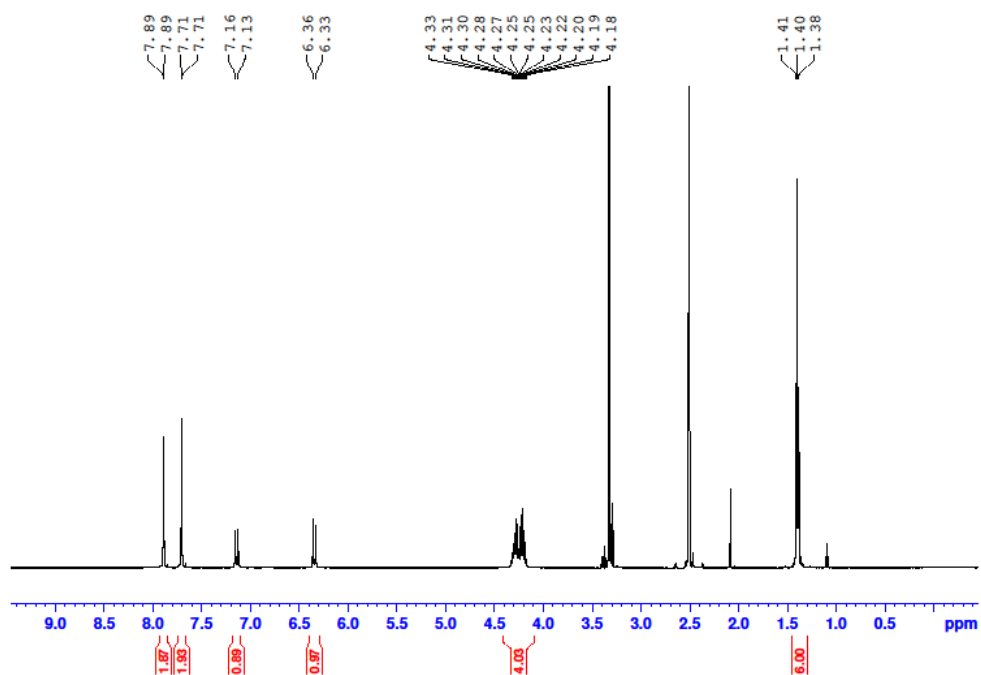


Figure A.92 <sup>1</sup>H-NMR spectrum of Au(I) homobimetallic complex **4.17**·(BF<sub>4</sub>)<sub>2</sub>.

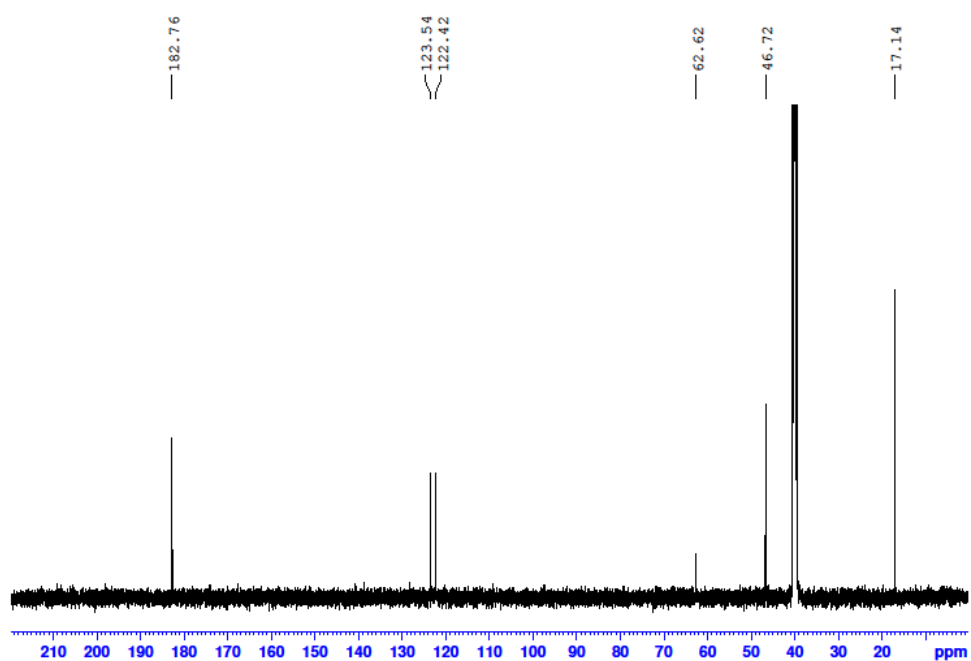


Figure A.93 <sup>13</sup>C-NMR spectrum of Au(I) homobimetallic complex **4.17**·(BF<sub>4</sub>)<sub>2</sub>.

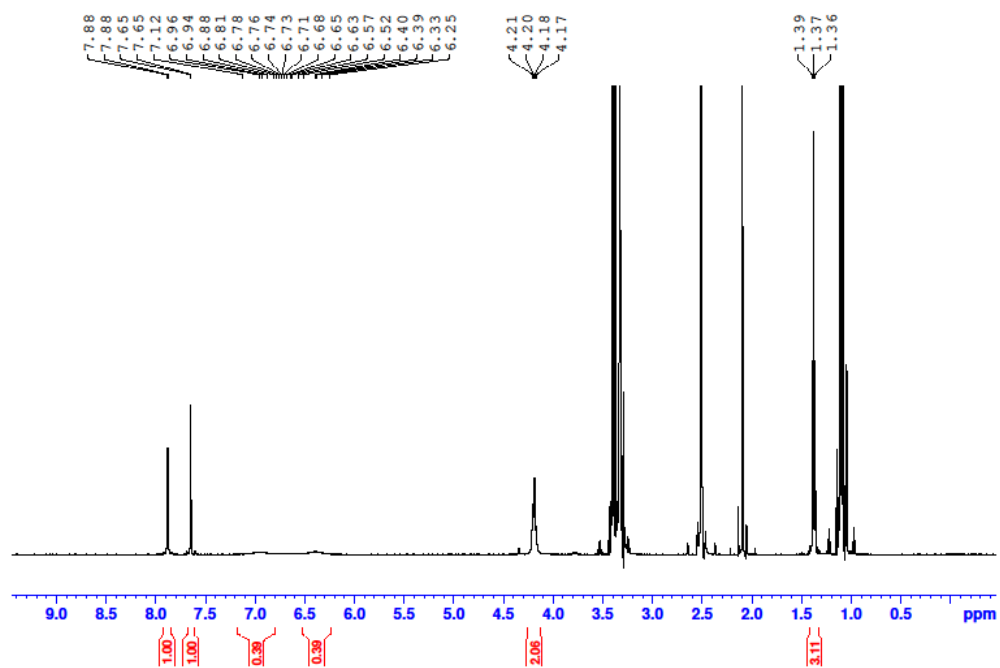


Figure A.94 <sup>1</sup>H-NMR spectrum of Au(I) homobimetallic complex **4.18**·(BF<sub>4</sub>)<sub>2</sub>.

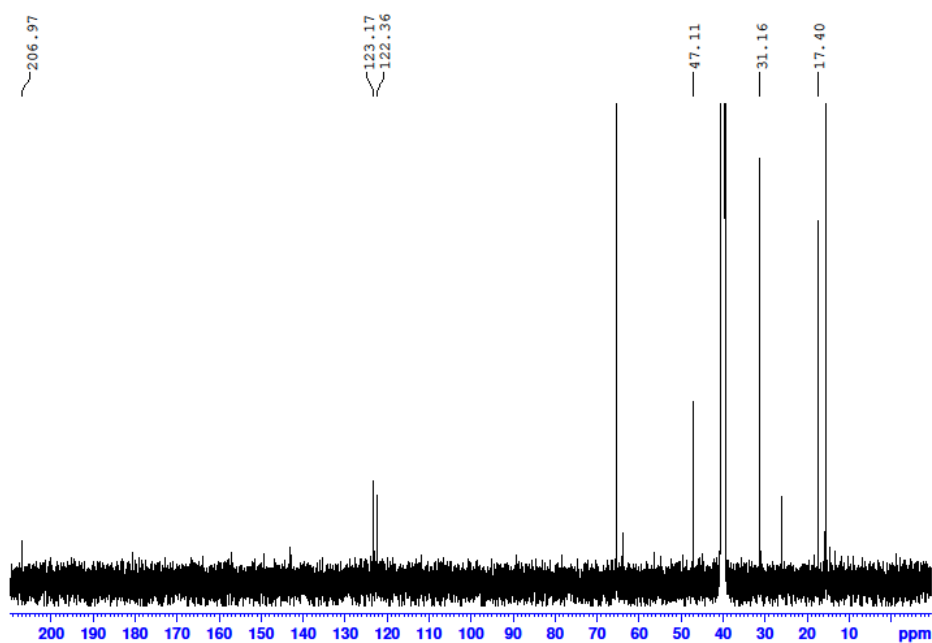


Figure A.95 <sup>13</sup>C-NMR spectrum of Au(I) homobimetallic complex **4.18**·(BF<sub>4</sub>)<sub>2</sub>.

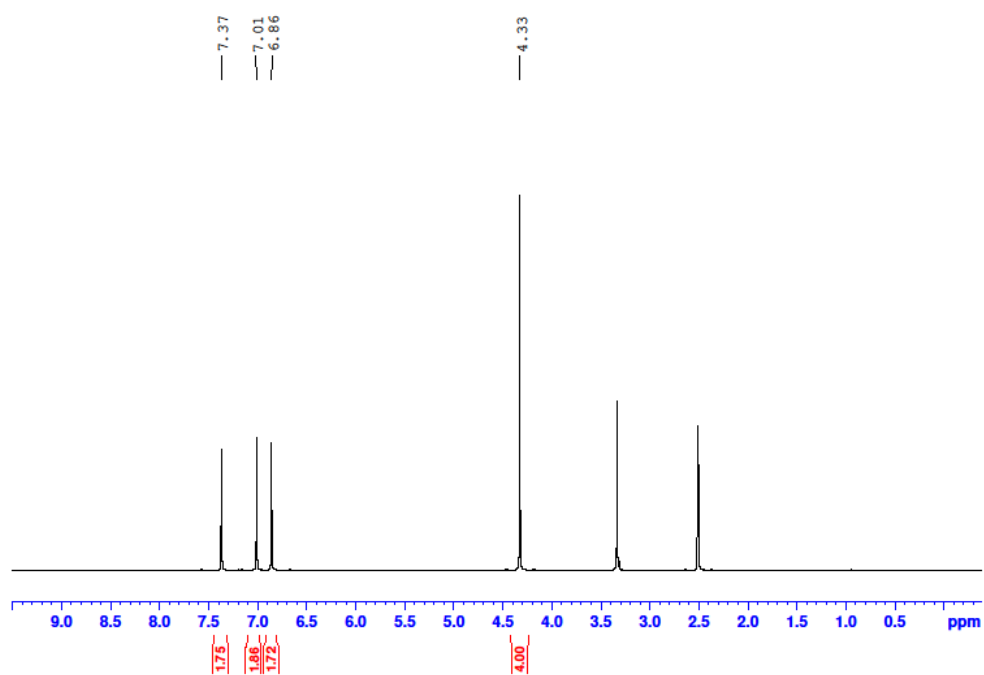


Figure A.96  $^1\text{H}$ -NMR spectrum of compound **4.19**.

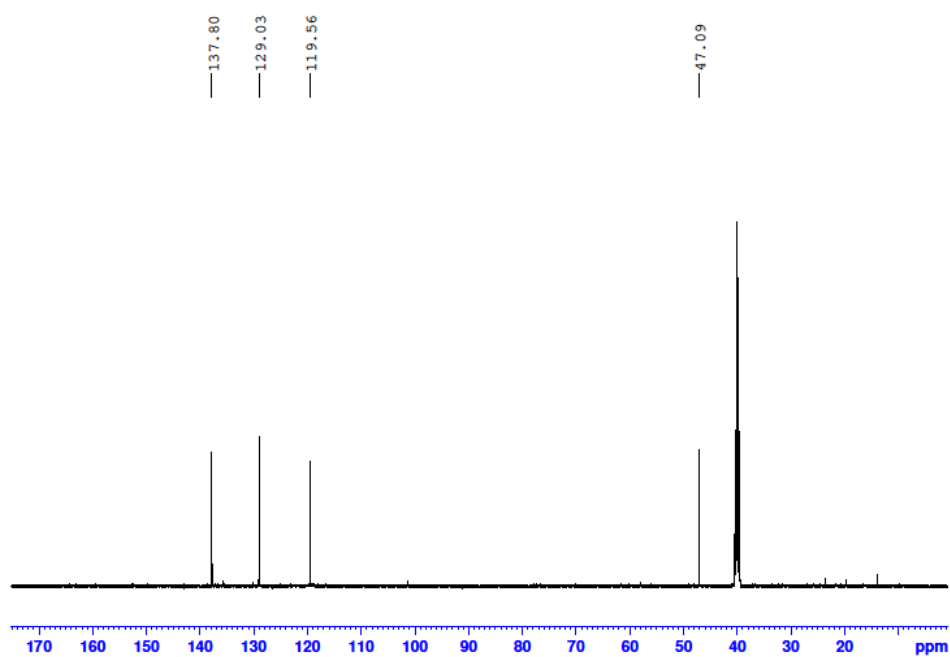


Figure A.97  $^{13}\text{C}$ -NMR spectrum of compound **4.19**.

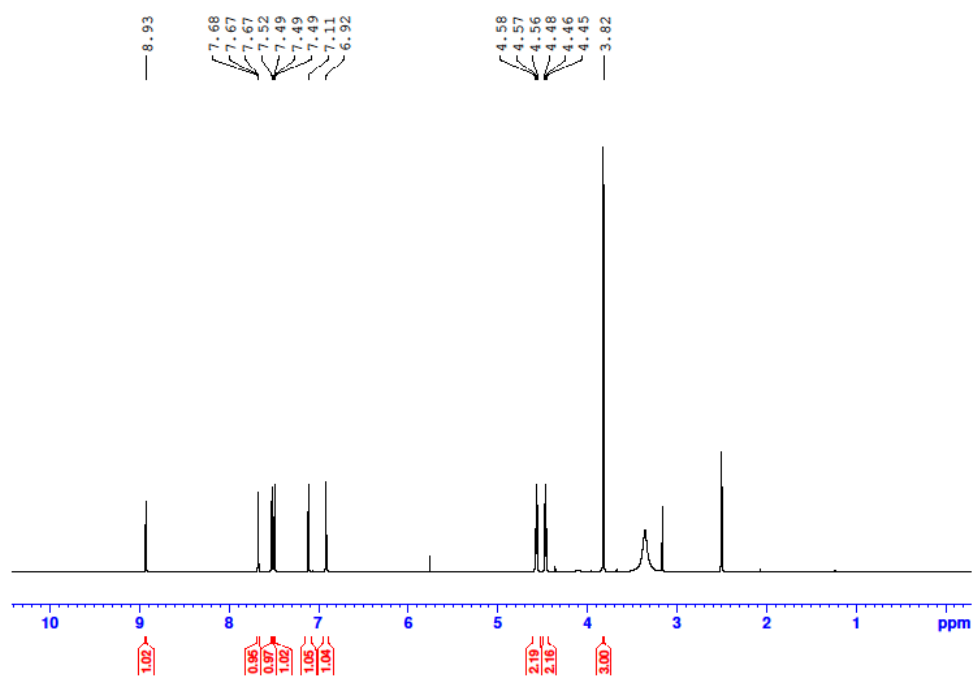


Figure A.98 <sup>1</sup>H-NMR spectrum of pro-ligand **4.20-I**.

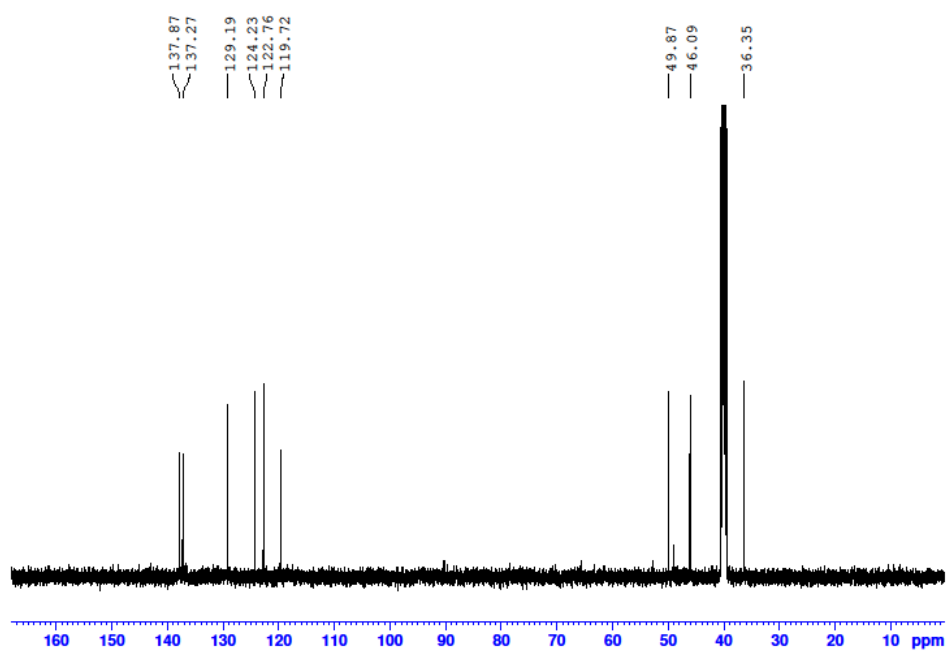


Figure A.99 <sup>13</sup>C-NMR spectrum of pro-ligand **4.20-I**.

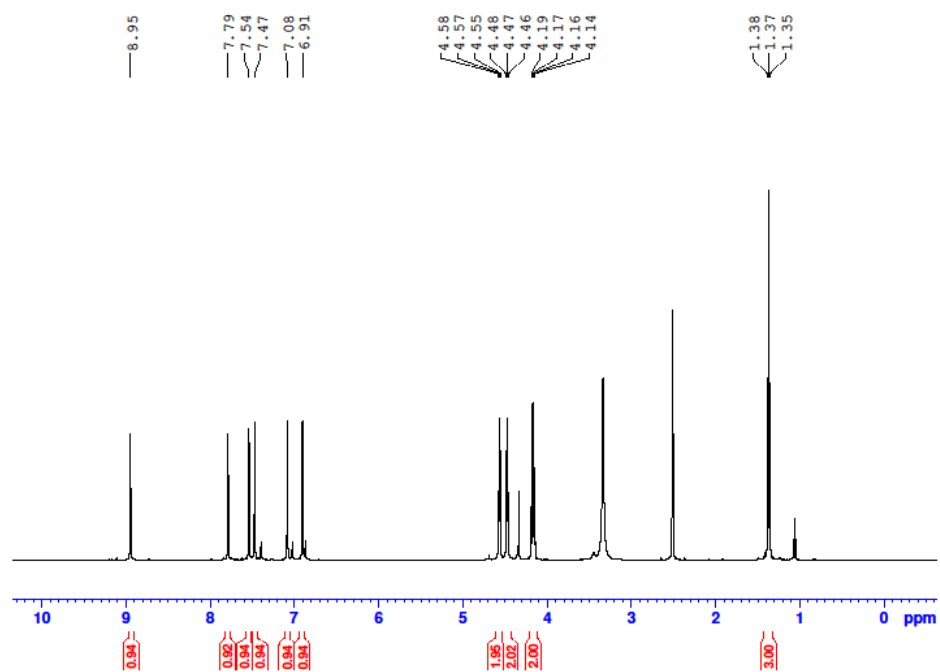


Figure A.100 <sup>1</sup>H-NMR spectrum of pro-ligand **4.21-I**.

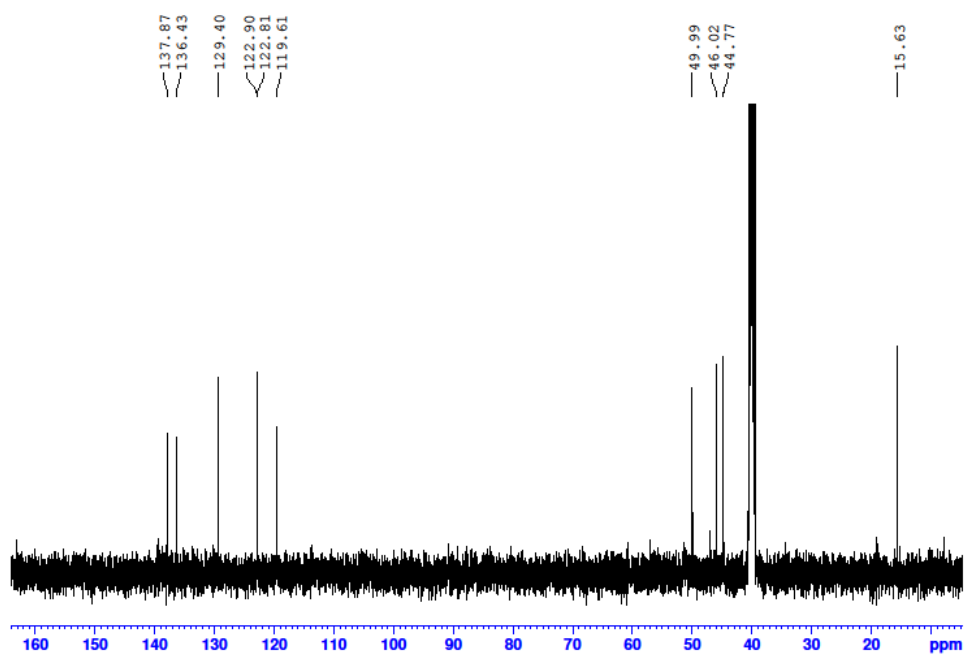


Figure A.101 <sup>13</sup>C-NMR spectrum of pro-ligand **4.21-I**.

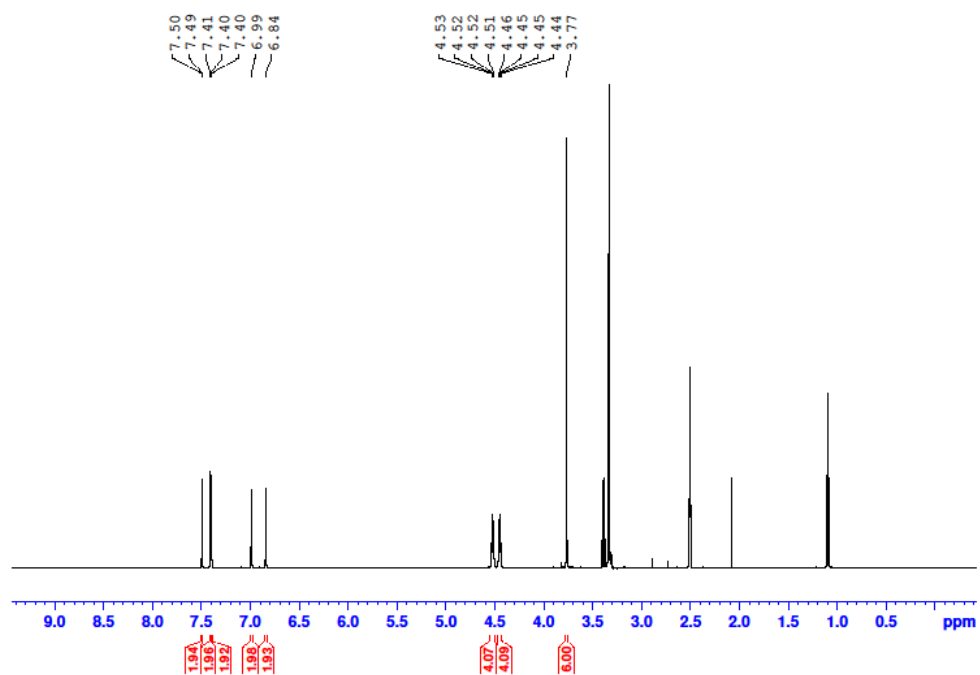


Figure A.102  $^1\text{H}$ -NMR spectrum of Au(I) monometallic complex **4.22**· $\text{BF}_4$ .

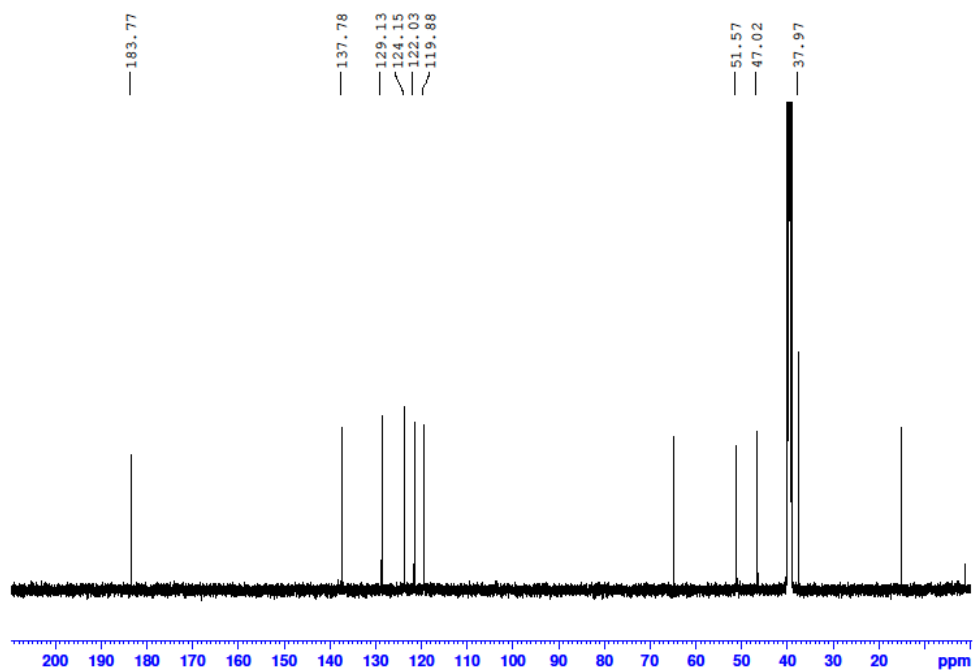


Figure A.103  $^{13}\text{C}$ -NMR spectrum of Au(I) monometallic complex **4.22**· $\text{BF}_4$ .

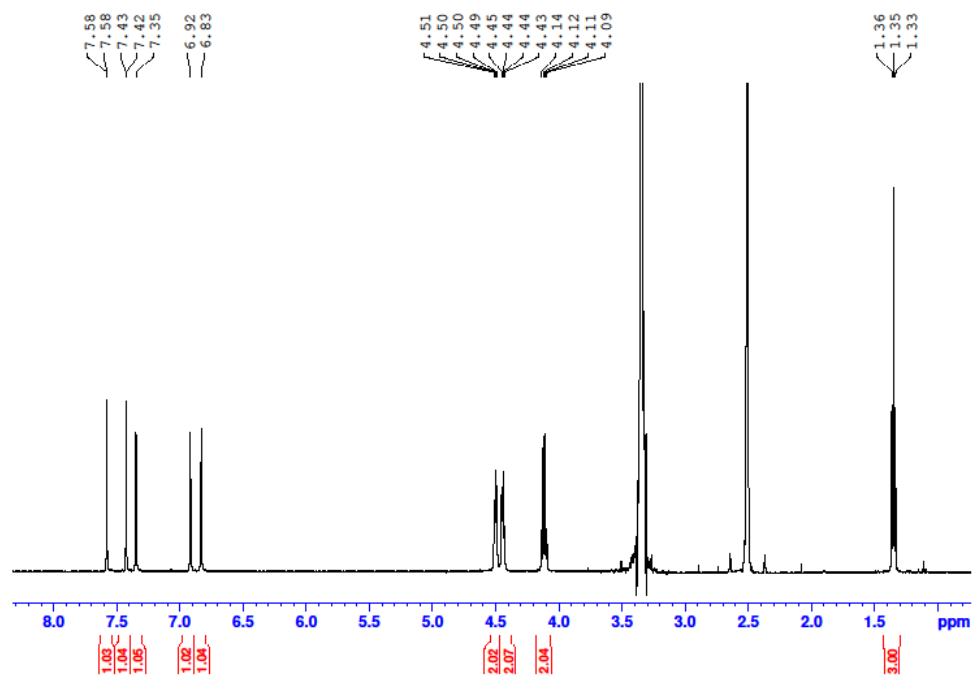


Figure A.104 <sup>1</sup>H-NMR spectrum of Au(I) monometallic complex **4.23**·BF<sub>4</sub>.

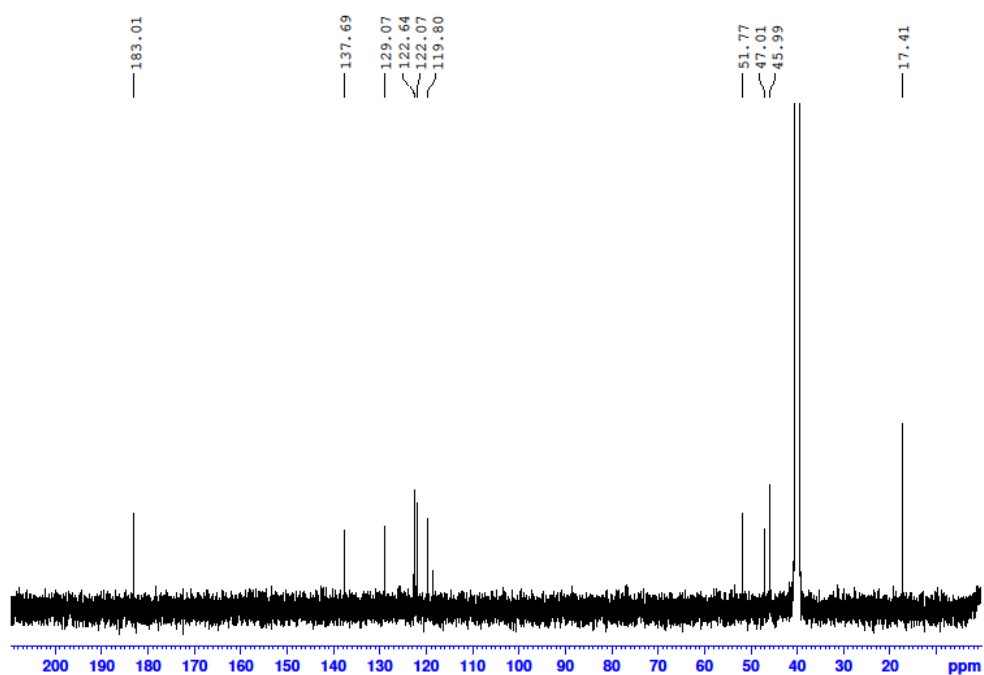


Figure A.105 <sup>13</sup>C-NMR spectrum of Au(I) monometallic complex **4.23**·BF<sub>4</sub>.



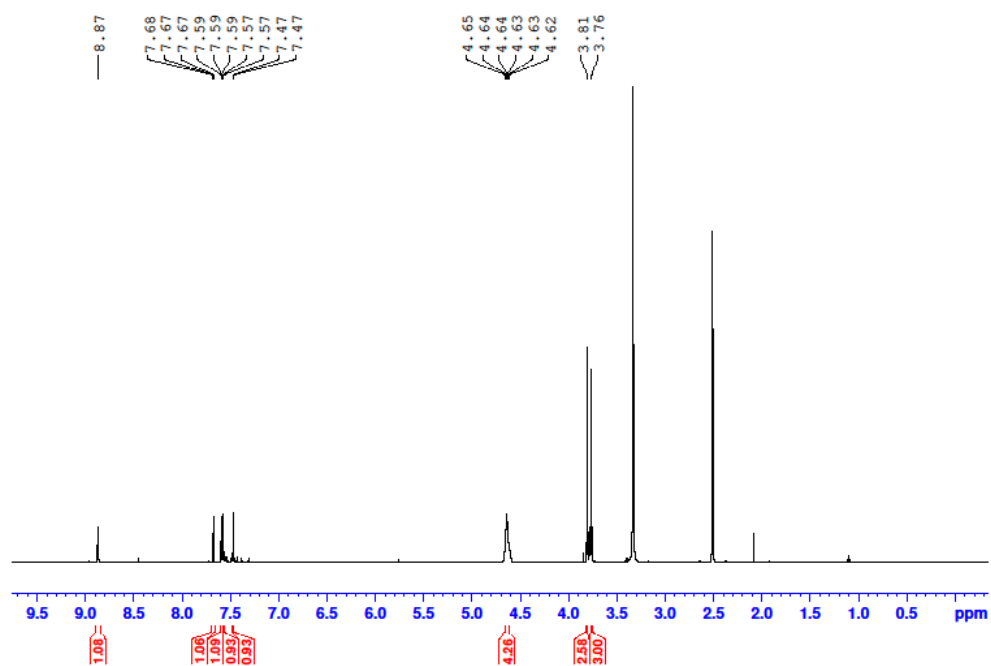


Figure A.106 <sup>1</sup>H-NMR spectrum of Au(I) monometallic complex **4.24**·(BF<sub>4</sub>)<sub>3</sub>.

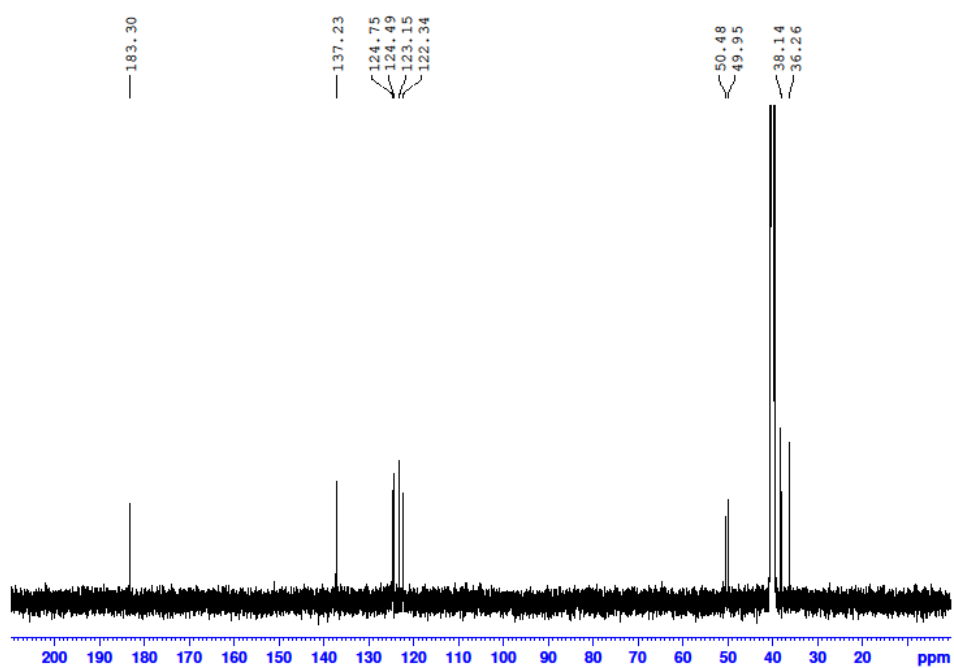


Figure A.107 <sup>13</sup>C-NMR spectrum of Au(I) monometallic complex **4.24**·(BF<sub>4</sub>)<sub>3</sub>.

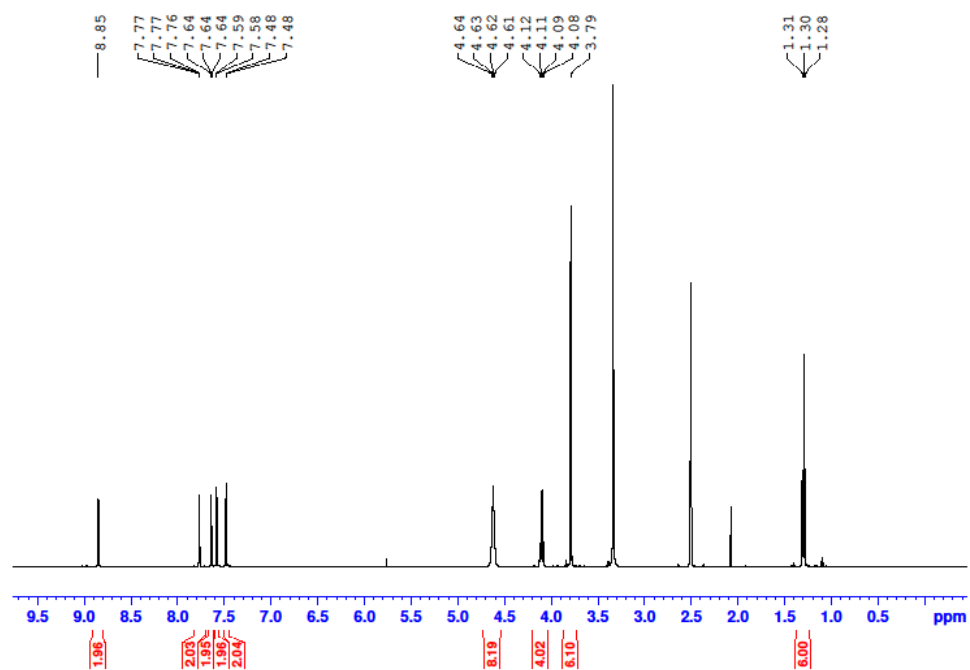


Figure A.108 <sup>1</sup>H-NMR spectrum of Au(I) monometallic complex **4.25**·(BF<sub>4</sub>)<sub>3</sub>.

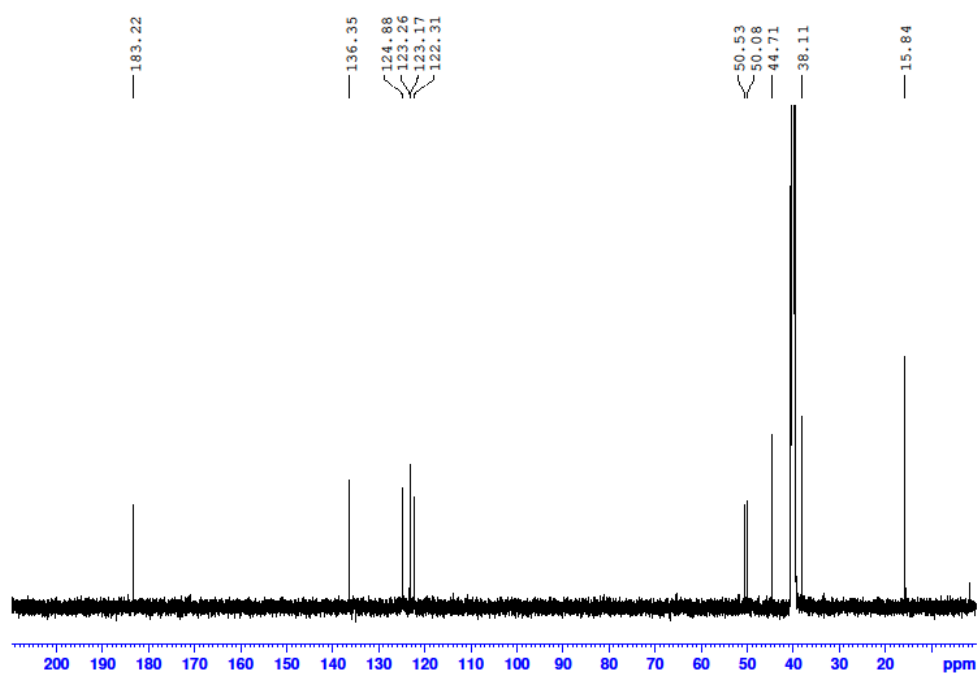


Figure A.109 <sup>13</sup>C-NMR spectrum of Au(I) monometallic complex **4.25**·(BF<sub>4</sub>)<sub>3</sub>.

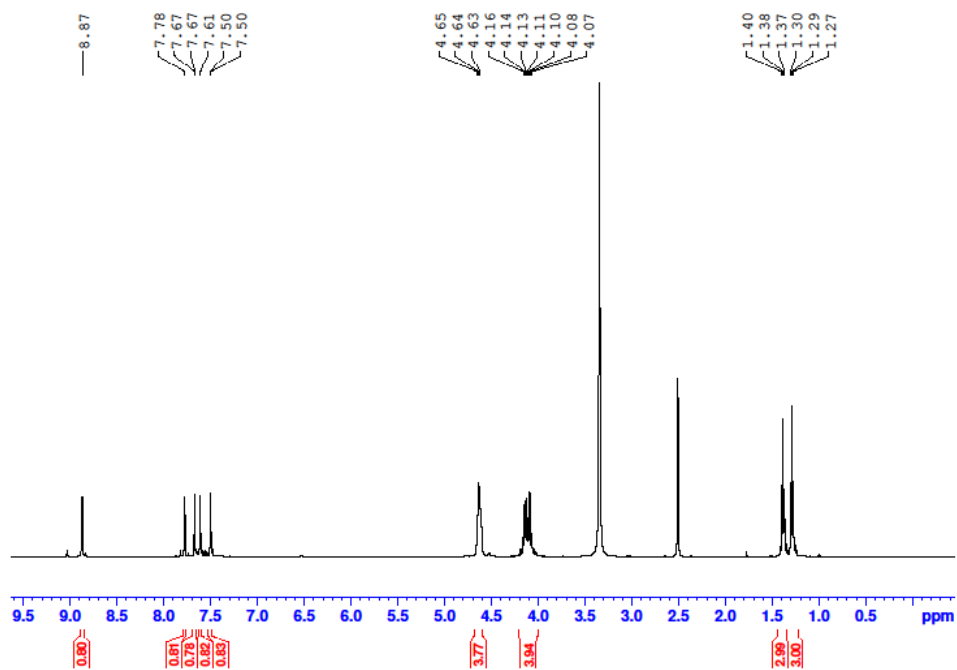


Figure A.110 <sup>1</sup>H-NMR spectrum of Au(I) monometallic complex **4.26**·(BF<sub>4</sub>)<sub>3</sub>.

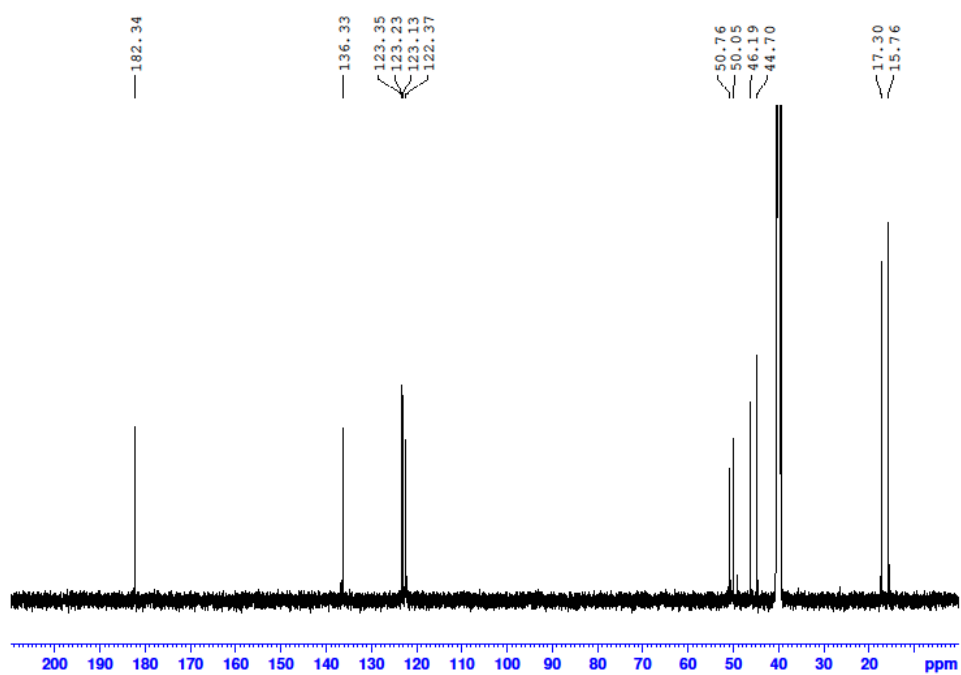


Figure A.111 <sup>13</sup>C-NMR spectrum of Au(I) monometallic complex **4.26**·(BF<sub>4</sub>)<sub>3</sub>.

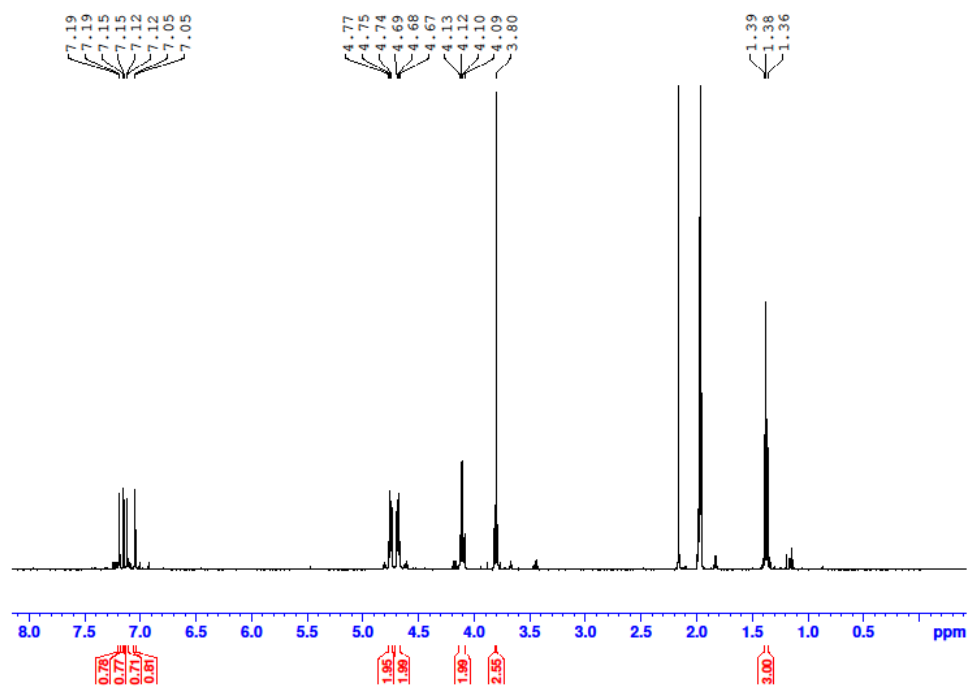


Figure A.112 <sup>1</sup>H-NMR spectrum of Au(I)-Ag(I) heterometallic complex **4.28**·(BF<sub>4</sub>)<sub>2</sub>.

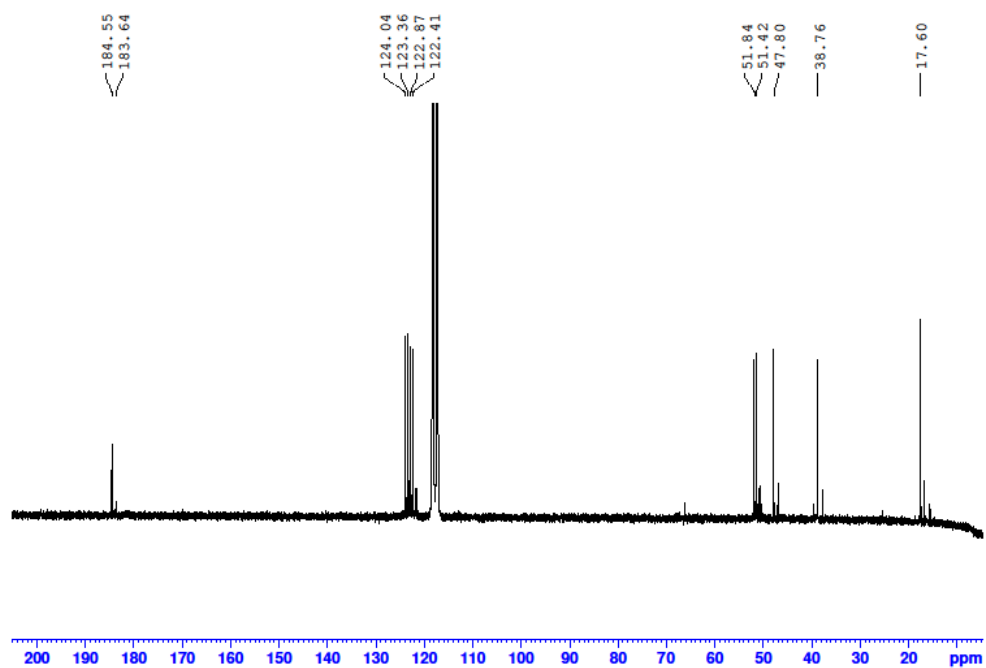


Figure A.113 <sup>13</sup>C-NMR spectrum of Au(I)-Ag(I) heterometallic complex **4.28**·(BF<sub>4</sub>)<sub>2</sub>.

#### A.4.2 Variable temperature NMR studies for Chapter 4

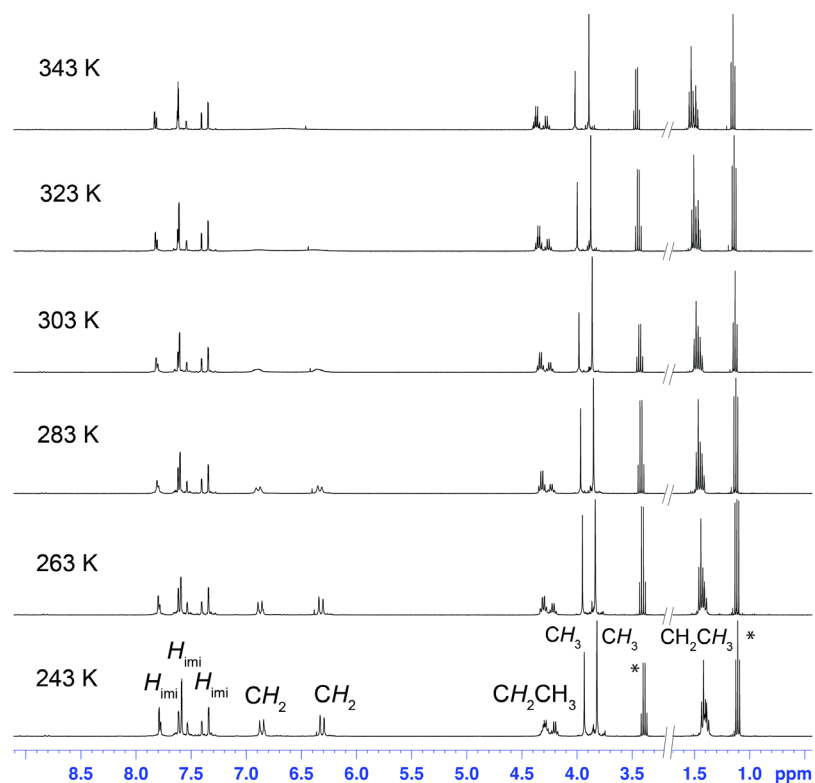


Figure A.114 Stacked  $^1\text{H}$ -NMR spectra of Au(I)-Hg(II) heterobimetallic complex **4.13**·(BF<sub>4</sub>)<sub>3</sub>.

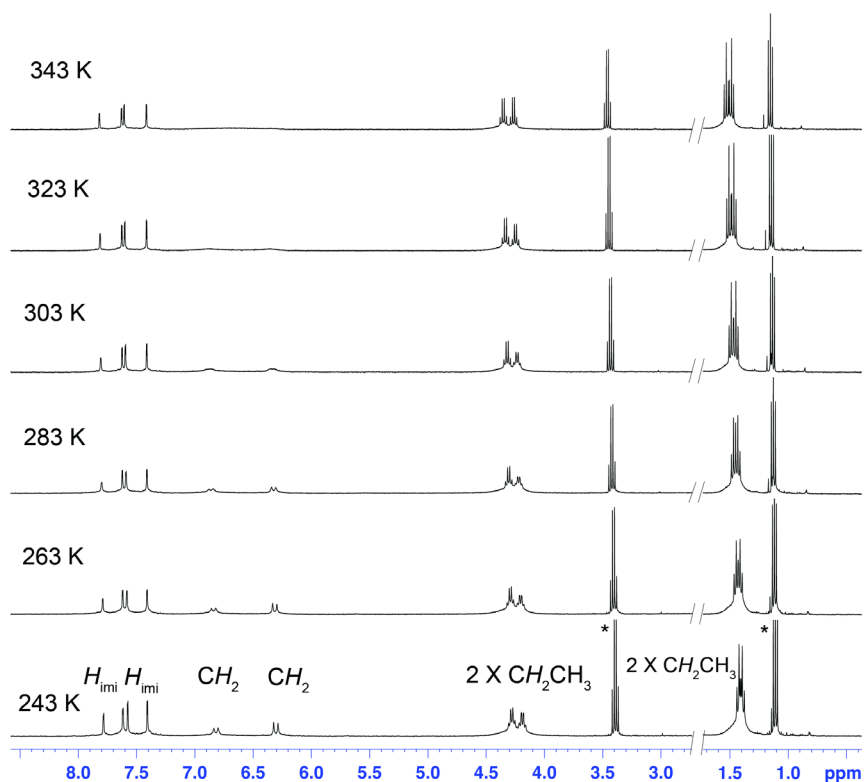


Figure A.115 Stacked  $^1\text{H}$ -NMR spectra of Au(I)-Hg(II) heterobimetallic complex **4.14**·(BF<sub>4</sub>)<sub>3</sub>.

## A.5 X-ray crystallography

### A.5.1 X-ray crystallography detail

Single crystals suitable for X-ray diffraction studies were grown as follows: **2.11·Br<sub>2</sub>** and **2.15·Br<sub>4</sub>** were grown by vapour diffusion of diethyl ether into a methanol solution of the title compound; **2.16·Br<sub>3</sub>PF<sub>6</sub>** was grown by vapour diffusion of diethyl ether into an acetonitrile solution of the title compound containing 2 drops of a solution of *tetra*-n-butylammonium bromide in acetonitrile; **2.17·Br<sub>4</sub>** was grown by slow evaporation of a methanol solution of the title compound; **2.21·Br<sub>2</sub>(PF<sub>6</sub>)<sub>4</sub>** was grown by vapour diffusion of ethyl acetate into an acetonitrile solution of the title compound; **2.26·(PF<sub>6</sub>)<sub>2</sub>**, **4.9·(BF<sub>4</sub>)<sub>3</sub>**, **4.9·(BF<sub>4</sub>)<sub>3</sub>**, **4.12·(BF<sub>4</sub>)<sub>2</sub>**, **4.12·(BF<sub>4</sub>)<sub>2</sub>** and **4.20·I** were grown by vapour diffusion of diethyl ether into an acetonitrile solution of the title compound; **(4.23)<sub>2</sub>·Na(CH<sub>3</sub>CN)Br** was grown by vapour diffusion of THF into an acetonitrile solution of the titled compound. Crystallographic data for all structures determined are given in Table A.1 and Table A.2. For all samples, crystals were removed from the crystallisation vial and immediately coated with paratone oil on a glass slide. A suitable crystal was mounted in paratone oil on a glass fibre and cooled rapidly to 173 K in a stream of cold N<sub>2</sub> using an Oxford low temperature device. Diffraction data were measured using a Rigaku Oxford Diffraction SuperNova X-ray Diffraction System mounted with Mo-K $\alpha$   $\lambda$  = 0.71073 Å and Cu-K $\alpha$   $\lambda$  = 1.54184. Data were reduced and corrected for absorption using the CrysAlis Pro program. The SHELXL2013-2 program was used to solve the structures with Direct Methods, with refinement by the Full-Matrix Least-Squares refinement techniques on F<sup>2</sup>. The non-hydrogen atoms were refined anisotropically and hydrogen atoms were placed geometrically and refined using the riding model. Coordinates and anisotropic thermal parameters of all non-hydrogen atoms were refined. All calculations were carried out using the program Olex2. Further XRD details are provided in the Supporting Information. CCDC 1885400-1885405 contains

the supplementary crystallographic data for this thesis. These data can be obtained free of charge from The Cambridge Crystallographic Data Centre via [www.ccdc.cam.ac.uk/data\\_request/cif](http://www.ccdc.cam.ac.uk/data_request/cif).

## A.5.2 XRD data for Chapter 2

Table A.1 Crystallographic data for compounds **2.11·Br<sub>2</sub>**, **2.15·Br<sub>4</sub>**, **2.16·Br<sub>3</sub>PF<sub>6</sub>**, **2.17·Br<sub>4</sub>**, **2.21·Br<sub>2</sub>(PF<sub>6</sub>)<sub>4</sub>** and **2.26·(PF<sub>6</sub>)<sub>2</sub>**

	<b>2.11·Br<sub>2</sub></b>	<b>2.15·Br<sub>4</sub></b>	<b>2.16·Br<sub>3</sub>PF<sub>6</sub></b>	<b>2.17·Br<sub>4</sub></b>	<b>2.21Br<sub>2</sub>(PF<sub>6</sub>)<sub>4</sub></b>	<b>2.26·(PF<sub>6</sub>)<sub>2</sub></b>
Empirical formula	C <sub>18</sub> H <sub>22</sub> Br <sub>4</sub> N <sub>4</sub>	C <sub>34</sub> H <sub>44</sub> Br <sub>4</sub> N <sub>8</sub> O <sub>2</sub>	C <sub>36</sub> H <sub>42</sub> Br <sub>3</sub> F <sub>6</sub> N <sub>10</sub> P	C <sub>35</sub> H <sub>44</sub> Br <sub>4</sub> N <sub>8</sub> O	C <sub>108</sub> H <sub>118</sub> Au <sub>6</sub> Br <sub>2</sub> F <sub>24</sub> N <sub>26</sub> O <sub>4</sub> P <sub>4</sub>	C <sub>42</sub> H <sub>50</sub> Br <sub>2</sub> F <sub>12</sub> N <sub>12</sub> P <sub>2</sub> Pd
Formula weight	614.03	916.41	999.49	912.42	3765.78	1279.1
Temperature/K	173.0(10)	122.96(10)	130.01(10)	150.00(10)	173.00(10)	100.00(10)
Crystal system	monoclinic	monoclinic	triclinic	Triclinic	triclinic	triclinic
Space group	<i>C2/c</i>	<i>P2<sub>1</sub>/c</i>	<i>P</i> -1	<i>P</i> -1	<i>P</i> -1	<i>P</i> -1
<i>a</i> /Å	14.3347(16)	12.8710(2)	10.8599(5)	11.4962(5)	14.9369(2)	13.7023(3)
<i>b</i> /Å	10.6333(7)	23.9257(4)	10.9352(5)	12.8708(5)	15.2472(2)	14.0092(3)
<i>c</i> /Å	15.7967(17)	12.1591(2)	17.9221(8)	13.9480(5)	29.5303(4)	15.4005(3)
$\alpha$ /°	90	90	78.193(4)	104.000(3)	87.0513(11)	109.735(2)
$\beta$ /°	121.734(15)	91.4195(16)	84.397(4)	97.228(4)	77.1272(12)	108.553(2)
$\gamma$ /°	90	90	85.653(4)	110.155(4)	87.0120(11)	94.107(2)
Volume/Å <sup>3</sup>	2047.8(4)	3743.22(11)	2069.96(16)	1829.64(14)	6541.98(16)	2584.34(10)
<i>Z</i>	4	4	2	2	2	2
$\rho_{\text{calc}}$ /cm <sup>3</sup>	1.992	1.626	1.604	1.656	1.912	1.644
$\mu$ /mm <sup>-1</sup>	7.872	5.586	4.566	5.691	7.454	2.054
<i>F</i> (000)	1192	1840	1004	916	3600	1280
Crystal size/mm <sup>3</sup>	0.08 × 0.08 × 0.06	0.1 × 0.08 × 0.04	0.05 × 0.02 × 0.01	0.01 × 0.01 × 0.002	0.1 × 0.07 × 0.02	0.03 × 0.02 × 0.02
Radiation	MoK $\alpha$ ( $\lambda$ = 0.71073)	CuK $\alpha$ ( $\lambda$ = 1.54184)	CuK $\alpha$ ( $\lambda$ = 1.54184)	CuK $\alpha$ ( $\lambda$ = 1.54184)	MoK $\alpha$ ( $\lambda$ = 0.71073)	MoK $\alpha$ ( $\lambda$ = 0.71073)
2 $\Theta$ range for data collection/°	6.064 to 52.738	7.39 to 130.166	8.194 to 148.988	6.71 to 130.14	5.6 to 60.64	6.476 to 49.416
Index ranges	-16 ≤ <i>h</i> ≤ 17, -13 ≤ <i>k</i> ≤ 13, -19 ≤ <i>l</i> ≤ 15	-15 ≤ <i>h</i> ≤ 13, -28 ≤ <i>k</i> ≤ 18, -14 ≤ <i>l</i> ≤ 14	-12 ≤ <i>h</i> ≤ 13, -13 ≤ <i>k</i> ≤ 13, -22 ≤ <i>l</i> ≤ 22	-13 ≤ <i>h</i> ≤ 13, -15 ≤ <i>k</i> ≤ 14, -16 ≤ <i>l</i> ≤ 16	-19 ≤ <i>h</i> ≤ 21, -20 ≤ <i>k</i> ≤ 21, -41 ≤ <i>l</i> ≤ 41	-16 ≤ <i>h</i> ≤ 16, -16 ≤ <i>k</i> ≤ 16, -18 ≤ <i>l</i> ≤ 16
Reflections collected	5867	12945	19369	14785	102731	29090
Independent reflections	2094 [ <i>R</i> <sub>int</sub> = 0.0253, <i>R</i> <sub>sigma</sub> = 0.0303]	6369 [ <i>R</i> <sub>int</sub> = 0.0218, <i>R</i> <sub>sigma</sub> = 0.0261]	8443 [ <i>R</i> <sub>int</sub> = 0.0398, <i>R</i> <sub>sigma</sub> = 0.0440]	6244 [ <i>R</i> <sub>int</sub> = 0.0311, <i>R</i> <sub>sigma</sub> = 0.0389]	34834 [ <i>R</i> <sub>int</sub> = 0.0320, <i>R</i> <sub>sigma</sub> = 0.0429]	8779 [ <i>R</i> <sub>int</sub> = 0.0352, <i>R</i> <sub>sigma</sub> = 0.0437]
Data/restraints/parameters	2094/0/118	6369/0/440	8443/0/511	6244/0/437	34834/1/1576	8779/0/646
Goodness-of-fit on <i>F</i> <sup>2</sup>	1.062	1.034	1.033	1.035	1.036	1.068
Final <i>R</i> indexes [ <i>I</i> ≥ 2 $\sigma$ ( <i>I</i> )]	<i>R</i> <sub>1</sub> = 0.0373, <i>wR</i> <sub>2</sub> = 0.0917	<i>R</i> <sub>1</sub> = 0.0321, <i>wR</i> <sub>2</sub> = 0.0845	<i>R</i> <sub>1</sub> = 0.0387, <i>wR</i> <sub>2</sub> = 0.0973	<i>R</i> <sub>1</sub> = 0.0301, <i>wR</i> <sub>2</sub> = 0.0746	<i>R</i> <sub>1</sub> = 0.0437, <i>wR</i> <sub>2</sub> = 0.0970	<i>R</i> <sub>1</sub> = 0.0397, <i>wR</i> <sub>2</sub> = 0.1010
Final <i>R</i> indexes [all data]	<i>R</i> <sub>1</sub> = 0.0468, <i>wR</i> <sub>2</sub> = 0.0973	<i>R</i> <sub>1</sub> = 0.0353, <i>wR</i> <sub>2</sub> = 0.0868	<i>R</i> <sub>1</sub> = 0.0512, <i>wR</i> <sub>2</sub> = 0.1059	<i>R</i> <sub>1</sub> = 0.0351, <i>wR</i> <sub>2</sub> = 0.0786	<i>R</i> <sub>1</sub> = 0.0639, <i>wR</i> <sub>2</sub> = 0.1069	<i>R</i> <sub>1</sub> = 0.0500, <i>wR</i> <sub>2</sub> = 0.1053
Largest diff. peak/hole / e Å <sup>-3</sup>	1.57/-1.15	1.39/-0.49	0.95/-0.63	1.01/-0.60	5.05/-5.20	1.42/-1.36



### A.5.3 XRD data for Chapter 4

Table A.2 Crystallographic data for compounds **4.9·(BF<sub>4</sub>)<sub>3</sub>**, **4.12·(BF<sub>4</sub>)<sub>2</sub>**, **4.17·(BF<sub>4</sub>)<sub>2</sub>**, **4.20·I**, **4.23·HBr<sub>2</sub>** and **(4.23)<sub>2</sub>·Na(CH<sub>3</sub>CN)Br<sub>3</sub>**.

	<b>4.9·(BF<sub>4</sub>)<sub>3</sub></b>	<b>4.12·(BF<sub>4</sub>)<sub>2</sub></b>	<b>4.17·(BF<sub>4</sub>)<sub>2</sub></b>	<b>4.20·I</b>	<b>4.23·Br</b>	<b>(4.23)<sub>2</sub>·Na(CH<sub>3</sub>CN)Br<sub>3</sub></b>
Empirical formula	C <sub>20</sub> H <sub>30</sub> AuB <sub>3</sub> F <sub>12</sub> N <sub>8</sub>	C <sub>20</sub> H <sub>26</sub> AgAuB <sub>2</sub> F <sub>8</sub> N <sub>8</sub>	C <sub>22</sub> H <sub>32</sub> Ag <sub>2</sub> B <sub>2</sub> F <sub>8</sub> N <sub>8</sub>	C <sub>9</sub> H <sub>13</sub> N <sub>4</sub> I	C <sub>20</sub> H <sub>29</sub> AuBr <sub>2</sub> N <sub>8</sub>	C <sub>23</sub> H <sub>33</sub> AuI <sub>1.5</sub> N <sub>8.5</sub> Na <sub>0.5</sub> O <sub>0.5</sub>
Formula weight	838.93	856.94	797.91	304.14	738.30	835.39
Temperature/K	150.00(10)	149.99(10)	150.00(10)	133.0(4)	149.98(10)	149.99(10)
Crystal system	monoclinic	monoclinic	triclinic	monoclinic	triclinic	orthorhombic
Space group	P2 <sub>1</sub> /m	I2/a	P-1	P2 <sub>1</sub> /c	P-1	Pbca
a/Å	7.8113(3)	13.49130(10)	8.72610(10)	6.8428(6)	10.7465(2)	23.03910(10)
b/Å	12.0497(4)	14.38060(10)	9.47660(10)	11.5230(5)	11.46525(18)	20.32320(10)
c/Å	16.2511(6)	17.91910(10)	9.62530(10)	17.2878(15)	12.0732(2)	27.3134(2)
α/°	90	90	82.3560(10)	90	65.8087(16)	90
β/°	99.996(3)	106.4520(10)	67.8470(10)	124.136(12)	85.8739(15)	90
γ/°	90	90	85.3190(10)	90	80.8541(15)	90
Volume/Å <sup>3</sup>	1506.40(10)	3334.20(4)	730.216(15)	1128.3(2)	1339.64(4)	12788.91(13)
Z	2	4	1	2	2	16
ρ <sub>calc</sub> /cm <sup>3</sup>	1.850	1.707	1.814	1.790	1.830	1.735
μ/mm <sup>-1</sup>	4.984	13.480	11.483	22.055	13.989	20.297
F(000)	814.0	1640.0	396.0	592.0	708.0	6376.0
Crystal size/mm <sup>3</sup>	0.05 × 0.02 × 0.02	0.04 × 0.04 × 0.02	0.07 × 0.06 × 0.04	0.04 × 0.02 × 0.02	0.08 × 0.05 × 0.03	0.09 × 0.08 × 0.02
Radiation	MoKα (λ = 0.71073)	CuKα (λ = 1.54184)	CuKα (λ = 1.54184)	CuKα (λ = 1.54184)	CuKα (λ = 1.54184)	CuKα (λ = 1.54184)
2θ range for data collection/°	6.426 to 49.424	8.016 to 142.512	9.422 to 136.784	9.856 to 148.96	8.028 to 142.452	6.642 to 130.176
Index ranges	-8 ≤ h ≤ 9, -14 ≤ k ≤ 12, -19 ≤ l ≤ 19	-15 ≤ h ≤ 16, -17 ≤ k ≤ 17, -21 ≤ l ≤ 17	-10 ≤ h ≤ 10, -11 ≤ k ≤ 11, -11 ≤ l ≤ 11	-8 ≤ h ≤ 8, -14 ≤ k ≤ 14, -21 ≤ l ≤ 21	-13 ≤ h ≤ 13, -14 ≤ k ≤ 12, -14 ≤ l ≤ 11	-27 ≤ h ≤ 26, -23 ≤ k ≤ 21, -32 ≤ l ≤ 32
Reflections collected	16113	33825	24497	9270	28172	231683
Independent reflections	2692 [R <sub>int</sub> = 0.1314, R <sub>sigma</sub> = 0.0748]	3241 [R <sub>int</sub> = 0.0279, R <sub>sigma</sub> = 0.0094]	2681 [R <sub>int</sub> = 0.0586, R <sub>sigma</sub> = 0.0188]	2315 [R <sub>int</sub> = 0.0333, R <sub>sigma</sub> = 0.0234]	5174 [R <sub>int</sub> = 0.0289, R <sub>sigma</sub> = 0.0154]	10898 [R <sub>int</sub> = 0.1136, R <sub>sigma</sub> = 0.0287]
Data/restraints/parameters	2692/2/266	3241/2/201	2681/0/192	2315/0/128	5174/225/283	10898/0/681
Goodness-of-fit on F <sup>2</sup>	1.135	1.084	1.114	1.086	1.044	1.043
Final R indexes [I > 2σ (I)]	R <sub>1</sub> = 0.0560, wR <sub>2</sub> = 0.1363	R <sub>1</sub> = 0.0217, wR <sub>2</sub> = 0.0593	R <sub>1</sub> = 0.0266, wR <sub>2</sub> = 0.0702	R <sub>1</sub> = 0.0303, wR <sub>2</sub> = 0.0846	R <sub>1</sub> = 0.0347, wR <sub>2</sub> = 0.0932	R <sub>1</sub> = 0.0495, wR <sub>2</sub> = 0.1389
Final R indexes [all data]	R <sub>1</sub> = 0.0648, wR <sub>2</sub> = 0.1394	R <sub>1</sub> = 0.0220, wR <sub>2</sub> = 0.0595	R <sub>1</sub> = 0.0266, wR <sub>2</sub> = 0.0702	R <sub>1</sub> = 0.0331, wR <sub>2</sub> = 0.0888	R <sub>1</sub> = 0.0351, wR <sub>2</sub> = 0.0935	R <sub>1</sub> = 0.0513, wR <sub>2</sub> = 0.1410
Largest diff. peak/hole / e Å <sup>-3</sup>	1.29/-1.43	0.62/-0.54	0.67/-1.18	0.62/-1.37	1.64/-1.66	4.01/-1.51